FISH OTOLITH CHEMISTRY AS AN INDICATOR OF PHYSIOLOGICAL, ECOLOGICAL AND ENVIRONMENTAL EVENTS

by
John M. Kalish B.S. (Miami), M.S. (Oregon State)

Department of Zoology

submitted in fulfillment of the requirements for the degree of
Doctor of Philosophy
University of Tasmania

December 1989

DECLARATION

This thesis contains no material which has been accepted for the award of any degree or diploma in any university, and to the best of my knowledge and belief, this thesis contains no copy or paraphrase of material previously published or written by any person, except where due reference is made in the text of the thesis.

John M. Kalish

TABLE OF CONTENTS

ABSTRACT

Fish otoliths are calcium carbonate aggregates in the membranous labyrinth of all teleost fishes. The deposition of these structures is affected by both physiological and environmental factors which can cause changes in both the rate of otolith depositon and in the composition of the material deposited. The rate of otolith deposition, particularly in regard to the alternation of calcium carbonate-rich and protein-rich zones, has been widely investigated in an attempt to understand processes of ageing and growth in fishes. Aspects of the chemistry of these structures, particularly trace elements and stable isotopes, that may vary in response to physiological and environmental change, have not been studied in detail and are the basis of this research.

The effects of temperature, somatic growth, otolith growth, condition factor, RNA/DNA ratio, age and season on the incorporation of Sr, Na, K and S into the sagittal otoliths of Australian salmon and blue grenadier were investigated by a combination of laboratory rearing experiments and monthly collections of wild fish. Microchemical analyses of otolith chemistry were carried out with a wavelength dispersive electron microprobe. There were significant differences in otolith Sr/Ca ratios among Australian salmon maintained in the laboratory at different temperatures and a slight positive correlation with temperature, but there was no evidence for a linear relationship between Sr/Ca ratio and temperature. Biologically significant relationships between other factors were not evident in laboratory-maintained fish. Furthermore, the variability of elemental ratios within temperature treatments and within individual otoliths was very significant. There were highly significant correlations between otolith chemistry and fish age in wild blue grenadier and it was hypothesized that the seasonal and age-related variation in otolith Sr content is largely the result of changes in the proportions of free and bound Ca and Sr present in the blood plasma and that this is in turn a function of the quantity and type of proteins present in the plasma. Data on the level of Sr present in the saccular endolymph and the sagittae of 12 fish species showed that there was a very strong relationship between the composition of the endolymph and the otoliths.

Seasonal collections of otoliths, blood plasma, saccular endolymph and biological data from *Pseudophycis barbatus* indicated that physiology was largely responsible for changes in endolymph composition. Measurements of weight, length, gonad weight, and Sr, Ca, Na, K, protein, triglyceride, phosphate and glucose in the plasma and endolymph were used to develop multivariate models to explain endolymph and otolith composition. It was possible to explain up to 98% of the variance in the endolymph Sr content of female *Pseudophycis barbatus*. The range of otolith Na and K content could be estimated using models in the geochemical literature. These results showed that otolith trace element composition was based on the interaction of physiological, ecological and environmental factors.

Life-history transects of otolith microchemistry in a range of species indicated

that the factors that ultimately effect otolith composition are generally not under strong environmental control. However, it was found that variations in otolith microchemistry can be useful in studies aimed at determining distributional relationships among contemporaneous individuals, particularly in studies seeking to identify nursery grounds or where there is an interest in fine resolution "stock" discrimination. Recognizable "signatures" in otolith life-history transects may result when co-occurring individuals experience extreme environmental conditions. In most species there appears to be little information that can be gained directly from the interpretation of otolith Sr/Ca, Na/Ca, K/Ca and S/Ca ratios. The complex interaction of factors affecting trace element levels in fish otoliths makes it virtually impossible to determine those factors which result in a particular quantity of Sr, Na, K or S in an otolith or, to use these elements as indicators of physiological or environmental change.

Otolith microchemistry of anadromous and nonanadromous salmonids was investigated to determine if there were differences among migratory and nonmigratory individuals and to determine if the habitat where vitellogenesis took place would affect the composition of the otolith primordia of the progeny. There were significant differences in otolith Sr/Ca ratios among adult anadromous and nonanadromous salmonids and the otolith Sr/Ca ratios in the primordia were greater in the progeny of anadromous salmonids than in the otolith primordia of the progeny of nonanadromous individuals.

Studies of oxygen and carbon isotopes in the otoliths of laboratory maintained *Arripis trutta* showed that oxygen isotopes were deposited near to equilibrium with seawater and, contrary to evidence presented in the literature, can be used to predict environmental temperatures. Approximately 30% of the otolith carbon was from metabolically derived sources. Oxygen isotopes in otoliths from a wide range of fish species were found to be deposited in equilibrium with seawater, while there are varying levels of carbon isotope disequilibria. The hypothesis that the magnitude of carbon isotope disequilibria is related to metabolic rate (VO_2) was developed and evidence in support of this hypothesis was presented.

Scanning and transmission electron microscope studies of fish otoliths showed the relationship between organic and inorganic material in microincrements and presented evidence for the complete cessation of calcium carbonate deposition during periods of stress. Ultrastructural observations showed that aragonite crystals in fish otoliths are highly variable in morphology and size and, thus, may be an important factor in determining within otolith variations in trace element chemistry.

ACKNOWLEDGEMENTS

There are many people who should be thanked for their assistance in making the completion of this thesis a reality and for listening to someone who was willing to spend several years studying "fish ears". The list includes a diverse range of people and possums. Also, this research would not have been possible without the co-operation of several organizations which provided equipment and facilities.

-My supervisor, Dr. Robert White, commented on a draft of this thesis and organized the financing of many elements of this research.

-Professor Michael Stoddart provided advice in some of the rougher sections.

-Nick Ware (Research School of Earth Sciences, Australian National University) taught me about electron microprobes and made the microprobe facilities at ANU available for a token fee. That's a good thing since I operated the ANU Cameca for 568.2 h and made 8796 analyses.

-Dr. June Olley and Stephen Thrower (CSIRO Division of Food Technology) made it possible to carry out the aquarium validation experiments by allowing me to use their constant temperature facilities at "Stowell".

- Jim Kiss (Hobart Repatriation Hospital) made available facilities for biochemical analyses and helped to lighten the work load.

-Dr. Des Richardson (Australian Newsprint Mills, Boyer) let me use the graphite furnace atomic absorption spectrophotometer at ANM every Monday.

-Dr. Charles Dragar discussed a wide range of chemical problems and provided sound advice.

-Dr. Peter Davies (Inland Fisheries Commission) provided advice on many topics and some of the trout and trout ova. He also made IFC facilities available, especially for some of the RNA/DNA analyses.

-Laurie Cook (Inland Fisheries Commission) showed me how to do RNA/DNA analyses and helped to collect trout.

-Dr. Alex McLaren (Research School of Earth Sciences, Australian National University) did the work on the TEM and discussed various aspects of crystallography and mineralogy.

-Wayne Kelly went out on most of the cod expeditions to Variety Bay and helped me extract the juices from all those fish and Adam Smolenski gave a hand when Wayne was on holiday.

-Mike Power and Christine CooK (U. Tas., Central Science Laboratory) helped the the stable isotope mass spectrometry.

-Wieslaw Jablonski (U. Tas., Central Science Laboratory) gave me "free-range" on the new Cameca SX-50 microprobe and the SEM.

-Simon Stephens let me use the Geology Department's specimen preparation facilities.

-Dr. Tim Davis (CSIRO Division of Fisheries Research) gave me free access to the low-speed diamond saw.

-Phil Robinson did the XRF analyses.
-Ted Ritchey caught the school of Australian salmon off Vansitart Island.
-Dr. Jeremy Lyle and John Kitchener (Tasmanian Department of Sea Fisheries) collected the orange roughy and brought me fresh specimens.
-Dick Williams (Australian Antarctic Division) game me the otoliths from the Antarctic fish.
-Ron Mawbey helped with sampling locations and the early collections of Australian salmon.
-Barry Rumbold ordered everything, knew where to get things, manipulated finances and deserves a lot more credit than he generally receives. The poor guy has to put up with all of us.
-Richard Holmes piloted the boat to Variety Bay and found the cod. He managed to order sunny days a large percentage of the time and was very handy with a 9/16 ring spanner. He also constructed many bits of equipment used in this research.
-Jane Andrew (Inland Fisheries Commission) reared the trout and provided trout ova.
-Mick "Moiré Fringe" O'Leary provided some of the more stunning artwork in the thesis and was always in on "gonna go downtown....".
-Numerous people helped with the beach seining including Stephen Reid, Ron Mawbey, Prem and Lee Hamr, Bill Buttemer, Vaughan Monamy, Sarah Monks and Rick Crossland. There are almost certainly others but your memory starts to go near the end.

Stephanie, the person who provided the greatest assistance, gets her own paragraph. She went on most of the beach seining expeditions, made sure that I didn't drowned while collecting mysids, helped to feed the fish, collected sludge infested trout on the Derwent under all conditions, made heaps of graphs, did loads of typing, read most of it, heard all of it and more. Most importantly, she provided mental support under all circumstances.

CHAPTER 1

GENERAL INTRODUCTION

1.1 INTRODUCTION

The following investigations consider the feasibility of applying data on the trace element and isotopic chemistry of aragonitic fish otoliths to studies of fish biology. These are approaches that have received some attention in recent years (Mulcahy *et al.*, 1979; Casselman, 1983; Radtke, 1984a, 1984b; Townsend *et al.*, 1989), but which have not been investigated to such a degree that their utility can be assessed conclusively. The major impetus for the research reported in this thesis was to develop new methods for the study of marine fishes. Many of the major questions in fish biology cannot be answered using currently employed methodologies. This is due to the combined effects of inaccessibility, mobility and longevity that are frequently attributable to many marine fish species. In some instances these problems can be overcome by increased effort, more time at sea, examination of a greater number of specimens and similar approaches. This is often highly impractical and very costly. An alternative approach involves the development or adaptation of methodologies that are new to the study of fishes.

The membranous labyrinth of all vertebrates contains some form of mineralized structure which mediates both vestibular and auditory functions. When large numbers of small calcium carbonate crystals are present, these structures are called otoconia (ear dust), whereas the organs are known as otoliths (ear stones) in teleost fishes which possess relatively large individual masses of calcium carbonate in each of the three otolith pouches, the saccule, utricule and lagena. Otoconia, generally in the form of calcitic or aragonitic prisms, grow to a finite size and display relatively little notable microstructure beyond that of the individual microcrystals and organic matrix of which they are composed (Mann *et al.*, 1983; Ross and Donovan, 1986). However, fish otoliths exhibit a relatively complex microstructure due to the cyclic/daily deposition of alternate layers of calcium carbonate rich and protein rich material. These alternating zones define the bipartite microstructure of fish otoliths called growth increments, microincrements or "daily" increments (Pannella, 1971; Brothers *et al.*, 1976; Campana and Neilson, 1985). This property of fish otoliths, which suggests that they are produced by a nearly continuous process of deposition

throughout life, makes them a potentially valuable source of information regarding the life of individual fish.

The distribution of trace elements and isotopes within an otolith may be a manifestation of the combined effects of a fish's physiology, life-history stage and environment. However, the interpretation of otolith chemistry as the ultimate product of numerous factors is extremely complex. The significance of variations in the chemical composition of both inorganic and biogenic calcium carbonate is poorly understood. Geochemical studies have shown that variations in the composition of calcium carbonate, and the degree to which trace elements may "contaminate" the calcium carbonate lattice, can be related to four major factors: (1) mineralogy of the skeletal fragment; (2) environmental features; (3) water chemistry; and (4) a "vital" or biological effect based on the physiology of the organism (Amiel *et al.*, 1973; Milliman, 1974; Veizer, 1983). As this study will demonstrate, the division of those properties that effect carbonate chemistry into four categories is an oversimplification given the extreme generality of each category. Reviews on the chemistry of both inorganic and biogenic carbonates can be found in Milliman (1974) and Reeder (1983).

A large number of investigations have attempted to use qualitative and quantitative changes in carbonate trace element and isotope chemistry as palaeoenvironmental indicators. The primary impetus for these studies was the belief that there were direct and quantifiable relationships between calcium carbonate composition and environmental variability. Although a large number of trace elements have been detected in calcium carbonates (Turekian and Wedepohl, 1961; Wolf *et al.*, 1967; Milliman, 1974; Veizer, 1983), the majority of investigations have concentrated on variations in the more abundantly occurring monovalent and divalent cations, which include Na^{+}, Mg^{++}, K^{+}, Mn^{++}, Fe^{++} and Sr^{++}, with by far the greatest emphasis on Sr^{++}, Mg^{++} and Na^{+}. The literature is extensive and will not be dealt with in detail here. However, it is important to indicate the general direction and conclusions of these investigations in order to appreciate the framework for this study.

Strontium, magnesium and sodium are major constituents of seawater and are generally found in readily detectable quantities in calcium carbonate. Almost 40 years ago scientists began to investigate the relationship between these elements in seawater and calcium carbonate (Kulp *et al.*, 1952; Chave, 1954a, 1954b; Thompson and

Chow, 1955; Turekian, 1955; Odum, 1957; Dodd, 1965; Land and Hoops, 1973). It was initially suggested that the quantities of these elements measured in calcium carbonate shells and coral skeletons would be a function of salinity alone, but this idea was soon modified to include temperature. In addition, it became evident that if any relationships did exist, then they operated differently in calcite and aragonite, the two most commonly occurring polymorphs of calcium carbonate (Lowenstam, 1954a, 1954b). In many instances, a relationship between temperature and/or salinity and the quantity of strontium and magnesium in the calcium carbonate test was found (Dodd, 1965, 1967; Hallam and Price, 1968), but these conclusions were made without consideration of other variables such as growth rates, light intensity, diet or sex. Others reported that there was no relationship between temperature and Sr or Mg in the calcium carbonate structures of molluscs and corals (Thompson and Chow, 1955; Pilkey and Goodell, 1963; Harriss, 1965; Moberly, 1968).

Kinsman and Holland (1969) provided laboratory-based empirical evidence to support the theory that the quantity of Sr present in inorganically precipitated aragonite was inversely correlated with temperature. The theoretical basis for this result also provided evidence for a relationship between Mg incorporation in calcite and temperature. This finding did not result in any detectable increase in publications in the area, but did provide some support to the earlier findings. Houck *et al.* (1977) and Smith *et al.* (1979) provided the first irrefutable evidence that the level of Sr in scleractinian corals could be used as an indicator of temperature. They measured coral growth rates, salinity, illumination and temperature in experiments with 5 coral species and found that the relationship existed in each of the species, but that the relationships were slightly different from that found by Kinsman and Holland (1969) for inorganic aragonite. Although Schneider and Smith (1982) were able to apply successfully the concept of Sr/Ca thermometry to cores of *Porites* spp., it has subsequently been found that these relationships do not always apply and are not consistent among or within species (Goreau, 1977; personal communication, Dr. S. V. Smith, Department of Oceanography, University of Hawaii). Both Buchardt and Fritz (1978) and Lorens and Bender (1980) found that Sr/Ca thermometry was not applicable to molluscs. Alternatively, Mg has been used with some success as an indicator of temperature and salinity in ostracods (Cadot *et al.*, 1972; Chivas *et al.*, 1986). Investigations of both Na and K in corals and bivalves are less common and in many cases have been restricted to the literature on inorganic precipitates (White,

1977; Lorens and Bender, 1980; Okumura and Kitano, 1986). These will be discussed further in the body of this thesis.

Despite general confusion and disagreement in the literature regarding the utility of Sr and Mg data as indicators of temperature (see Rosenberg, 1980 for a summary of the data on molluscs), it is evident that, in some cases, these data can provide valuable information. Radtke and Targett (1984), Radtke (1984b, 1989) and Townsend *et al.* (1989) presented evidence for a relationship between temperature and otolith Sr levels. However, these data were not conclusive because these researchers did not measure other variables during their investigations and, in some cases, the interpretation of the data was largely subjective. In addition, they did not consider the significance of other readily detectable trace elements in fish otoliths.

There is a need for clarification of the relationships between calcium carbonate trace element chemistry and environmental and physiological variables for a wide range of marine organisms. The present study was designed to determine the relationships between otolith composition and physiology, life-history and environment, and to investigate the application of these relationships to problems in fish biology. Because of the relative lack of background knowledge in this area, the approach is wide ranging and encompasses the fields of oceanography, fish physiology, ecology and geochemistry. Although the study is of a broad general interest, it is intended for scientists involved in the general area of fish biology. As such, I have included below, a brief section on electron microprobe analysis. Basic geochemical principles are discussed in the relevant chapters and further information can be obtained from the references therein.

1.2 APPLICATION OF ELECTRON MICROPROBE ANALYSIS TO THE STUDY OF FISH OTOLITH MICROCHEMISTRY

The utility of the electron microprobe is based on the fact that x-rays, photons of electromagnetic radiation, emitted from a substance display a frequency that is characteristic of the element from which they are produced. This fact, coupled with the finely focused electron beam capabilities of the electron microscope, produced the first electron microprobe in 1949 (Castaing and Guinier, 1949). There is a large body of both theoretical and empirical literature that is related to the coupling of these principles (Reed, 1975; Goldstein *et al.*, 1981). These are discussed only briefly and then considered in relation to the capabilities and limitations of these methods in

the analysis of calcium carbonate samples and fish otoliths.

Two forms of x-rays can be produced when electrons bombard a sample: characteristic x-rays and continuum x-rays. Electron bombardment can result in the ejection of an electron from an element if the kinetic energy of the bombarding electrons is sufficient. If the ejected electron is from an inner atomic shell (K, L, M. etc.) then the atom will be in an ionized state. The atoms response to this ionization involves relaxation to the ground state. This requires the transition of an electron from an outer shell to fill the electron vacancy. During this transition a quantum of energy is released, in the form of an x-ray, that is equal to the difference in the potential of the atom before and after ionization (Goldstein *et al.*, 1981). The energy of x-rays resulting from the ionization of electrons from a specific element and electron shell are defined precisely (Bertin, 1975). The quantification and identification of these characteristic x-rays is the basic goal of electron microprobe analysis. In addition, continuum x-rays are produced which result in the formation of a continuous spectrum or 'bremsstrahlung' (braking radiation). This form of background radiation results when x-ray photons produced by electron bombardment are decelerated by collisions with other atoms in the sample.

Two forms of electron microprobe, energy dispersive (ED) and wavelength dispersive (WD) can be used to identify and quantify the x-rays produced from the electron bombardment of a sample. The electron probe forming component of the system is similar, but there are large differences in the functioning of the spectrometers which actually detect the x-ray energy. Operation of the WD spectrometer is based on Bragg's law which indicates that the diffraction of an x-ray by a crystal is dependent on the wavelength of the x-ray and the spacing between the planes of the crystal. By adjusting the angle of the appropriate crystal relative to the incident x-rays, it is possible to selectively diffract x-rays of a specific wavelength. The selected x-rays are then quantified by a gas flow proportional counter (Reed, 1975; Goldstein *et al.*, 1981). Energy dispersive spectrometers are equipped with liquid nitrogen cooled solid state detectors. These devices are capable of acquiring a spectrum which relates to the energy range of the x-rays that impinge upon the detector. As there is no energy or wavelength segregating device analogous to the WD spectrometer crystal in place before the silicon detector, all x-rays are detected. After amplification, the electrical pulse produced by the detector is measured and passed to a multichannel analyzer (MCA), generally with 1024 channels, which sorts

the pulses by voltage. This results in a spectrum of the x-rays produced by electron bombardment of the sample (Statham, 1981).

There are several trade-offs involved in the use of a WD or ED spectrometers. In a WD spectrometer it is necessary to alter the position of the diffracting crystal (and, in many instances change the type of crystal) in order to detect different elements. To make these changes the position of the crystal is altered mechanically. This is not necessary in the ED spectrometer as this device is designed to collect an entire spectrum simultaneously. However, although the WD spectrometer lacks speed of operation, it is far superior to the ED spectrometer in terms of sensitivity and detection limits. The ED spectrometer is plagued by both high and complex background radiation due to limited energy resolution, whereas the energy resolution of the WD spectrometer is very high and background radiation can be readily determined. Also, recent years have seen tremendous improvements in the speed and reliability with which a WD spectrometer can precisely alter the position of a diffracting crystal. Furthermore, WD microprobes generally have from 3 to 5 separate spectrometers, allowing for the precise quantification of up to 5 elements simultaneously. The advantages and disadvantages of ED and WD spectrometers are discussed in greater detail in the references already cited.

The true test of the utility of ED versus WD spectrometry is dependent on the intended application. The following discussion will clarify the reasons for selecting WD spectrometers for the analysis of trace elements in fish otoliths. It is worthwhile to consider this from a more general viewpoint before discussing calcium carbonate and otoliths specifically. A primary consideration in quantitative estimation of trace elements by microprobe analysis is the concept of detection limits. Calculation of the minimum concentration that can be detected, also called the detectability limit C_{DL} is by (Goldstein *et al.*, 1981)

$$C_{DL} = \frac{C_s}{\bar{N}_s - \bar{N}_{sb}} \frac{2^{\frac{1}{2}} t_{n-1}^{1-\alpha} S_c}{n^{\frac{1}{2}}}$$

where

C_S = concentration of element in the standard

N_s = mean number of counts obtained from the standard

N_{sb} = continuum background for the standard

t = Student t value for a 1-a confidence level and for n-1 degrees of freedom

S_c = standard deviation of the measured counts

n = the number of times that counts were collected

A more simplistic approach considers an element to be detected if the mean total number of counts N exceeds the background by $3(N_B)^{1/2}$, where N_B is the number of background counts (Goldstein *et al.*, 1981). Typical values for peak and background counts in this study, and the associated detection limits, are presented in Table 1.1.

Table 1.1 Estimates of detection limits for typical wavelength dispersive electron microprobe data collected in this study. Counting times used can be found in Tables 2.1 and 5.1.

Element	Peak counts	Background counts	$3(N_B)^{1/2}$
Ca	85,000	600	73.5
Sr	2,000	950	92.5
Na	1,200	230	45.5
K	600	450	63.6
S	400	180	40.2

Under the conditions presented in Table 1.1 all the elements listed are easily detected.

Clearly, the detectability limit increases as the level of the background increases. This is the area where the WD microprobe is far superior to the ED microprobe. High background combined with relatively poor energy resolution frequently make the ED microprobe inadequate for studies of trace elements.

To indicate the difficulties that can be encountered when measuring trace elements with an electron microprobe I will consider the quantitative estimation of strontium. This example is particularly relevant because of the importance of strontium to this study. Under optimal operating conditions the minimum detectability limit for a wavelength dispersive (WD) electron microprobe is approximately 10 times lower than that of an ED microprobe for all elements (Geller 1977; Goldstein *et al.* 1981). Generally, the minimum detection limits attainable with an ED spectrometer are on the order of 0.10 wt% (1000 ppm) and these

conditions are frequently not realized due to various factors. The range of Sr concentrations measured in the following study was approximately 300-5000 ppm and all marine fish otoliths investigated to date appear to contain Sr in excess of 1000 ppm (Radtke, 1987; Edmonds, *et al.* 1989; Kalish, 1989). Theoretically the ED spectrometer should be capable of making all otolith Sr measurements in marine fish and some of those from freshwater fish. However, the detection and accurate quantitative estimation of Sr creates special problems for the ED microprobe.

The x-ray line that is used to detect Sr at 1.806 keV (L_α) is affected by the silicon escape peak associated with the large Ca K_α peak produced when measuring specimens that are largely calcium (aragonite fish otoliths are approximately 38 wt% Ca). The silicon escape peak results from the production of Si K_α photons following absorption of relatively high energy (>1.841 keV) photons by the silicon detector of an ED spectrometer (Reed and Ware, 1972). The energy of the photon producing the escape peak is E_x-E_{Si}, where E_x is the incident photon energy and E_{Si} is the energy of a Si K_α photon (1.739 keV). The silicon escape peak due to Ca K_α would have an energy of 1.951 keV (3.690 keV-1.739 keV) and an intensity 0.78% that of the Ca K_α peak (Reed, 1975). Such a peak, within less than 150 eV of the Sr peak, would create significant errors in the estimation of low levels of Sr. Measurements of trace levels of phosphorus with the K_α line (2.013 keV) would be even more vulnerable to errors because of the closer proximity to the Ca K_α derived silicon escape peak. Other errors can result from a silicon internal fluorescence peak (Reed and Ware, 1972) and the silicon absorption edge (Goldstein *et al.*, 1981; Statham, 1981), both artefacts of the ED spectrometer and associated silicon detector, and of particular interest to the determination of trace levels of Sr. These sources of error are not present when using a WD electron microprobe.

There are numerous other potential sources of error in otolith trace element studies carried out with ED electron microprobes. These errors can occur due to the relatively poor energy resolution of the ED spectrometer and the resultant inability to discriminate between x-ray lines separated by less than approximately 150 ev (Statham 1981). Furthermore, the presence of a greater proportion of continuum background radiation or "bremsstrahlung" in the ED spectrometer, due to decreased energy resolution, results in a five-fold increase in the peak to background ratio in a WD spectrometer over an ED spectrometer (Reed 1975).

These factors, and others, make it necessary to view with caution studies with

ED microprobes that investigate the distribution of large numbers of trace (<0.5 wt%) elements, particularly without reference to criteria for determining detection levels or precision. Using an ED microprobe, Mulligan *et al.* (1987) claim to have detected 34 trace elements in the otoliths of striped bass *Morone saxatilis* from the Chesapeake Bay region on the central east coast of North America. They do not report any criteria for determining detection limits and, on the basis of their sample x-ray spectrum (Fig. 2 in Mulligan *et al.*, 1987) it is difficult to acknowledge the presence of Cr (which they highlight), let alone the wide range of rare earth elements they claim to have detected. The rare earth elements are generally at levels below 1.0 ppm in carbonates (Milliman, 1974; Veizer, 1983) and would be impossible to detect with either an ED or WD electron microprobe. Furthermore, in the ED microprobe there would be extensive overlap of x-ray lines for the rare earths and for many of the other elements they claim to have detected.

In an investigation of otolith composition using x-ray fluorescence spectroscopy (XRF) Cu, Cd, Cr and V were below the detection limits of the instrument (<3.0 ppm), Ni was found at levels averaging 2.0 ppm and Fe, Zn and Ba levels were below 10 ppm in the 4 species studied (Appendix 1). Edmonds *et al.* (1989) used inductively coupled plasma atomic emission spectroscopy (ICP-AES) to study otolith composition of the pink snapper (*Chrysophrys auratus*) for stock discrimination and their data indicate that Mg, Si, and Fe are at levels below the detection limits achievable using either ED or WD microprobe analysis.

With the above results in mind it appears that with a WD electron microprobe the only elements that can be reliably quantified in otoliths are Ca, Na, Sr, K, S and, in some cases, Cl. However, for Cl, the presence of this element in the most frequently used mounting medium, epoxy, makes the quantitative determination of this element difficult. If it is desired to detect Cl an alternative mounting medium should be considered. The utility of ED microprobe analysis to studies of the quantitative composition of fish otoliths seems to be limited to Ca and, in some rare instances Na and Sr. It is important to have a good understanding of automated instruments such as the modern electron microprobe before attempting to interpret the data that can be produced.

1.3 ORGANIZATION OF THESIS

This study began with the hypothesis that environmental variation would have a

direct effect on the trace element composition of fish otoliths. Tests of this basic hypothesis are considered in Chapter 2, through studies of both laboratory maintained and wild fish. Failure to accept this hypothesis precipitated an investigation of seasonal variation in the composition of blood plasma, endolymph and otoliths in wild fish (Chapter 3). Chapters 4 and 5 investigate the utility of otolith trace element data in a range of species, given the understanding that was developed in the previous chapters. Chapter 4 considers wholly marine species, whereas Chapter 5 applies otolith microchemistry data to studies of diadromous fishes.

Two chapters (6 and 7) investigate variation in fish otolith stable oxygen and carbon isotope composition. Chapter 6 presents laboratory data aimed at validating the effects of temperature on otolith oxygen and carbon isotopes. These data, combined with information available in the literature, are used to develop an understanding of carbon and oxygen isotopic disequilibria (Chapter 7).

The penultimate chapter (Chapter 8) is a visual study employing both scanning and transmission electron microscopy to gain insight into the large variability that exists in otolith chemistry, even at relatively small scales. The General Discussion (Chapter 9) stresses the importance of scale and the need for a carefully orientated systems approach when investigating problems that involve the interaction of organisms, their physiology and the environment.

CHAPTER 2

VALIDATION OF THE EFFECTS OF PHYSIOLOGY, AGE AND ENVIRONMENT ON OTOLITH COMPOSITION

2.1 INTRODUCTION

Otoliths have been used successfully for estimating the age of teleost fishes for many years (Bagenal, 1974; Prince and Pulos, 1983; Summerfelt and Hall, 1987). Recent research has emphasized the formation and significance of microstructural increments and the validity of daily ageing techniques (Campana and Neilson, 1985). Relatively few studies have considered the significance of otolith composition, particularly relating to inorganic constituents (Degens *et al.*, 1969; Gauldie and Nathan, 1977; Gauldie *et al.*, 1980, 1986; Radtke, 1984b; Radtke and Targett, 1984; Morales-Nin, 1986, 1987), despite much other work on the trace element composition of calcium carbonate structures of foraminiferans (Berger *et al.*, 1981), bivalves (Rhoads and Lutz, 1980), corals (Smith *et al.*, 1979; Schneider and Smith, 1982), ostracods (Chivas *et al.*, 1985, 1986) and many others (Milliman, 1974) in relation to palaeooceanography, palaeolimnology and related fields.

Strontium incorporation in biogenic carbonates, such as fish otoliths, is of special interest because of its potential utility as an indicator of past environmental temperatures. Laboratory studies on the composition of inorganically precipitated aragonite, the form of calcium carbonate of which most teleost otoliths are composed, have shown that the distribution coefficient K_{Sr}, defined as the ratio of Sr/Ca within the aragonite to the Sr/Ca of the solution from which the aragonite is precipitated, is negatively correlated with temperature (Kinsman, 1969; Kinsman and Holland, 1969). A similar relationship between Sr/Ca ratios and temperature exists in aragonitic corals (Houck *et al.*, 1977; Smith *et al.*, 1979, Schneider and Smith, 1982), although the Sr/Ca distribution coefficients for the corals differed significantly from those of inorganically precipitated aragonite, presumably due to biological fractionation. However, both Weber (1973) and Thompson and Livingston (1970) concluded that species, growth rate, metabolism and other biological factors, rather than temperature, affected the incorporation of Sr in the aragonite matrix of corals. Radtke (1984b, 1989) found that Sr/Ca ratios measured in cod (*Gadus morhua*) and *Fundulus heteroclitus* otoliths were inversely correlated with temperature, but with a much greater biological

fractionation effect than for corals. Conversely, Buchardt and Fritz (1978) and Lorens and Bender (1980) found that K_{Sr} was not affected by temperature for a freshwater gastropod (*Limnaea stagnalis*) or the blue mussel (*Mytilus edulis*).

Conflicting results among inorganic precipitate studies and biogenic calcification studies on corals, mollusks and fish otoliths make it necessary to carry out a more detailed and conclusive study before the nature of Sr/Ca variations in fish otoliths can be fully understood. This investigation considers the effects of temperature, somatic growth, otolith growth, condition, RNA/DNA ratio and season on the incorporation of Sr, Na, K and S into the sagittal otoliths of a percoid teleost, the Australian salmon (*Arripis trutta* Bloch et Schneider) through studies on both wild and laboratory-maintained fish. The relationship between age, season and otolith chemistry is also investigated in blue grenadier (*Macruronus novaezelandiae* Hector). Finally, this study presents the first measurements of Sr in saccular endolymph and the relationship between endolymph and otolith Sr/Ca ratios in 12 fish species.

2.2 MATERIALS AND METHODS

Investigations involved a combination of controlled laboratory experiments and collection of wild specimens. It was considered best to study otolith microchemistry in juveniles to eliminate potential variability that would result from both sex and the level of maturity. Juvenile Australian salmon were selected for the laboratory experiments because small juveniles (<8 cm) are readily captured in Tasmanian waters throughout the year, and initial trials showed that they can be maintained in captivity and display rapid growth rates. The availability of juvenile Australian salmon throughout the year was critical because this made it possible to compare the otolith composition of juveniles in the wild over a wide range of temperatures with fish reared in the laboratory over a similar temperature range, and to investigate seasonal effects, if any, on otolith chemistry. Analyses of the otolith chemistry of mature wild fish were required to investigate the effects of sex, stage of maturity, age and season. Blue grenadier were best suited to this phase of the study because of the availability of otoliths and the level of understanding of the ecology and life history of the species.

2.2.1 Collection and analyses: wild fishes

For estimation of the monthly variation in otolith elemental ratios of juvenile Australian salmon, fish were collected by beach seine each month from May 1987 to

April 1988. Fish were returned to the laboratory in seawater-filled drums within 1 h of capture. They were killed in a benzocaine/seawater solution and weighed to the nearest 0.1 gm and measured to the nearest 0.5 mm with vernier calipers. The bulk of both the right and left epaxial muscle was removed and skinned and placed in individual cyrotubes and frozen in liquid nitrogen for later analysis of RNA/DNA ratios. Sagittal otoliths were extracted from fresh specimens, the adhering otolith capsule was removed using fine forceps and the otoliths were further cleaned in a sodium hypochlorite solution (12 $g \cdot l^{-1}$ available chlorine), then ultrasonically cleaned in deionized water and finally rinsed several times in deionized water. Cleaned otoliths were placed on glass slides and oven dried at 50°C for 10 h. After cleaning and drying, otolith rostral length was measured to the nearest 0.01 mm with a binocular microscope equipped with a graticule and then weighed to the nearest 0.1 mg. Otoliths were stored in glass vials in a light-proof box.

RNA/DNA ratios, an indicator of rates of protein synthesis and growth (Bulow, 1987), were determined in wild Australian salmon using the modified Schmidt and Thannhauser method (Munro and Fleck, 1966) as outlined by Buckley and Bulow (1987). Approximately 0.06 gm of skinned muscle tissue was homogenized in 3 ml of deionized water and 1.4 ml of this homogenate was used for the extraction of both RNA and DNA through a series of hydrolysation and centrifugation steps (Buckley and Bulow, 1987). Concentrations of RNA and DNA extracted from muscle tissue samples were estimated by measuring absorbance at 260 nm. RNA/DNA ratios were calculated from the actual concentrations of RNA and DNA measured in the tissue.

Blue grenadier (*Macruronus novaezelandiae*) otoliths were obtained from fish collected from April 1984 to December 1985 in demersal trawls along the Tasmanian continental slope at depths of 400 to 700 m. Fish were weighed, measured and sexed, and otoliths were removed and stored dry in envelopes at sea and later transferred to glass vials. Otoliths were prepared for microprobe analysis as discussed below.

Blue grenadier ages were estimated from the transverse thin sections of otoliths prepared for microprobe analysis. Age estimates were determined by enumerating the number of hyaline zones (winter growth zones) visible, with 1 August, the approximate time of peak spawning, selected as the birth date as in Kenchington and Augustine (1987).

2.2.2 Constant-temperature experiments

Australian salmon were collected by beach seine each month from February to June 1987 off Cremorne Beach in southeastern Tasmania. Healthy juveniles were placed in seawater-filled plastic drums and transported to the laboratory within 2 h of capture and acclimated to the laboratory temperature (15±1°C).

Otoliths were marked for later measurements of otolith growth, and for discrimination between old (growth in the sea) and new (growth in the laboratory) otolith material by keeping the fish in ambient temperature filtered seawater containing 250 $mg \cdot l^{-1}$ oxytetracycline hydrochloride (OTC) for 16 h (1800 to 1000), after which they were transferred to drums with fresh seawater.

After the immersion period in OTC, individuals were selected at random and anesthetized in a solution of 0.1g MS-222 l^{-1} of seawater, measured to the nearest 0.1 mm with vernier calipers, and weighed to the nearest 0.01 g after being blotted dry on absorbent paper. Using iris scissors, each fish was given a unique combination of dorsal fin spine clips and placed in a plastic drum with fresh seawater and designated for a particular experimental aquarium. The fish were then transferred to the aquarium facility, acclimated to a selected temperature within 10 h and transferred to the appropriate experimental aquarium.

Constant-temperature rearing experiments were carried out twice (EXP1 and EXP2) with one aquarium each at 13.0, 16.0,19.0 and 22.0 ± 0.2°C and salinity of 34.8 ± 0.2°/oo. A 14 h light : 10 h dark photoperiod was provided, incorporating a gradual change from light to dark, with light intensities of 2000 and <20 lx, respectively. Fish were maintained in 250 l insulated, opaque polypropylene aquaria with separate recirculating water filter systems and temperature control. Temperature was recorded twice each day and pH, salinity, ammonia, nitrite, nitrate and phosphate levels were determined once each week. Before experimental fish were placed in aquaria, ammonia and nitrite-nitrogen levels were stabilized below 1.0 $mg \cdot l^{-1}$ while pH fluctuated between 7.8 and 8.1. A 10% water change was carried out each day in order to maintain water quality. Calcium and strontium concentrations in the aquaria were measured at the beginning and end of each experiment by flame atomic absorption spectrophotometry following established procedures (Fabricand *et al.*, 1966; Fabricand *et al.*, 1967). Calcium and strontium concentrations ranged from 9.6 to 10.7 mM l^{-1} and 82 to 92 μM^{-1}, respectively.

Fish were fed to satiation once each morning (0900) with freshly caught live

mysids, predominantly *Tenagomysis* sp., a regular item in the diet of Australian salmon. There were no fish mortalities during the course of these constant-temperature experiments. Most fish were maintained in captivity for 19 or 36 days with some individuals being maintained for up to 66 days.

At the end of each experiment, fish were killed in a benzocaine/seawater solution, weighed, measured and then frozen for later extraction of sagittal otoliths. Sagittal otoliths were extracted from thawed specimens, and treated in the same way as for the wild Australian salmon.

2.2.3 Preparation of microprobe specimens and microprobe analysis

Whole sagittal otoliths were mounted in "Araldite D" epoxy resin (Ciba-Geigy) and polymerized in an oven at 40°C for a minimum of 24 h. Several transverse sections of approximately 200 μm thickness were obtained from the otolith, including one section containing the primordium, with a low speed saw (Struers Accutom) equipped with a diamond cut-off wheel.

Before further processing, those otoliths that had been marked with OTC were observed and photographed with both transmitted visible light and incident ultraviolet-light excitation on a Leitz Diaplan microscope. The microscope was equipped with a PLOEMOPAK 4 incident light illuminator and oxytetracycline bands in the otoliths were made visible with a D filter block incorporating a 355-425 nm excitation filter, a 455 nm dichroic mirror and a 460 nm barrier filter (Leitz-Wetzlar). Photographs were used to mark the position of subsequent microprobe measurements and were also used to determine otolith growth in the plane of each of these measurements. Two examples of Australian salmon otolith sections photographed with both transmitted visible light and incident-ultraviolet light are shown in Fig. 2.1.

After sections were photographed, they were affixed to glass slides with epoxy. After drying, sections were ground with several grades of carborundum paper (wet/dry paper 600 to 1200 grade) until the primordium was reached, or, for sections not containing the primordium, to a thickness of approximately 100 μm. Otoliths were then polished on a lapping wheel with 0.25 μm aluminum paste (Linde A in water) and then finished with 0.25 μm diamond paste. After polishing, otolith sections were cleaned in an ultrasonic bath in reagent-grade mineral spirits followed by ultrasonic cleaning in deionized water. Specimens were oven dried at 40°C for a minimum of 24 h, lightly wiped with a lint-free cloth wetted with ether and carbon coated with a film

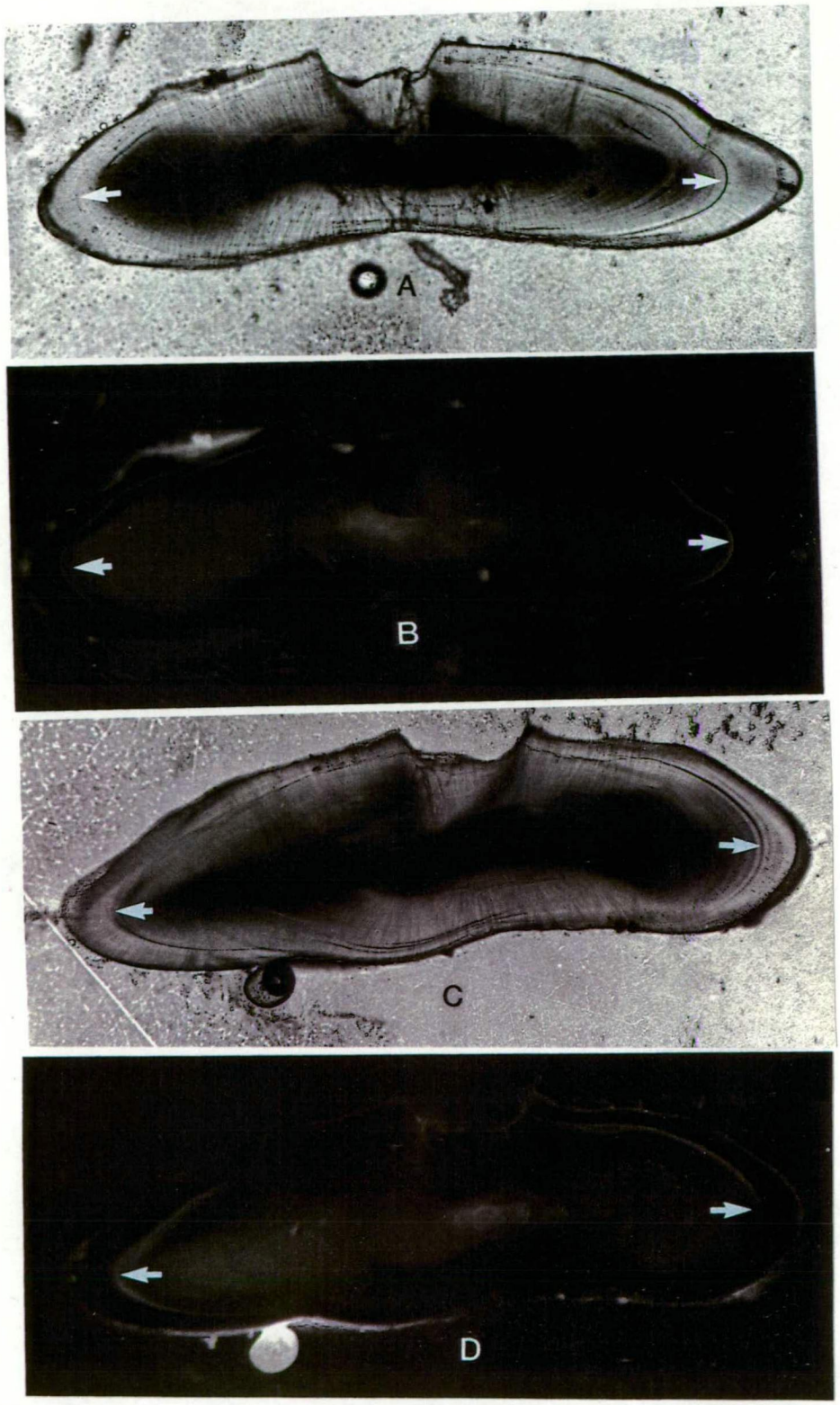

Fig. 2.1 Light micrographs of transverse sections form two Australian salmon sagittae. Both otoliths are from fish maintained in the 16°C treatment. Micrographs were taken with transmitted light (A and C) and incident uv-light (B and D). The location of the uv-light fluorescent OTC mark and the corresponding stress-related check mark are indicated. (A) and (B) are from a fish maintained in captivity for 23 days (45 mm before captivity and 53 mm SL when sacrificed); (C) and (D) are from a fish maintained in captivity for 23 days (42 mm before captivity and 51 mm SL when sacrificed).

of approximately 25 nm.

Electron microprobe analyses were carried out using wavelength dispersive spectrometers on a Cameca Camebex Microbeam microprobe. Analyses were made with a square raster of 12.5 x 12.5 μm. Probe current and accelerating voltage were 10 nA (measured on copper) and 15 kV, respectively. A large window combined with low current and long counting times was employed to minimize specimen damage and maintain acceptable counting statistics. Elements analysed included calcium, strontium, sodium, potassium and sulphur. Details of the microprobe counting procedures, precision and standards are outlined in Table 2.1. Background was measured at offsets both above and below peak position for 50% of the peak counting time. The average counts from these two background measurements were subtracted from the peak. Background measurements were made with each analysis. Corrected x-ray intensity ratios were calculated using the ZAF method (Reed, 1975) and the final elemental ratios are normalized atom ratios based on concentrations derived from the standards.

The locations on an otolith selected for microprobe analysis varied depending on the specimen. Analyses on the otoliths of laboratory reared Australian salmon were carried out at 6 predetermined locations around the otolith edge and always in the material precipitated during captivity. This provided elemental data from material produced at different otolith growth rates. For both wild Australian salmon and blue grenadier microprobe analyses were done at the otolith edge along the plane of most rapid growth, on the dorsal and ventral edges of the transverse sections. In the juvenile Australian salmon this would usually result in measuring a section of otolith produced over a period of, at most, two weeks. However, in the much older blue grenadier, otolith growth, even along a single plane, would vary significantly with age. In the case of blue grenadier older than 15 years of age, a 12.5 x 12.5 μm window would encompass otolith material produced over a period of up to 2 months.

2.2.4 Endolymph collection and analysis

Eleven species of fish were collected by handline in Storm Bay, southeast Tasmania, by gill net in the Derwent River estuary during the months of February, March and April, and freshwater trout were obtained from a local trout farm. All collections of endolymph from marine species were carried out at sea immediately after an individual was captured. Endolymph from freshwater trout was collected in the

Table 2.1 Electron microprobe analytical data for fish otolith analyses. Details of counting times, counting precision and materials used as standards.

Spectrometer/ Crystal	Element	Peak counting time (s)	Counting precision	Standard Material	Standard Composition	Source
1/PET	Ca-K_α	20s	~55,000 counts collected	Calcite	CaO 56.10%	USNM 136321
			0.5%		CO_2 44.01%	Jarosewich & MacIntyre (1983)
1/PET	K-K_α	180	3.4% when K/Ca=$2x10^{-3}$	Anorthite	SiO_2 44.00%	USNM 137041
					Al_2O_3 36.03%	Jarosewich *et al.* (1980)
					CaO 19.09%	
					FeO 0.62%	
					Na_2O 0.53%	
					K_2O 0.03%	
2/PET	S-K_α	200	6.3% when S/Ca=$1x10^{-3}$	Troilite	FeO 63.21%	BMR Museum (Australia)
					SO_3 37.23%	Ramdohr and Goresy (1971)
					Cr_2O_3 0.50%	
					ZnO 0.03%	
3/TAP	Na-K_α	100	2.7% when Na/Ca=$1.5x10^{-2}$	Anorthite	Same as for K above	
3/TAP	Sr-L_α	100	3.5% when Sr/Ca=$2x10^{-3}$	Strontianite	SrO 67.67%	USNM 10065
			2.9% when Sr/Ca=$3x10^{-3}$		CO_2 30.23%	Jarosewich & White (1987)
					CaO 1.90%	

laboratory. Endolymph was also collected from recently captured specimens of orange roughy (*Hoplostethus atlanticus*).

Because strontium and calcium are present only at trace levels in the endolymph fluid, it must be collected in a manner that minimizes the potential for contamination. Fish were killed by a blow to the head and the brain was immediately exposed. The brain was removed with forceps and any fluid remaining in the brain cavity was absorbed with lint-free paper making the sacculi containing the sagittal otoliths visible. The membrane between the brain cavity and the sacculus was punctured with the autopipette tip used for endolymph collection. In most cases, the otoliths were kept in place while the endolymph was removed with an autopipette with a standard low-volume tip, or, if necessary, a special ultra-fine pipette tip. When the otoliths obstructed most of the sacculus, they were removed with plastic forceps before the endolymph was collected. The amount of endolymph fluid collected from individual fish ranged from 5 to 1500 µl. The small amount of fluid collected from the majority of species was adequate to carry out only Sr and Ca analyses. Immediately after collection the endolymph was placed on ice and subsequently stored at 4°C prior to analysis.

The strontium concentration in endolymph samples was measured using the method of standard additions by graphite furnace atomic absorption spectrophotometry (GFAAS) on a Varian AA-1475 spectrophotometer equipped with a GTA-95 graphite furnace and an autosampler. Argon was used as the purging gas in the graphite furnace. Samples were diluted up to 200 times with a 0.25% solution of an ionic detergent, Triton X-100, and 20 µl of diluted sample were injected by autosampler into a walled, pyrolytically coated graphite tube. Furnace conditions were: drying at 90°C for 60 sec; ramp ashing from 90 to 700°C for 20 sec; ashing at 2600°C for 1 sec; and atomization, with no gas flow, at 2600°C for 3 sec. Examples of a GFAAS calibration curve and absorption peak for strontium are shown in Fig. 3.1. Endolymph calcium concentrations were measured in sample aliquots diluted fifty-fold with 0.1% lanthanum chloride in solution with 100 meq sodium and 50 meq potassium·l^{-1}. Calcium anlyses were determined by flame atomic absorption spectrophotometry using a nitrous oxide/acetylene flame.

2.2.5 Analytical procedures

Differences among data were determined by analysis of variance, with a nested design being employed when it was desirable to consider the variability in elemental ratios measured within a single otolith. A relationship was considered significant when $p<0.05$. Differences between pairs of means were tested *a posteriori* using a Student-Neuman-Keuls (SNK) multiple range test (Sokal and Rohlf, 1969).

2.3 RESULTS

2.3.1 Experimental Australian salmon

Strontium/calcium, Na/Ca, K/Ca and S/Ca ratios from the two experimental runs at the four temperatures were examined independently for a significant variance component due to temperature using a two-tiered nested analysis of variance (Table 2.2). Significant variation among treatments was found only for K/Ca in EXP1 ($p<0.01$), Sr/Ca in EXP2 ($p<0.001$) and S/Ca in EXP2 ($p<0.001$), with nearly significant variation among treatments in Sr/Ca in EXP1 ($p=0.066$). Trend analysis showed that there was evidence for a linear trend in Sr/Ca, but not K/Ca or S/Ca, with temperature.

Although there was a significant difference among Sr/Ca ratios at the four experimental temperatures for the combined data from EXP1 and EXP2 ($F=6.6$; $df=3,96$; $p<0.001$) Model 1 linear regression (Sokal and Rohlf, 1981) indicated that there was no evidence for a linear relationship between temperature and Sr/Ca ($F=6.6$; $df=1,2$; $p>0.10$) (Fig. 2.2). There were no significant relationships between temperature and Na/Ca, K/Ca and S/Ca ratios.

The two-tiered nested ANOVA (Table 2.2) and the associated variance components indicated that the majority of variance in the elemental ratios was attributable to variance within a single treatment and, most important, to measurements of otolith microchemistry made within a single otolith. This indicated that the main sources of variance would be attributable to factors associated with individual fish, such as growth rate, condition factor, RNA/DNA ratios, and within an otolith, such as growth of the otolith along a single plane, crystal size or calcification rate.

There were large differences in fish growth rate and only small differences in condition factor ($CF=W/L^3$) both among and within the four treatment temperatures (Fig. 2.3). A significant logarithmic regression ($r^2=0.20$; $p<0.01$) between growth

Table 2.2 Summary of mixed model one-way nested analysis of variance results of *Arripis trutta* otolith microchemistry from 2 constant-temperature experiments. Percentages are variance components.

Variance of elemental ratios in constant-temperature Experiment 1

Source of variation	Sr/Ca	Na/Ca	K/Ca	S/Ca
Temperature	F=2.61; df=3; ns	F=1.55; df=3; ns	F=3.59; df=3; p=.022	F=0.03; df=3; ns
Individual fish otoliths	F=1.92; df=34; p=.003 11.7%	F=2.00; df=36; p=.001 12.5%	F=1.99; df=36; p=.001 12.3%	F=2.17; df=36; p=.0003 14.4%
Within otolith variability	df=230; 88.3%	df=246; 87.5%	df=246; 87.7%	df=245; 85.6%

Variance of elemental ratios in constant-temperature Experiment 2

Source of variation	Sr/Ca	Na/Ca	K/Ca	S/Ca
Temperature	F=6.23; df=3; p=.001	F=1.38; df=3; ns	F=1.92; df=3; ns	F=6.10; df=3; p=.001
Individual fish otoliths	F=1.69; df=56; p=.003 10.8%	F=3.77; df=58; p<.00001 32.6%	F=5.65; df=58; p<.00001 44.8%	F=1.20; df=58; ns 3.3%
Within otolith variability	df=286; 89.2%	df=295; 67.4%	df=295; 55.2%	df=295; 96.7%

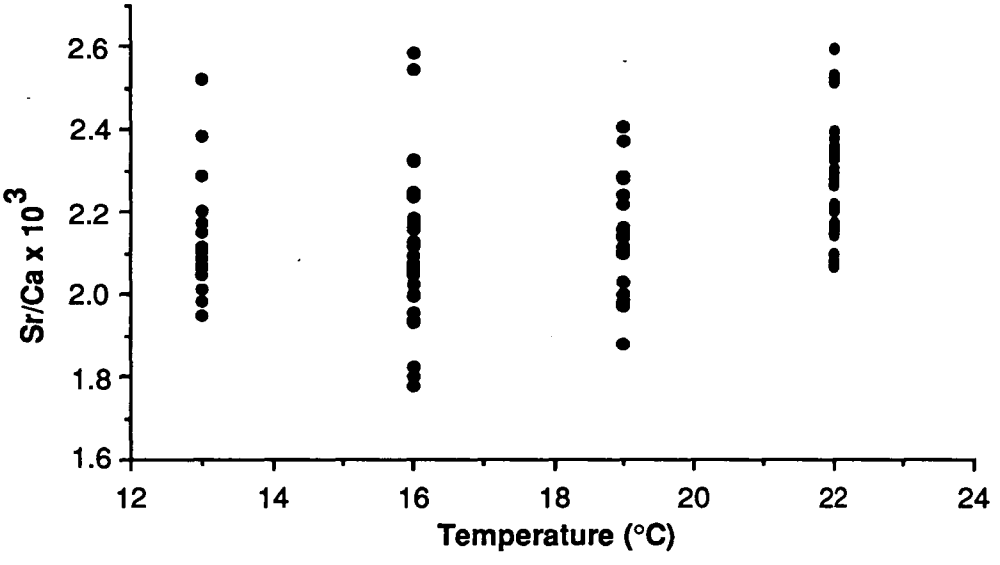

Fig. 2.2 Otolith Sr/Ca ratios from juvenile *Arripis trutta* plotted against temperature. Data are from the two constant-temperature experiments. Mean Sr/Ca ratios at each temperature are: 13°C, 0.00213; 16°C, 0.00211; 19°C, 0.00216; 22°C, 0.00228. Each data point represents a mean of multiple Sr/Ca ratio determinations from an individual sagitta. Total n=100.

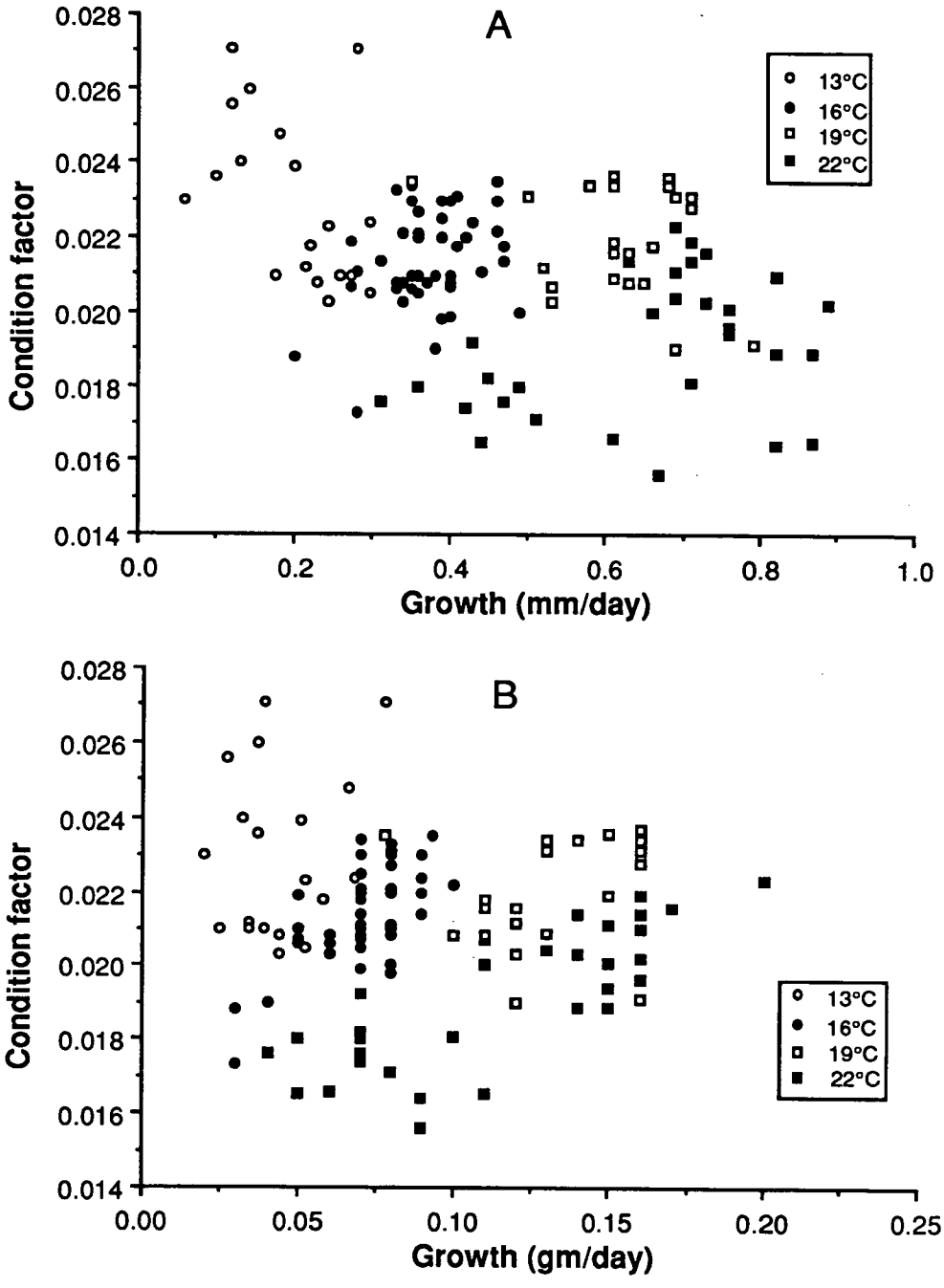

Fig. 2.3 Graphs of condition factor ($CF = W/L^3$) against growth rate (a) mm day^{-1} and (b) gm day^{-1} for aquarium-maintained *Arripis trutta* at four temperatures.

(mm/day) and condition factor indicated that the slower growing fish, particularly those at the lower temperatures, were in slightly better condition. Although there were significant differences among growth rate and condition factor for the fishes reared at the different temperatures there was no clear evidence for a biologically significant relationship with Sr/Ca, Na/Ca, K/Ca or S/Ca ratios measured in the otoliths. However, the Sr/Ca ratios obtained from individuals in the 13°C tank were negatively correlated with growth in length and weight (r^2=0.50; p<0.0001) with two sick, slow-growing fish having high otolith Sr/Ca ratios. These two fish were suffering from a fungal infection resulting in fin erosion with one individual losing the majority of its caudal fin.

Correlation analysis showed that measurements of otolith growth made along orthogonals between individual microprobe measurements and the OTC check mark were significantly correlated with Na/Ca (r^2=0.07; p<0.001), K/Ca (r^2=0.07; p<0.001) and S/Ca (r^2=0.05; p<0.01) ratios (Fig. 2.4), but less than 10% of the variance was explained by these relationships. There was no correlation between Sr/Ca ratio and otolith growth. On the basis of these results it is clear that otolith growth data, and probably variations in calcification rate, cannot explain the large variance component attributable to variation within an individual otolith.

Various combinations of the measured variables were used to develop multiple regression models in an attempt to predict Sr/Ca, Na/Ca, K/Ca and S/Ca ratios. Variables included in the models were fish length and weight (before and/or after captivity), condition factor, days in captivity, mean growth in mm·day^{-1} and gm·day^{-1}, total otolith growth and mean otolith growth (μm·day^{-1}), temperature and otolith elemental ratios. However, none of the models were capable of explaining more than 15% of the variance for any of the elemental ratios.

Total trace ions in the newly formed otolith material in aquarium-maintained fish were estimated by summing the mean ratios of Sr/Ca, Na/Ca, K/Ca and S/Ca determined for each otolith. The mean values for total ions in otoliths were 0.0227, 0.0230, 0.0233 and 0.0218 μM at 22, 19, 16 and 13°C, respectively. One-way ANOVA indicated a significant difference among the means (F=10.74; df=3,96; p<.001), however, trend analysis showed that there was no systematic variation with temperature.

Otolith material produced by the Australian salmon in captivity was generally hyaline (in transmitted light) and in many cases microincrements were not clearly

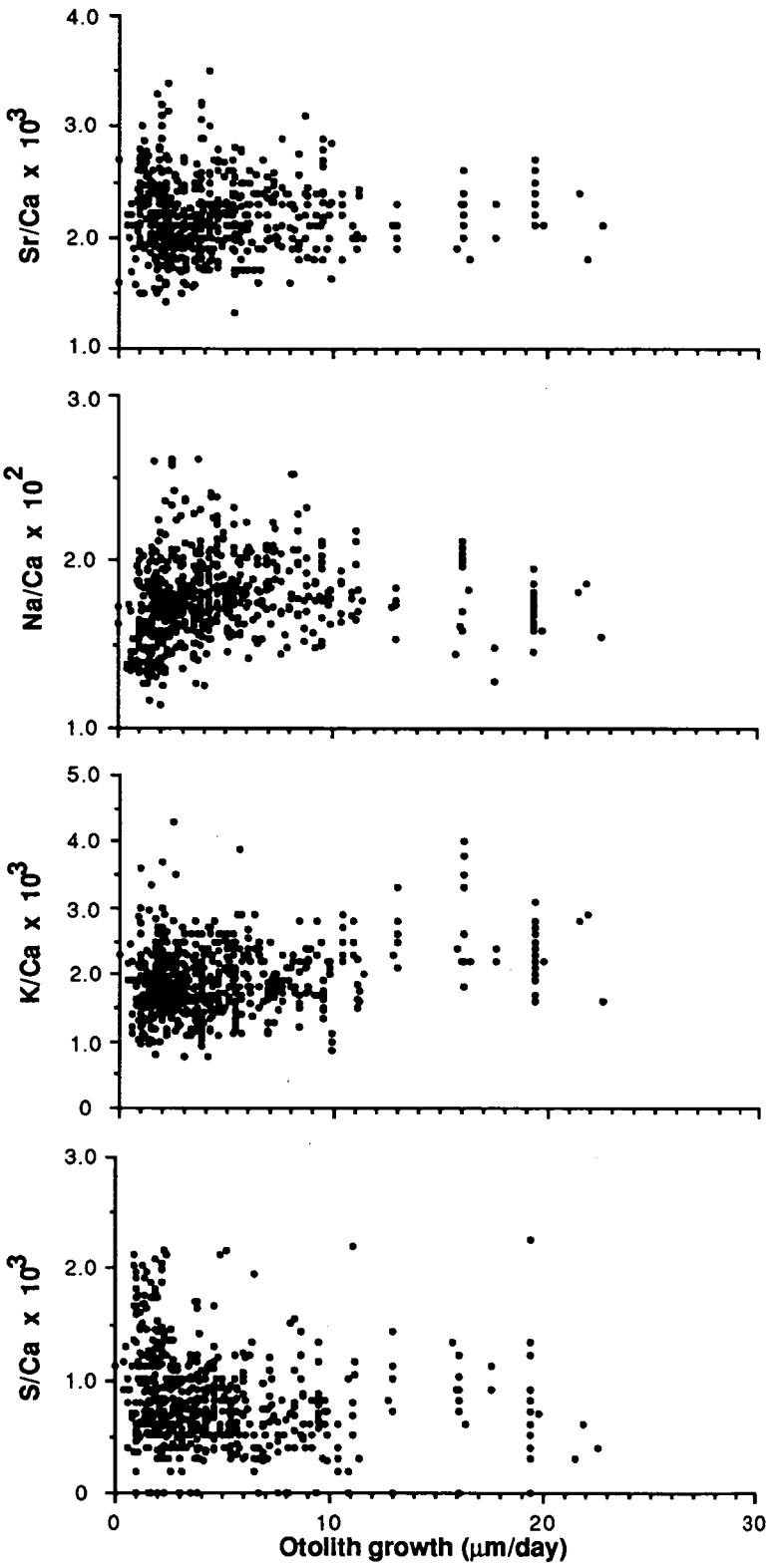

Fig. 2.4 Plots of elemental ratio measurements from aquarium maintained *Arripis trutta* against mean daily otolith growth (μm/day), over the duration of the experiment. Otolith growth measured along the growth axis orthogonal to the otolith microincrement containing the microprobe measurement. Zero values in the plot of S/Ca against otolith growth indicate S levels below the detection limit of the microprobe.

Fig. 2.5 Light micrographs and SEM of juvenile Australian salmon otoliths (transverse sections, approximately 100 μm thick) illustrating the irregular nature of microincrements in captive versus wild fish. Arrows indicate the location of the stress induced check mark and fluorescent OTC mark in fish maintained in captivity. Light micrographs are magnified 135X. (A) Fish maintained in captivity for 19 days at 22°C (45 mm before captivity and 60.5 mm when sacrificed). Nineteen microincrements are visible with an average width (discontinuous zone plus incremental zone) of approximately 16 μm; (B) Fish maintained in captivity for 24 days at 16°C (46.5 mm before captivity and 49.5 mm when sacrificed). Only a few microincrements are visible; (C) Fish maintained in captivity for 66 days at 16°C (43.5 mm before captivity and 61.5 mm when sacrificed). Less than 66 microincrements are visible; (D) Wild 77.0 mm Australian salmon not maintained in captivity; (E) Wild 70.0 mm Australian salmon not maintained in captivity; (F) EDTA etched otolith section from a captive Australian salmon maintained at 22°C.

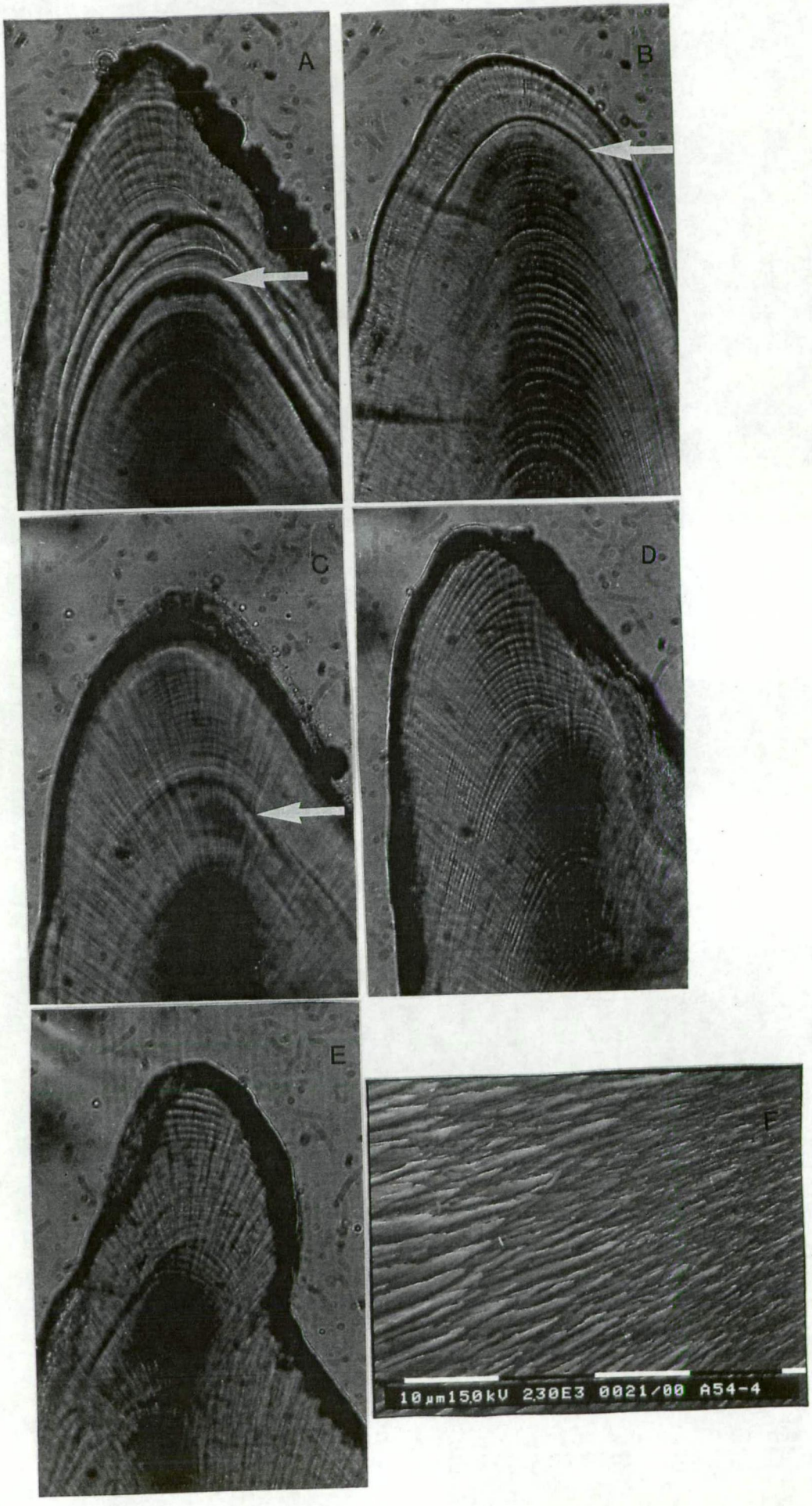
A
B
C
D
E
F
10µm15.0kV 230E3 0021/00 A54-4

visible (Fig. 2.5). Etching of the otolith material with 0.2 M EDTA (pH=8.0) or 1.0 N HCl and observation with an SEM frequently failed to make microincrements visible (Fig. 2.5). The transparency of the otolith material formed in captivity would indicate a relatively low level of organic matrix in these regions. A low level and, perhaps, even distribution of otolith protein was probably responsible for the low contrast of the microincrements in the otoliths of these laboratory maintained fish. This uniformity along with the relative difficulty in resolving microincrements is frequently encountered in laboratory maintained fish (Campana and Neilson, 1985).

2.3.2 Wild Australian salmon

Microchemical data from the otoliths of juvenile Australian salmon collected at Cremorne, Tasmania each month for one year show significant variations during the year in Sr/Ca ($F= 4.5$; $df=11,67$; $p<0.0001$), Na/Ca ($F=13.5$; $df=11,65$; $p<0.0001$), K/Ca ($F=4.3$, $df=11,66$; $p<0.0001$) and S/Ca ($F=3.6$; $df=11,65$; $p<0.001$) ratios (Fig. 2.6). These data, obtained from within 20 μm of the otolith edge, show the chemical composition of otolith material formed within, at most, the previous 2 weeks, based on counts of otolith microincrements. During periods of rapid growth the chemical measurements are representative of otolith material produced in the two to three days before capture. The most notable features of these monthly measurements of Australian salmon otolith chemistry are the gradual decline of the Sr/Ca ratio over the winter months to a low in October followed by a sharp increase over the summer months and the almost opposite trend of increasing Na/Ca in the winter followed by a decline to a minimum in the summer months. Among the element ratios only Na/Ca was correlated with temperature. However, the Na/Ca data vary out of phase with temperature and any direct significance to this correlation is questionable. Monthly temperatures at the Cremorne collection site are shown in Fig. 2.7a.

RNA/DNA ratios measured in wild juvenile Australian salmon varied seasonally (Fig. 2.7b), however, variability was large perhaps due, in part, to variations in the size of fish used in the RNA/DNA determinations (Fig. 2.7c). In a month where the variation in fish length was very great (February) there was a significant negative correlation between RNA/DNA and fish length ($r^2=0.74$, $p<0.01$). RNA and DNA concentrations for all fish ranged from 1572 to 4560 $\mu g \cdot g^{-1}$ and 350 to 751 $\mu g \cdot g^{-1}$, respectively. Na/Ca ratios were negatively correlated with RNA/DNA ratios ($r^2=0.08$, $p<0.03$) and condition factor ($r^2=0.25$, $p<0.01$), but these correlations are too low to

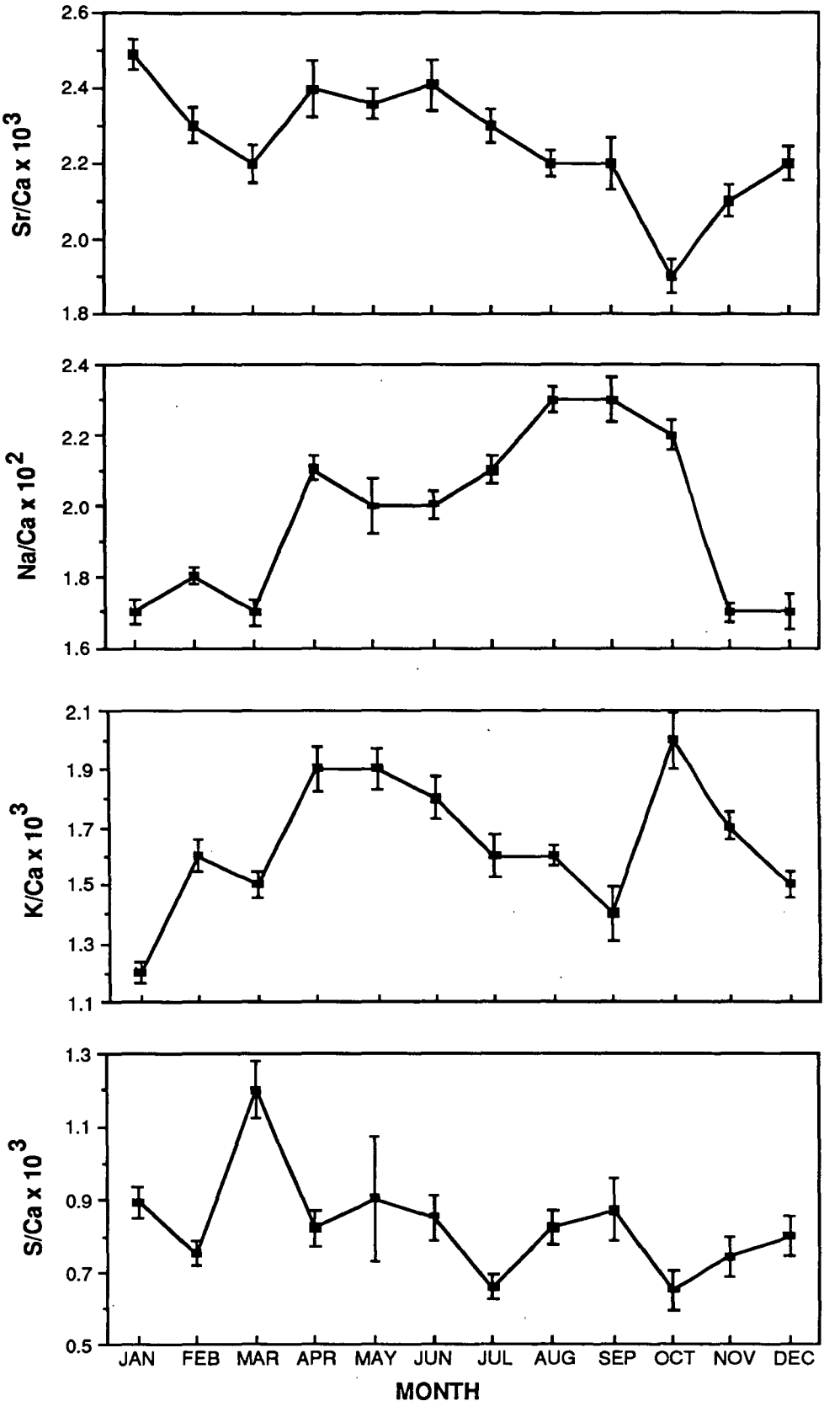

Fig. 2.6 Monthly measurements of elemental ratios from the otolith edge of *Arripis trutta* collected at Cremorne Beach. Points are mean values with 1 SE.

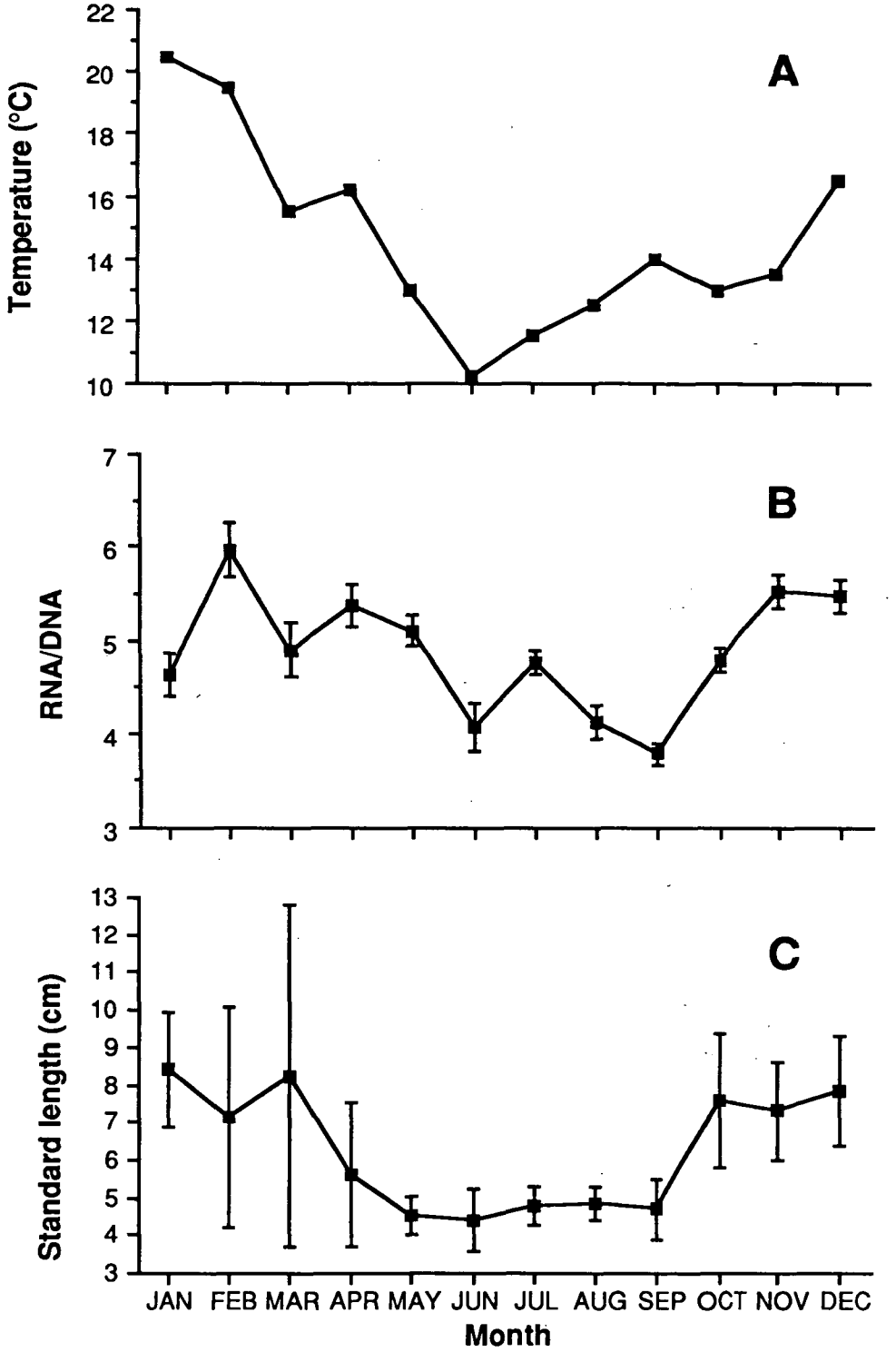

Fig. 2.7 (A) Record of monthly temperatures at Cremorne Beach, Tasmania, determined on dates of fish collection. (B) Monthly variations in RNA/DNA ratios from *Arripis trutta* collected at Cremorne Beach. Points are mean values with 1 SE. (C) Monthly variation in length of *Arripis trutta* collected at Cremorne Beach. Points are mean values with bars indicating range.

be biologically meaningful. No other correlations among physiological data and otolith composition were found.

2.3.3 Blue grenadier otoliths

Otolith-based age estimates for blue grenadier were verified by fitting the von Bertalanffy function to both the length and weight at age data and comparing the resultant parameters with those obtained by Kenchington and Augustine (1987). The parameters of the von Bertalanffy growth functions are shown in Table 2.3 and the curves appear in Fig. 2.8. The 99% confidence limits of all von Bertalanffy parameters for both weight and length models overlapped with those of Kenchington and Augustine (1987).

There were significant age-related differences in Sr/Ca, Na/Ca, K/Ca and S/Ca ratios in blue grenadier otoliths (Fig. 2.9). When the 5 one-year-old fish collected in September were excluded from the data set, the relationship between S/Ca and age is no longer significant. Logarithmic regressions provide the best fit for the Sr/Ca, Na/Ca and K/Ca data and appear in the caption of Fig. 2.9. The three fish of 10, 12 and 15 years of age with Sr/Ca ratios greater than 0.0055 are females that displayed significant gonad development (gonad stage ≥ 2) (Fig. 2.9). The data showed no significant differences between males and females although a larger sample size would be required to confirm the validity of this result.

Because the age distributions within monthly blue grenadier samples were different it was not valid to consider seasonal variability in otolith composition by analysis of these data. Therefore, the residuals from the regressions between age and elemental ratio were considered when investigating seasonal variations in otolith composition. Comparison, by one-way ANOVA, of the Sr/Ca, Na/Ca, K/Ca and S/Ca ratio deviations determined by microprobe measurements at the edge of blue grenadier otoliths showed that there were significant differences among monthly samples for Sr/Ca ($F=2.1$; $df=10,66$; $p=0.04$), Na/Ca ($F=2.3$; $df=10,66$; $p=0.02$), K/Ca ($F=2.2$; $df=10,66$; $p=0.03$) and S/Ca ($F=7.0$; $df=10,66$; $p<0.0001$) data (Fig. 2.10). The seasonal cycle of otolith composition for blue grenadier is very different from that of the juvenile Australian salmon. This is probably due to the fact that different life history stages were examined for the two species and, that they inhabit very different environnments which probably display dissimilar seasonal cycles in food abundance and other variables.

Table 2.3 Parameters of von Bertalanffy growth curves for *Macruronus novaezelandiae* estimated (a) by length and (b) by weight.

(a)	L_∞	K	t_0	N
	93.1±1.4	0.284±0.018	-1.03±0.11	77
(b)	W_∞	K	t_0	N
	3.48±0.41	0.155±0.033	0.42±0.15	77

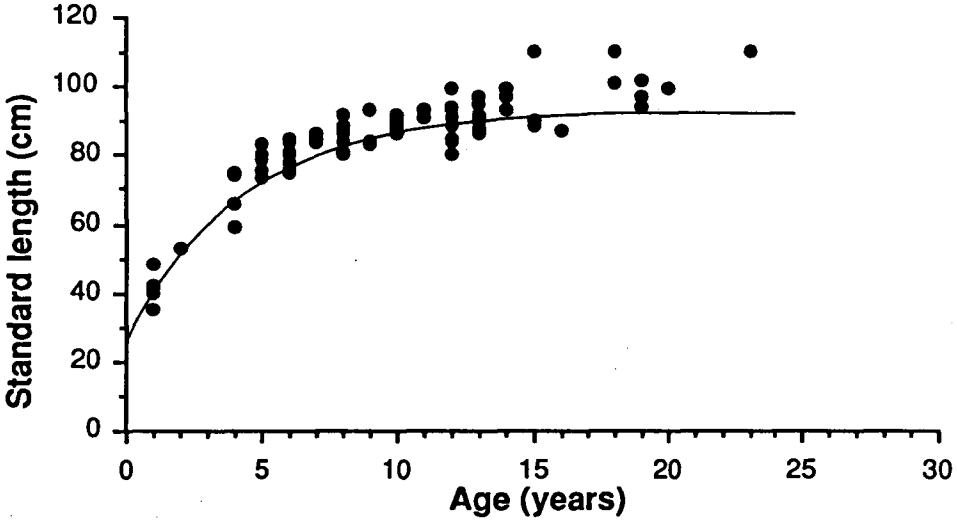

Fig. 2.8a Von Bertalanffy growth curve by length for *Macruronus novaezelandiae. N=77.*

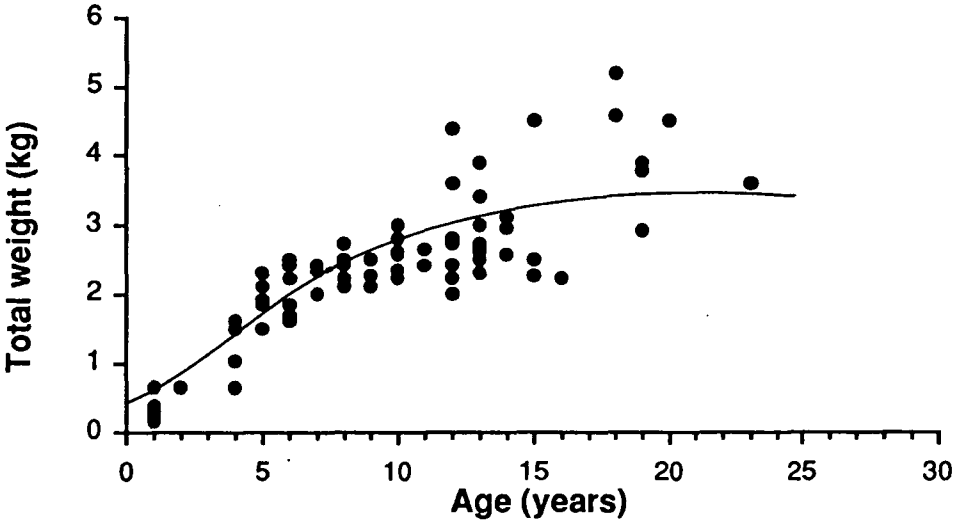

Fig. 2.8b Von Bertalanffy growth curve by weight for *Macruronus novaezelandiae. N=77.*

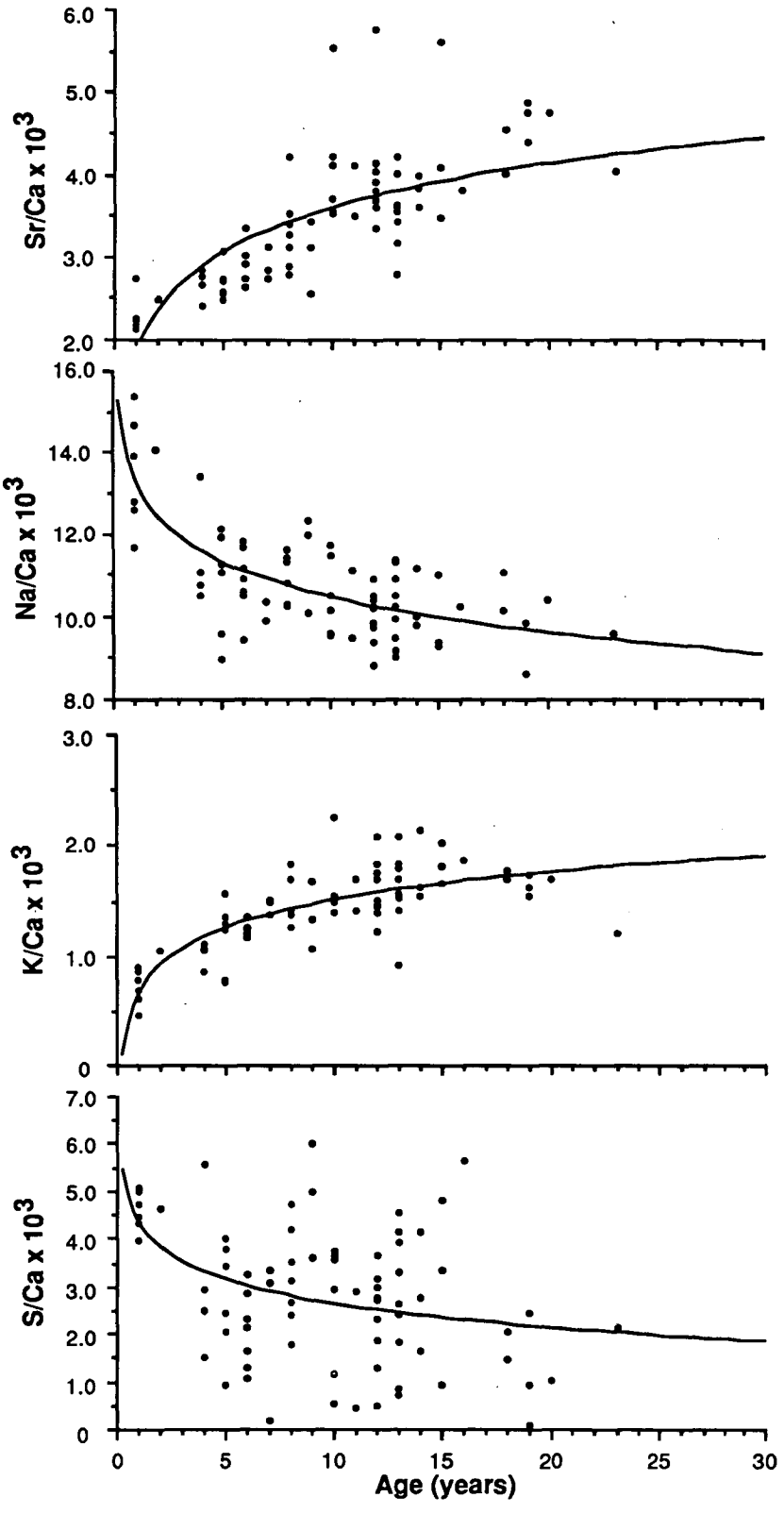

Fig. 2.9 Plots of elemental ratios from the otolith edge of *M. novaezelandiae* against age determined from otolith sections. Logarithmic regression equations for blue grenadier elemental ratios vs. age in years (A) are as follows: $Sr/Ca=(0.00203)(A^{0.2409})$, ($r^2=0.62$, $P<0.0001$); $Na/Ca=(0.01330)(A^{0.1057})$, ($r^2=0.48$, $P<0.0001$); $K/Ca=(0.00072)(A^{0.3136})$, ($r^2=0.64$, $P<0.0001$); $S/Ca=(0.00043)(A^{-0.2125})$, ($r^2=0.15$, $P<0.001$). For each relationship, n=77.

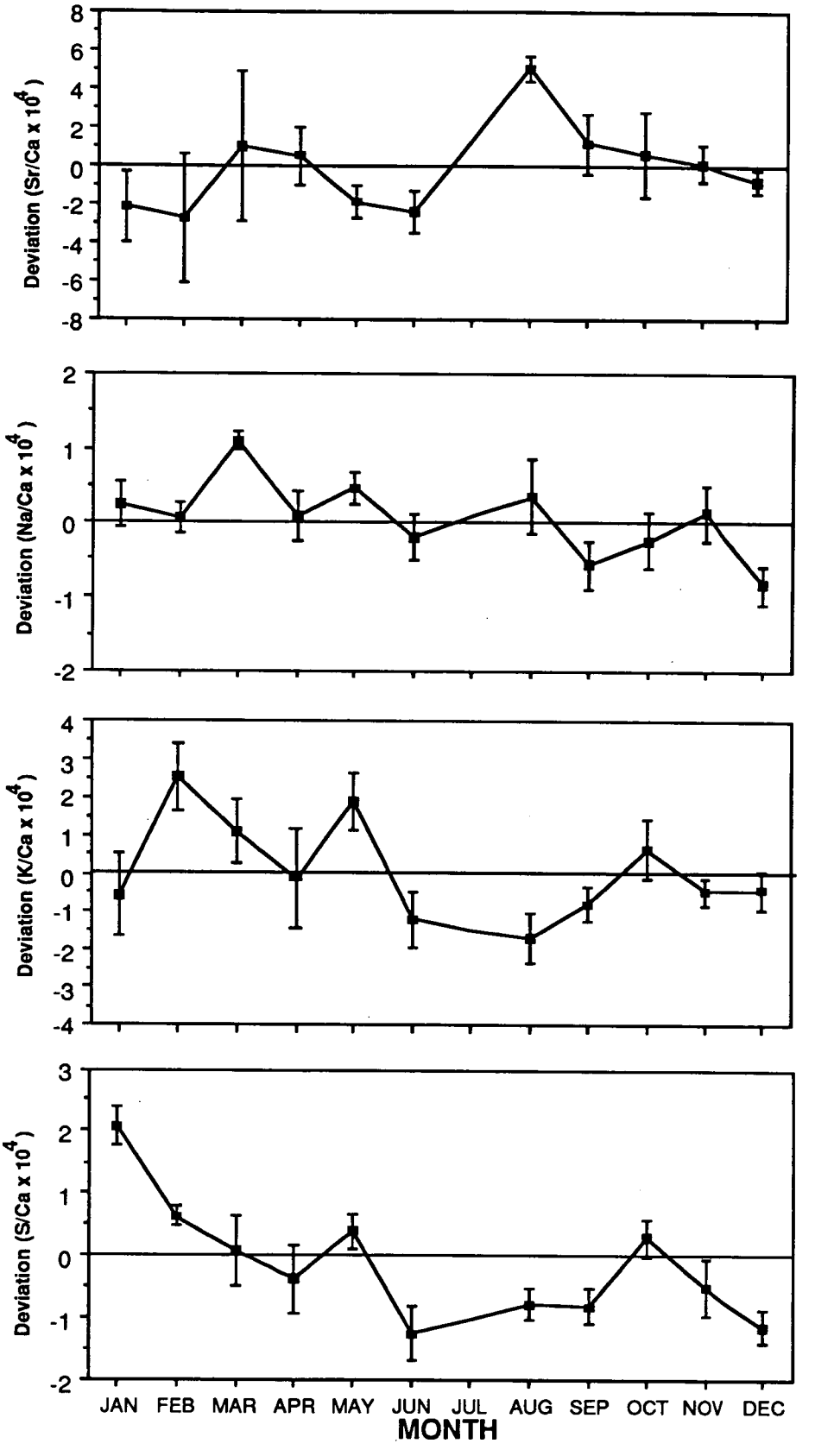

Fig. 2.10 Monthly variations in the residuals from the relationships of elemental ratios against fish age for *Macruronus novaezelandiae*. Points are mean values with 1 SE.

2.3.4 Endolymph

Endolymph and otolith Sr/Ca ratio data collected from 12 different species and 44 individuals are plotted in Fig. 2.11. These fish were all collected within a temperature range of 16.0° to 17.5°C within a period of less than 30 days. All specimens, with the exception of the freshwater brown trout (*Salmo trutta*) were collected in seawater. Of the species collected in marine waters only brown trout and black bream (*Acanthopagrus butcheri*) enter freshwater. Endolymph Sr and Ca concentrations ranged from 0.94 to 20.4 μM and 0.78 to 1.55 mM, respectively. Standard deviations for measurements of endolymph composition were typically less than 2% of the mean value based on triplicate analyses and standard deviations of otolith Sr/Ca ratios determined by microprobe are approximately 1.5% of the plotted value. The linear relationship between endolymph and otolith Sr/Ca was highly significant ($r^2=0.82$, $p<0.0001$) and can be represented by $O_{Sr}=0.00181+0.2453(E_{Sr})$, where O_{Sr} and E_{Sr} are the otolith and endolymph Sr/Ca ratios, respectively.

The fish caught in marine waters were collected within a narrow range of salinities (34.6 to 35.2‰). Therefore, with the exception of the freshwater brown trout, variations in endolymph Sr/Ca ratios measured here are due to interspecific and physiological differences. The data do show evidence of clustering for each species and may indicate that interspecific differences are a more significant factor in determining the variability of endolymph Sr/Ca ratios than individual or intraspecific physiological factors. However, further study is required before this can be determined conclusively.

Brown trout from freshwater have much lower endolymph and otolith Sr/Ca ratios than sea-run brown trout returning from the sea to freshwater. The depletion of Sr in all freshwaters relative to seawater indicates that measurements of variations in otolith Sr/Ca ratios may have wide application in studies of diadromous fishes as has been demonstrated by Casselman (1982) in a study of American eel *Anguilla rostrata* otoliths. This study has found no evidence that endolymph or otolith Sr/Ca ratios as low as those found in freshwater trout occur in fish that spend their entire lives in marine waters.

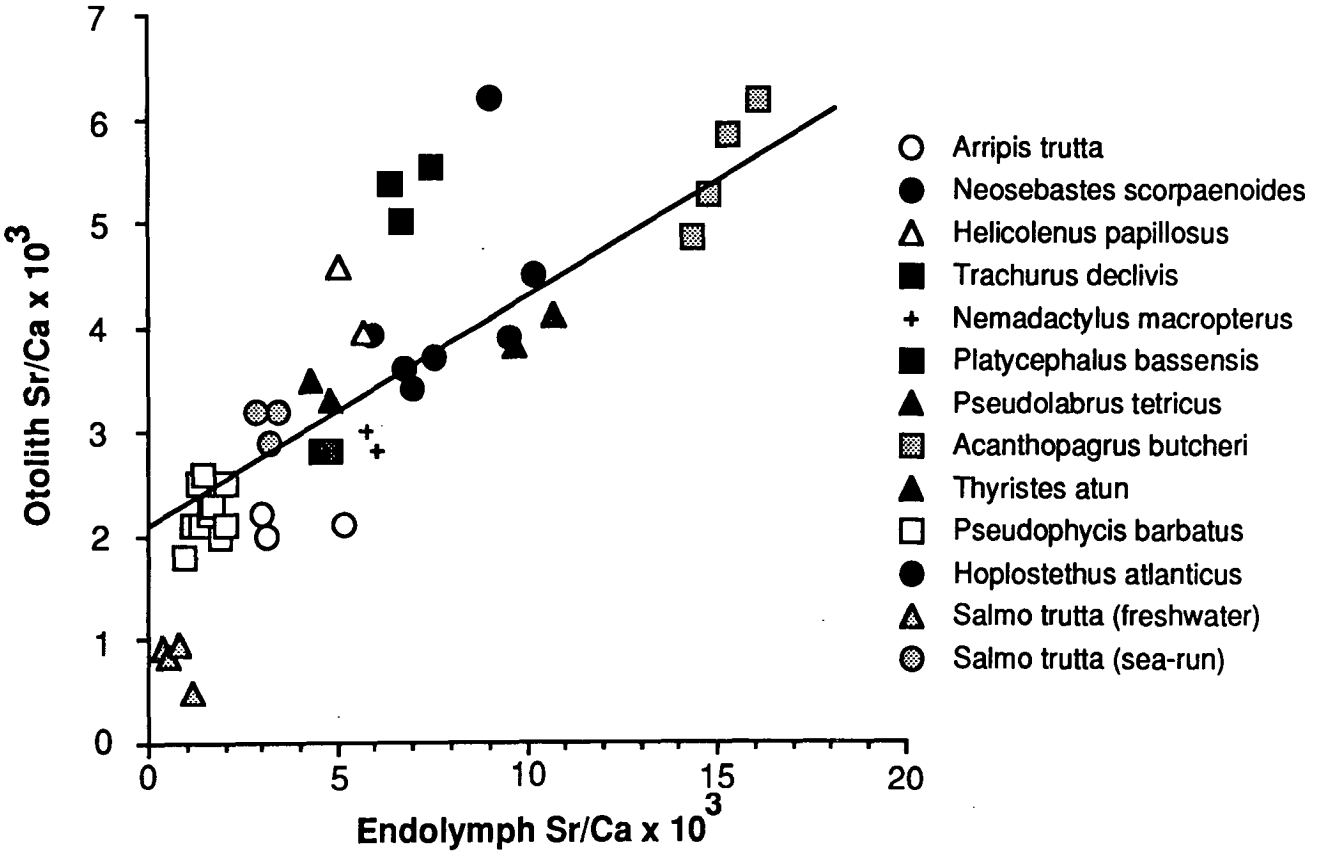

Fig. 2.11 Relationship between otolith Sr/Ca ratio determined along otolith edge and endolymph Sr/Ca ratio in 11 marine and one freshwater fish species. Linear regression is described by $O_{Sr}=0.00181+0.2453(E_{Sr})$, ($r^2=0.82$, $P<0.0001$, $n=44$). Error bars are not included because they are too small for the scale of the graph.

2.4 DISCUSSION

2.4.1 Temperature and otolith composition

Experimental data show that incorporation of Sr into the otoliths of Australian salmon is not negatively correlated with temperature and, in fact, there is no clear relationship between otolith Sr/Ca ratio and temperature. Thus, application of the relationship whereby increasing amounts of Sr are incorporated into an aragonite matrix with decreasing temperature (Kinsman and Holland, 1969) does not seem valid for Australian salmon otoliths. Because of the negative results of these experiments it was felt that some alternate test should be carried out to provide evidence that the Australian salmon otoliths were precipitated under temperature conditions that were adequate to have an effect on the composition of the otoliths. Therefore, oxygen stable isotope analyses were carried out on the second otolith from each Australian salmon otolith pair used for microprobe analysis. The relationship between temperature and oxygen isotope deposition in biogenic calcium carbonate is well established (Berger *et al.*, 1981) and a similar relationship was found for the Australian salmon otoliths (see Chapter 6). The Sr/Ca data from the controlled-temperature experiments are corroborated by data on wild Australian salmon and blue grenadier which showed no correlation with temperature and are in agreement with the results of Buchardt and Fritz (1978) and Lorens and Bender (1980) who found no relationship between the incorporation of Sr and temperature in molluscs with aragonite shells.

Radtke (1984) found that there was a significant inverse relationship between the otolith Sr/Ca ratio and temperature in laboratory-reared Atlantic cod (*Gadus morhua*) and that the slope of this relationship was not significantly different from the data obtained by Kinsman and Holland (1969) for inorganically precipitated aragonite. The cod otolith data did show a marked biological fractionation effect with otolith aragonite being depleted in Sr relative to the inorganically precipitated aragonite. Although a Sr/Ca versus temperature relationship was found by Radtke (1984) there is no direct evidence that the kinetic mechanism invoked by Kinsman and Holland (1969) was the causative factor. Over the experimental temperature range of the cod rearing experiments (4.3-7.8°C) there may have been other metabolic effects related to factors such as growth or condition that might alter the Sr/Ca ratio present in the endolymph surrounding the otolith. This will be discussed in more detail at a later stage.

Consideration of Sr/Ca ratio data obtained from the inorganic precipitate

experiments of Kinsman and Holland (1969) and from otoliths (Radtke and Targett,1984; Radtke, 1984b, 1987) further support the conclusion that otolith Sr/Ca ratios cannot be used effectively as a predictor of temperature. Kinsman and Holland (1969) carried out inorganic precipitate experiments at temperatures of 16 to 90°C with only two treatments (16 and 30°C) within the range of environmental temperatures generally found in aquatic environments. Examination of their data at 16° (n=10) and 30°C (n=13) shows that there is no significant difference between the K_{Sr} at the two temperatures (t-test; $p>0.4$). Furthermore, the application of the Kinsman and Holland relationship to aquatic environments would frequently require extrapolation beyond the temperature range of the data.

Radtke and Targett (1984) postulate an environmental thermometer based on Sr/Ca ratios in otoliths of the Antarctic fish *Notothenia larseni*, however, their data do not support this hypothesis. Specimens of *N. larseni* for their research were collected at South Georgia Island on 19 May, well past the austral summer and into the months of decreasing ocean temperatures in waters around South Georgia (North, 1988), yet their measurements of Sr/Ca ratios at the otolith edge, the material produced just prior to capture, were still decreasing and would indicate that ocean temperatures experienced by the fish were still increasing. This implies a positive correlation, if any, between temperature and otolith Sr/Ca. Furthermore, if the Sr/Ca thermometer was assumed to be applicable to their specimen of *N. larseni*, one would conclude that the winter otolith growth rate was equal to, if not greater than, that in the summer months. However, data on the growth of Antarctic fishes indicate a marked seasonality in growth with increased growth in summer months (Macdonald *et al.*, 1987). Finally, if we apply the slope from the regression equation for Sr/Ca x 10^3 (R) versus temperature in °C (T) for inorganic aragonite from Kinsman and Holland (1969) where R=10.66-0.039T, to the data of Radtke and Targett (1984) we find that the temperatures experienced by the fish in question (range of Sr/Ca ratios 0.0025-0.0080) would have ranged over 141°C degrees. Alternatively, using the Sr/Ca x 10^3 versus temperature relationship obtained by Radtke (1984b) in experimental work with cod (*Gadus morhua*) where R=4.19-0.13T, the temperature range is 42°C. Similarly impossible temperature ranges are obtained using published data for Hawaiian snapper (*Pristipomoides filamentosus*) (Radtke, 1987).

It has been suggested that increased environmental temperature results in an increase in the total quantity of trace elements incorporated into aragonitic fish otoliths

(Gauldie and Nathan, 1977; Gauldie *et al.*, 1980; Gauldie *et al.*, 1986). The results of constant-temperature experiments in this study do not support this hypothesis in relation to the total trace ions in fish otoliths resulting from Sr, Na, K and S. However, there was some evidence of an increase in otolith Sr/Ca ratio with increased temperature (Fig. 2.2). This relationship is probably not a direct one, with the effects of temperature on physiology and the resultant alteration in the composition of the endolymph, the most likely agent. Although the apparent effect of temperature is slight, the trend was evident in the two independent constant-temperature experiments, thus, it seems likely that there is some biological significance to this relationship. Attempts to explain any variability directly or indirectly attributable to temperature will first require a greater understanding of the variability both within treatment temperatures and individual otoliths.

2.4.2 Endolymph and otolith composition

The Sr/Ca ratio of the otolith aragonite increases linearly as the Sr/Ca ratio of the endolymph increases (Fig. 2.11) even when considering a range of species from different taxonomic orders and confirms that solution chemistry is a major factor in determining the Sr/Ca ratio in the otolith. The distribution coefficient, K_{Sr}, at approximately 18°C, calculated from the slope of the data in Fig. 2.11, is 0.255±0.052, and not significantly different from the distribution coefficients of 0.23±0.04 (Lorens and Bender, 1980) and 0.237±0.027 (Buchardt and Fritz, 1977) for the molluscs *Mytilus edulis* and *Limnaea stagnalis*. Kinsman and Holland (1969) obtained a distribution coefficient of 1.15 at 20°C for aragonite which is similar to distribution coefficients of 1.0 to 1.3 obtained for aragonitic ooids, aggregates, algae (Milliman, 1974) and corals (Smith *et al.*, 1977).

It is difficult to explain the differences in distribution coefficients among fish otoliths, molluscan shells and other organisms with the data available, however, these results may provide some insight into mechanisms of biogenic calcification. The similar Sr distribution coefficients for fish otoliths and molluscan shells may indicate that a similar mechanism is involved in the production of biogenic calcium carbonate in these organisms. Concomitantly, it may imply that the calcification mechanism in corals and algae is different from that in otoliths and mollusc shells. The lower distribution coefficient for molluscs and fish otoliths indicates that some form of biological fractionation is occurring. Biological fractionation may result from

differences in kinetics or from site-specific differences in a calcium-binding protein involved in calcification. If a discriminatory calcium-binding protein were involved in otolith formation there would be a fractionation effect during otolith crystallization and a relatively low distribution coefficient would result. The higher distribution coefficient in corals and algae, similar to that for inorganic precipitates, may be due to a calcium-binding protein which does not discriminate between Ca and Sr ions or a calcium-binding protein may not be involved in ordering the ions during the calcification process.

2.4.3 Seasonal and age-related variation in otolith composition

Microchemical data from the otoliths of monthly collections of Australian salmon failed to show that a relationship existed between temperature and the incorporation of trace elements studied, but there were significant seasonal variations in otolith trace element composition. Although the size range of Australian salmon used in these measurements overlapped in most months (Fig. 2.7c), it was difficult to collect individuals from a similar size range despite the protracted recruitment period of this species to Tasmanian waters. As a result, it may be difficult to interpret seasonal variations in otolith elemental ratios due to potential bias resulting from size-related factors. Size was shown to affect RNA/DNA ratios and, similarly, it may obscure any relationship between measurements associated with growth and otolith chemistry.

There are numerous physiologically based hypotheses that might be presented as plausible explanations for the observed seasonal variations in otolith microchemistry. On the basis of the data relating endolymph Sr to otolith Sr, it appears that explanations for changes in endolymph composition would largely explain variations in otolith Sr. Although similar conclusions might be drawn for the incorporation of Na, K and S into the otolith aragonite matrix, it is not possible to do so with the data presented here. However, studies on calcium carbonate precipitation do lend support to the importance of the composition of the precipitating fluid in determining the composition of the precipitate (Kitano *et al.*, 1975; White, 1977; Lorens and Bender, 1980; Busenberg and Plummer, 1985; Okumura and Kitano, 1986). One mechanism that may alter the endolymph Sr/Ca ratio and that would respond to numerous physiological changes is dependent on levels of calcium-binding proteins present in the blood. According to Mugiya (1966) and Mugiya and Takahashi (1985) the level of free calcium in the plasma is directly proportional to, if not equal to, the Ca in the endolymph. Therefore

a reduction in free plasma calcium due to an increase in calcium-binding proteins, such as albumin or vitellogenin, in the blood would result in reduced Ca in the endolymph. Numerous studies have found seasonal variations in the levels of blood protein in fishes (Booke, 1964; Das, 1965; Mugiya, 1964, 1966; Mulcahy, 1967; Snieszko, 1972; Heming and Paleczny, 1987). Furthermore, if Sr levels remained constant in the plasma at this time, the net result would be a relative increase in the quantity of Sr in the endolymph, as calcium-binding proteins selectively bind Ca over Sr, despite the similarity of the two ions (Ichikawa, 1960; Oguri *et al.*, 1965; Comar, 1967; Wadkins and Peng, 1981; Rosenthal, 1981; Isa and Okazaki, 1987). The increase in the endolymph Sr/Ca ratio would result in an increase in the otolith Sr/Ca ratio as previously shown.

The relationship between otolith Sr/Ca ratio and age in blue grenadier (Fig. 2.9) may be related to relative protein growth, most easily represented as weight, during the life span of the fish. A logarithmic expression best describes the relationship between blue grenadier otolith Sr/Ca and age, similar to relationships typically used to describe growth such as the von Bertalanffy growth function. The asymptotic maxima (Sr and K) and minima (Na and S) are reached at the age of about 10 years, similar to the age at which mean maximum weight is achieved as estimated by von Bertalanffy growth curves for blue grenadier (Fig. 2.8) (Kenchington and Augustine, 1987). This implies that the incorporation of certain trace elements into the otolith may be related to growth. Growth in weight in blue grenadier appears to continue well beyond the time when growth in length has ceased, based on data from this study and Kenchington and Augustine (1987). Furthermore, the increased variance in fish weight with age indicates that the highest absolute weight growth rates may occur in older fish. This variance may be due to seasonal weight changes and the effect of examining fish collected over the whole year for a single weight-at-age function. During the life of a fish, growth in both length and weight is best represented by an oscillating growth function (Ursin 1963; Pitcher and Macdonald 1973; Shul'man 1974; Moreau 1987). Shul'man (1974), Pitcher and Macdonald (1973), Moreau (1987) and others have described oscillating seasonal weight-growth functions which indicate an increased seasonal growth rate in later life, that is, an increase in the amplitude of growth cycles, due to recovery from weight loss following low winter rations and/or spawning. If large weight fluctuations are occurring in older blue grenadier, high levels of calcium-binding proteins would be present in the plasma during growth periods, potentially

increasing the endolymph and otolith Sr/Ca ratio. Das (1965) found that blood protein increased with age in Indian carp (*Catla catla*) and Lockhart and Metner (1984) found that serum protein levels increased with increasing length-weight measurements in white suckers (*Catostomus commersoni*). Also, age-related increases in otolith Sr/Ca may be linked to increases in fecundity and gonado-somatic index (GSI) with age, as discussed below.

The changes in blue grenadier otolith chemistry are not likely to be related to ontogenetic changes in distribution. There are age-related changes in all elemental ratios and, specifically, the changes in Sr/Ca ratio with age are too great to suggest a temperature-mediated effect. Furthermore, there is no evidence to suggest that blue grenadier older than 5 years of age display any significant changes in habitat or distribution other than during the spawning season.

The seasonal variation in Sr/Ca ratios in blue grenadier may be related to spawning and growth. Gunn *et al.*, (1989) concluded from both larval collections and a gonado-somatic index that blue grenadier spawn off the west coast of Tasmania from June through August. Fish collected on the west coast had high GSI's from June through August, whereas those collected from eastern and southeastern Tasmania had low GSI's throughout the year with only a minor peak occurring in June off southeastern Tasmania. The relatively high Sr/Ca ratios occurring in blue grenadier otoliths collected in August (Fig. 2.10) may be a direct result of high plasma protein levels during the period of gonad maturation and spawning. Booke (1964), Woodhead (1968) and others have shown that during the period leading up to spawning there is a gradual increase in levels of both plasma calcium and plasma protein, which are both involved in the synthesis of gonad tissue. Furthermore, the increase is in bound calcium only as the increased calcium is destined almost exclusively for the gonads (Bailey, 1957; Urist and Schjeide, 1961; Simkiss,1974). Again, the same mechanism invoked earlier, whereby levels of free or diffusible calcium are reduced due to increases in calcium-binding plasma proteins could result in an increase in the Sr/Ca ratio in the endolymph and, thus, an increase in the otolith Sr/Ca ratio. Older fish frequently have a greater relative investment in reproduction, represented by an increase in GSI (Woodhead, 1979), and this may further increase the level of calcium-binding protein and the otolith Sr/Ca ratio.

An increase in the Sr/Ca ratio due, in part, to cooler winter temperatures is questionable for blue grenadier since they are generally collected at depths of

400-700 m where there is only a minor seasonal variation in temperature of 7° to 10°C (unpublished data, Commonwealth Scientific and Industrial Research Organization, Division of Fisheries Research, Australia). High otolith Sr/Ca ratios in the March and April samples may be associated with high levels of plasma protein due to summer feeding and rapid growth.

Both the age-related and monthly variations in S/Ca ratios in blue grenadier otoliths may be a result of variations in the levels of protein incorporated into the otolith. Sulphur is present in two of the amino acids detected in otolith protein, cysteine and methionine (Degens *et al.*, 1969; Morales-Nin, 1986; Radtke, 1984). Mugiya (1968) and Mugiya and Iketsu (1987) detected sulphated acid mucopolysaccharides, another potential source of organic sulphur in otoliths. Estimates of the total quantity of organic matter present in otoliths are highly variable ranging from 0.2 to 10% (Degens *et al.*, 1969; Radtke, 1984; Morales-Nin, 1986). Despite the great variability in both total protein and the relative abundances of the various amino acids, it is evident that both cysteine and methionine make a relatively small contribution to the total mass of the otolith. If it is assumed that 1% of the otolith amino acids are either cysteine or methionine (26.5 and 21.5% sulphur by weight respectively), as estimated by Degens *et al.*, (1969) and Radtke (1984), then an otolith that is 5% protein would contain 0.012% or 3.7 μM sulphur due to protein. Total sulphur measured with the electron microprobe in blue grenadier otoliths ranged from approximately 1.0 to 20 μM. Thus, variations in the quantities of protein, or more specifically, sulphur-containing amino acids in fish otoliths could be an important factor affecting the total sulphur measured in otoliths. The monthly variations in otolith S/Ca support this hypothesis. The high S/Ca ratios measured in the summer months are associated with protein-rich opaque zones and during the fall and winter there is a drop in otolith S associated with spawning and the formation of low-protein hyaline zones.

The negative correlation between otolith S/Ca and age, although weak, is further evidence that a significant portion of the S is attributable to protein. Morales-Nin (1986) found that levels of otolith protein were higher in sea bass (*Dicentrarchus labrax*) less than one year of age, with no significant difference in the percentage of otolith protein among fish aged one year and greater. The blue grenadier otolith S/Ca data presented here shows a similar trend with one year old fish having higher S/Ca ratios, indicative of more protein.

Levels of both sodium and potassium in fish blood are maintained at fairly constant levels due to the importance of these ions in maintaining osmotic balance and nervous functions. Alterations in the levels of these constituents are usually associated with extreme changes in physiology or condition. Changes in plasma potassium levels are especially critical because of the importance of potassium in maintaining membrane resting potentials. The varied results obtained in studies of plasma sodium and potassium levels make it impossible to extrapolate these data to endolymph composition and, ulitmately, otolith composition. Detailed studies of the variability in plasma and endolymph constituents of marine species are necessary before a valid interpretation of otolith Na and K levels can be attempted.

2.4.4 Physical considerations

This discussion has concentrated on biological arguments to explain the variations observed in otolith trace element chemistry. It must be pointed out that, as in all biological systems, there are underlying physical mechanisms that are ultimately responsible for the quantity of a particular trace element that is incorporated into the aragonite matrix of an otolith (Kinsman and Holland, 1969; White, 1977; Onuma *et al.*, 1979; Lorens, 1981; Veizer, 1983; Okumura and Kitano, 1986). The quantities of Sr, Na, K and S that were measured in fish otolith aragonite are clearly within the range one would expect on the basis of experiments with inorganic carbonate precipitates. In fact, the Sr content of otolith aragonite is close to that of the most stable aragonite on the basis of thermodynamic studies of aragonite-strontianite solid solutions (Plummer and Busenberg, 1987). Otolith aragonite stability may be critical in preventing dissolution of the otolith in the sacculus due to undersaturation, with respect to Ca, of the endolymph. However, despite any parallels with studies of inorganic carbonates, the variability that has been observed in otolith trace element chemistry cannot be adequately explained on the basis of physical principles alone. On the scale of a single otolith it is apparent that there are four levels of variability effecting trace element composition: 1) temporal variability which may be largely explained by the physiology of an individual fish and related changes in the composition of the endolymph; 2) spatial variability represented on scales of 5 to 10 μm as measured by the electron microprobe and within a single increment around an otolith that may be due to inhomogeneity in the distribution of proteins and trace elements in the endolymph; 3) submicron processes at the otolith-endolymph interface that may be

dominated by such factors as the orientation of aragonite crystal faces, crystal surface area and the degree of solution saturation (Wiechiers *et al.*, 1975; Morse, 1986), and; 4) processes at the molecular level and below relating to both the forces within aragonite crystals and kinetic and thermodynamic properties (Saxena, 1973; Onuma *et al.*, 1979, Busenberg and Plummer, 1985; Plummer and Busenberg, 1987).

The data are unable to explain the high variability in elemental ratios measured within individual otoliths in the constant temperature experiment and within a single growth zone such as around the edge of the otolith. There was no meaningful correlation between element ratio and otolith growth that would explain the variability at this level. Weber (1973) and Thompson and Livingston (1970) concluded that their data showed a relationship between coral growth and Sr/Ca ratio, however, this interpretation of their results has not been universally accepted (Smith *et al.*, 1979, Chalker, 1981). In any case, we must be careful when comparing carbonates of such different origins as coral skeletons and fish otoliths as there may be differences in the calcification mechanism.

2.5 SUMMARY

This study has demonstrated that temperature plays a very minor role, if any, in the determination of Sr/Ca, Na/Ca, K/Ca and S/Ca ratios in fish otoliths. It has also demonstrated that there is considerable variability in otolith chemistry both within and among otoliths. These conclusions are particularly important in light of the current interest in the application of methods of instrumental analysis, particularly the electron microprobe, to the study of the microchemistry of fish otoliths. Although seasonal cycles and other periodic trends are occasionally evident in Sr/Ca ratio data collected from some species (see Chapter 4) (Radtke, 1984) the causative factor for these cycles is still open to conjecture. It is important to note that, more often than not, microchemical transects of otoliths have failed to show any discernible periodicity (see Chapter 4) (Radtke, 1987). If endolymph Sr/Ca ratios vary in relation to the levels of free/diffusible calcium in the plasma, there would be many factors, both an inter- and intraspecific, that could ultimately affect otolith Sr/Ca ratios. The number and complexity of these factors makes the potential for error in the interpretation of otolith Sr/Ca data very great.

Before interpretation of variations in otolith chemistry is attempted, it is clearly necessary to carry out various validation experiments and to develop an understanding

of the relationships among plasma, endolymph and otolith composition. As an alternative or, preferably, an adjunct to validation experiments, it would be valuable to determine annual variations in otolith composition from measurements obtained from the otolith edge of numerous specimens of known physiological state as has been done here for blue grenadier and Australian salmon. In some species this may result in an understanding of data obtained from microprobe transects of individual otoliths.

CHAPTER 3

SEASONAL VARIATION IN THE COMPOSITION OF BLOOD PLASMA, ENDOLYMPH AND OTOLITHS OF BEARDED ROCK COD *PSEUDOPHYCIS BARBATUS*

3.1 INTRODUCTION

Seasonal variations in the nature of otolith material have long been the basis for age determination in many fish species. Generally, the alternation of opaque and hyaline zones in otoliths has been associated with variations in fish growth rate (Blacker, 1974). Investigations of the relationships between certain physiological parameters and the occurrence of these opaque and hyaline zones has been plagued with confusion, but it is generally agreed that the difference in optical density between the two zones is due to the relative quantity of organic matrix present (Dannevig, 1956; Irie, 1955, 1960; Blacker, 1969; Mugiya *et al.*, 1985). Although a clear link between physiological state, associated with periods of fast or slow growth, and the production of otolith zones of differing optical density has been established, no study has considered the influence of these same physiological parameters on the composition of the blood, the endolymph, the fluid surrounding the otoliths and, ultimately, the trace element composition of the otoliths.

Only a handful of studies has examined the composition of fish endolymph and, in only about one half of these studies, were the investigators interested in endolymph composition in relation to the formation of otoliths. Enger (1964), Fänge *et al.* (1972), Watanabe and Miyamoto (1973) and Mugiya and Takahashi (1985) investigated the composition of fish endolymph to gain insight into the ionic composition of this fluid and the role of endolymph in the maintenance of saccular ionic potentials. Calcification studies by Mugiya (1964, 1966a, 1966b) and Mugiya and Takahashi (1985) remain the primary works on the relationship between fish endolymph composition and otolith calcification. These workers concentrated on aspects of endolymph composition that were particularly relevant to the seasonal formation of otolith opaque and hyaline zones and were primarily concerned with seasonal changes in the protein and calcium content of endolymph. Mugiya (1966b) determined seasonal changes in levels of magnesium in the endolymph and blood plasma of a salmonid, *Oncorhynchus mykiss* and a flatfish, *Kareius bicoloratus*, but

but he did not relate these measurements to the composition of the otolith. Thus, no study until Kalish (1989) has related the trace element composition of fish endolymph to otolith composition.

Biogenic calcium carbonates are, in many cases, not deposited in equilibrium with seawater and both mineralogy and composition generally differ from the composition predicted on the basis of relationships derived from studies of inorganic precipitates (see Chapter 1). Understanding the conditions and processes that result in the observed compositions of biogenic carbonates is a basic requirement for the interpretation of mineralogical and microchemical data. Although it may be feasible, in some cases, to interpret microchemical data on the basis of a basic knowledge of the ecology and environment of the calcium carbonate producing organism, such data are generally inadequate (Kalish, 1989).

Geochemical studies have generally operated under the assumption that variations in the composition of calcium carbonate, and the degree to which trace elements may "contaminate" the calcium carbonate lattice, can be related to four major factors: (1) mineralogy of the skeletal fragment (calcite, aragonite or vaterite) ; (2) environmental features (e. g. temperature and salinity); (3) water chemistry; and (4) a "vital" or biological effect based on the physiology of the organism. Although these relationships have been actively studied through both laboratory and field experiments, for a wide range of biological systems, there is only a cursory understanding of the factors affecting trace element deposition. Furthermore, for many organisms that produce calcareous deposits internally, such as in the case of fish otoliths and squid statoliths, the nature of the fluid surrounding the carbonate structure has received little or no attention, despite the fact that these fluids are probably of great importance.

The maintenance of internal composition, particularly of body fluids, is generally placed under the label of homeostasis. In cases where an element or metabolite is an essential component of some structure or required in a physiological process, the element or compound in question may be carefully regulated. However, it is clear that the chemistry of an organism will change depending on it's physiological, reproductive or life history status, as well as on the season. The degree to which such changes are manifested in the blood plasma has been studied intensively in salmonids (Hille, 1982). However, few studies have considered these relationships in wild marine fish and, as indicated earlier, no studies have considered such

interactions in endolymph.

This study seeks to determine the relationships, if any, between ambient temperature, fish length, weight, sex, age, condition, gonad weight, the composition of blood plasma, endolymph and otoliths. The ultimate goal of this chapter is to identify those factors that are most important in controlling the trace element composition of fish otoliths and to relate these data to seasonal variations in otolith trace element composition. A later section will consider how these data may relate to otolith life-history transects of the species investigated.

3.2 MATERIALS AND METHODS

3.2.1 Selection of study species

Bearded rock cod (*Pseudophycis barbatus*) were selected for study because of their year round availability and relative ease of capture, their large sagittal otoliths and the associated large sacculus which contains adequate quantities of endolymphatic fluid for carrying out the required analyses without pooling fluid from more than one fish. Gadoids typically have large otoliths making them an obvious first choice. Their suitability became even more evident during a comparative study of the endolymph strontium content in fishes from the environs of Storm Bay (Chapter 2). Other species that were considered for this study were either difficult to capture and/or they contained inadequate quantities of endolymph to carry out the analyses without pooling samples. Furthermore, in most species the endolymph was too difficult to remove without contamination from cerebrospinal fluid. Although these factors made cod the only suitable choice for this study, they were not necessarily ideal, primarily due to the lack of any clearly defined "seasonal cycles" in otolith composition and because the long-term variability in otolith composition was not always very great. There were additional problems, related to otolith growth in mature cod, that make it difficult to determine the composition of the most recently formed otolith material and these points will be discussed in a later section. However, none of the species I investigated in southeast Tasmanian waters was found to have clearly discernible seasonal cycles in otolith elemental ratios (Sr/Ca, Na/Ca, K/Ca and S/Ca) based on otolith transects with a wavelength dispersive electron microprobe.

3.2.2 Collection of blood, endolymph and otoliths

Cod were collected from March 1987 to February 1988 by handline fishing in Variety Bay, on the Storm Bay side of Bruny Island. Two fishing locations, separated by about 100 m, over rocky reefs at depths of 20 to 25 m were located within Variety Bay and these regions were used as collection sites throughout the study.

All sample collection was done at sea immediately after capture of individual fish. Within 30 sec of being hooked fish were brought to the surface where they were killed by a blow to the head. Individuals were weighed to the nearest 10 g with a spring balance and the standard length measured. The tail was cut off in the region of the caudal peduncle for collection of blood from the dorsal aorta. Blood was collected by placing a capillary tube containing about 2 µl lithium heparin (0.25 mg ml^{-1}) against the dorsal aorta and collecting blood from the capillary tube in 1.5 ml plastic centrifuge tubes. Korcock *et al.* (1988) have shown that blood collection from stunned specimens and the use of heparin result in the least change in parameters frequently measured in fish blood. Whole blood was placed on ice and centrifuged within 2 h of collection.

Endolymph was collected immediately after blood collection. Before exposing the brain, gill arches were cut and the fish was placed in seawater and agitated by hand for around 30 sec to ensure the removal of the greatest amount of blood possible. This step helped to eliminate problems of contamination of endolymph with blood. The brain was exposed and removed with forceps and any fluid remaining in the brain cavity was absorbed with lint-free paper making the sacculi containing the sagittal otoliths visible. The membrane between the brain cavity and the sacculus was punctured with the autopipette tip used for endolymph collection. In most cases, the otoliths were kept in place while the endolymph was removed with an autopipette with a standard low volume (10 to 250 µl) tip. When the otoliths obstructed most of the sacculus they were removed with plastic forceps before the endolymph was collected. Sample volume collected from individual fish ranged from 50 to 500 µl, low volume collections typically resulting from complications during the sampling and, in many cases, contamination, during the sampling process, with blood or cerebral-spinal fluid. Endolymph samples were stored on 0.5 ml plastic centrifuge tubes. Immediately after collection the endolymph was placed on ice and subsequently stored at 4° C prior to analysis. Analytical methods were similar for constituents of blood plasma and endolymph unless otherwise specified.

Only sagittal otoliths were collected in this study. Otoliths were extracted from the sacculus and the adhering otolith capsule was removed. Sagittae were rinsed in freshwater and then stored in individual glass vials. Preparation of otolith samples for microprobe analysis is discussed below.

3.2.3 Analysis of metabolites and ions

3.2.3.1 *Phosphate*

Inorganic phosphate levels were determined using the methods outlined by Daly and Ertingshausen (1972), as modified by Wang *et al.* (1983). Acidified ammonium molybdate was added to approximately 10 µl of sample which resulted in the formation of phosphomolybdic acid. The quantity of phosphomolybdic acid was then determined by UV spectrophotometry at 340 nm and 30°C.

3.2.3.3 *Triglycerides*

Total triglycerides in plasma and endolymph were determined by the enzymatic hydrolysis of the triglycerides followed by the measurement of the resulting glycerol by spectrophotometry at 540 nm and 25°C. The method is detailed by Wahlefeld (1974) and the reagents used were from a Boehringer Mannheim Diagnostic Kit (Triglycerides GPO-PAP).

3.2.3.4 *Glucose*

Glucose was determined by the enzymatic method of Bondar and Mead (1974). Glucose was reacted with ATP and the enzyme hexokinase resulting in D-glucose-6-phosphate which was reacted with glucose-6-phosphate dehydrogenase in the presence of NAD (nicotinamide adenine dinucleotide). This resulted in the formation of reduced NAD (NADH) which was measured spectrophotometrically at 340 nm. Reagents were from a Roche Diagnostic Kit (Glucose HK).

3.2.3.5 *Protein*

The majority of the protein assays were carried out using the protein-dye binding method of Bradford (1976) although some plasma protein analyses were done using the biuret assay (Kingsley, 1939). The protein-dye binding method was used because of it's greater sensitivity. This increased sensitivity was required to measure the low levels of protein in the endolymph. There were no significant differences in

the results obtained using the two methods. The method of Bradford (1976) involves the binding of Coomasie Brilliant Blue G-250 to the protein which results in a shift in absorption maximum for the dye from 465 nm to 595 nm.

3.2.3.6 *Albumin*

Albumin was determined using the bromcresol green (BCG) binding assay, where the binding of albumin to BCG results in a shift in the absorbance maxima of BCG (Doumas *et al.*, 1971). The change in absorbance at 630 nm is proportional to the quantity of albumin in the sample. The reagent used was from an albumin test kit (Roche Reagents).

3.2.3.7 *Strontium, calcium, sodium, potassium*

Strontium concentrations in endolymph and plasma samples were measured by graphite furnace atomic absorption spectrophotometry on a Varian AA-1475 spectrophotometer equipped with a GTA-95 graphite furnace and an autosampler. Argon was used as the purging gas in the graphite furnace. Samples were diluted up to 200 times with a 0.25% solution of an ionic detergent, Triton X-100, and 20 µl of diluted sample were injected by autosampler into a walled, pyrolytically coated graphite tube. Furnace conditions were: drying at 90°C for 60 sec; ramp ashing from 90 to 700°C for 20 sec; ashing at 2600°C for 1 sec; and atomization, with no gas flow, at 2600°C for 3 sec. Based on initial results using the method of standard additions, there was no evidence of significant interferences in strontium analyses (Fig. 3.1).

Plasma and endolymph calcium concentrations were determined by flame atomic absorption spectrophotometry using a nitrous oxide/acetylene flame. Magnesium concentrations were also determined by flame atomic absorption spectrophotometry but using a air/acetylene flame. Potassium and sodium analyses were performed by atomic emission spectroscopy.

3.2.4 Characterization of plasma and endolymph proteins

Variations in serum proteins and comparison with endolymph proteins were carried out by electrophoresis on mylar supported cellulosic media in a barbital-sodium barbital buffer of pH 8.6, ionic strength 0.06 M. Endolymph samples were concentrated before electrophoresis because of the low concentration of proteins in

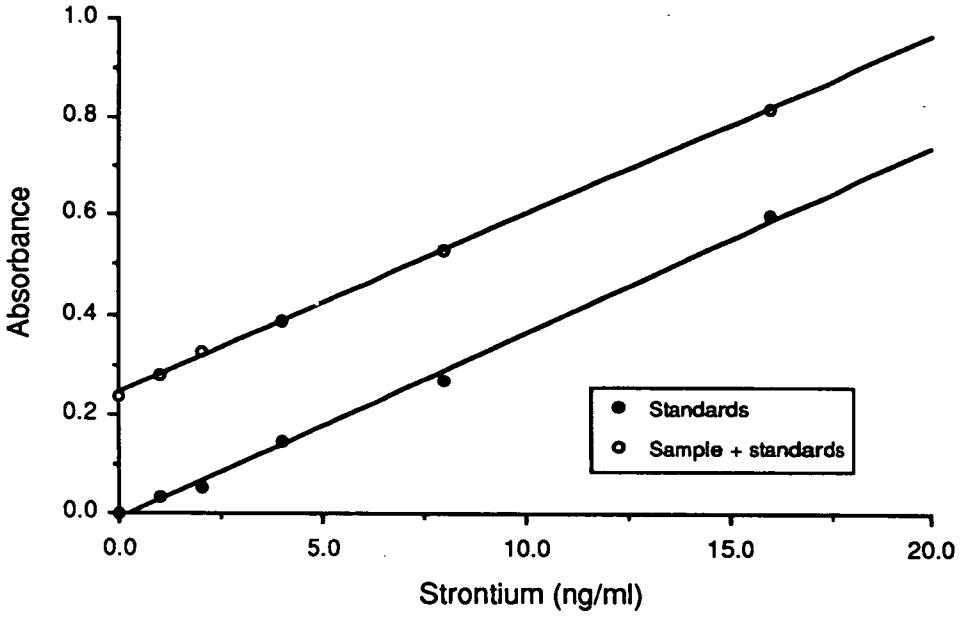

Figure 3.1a Example of graphite furnace atomic absorption spectroscopy calibration curve for strontium standards in 0.25% Triton X-100 and an example of a diluted cod endolymph sample run using the method of standard additions.

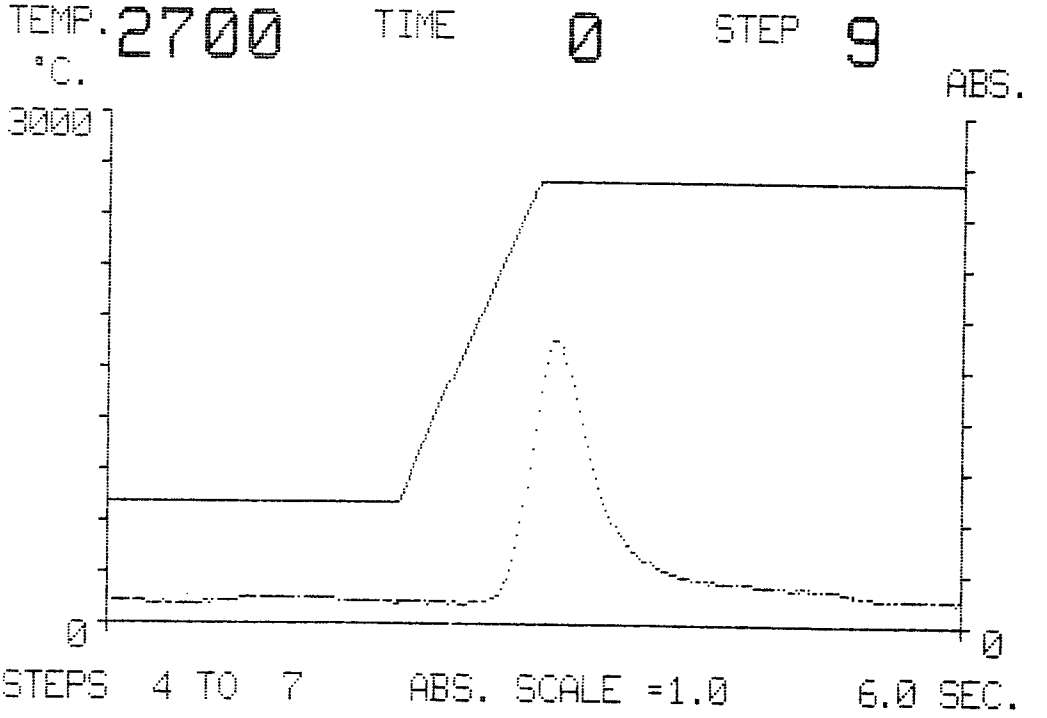

Figure 3.1b Example of a strontium absorption peak produced from a cod endolymph sample analysed by GFAAS. The X-axis is a time scale running from 0 to 6 sec. The solid line is the temperature profile in the graphite tube during the ashing and atomization phases of the program.

endolymph. Strips were stained with Ponceau S and then rinsed in 5% acetic acid. The optical density of the electrophoresed proteins was measured in an automated densitometer which also plotted the optical density against the distance migrated by the proteins.

Estimation of the molecular weights and calcium binding capabilities of endolymph and plasma proteins was carried out by gel filtration on a 2.6 x 30 cm column packed with Sephadex G-100 Fine gel filtration medium (Pharmacia, Uppsala, Sweden). Sample volumes were 1.5 ml for both plasma and endolymph. The column was equilibrated and samples were run with 0.02 M Tris-HCl buffer, pH 8.2, containing 0.33 M NaCl. Flow rates through the column were maintained at approximately 30 ml h^{-1} using a peristaltic pump. Continuous absorbance was measured at 280 nm and 1.5 ml fractions were collected in an automated fraction collector. The gel column was calibrated using SDS Molecular Weight Markers (Sigma Chemical Company, St. Louis, U.S.A.) and Blue Dextran. Calcium concentrations in the gel filtration fractions were determined by flame atomic absorption spectrophotometry using a nitrous oxide/acetylene flame.

3.2.5 Microprobe analysis of otoliths

Wavelength dispersive electron microprobe analysis was used to determine the concentrations of Ca, Sr, Na, K and S in the marginal increment of the cod sagittae. Sample preparation was similar to that for blue grenadier otoliths discussed in Chapter 2. Analyses were done with a Cameca SX-50 wavelength dispersive electron microprobe. Microprobe analyses were carried out on transverse sections through the otolith primordium and a 10 x 10 μm window (scanning raster) was employed. Beam current was 10 nA measured on copper and the accelerating voltage was 15 kV. The crystal configuration, standards and counting procedures were similar to those employed for the analyses discussed in Chapter 2 (Table 2.1). A minimum of 5 microprobe measurements were made at predetermined locations on the marginal increment of each transverse section. Results are presented as ratios of atomic concentrations.

3.2.6 Estimation of age and growth

Cod ages were estimated from transverse thin sections of otoliths prepared for microprobe analysis. Age estimates for individuals less than 5 years of age were

determined by enumerating the number of opaque zones (winter growth zones) visible with transmitted light. A Von Bertalanffy function was fitted by an iterative procedure to both the length and weight at age data.

3.2.7 Models

Various forms of models were investigated in an attempt to explain the variability in otolith and endolymph composition. In general, two forms of models were considered: (1) multiple regression models; (2) models in the geochemical literature that were derived from empirical data alone; and (3) geochemical models based on a combination of theoretical principles and empirical data.

Data on blood plasma, endolymph and otolith composition, fish length, weight, condition, reproductive state, age and water temperature were used to derive multiple regression models of the form:

$$Y = a + b_1X_1 + b_2X_2 + \cdots + b_nX_n$$

Multiple regression models were constructed using an interactive stepwise method with a significant F-statistic ($p \leq 0.05$) as the major statistical criterion for inclusion in the model. However, only those independent variables that were deemed biologically relevant and that would ultimately aid in the prediction of the dependent variable were considered. It was not believed appropriate, for example, to utilize a constituent of the endolymph to aid in the prediction of another endolymph variable. In such instances, it would be more appropriate to measure the dependent variable directly. Of course, the measurement of one endolymph variable might help to predict one or more dependent endolymph variables. Also, before consideration for inclusion in the model independent variables were plotted against dependent variables, along with the resultant standardized residuals and these plots were inspected to confirm that the assumptions of the regression analysis were not violated (Draper and Smith, 1981; Sokal and Rohlf, 1981). Where skewness was evident, a log transformation was applied to the independent variable data.

Details of the geochemical models are discussed in the relevant sections.

3.3 RESULTS

All cod were collected from a depth range of 20 to 25 m based on echo sounder readings. The seasonal variations in temperature and salinity at 20 m in Variety Bay (Fig. 3.2) are very similar to those measured at the surface and they are indicative of a well-mixed system comprised of Tasman Sea surface waters and free of any major fresh water inputs due to run-off and precipitation or the effects of evaporation. These conditions were essential to ensure relatively constant water chemistry conditions at the collection site.

There were some significant changes in both fish weight and length over the sampling period with fish of relatively constant size being collected from February to July at which point there was a gradual increase in both weight and length for females and length only for males (Fig. 3.3a, 3.3b). The number of fish collected each month is shown below in Table 3.1.

Table 3.1 Number of cod *Pseudophycis barbatus* collected each month.

Date of collection	Males	Females	Total
8 February	8	7	15
25 March	2	9	11
17 April	12	9	21
22 June	10	5	15
29 July	5	5	10
8 September	10	6	16
19 October	9	8	17
6 December	5	5	10

Condition factor appeared to vary independently of the changes in the size of the fish collected over the year (Fig. 3.3c). Both males and females showed an increase in condition factor in June, the first month of winter, followed by a sharp drop in condition in July. The decrease in condition in July was associated with an increase

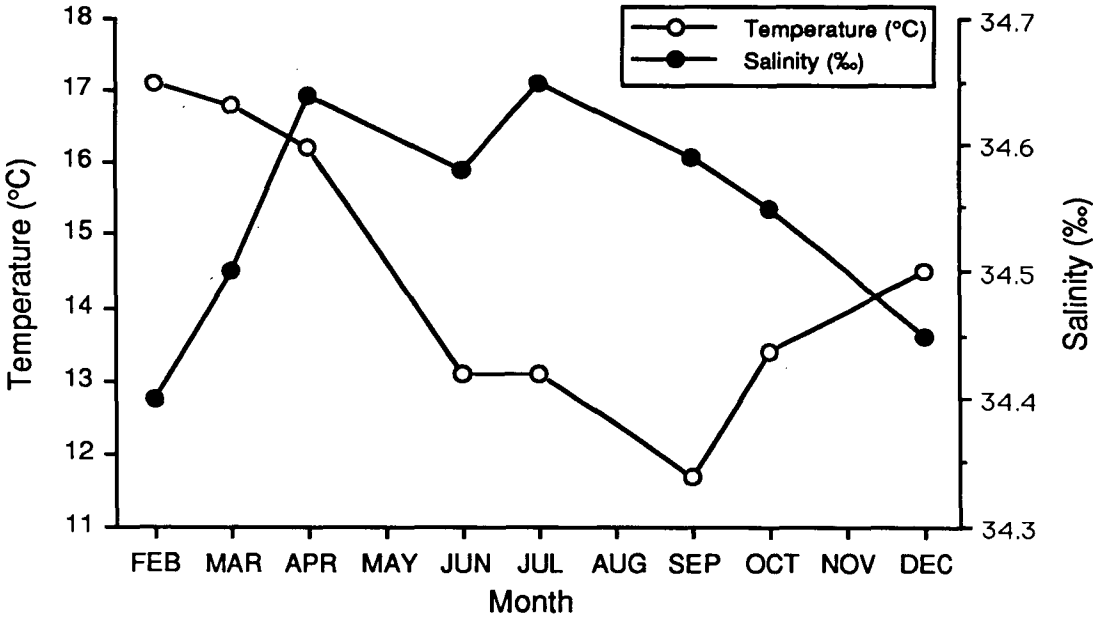

Figure 3.2 Seasonal variation in temperature (°C) and salinity (‰) at 20 m in Variety Bay. Data were collected over the reef where cod were captured.

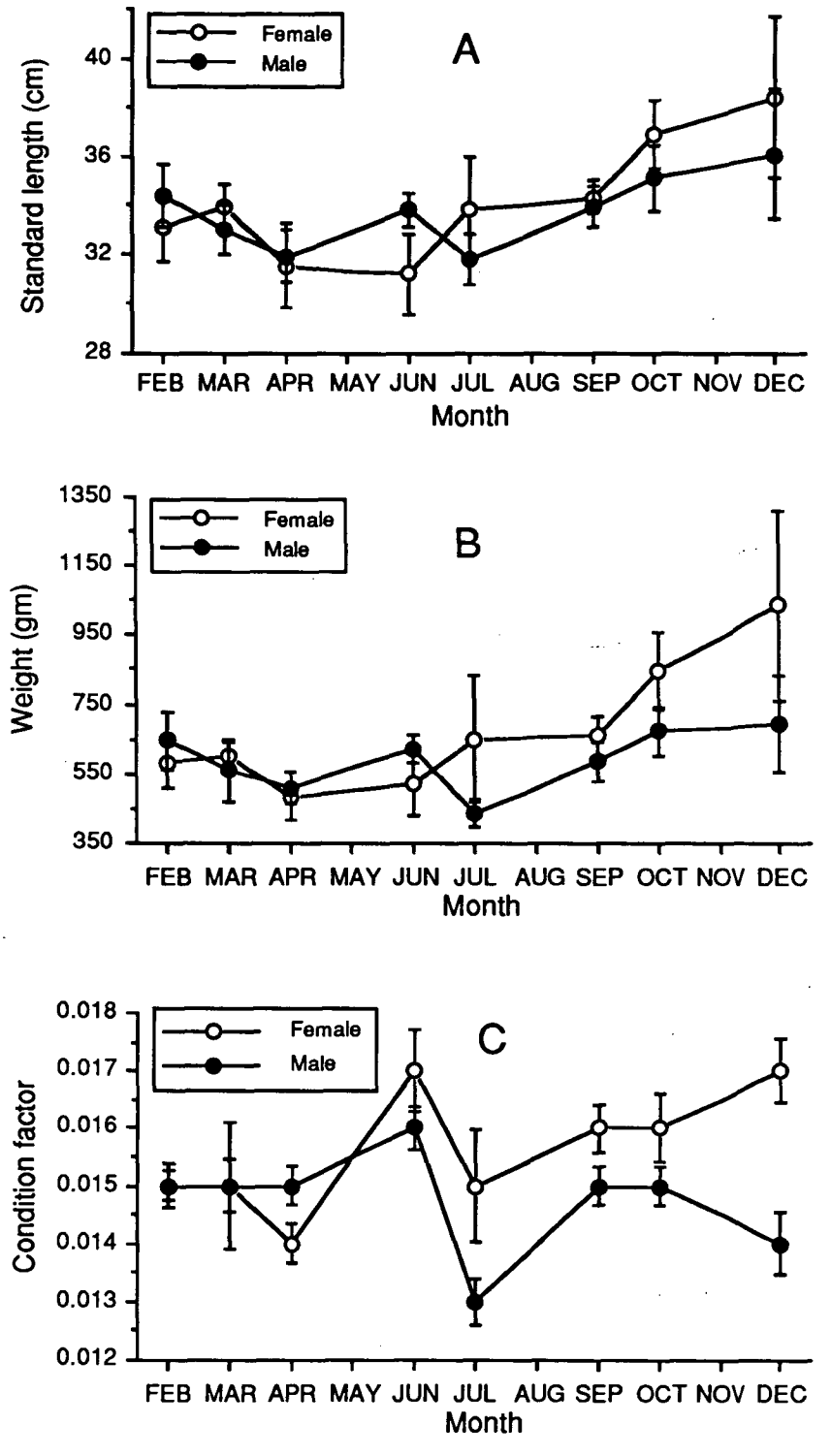

Figure 3.3 Seasonal variation in length (A); weight (B); and condition factor (W/L^3) (C); of cod collected from Variety Bay. Error bars are ±1 S.E.

in gonad weight and gonadosomatic index indicating preparation for spawning (Fig. 3.4). Condition returned to the pre-winter levels in the spring in the males and increased beyond pre-winter levels for the female fish. Male condition drops off again in December, but increased to June pre-spawning levels in the females.

The age structure of the samples collected can be determined from the plots of both length and weight at age (Fig. 3.5). There were some significant changes in the mean age of fish collected over the sampling period (Fig. 3.6), but relationships among the chemical variables measured in the plasma, endolymph and otoliths and fish age were not significant. Therefore, it was not necessary to account for fish age when comparing data from different months as was done with blue grenadier (see Chapter 2).

On the basis of examination of the cod otoliths, and subsequent age estimation, it was evident that otolith growth in the fishes collected for this study was relatively slow in the periods just prior to capture. This is due to the fact that a large percentage of the fish collected were approaching the asymptotic length; this is clearly indicated by the Von Bertalanffy growth function (Fig. 3.5, Table 3.2).

Table 3.2 Parameters of von Bertalanffy growth curves for *Pseudophycis barbatus* estimated (a) by length (cm) and (b) by weight (g).

(a)	L_∞	K	t_0	N
	34.8±0.3	0.649±0.038	1.16±0.06	115
(b)	W_∞	K	t_0	N
	759±30	0.277±0.030	1.19±0.13	115

Therefore, it is not unlikely that, in some instances, the 10 x 10 μm window used for microprobe measurements would encompass otolith growth over as much as several months. As a result, some of the relationships that are evident among otolith composition and the physiological and environmental variables may be somewhat obscured.

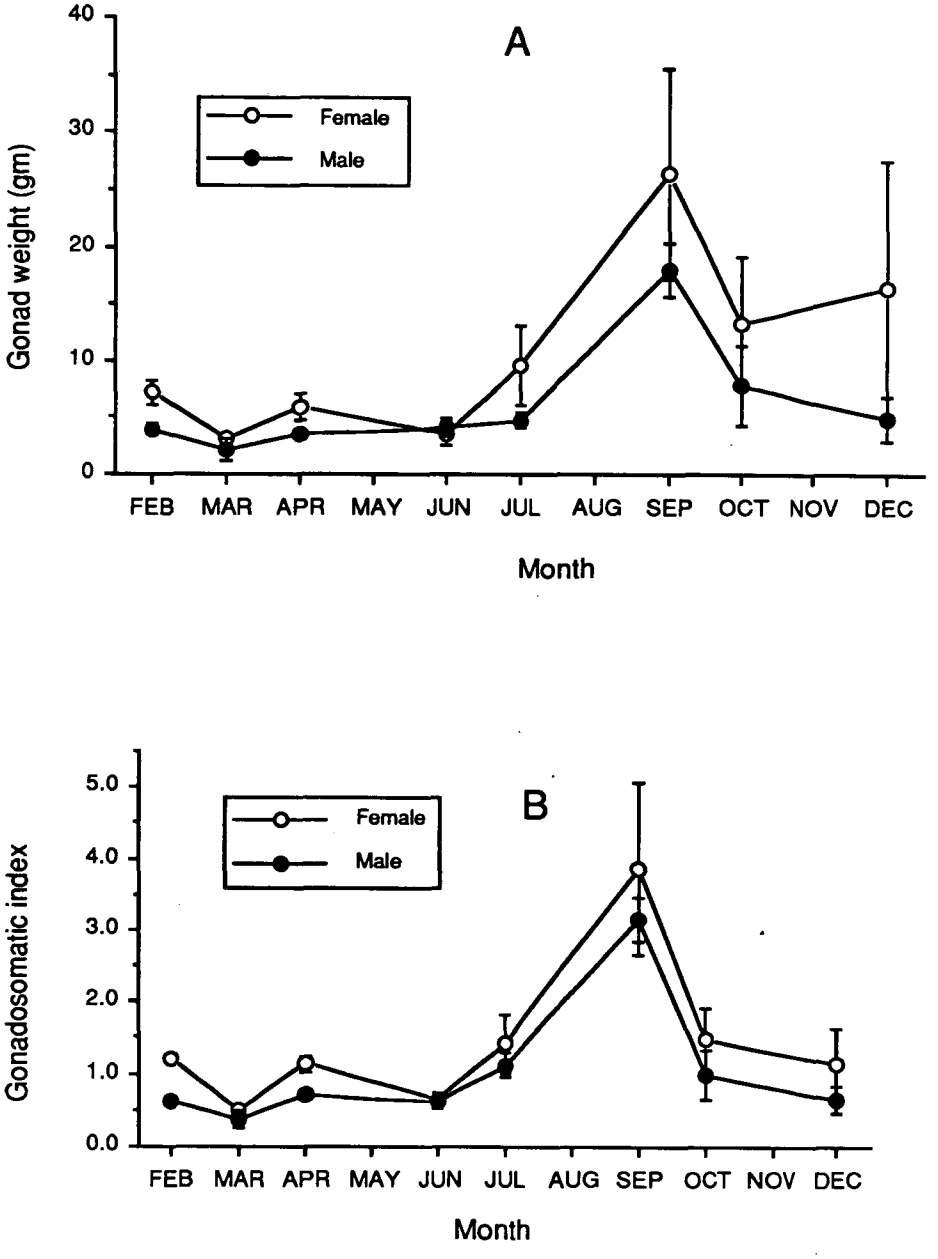

Figure 3.4 Seasonal variation in gonad weight (A); and gonadosomatic index (B); of cod collected from Variety Bay. Error bars are ±1 S.E.

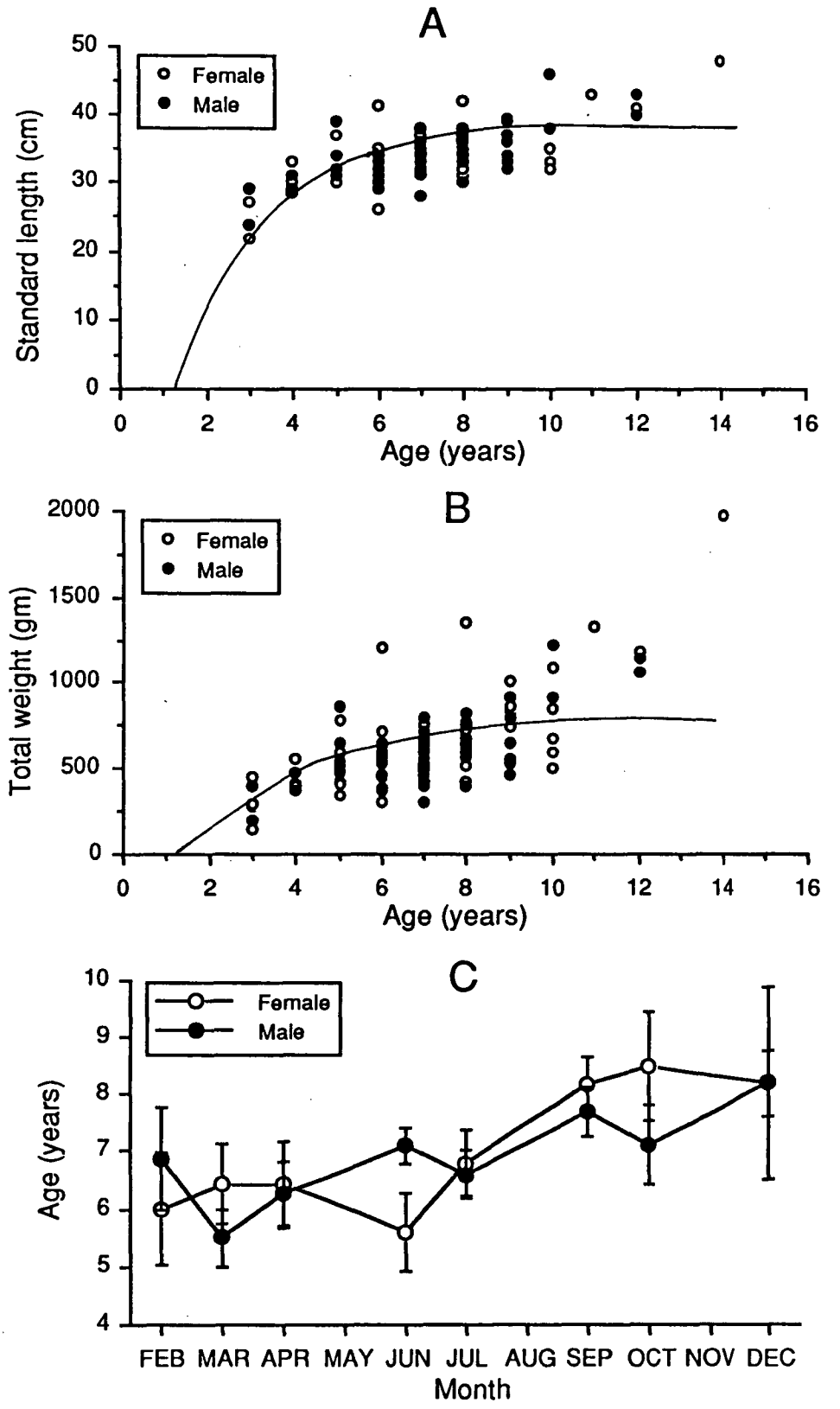

Figure 3.5 Von Bertalanffy growth curves by length (A) and weight (B) for cod collected from Variety Bay and seasonal variation in age of cod collected from Variety Bay (C).

3.3.1 Plasma and endolymph metabolites

There are numerous cycles and interactions evident in the levels of the constituents measured in blood plasma, endolymph and the otoliths of the cod and, in many cases, these appear to be related to season. The results of two-way ANOVA for each variable are presented in Table 3.3, where the sources of variation are month and sex as well as the interaction between these two independent sources. Each variable is discussed in greater detail below.

A gradual increase in total plasma protein from February to peak levels in June coincided with the June peak in condition factor in both males and females (Fig. 3.6). However, male plasma protein decreased to the levels measured in February, while the female plasma protein remained stable from June to October. Both sexes showed the highest level of plasma protein, in December. Levels of total plasma proteins in males and females ranged from 21.0 to 61.7 g l^{-1} and 18.6 to 54.6 g l^{-1}, respectively.

Total endolymph protein for both sexes ranged from 0.5 to 8.4 g l^{-1}, well below the levels measured in the plasma but, followed, in part, the same seasonal pattern as total plasma protein (Fig. 3.7). Endolymph protein levels were at their lowest in February and March and, like plasma proteins, began to increase in April. However, the peak in endolymph protein was not reached until July in the males and September in the females. These peaks in endolymph protein may be related to the development of the gonads as indicated by the gonadosomatic index (Fig. 3.4).

There were no significant seasonal or sex related variations in plasma glucose based on 2-way ANOVA and the interaction between these two sources of variation was not significant (Fig. 3.8). However, there were significant seasonal variations in glucose measured in the endolymph ($F=6.42$, $p<0.0001$). Both males and females showed an initial gradual increase in the level of endolymph glucose during March and April (Fig. 3.9). This gradual increase continued through September in the males but, in the females, there was a very sharp increase from July to September with peak levels being reached in September, coincident with the peak in gonadosomatic index. Endolymph glucose is both coincident and highly correlated with the gonadosomatic index (all fish, $r^2=0.33$, $n=115$, $p<0.0001$; females only, $r^2=0.59$, $n=54$, $p<0.0001$) (Fig. 3.10).

Plasma glucose levels, were more than 6 times the level measured in the endolymph, although the two variables were significantly correlated (all fish, $r^2=0.06$, $n=115$, $p<0.05$; males only, $r^2=0.21$, $n=61$, $p<0.0001$). Despite the large

Table 3.3 Results of two-way analysis of variance comparing *Pseudophycis barbatus* blood plasma and endolymph data by month and sex.

Plasma protein ($g\ l^{-1}$)

Source	df	Sum of squares	Mean squares	F	P
Analysis of variance					
Months	7	2221.140	317.305	7.083	<0.0001
Sex	1	0.005	0.005	0.000	1.0000
Months x Sex	7	371.709	53.101	1.185	0.3179
Error	99	4435.100	44.799		

Endolymph protein ($g\ l^{-1}$)

Source	df	Sum of squares	Mean squares	F	P
Analysis of variance					
Months	7	211.747	30.250	21.429	<0.0001
Sex	1	0.245	0.245	0.173	1.0000
Months x Sex	7	10.133	1.448	1.025	0.4186
Error	99	139.748	1.412		

Plasma calcium ($mM\ l^{-1}$)

Source	df	Sum of squares	Mean squares	F	P
Analysis of variance					
Months	7	12.129	1.733	5.976	<0.0001
Sex	1	1.296	1.296	4.469	0.0350
Months x Sex	7	0.643	0.092	0.317	0.9441
Error	99	28.706	0.290		

Endolymph calcium ($mM\ l^{-1}$)

Source	df	Sum of squares	Mean squares	F	P
Analysis of variance					
Months	7	2.772	0.396	4.564	0.0002
Sex	1	0.000	0.000	0.001	1.0000
Months x Sex	7	0.977	0.140	1.609	0.1408
Error	99	8.591	0.087		

Plasma strontium ($\mu g\ l^{-1}$)

Source	df	Sum of squares	Mean squares	F	P
Analysis of variance					
Months	7	8675594.000	1239370.000	22.370	<0.0001
Sex	1	44422.340	44422.340	0.802	1.0000
Months x Sex	7	359467.000	51352.420	0.927	0.5099
Error	99	5485030.000	55404.310		

Endolymph strontium ($\mu g\ l^{-1}$)

Source	df	Sum of squares	Mean squares	F	P
Analysis of variance					
Months	7	1613860.000	230551.100	17.441	<0.0001
Sex	1	5312.963	5312.963	0.402	1.0000
Months x Sex	7	201479.100	28782.730	2.177	0.0423
Error	99	1308660.000	13218.800		

Plasma sodium ($mM\ l^{-1}$)

Source	df	Sum of squares	Mean squares	F	P
Analysis of variance					
Months	7	2707.481	386.783	8.432	<0.0001
Sex	1	80.117	80.117	1.747	1.0000
Months x Sex	7	201.302	28.757	0.627	0.7342
Error	99	4540.960	45.868		

Endolmyph sodium ($mM\ l^{-1}$)

Source	df	Sum of squares	Mean squares	F	P
Analysis of variance					
Months	7	1360.380	194.339	4.203	0.0005
Sex	1	2.790	2.790	0.060	1.0000
Months x Sex	7	210.454	30.065	0.650	0.7149
Error	99	4577.090	46.233		

Plasma potassium ($mM\ l^{-1}$)

Source	df	Sum of squares	Mean squares	F	P
Analysis of variance					
Months	7	139.112	19.873	9.137	<0.0001
Sex	1	0.515	0.515	0.237	1.0000
Months x Sex	7	35.327	5.047	2.320	0.0310
Error	99	215.325	2.175		

Endolymph postassium ($mM\ l^{-1}$)

Source	df	Sum of squares	Mean squares	F	P
Analysis of variance					
Months	7	523.373	74.767	2.411	0.0254
Sex	1	54.005	54.005	1.741	1.0000
Months x Sex	7	169.337	24.191	0.780	0.6070
Error	99	3070.540	31.016		

Plasma triglycerides ($mM\ l^{-1}$)

Source	df	Sum of squares	Mean squares	F	P
Analysis of variance					
Months	7	158.683	22.669	6.606	<0.0001
Sex	1	5.155	5.155	1.502	1.0000
Months x Sex	7	203.097	29.014	8.454	<0.0001
Error	99	339.751	3.432		

Endolymph triglycerides ($mM\ l^{-1}$)

Source	df	Sum of squares	Mean squares	F	P
Analysis of variance					
Months	7	4.138	0.591	4.192	0.0005
Sex	1	0.596	0.596	4.227	0.0401
Months x Sex	7	3.145	0.449	3.185	0.0045
Error	99	13.962	0.141		

Plasma glucose ($mM\ l^{-1}$)

Source	df	Sum of squares	Mean squares	F	P
Analysis of variance					
Months	7	36.578	5.225	1.623	0.1370
Sex	1	7.257	7.257	2.253	1.0000
Months x Sex	7	20.999	3.000	0.932	0.5134
Error	99	318.818	3.220		

Endolymph glucose ($mM\ l^{-1}$)

Source	df	Sum of squares	Mean squares	F	P
Analysis of variance					
Months	7	5.572	0.796	6.422	<0.0001
Sex	1	0.262	0.262	2.116	1.0000
Months x Sex	7	1.261	0.180	1.453	0.1922
Error	99	12.270	0.124		

Plasma phosphate ($mM\ l^{-1}$)

Source	df	Sum of squares	Mean squares	F	P
Analysis of variance					
Months	7	14.085	2.012	2.351	0.0289
Sex	1	0.021	0.021	0.024	1.0000
Months x Sex	7	23.350	3.336	3.897	0.0009
Error	99	84.740	0.856		

Endolymph phosphate (mM l^{-1})

Source	df	Sum of squares	Mean squares	F	P
Analysis of variance					
Months	7	17.426	2.499	5.939	<0.0001
Sex	1	1.330	1.330	3.174	0.0742
Months x Sex	7	6.814	0.973	2.322	0.0308
Error	99	41.495	0.419		

Otolith Sr/Ca

Source	df	Sum of squares	Mean squares	F	P
Analysis of variance					
Months	7	920.881	131.554	6.218	<0.0001
Sex	1	0.767	0.767	0.036	1.0000
Months x Sex	7	96.195	13.742	0.649	0.7156
Error	99	2094.713	21.159		

Otolith Na/Ca

Source	df	Sum of squares	Mean squares	F	P
Analysis of variance					
Months	7	12803.510	1829.073	14.753	<0.0001
Sex	1	1491.044	1491.044	12.026	<0.0001
Months x Sex	7	1402.070	200.296	1.616	0.1390
Error	99	12274.020	123.980		

Otolith K/Ca

Source	df	Sum of squares	Mean squares	F	P
Analysis of variance					
Months	7	79.134	11.305	2.418	0.0249
Sex	1	10.570	10.570	2.261	1.0000
Months x Sex	7	31.164	4.452	0.952	0.5290
Error	99	462.772	4.674		

Otolith S/Ca

Source	df	Sum of squares	Mean squares	F	P
Analysis of variance					
Months	7	101.656	14.522	8.356	<0.0001
Sex	1	4.890	4.890	2.813	1.0000
Months x Sex	7	15.147	2.164	1.245	0.2853
Error	99	172.061	1.738		

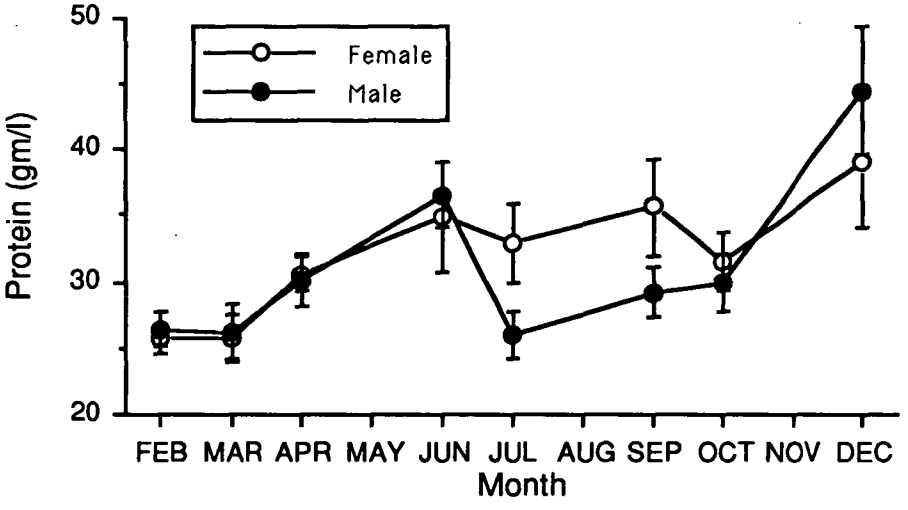

Figure 3.6 Seasonal variation in the total plasma protein (gm/l) in cod collected from Variety Bay.

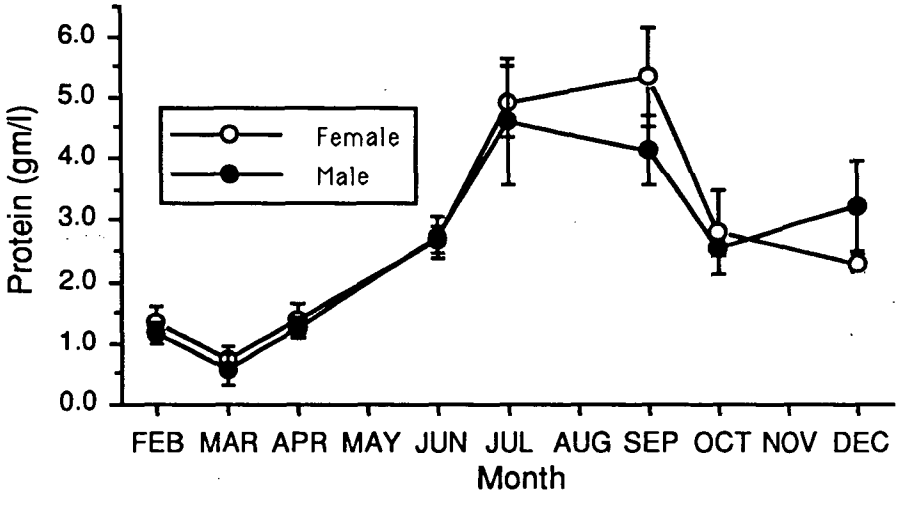

Figure 3.7 Seasonal variation in the total endolymph protein (gm/l) in cod collected from Variety Bay.

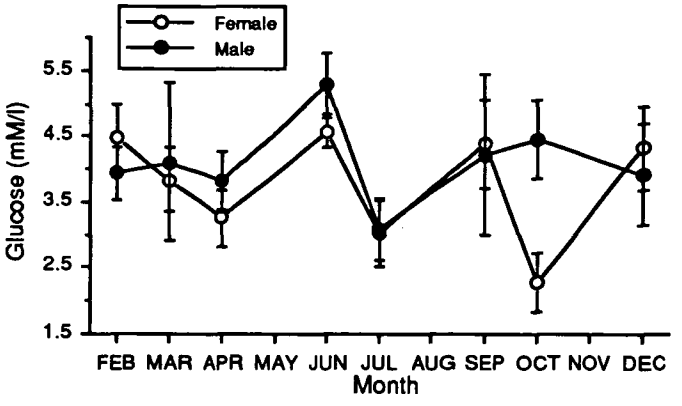

Figure 3.8 Seasonal variation in plasma glucose (mM/l) in cod collected from Variety Bay. Error bars are ±1 S.E.

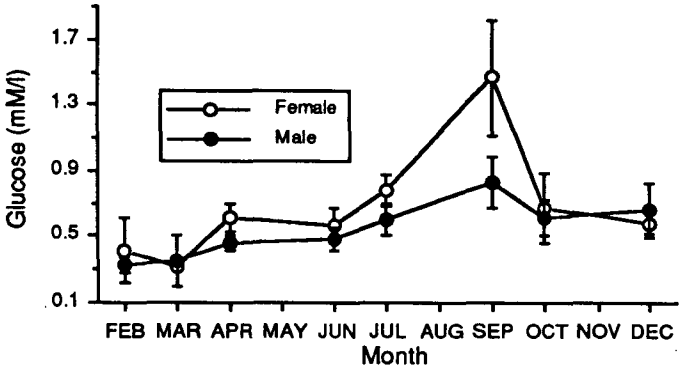

Figure 3.9 Seasonal variation in endolymph glucose (mM/l) in cod collected from Variety Bay. Error bars are ±1 S.E.

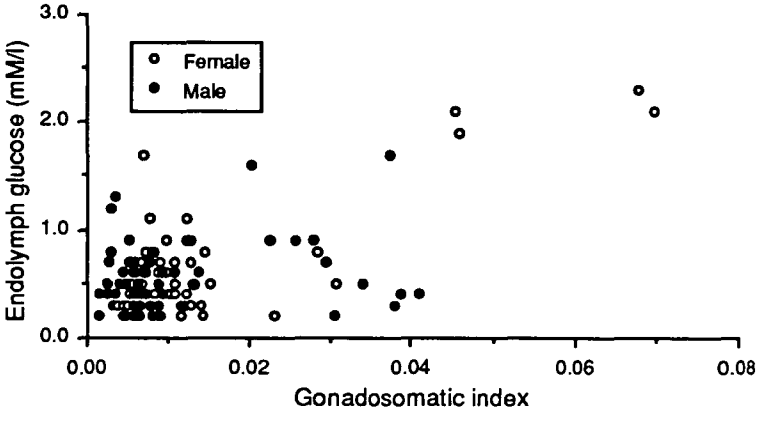

Figure 3.10 Plot of endolymph glucose against gonadosomatic index in cod. Males, N=61; Females, N=54.

differences in the mean endolymph glucose measured in September in males (0.83 mM l^{-1}) and females (1.47 mM l^{-1}) there was no significant difference detected among the sexes ($F=2.12$, $p=1.00$) or based on the interaction of month and sex ($F=1.45$, $p=0.19$). This was probably due to the wide range of values obtained for males (0.3 to 1.7 mM l^{-1}) and females (0.2 to 2.3 mM l^{-1}) during that month. Nevertheless, there was some evidence for a greater seasonal increase in glucose in females than in males.

Plasma phosphate levels varied significantly over the year ($F=2.35$, $p=0.03$), but not by sex (Fig. 3.11). However, there was a significant interaction between month and sex ($F=3.90$, $p=0.0009$) indicating sex related differences in plasma phosphate over the year. Both males and females showed minor variations in plasma phosphate from February to July, but in September there was a sharp increase in the phosphate measured in the females. This rise was matched in the males by a more gradual increase in phosphate which peaks in December. However, during the period of increasing phosphate in the males, the females showed a decline to the lowest levels of the year in December.

Seasonal variations in endolymph phosphate (Fig. 3.12), most notably in the females, were very similar to the variations measured in endolymph glucose with peak values being reached in September. Males showed a gradual increase in endolymph phosphate from March to July, like glucose, but peak levels were reached one month earlier. Endolymph phosphate and glucose were very highly correlated for both sexes ($r^2=0.73$, $n=115$, $p<0.0001$), and particularly in the females ($r^2=0.88$, $n=54$, $p<0.0001$) (Fig. 3.13). Endolymph phosphate was also highly correlated with total protein in the endolymph ($r^2=0.61$, $n=115$, $p<0.0001$) (Fig. 3.14). Unlike endolymph glucose, there were significant variations among months ($F=5.94$, $p<0.0001$) as well as a significant interaction between months and sex ($F=2.32$, $p=0.03$). The variation between sexes was nearly significant ($F=3.17$, $p=0.07$). Peak female plasma and endolymph phosphate levels are both reached in September.

Seasonal variations in plasma triglyceride levels were highly significant ($F=6.61$, $p<0.0001$) and followed a similar pattern to phosphate (Fig. 3.15). In females there was a gradual increase in triglycerides until the peak in October and a subsequent sharp decline to the lowest values of the year in December. The similarity of these two patterns was accentuated by the correlation between female plasma phosphate and triglyceride ($r^2=0.34$, $n=54$, $p<0.01$). There was a strong interaction between month

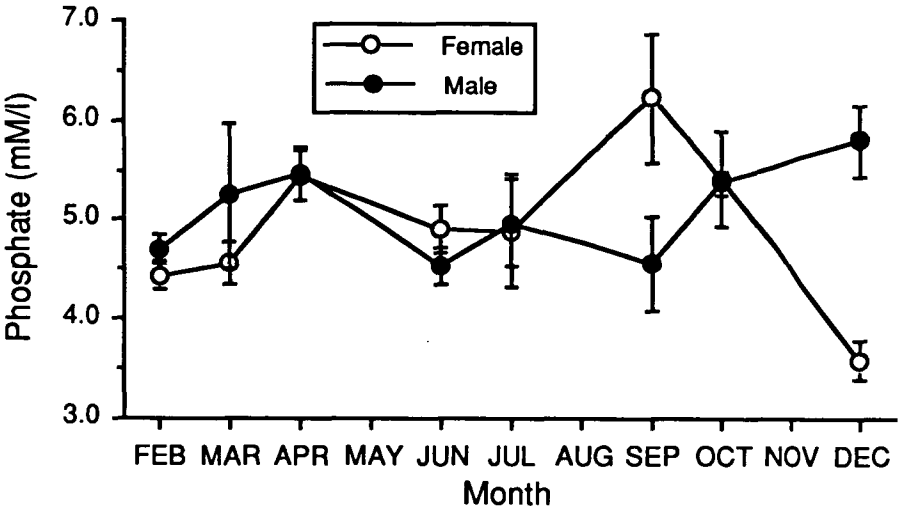

Figure 3.11 Seasonal variation in plasma phosphate (mM/l) in cod collected from Variety Bay. Error bars are ±1 S.E.

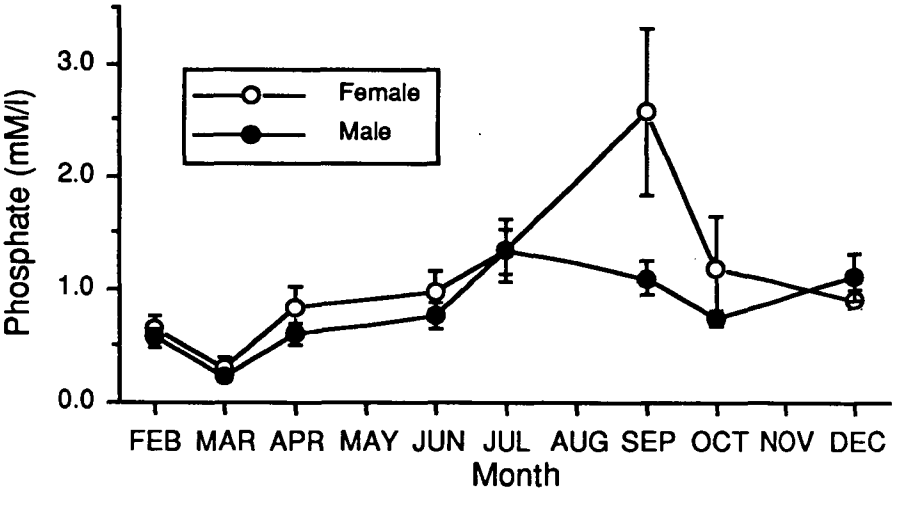

Figure 3.12 Seasonal variation in endolymph phosphate (mM/l) in cod collected from Variety Bay. Error bars are ±1 S.E.

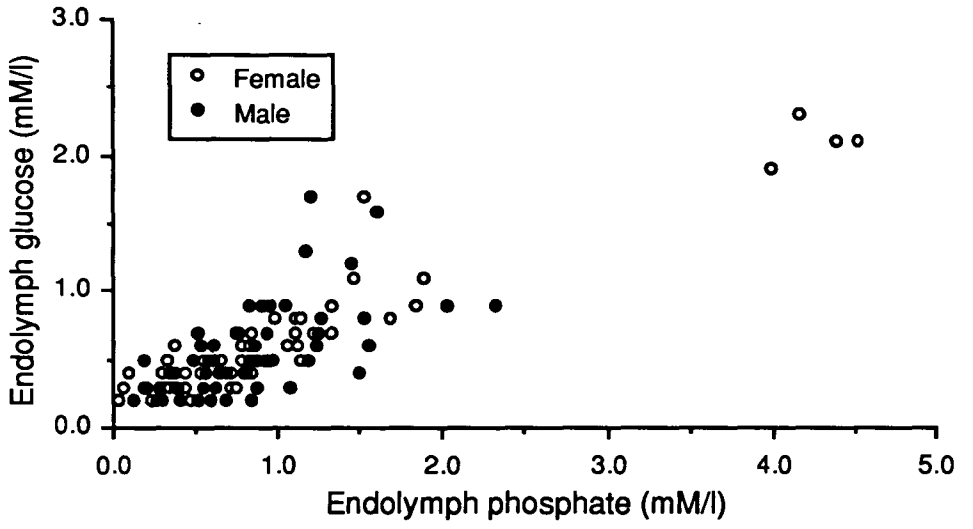

Figure 3.13 Plot of endolymph glucose against endolymph phosphate in cod. Males, N=61; Females, N=54.

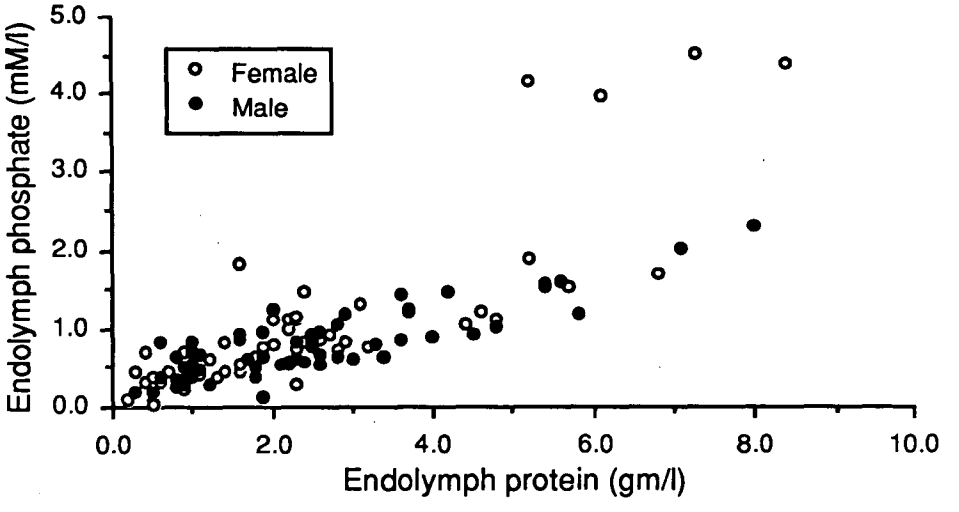

Figure 3.14 Plot of endolymph phosphate against endolymph protein in cod. Males, N=61; Females, N=54.

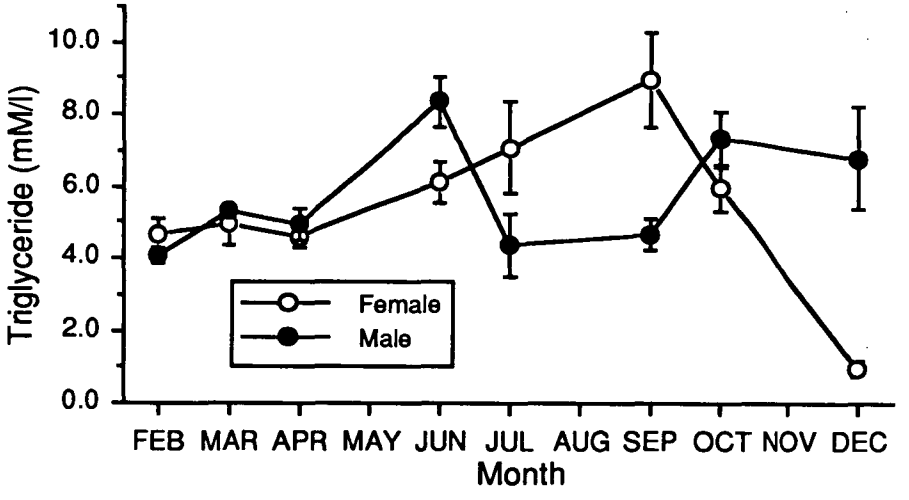

Figure 3.15 Seasonal variation in plasma triglycerides (mM/l) in cod collected from Variety Bay. Error bars are ±1 S.E.

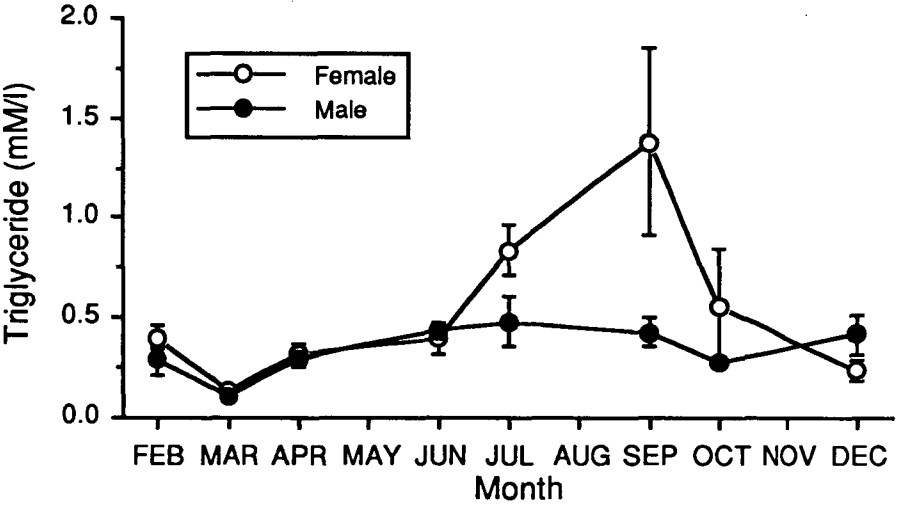

Figure 3.16 Seasonal variation in endolymph triglycerides in cod collected from Variety Bay. Error bars are ±1 S.E.

and sex ($F=8.45$, $p<0.0001$), the male pattern of variation being markedly different from that shown by the females. In males, triglycerides were constant from March to April, increased slightly in June, dropped to previous levels and increased again in October and December.

The seasonal pattern seen in endolymph glucose and phosphate was again apparent in endolymph triglyceride (Fig. 3.16). Seasonal ($F=4.19$, $p=0.0005$), sex-related ($F=4.23$, $p=0.04$) and interaction ($F=3.19$, $p=0.0045$) variations are all significant for the endolymph triglyceride data. Females showed a distinct peak in triglycerides in September and male levels were fairly constant with some evidence of a peak occurring in July. The endolymph triglyceride data were strongly correlated both with the glucose ($r^2=0.61$, $n=115$, $p<0.0001$) and the phosphate ($r^2=0.80$, $n=115$, $p<0.0001$) data and, again, these correlations were strongest when the female data were considered separately ($r^2=0.78$, $n=54$, $p<0.0001$ for glucose and $r^2=0.87$, $n=54$, $p<0.0001$ for phosphate) (Fig. 3.17 and 3.18).

3.3.2 Plasma and endolymph ions

There were significant variations in plasma calcium by month ($F=5.98$, $p<0.0001$) and by sex ($F=4.47$, $p=0.035$), but there was no significant interaction between these two variables ($F=0.32$, $p=0.94$). The seasonal patterns shown by the two sexes were similar with a gradual decrease in plasma calcium from February to June, followed by a sharp increase from June to peak calcium levels in September/October (Fig 3.19). Calcium levels declined in December to levels that were similar to those measured in February. Mean plasma calcium in females was 1.91 ± 0.55 mM l^{-1} and 1.70 ± 0.65 mM l^{-1} in males.

Endolymph calcium levels were significantly lower than plasma calcium levels (paired t-test, $t=8.28$, $n=115$, $p<0.0001$) and showed different, but significant, seasonal variation ($F=4.56$, $p=0.0002$) (Fig. 3.20). The most notable point of the seasonal cycle in endolymph calcium was the peak in the females in September, coincident with the September peak in the gonadosomatic index. This peak was followed by a relatively sharp decline in endolymph calcium in both males and females. Variations between males and females and the interaction between month and sex were not significant.

Plasma sodium levels varied significantly through the year ($F=8.43$, $p<0.0001$), and showed evidence for two cycles during the year with peaks in June and

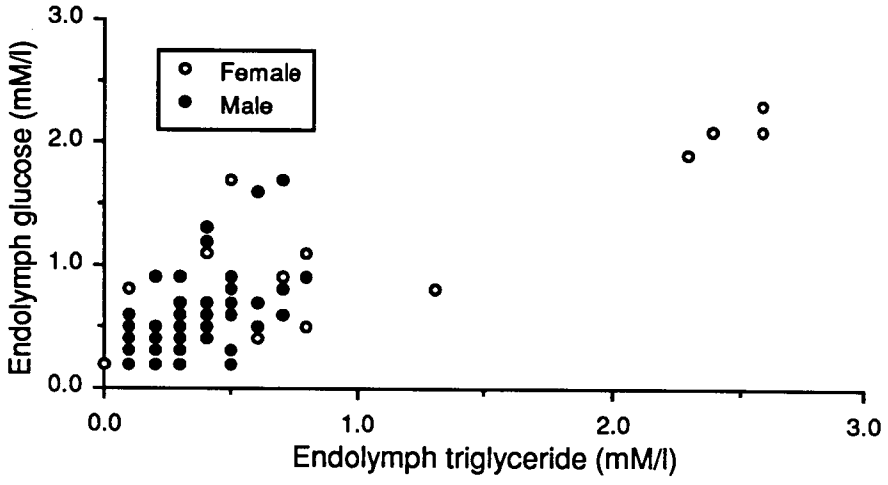

Figure 3.17 Plot of endolymph glucose against endolymph triglyceride in cod. Males, N=61; Females, N=54.

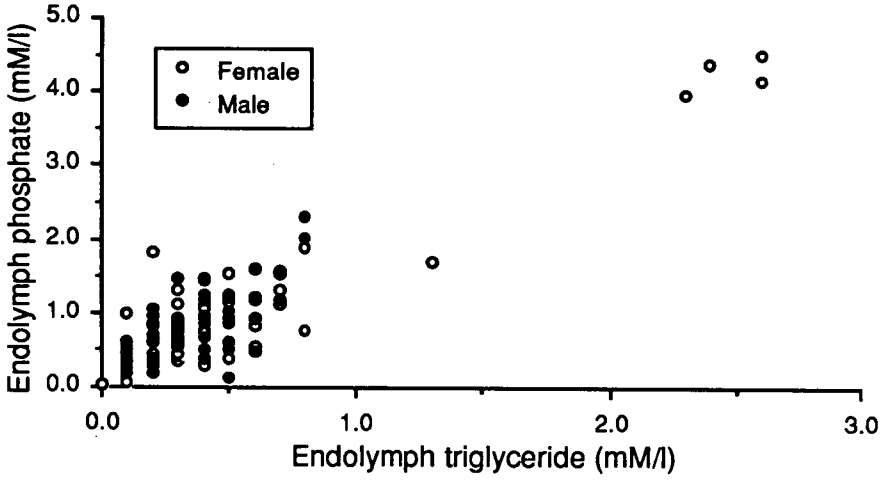

Figure 3.18 Plot of endolymph phosphate against endolymph triglyceride in cod. Males, N=61; Females, N=54.

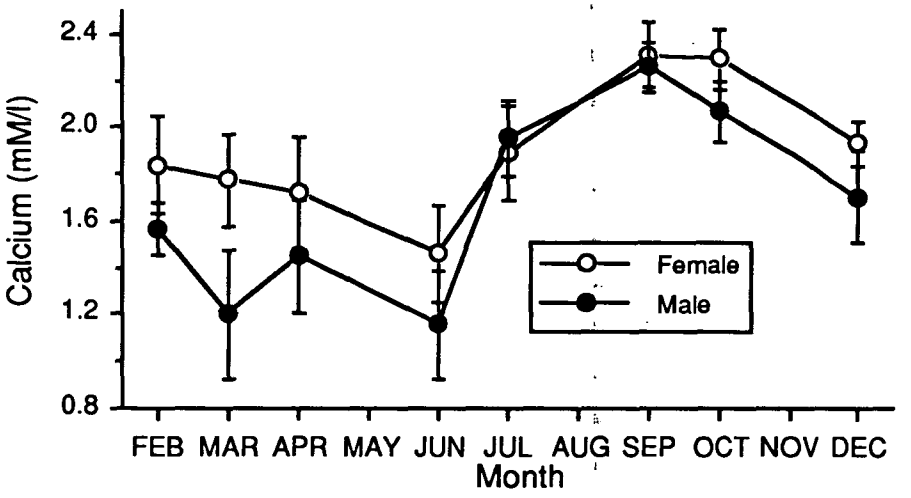

Figure 3.19 Seasonal variation in plasma calcium (mM/l) in cod collected from Variety Bay. Error bars are 1 S.E.

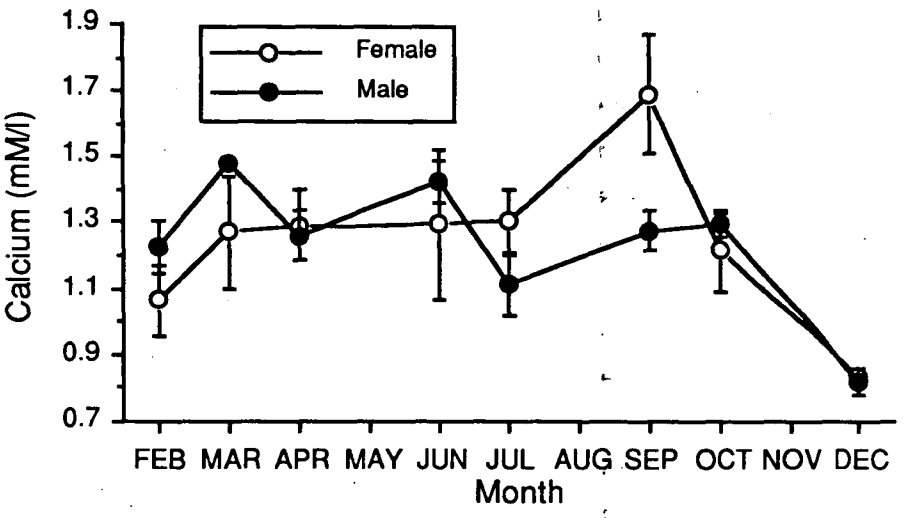

Figure 3.20 Seasonal variation in endolymph calcium (mM/l) in cod collected from Variety Bay. Error bars are 1 S.E.

September and troughs in March and December (Fig. 3.21). The seasonal cycles were very similar for both sexes as were the mean plasma sodium levels for males (185±8 mM l^{-1}) and females (183±8 mM l^{-1}). The drop in plasma sodium in July was not due to analytical error as the endolymph samples from July were analysed at the same time and on the same instrument, yet they showed no decrease in sodium at this time. The significant seasonal variation of sodium in the endolymph ($F=4.20$, $p=0.0005$) was very different from that measured in the plasma although males and females again showed similar patterns of variation (Fig. 3.22). Mean levels were roughly 60% of that measured in the plasma.

Plasma and endolymph potassium varied significantly over the year ($F=9.14$, $p<0.0001$ for plasma and, $F=2.41$, $p=0.025$ for endolymph) and, both showed the same general seasonal cycle (Figs. 3.23 and 3.24). Potassium levels reached their maximum in March and September and minimum in June and December and these cycles were similar for both sexes. Mean potassium levels were 7.10±1.83 mM l^{-1} and 67.15±5.76 in the plasma and the endolymph, respectively. There was a significant correlation between endolymph Na and endolymph K ($r^2=0.36$, $n=115$, $p<0.001$) (Fig. 3.25), but there was no such relationship in the blood plasma. This is probably due to the relative importance of K^+ and Na^+ in maintaining ionic potentials in the sacculus as opposed to the blood.

Plasma strontium levels showed significant variation through the year ($F=22.37$, $p<0.0001$), with little difference between the levels measured in males and females (Fig. 3.26). The data were somewhat unusual in that there was a large discrepancy between the February and December samples with mean strontium levels of 8.33±1.42 and 18.05±3.65 μM l^{-1}. For the present it must be assumed that strontium levels might drop relatively rapidly in December and January. Plots of the ratio of plasma strontium to plasma calcium over the year (Fig. 3.27) showed even more pronounced cycles than when the elements were considered alone. This is due to the fact that the relative increases and decreases in plasma strontium and calcium were opposing. The plot of plasma Sr/Ca against month showed evidence for two cycles per year.

Endolymph strontium shows significant seasonal variability ($F=17.44$, $p<0.0001$) as well as a significant interaction between month and sex ($F=2.12$, $p<0.04$). In the females, strontium levels were similar in February and March, but increased almost monotonically from March to September (Fig. 3.28). The mean

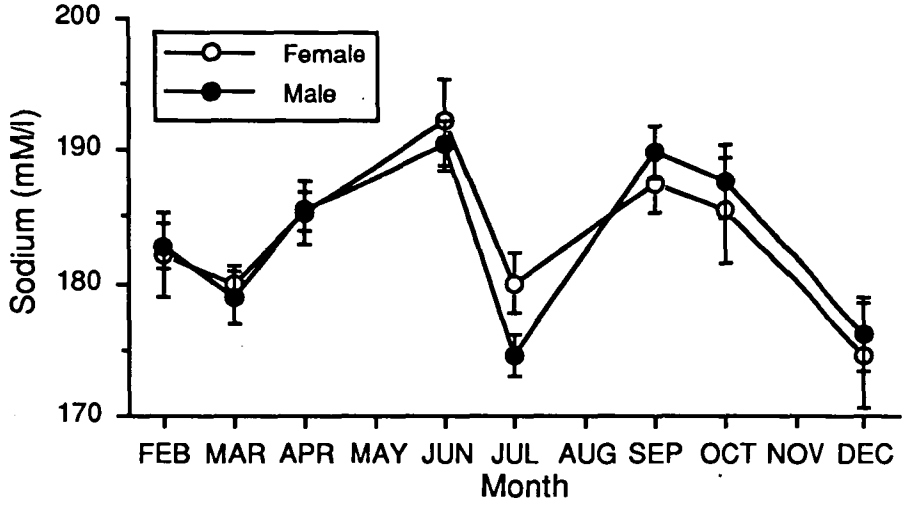

Figure 3.21 Seasonal variation in plasma sodium (mM/l) in cod collected from Variety Bay. Error bars are ±1 S.E.

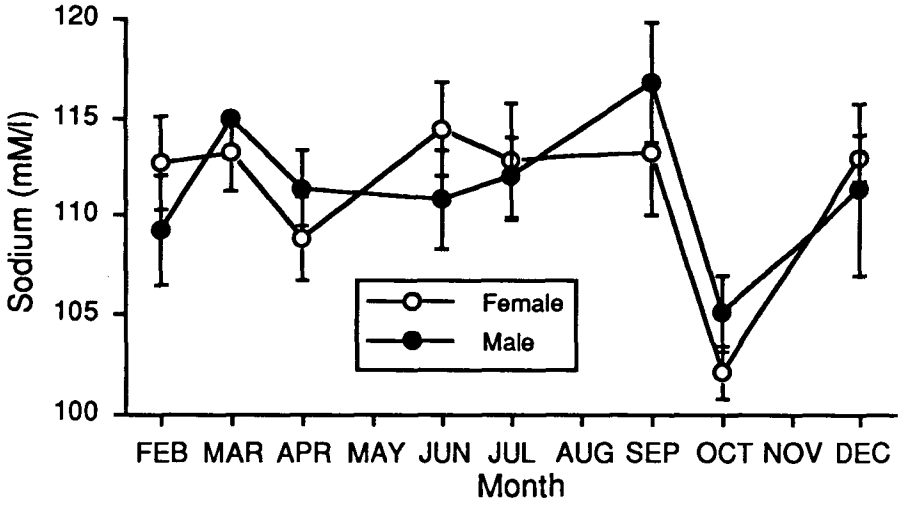

Figure 3.22 Seasonal variation in endolymph sodium (mM/l) in cod collected from Variety Bay. Error bars are ±1 S.E.

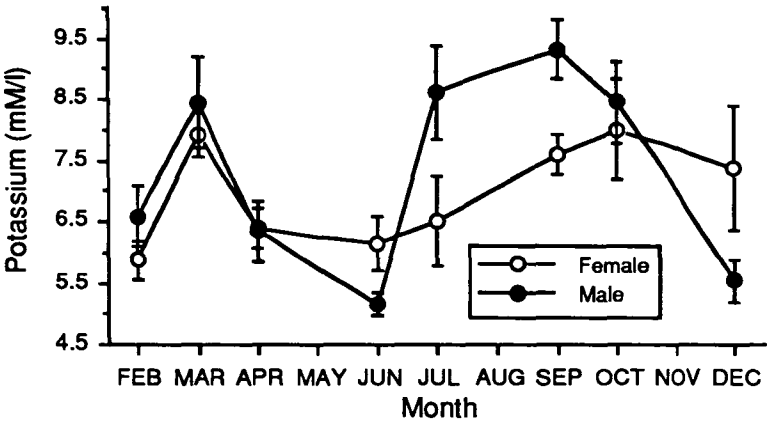

Figure 3.23 Seasonal variation in plasma potassium (mM/l) in cod collected from Variety Bay. Error bars are ±1 S.E.

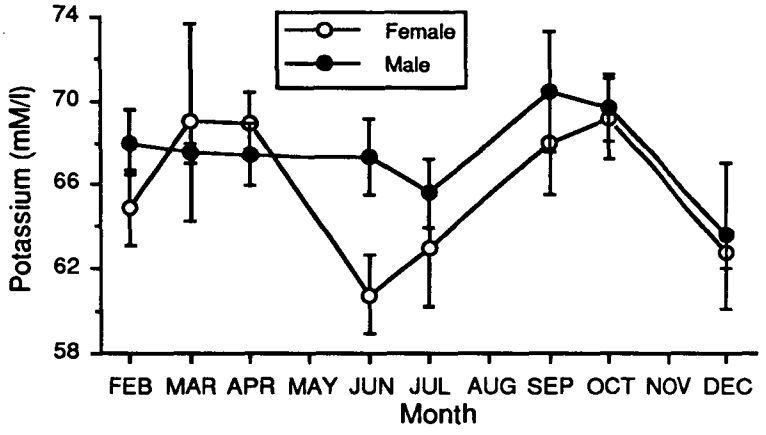

Figure 3.24 Seasonal varition in endolymph potassium (mM/l) in cod collected from Variety Bay. Error bars are ±1 S.E.

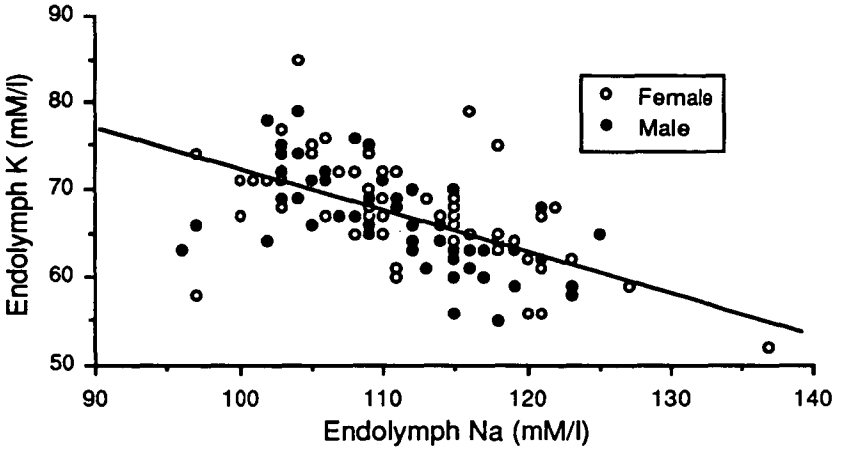

Figure 3.25 Plot of endolymph K (mM/l) against endolymph Na (mM/l) in cod. The equation describing the line fit by linear regression is $y = -0.47x + 119.37$, $r=0.60$, $N=115$.

Figure 3.26 Seasonal variation in plasma strontium (μM/l) in cod collected from Variety Bay. Error bars are ±1 S.E.

Figure 3.27 Seasonal variation in plasma Sr/Ca ratio in cod collected from Variety Bay. Error bars are ±1 S.E.

Figure 3.28 Seasonal variation in endolymph strontium (μm/l) in cod collected from Variety Bay. Error bars are ±1 S.E.

Figure 3.29 Seasonal variation in endolymph Sr/Ca ratio in cod collected from Variety Bay. Error bars are ±1 S.E.

Fig. 3.26

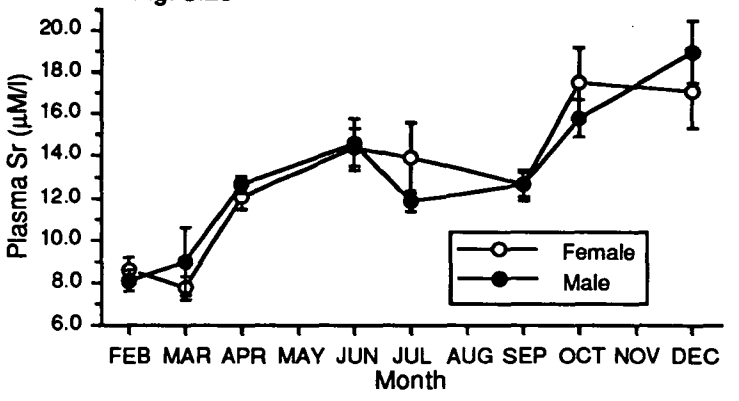

Fig. 3.27

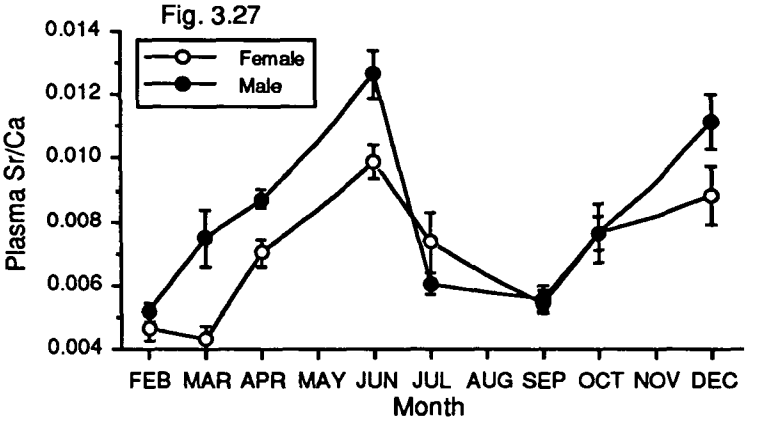

Fig. 3.28

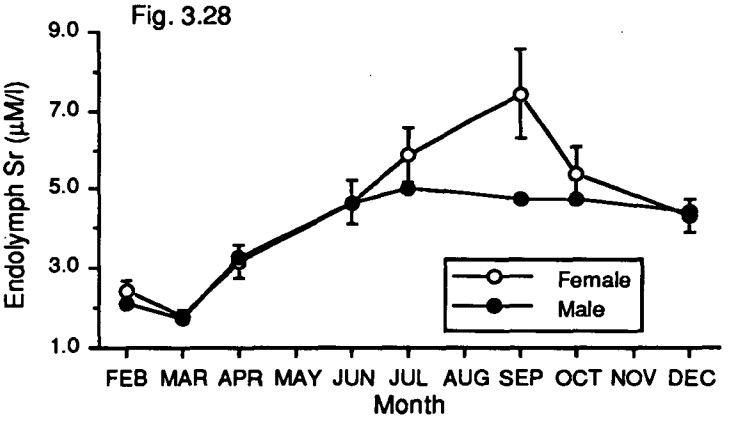

Fig. 3.29

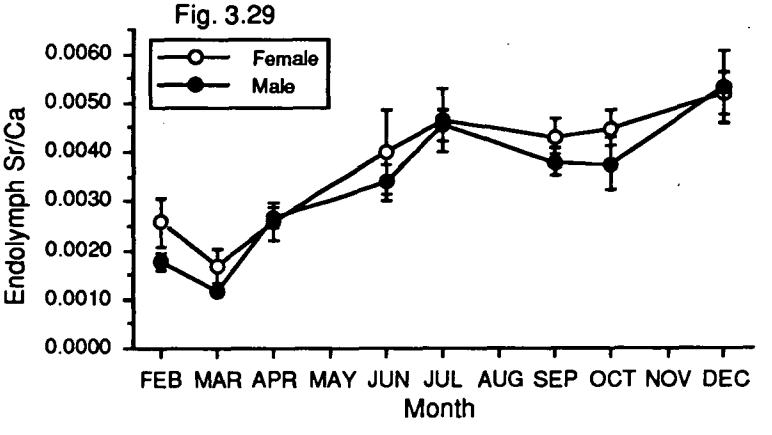

level at the peak in September was 7.43±2.80 μM l^{-1}, more than 4 times the mean level of 1.79±0.45 μM l^{-1} measured in March. In males, the pattern of variation from February to June was almost identical to that of the females. However, unlike the females, there was virtually no change in endolymph strontium from June to December. Quantities of strontium in the male and female endolymph were almost identical in December.

Plots of the variation in endolymph Sr/Ca ratio versus month (Fig. 3.29) showed seasonal variation that was very similar to that of plasma strontium and, there was also a strong correlation between endolymph Sr/Ca and plasma strontium (r^2=0.36, n=115, p<0.0001) (Fig. 3.30). This correlation was more significant than the correlation between endolymph Sr and plasma Sr (r^2=0.26, n=115, p<0.0001) (Fig. 3.31a) due to the fact that the four female fish with very high endolymph strontium levels (>9.1 μM l^{-1}), seemingly independent of their plasma strontium level, also had relatively high plasma calcium (>2.2 mM l^{-1}). Therefore, it is evident that, although the endolymph strontium level in cod is closely related to plasma strontium, other factors must clearly play a part in determining the quantity of strontium in the endolymph. A plot of endolymph Sr/Ca versus plasma Sr/Ca (Fig. 3.31b) shows that the plasma Sr/Ca ratio was relatively constant among cod sampled over the year, with the exception of several male cod that had relatively low plasma calcium levels.

Endolymph strontium was strongly correlated with several other variables, particularly those indicative of the seasonal development of the female gonads before spawning. Correlations with gonad weight (all fish, r^2=0.29, n=115, p<0.0001; females only, r^2=0.39, n=54, p<0.001) and gonadosomatic index (all fish, r^2=0.35, n=115, p<0.0001; females only, r^2=0.56, n=54, p<0.0001) (Fig. 3.32) were most notable. It is important to note that, while endolymph strontium was significantly correlated with GSI, there was no such correlation between plasma strontium and GSI (all fish, r^2=0.0003, n=115, p>0.5). There was also a very strong negative correlation between endolymph strontium and temperature (all fish, r^2=0.47, n=115, p<0.001; females only, r^2=0.59, n=54, p<0.001) (Fig. 3.33). However, this relationship may be indirectly linked to the development of the gonads during the winter as will be discussed in a later section. There were also strong correlations between endolymph Sr and endolymph protein (r^2=0.57, n=115, p<0.0001) (Fig. 3.34), endolymph phosphorus (r^2=0.60, n=115, p<0.0001) (Fig. 3.35) and endolymph glucose (r^2=0.42, n=115, p<0.001) (Fig. 3.36).

Figure 3.30 Plot of endolymph Sr/Ca ratio against plasma strontium (μM/l) in cod. Males, N=61; Females, N=54.

Figure 3.31a Plot of endolymph strontium (μM/l) against plasma strontium (μM/l) in cod. Note the 4 female fish with endolymph strontium levels above 9.1 μm/l. Males, N=61; Females, N=54.

Figure 3.31b Plot of endolymph Sr/Ca ratio against plasma Sr/Ca ratio in cod. Males, N=61; Females, N=64.

Fig. 3.30

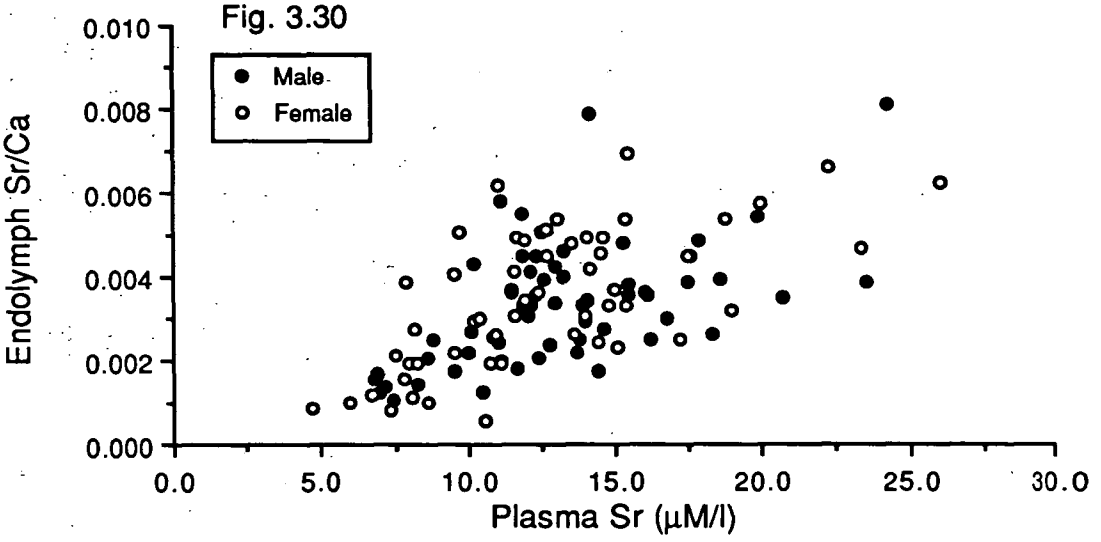

Fig. 3.31a

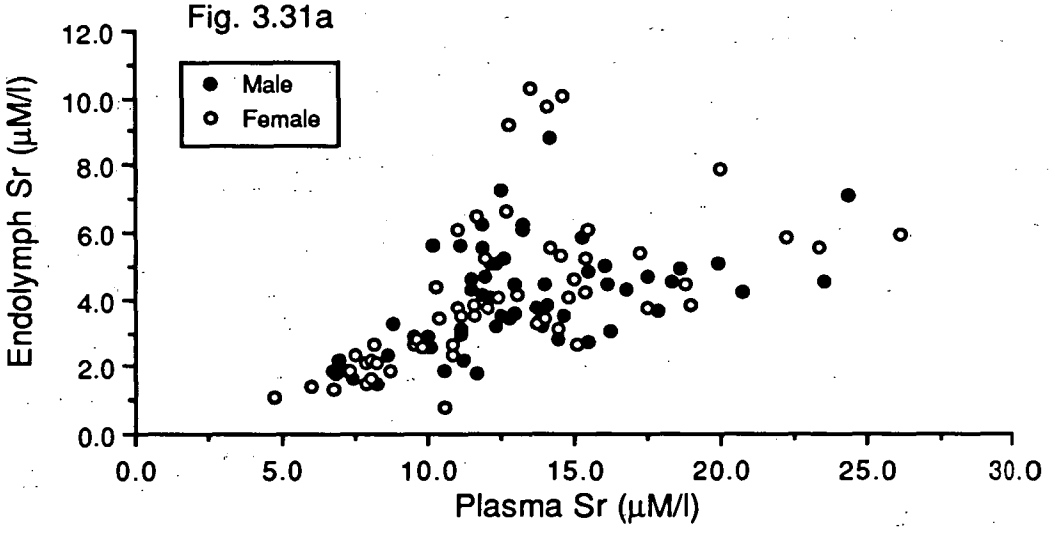

Fig. 3.31b

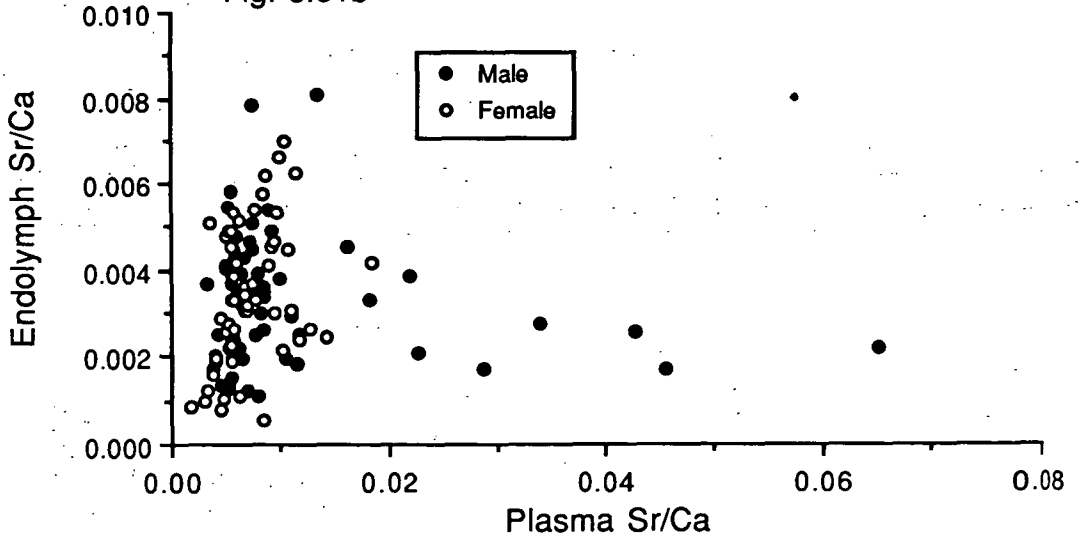

Figure 3.32 Plot of endolymph strontium (μM/l) against gonadosomatic index in cod. Males, N=61; Females, N=54.

Figure 3.33 Plot of endolymph strontium (μM/l) in cod against temperature (°C) at 20 m in Variety Bay. Although these variables were significantly correlated (all fish, r^2=0.47, n=115, p<0.001) the relationship between these variables was not significant on the basis of Model 1 linear regression (F=3.03, df=1,5, p>0.10). The lines based on linear regression, although not significant, are shown in the figure to help clarify the positions of the endolymph Sr data, relative to temperature, attributable to the two sexes.

Figure 3.34 Plot of endolymph strontium (μM/l) against endolymph protein (g/l) in cod. Males, N=61; Females, N=54.

Fig. 3.32

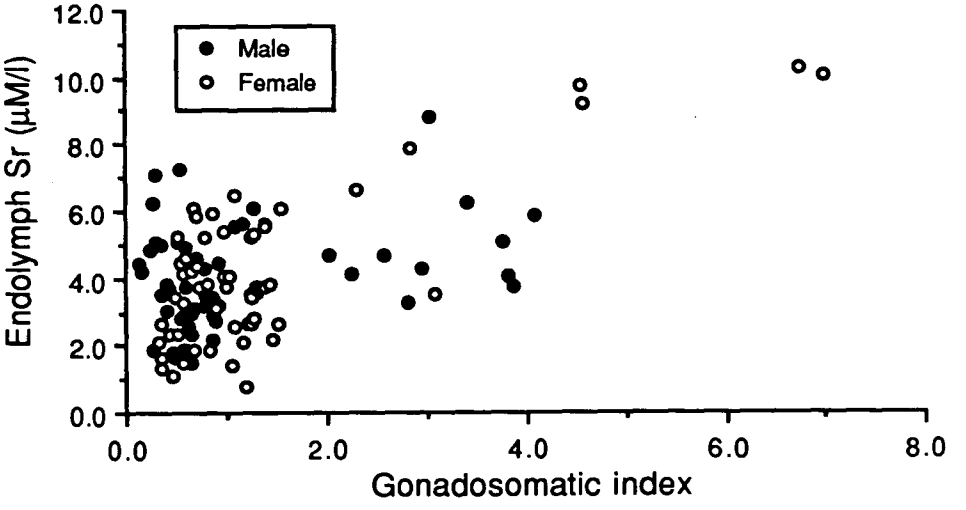

Fig. 3.33

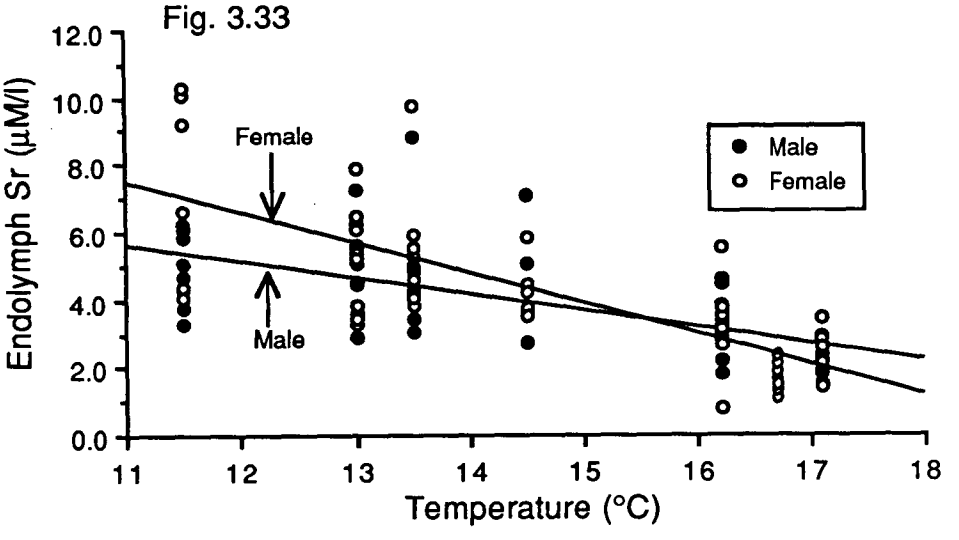

Fig. 3.34

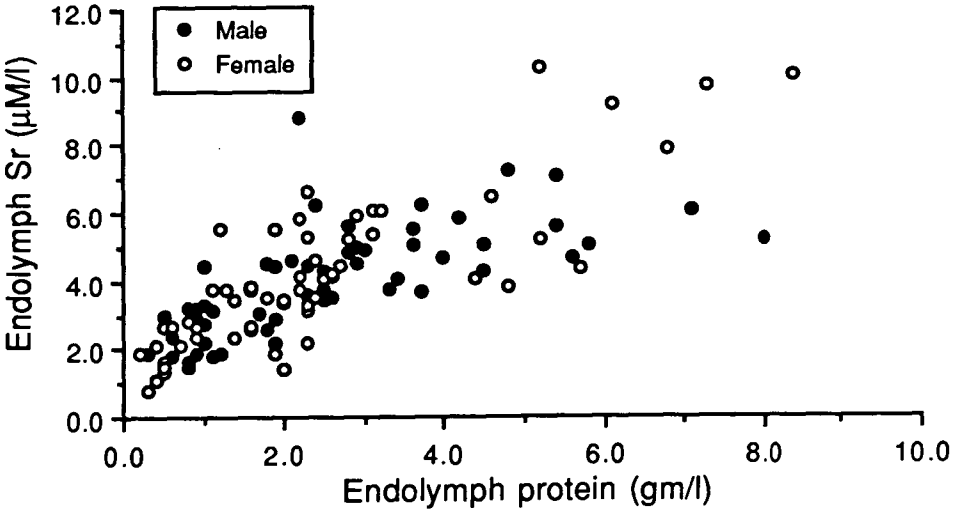

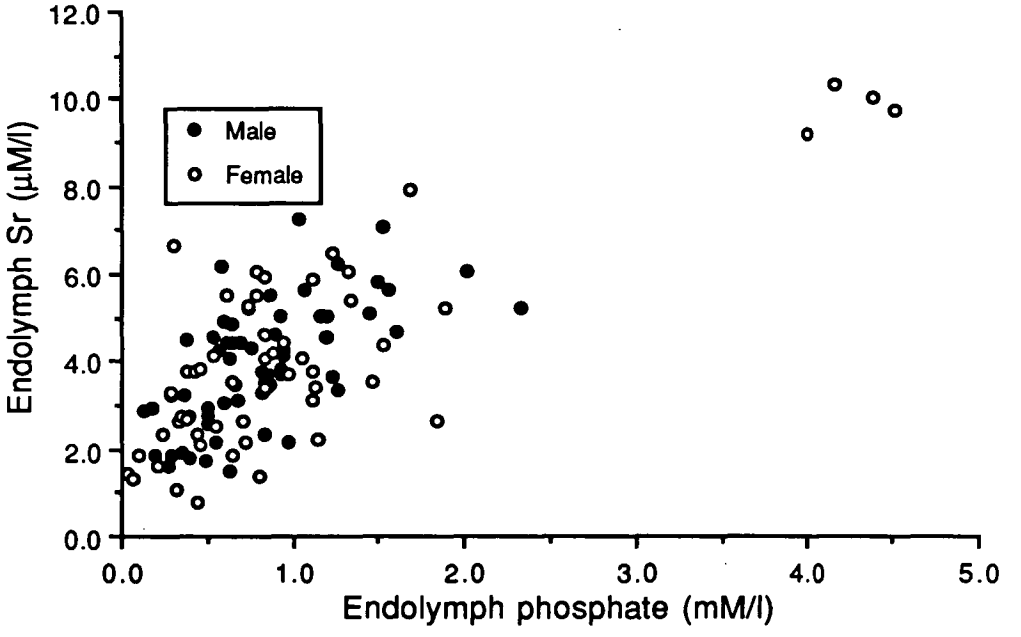

Figure 3.35 Plot of endolymph Sr against endolymph phosphate in cod. Males, N=61; Females, N=54.

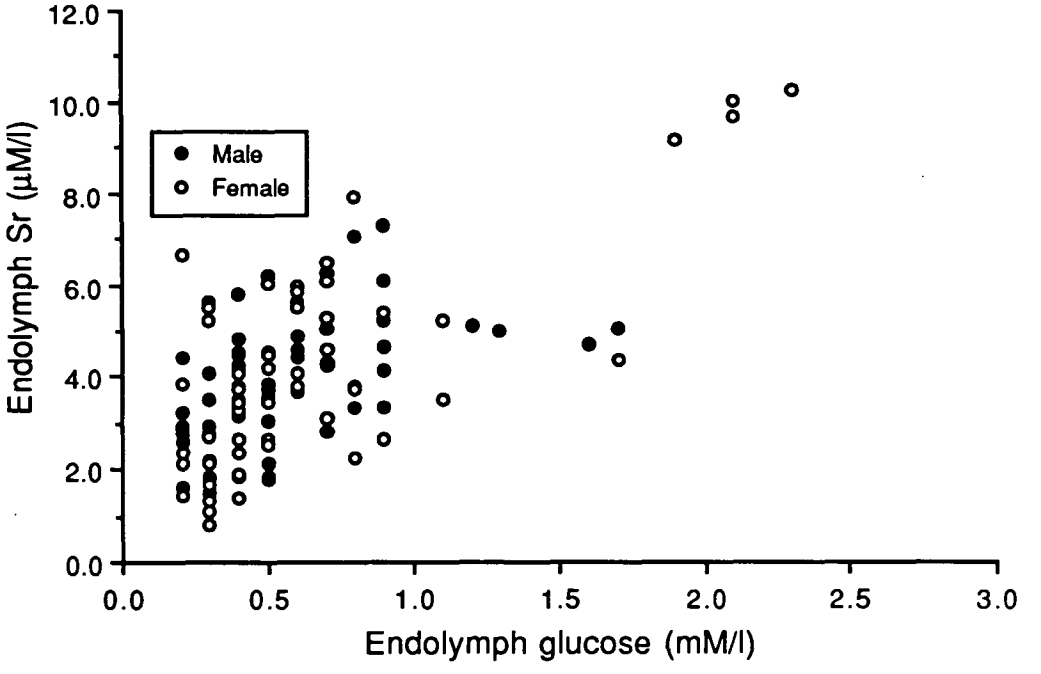

Figure 3.36 Plot of endolymph Sr against endolymph glucose in cod. Males, N=61; Females, N=54.

3.3.3 Otolith composition

Measurements by wavelength dispersive electron microprobe of the composition of the cod otolith material formed previous to capture show that there were significant seasonal variations in otolith Sr/Ca ($F=6.22$, $p<0.0001$), Na/Ca ($F=14.75$, $p<0.0001$), K/Ca ($F=2.42$, $p=0.025$) and S/Ca ($F=8.36$, $p<0.0001$) ratios (Figs. 3.37 to 3.40). Only Na/Ca ratios showed evidence of variability related to sex ($F=12.03$, $p<0.0001$). There was no indication of any significant interaction between month and sex for any of the chemical ratios measured.

Otolith Sr/Ca ratios showed one major cycle over the year with the lowest levels occurring in the summer months. Levels measured during the fall, winter and spring did not appear to differ significantly. The otolith Sr/Ca data were positively correlated with the quantity of Sr measured in the endolymph ($r^2=0.32$, $n=115$, $p<0.0001$) (Fig. 3.41), although the similarities between the seasonal changes exhibited by the two variables were very general with both showing relatively low levels in February and March and increasing to a plateau in the following months.

Variations in otolith Na/Ca, K/Ca and S/Ca were different from those exhibited by the Sr/Ca data. Otolith Na/Ca showed a distinct peak in March in both sexes, but was relatively constant throughout the rest of the sampling period (Fig. 3.38). K/Ca data showed greater variability with the most notable feature being a drop in otolith K/Ca in the winter (July in males and September in females) that gradually returned to higher levels in the spring and early summer (Fig. 3.39). Otolith S/Ca data showed a relatively distinct single seasonal cycle which was similar for both sexes (Fig. 3.40). There was a peak in S/Ca during the summer followed by a sharp decline in the fall to a minimum in June. The S/Ca ratio gradually increased during the latter part of winter and spring, finally returning to the peak summer levels.

Relatively few magnesium analyses were performed because of the low concentration of this ion in the plasma, endolymph and otoliths and, thus, the probability that magnesium has little or no effect on the incorporation of other ions into the otolith. Estimates of the quantity of magnesium in blood plasma and endolymph were 0.57 ± 0.09 mM l^{-1} ($n=10$) and 0.19 ± 0.04 mM l^{-1} ($n=10$), respectively.

Figure 3.37 Seasonal variation in otolith Sr/Ca ratio, measured along the otolith margin by wavelength dispersive electron microprobe, in cod collected from Variety Bay. Error bars are ±1 S.E.

Figure 3.38 Seasonal variation in otolith Na/Ca ratio, measured along the otolith margin by wavelength dispersive electron microprobe, in cod collected from Variety Bay. Error bars are ±1 S.E.

Figure 3.39 Seasonal variation in otolith K/Ca ratio, measured along the otolith margin by wavelength dispersive electron microprobe, in cod collected from Variety Bay. Error bars are ±1 S.E.

Figure 3.40 Seasonal variation in otolith S/Ca ratio, measured along the otolith margin by wavelength dispersive electron microprobe, in cod collected from Variety Bay. Error bars are ±1 S.E.

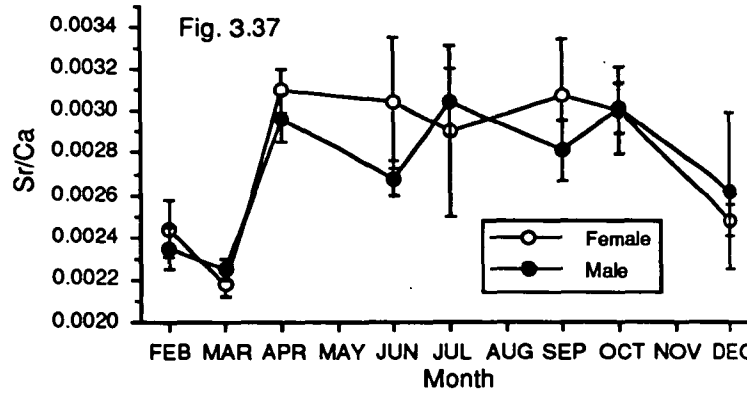
Fig. 3.37
Sr/Ca
0.0034
0.0032
0.0030
0.0028
0.0026
0.0024
0.0022
0.0020
Female
Male
FEB MAR APR MAY JUN JUL AUG SEP OCT NOV DEC
Month

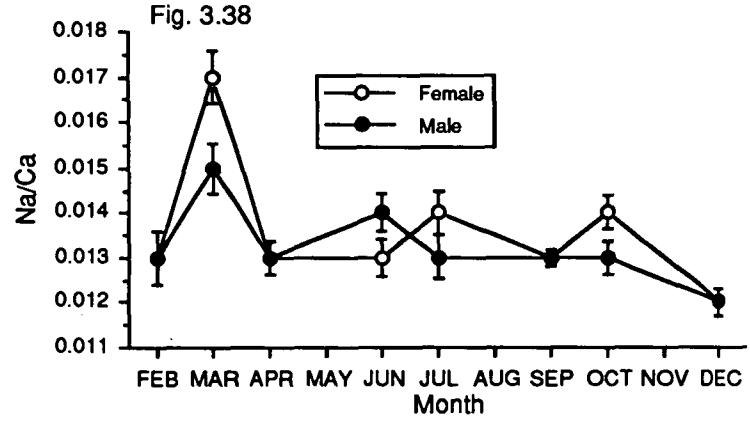
Fig. 3.38
Na/Ca
0.018
0.017
0.016
0.015
0.014
0.013
0.012
0.011
Female
Male
FEB MAR APR MAY JUN JUL AUG SEP OCT NOV DEC
Month

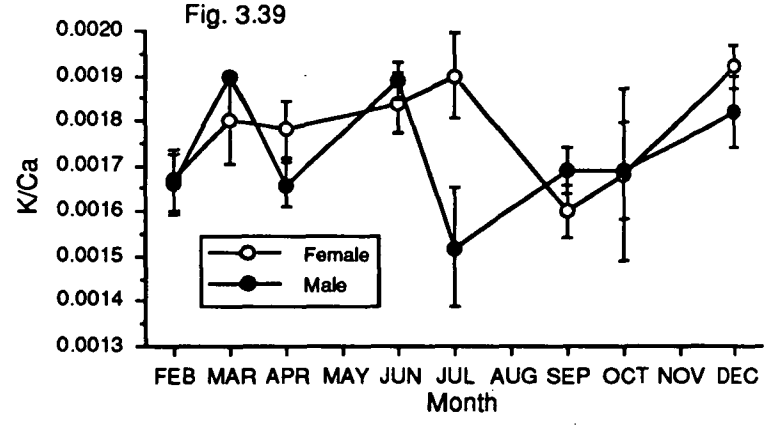
Fig. 3.39
K/Ca
0.0020
0.0019
0.0018
0.0017
0.0016
0.0015
0.0014
0.0013
Female
Male
FEB MAR APR MAY JUN JUL AUG SEP OCT NOV DEC
Month

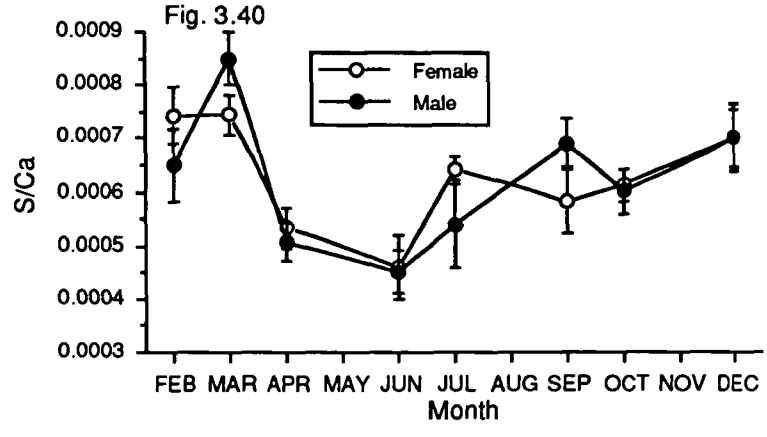
Fig. 3.40
S/Ca
0.0009
0.0008
0.0007
0.0006
0.0005
0.0004
0.0003
Female
Male
FEB MAR APR MAY JUN JUL AUG SEP OCT NOV DEC
Month

3.3.4 Multiple regression models of strontium in endolymph and otoliths

Numerous significant correlations were found among endolymph and otolith Sr data and the environmental and physiological variables (Table 3.4). Although the most significant correlations with endolymph Sr were other endolymph variables, these data were not considered in the models for reasons discussed earlier. Furthermore, endolymph variables such as protein, glucose, calcium, phosphate and triglycerides were all highly correlated with GSI, a variable considered for inclusion in the endolymph Sr models.

Multiple linear regression models were clearly more effective at explaining the variation in endolymph Sr measured in female rather than male fish. Details of the variables included in the models are shown in Table 3.5. A model containing 3 variables (temperature, GSI and plasma Sr) was able to explain 84% of the variance in the endolymph Sr data from female cod, whereas a multiple regression model, also containing 3 variables (temperature, plasma Sr and plasma Ca) could only explain 49% of the variance in male endolymph Sr data. When both sexes were combined the multiple regression model included 5 variables (temperature, gonad weight, plasma Sr, fish weight and plasma K) and explained 69% of the variance in the data. All three models involved ambient temperature and plasma Sr.

Like the endolymph Sr models, the otolith Sr multiple linear regression models were more effective at explaining the variance in the female cod (Table 3.6). A model containing 6 variables (fish length, GSI, plasma Sr, plasma Ca, condition factor and age) explained 69% of the variance in the female cod otolith Sr data. The best model for male otolith Sr data explained only 44% of the variance and contained 3 variables (fish weight, endolymph Sr and endolymph protein). A model to predict otolith Sr in both males and females was marginally better than the model for males and explained 52% of the variance with 6 variables (fish weight, gonad weight, endolymph Sr, plasma Sr, endolymph protein and condition factor).

3.3.5 Models of sodium and potassium precipitation in otoliths

White (1977) investigated experimentally the coprecipitation of sodium and potassium in aragonite and, on the basis of his results he was able to derive an empirical relationship that described the incorporation of these two alkali metal ions in aragonite. Further, he was able to justify his empirically derived model on theoretical

Table 3.4 Correlation coefficients for physiological and environmental variables significantly correlated ($P<0.05$) with endolymph and otolith strontium variables (Total N=115; Females N=54; Males N=61).

	Endolymph Sr			Otolith Sr/Ca		
	Females	Males	Both sexes	Females	Males	Both sexes
Temperature	-.768	-.635	-.685	-.38		-.295
Length				-.281		-.265
Weight				-.267	-.295	-.275
Condition factor					-.261	-.234
Age			.234			
Gonad weight	.623	.337	.538	.263		.19
GSI	.745	.31	.589	.467		.329
Plasma protein	.533		.312			
Plasma Sr	.549	.474	.512	.547	.363	.468
Plasma Ca	.296	.393	.329			
Plasma Na				.285		
Plasma K						
Plasma glucose						
Plasma triglyceride	.574		.377	.36		.215
Plasma phosphate	.338		.231	.371		.272
Endolymph protein	.823	.673	.754	.48		.327
Endolymph Sr	1.00	1.00	1.00	.583	.534	.562
Endolymph Ca	.388		.263			
Endolymph Na		.284				
Endolymph K						
Endolymph glucose	.734	.377	.616	.456		.319
Endolymph triglyceride	.80	.42	.692	.478		.347
Endolymph phosphate	.793	.547	.718	.52		.391

Table 3.5 Multiple linear regression model coefficients and associated statistics for estimation of endolymph Sr (mM) in cod.

Variable	Coefficient	SE	P
Females (N=51)			
Temperature	-0.00045	8.43×10^{-5}	<0.0001
GSI	0.001	9.55×10^{-5}	<0.0001
Plasma Sr	0.142	0.034	<0.0001
Constant (a)	0.008		
Multiple correlation, R=0.917			
Males (N=64)			
Temperature	-0.00036	8.01×10^{-5}	<0.0001
Plasma Sr	0.117	0.039	<0.005
Plasma Ca	0.001	0.000224	<0.025
Constant (a)	0.007		
Multiple correlation, R=0.703			
Both sexes (N=115)			
Temperature	-0.00038	6.52×10^{-5}	<0.0001
Fish weight	-2.08×10^{-6}	4.81×10^{-7}	<0.0001
Gonad weight	9.71×10^{-5}	1.22×10^{-5}	<0.0001
Plasma Sr	0.152	0.028	<0.0001
Plasma K	-0.00016	5.74×10^{-5}	<0.01
Constant (a)	0.009		
Multiple correlation, R=0.832			

Table 3.6 Multiple linear regression model coefficients and associated statistics for estimation of otolith Sr/Ca ratios in cod.

Variable	Coefficient	SE	P
Females (N=51)			
Fish length	-6.96×10^{-5}	1.55×10^{-5}	<0.0001
GSI	0.000219	3.48×10^{-5}	<0.0001
Plasma Sr	0.073	0.011	<0.0001
Plasma Ca	-0.000218	9.23×10^{-5}	<0.025
Condition	-0.087	0.034	<0.020
Age	7.58×10^{-5}	3.00×10^{-5}	<0.020
Constant (a)	0.005		
Multiple correlation, R=0.829			
Males (N=64)			
Fish weight	-6.97×10^{-7}	2.32×10^{-7}	<0.005
Endolymph Sr	0.25	0.04	<0.0001
Endolymph protein	-0.000129	3.60×10^{-5}	<0.001
Constant (a)	0.003		
Multiple correlation, R=0.662			
Both sexes (N=115)			
Fish weight	-8.28×10^{-7}	1.78×10^{-7}	<0.0001
Gonad weight	1.49×10^{-5}	5.12×10^{-6}	<0.005
Endolymph Sr	0.128	0.036	<0.001
Plasma Sr	0.04	0.011	<0.001
Endolymph protein	-7.05×10^{-5}	2.94×10^{-5}	<0.025
Condition	-0.07	0.027	<0.020
Constant (a)	0.003366		
Multiple correlation, R=0.720			

Figure 3.41 Plot of otolith Sr/Ca ratio, measured along the otolith margin, against endolymph strontium (μM/l) in cod. Males, N=61; Females, N=54.

Figure 3.42 Plot of otolith Na/Ca ratio, measured along the otolith margin, against the predicted Na/Ca ratio in aragonite based on the empirically derived model from White (1977). The model is explained in the text. Although the range of Na/Ca values measured in the otoliths overlaps with the range of Na/Ca ratios based on the model, the two variables are not correlated.

Figure 3.43 Plot of otolith Na/Ca ratio, measured along the otolith margin, against the predicted Na/Ca ratio in aragonite based on the model from White (1977) times the log of the endolymph protein (g/l) content. Only the data from the female cod (N=54) are shown.

Fig. 3.41

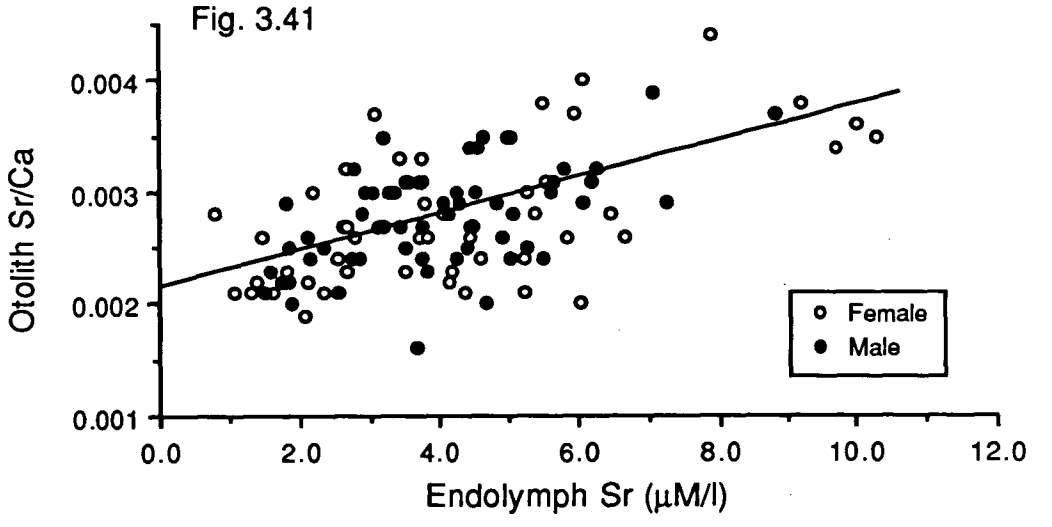

Fig. 3.42

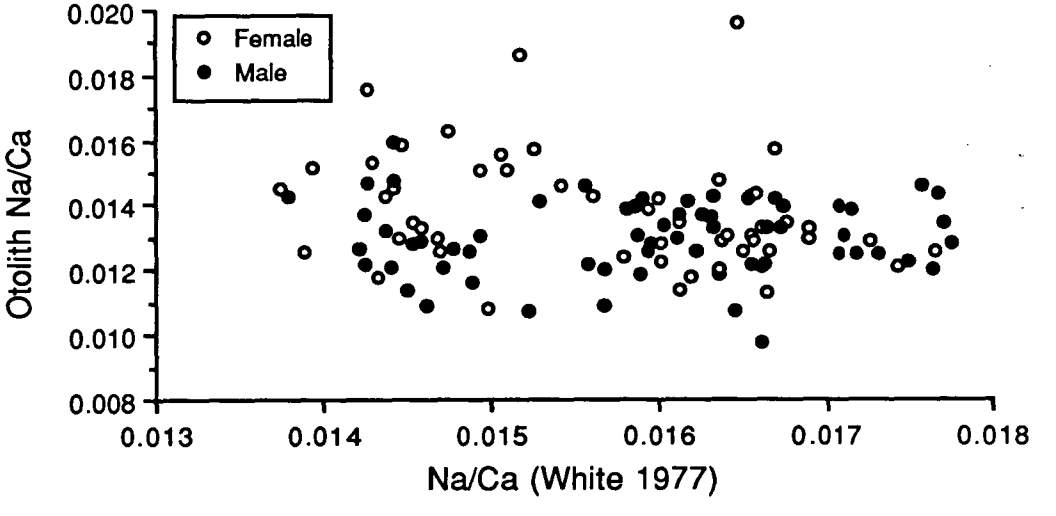

Fig. 3.43

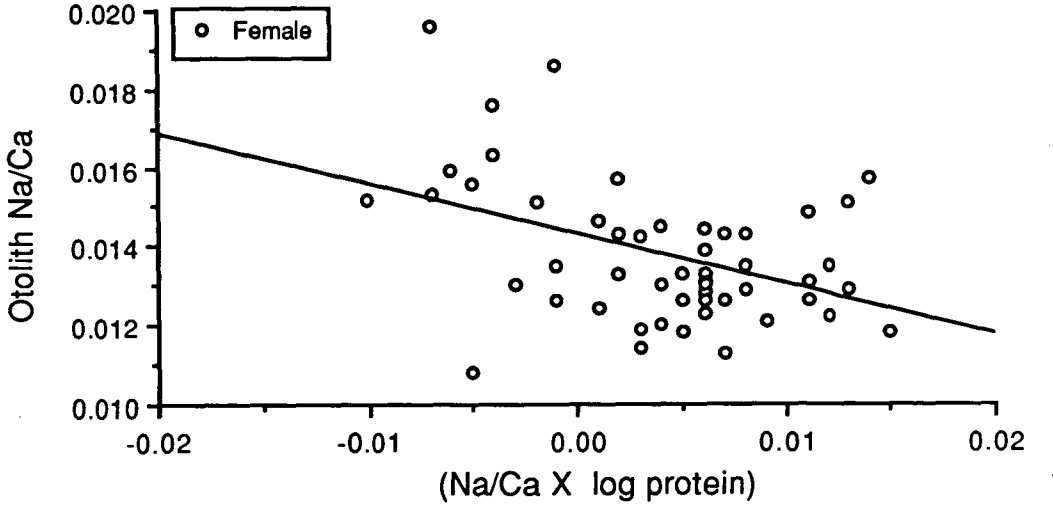

grounds. In this section I will present these models along with a brief explanation regarding their derivation and theoretical justification.

The theoretical basis for White's (1977) model is that both sodium and potassium ions substituted for calcium in the aragonite matrix. White's (1977) empirical model follows the assumption that the distribution of incorporation sites in the aragonite crystal is heterogeneous, similar to the assumptions of Kinsman and Holland (1969) in developing a model of Sr^{2+} coprecipitation in aragonite. White's (1977) linear logarithmic model takes the form:

$$\log X_{Na_2CO_3,\, K_2CO_3} = C_0 + C_1 \log \frac{a^2_{Na^+,\, K^+}}{a_{Ca^{2+}}} \qquad \text{(Eq 3.1)}$$

where X is the mole fraction of sodium or potassium in the aragonite solid, a_m represents the aqueous activity of the sodium or potassium ions, a_{ca2+} is the aqueous activity of the calcium ions and C_0 and C_1 are the intercept and slope, respectively.

The above relationship (Eq. 3.1) is applicable to a system where the coexistence of cations such as potassium and sodium does not affect coprecipitation. White (1977) found that the coprecipitation of sodium in aragonite was not affected by the presence of potassium in the aqueous solution, and, thus, Equation 3.1 was valid, whereas potassium was affected by the presence of sodium. Pure potassium or sodium systems are probably rare, if not nonexistent in nature, and White (1977) proposed an empirical relationship for estimating the coexisting sodium and potassium distributions in aragonite precipitated from solutions containing both sodium and potassium:

$$\log \frac{X_{K_2CO_3}}{X_{Na_2CO_3}} = -0.990 + 0.312 \log \frac{a^2_{K^+}}{a^2_{Na^+}} \qquad \text{(Eq 3.2)}$$

which is a least squares fit to his experimental data.

White (1977) observed that temperature effected both the slopes and intercepts of the sodium and potassium coprecipitation relationships. I have used his temperature/coprecipitation data to calculate the coefficients C_0 and C_1 for use in Equation 3.1 for sodium and potassium. Unfortunately, White (1977) does not present data that relates to the effect of temperature on the precipitation of potassium in the presence of sodium. Table 3.7 below presents the regression equations I used for estimating the effects of temperature C_0 and C_1. They are derived from the raw data presented in White (1977). These relationships were input into Equation 3.1 to produce models of sodium and potassium precipitation in cod otoliths.

Table 3.7 Regression relationships between temperature (T) and C_0 and C_1 for input into Equation 3.1. Data for these relationships was taken from White (1977).

Sodium

$C_0 = -2.015 + -0.0162\ T \quad (r^2 = 0.98)$

$C_1 = -0.0963 + 0.99174\ T \quad (r^2 = 0.79)$

Potassium

$C_0 = -2.45 + -0.0254\ T \quad (r^2 = 0.99)$

$C_1 = 0.1553 + 0.00258\ T \quad (r^2 = 0.86)$

The ion activity coefficients, γ_i, of Na, K and Ca in the precipitating solution, in this case the endolymph, were calculated according to the Debye-Hückel method (Garrels and Christ, 1965; Pytkowicz, 1983):

$$-\log\gamma_i = \frac{A z_i^2 \sqrt{I}}{1 + å_i B\sqrt{I}} \qquad \text{(Eq. 3.3)}$$

where z_i is the charge of the i^{th} ion in solution, I is the ionic strength, calculated below, å is a constant that is dependent upon the effective diameter of the ion in

solution and A and B are constants (see Garrels and Christ, 1965). The calculated activity coefficients were in agreement with published values (Pytkowicz, 1983).

Ionic strength (I), used in the calculation of the Debye-Hückel activity coefficient, of cod endolymph was calculated based on the mean endolymph composition for both sexes (Table 3.8).

Table 3.8 Annual mean composition ($M \cdot l^{-1}$) of cod endolymph from both sexes used to estimate the ionic strength (I) of cod endolymph.

Na^+	Ca^{++}	K^+	Mg^{++}	HCO_3^-	Cl^-
0.111	0.00125	0.067	0.0005	0.005	0.15

Ionic strength is defined as (Garrels and Christ, 1965):

$$I = \frac{1}{2} \sum m_i z_i^2 \qquad \text{(Eq. 3.4)}$$

where m_i is the molality of the *i*th ion and z_i is the charge of the *i*th ion in solution. The summation takes into account both positive and negative ions. On the basis of the endolymph composition in Table 3.8 the estimated ionic strength is 0.17.

Application of White's (1977) model of sodium coprecipitation in aragonite (Equation 3.1) to the cod endolymph data results in estimates of aragonite sodium content that are within the range of Na measured in cod otoliths. The mean otolith Na/Ca ratio based on the model is 0.016±0.0011 and 0.017±0.0015 in the males and females, respectively, which is similar to the values of 0.013±0.0012 for males and 0.014±0.0018 mM for females measured in the otoliths by electron microprobe. However, an unpaired t-test indicates that there are significant differences between the Na/Ca estimates from the model and Na/Ca ratios measured in the cod otoliths ($t=14.1$, $n=115$, $p<0.0001$). Furthermore, the values derived from the application of the model to the endolymph data are not significantly correlated with the otolith Na/Ca data (Fig. 3.42) In an attempt to explain the discrepancy among these data the model

data were adjusted by multiplying by the logarithm of the endolymph protein content. This resulted in a slightly significant linear regression between the model data and the otolith data for both sexes (r^2=0.09, n=115, p<0.05). If the female data are considered alone the regression becomes more significant (r^2=0.19, n=51, p<0.01) (Fig. 3.43), but the relationship is not significant for the male data alone.

As for the Na otolith data, the application of White's (1977) model for the coprecipitation of K in aragonite, in the presence of Na, (Equation 3.2) gives results within the range of K values measured in cod otoliths. The modeled estimate of K/Ca in otolith aragonite for both sexes is 0.0020±0.0003 , which is close to the value of 0.0017±0.00023 measured in the otoliths by electron microprobe, but a t-test indicates that these results are significantly different (t=6.7, n=115, p<0.0001). There is no significant correlation among these data even when the protein content of the endolymph is taken into consideration.

3.3.6 Characterization of plasma and endolymph proteins

Results of cellulose acetate electrophoresis showed that there were large differences in the relative protein composition of cod plasma over the year and somewhat smaller differences within samples from the same collecting trip. These differences are evident in the electrophoretic patterns of fish plasma, of which some examples appear in Fig. 3.44, and in the elution diagrams derived from the electrophoretic data (Fig. 3.45). Individual elution diagrams are explained in the appropriate figure captions. Evidence of the potential variation in the calcium-binding capacity of fish plasma from various individuals can be realized by examination of the differences in the quantities of the albumin and globulin fractions in the plasma and, the albumin/globulin ratio (A/G ratio) derived from the elution diagrams. Spectrophotometric measurement of albumin in the plasma samples also highlighted the variability of these data (Table 3.9).

As with other physiological data, the blood protein data appeared to be more useful in investigations of variations in the chemical makeup of the female cod. However, only a fraction of the cod samples were analysed electrophoretically (27 of 115 samples) and, thus, the results are tentative. In female fish the ratio of albumin to globulins (A/G) was negatively correlated with temperature (r^2=0.35, n=14, p=0.033), and positively correlated with plasma triglycerides (r^2=0.38, n=14, p=0.025). Plasma albumin was negatively correlated with temperature (r^2=0.43,

Table 3.9 Total plasma protein, albumin and A/G ratio data from selected cod.

Date of collection	Sex	A/G	Albumin	Protein
17 April	M	1.16	15	37.4
17 April	M	1.61	13	32.7
17 April	F	1.54	8	24.0
17 April	F	0.77	11	36.4
22 June	M	1.50	10	26.5
22 June	M	3.35	11	41.3
22 June	F	1.17	13	35.2
22 June	F	1.25	10	50.5
29 July	M	1.79	11	32.4
29 July	F	2.84	12	41.0
8 September	M	0.96	13	38.2
8 September	M	1.70	14	30.6
8 September	F	3.55	16	42.3
8 September	F	0.88	17	41.1
19 October	M	1.70	9	34.8
19 October	M	1.26	11	25.8
19 October	F	1.59	7	32.1
6 December	M	1.20	11	33.2
6 December	M	0.77	13	37.7
6 December	M	1.57	12	43.2
6 December	M	0.81	11	61.7
6 December	M	0.88	11	46.5
6 December	F	0.91	9	23.5
6 December	F	0.48	9	39.9
6 December	F	0.81	8	38.4
6 December	F	0.78	9	38.8

Table 3.10 Multiple linear regression model coefficients and associated statistics for estimation of endolymph Sr/Ca ratios in female cod. Unlike the model presented in Table 3.5, blood protein data are included in this model.

Variable	Coefficient	SE	P
Females (N=12)			
Albumin/globulin ratio	0.001	9.44×10^{-5}	<0.0001
Total plasma protein	4.08×10^{-5}	8.79×10^{-6}	<0.0001
Fish length	-0.00027	4.99×10^{-5}	<0.0001
Fish weight	1.35×10^{-6}	5.78×10^{-7}	<0.01
GSI	0.001	3.52×10^{-5}	<0.0001
Plasma Sr	0.08	0.022	<0.0001
Constant (a)	0.01		
Multiple correlation, R=0.992			

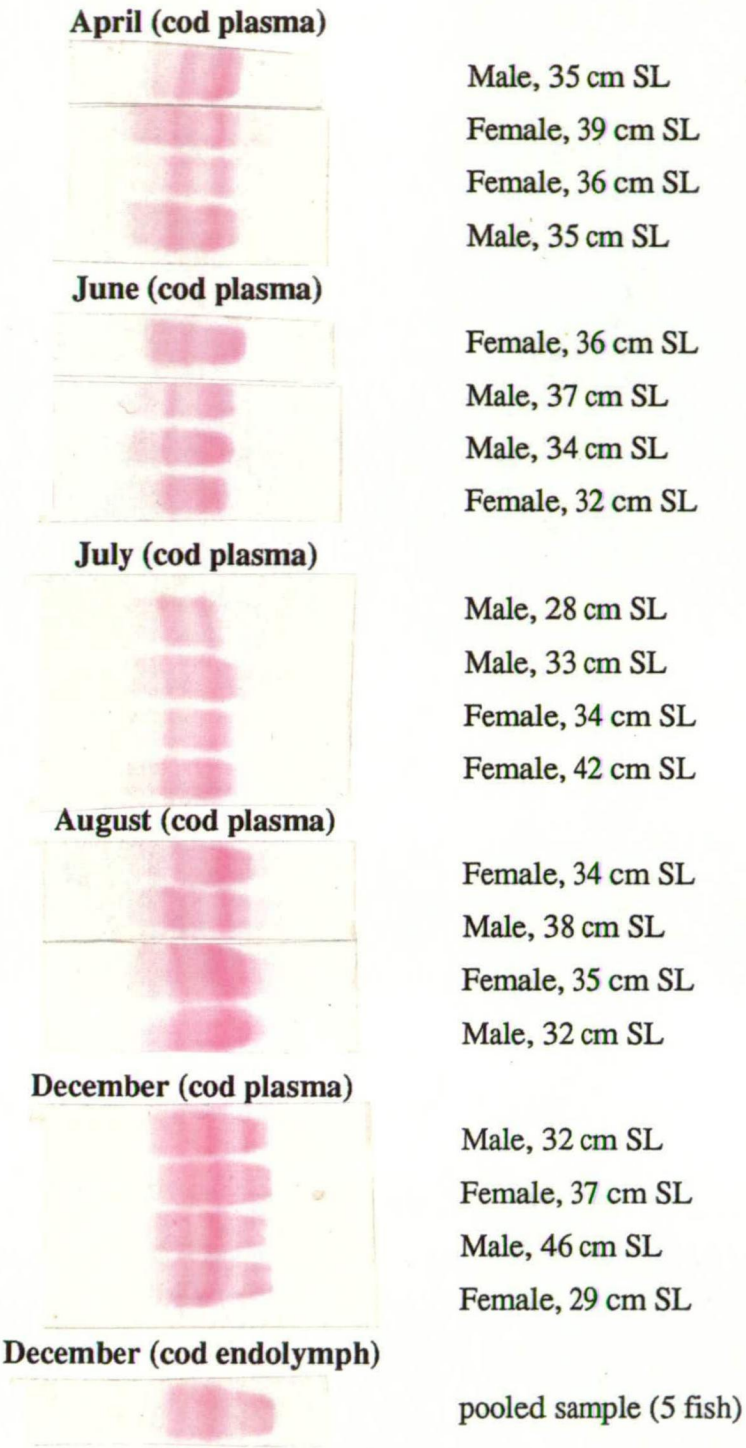

Fig. 3.44 Electrophoretic patterns of samples of *Pseudophycis barbatus* plasma and endolymph. The plasma samples are separated by month. The endolymph sample was concentrated before analysis. Direction of migration is from left to right.

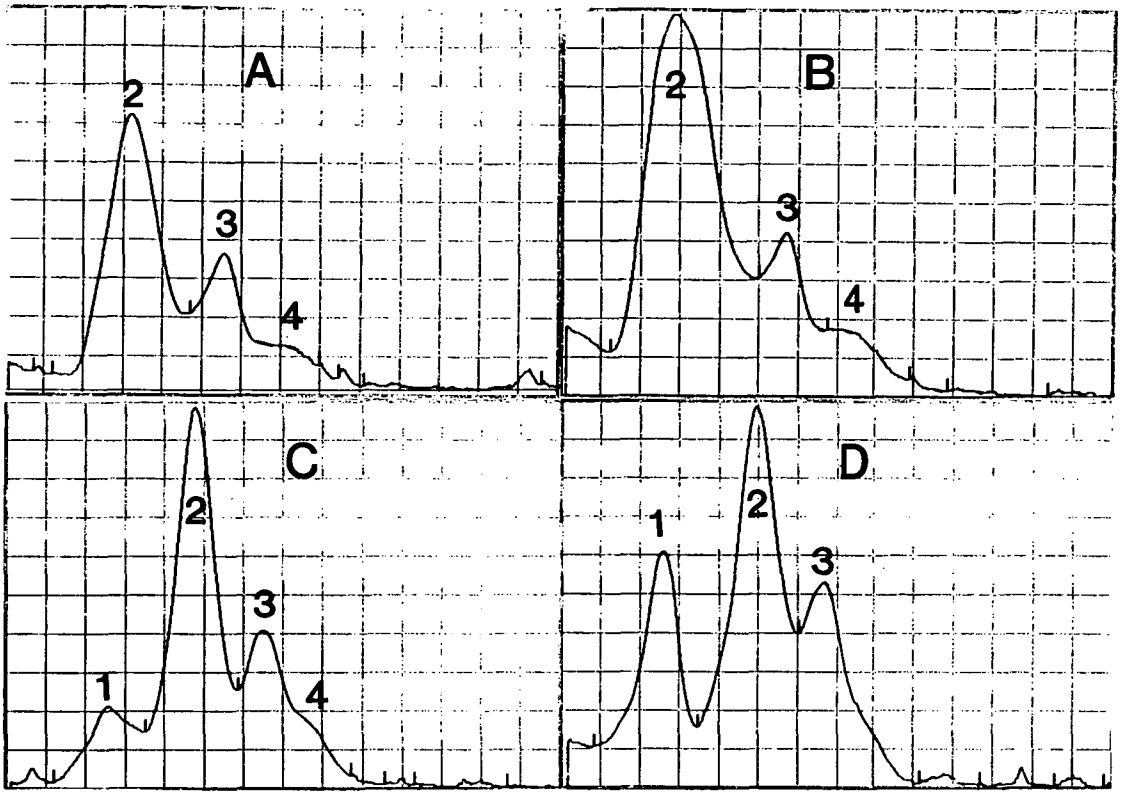

Fig. 3.45 Elution diagrams derived from electrophoretic data shown in Fig. 3.44. The direction of migration is from right to left in these diagrams. Protein fractions did not separate very well and in some instances run times were increased in attempts to improve separation. Fractions are labelled as follows: 1=prealbumin; 2=albumin; 3= α globulin and β globulin; 4= γ globulin. Generally, the albumin fraction migrated the greatest distance although in C and D there are varying levels of prealbumin. (A) collected April, male, 35 cm Sl, A/G ratio=1.61; (B) collected June, male, 34 cm SL, A/G ratio=2.17; (C) collected December, male, 46 cm SL, A/G ratio=1.20; (D) collected December, female, 37 cm SL, A/G ratio=0.84.

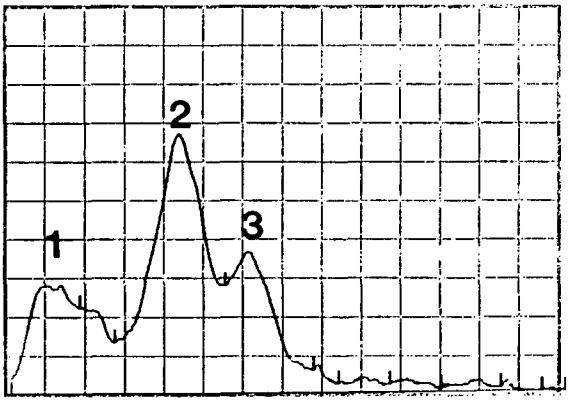

Fig. 3.46 Elution diagram from a pooled sample (5 fish) of *Pseudophycis barbatus* endolymph. Fish were collected in December. Fractions are labelled as in Fig. 3.45 although these fractions may be somewhat different from those found in the plasma.

n=14, p=0.011) and positively correlated with endolymph Sr (r^2=0.58, n=14, p=0.002), GSI (r^2=0.59, n=14, p<0.001), plasma triglycerides (r^2=0.58, n=14, p=0.002), endolymph protein (r^2=0.55, n=14, p=0.003), endolymph glucose (r^2=0.46, n=14, p=0.008), endolymph calcium (r^2=0.29, n=14, p=0.05), endolymph phosphate (r^2=0.61, n=14, p<0.001) and endolymph triglycerides (r^2=0.67, n=14, p=0.0004). These variables were not significantly correlated in the male fish. Incorporation of the variable A/G ratio into a multiple regression model to predict the endolymph Sr was capable of explaining 98.5% of the total variance in female endolymph Sr levels (Table 3.10). The model included the variables A/G ratio, plasma protein, fish length, fish weight, gonad index and plasma Sr.

Cellulose acetate electrophoresis of concentrated cod endolymph indicated that the gross protein composition of endolymph was not greatly different from that found for the plasma (Figs. 3.44 and 3.46). As in a majority of the plasma samples, there were large prealbumin and albumin fractions. Other fractions, presumably globulins, were not well separated.

Gel filtration of cod plasma and endolymph and subsequent calcium analyses of the fractions indicated that both the relative distribution of proteins as well as the calcium-binding fractions were not grossly different. There was no evidence for a unique calcium-binding protein in the endolymph, but this could be an artefact of the relative insensitivity of the separation procedure employed at certain molecular weights. Also, there was some difficulty in accurately determining calcium concentrations due to excessively high background levels in the samples when analysing the fractions by atomic absorption spectrophotometry. These protein separation trials were largely exploratory and serve to highlight the utility of these techniques.

The results of column chromatography of the standards (Fig. 3.47) can be compared with plasma and endolymph data to get estimates of the molecular weights of the fractions eluted (Fig. 3.48 and 3.49). It can be seen that calcium binding occured in similar molecular weight regions of the column elution volume in both the cod plasma (Fig. 3.48) and the cod endolymph (Fig. 3.49a). Orange roughy endolymph resulted in an elution diagram (Fig. 3.49b) similar to that found for cod endolymph, but calcium determinations were not made on these fractions. In general there was an overall similarity between the cod plasma and endolymph and the orange roughy endolymph.

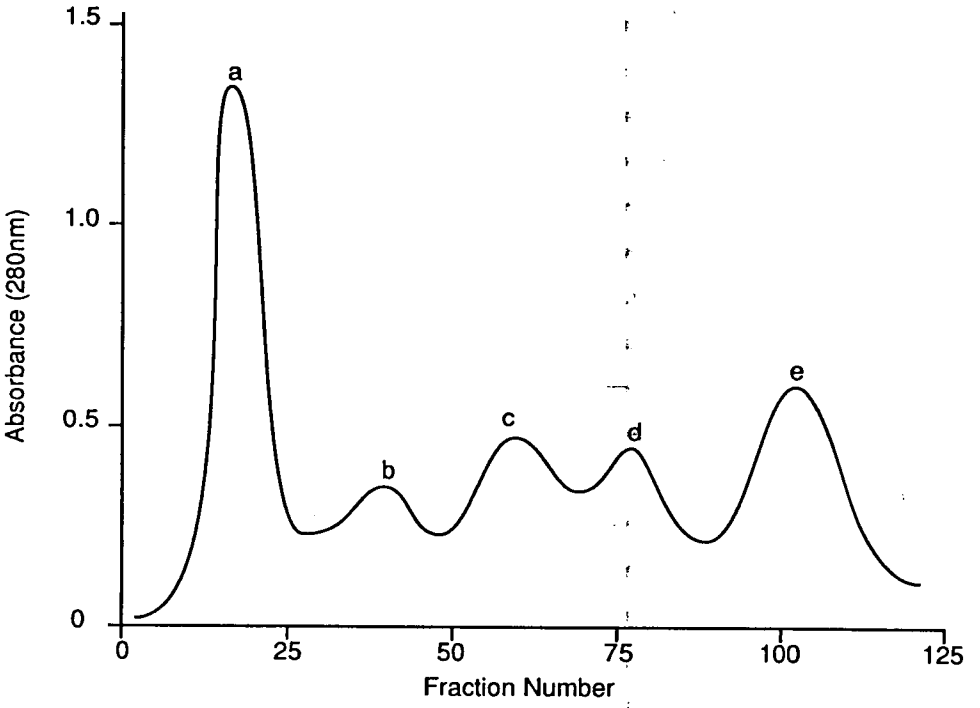

Fig. 3.47 Sephadex G-100 column chromatography of standards showing the relative distribution of the different molecular weight fractions. Standard peaks, indicated by letters on chromatogram, and their molecular weights: (a) Blue Dextran (2,000K); (b) egg albumin (45K); (c) pepsin (34.7K); (d) trypsinogen (24K); and (e) lysozyme (14.3K).

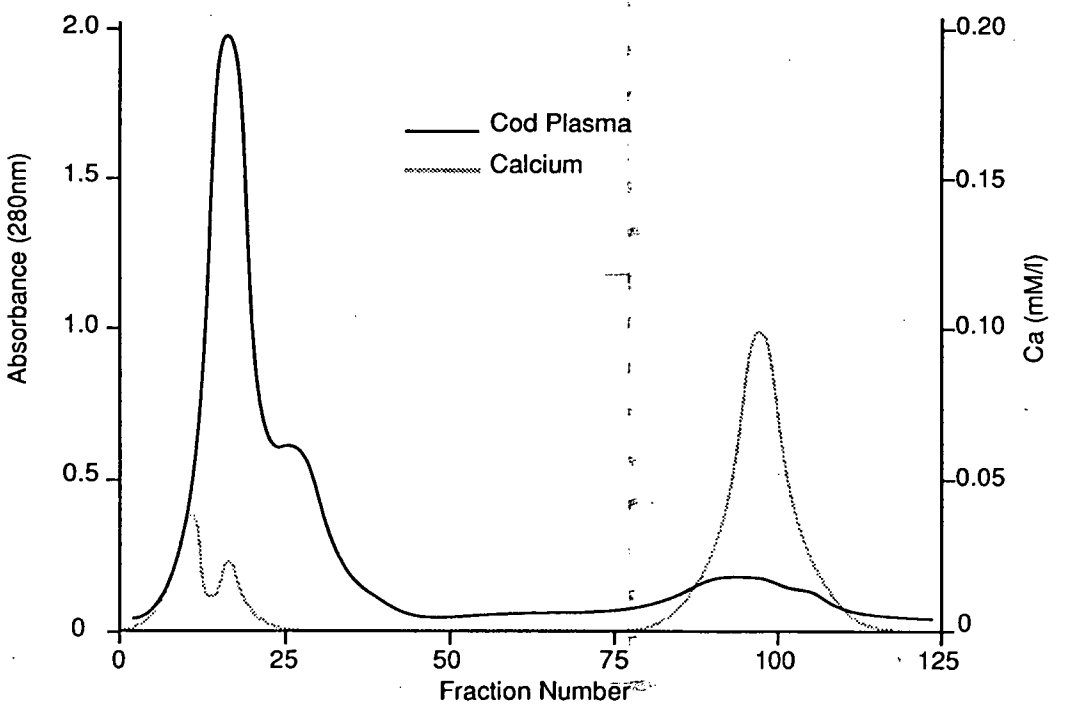

Fig. 3.48 Sephadex G-100 column chromatography of *Pseudophycis barbatus* plasma. Individual was a female (48 cm SL; 2160 g; 2.8 GSI) collected from Variety Bay on 6 December 1988. First calcium peak at (fraction 10-12) may be associated with vitellogenin. Large calcium peak is free calcium or calcium bound to small molecules.

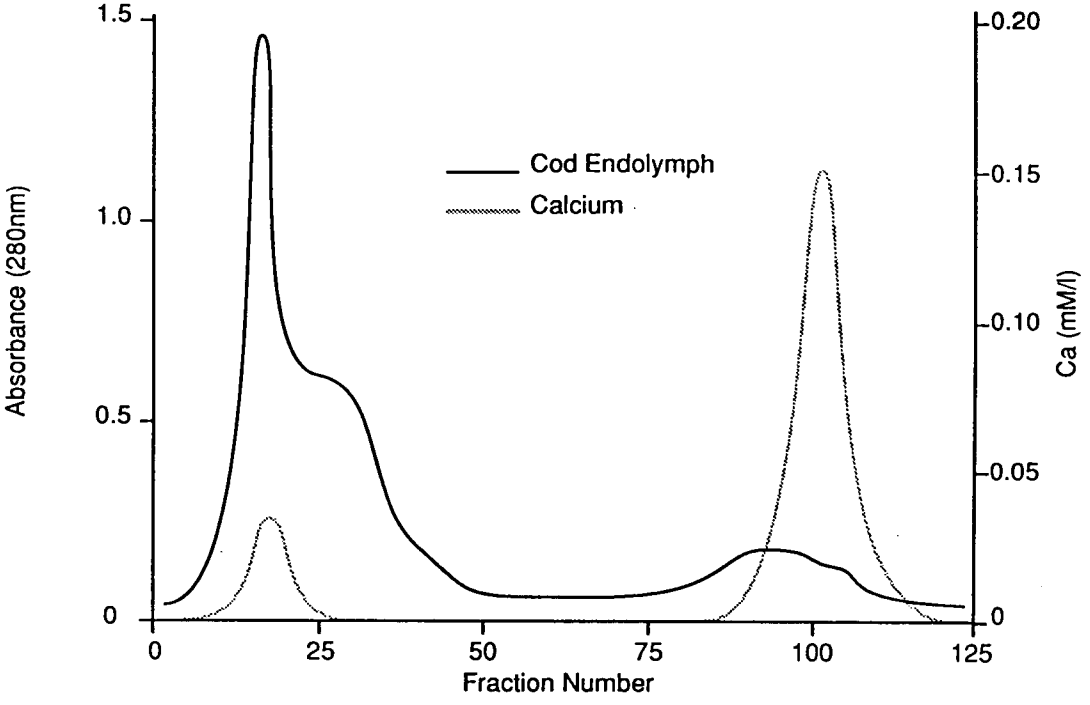

Fig. 3.49a Sephadex G-100 column chromatography of *Pseudophycis barbatus* endolymph. Sample was pooled from 5 fish collected from Variety Bay on 6 December 1988. First calcium peak (fraction 18-22) is associated with a protein with a molecular weight between 50K and 100K, probably an albumin. Large calcium peak is free calcium or calcium bound to small molecules.

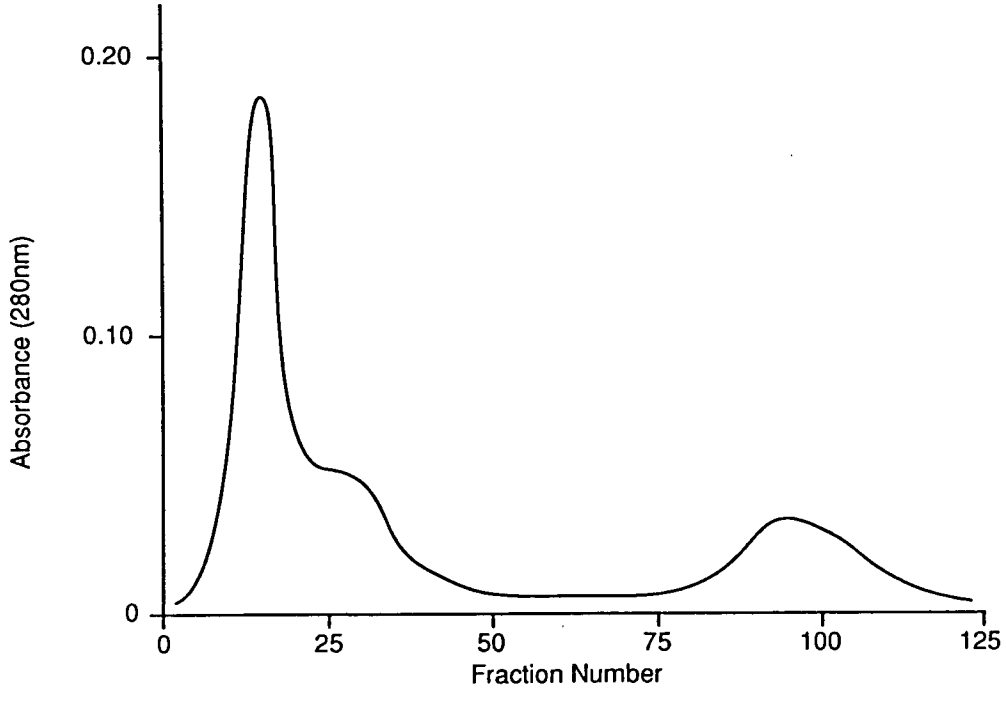

Fig. 3.49b Sephadex G-100 column chromatography of *Hoplostethus atlanticus* endolymph. Sample was pooled from 3 fish collected off the east coast of Tasmania on 2 November 1988.

3.4 DISCUSSION

The data on blood plasma, endolymph and otolith composition indicate that, while there is a fair degree of interaction among these body components, these relationships are not necessarily simple or straightforward.

3.4.1 Plasma and endolymph metabolites

The data on the cod present clear evidence of the influence of season on the composition of blood plasma and endolymph and indicate that a major influence on the composition of these body constituents is the development of the gonads before spawning.

3.4.1.1 *Plasma glucose, phosphate and triglyceride*

Variations in plasma glucose are considered difficult to measure in wild fishes because of the effects of stress and exertion, in relation to capture, on levels of plasma glucose (Chavin and Young, 1970; Wardle, 1972; White and Fletcher, 1985). However, Black *et al.* (1960) found that exercise did not have a significant effect on blood glucose levels in wild rainbow trout (*Onchorynchus mykiss*). Unfortunately, Wardle (1972) considers the elevated glucose levels after capture as stress related alone, and he relates these data to "unstressed" fish that were maintained unfed while in captivity. He does not consider the relative glucose levels of animals in the fed and unfed state. In addition to capture related stress, it is important to consider environmental stress (Wedemeyer, 1981), temperature (Umminger, 1969), sex, size, age, reproductive condition (Chavin and Young, 1970; Leach and Taylor, 1977) and the time since last feeding. The ingestion of carbohydrates causes an increase in plasma glucose (Lehninger, 1970); this effect is clearly illustrated in research on the sand dab (*Limanda limanda*) (Fletcher, 1984).

The large number of variables affecting plasma glucose make it difficult, in this case, to determine how representative the glucose data are of normal glucose levels in undisturbed cod in the wild. Wardle (1972) estimated normal blood glucose levels in adult plaice (*Pleuronectes platessa*) as 0.8 to 1.4 $mM \cdot l^{-1}$ and, White and Fletcher (1985) found levels varied seasonally from about 0.8 to 2.0 $mM \cdot l^{-1}$ for the same species. Fletcher (1984) found that plasma glucose levels remained between 1.1 and 1.4 $mM \cdot l^{-1}$ and did not vary seasonally in *Limanda limanda*. In each of these three studies the blood glucose levels were measured in fish which had been maintained in

captivity without feeding for a period of a least one week. Fletcher (1984) found that feeding dramatically increased plasma glucose in *Limanda limanda* to more than 6.4 $mM \cdot l^{-1}$ in summer and 3.4 $mM \cdot l^{-1}$ in winter. The effects of feeding were evident almost immediately and the plasma glucose levels remained elevated for up to 50 h in these animals. Bergot (1979) found that plasma glucose levels reached their peak in rainbow trout 6 h after a glucose enriched meal. Because the majority of the cod used in this study were collected between 1100 h and 1400 h, approximately 5 to 8 h after first light, when feeding probably commences, high plasma glucose levels would be expected. Therefore, it would be unreasonable to estimate the effects of stress on the cod collected in this study on the basis of unfed fish maintained in captivity. On the basis of the studies cited above, it is difficult to determine if the mean plasma glucose level of 3.9 ± 1.7 $mM \cdot l^{-1}$ measured in cod is indicative of natural levels or the result of stress.

Measurements of total phosphate are not likely to be affected by the immediate effects of capture related stress and, thus, provide information that can be readily related to the physiological state of the animal. However, interpretation of data on total phosphate can be subject to difficulties due to the numerous potential sources of phosphate in the blood. In fish, phosphates can be associated with various phospholipids which are most important as constituents of cell membranes and organelles and are probably the most concentrated lipids in fish plasma (Robinson and Mead, 1973). Phosphate-bearing compounds that can be found in fish plasma include numerous phosphorylated compounds relevant to energy transfer, phospholipoproteins such as vitellogenin which are involved in the process of egg formation and may be precursors of the egg yolk proteins, phosvitin and lipovitellin. It must be understood that levels of inorganic phosphate were measured in this study but that these values are generally altered on the basis of the presence of breakdown products associated with the decomposition of organic compounds present in the blood (Gross, 1976; Craik and Harvey, 1984a).

The fact that there were significant differences, both seasonally and on the basis of the interaction of season and sex, is a good indication that, in part, seasonal variations in phosphate were attributable to the presence of a phospholipoprotein such as vitellogenin. This conclusion is supported by the September peak in phosphate in female cod that coincides with the peak in gonadosomatic index. Similar results were also obtained by Petersen and Emmersen (1977) who found increased serum

phospholipid levels in the flounder (*Platichthys flesus*) at the onset of seasonal ovarian development and through the spawning period. McCartney (1967) found that serum phospholipid levels increased in rainbow trout just prior to and, during spawning and, therefore, could not conclude that the changes in phospholipids were directly related to the development of the ovaries.

White *et al.* (1986) found no clear pattern in plaice serum phospholipids and concluded that these levels were unaffected by ovarian development in this species, although their data do show a peak in serum phospholipid in February that could be related to gonadal development before the February-March spawning period. White *et al.* (1986) obtained mean phospholipid levels in February of 363±12 $mg \cdot 100ml^{-1}$ for female plaice and 329±19 $mg \cdot 100ml^{-1}$ for males and indicate that there were no significant differences between female and male phospholipid levels throughout the year. Therefore, they conclude that the proteins involved in ovarian development, such as vitellogenin are not affecting their values. Although it is not totally clear, it appears that White *et al.* (1986) tested for significant differences in serum lipids between sexes and months separately by one-way analysis of variance and they did not consider the potential interaction between month and sex by using a two-way design. On the basis of the mean values for male and female serum phospholipids in February it seems probable that such an interaction exists as in female cod.

The sharp drop in female cod plasma phosphate levels from the September maximum to a December minimum, well below phosphate levels measured in male cod indicates that these variations are sex related and, presumably, related to the spawning cycle. Fletcher (1984) and White *et al.* (1986) obtained the opposite result and, attributed increases in plasma phospholipids after spawning in *Limanda limanda* and *Pleuronectes platessa* to the reabsorption of ovarian material which is predominantly lipid, specifically phospholipid.

In female cod, the low levels of plasma phosphate may be related to the rebuilding of the body tissues and reserves after the draining period of gonadal development leading up to spawning. This interpretation would be consistent with data presented by Craik and Harvey (1984b) which considers seasonal changes in plasma phosphate associated with the development of eggs.

Levels of lipid in the plasma can vary in response to gonadal development, as just discussed, or to levels of feeding. Lipids, primarily in the form of triglycerides stored in the liver, are mobilized during periods of starvation (Lehninger, 1976). In

"fatty" fish species interstitial fat in the muscle tissue may also serve as a storage site for triglycerides (Larsson and Fänge, 1977; Fletcher, 1984; White *et al.*, 1986), but it is only in times of extreme deprivation that cell constituents such as the phospholipids are broken down for use as an energy source (Lech, 1970).

The marked similarity between seasonal cycles of plasma phosphate and triglyceride levels in female cod and the correlation between these variables (females only, r^2=0.34, n=54, p<0.0001) was an additional indication of the dominance of spawning in controlling metabolite levels in the blood plasma. Furthermore, there was a strong positive correlation between the gonadosomatic index and plasma triglyceride levels in the females (females only, r^2=0.42, n=54, p<0.0001) and both data sets show evidence of similar seasonal cycles. These relationships were not evident in the male cod (males only, r^2=0.02, n=61, p>0.05). Elevated triglyceride levels in the plasma are indicative of periods of stress due to starvation or the need to satisfy energy requirements that cannot be met by ingested food alone. Mobilization of triglycerides stored in the liver may be the principle source of energy after tissue and liver glycogen reserves are utilized, although the function of these storage molecules may vary to some degree for different species (Lech, 1970, White *et al.*, 1986). Triglycerides released into the blood from the liver are hydrolyzed by various lipases resulting in free fatty acids (FFA) and glycerol. The glycerol is ultimately converted to glucose for energy, whereas the FFA may be used to produce energy through the fatty acid oxidation cycle or, alternatively, they can be utilized in the production of plasma lipoproteins such as the egg yolk precursor, vitellogenin (Lech, 1970). Therefore, increased levels of plasma triglycerides may occur in response to the females need to meet energy requirements during the buildup of the gonads before spawning and may also provide material necessary for the production of egg yolk.

The fall in plasma triglycerides in the females after the spawning related peak in September was almost identical to that found for phosphates and suggests that, in the second half of the year at least, the triglyceride and phosphate levels were very closely linked. In these circumstances, it seems reasonable to conclude the two metabolites were, ultimately, portions of the same phospholipoproteins involved in egg production and that the decreases in phosphate and triglyceride in the Spring were due to the need for females to rebuild their body tissues and liver triglyceride stores before the next spawning season. Presumably these constituents were near exhaustion from the stress of gonad production and spawning.

3.4.1.2 *Endolymph glucose, phosphate and triglyceride*

Endolymph glucose, phosphate and triglyceride levels were clearly affected by the seasonal cycle of spawning in the females. These data were more convincing in this respect than the data from plasma. Peaks in levels of glucose, phosphate and triglyceride in the female endolymph showed peaks that correspond with the peak in gonadosomatic index in September. There was little variation during the remainder of the year and the levels were relatively constant in the males. These data indicate that readiness for spawning may be more easily determined on the basis of metabolites measured in the endolymph rather than in the plasma.

3.4.2 Ions in endolymph and otoliths

3.4.2.1 *Strontium and calcium*

Seasonal cycles in plasma calcium have been described for many marine and freshwater species. Increases in plasma calcium have been attributed to the development of the female gonads in *Salvelinus fontinalis* (Booke, 1964), *Carassius auratus* (Oguri and Takada, 1967), *Gadus morhua* (Woodhead, 1968), *Oncorhynchus mykiss* (Whitehead *et al.*, 1980) and many others. Spawning related increases in male plasma calcium were not detected in some cases (Booke, 1964; Oguri and Takada, 1967) or levels of plasma calcium were considered to be lower than those measured in the females (Whitehead and Bromage, 1978). Data on cod indicate that both males and females became hypercalcemic during the spawning season. However, in all months except July, male cod had significantly lower levels of plasma calcium than females with annual mean values of 1.70 ± 0.65 $mM \cdot l^{-1}$ and 1.91 ± 0.55 $mM \cdot l^{-1}$, respectively.

Unlike the plasma calcium data, only the female endolymph calcium data showed evidence for a relationship with gonadosomatic index (females only, $r^2=0.28$, $n=54$, $p<0.001$; males only, $r^2=0.003$, $n=61$, $p>>0.50$). This is not surprising in view of the fact that only the female endolymph showed spawning related increases in glucose, phosphate and triglycerides. Mugiya (1966b) found seasonal changes in endolymph calcium in *Oncorhynchus mykiss* and a flatfish, *Kareius bicoloratus*, but he did not separate males and females. Therefore, the variations that he discusses may be misrepresentations of the endolymph calcium variations in each sex. However, Mugiya (1966b) still found a relationship between the seasonal variations in serum and endolymph calcium. Mugiya (1966b) separately measured total and

diffusible calcium in both the serum and endolymph and found that the diffusible calcium in the serum more closely reflected the seasonal variations in endolymph calcium. Furthermore, his quantities of diffusible calcium in the serum were very similar to the total amount of calcium found in the endolymph and, thus, Mugiya (1966b) concluded that the seasonal variation in total endolymph calcium was related to the change in the quantity of plasma proteins which, in turn, has been shown to be directly related to the relative proportions of bound and diffusible calcium in some organisms (Levine and Williams, 1982).

Over the 12 months of his study, Mugiya (1966b) found that the total Ca measured in the endolymph was 65.6% and 66.7% of the total Ca measured in the blood serum in *Kareius bicoloratus* and *Oncorhynchus mykiss*, and that these percentages corresponded with the proportion of diffusible calcium (ionized and complex-bound) to total calcium in the plasma. Similar results were obtained in this study, with female cod endolymph containing 65.5% and male endolymph containing 73.7% of the total quantity of Ca measured in the blood plasma. Andreasen (1985) investigated variations in the free (ionized) and total calcium concentrations in the blood plasma of *Oncorhyncus mykiss* and found a very strong correlation (r^2=0.99) between these two forms of calcium with 67% of the total calcium being in the ionized form. These results provide evidence of the significance of levels of plasma proteins in mediating the levels of calcium in fish endolymph. Data on human plasma indicate that 38% of plasma calcium is in the protein-bound form and 62% is diffusible, that is, ionized or complex-bound calcium (Sena and Bowers, 1988). These data indicate that general principles applicable to the proportions of free and bound calcium in human plasma and serum may be applicable to studies of fish plasma and serum.

Furthermore, the fact that a greater percentage of the total plasma calcium occurs in the endolymph in males was indicative of higher levels of calcium-binding proteins in the female plasma. During the winter period of gonadal development female plasma protein levels were consistently greater than in males. It was likely that these increased plasma protein levels and the concomitant reduction in the relative proportion of calcium in the endolymph were attributable to the calcium-binding egg yolk precursor protein, vitellogenin.

Although the physical properties and behavior of Ca^{2+} and Sr^{2+} are very similar, the seasonal variations in the distributions of these two ions in cod plasma

and endolymph were somewhat different. The notable similarity between these data was the September peak in both endolymph strontium and calcium in the females, which was probably related to development of the ovaries. Evidence for interaction amongst these variables was provided by multiple regression analysis (Table 3.5). The basis for these relationships was probably due to the total quantity of calcium-binding protein present and the relative discrimination of these proteins in binding Ca^{2+} over Sr^{2+}. Taking these points into account, an increase in plasma protein in the females as vitellogenin, and an associated increase in plasma calcium would be expected to result in an increase in the relative proportion of protein-bound calcium in the plasma and an associated reduction in the percentage of the total plasma calcium measured in the endolymph. In female cod there was an increase in total plasma calcium during the period of gonad development from approximately 1.5 $mM \cdot l^{-1}$ to 2.3 $mM \cdot l^{-1}$, whereas endolymph calcium increased from 1.3 $mM \cdot l^{-1}$ to 1.7 $mM \cdot l^{-1}$, an increase of exactly half that estimated in the plasma. This indicates that, to a large extent, the increase in plasma calcium in females was largely due to calcium in the protein-bound form. This conclusion is supported by information presented in Simkiss (1974).

Seasonal increases in male cod plasma calcium were greater than in females and mean monthly values ranged from 1.2 $mM \cdot l^{-1}$ to 2.3 $mM \cdot l^{-1}$, yet there were no significant changes in endolymph calcium that could be related to spawning. This indicates that there are factors, in addition to proteins related to gonad development, that are affecting the quantities of Ca^{2+} and Sr^{2+} in the plasma and, ultimately, the endolymph.

Because of the similar physical properties of Ca^{2+} and Sr^{2+}, it might be expected that the variations in the two ions would be similar, but this does not occur. In female cod plasma mean monthly strontium values ranged from 8.1 $\mu M \cdot l^{-1}$ to 17.2 $\mu M \cdot l^{-1}$, while in the endolymph the range was from 1.8 $\mu M \cdot l^{-1}$ to 7.4 $\mu M \cdot l^{-1}$. Unlike for calcium, the strontium levels in the plasma and the endolymph did not overlap and, while the relative variation in plasma calcium and plasma strontium values were similar, the maximum endolymph strontium values were more than 4 times the minimum value compared with a 30% increase in endolymph calcium. These differences may be attributable to the relative discrimination against strontium by calcium-binding proteins. Therefore, increases in plasma calcium and strontium due to similar physiological needs, such as gonad development are reflected in the plasma

in a proportional manner. However, the increases in endolymph calcium and strontium are not comparable because the endolymph component of these ions is, most likely, a function of the amount of calcium-binding protein and, thus, the proportion of protein-bound to diffusible calcium and strontium in the plasma. This, in turn, is due to the fact that calcium-binding proteins selectively bind calcium over strontium. The degree of discrimination between these ions will vary from protein to protein and will, of course, be dependent on other characteristics of the plasma such as pH and the quantities of other ions present. The data on female cod plasma indicated that a 9.1 $\mu M \cdot l^{-1}$ increase in plasma strontium corresponded to a 5.6 $\mu M \cdot l^{-1}$ increase in endolymph strontium, compared with a 0.8 $mM \cdot l^{-1}$ increase in plasma calcium and a 0.4 $mM \cdot l^{-1}$ increase in endolymph calcium. This may be an indication that 50% of the increased calcium and 38% of the increased strontium in the plasma is in the protein-bound form and provides additional evidence for discrimination against strontium in preference for calcium.

The major deviation from the linear relationship between plasma Sr and endolymph Sr/Ca (Fig. 3.30) was attributable to five fish with endolymph Sr levels in excess of 8 $\mu M\ l^{-1}$. These high endolymph Sr levels were associated with individuals with a high GSI, specifically four female and one male fish (Fig. 3.32). Relationships involving levels of endolymph and plasma phosphate, glucose and triglycerides serve to further identify the physiological condition of these individuals in spawning condition. The highest Sr/Ca ratios measured in the otoliths of blue grenadier were from three female fish (Chapter 2), each with relatively high GSI's and, as in the cod, this is probably indicative of a high endolymph Sr/Ca ratio that can be associated with gonad development.

Increases in endolymph Sr were significantly related to increases in plasma protein. However, it is likely that this relationship was due, not to increases in plasma protein in general, but to increases in specific plasma proteins. For this reason a preliminary investigation was made into the seasonal variations in plasma proteins to determine if there were significant changes over the year and among individuals. The data indicate very significant changes in the levels of the major plasma protein components, specifically globulins and albumin. Albumin, besides acting in osmotic regulation and the transport of other plasma constituents, is the major calcium-binding protein present in blood plasma (Lehninger, 1975). The large variations in albumin could have a very significant impact on the relative proportions

of diffusible and non-diffusible calcium present in the plasma and, ultimately, the composition of the endolymph.

Radtke (1984b), Radtke (1989), Radtke and Morales-Nin (1989) and Townsend *et al.* (1989) attempt to explain the variations in otolith Sr/Ca ratios in terms of temperature. Townsend *et al.* (1989) infer both the distribution and recruitment patterns of larval herring, *Clupea harengus*, on the basis of a relationship between otolith Sr/Ca ratios and temperature. These interpretations are probably misleading as well as oversimplifications of the actual mechanism that results in variations in otolith Sr/Ca ratios. I have demonstrated a negative correlation between temperature and both plasma Sr and endolymph Sr. On this basis, it seems that physiological changes are resulting in changes in the level of Sr in both the plasma, the endolymph and, ultimately the otolith. The temperature related changes in plasma Sr, in the case of adult cod, were probably associated with gonadal development and, thus, can be related to changes in plasma Ca. The relationship between endolymph Sr and temperature was probably a further manifestation of the physiological changes associated with reproduction and the related changes in the plasma protein complement.

Changes in the endolymph composition associated with adult fish during gonad development cannot be used to explain changes in otolith Sr/Ca ratios measured in larvae and juveniles. However, a calcium-binding protein mechanism can also be operating in the larvae and juveniles. These points are considered in Chapters 2 and 4, and are also implied by the data presented in Townsend *et al.* (1989). As stated previously changes in growth rate, age, physiology and health can affect the protein complement of fish. The exact nature of these changes is beyond the scope of this study but, in some instances, it is possible to gain an insight into the mechanisms involved. For example, Townsend *et al.* (1989) discard their Sr/Ca ratio versus temperature validation data (their Figure 6a) on the basis that the data do not fit their hypothesis. Apart from this being poor scientific practice, they do suggest reasons for the failure of the validation that agree with data presented earlier in this study. They postulate that what they believe to be inappropriately high otolith Sr/Ca ratios at higher temperatures were due to stress and the resultant reduced ability of the fish to discriminate physiologically between Ca and Sr. Two *Arripis trutta* in my validation study (Chapter 2) were stressed with fin rot and had relatively low condition factors. These individuals also had the highest mean otolith Sr/Ca ratios (0.0034) of any of

the captive Australian salmon. I also found consistent evidence for increased Sr/Ca ratios in stressed, wild juvenile Australian salmon from Bream Creek Lagoon and these data are presented and discussed in Chapter 4. However, although the "stressed" fish in Townsend *et al.* (1989) had higher otolith Sr/Ca ratios than they expected these ratios were still lower than those measured in other, supposedly unstressed, individuals. Nevertheless, stress may change the protein complement and ultimately affect the relative proportions of Ca and Sr in the endolymph.

Although there is clearly a relationship between the quantity of Sr in the endolymph and the otolith (Fig. 3.41), the correlation between the two data sets is not as good as had been anticipated. As is indicated below in the discussion of the results of the linear multiple regression models, the interaction of several variables may ultimately play a part. However, it is also important to reiterate the difficulties that arise when using measurements of the outer otolith margin composition as an indicator of the composition of the most recently formed portions of the otolith. Because of sample destruction during electron microprobe analysis of readily vaporized minerals such as carbonates, it is necessary to use a scanning raster or a defocussed electron beam. Ideally, the minimum size for a square window that would minimize sample destruction is 10 x 10 μm. In the fast growing juvenile *Arripis trutta* used in the validation experiments there is clearly more than 10 μm of recently formed otolith material available for analysis. But in the slow growing adult cod, 10 μm of otolith material may encompass aragonite deposited in the last several months, particularly in the winter periods when the growth rate would be lowest. The result is the comparison of a temporally discrete endolymph sample with an integrated sample of otolith composition, not an ideal situation.

The results of the linear multiple regression models, while of little practical use in actual prediction, provide a valuable insight into those factors that ultimately influence the Sr content of both fish endolymph and otoliths. Most importantly, in view of the present interest in fish otoliths as predictors of environmental temperature, is the fact that the variable ambient temperature was the first variable selected in models to predict the Sr content of fish endolymph (Table 3.5). This illustrates that, in the otoliths of adult cod at least, temperature does not appear to directly influence the Sr content of fish otoliths. Furthermore, temperature does not appear as a variable in any of the multiple regression models to predict otolith Sr (Table 3.6). Alternatively, as hypothesized on the basis of data presented in Chapter 2, the effect of temperature

or, perhaps more generally, the effect of seasonal changes in physiology which are associated with changes in temperature, are the primary force in altering the composition of fish endolymph and, concomitantly, fish otoliths. This conclusion is highlighted by the relationship that also exists between the Sr content of blood plasma and endolymph, evident in both male and female fish.

Both species that have been studied most intensively in these investigations as mature adults, blue grenadier and cod, spawn during the coldest winter months, and, thus, it is plausible that the occurrence of peak otolith Sr levels in the winter is largely associated with the physiological changes related to gonad development. This hypothesis is supported, in part, by the occurrence of peak otolith Sr levels measured in the summer and fall in juvenile Australian salmon. However, the presence of a definable peak at any time of the year in juvenile fish clearly implicates the importance of factors other than reproduction in the control of otolith microchemistry. Gonadosomatic index was the second most important variable in the prediction of endolymph and otolith Sr in female cod, whereas neither GSI or gonad weight was used to predict the dependent variable in male cod. In view of these results it would be important to investigate variations in endolymph and otolith composition in a species that spawned in the summer.

The distribution coefficient K_{Sr}, defined by,

$$\left(\frac{Me}{Ca}\right)_{CaCO_3} = K_{Me}\left(\frac{Me}{Ca}\right)_{solution} \qquad \text{(Eq. 3.5)}$$

where Me and Ca refer to the molar concentrations of the trace metal and calcium present in the solid phase calcium carbonate and in the precipitating solution, found for the cod was significantly different from that found in Chapter 2 based on a wide range of fish species (Fig. 3.50). The distribution coefficient, K_{Sr}, for the cod data only is 0.146±0.31 compared with 0.255±0.052 for the multi-species estimate. The two slopes were compared by the use of a t-test (Zar, 1974) and were found to be significantly different ($t=25.6$, $df=152$, $P<0.0001$). However, inspection of the two data sets indicates that there is considerable overlap and the precipitation of

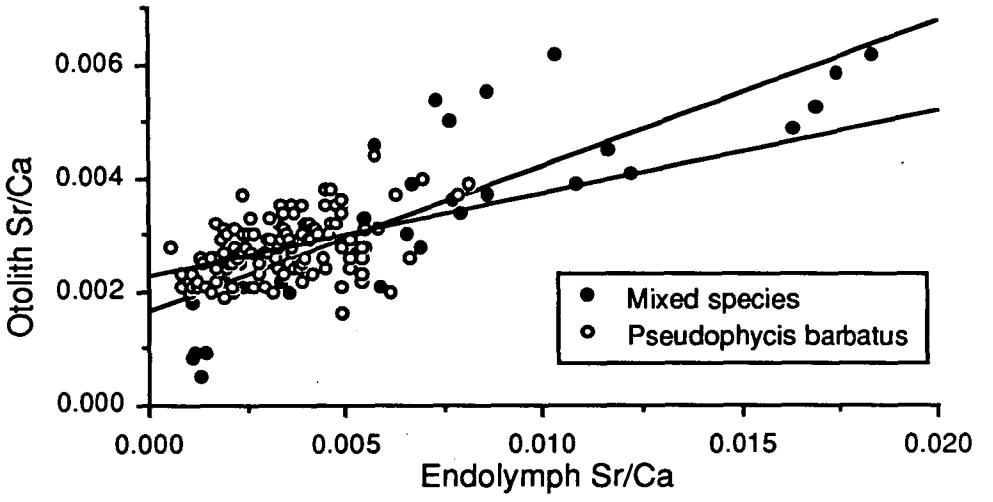

Figure 3.50 Comparison of the relationship between otolith Sr/Ca and endolymph Sr for the cod data and similar data from several species (see Chapter 2). The line for the cod data is described by the equation O_{Sr}= 0.0023 + 0.1456(E_{Sr}), (r^2 = 0.19, P<0.001, n = 115) and for the mixed species data the line is described by O_{Sr}= 0.0018 + 0.2453(E_{Sr}), (r^2 = 0.82, P<0.0001, n = 44). The slopes of the two lines are significantly different (t = 25.6, df = 152, P<0.001).

endolymph Sr/Ca to form the otolith is probably dominated by similar properties in all species considered. In both cases the values for K_{Sr} are low when compared with data obtained from corals and some bivalves which have K_{Sr} values of approximately 1.0. This point is discussed briefly in Chapter 2.

Low K_{Sr} values for fish otoliths in general may be due, in part, to the potential effect of precipitation rate on trace element incorporation. Unfortunately, few studies have considered the effect of aragonite or calcite precipitation rate in inorganic systems, let alone in biogenic carbonates. However, it is generally accepted that precipitation can play a major role in determining distribution coefficients (Ohara and Reid, 1973) and, even in investigations of inorganic precipitates, inter-study differences in distribution coefficients are attributed to differences in the rate of precipitate formation (Okumura and Kitano, 1986). Lorens (1981) investigated the effect of precipitation rate on the incorporation of Sr, Cd, Mn and Co in calcite. His data indicated that K_{Sr} increased with increasing precipitation rate, whereas K_{Cd}, K_{Mn} and K_{Co} decreased with increasing precipitation rate.

The partial dependence of the distribution coefficient on crystal growth rate is based on the interaction between metal ions and the morphologically variable crystal surface (Kinsman and Holland, 1969; Lorens, 1981; Morse, 1983) (see Chapter 8 regarding the morphology of otolith aragonite crystals). The crystal surface is heterogeneous in terms of morphology and, thus includes sites of different energies (Burton *et al.*, 1951). During crystal growth cations become incorporated in these sites and with further crystal growth the coordination of the cation increases until it is a fully coordinated component of the crystal lattice. The amount of time required for full coordination of a particular cation site will vary depending on the initial degree of coordination of the site. At slow crystal growth rates all cation sites would have adequate time to reach equilibrium with the precipitating solution and, in these instances, the resulting distribution coefficient would be near the value expected for an equilibrium distribution coefficient. Alternatively, if crystal growth were proceeding at a very rapid rate, in a similar system with a complex distribution of cation sites with differing coordination, then an individual cation might become incorporated before equilibration, irregardless of the initial coordination of the cation site. In these circumstances, the distribution coefficient would be indicative of the level of coordination for which equilibration could be achieved in the time available (Kinsman and Holland, 1969; Lorens, 1981). Simply, slow precipitation rates would

result in low distribution coefficients indicative of equilibrium between the precipitating solution and the solid, whereas fast rates of precipitation could result in high distribution coefficients that are more an indicator of the initial number of cation sites suitable for the incorporation of particular cation such as Sr.

Precipitation rate relationships as described above may be an important determinant of the distribution coefficient. Although it is difficult to accurately estimate the crystal growth rate of fish otoliths it is probably not unreasonable to conclude that their crystal growth rate is slower than that of coral or molluscan calcium carbonate during comparable growth phases. If this were true, then the slower precipitation rates in fish otoliths may explain the relatively low distribution coefficients for Sr when compared with corals and molluscs. Before accepting these conclusions it is important to recall the results of the validation experiments discussed in Chapter 2 where there was no evidence that otolith growth rates had an effect on the Sr/Ca ratio measured in the otoliths of juvenile *Arripis trutta*. However, this point does not exclude the possibility that the value for K_{Sr} had changed. Unfortunately, it was impossible to estimate the levels of Sr and Ca in the endolymph and, thus, values of K_{Sr} in these small fish because of the inadequate quantities of endolymph that could be extracted from each fish ($\approx$ 2 µl). Furthermore, it is possible that all but the most extreme ranges of crystal growth rate are obscured by other physiological factors. Therefore, on the basis of the data available it seems impossible to draw a definitive conclusion as to the effect of aragonite precipitation rate on the value of K_{Sr}.

3.4.2.2 *Sodium, potassium and sulphate*

The data on sodium and potassium are conspicuous due to the lack of any notable correlations with other physiological data. This is not altogether surprising due to the fact that sodium and potassium levels are very important physiologically and are maintained within relatively narrow limits under all but the most extreme physiological conditions (Love, 1980). However there were significant seasonal variations in sodium and potassium in the endolymph and otoliths.

Despite the difficulty in explaining the basis for seasonal variations in Na and K levels the data are still interesting in light of their agreement with theoretical and empirically based models of alkali metal coprecipitation in inorganic precipitates (Kitano *et al.*, 1975; White, 1977; Busenberg and Plummer, 1985; Okumura and

Kitano, 1986). Several studies have attempted to relate the sodium and potassium content of biogenic carbonates to data obtained from studies of inorganic precipitates. In many cases the range of Na and K concentrations predicted by the models are not an adequate estimate of the data obtained from biogenic carbonates.

The initial impetus for investigations of the sodium content of carbonates was the possibility that these data could yield information on the salinity of the waters from which the carbonates were precipitated (Land and Hoops, 1973). There are several factors that could make inferences regarding salinity difficult. Most importantly, the composition of the solution from which precipitation actually occurs, in regards to sodium and calcium at least, must be directly related to the composition of the ambient water. In corals and molluscs (Crenshaw, 1972; Wada and Fujinuki, 1976; Lorens, 1978; Wilbur and Saleuddin, 1983) this assumption seems to be satisfied. Lattice-bound sodium must be distinguishable from sodium that is trapped or absorbed as well as sodium that is a component of any organic compounds incorporated in the biogenic carbonate (Land and Hoops,1973). Amiel *et al.* (1973) found that 90% of the sodium in aragonitic corals was incorporated in the mineral fraction with the remaining 10% being adsorbed or related to organic compounds. These results are in agreement with the findings of Billings and Ragland (1968) who also concluded that about 10% of the sodium in corals was incorporated in an organic phase. Lorens and Bender (1980) found a significant relationship between the Na/Ca ratio of the extrapallial fluid and the Na/Ca ratios in the aragonitic portion of the shells of *Mytilus edulis*. This relationship was of a similar form to that found by both White (1977) and Okumura and Kitano (1986) for precipitates from inorganic solutions but the intercept of the relationships was significantly different. The net result was that Na/Ca ratios in *Mytilus edulis* aragonite were 50 to 100% greater than that predicted on the basis of inorganic studies. Lorens and Bender (1980) suggest that this may be due to differences in the ion activity coefficients for sodium and calcium. Generally, these effects would be relatively small on the basis of the empirical and theoretical relationships described by White (1977) (Equation 3.1). Lorens and Bender (1980) indicated doubt that Na was biologically concentrated in a shell organic component, but they have little evidence to refute this possibility.

The fact that data presented here on endolymph Na, K and Ca can be used to provide an estimate of the range of Na and K in the fish otolith accentuates several points. Firstly, the mean endolymph Na/Ca (0.111/0.00125 = 88.8) and K/Ca

(0.0671/0.00125 = 53.7) ratios are very different from the same ratios found in seawater and, concomitantly, coral fluids and molluscan extrapallial fluid. In seawater Na/Ca and K/Ca ratios are 45.4 (0.468/0.0103) and 0.99 (0.0102/0.0103), respectively. These extreme differences may alter the kinetic properties of the solutions and, thereby, result in different precipitates. White (1977) found significant differences in the kinetics of solutions with different levels of Na and Ca. More importantly, if White's (1977; Table 1 and Fig. 1) data are examined it is evident that, fortuitously, his experimental solutions more closely follow the composition of fish endolymph, than the composition of seawater or the fluids of molluscs and corals. In fact, his data are modelled on the basis of log (a^2_{Na}/a_{Ca}) for an estimation of the level of Na and Ca in the solutions and, to obtain values of log (a^2_{Na}/a_{Ca}) similar to seawater it is necessary to consider, on the basis of White's (1977) study a solution with approximately 0.001 M Ca and 0.100 M Na, almost precisely what is found in fish endolymph, but very different from seawater. It seems, under these conditions, White (1977) has produced a model for the precipitation of aragonite from a fish endolymph-like fluid rather than a fluid with characteristics similar to seawater! The inorganic systems he employed for investigating the precipitation of K in the presence of Na are more general, but they also provide a good inorganic model of the fish endolymph system. On the basis of these factors it is not surprising that the inorganic model is more successful at predicting fish otolith composition rather than coral or shell composition.

Several studies have considered the relationship between the composition of the precipitating fluid and the calcium carbonate precipitate without making measurements of the precipitating fluid composition (Kinsman, 1969; Buchardt and Fritz, 1978; Smith *et al.*, 1979; Lorens and Bender, 1980, Townsend *et al.*, 1989). On this basis the distribution coefficient (Equation 3.5) actually serves as an indicator of the relationship between the ambient seawater or freshwater environment and the composition of the carbonate. There are obvious difficulties in attempting to determine the relationship between the precipitating fluid and the precipitate while assuming the composition of the solution is the same as that of the ambient environment, although in some cases this assumption may be valid, particularly when dealing with corals and molluscs.

Quantities of sulphate, measured as sulphur, in the cod otoliths varied over a similar single cycle over the year in both males and females (Fig. 3.40). The levels of

sulphate detected in the cod otoliths, mean of 6.1±1.6 mM kg^{-1}, were fairly low, but not inconsistent with data from other biogenic aragonites (Kitano *et al.*, 1975; Busenberg and Plummer, 1985). It is impossible to draw any definitive conclusions regarding the seasonal variability in the S/Ca ratio data, but, as was indicated by data from wild juvenile *Arripis trutta* and adult *Macruronus novaezelandiae* (see Chapter 2), there is a definite summer maximum and winter minimum associated with these data. Although little information is available to determine the proximal causes for the consistent seasonal variations in S/Ca ratios among three unrelated fish species, the fact that there is correspondence among these data lends support to the argument that the variability is linked to the same processes that result in the formation of "protein-rich" otolith zones (fast growth) during the summer and "protein-poor" zones (slow growth) in winter. The range of sulphur levels measured in cod is approximately 4 to 10 μM kg^{-1} and, as in the blue grenadier and Australian salmon, a reasonable proportion of this total may be incorporated into the otolith as organics in the form of two sulphur containing amino acids, cysteine and methionine, that are found in fish otoliths (see Chapter 2). Lorens and Bender (1980) concluded that sulphur measured in the calcite of *Mytilus edulis* was incorporated as part of the shell organic matrix.

Alternate theories regarding the incorporation of sulphur into calcium carbonate do not preclude the possibility that the sulphur is a component of the organic matrix. It has been suggested that the Na present in calcium carbonate occurs partly as sodium sulfate (Na_2SO_4) (Kitano *et al.*, 1975; Busenberg and Plummer, 1985). The extent to which this occurs is not known. However, a manifestation of this property may be the occurrence of Na/Ca and S/Ca ratio maxima in cod otoliths both in March (Fig. 3.38 and 3.40).

3.5 SUMMARY

Seasonal variation in the chemistry of cod, *Pseudophycis barbatus*, plasma, endolymph and otoliths was investigated to determine the effects of physiology and environment on the trace element composition of otoliths. Cod blood, endolymph and otoliths were collected from freshly caught fish at sea. Quantities of protein, triglycerides, phosphate, glucose, calcium, sodium, potassium and strontium were determined in the blood plasma and the endolymph. These data, in conjunction with temperature data and basic biological information such as length, weight, sex, gonad

weight, condition and age were used to explain the levels of Sr, Na, K, and S found in cod otoliths and, in some cases, the data were capable of explaining a large percentage of the seasonal variation in otolith chemistry.

The results clearly indicate that temperature does not directly affect the Sr, Na, K or S content of otoliths, but, in adult cod, that changes in temperature are associated with major physiological changes, specifically the development of the gonads. These seasonal physiological changes are associated with changes in the chemistry of the blood plasma and the endolymph, which result in differences in the trace element composition of otolith material.

A brief investigation of the variability in the relative protein composition of the plasma indicates that there are large intraspecific and seasonal variations in protein complement, notably the albumins and globulins. These changes may ultimately affect the composition of endolymph and otoliths due to differences in metal-binding capacity. This is an area of potential further investigation.

These data show that the interpretation of otolith microchemistry data cannot be based on temperature data alone and, thus, corroborate hypotheses generated in Chapter 2. In the case of cod, the negative correlation between temperature and otolith Sr is a fortuitous one, with changes in physiology being the major force. In other species changes in physiology similar to those observed here are likely to occur at very different times of the year. Therefore, before the interpretation of otolith microchemistry data is undertaken, the researcher must carefully consider the various environmental and physiological factors unique to each species.

CHAPTER 4

USE OF OTOLITH MICROCHEMISTRY IN STUDIES OF STOCK SEPARATION, NURSERY GROUNDS, AGE ESTIMATION AND SCHOOL COHESIVENESS

4.1 GENERAL INTRODUCTION

A wide range of biological structures in both plants and animals grow in such a manner that their production can be related to time. They can range from trees, to teeth, molluscan shells and fish otoliths. In most cases, the growth processes resulting in these structures are not constant, particularly in long-lived organisms. Nevertheless, regular periodicities in the morphology of these structures are frequently evident and their spatial distribution is based on temporal phenomena. These morphological periodicities are typically manifestations of seasonal variations in the suitability of a habitat for growth. This is the case for the production of annuli in trees, visualized as latewood (slow growth) or earlywood (fast growth) (Fritts, 1976) as well as the annuli in molluscan shells or fish otoliths, identified as hyaline (slow growth) and opaque (fast growth) zones. Concomitant with variations in environmental conditions that are capable of effecting extreme changes in growth rate are changes in both the physiology and composition of the organism. These changes, particularly those related to factors such as temperature, starvation and reproduction, are discussed in some detail in Chapters 2 and 3, and in Love (1970, 1980). On the basis of these principles, and data presented in earlier portions of this thesis, it seems plausible that some record of physiological and/or environmental variation would reside within those structures where variations in growth rate are clearly manifested. However, as previously discussed, the ability to interpret variations in the chemical composition of such structures is severely hampered by the interaction of a large number of variables.

Although the combined physiological and environmental basis for time related changes in the composition of otolith material may often be obscure, the value of these periodicities is not necessarily negated. Time-related variations in otolith chemistry may be useful in investigating several aspects of fish biology and may provide a level of understanding beyond what is achievable using visual methodologies alone. Changes in otolith morphology and crystallography are, in

many cases, not reflected in any readily detectable change in otolith chemistry and, likewise, changes in otolith chemistry are not always manifested in the structure of the otolith. As such, variations in otolith chemistry can provide another level of information for investigating the biology of fishes.

Extreme environmental and physiological events such as starvation and reproduction can result in the formation of check marks in the otoliths of fishes (Campana, 1983; Campana and Neilson, 1985). These marks can occur at any time during the year and their presence can serve as a relative time marker for those individuals experiencing the same conditions. These same events may cause changes in the chemistry of the otoliths. A specific example of this type of event in wild fish is presented in Section 4.2. A series of similar events over virtually any time frame may serve to identify an individual as being from a particular habitat. All individuals of the same size and growth rate might display similar marks or chemical variations within their otoliths. Recognition of similar chemical periodicities or variations within a group of fish from the same population, stock or school may have several implications: (1) individuals are genetically related; (2) individuals have experienced similar environmental conditions; and, (3) similar physiological responses to the environment coupled with endogenous rhythms, perhaps in conjunction with ontogenetic physiological and habitat changes.

Despite ambiguity in the interpretation of the physiological basis for chemical variations in fish otoliths, I investigated the utility of these data in studies of nursery grounds, stock separation, age estimation, school cohesiveness, and diadromy. The theoretical basis for each investigation is considered in an introduction to the relevant section. Each section is treated as an independent entity, but information from each section is developed from a base established in the previous sections. These studies have considered fish from several different habitats and of numerous ages. I also consider the repeatability of data collected from otolith microchemistry "life-history" transects. The utility of otolith chemistry in studies of diadromy, because of it's clear and considerable value in such studies, is considered separately in Chapter 5.

4.2 Intercomparison of microchemical transects within individuals

4.2.1 Introduction

A basic assumption in studies of microchemical variations across otoliths is that these variations are consistent within individuals. On the basis of data presented in

Chapter 2, there are very significant variations in otolith chemistry within similar regions of an otolith, even in fish that are maintained under uniform, controlled environmental conditions. The existence of this variability obviously makes it difficult, if not impossible, to draw precise conclusions regarding the physiology of individual fish and the environmental conditions that they have experienced. This variability does not preclude the feasibility of detecting general trends or patterns in otolith microchemistry transects. However, before it is possible to draw general conclusions regarding the patterns of variation in microchemical transects it is necessary to investigate the variation that exists in multiple transects from individual otoliths. The essential criterion of these data is that the transects show relative increases and decreases in elemental ratios at similar positions on an otolith. Without this agreement, the intercomparison of microchemical transects among fish would have little value. This study investigates the differences that exist between multiple otolith microchemistry transects, from the same otolith, made with a wavelength dispersive electron microprobe. These relationships are considered in several species.

4.2.2 Materials and methods

Australian salmon (*Arripis trutta*), blue grenadier (*Macruronus novazelandiae*), cod (*Pseudophycis barbatus*) and Ray's bream (*Brama brama*) sagittae were prepared as described for blue grenadier in Chapter 2.

Due to the large quantities of data that are required to accumulate life-history transects, the protocol for collection of wavelength dispersive electron microprobe data has been altered for a large portion of the data considered in this chapter. To some extent, analytical precision has been sacrificed for the sake of speed of analysis. Data were collected on a Cameca Camebax Microbeam or Cameca SX-50 wavelength dispersive electron microprobe. Both microprobes were equipped with 2 vertical and 1 horizontal wavelength dispersive spectrometers and an energy dispersive spectrometer A beam current of 25 nA (measured on copper) and an accelerating voltage of 15 kV were used. Spectrometer scheduling was similar to that outlined in Chapter 2, but the counting times have been reduced to accommodate the increased beam current and to minimize specimen damage from the electron beam. Counting times were as follows:

Calcium	Strontium	Sodium	Potassium	Sulphur
20 sec	30	30	40	60

with background measured at 50% of the peak counting time at offsets both above and below the peak. Errors were similar to those estimated for microprobe analysis in Chapter 2.

Throughout this chapter life-history transects were collected from transverse sections of sagittae unless indicated otherwise. The life history transects begin at the primordium (otolith distance=0) and move towards either the dorsal or ventral otolith edge. In this particular section where multiple transects of single otoliths are considered, the transects were made from the primordium to both the dorsal and ventral edge of the sagitta.

In order to make it easier to visualize data from microprobe transects, data were smoothed with a 3-point moving average. Because of the errors inherent in the data collection system all transects contain a certain element of "noise". The magnitude of this noise can be determined from the information presented in Table 2.1. The 3-point moving average, thus, is an effective means of filtering noise. The solid line in microchemical transects is based on a 3-point moving average, whereas the data points are the actual atom ratios normalized to calcium.

4.2.3 Results and Discussion

Comparison of microprobe transects within a single otolith highlights a major problem in the interpretation of microchemical data. Inspection of replicate otolith Sr/Ca, Na/Ca, K/Ca, and S/Ca transects from two small cod (31 cm SL) show that there are large differences in otolith microchemistry within otoliths (Fig. 4.1). In Chapter 2 I demonstrated that the largest percentage of the variance in otolith microchemistry among individuals maintained in a controlled environment was attributable to variation within an otolith. Although the relative peaks and troughs in elemental ratios can be highlighted, as has been done in the cod Sr/Ca ratio transects (Fig. 4.1a), the relationship between these data is not immediately obvious. This is even after the data from the shorter otolith transects have been "stretched" so that they are easier to compare with the longer transects. In fact, the apparent relationship between transects from within an otolith is not markedly greater than that among sagittae from two fish of similar length and different sex, in the case of these two cod.

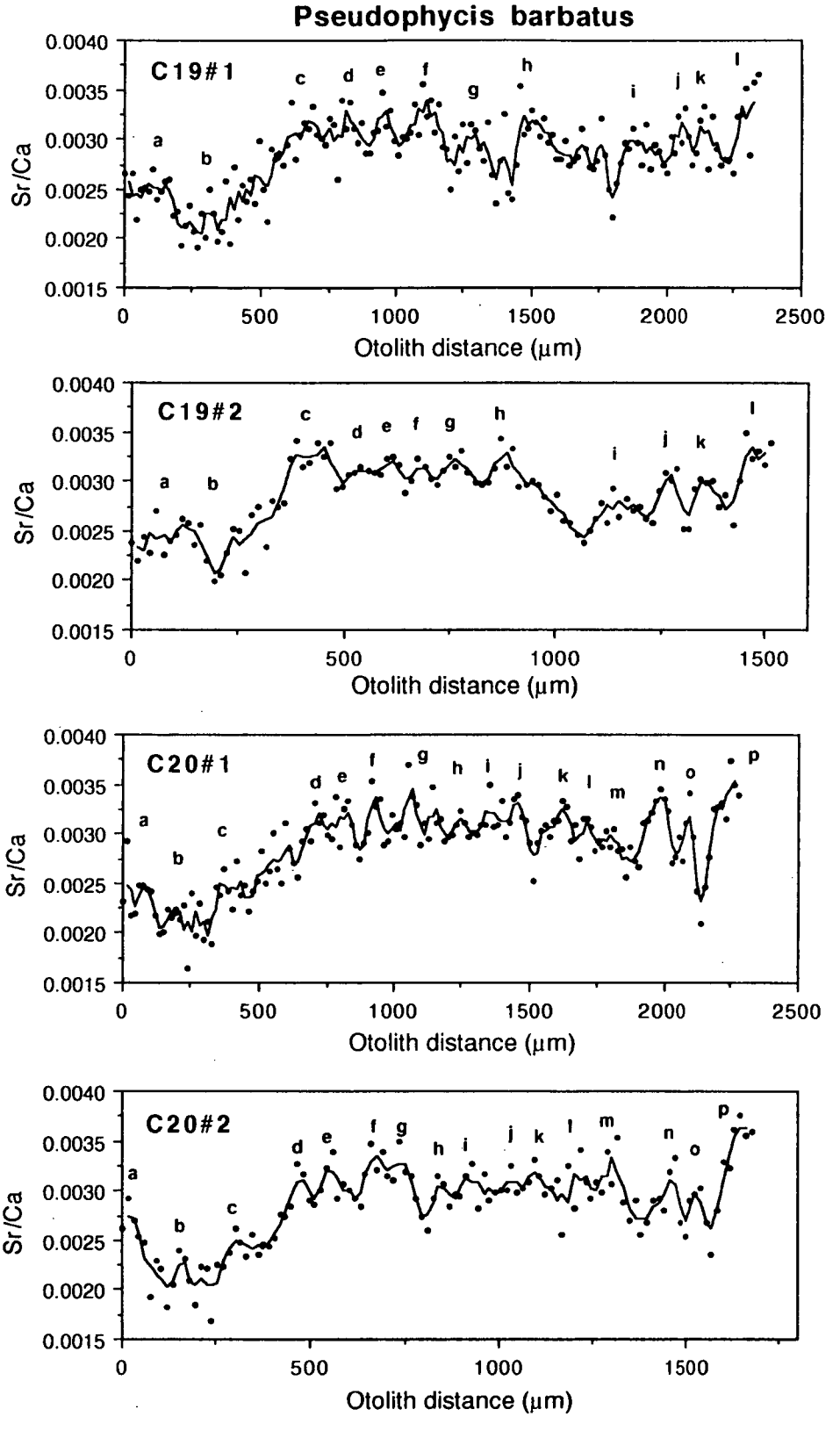

Fig. 4.1a Comparison of multiple Sr/Ca ratio transects across sagittae from two *Pseudophycis barbatus* caught in Variety Bay on 17 April 1988. Transect #1 is from the primordium (0) to the dorsal otolith edge; transect #2 is from the primordium (0) to the ventral otolith edge. C19-31 cm, 480 gm, male; C20-31 cm, 420 gm, female. Letters highlight common features of transects from within each otolith and are not for comparison between fish.

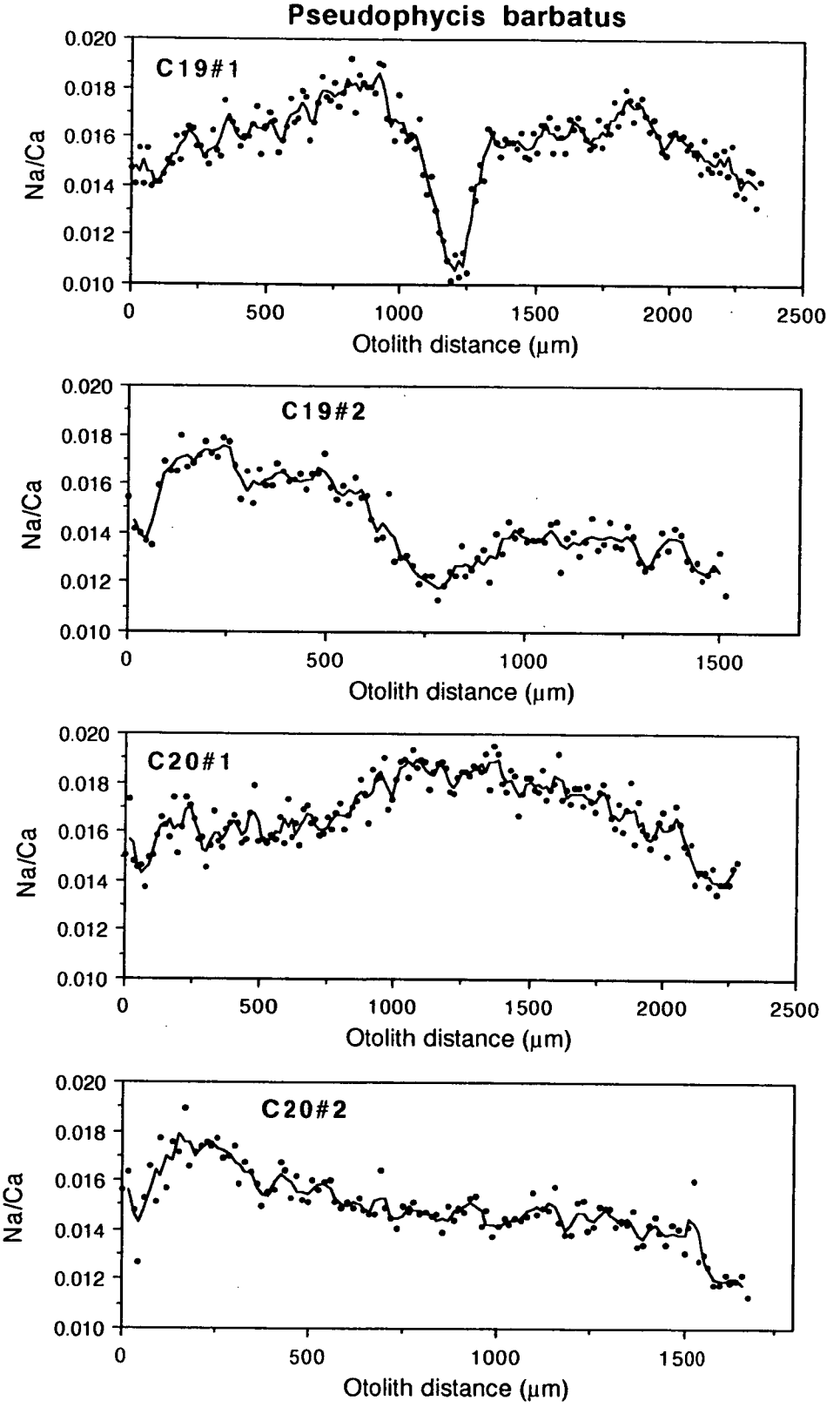

Fig 4.1b Comparison of multiple Na/Ca transects across sagittae from two *Pseudophycis barbatus* caught in Variety Bay on 17 April 1988. Other details as in Fig. 4.1a.

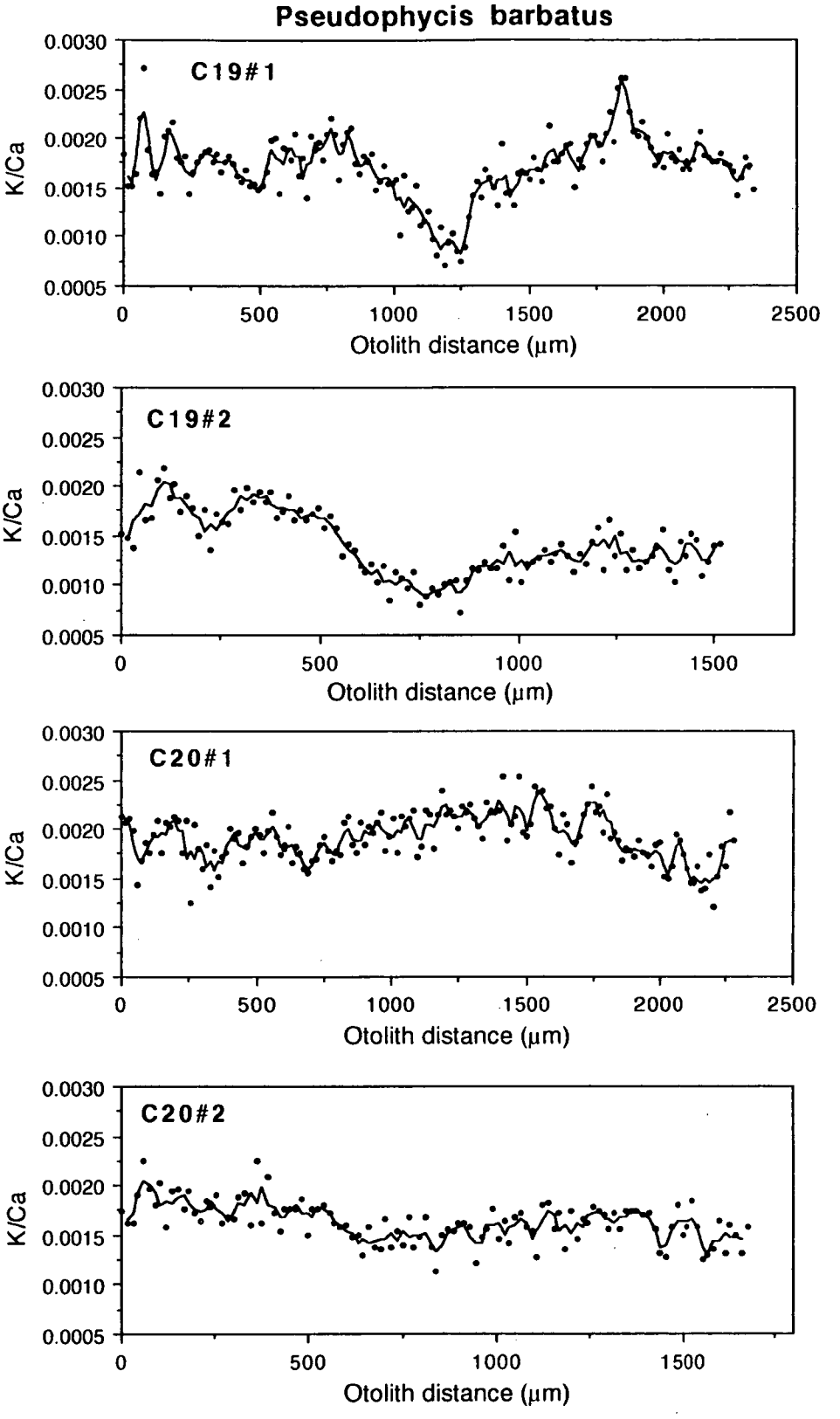

Fig 4.1c Comparison of multiple K/Ca transects across sagittae from two *Pseudophycis barbatus* caught in Variety Bay on 17 April 1988. Other details as in Fig. 4.1a.

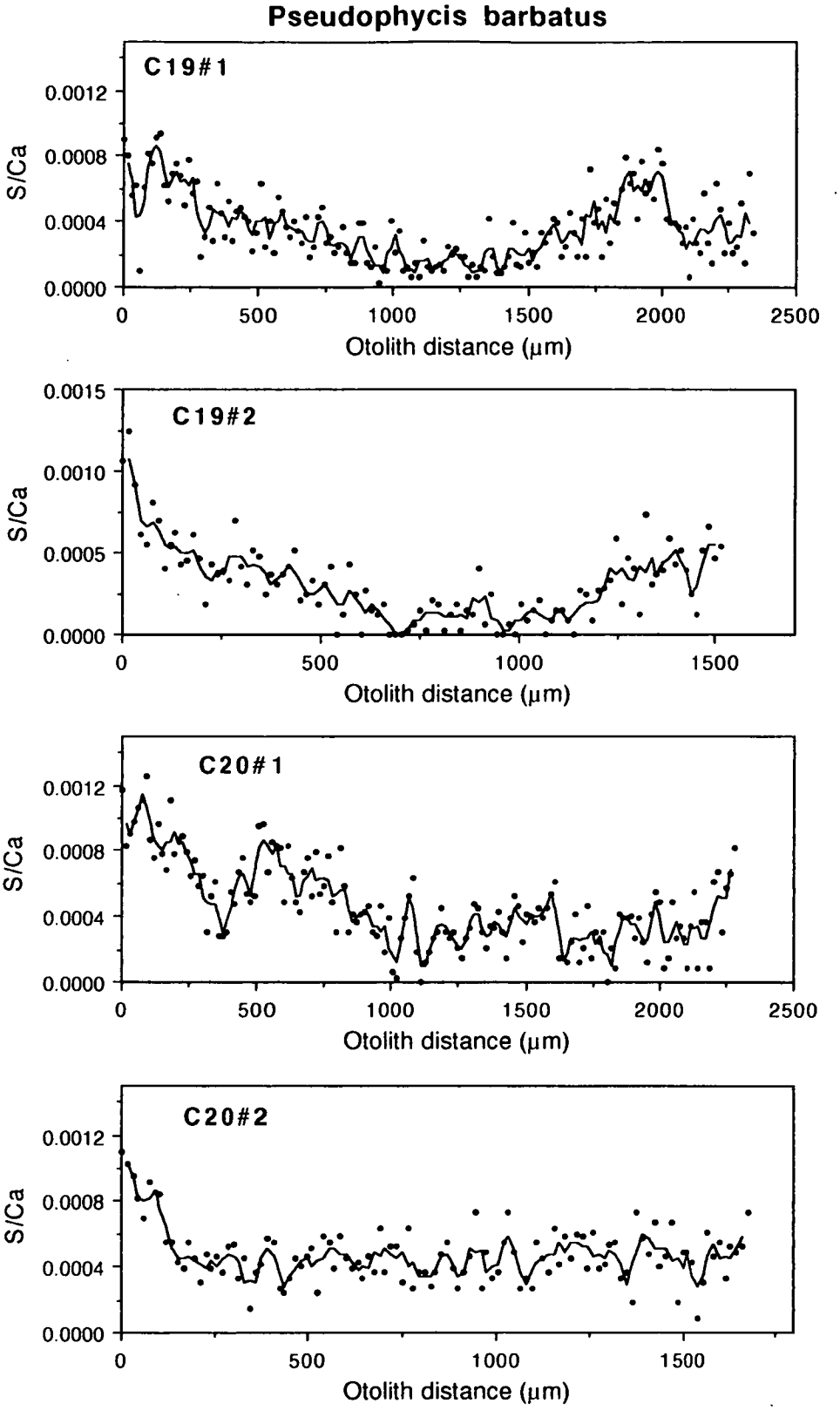

Fig 4.1d Comparison of multiple S/Ca transects across sagittae from two *Pseudophycis barbatus* caught in Variety Bay on 17 April 1988. Other details as in Fig. 4.1a.

Inspection of the cod Na/Ca data (Fig. 4.1b) shows even greater differences within an otolith than do the Sr/Ca data. For example, compare the drop in Na/Ca ratio at 1250 μm in transect C19#1 with that at 750 μm in transect C19#2. Since these data were collected from the same otolith, the drop in Na/Ca is undoubtedly a manifestation of the same physiological phenomena, yet the otolith transects are very different. Similar problems arise in K/Ca (Fig. 4.1c) and S/Ca (Fig. 4.1d) data in the cod.

Differences between transects from a single blue grenadier (Fig. 4.2a and 4.2b) are even more marked than those found in cod. These transects were taken on a single transverse section through the primordium of a 1+ year old blue grenadier. One transect was from the primordium to the dorsal otolith margin (Fig. 4.2a), the other from the primordium to the ventral margin (Fig. 4.2b). The Sr/Ca ratio data show a basic overall similarity and specific peaks from the two transects can be aligned with one another. However, this task requires some degree of subjectivity combined with "training". One factor that may make it difficult to compare the two transects is the fact that the overall range in otolith Sr/Ca ratios is not great in this specimen. Therefore, what appears as a relatively small change in one transect may not be visible in a different transect of the same otolith. It is very difficult, if not impossible to detect similarities among the Na/Ca, K/Ca or the S/Ca data collected in the two transects. This is partly due to the fact that the natural variability of the otolith is partially "swamped" by the variability that is related to the data collection process.

Differences as great as those found in the blue grenadier transects illustrated in Fig. 4.2 are the extreme. In most cases, a relationship is evident among Sr/Ca transects collected from single otoliths as illustrated by the Ray's bream Sr/Ca data in Fig. 4.3, although these similarities are generally qualitative rather than quantitative. It is possible to align the major peaks in data such as these, but it is important to realize that the relative height and position of the peaks may be altered due to both the frequency of the sampling and the spatial orientation of the samples. Similarities among Na/Ca, K/Ca and S/Ca data are generally less clear than for Sr/Ca ratio data.

Differences among otolith microchemical transects from within a single otolith are not always clearly related, particularly for Na/Ca, K/Ca and S/Ca data. This problem accentuates the significance of otolith microchemical variability as discussed in Chapter 2. These results suggest that microchemical data are very difficult, if not impossible to interpret in terms of absolute changes in a fish's physiology or

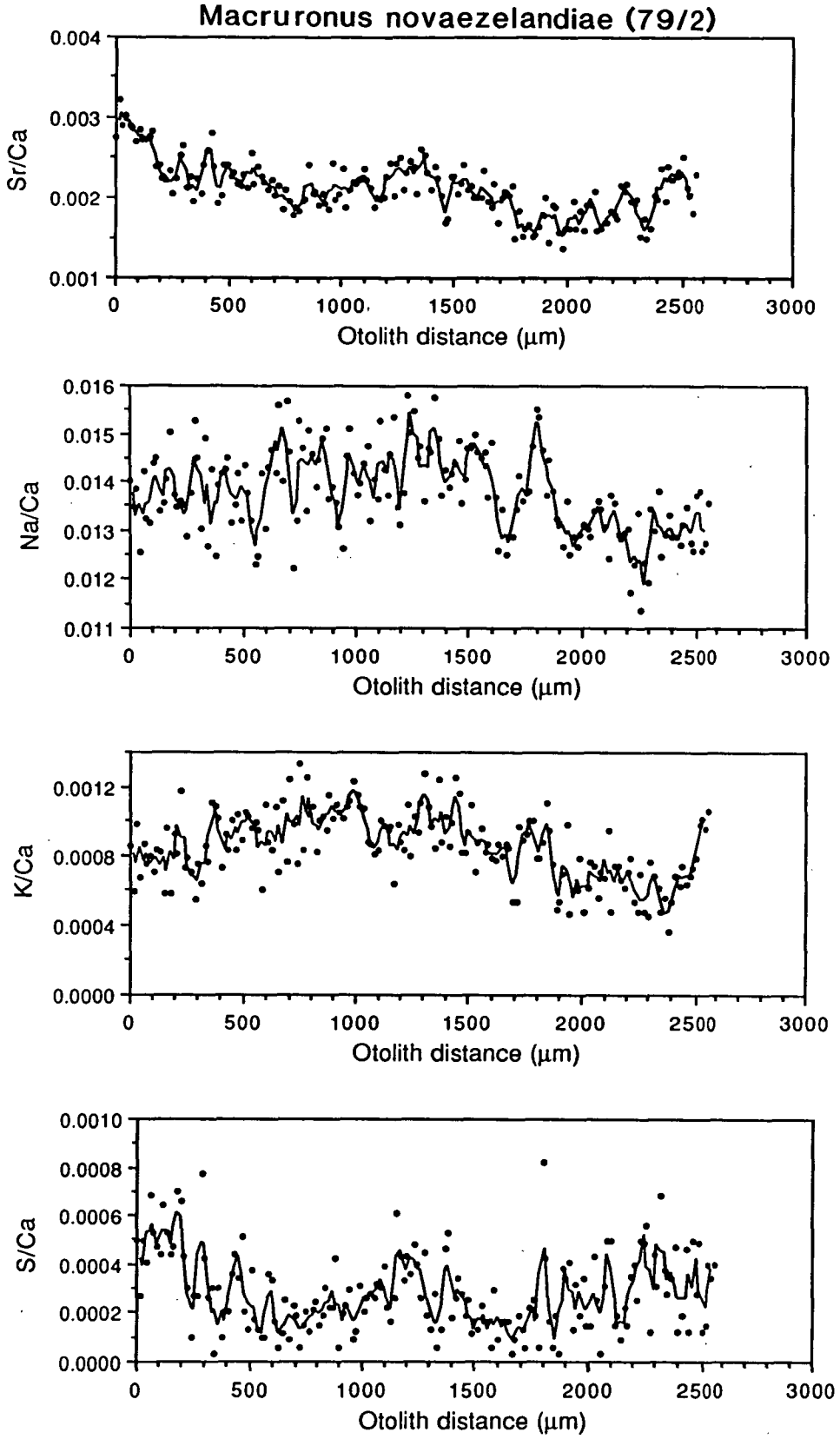

Fig 4.2a Microprobe transect of a *Macruronus novaezelandiae* sagitta from the primordium (0) to the dorsal otolith edge. Male, 41 cm SL, 210 gm caught October 1984. These data should be compared with those presented in Fig. 4.2b.

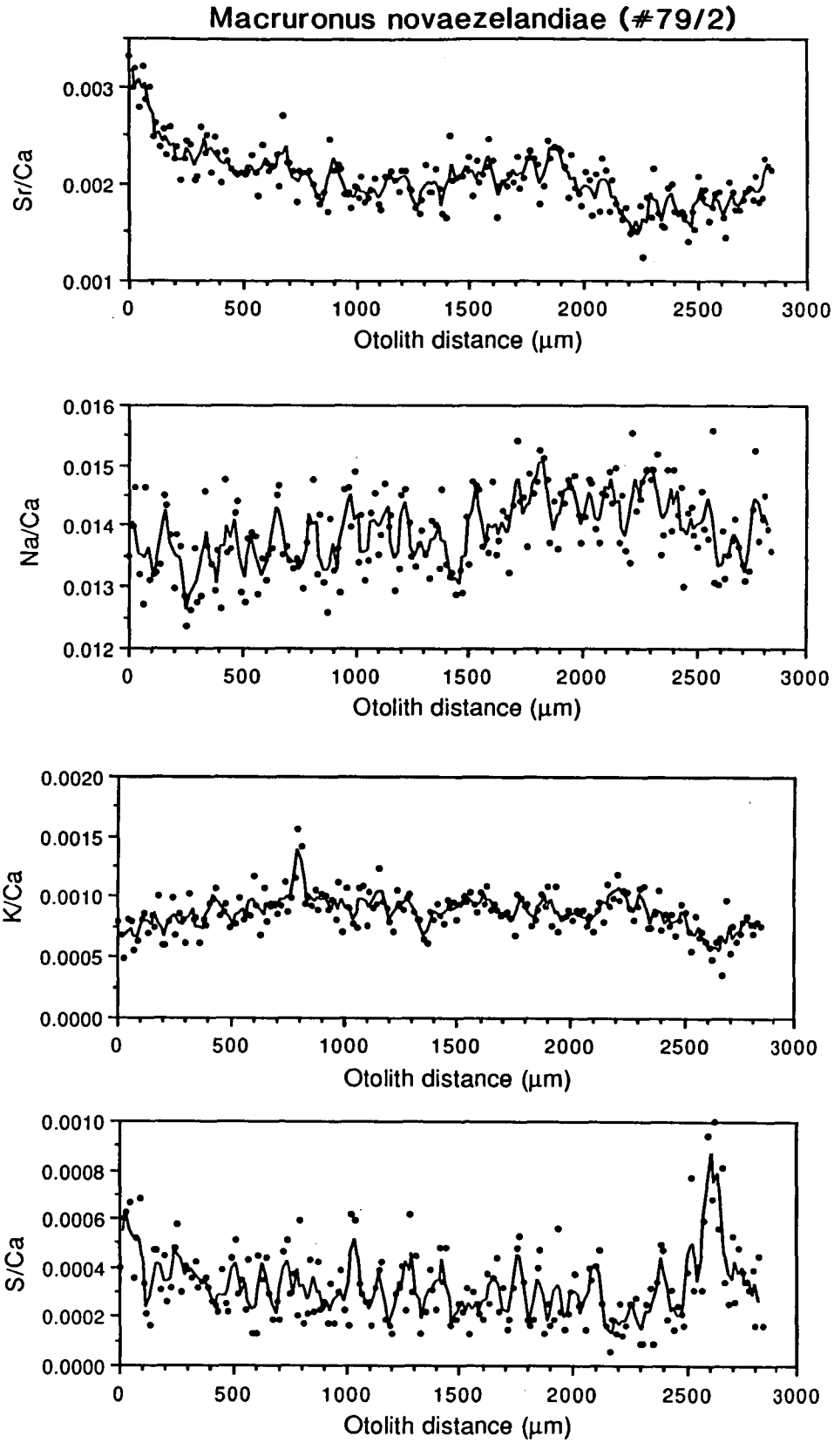

Fig 4.2b Microprobe transect of a *Macruronus novaezelandiae* sagitta from the primordium (0) to the ventral otolith edge. Male, 41 cm SL, 210 gm caught October 1984. These data should be compared with those presented in Fig. 4.2a.

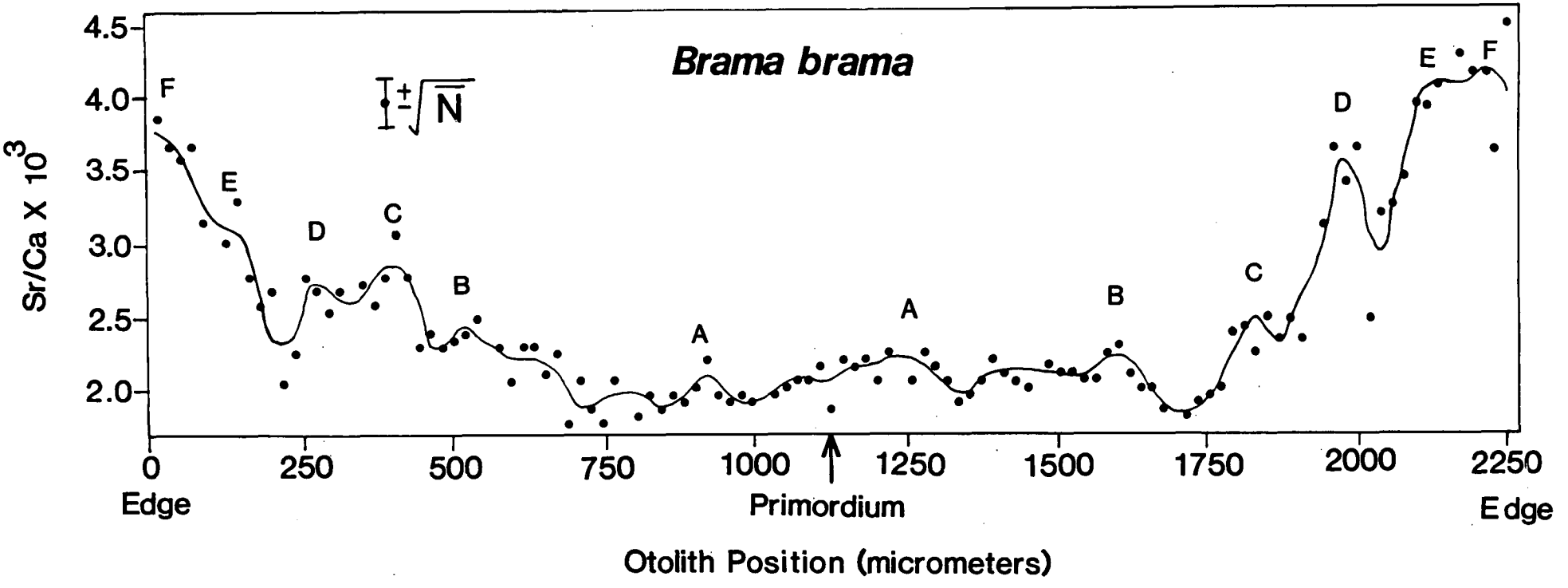

Fig. 4.3 Sr/Ca ratios from an electron microprobe transect across a sagitta transverse section of an adult Ray's bream, *Brama brama*, (45.5 cm SL) collected off Maria Island, Tasmania in February 1985. Otolith position 0 μm is at the dorsal otolith edge, the primordium is at 1125 μm and the ventral otolith edge is at 2250 μm. The error bar indicates the magnitude of a single standard deviation based on the mean number of counts at each point in the microprobe transect.

environment. However, the data may still be of use in distinguishing relative changes or as a form of signature for individuals or groups of individuals with a similar environmental and physiological history, as will be discussed in the following sections.

4.3 Formation of a chemical "check": a natural experiment

4.3.1 Introduction

A large proportion of this chapter is based on the idea that certain combinations of physiological and environmental factors will result in specific changes in the trace element composition of an otolith. The fact that these processes act together to mediate changes in otolith chemistry has been show in Chapter 3. Also, these data provided evidence that the otoliths from fish within a small region (such as the rocky reef in Variety Bay) can respond in a similar manner to these combined physiological and environmental conditions. However, it still remains to be shown that a group of fish experiencing similar environmental conditions will produce a distinct chemical "check" that can be recognized during a chemical transect of an otolith made with an electron microprobe.

This section presents the results of a natural experiment where a group of juvenile Australian salmon became stranded in the lower reaches of a beach-dammed river. These fish were exposed to unusual conditions for an unknown period of time and would be expected to retain some chemical mark on the otoliths indicative of this period of stress. Such a mark would become a component of the signature of these fish and, could be used subsequently in "stock" identification.

4.3.2 Materials and methods

Juvenile Australian salmon were collected by beach seine from the lower reaches of Bream Creek Lagoon behind Marion Bay Beach on the east coast of Tasmania (Fig. 4.4) on 27 February 1988. Details of the fish collected from Bream Creek Lagoon are shown in Table 4.1. Sagittal otoliths were prepared for microprobe analysis as for juvenile Australian salmon in Chapter 2 and microprobe counting procedures are similar to those outlined in the previous section.

The Bream Creek collection site was very different from the other juvenile Australian salmon collection sites, discussed later, for several reasons. Bream Creek is a slow moving stream that flows parallel to Marion Bay Beach for several

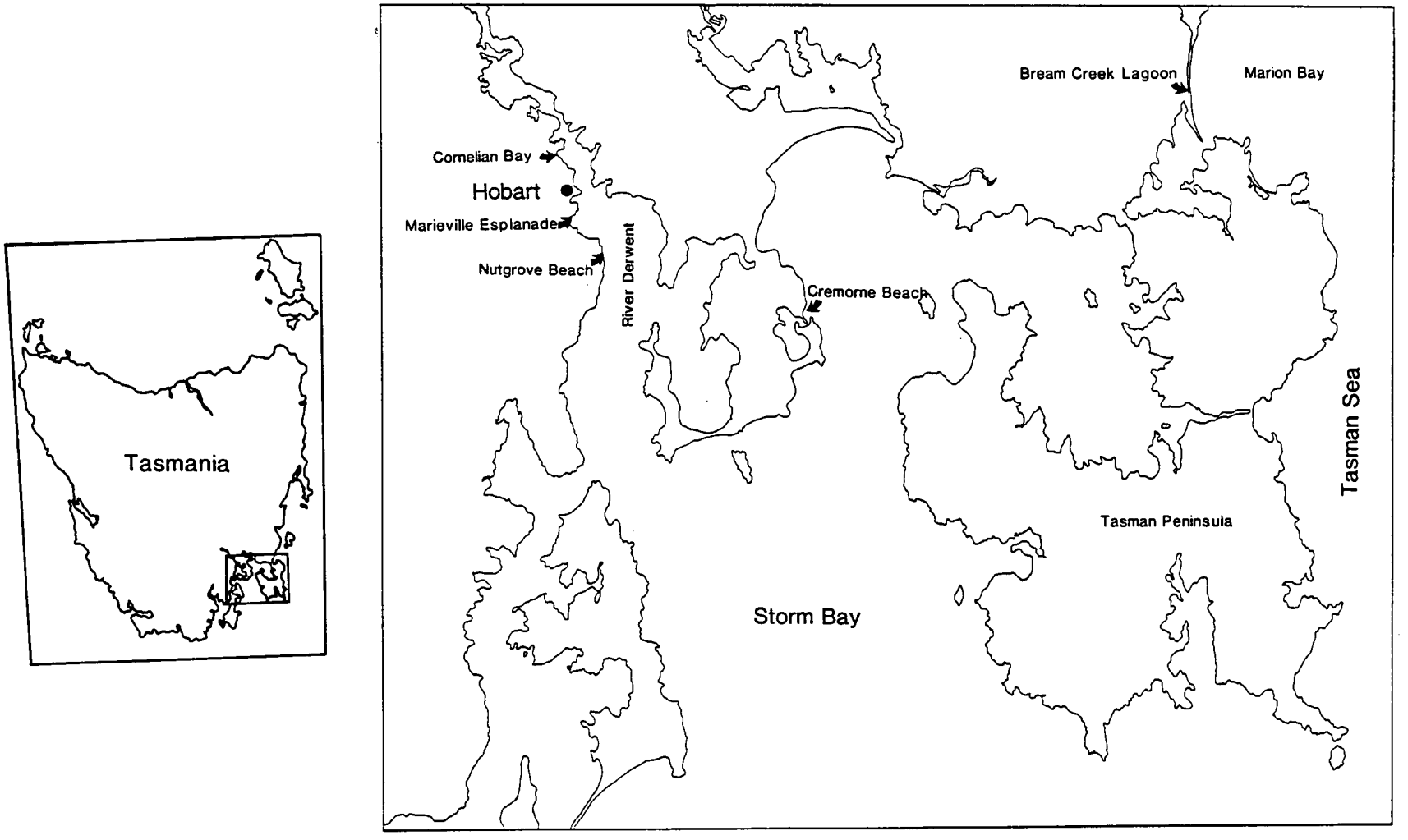

Fig. 4.4 Map showing *Arripis trutta* collection sites discussed in Sections 4.3 and 4.4.

Table 4.1 Fish and otolith length and weight data for *Arripis trutta* collected from Bream Creek Lagoon on 27 February 1988. The otolith data are based on the right sagitta. Complete microprobe transects of sagittae were carried out on those individuals marked with an asterisk and the transects are shown in Fig. 4.5.

	Fish		Condition	Otolith	
Fish no.	length (mm)	weight (gm)	factor	length (mm)	weight (mg)
AS222*	81.0	8.30	0.0156	4.35	7.4
AS223*	86.0	10.53	0.0165	4.72	8.0
AS224	69.5	6.22	0.0185	3.95	6.2
AS225	94.0	15.62	0.0188	5.05	9.4
AS226	142.0	50.68	0.0177	7.00	19.8
AS227	105.5	21.88	0.0186	5.40	11.1
AS228	82.0	9.76	0.0177	4.35	7.2
AS229*	76.5	8.62	0.0193	4.25	7.4
AS230*	80.0	8.62	0.0168	4.45	8.2
AS231*	89.5	11.72	0.0163	4.70	8.0
AS232*	77.5	8.40	0.0180	4.25	7.2
AS233*	77.0	6.93	0.0152	4.50	8.1
AS234*	92.5	13.03	0.0165	4.85	8.8
AS235*	76.5	8.42	0.0188	4.25	6.5
AS236*	74.5	7.84	0.0190	4.00	6.3

kilometers behind a series of grass covered dunes and can be classified as a beach-dammed river. The creek emerges from behind the dunes onto Marion Bay Beach and, for the majority of the year, does not actually flow directly into the sea, but through seepage channels in the sand. On the basis of the salinity of the lower reaches of Bream Creek which is frequently higher than 20 ‰ salinity, it is evident that there is also a large influx of saltwater into the creek. At certain times of the year, notably high tides that are coincident with higher river flows, Bream Creek cuts a channel perpendicular to the beach and flows directly into Marion Bay. Because Marion Bay Beach is an exposed beach it is prime habitat for Australian salmon (Last, 1983). As a result, it is not surprising that, during periods when Bream Creek flows directly into the sea, juvenile Australian salmon enter the creek. In some instances, these juvenile salmon become trapped in the stream when the tides recede and the river flows decrease.

Australian salmon were collected from Bream Creek on 27 February 1988 when the river flow fell about 150 m short of Marion Bay. It is not known for how long a period the creek had been isolated from the bay when these fish were collected, although observations of Australian salmon in the creek 5 days before the collections actually precipitated the collection trip.

Data from these fish were compared with fish collected from Cremorne Beach on 10 February 1988. Data from these Cremorne Beach fish is considered further in Section 4.4.

4.3.3 Results and Discussion

Based on rainfall and tidal conditions near the time of collection it seems likely that the Australian salmon collected from Bream Creek had been stranded there for at least 2 weeks. The creek salinity and temperature were 25.5‰ and 25.0°C at 1730 h on the day the salmon were collected. Salmon from the creek were in relatively poor condition, being visibly thin and they had a low mean condition factor (0.0176±0.0013, mean±SD) when compared with salmon collected at the Cremorne Beach site on 10 February 1988 (0.0202±0.0008). The condition factors of the fish at these two sites were significantly different (unpaired t-test; $t=7.16$, $df=32$, $p<0.0001$). Furthermore, the mean condition of the Bream Creek fish was lower than the condition of more than 90% of the experimental aquarium maintained fish (Chapter 2).

Otolith microchemistry life-history transects for Sr/Ca, Na/Ca, K/Ca and S/Ca from 10 Australian salmon collected in Bream Creek and selected at random are shown in Fig. 4.5. Transects from several fish show a basic similarity, but the most interesting aspect of the data is the uniformity in the relative change of the data in the final microprobe measurements near the otolith margin. In all cases, the Sr/Ca ratios in the final microprobe measurements are increasing (Fig. 4.5a). The mean Sr/Ca ratio at the otolith margin of the Bream Creek fish is 0.00284±0.00057 (n=30, 3 measurements along the edge of transverse sections from 10 sagittae from 10 fish), significantly higher than that measured at the margin of the February caught Cremorne Beach fish where the Sr/Ca ratio was 0.00227±0.00025 (n=50) ($t=9.61$, $df=78$, $p<0.0001$). For comparison, the mean Sr/Ca ratio for all the Australian salmon from the controlled temperature experiments was 0.00217±0.00029 Also, the majority of S/Ca data (88%) are increasing (Fig. 4.5d), whereas the majority of both the Na/Ca (88%) and K/Ca (90%) data are decreasing (Fig. 4.5b and 4.5c) at the otolith margin. Data from fish collected at Cremorne Beach on 10 February do not show a similar relative change in otolith chemistry in the final increments (see Appendix 2). Furthermore, the changes in otolith chemistry along the margins of the Bream Creek fish are not consistent with changes in otolith chemistry determined on the basis of monthly collections of Australian salmon from Cremorne Beach (Chapter 2).

The Bream Creek data are particularly interesting because they provide further evidence in support of the hypothesis, presented in Chapters 2 and 3, that a low condition factor ($CF=W/L^3$), resulting from illness or environmental extremes and stress, can ultimately affect the trace element composition of fish otoliths. Increasing Sr/Ca ratios occurred in these fish even though the salinity of the water from which they were captured was reduced (25.5‰) and the daytime water temperature was very high (25°C). Data on brown trout, *Salmo trutta*, endolymph and otoliths (Chapter 2) and additional data on other salmonid species (Chapter 5) showed that reduced salinity can result in a decrease in the Sr/Ca ratio in the otoliths. This is because Ca is maintained at relatively constant levels in fish plasma and, concomitantly endolymph, regardless of the levels present in the environment, whereas the "non-essential" element Sr is present in the plasma at levels that are related to the levels present in the environment. This makes it even more likely that the increased otolith Sr/Ca ratios observed here were the result of physiological factors.

The suggestion that otolith Sr/Ca ratios are inversely correlated with

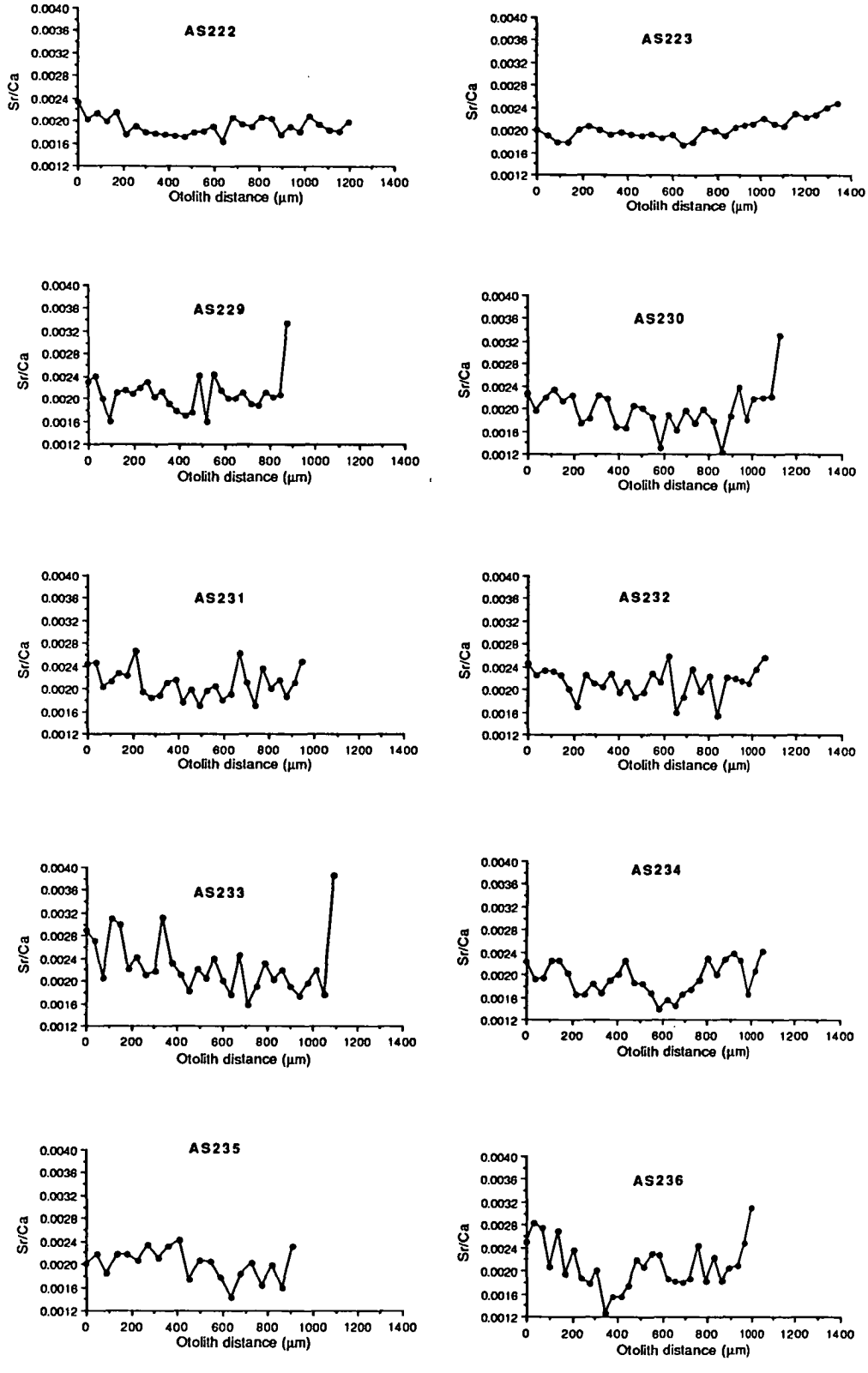

Fig. 4.5a Plots of Sr/Ca data from microprobe transects across the sagittae (0 µm=primordium) of 10 juvenile Australian salmon (see Table 4.1) collected from Bream Creek on 27 February 1988. Note that the last one or two points of the transects show an increase in the otolith Sr/Ca ratio.

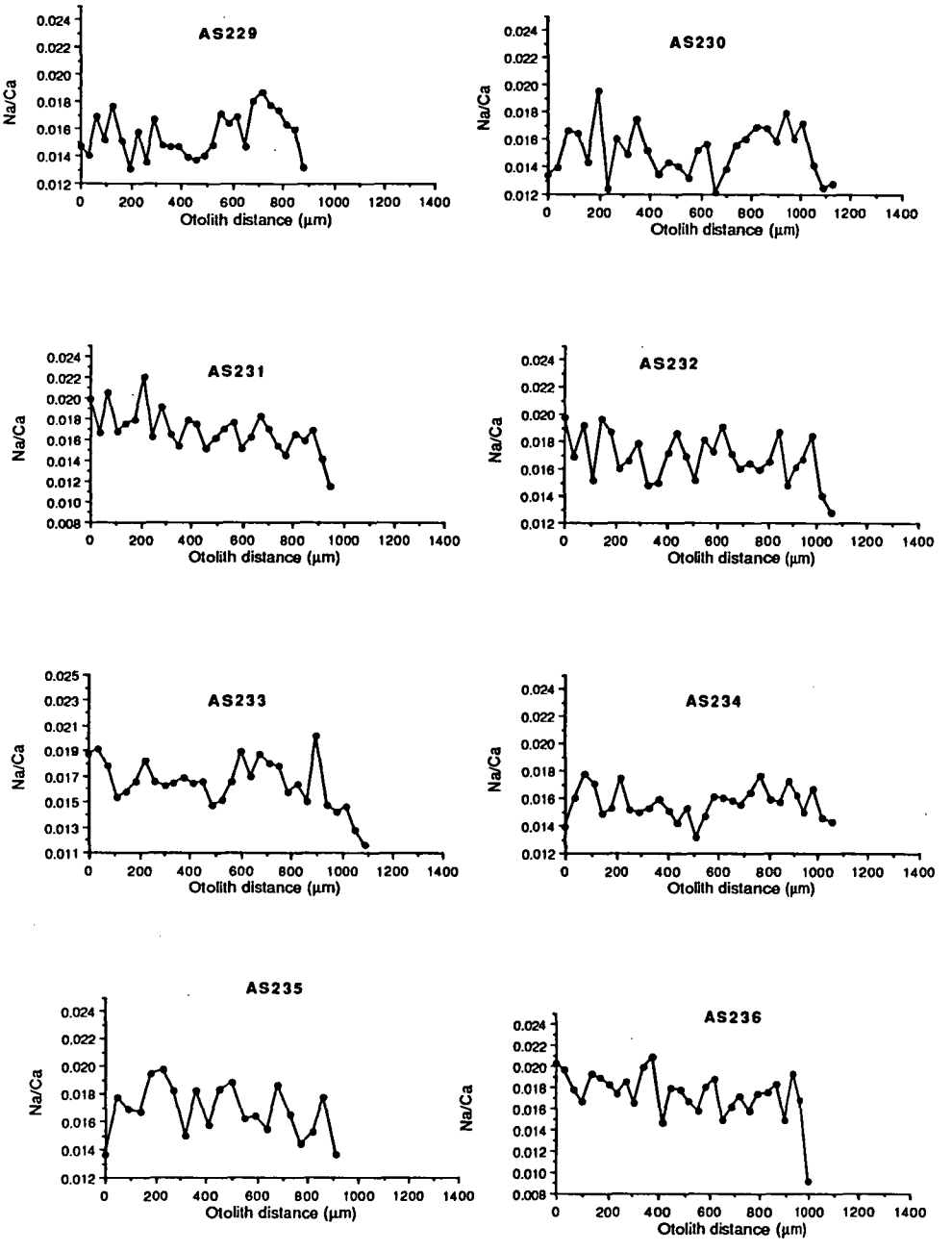

Fig. 4.5b Plots of Na/Ca data from microprobe transects across the sagittae (0 µm=primordium) of 8 juvenile Australian salmon (see Table 4.1) collected from Bream Creek on 27 February 1988. Note that the last one or two points of the transects show a decrease in the otolith Na/Ca ratio. Because of spectrometer failure the data from AS222 and AS223 are not shown.

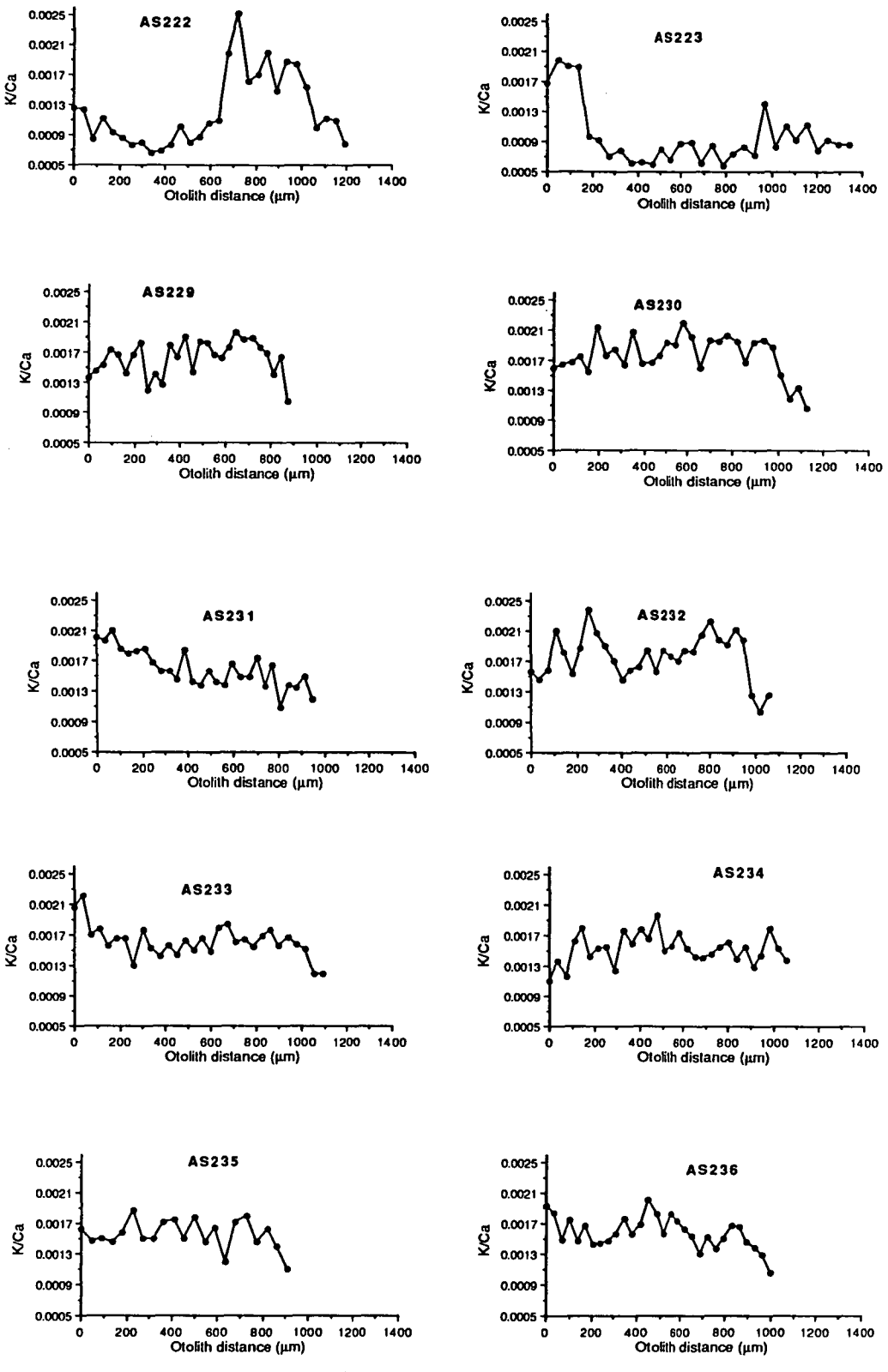

Fig. 4.5c Plots of K/Ca data from microprobe transects across the sagittae (0 µm=primordium) of 10 juvenile Australian salmon (see Table 4.1) collected from Bream Creek on 27 February 1988. Note that, in the majority of fish, the last one or two points of the transects show a decrease in the otolith K/Ca ratio.

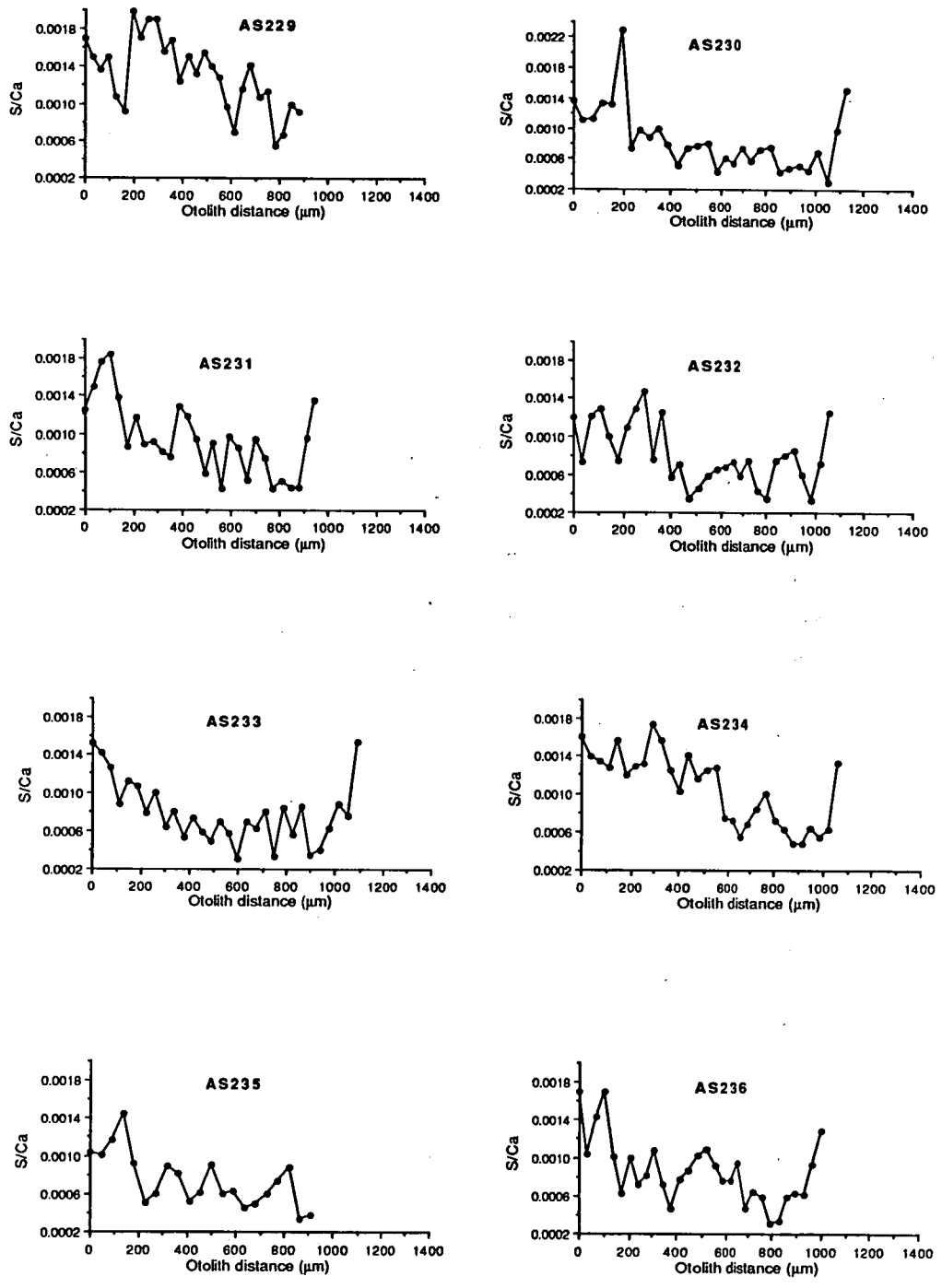

Fig. 4.5d Plots of S/Ca data from microprobe transects across the sagittae (0 µm=primordium) of 8 juvenile Australian salmon (see Table 4.1) collected from Bream Creek on 27 February 1988. Note that, in the majority of fish, the last one or two points of the transects show an increase in the otolith S/Ca ratio. Because of spectrometer failure the data from AS222 and AS223 are not shown.

temperature (Radtke, 1984; Radtke and Targett, 1984; Townsend et al., 1989) appears invalid for these fish collected from Bream Creek. This is because the temperatures recorded in Bream Creek were high and well above the sea surface temperature at Marion Bay (16.4°C). Moderate summer nighttime temperatures (mean February temperature of 17.9°C (Bureau of Meteorology, Hobart)) on the east coast of Tasmania would not lower the temperature of Bream Creek below that measured at the sea surface.

The changes in Na/Ca, K/Ca and S/Ca ratios on the otolith margin of the Bream Creek Australian salmon may also be a manifestation of the extreme environment and the resultant stress. Love et al. (1968) starved cod (*Gadus morhua*) and found that starvation resulted in a drop in the levels of Na and K in the blood plasma. These changes may also result in similar alterations in the composition of the endolymph and a concomitant reduction in the Na/Ca and K/Ca ratio of the otolith. Of course, based on findings presented in Chapter 3, the relationships may not be so simple and a wide range of factors is probably operating on otolith chemistry. The increase in S/Ca ratios at the otolith margin may be due to the formation of a protein rich check mark during the period of stress (Campana, 1983).

Although it may be difficult to give a completely satisfactory explanation for the changes in trace element composition along the otolith margin of the Bream Creek fish, it is clear that the changes are related to the extreme environment experienced by these fish. The fact that the relative change in otolith Sr/Ca ratios was consistent for all fish is an indication that environmental stress can produce a potentially recognizable chemical "signal" among a group of co-occurring fish. The occurrence of multiple chemical checks of this nature, among a group of fishes, can combine to produce a form of chemical signature unique to that group of fish. Detection of these markers and characterization of the chemical signature may be useful in the discrimination of population subunits or stocks. The identification of these unique patterns by electron microprobe analysis is an objective operation. However, the factors that effect the patterns of otolith chemistry may be of too fine a scale, both spatially and temporally, to be useful in stock discrimination.

4.4 Juvenile *Arripis trutta*: characterization of nursery grounds and stock discrimination

4.4.1 Introduction

A large number of fish species use coastal habitats as nursery grounds for the development of juveniles. These nursery grounds are often widespread and the juveniles may recruit to a large number of different localities, each with slightly differing physical and biological characteristics. The fish migrate to the adult habitat after growth and development in these nursery areas . At present, it is generally impossible to distinguish animals from different nursery grounds after they have moved out of these areas. However, transects of otolith microchemistry from juveniles collected from a similar habitat may serve as signatures for fish from various nursery grounds and these signatures may be recognizable in adult fish. Evidence that unique patterns in otolith chemistry would exist among fish that occurred in a similar habitat was presented in the previous section. This may serve as a form of "stock" discrimination in wild fish populations.

The life-history of the Australian salmon makes them well-suited to a study of the variability of recruitment habitats on the basis of otolith microchemistry. This factor combined with their year round availability in Tasmanian coastal waters and the relatively detailed knowledge of the species' otolith chemistry further enhances the value of this species to the study.

Australian salmon (*Arripis trutta*) are a migratory species with an extensive drift to nursery grounds. Spawning of Australian salmon is believed to occur over the continental shelf of New South Wales and Victoria (Stanley and Malcom, 1977). Eggs and larvae drift, presumably within the East Australian Current, to the coastal waters of Tasmania, where juveniles of approximately 30 to 35 mm SL, and about 120 days of age (based on counts of otolith microincrements) recruit to the lower reaches of estuaries and ocean beaches. Older juveniles (1+ years) are found over the continental shelf and gradually move northwards with increasing age. Fish three years of age and older are generally found in the waters of Bass Strait or off the Victorian and New South Wales coasts (Stanley, 1978).

This investigation considers the variability in otolith Sr/Ca, Na/Ca, K/Ca and S/Ca ratio data obtained from life-history transects along transverse sections of the sagittae of 110 juvenile Australian salmon collected from nursery grounds in the waters of southeastern Tasmania. The data are interpreted in an attempt to determine

the feasibility of identifying unique nursery ground "signatures" that could be used to identify the nursery grounds used by individual adult fish. These data would be useful in studies of stock separation, and, thereby, fisheries and habitat management.

4.4.2 Materials and methods

Juvenile Australian salmon were collected by beach seine at different times of year from 1985 to 1988. Several collection localities were used and these are shown in Fig. 4.4. The majority of the collection sites are exposed or semi-exposed beaches in Storm Bay and the Derwent River estuary. The date, locality, water temperature and number of fish from which otolith microchemistry life-history transect data were collected is shown in Table 4.2.

Sagittal otoliths were prepared for microprobe analysis as for juvenile Australian salmon in Chapter 2 and microprobe counting procedures are similar to those of the previous section. Electron microprobe measurements were done with a square raster of 12.5 x 12.5 μm. It was determined that it would be more important to collect data from a large number of samples and decrease the sample frequency. This was because the investigation was aimed at determining gross differences among microchemical time series and was not seeking to investigate the nature of variability in microprobe measurements. These problems are investigated in other portions of this thesis. On this basis it was determined that a spacing of approximately 50 μm between consecutive center points of microprobe measurements would be adequate.

Because individual data records were relatively short it was impractical to employ cross-correlation analysis to compare the various life-history transects. Due to the nature of the data it was felt that a subjective form of analysis was most appropriate. A similar rationale was employed by Rosenberg and Jones (1975) and Rosenberg (1980) in comparing microprobe data collected from transects of molluscan shells but, before making comparisons, they smoothed their data by recombination of the most significant frequencies based on Fourier analysis of the original data. In this study, unsmoothed data were compared initially, but, in some cases, smoothing has been employed to clarify relationships among transects.

4.4.3 Results and Discussion

A sample of the data collected from the life-history transects of juveniles from several localities is presented in Figs. 4.6 to 4.8 and these will be considered in

Table 4.2 Collection data for juvenile *Arripis trutta* used in the investigations of nursery areas and stock identificaion by identification of microchemical signatures in sagittal otoliths. The 'number of fish' refers to the number of individuals from which otolith microchemistry transect data were collected. The microchemical data from the sagittae of a small number of these fish are shown in this chapter. The remainder of the Sr/Ca transects appear in Appendix 2.

Date	Location	Temperature (°C)	Number of fish
13/11/85	Marieville Esplanade	16.3	5
14/10/86	Nutgrove Beach	15.3	6
28/3/87	Cremorne Beach	15.5	10
19/4/87	Cremorne Beach	15.2	20
8/6/87	Cremorne Beach	11.3	9
18/6/87	Cornelian Bay	9.0	3
26/9/87	Cremorne Beach	14.5	5
9/1/88	Cremorne Beach	20.5	12
10/2/88	Cremorne Beach	19.6	16
27/2/88	Bream Creek Lagoon	25.0	10
1/4/88	Cremorne Beach	17.0	11

greater detail below. The remainder of the data (Sr/Ca ratio transects only) appear in Appendix 2. It is evident from these data that the variability in otolith Sr/Ca, Na/Ca, K/Ca and S/Ca ratios determined from microprobe transects across otolith sections can be very great. In many cases, it is difficult to detect any significant degree of similarity among chemical transects within collection sites, among collection sites and among years. The only notable similarity among the juvenile microchemical transects is the initial decrease in otolith Sr/Ca ratio from the relatively high level measured in the primordium. This is probably more a function of the physiology of the embryonic and larval stage and not due to the interaction of environmental and physiological factors. This conclusion is supported by the fact that a large number of species show an initially high value in otolith Sr/Ca ratio in the earlier formed portions of the otolith. However, in some cases the otolith elemental data do provide very clear evidence for "relatedness" among individuals.

In most cases, intercomparison of the relatively short otolith microchemistry transects from the juvenile Australian salmon is difficult. Increasing the frequency of sampling may help to overcome these difficulties, but this becomes impractical due to the time and costs involved in sampling and the need for relatively large sample sizes. Subjective comparison of the relative positions of peaks, before or after smoothing is an alternative, but, for obvious reasons, it is not altogether satisfactory. Nevertheless, I will present some examples involving this form of analysis to indicate the nature of the results from such comparisons. Due to the quantity of data collected (otolith transects from 110 individuals were made) only a few representative examples are presented.

One of the better examples is from 3 fish collected in Cornelian Bay in June 1986. Cornelian Bay is a protected shallow bay in the upper reaches of the Derwent River estuary and would not be classified as suitable habitat for juvenile Australian salmon (Last, 1983). The fish were collected in water less than 1.0 m deep and the temperature was 9.0°C. Only 3 salmon were collected at the site. The elemental data shown (Fig. 4.6a and 4.6b) are from otolith transects of transverse sections from the primordium to the otolith edge. However, the transects of AS188 and AS190 were along the shorter dorsal axis of the transverse sections, whereas the transect of AS189 was along the longer ventral axis. The fish were different lengths with AS188, AS189 and AS190 being 51.5, 44.5 and 50.0 mm SL, respectively. However, counts of microincrements were similar among the three fish, indicating that AS189

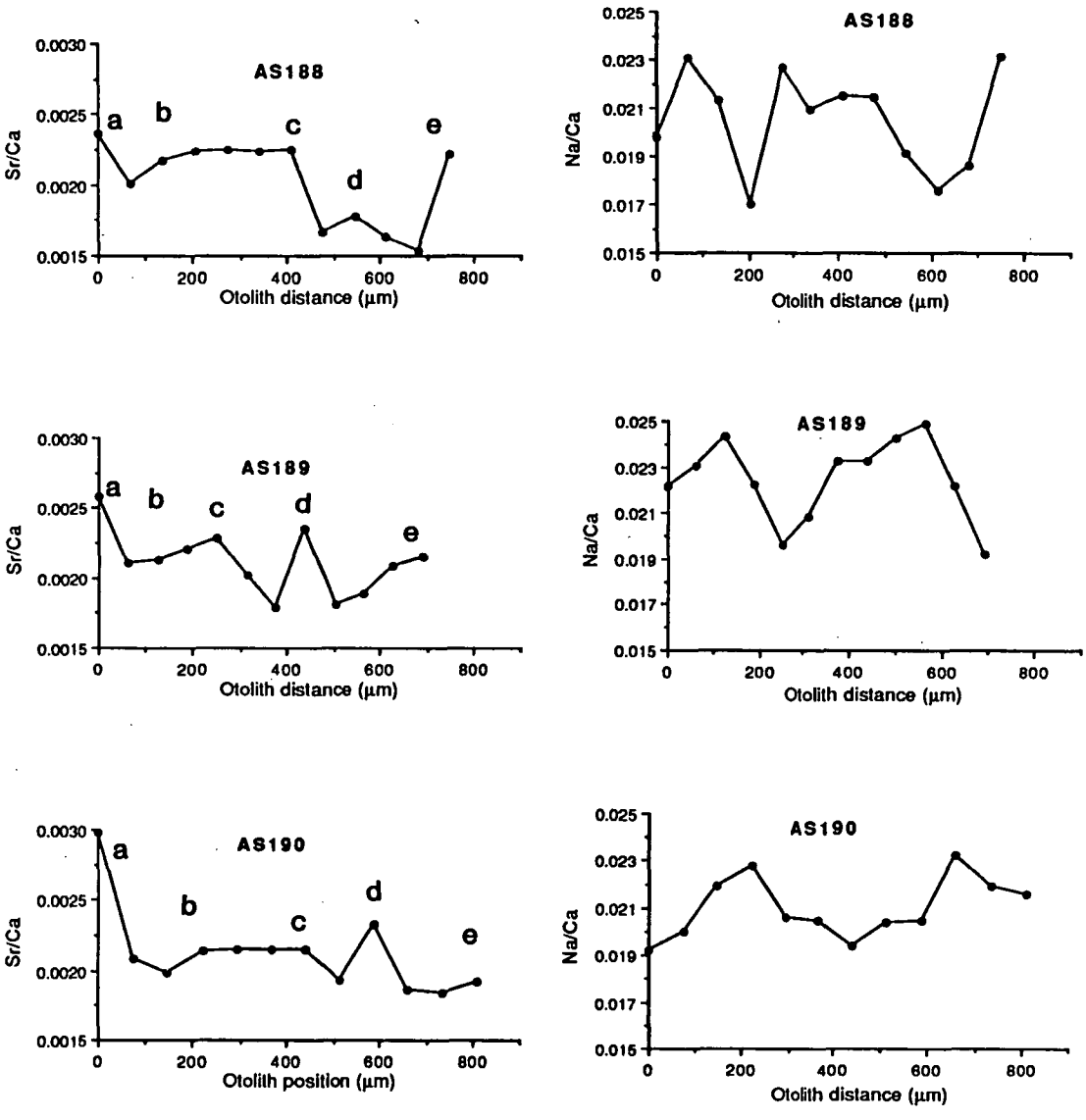

Fig. 4.6a Plots of Sr/Ca and Na/Ca data from microprobe transects across the sagittae (0 µm=primordium) of 3 juvenile Australian salmon collected from Cornelian Bay on 18 June 1987. Common features of the Sr/Ca ratio transects are lettered for comparison.

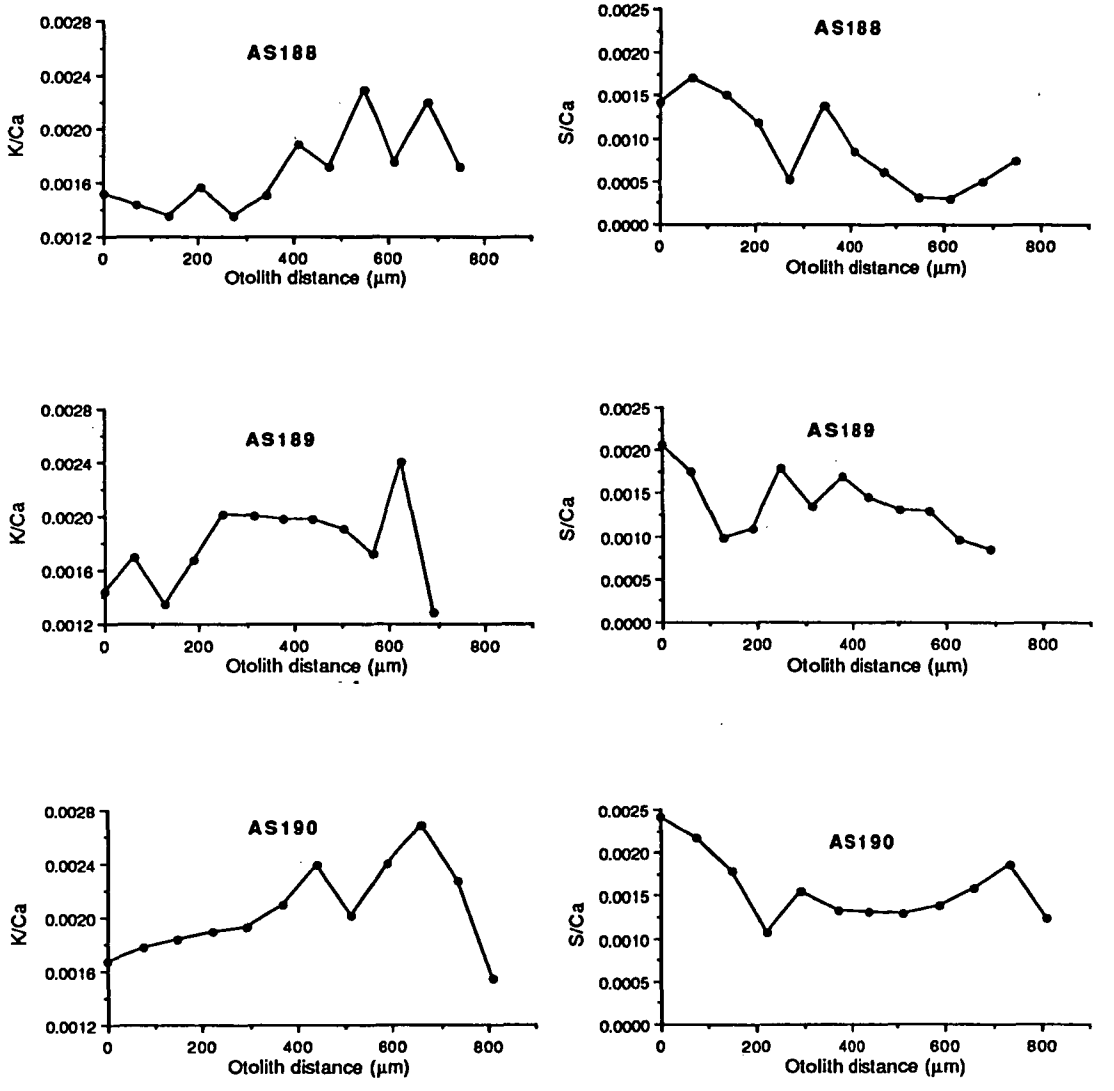

Fig. 4.6b Plots of K/Ca and S/Ca data from microprobe transects across the sagittae (0 µm=primordium) of 3 juvenile Australian salmon collected from Cornelian Bay on 18 June 1987.

was probably a relatively slow growing fish. Despite these differences, the microchemical data, and Sr/Ca ratios in particular, from the three fish are similar (Fig. 4.6a). It is important to realize that the magnitude of variation in the peaks and troughs may simply be an artefact of the sampling frequency. This is highlighted by the fact that the segment B to C in the Sr/Ca data (Fig. 4.6a) is at the same level (≈0.0022) in each of the fish. There is also some indication of similarity among the Na/Ca, K/Ca and S/Ca data, but the relative position of the peaks among the 3 fish are not altogether consistent with the Sr/Ca ratio data.

Further examples of otolith transects from juveniles that showed an overall similarity are illustrated in Fig. 4.7 and 4.8. Figure 4.7 compares the raw data and the smoothed data (3-point moving average) for 4 element ratios from 2 individuals collected at Cremorne Beach on 19 April 1987. The raw data on the left hand side of the page show similar trends, but these similarities become more evident after smoothing. The data from these two individuals illustrate the fact that if like trends are evident in one of the elemental ratio transects, then there is generally a similar relationship for the other elemental ratios. Sr/Ca ratio data from 8 juvenile Australian salmon, also collected at Cremorne Beach on 19 April 1987, are illustrated in Fig. 4.8. The data have not been smoothed, but certain "common" features of the transects have been highlighted. The same features have also been highlighted in the Sr/Ca ratio transects presented in Fig. 4.7. In some of the transects, notably B47, AS42, AS44 and AS46 the position of Sr/Ca peaks can be related among fish. In other instances this is more difficult and requires a certain degree of subjectivity. The transect presented in B50 was made along a transverse section but along a slightly longer axis (primordium to dorsal edge, rather than primordium to ventral edge). Nevertheless, the peaks labelled a, b, c and d can be related to those found in the other otoliths. There are further examples of transects that show a notable resemblance to one another, however, the percentage of transects that appear to be unique is much greater.

There is good evidence to support the hypothesis that Australian salmon of similar size/age, exposed to similar environmental conditions will display comparable trends in otolith chemistry from the primordium to the otolith edge. Because multiple transects from the primordium to the otolith edge within a single otolith show a fair degree of variability, the agreement between these coexisting juveniles is good evidence that individuals have experienced similar environments over relatively long

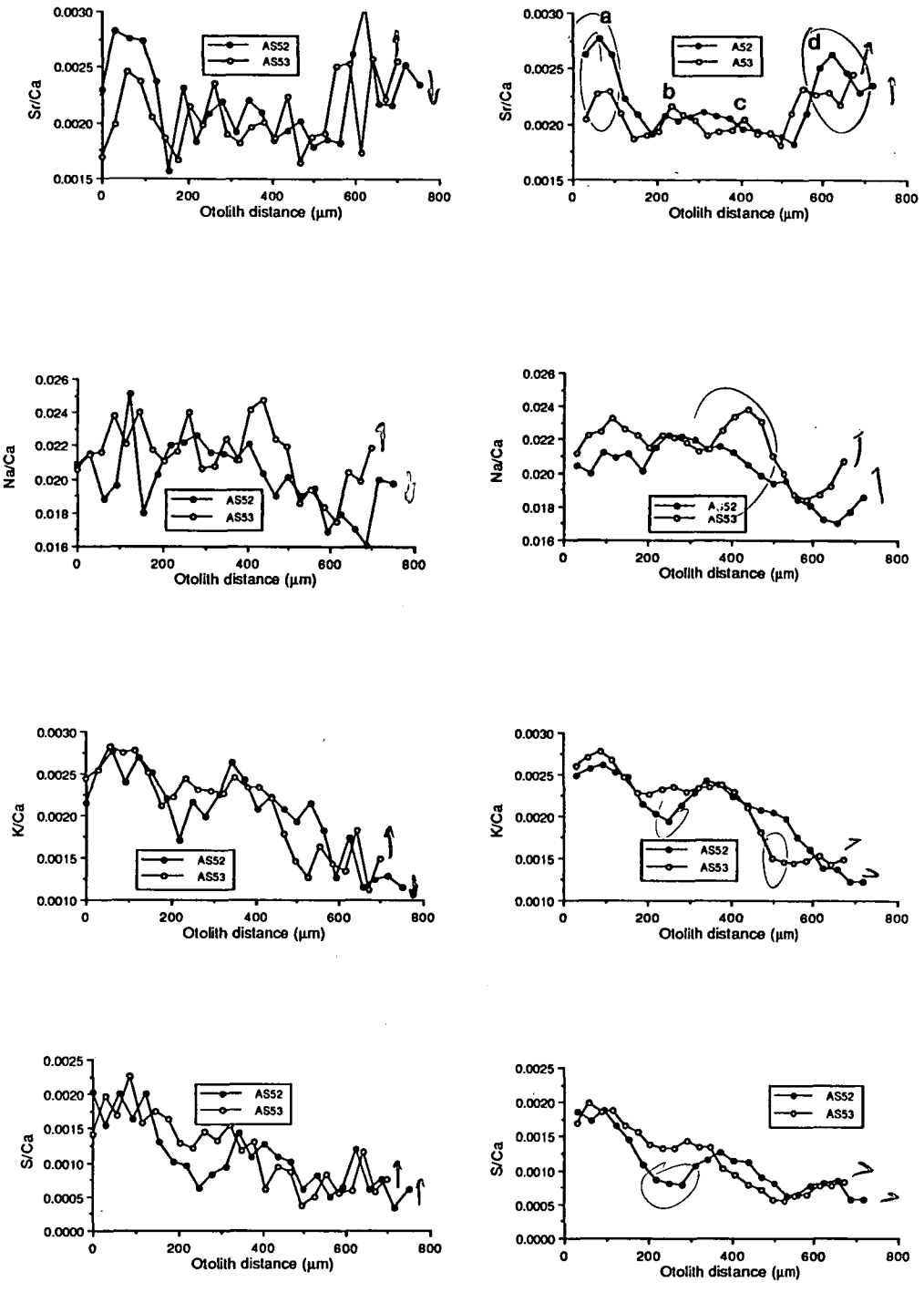

Fig. 4.7 Plots of Sr/Ca, Na/Ca, K/Ca and S/Ca data from microprobe transects across the sagittae (0 µm=primordium) of 2 juvenile Australian salmon (AS52, 45.5 mm SL; AS53, 43.0 mm SL) collected from Cremorne Beach on 19 May 1987. Plots on the left side of the page show the raw data and plots on the right side of the page show the same data after smoothing by a 3-point moving average. Features of the Sr/Ca ratio transects are lettered for comparison with Sr/Ca ratio data in Fig. 4.8.

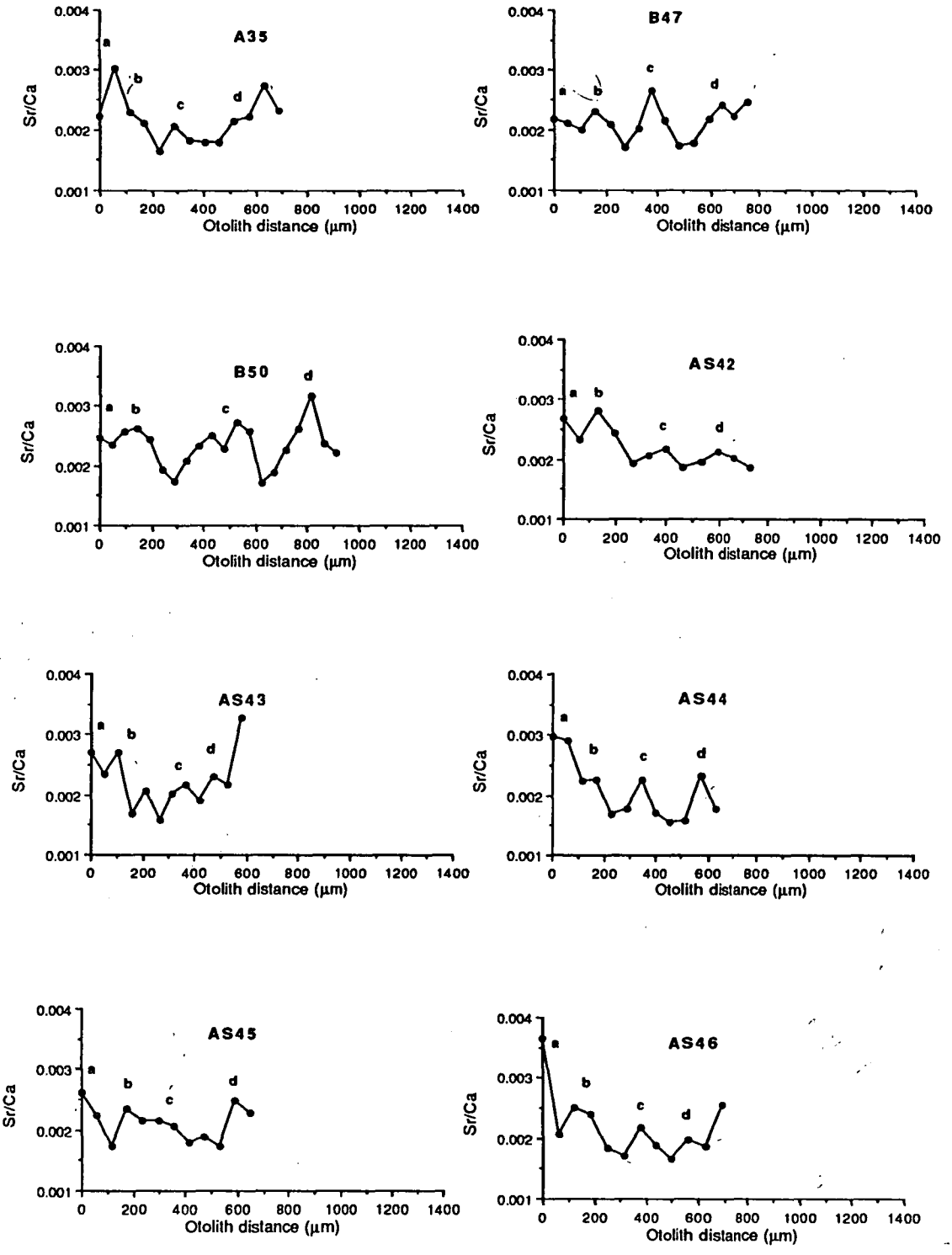

Fig. 4.8 Plots of Sr/Ca ratio data from microprobe transects across the sagittae (0 µm=primordium) of 8 juvenile Australian salmon (length range from 37 to 43 mm SL) collected from Cremorne Beach on 19 May 1987. Common features of the Sr/Ca ratio transects are lettered for comparison among fish and with Sr/Ca ratio data in Fig. 4.7.

periods of time. I was unable to find similar agreement in otolith microchemical trends among individuals collected at the same time of year but from different, albeit nearby, locations. This suggests that similarities in microchemical transects are due to individuals being influenced by similar localized environmental conditions, most likely in combination with physiological characteristics of the particular life-history stage and of the individual in question.

Because trends in otolith microchemistry across juvenile Australian salmon otoliths collected from similar sites at different times of the year and different years were only related in a superficial manner, it would be difficult to attribute any unique microchemical pattern to a particular nursery ground. However, in those instances where there is a very good correspondence among microchemical transects, such as in the Cornelian Bay fish, it seems likely that the microchemical signature could act as a natural tag or marker for an individual from that particular area. Of course, the reliability of such a signature would be increased if there were features that appeared to be unique to those individuals, as was probably being produced in the Bream Creek salmon. Unfortunately, the large number of nursery ground habitats coupled with extensive dispersal and large population size, makes the utilization of such nursery ground markers as a form of stock identification impractical for most fish species. The impracticality of using otolith microchemical transects as natural tags is more a function of cost and the difficulty involved in obtaining large numbers of transects, than due to the nature of the microchemical signature. Alternative microchemical methods, such as those involving chemical analysis of small portions of otoliths by inductively coupled argon plasma emission spectrometry (ICP) (Edmonds et al., 1989), or by inductively coupled argon plasma-mass spectrometry are more efficient and less costly than techniques involving the identification of time related changes in otolith microchemistry by electron microprobe analysis. Also, because I was unable to detect any significant similarity among otoliths from different localities within the Storm Bay region it seems likely that, even if microprobe analysis was feasible, it would provide a far greater spatial and temporal resolution than is necessary.

4.5 Adult *Arripis trutta*: school cohesiveness

4.5.1 Introduction

Variations in otolith composition may be useful in developing an understanding

of school cohesion. Because of the multiplicity of factors involved in determining the trace element composition of fish otoliths, it is highly unlikely that individuals that display similar variations in otolith trace element chemistry across an otolith (over time) would have lived in widely differing habitats. Although it is clear from this research that certain life-history changes will be reflected in otolith composition, it seems that variations in the nature of the environment may, to varying degrees, effect patterns that would be attributable to life-history changes alone. This point is considered in some detail in the section on juvenile *Arripis trutta* and the characterization of nursery grounds and "stock" identification (Section 4.4). The net outcome of those results was that individuals of the same age which display similar variations in otolith microchemistry have probably lived in close proximity to one another. This conclusion makes otolith microchemistry potentially useful in studies of school cohesion.

The application of otolith microchemistry to investigate school cohesion is analogous to studies of growth lines or growth increments in molluscs (Clark, 1968, 1975; Dillon and Clark, 1980) and trees (Fritts, 1976) that attempt to determine contemporaneity within or among populations. Dillon and Clark (1980) suggest, in their conclusion, that the major difficulties in using growth lines in analyses of contemporaneity in populations involve objective determination of which growth lines to count for use in subsequent correlation and cluster analysis. However, in using microprobe transects from otoliths rather than growth lines it is possible to eliminate a large degree of the subjectivity that would be involved in quantification of growth increments.

The degree to which fish schools are maintained as discrete elements of a fish stock is unknown for most fish species. It has been suggested that the shoaling behavior has evolved through kin selection, thus, inferring that fish within a shoal are related in some way (Pitcher, 1986). However, the existence of kinship is difficult to determine in fish schools. Some work on school population structure has been carried out on yellowfin tuna (*Thunnus albacares*) by using electrophoresis (Sharp, 1978). However, electrophoretic data are more relevant to population structure and variation among schools rather than variation within a school. Determination of mitochondrial DNA haplotypes by restriction enzyme analyses may be more useful in resolving the degree of relatedness among fish in a school, but even this technique probably lacks the required sensitivity for this form of discrimination. This study

investigates the degree of uniformity among otolith microchemistry life-history transects from individuals collected from the same school. It is hoped that this will provide some insight into the utility of otolith microchemistry as a tool for the study of school cohesion.

4.5.2 Materials and methods

Adult Australian salmon, *Arripis trutta*, were collected by purse seine from a single set near Vansitart Island, in the Furneaux Group northeast of Tasmania, in March 1986. The fish collected in the set were from a single school (personal communication, Mr. Tom Ritchey, Ritchey Fishing Co., Devonport, Tasmania). One hundred and twenty five fish were selected from the catch at random and frozen. Sagittae were removed from fish after defrosting, cleaned in distilled water and oven dried at 40°C. Fish age, based on scales and otolith sections, weight, length and sex were determined. Right otoliths from 20 fish were selected at random and prepared for microprobe analyses as discussed in Chapter 2. Electron microprobe analyses were made using a square raster of 12.5 x 12.5 μm. A sample of this size encompasses growth over a period of approximately 2 weeks in these summer caught fish.

Comparison of adult Australian salmon otolith life-history transects was by cross correlation of the spatial/time series obtained for each element and cluster analysis. The overall approach is similar to that applied by Dillon and Clark (1980) to studies of growth line contemporaniety in bivalves. Cross correlations for each potential pair of elemental series were performed over ±7 lags. The largest positive cross correlations were then selected from the lagged data and tabulated in a matrix of correlation coefficients. These analyses resulted in 4 matrices, one each for Sr/Ca, Na/Ca, K/Ca and S/Ca data, of correlation coefficients which were subsequently used to create an additional matrix of the mean positive correlation coefficient based on all 4 elemental ratios for all possible pairs of fish. The results of these calculations are tabulated in a single matrix (Appendix 3).

Correlation coefficient data were used in an "unweighted pair group method using arithmetic averages" (UPGMA) cluster analysis to group fish into "sub-school components" and to determine the degree of "relatedness" within the school (Sokal and Michener, 1958; Sokal and Sneath, 1963). The results from the UPGMA cluster analysis were used to construct dendograms for visualization of the

interschool relationships. It must be stressed that the results of these data are not intended to infer any form of genetic relatedness, but are meant only to highlight any similarities in otolith chemistry among individuals from the single school. Presumably, these similarities are due to a combination of genetic, environmental and physiological factors, as in the juvenile Australian salmon.

4.5.3 Results and Discussion

To investigate school cohesion it was considered important to collect fish from a school with individuals of similar size and age. There is some variation in length and weight, but estimation of ages of all fish collected on the basis of scales, and 20 individuals on the basis of otolith sections, indicates that the range of ages was from 3 to 3+ years. Age, fish length and weight, otolith length and weight and the sex of the 20 individuals selected for microprobe analysis are shown in Table 4.3. There is a fair degree of uniformity in the fish collected from the school, but there is some disparity in the data due to differences of perhaps 6 months in the birth dates of individuals.

The otolith transect data for the 20 fish are shown in Figs. 4.9 to 4.12. The points represent the actual elemental ratios, whereas the solid line is based on a 3-point moving average. The moving average is presented so that general trends can be detected more readily. This manipulation of the time series is also justified because it acts as a filter to remove variations in the data that are largely a function of the variability inherent in the data collection process. Although the fish have been estimated to be 3 to 3+ years of age on the basis of scales and otolith sections, there is no clear evidence for a similar number of cycles in any of the otolith chemistry data.

Visual inspection of the Sr/Ca , Na/Ca, K/Ca and S/Ca data to detect similarities is not only difficult, but overly subjective as well. Inspection of the juvenile transects from the previous section was a relatively simple task because of the relative shortness of the data record and the small number of data points. Due to the problems discussed in the Materials and Methods (Section 4.5.2) and below, a similar form of comparison would not be as productive for these older fish unless there were clearly similar features in the chemical record.

There was statistical evidence for similarities in otolith microchemical transects among fish from the single school. The significant cross correlations are tabulated in matrices in Appendix 3. Dendograms based on UPGMA cluster analysis applied to

Table 4.3 Basic biological data on *Arripis trutta* collected from Vansitart Island and used in the investigation of school cohesiveness. The otolith data are based on the right sagittae.

Fish no.	Fish		Otolith		Sex	Age
	length (cm)	weight (gm)	length (cm)	weight (mg)		
TR11	40.5	1193	1.23	64.8	M	3+
TR22	37.0	981	1.15	65.8	M	3+
TR28	37.5	1045	1.31	72.2	F	3+
TR34	35.0	808	1.26	62.1	F	3+
TR35	40.0	1204	1.25	67.7	M	3+
TR40	34.5	777	1.12	60.5	M	3
TR42	35.0	805	1.20	61.9	F	3
TR43	32.0	653	1.16	52.6	M	3
TR44	38.0	1103	1.25	63.5	F	3
TR45	39.5	1185	1.20	71.4	M	3+
TR46	36.0	984	1.16	60.5	M	3
TR47	35.0	821	1.23	61.9	M	3
TR48	33.0	774	1.19	55.8	M	3
TR49	32.5	694	1.08	51.4	F	3
TR50	37.5	978	1.27	68.1	M	3+
TR52	39.5	1127	1.17	66.6	M	3+
TR54	38.0	1222	1.27	70.7	M	3+
TR55	36.5	967	1.15	55.6	M	3
TR57	34.5	726	1.15	6.11	M	3
TR59	34.5	778	1.22	64.8	M	3

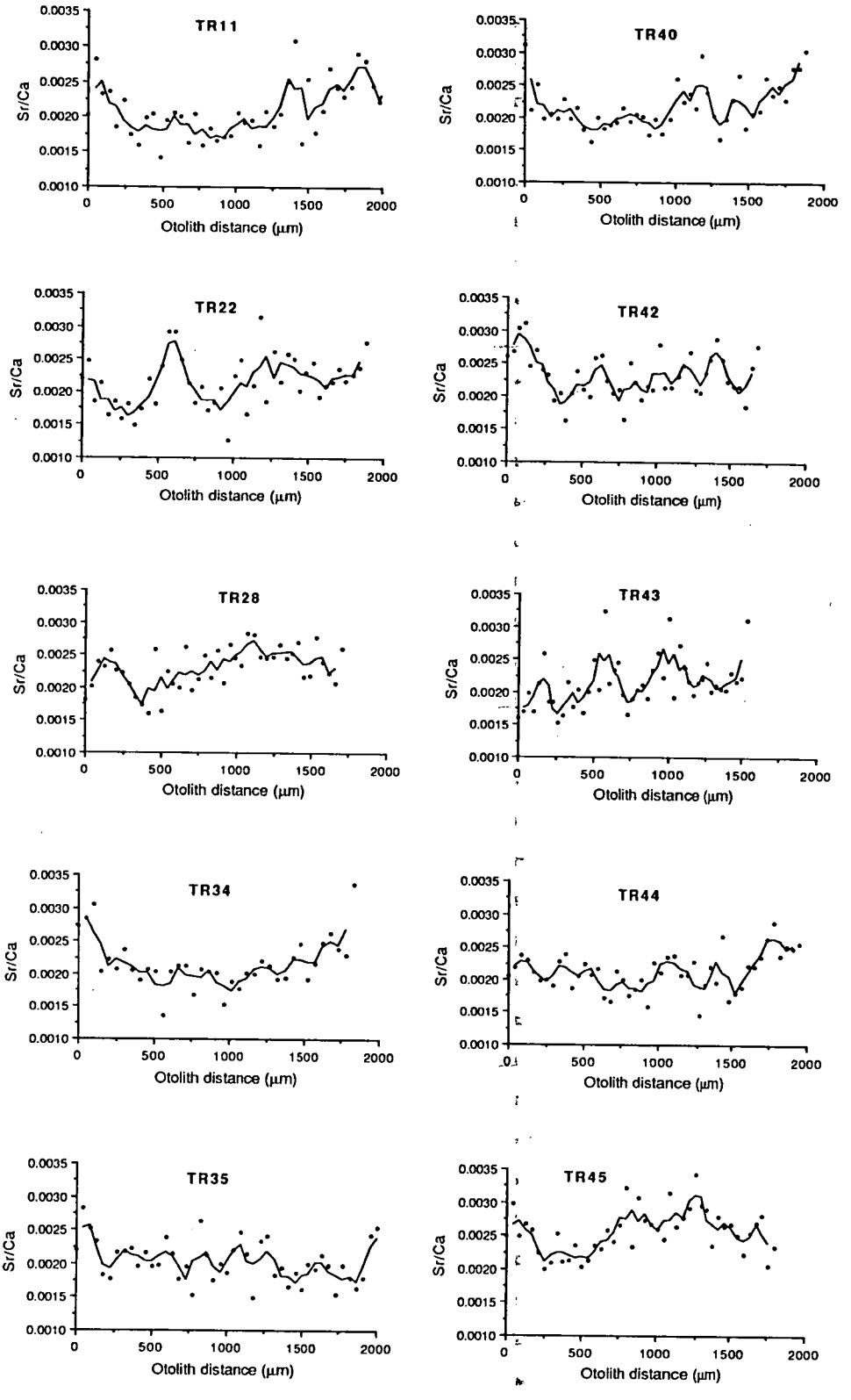

Fig. 4.9 Plots of Sr/Ca ratio data from microprobe transects across the sagittae (0 μm=primordium) of 20 Australian salmon collected near Vansitart Island in March 1986. Points are the raw data and the line represents data after smoothing with a 3-point moving average. Data on the length, weight, sex and age of these fish can be found in Table 4.3.

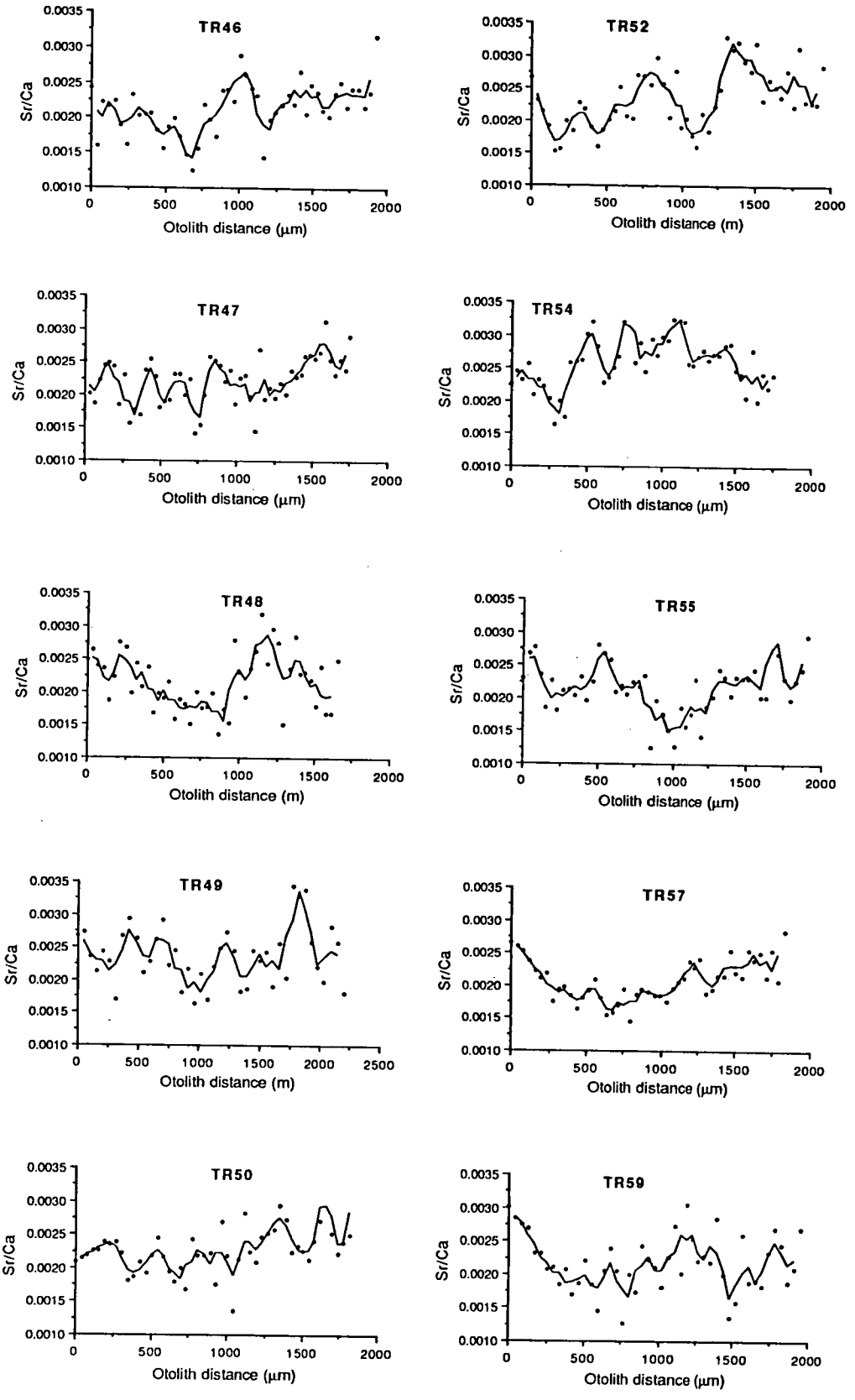

Fig. 4.9 (continued)

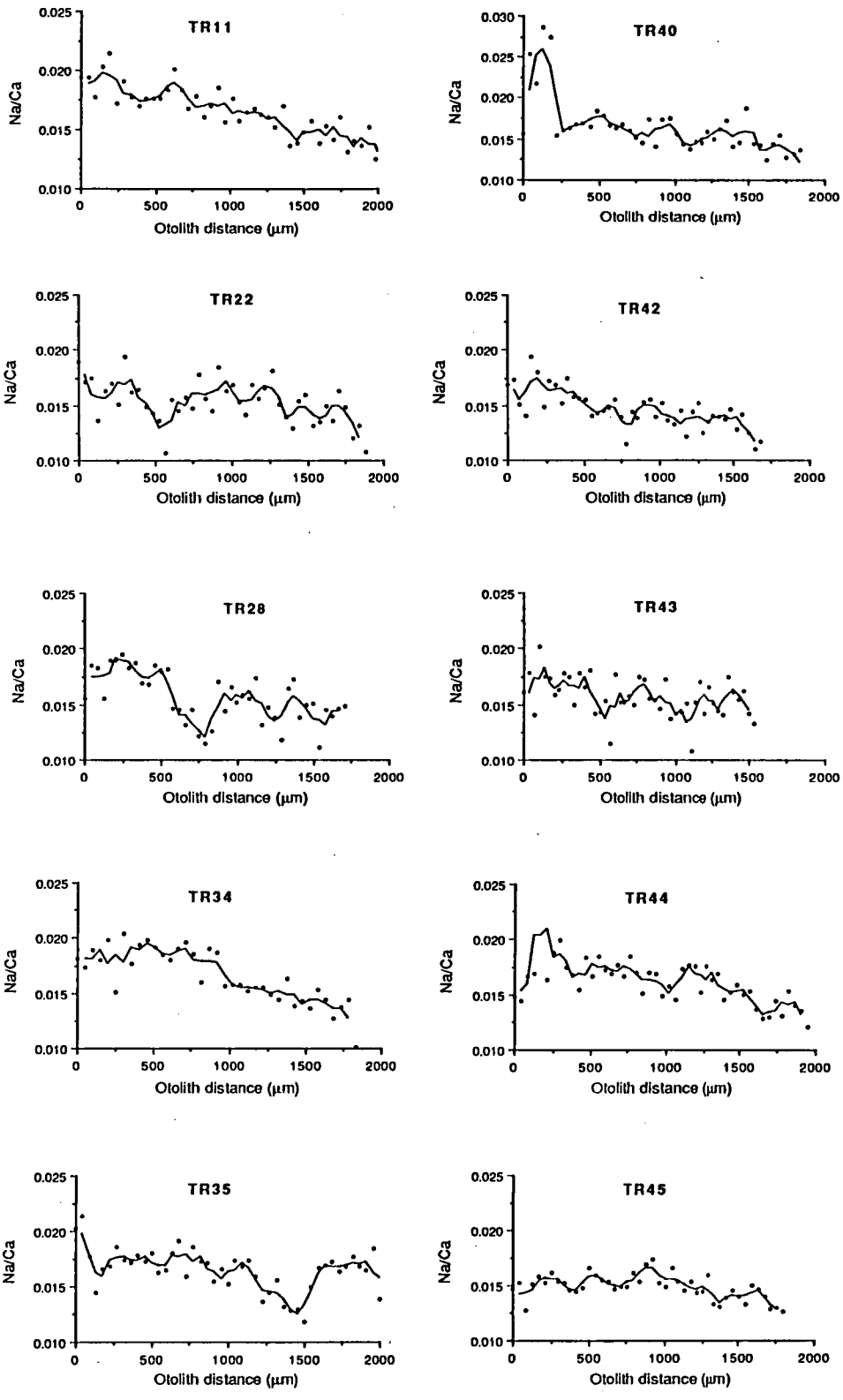

Fig. 4.10 Plots of Na/Ca ratio data from microprobe transects across the sagittae (0 µm=primordium) of 20 Australian salmon collected near Vansitart Island in March 1986. Points are the raw data and the line represents data after smoothing with a 3-point moving average. Data on the length, weight, sex and age of these fish can be found in Table 4.3.

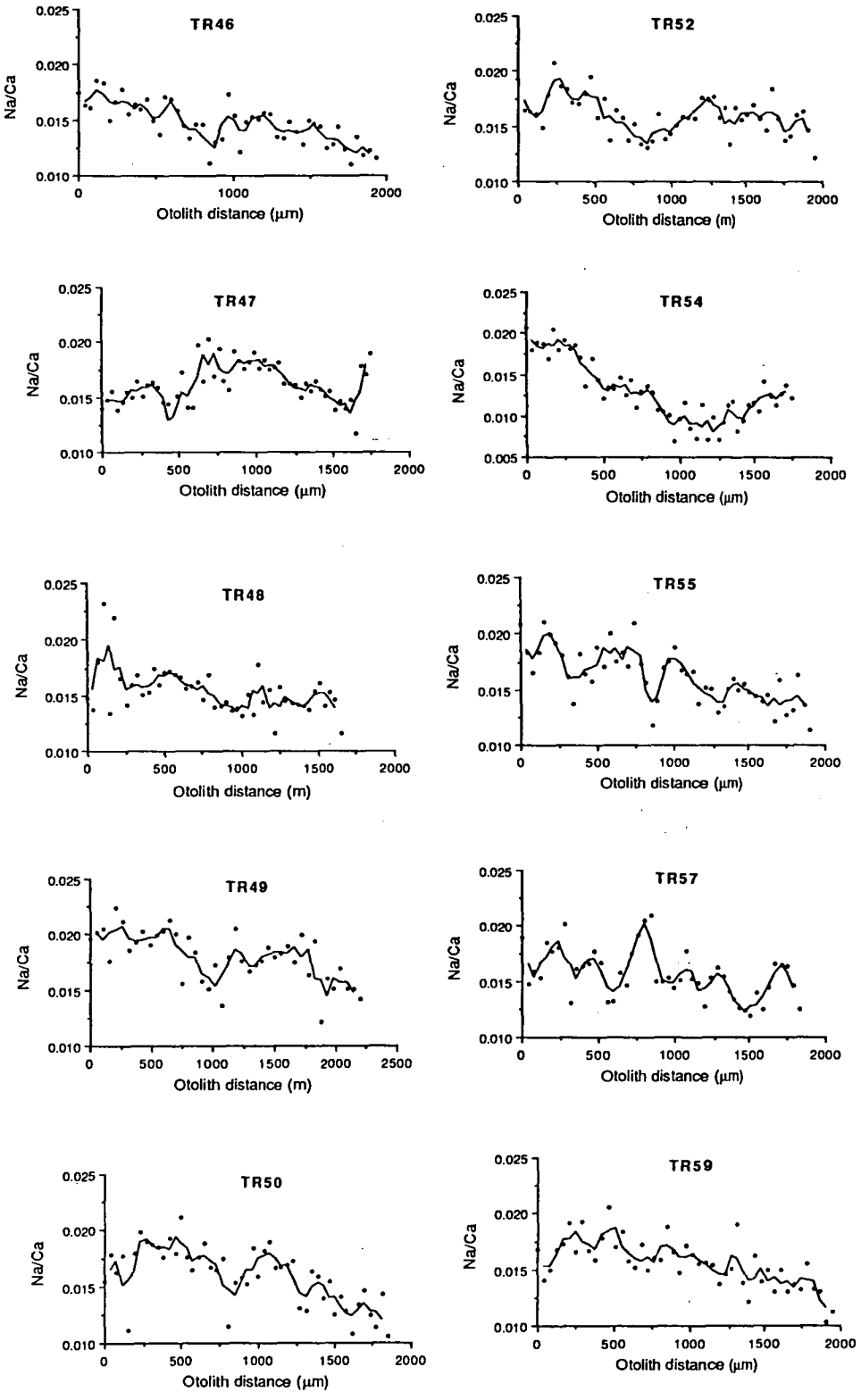

Fig. 4.10 (continued)

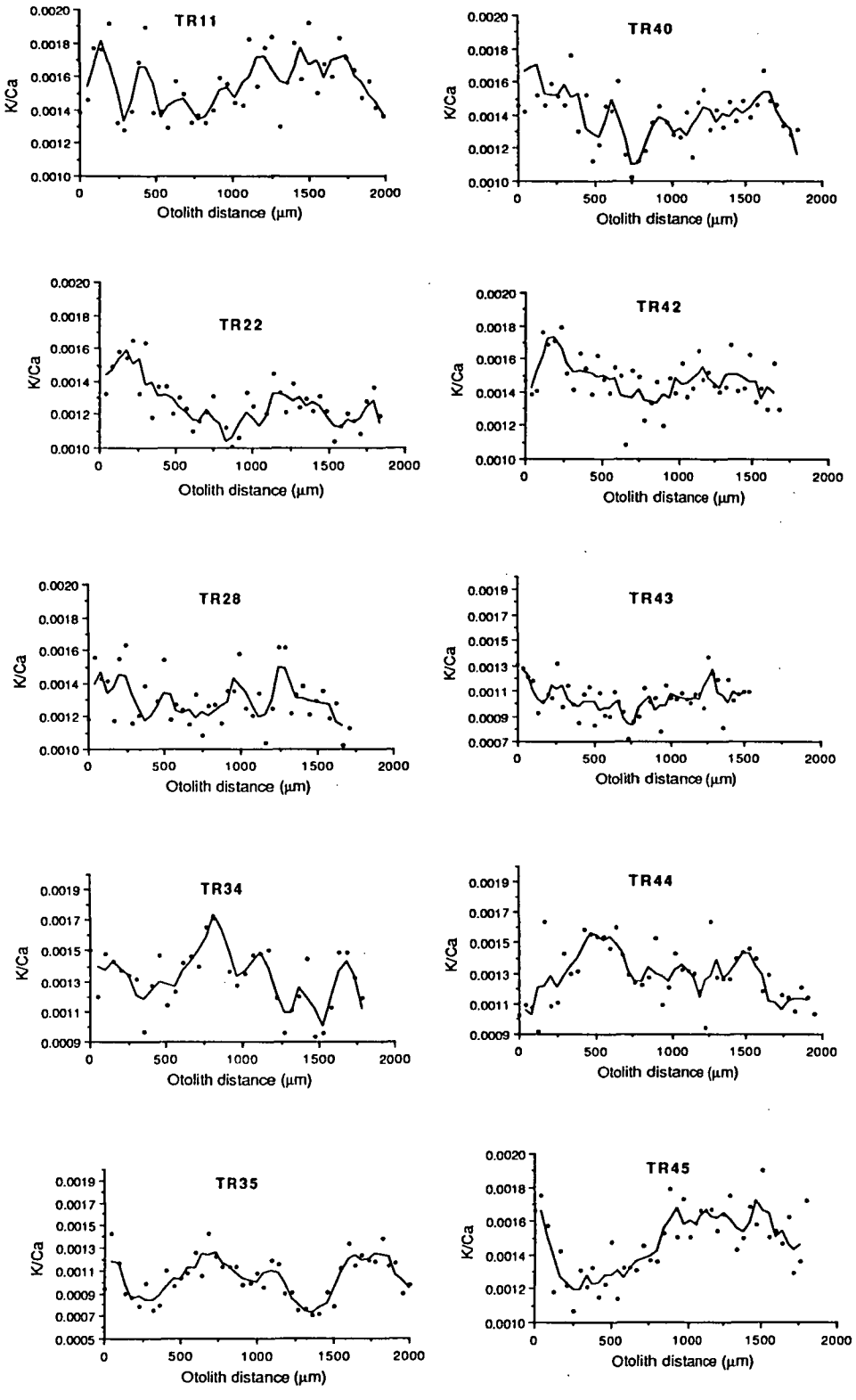

Fig. 4.11 Plots of K/Ca ratio data from microprobe transects across the sagittae (0 µm=primordium) of 20 Australian salmon collected near Vansitart Island in March 1986. Points are the raw data and the line represents data after smoothing with a 3-point moving average. Data on the length, weight, sex and age of these fish can be found in Table 4.3.

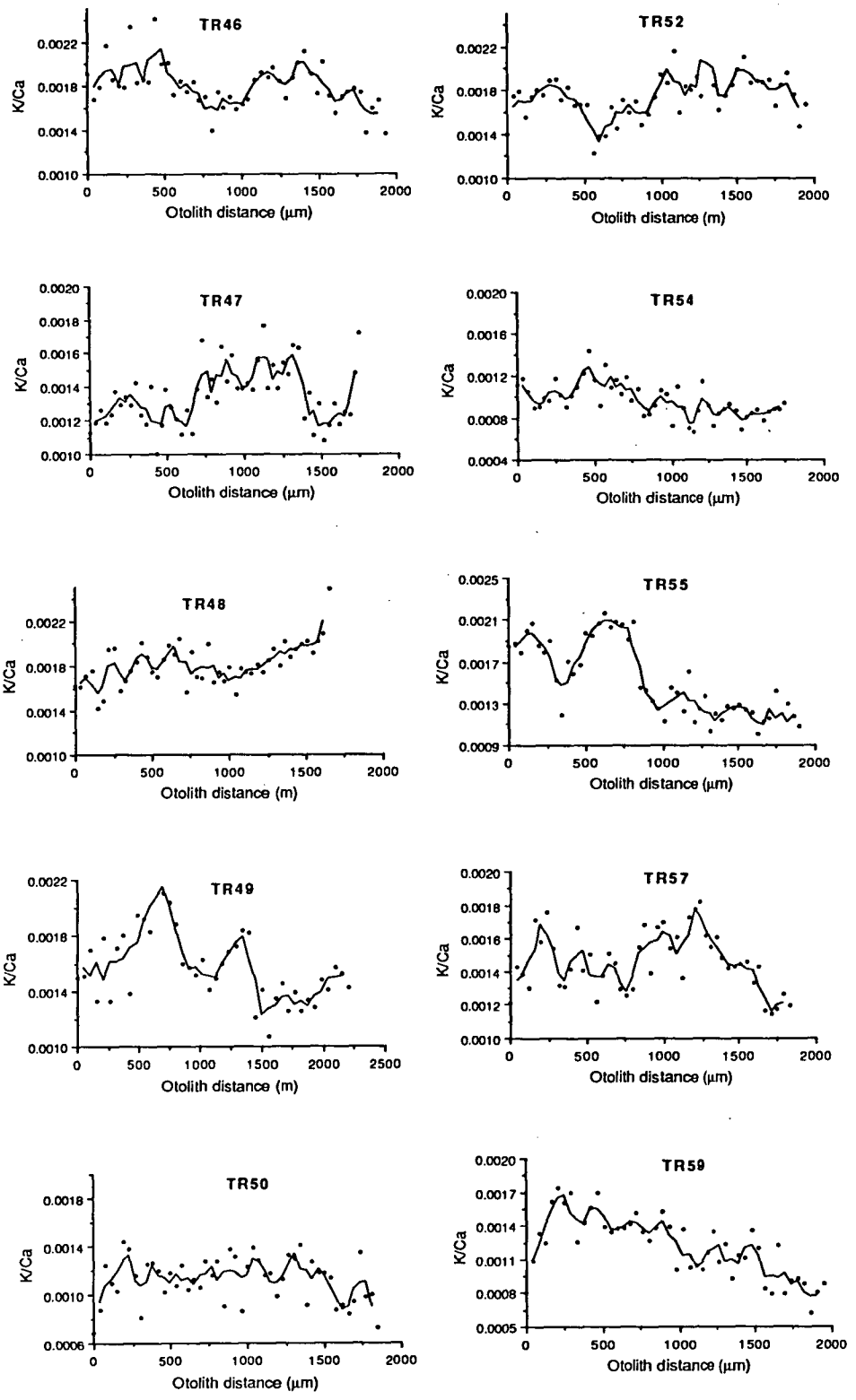

Fig. 4.11 (continued)

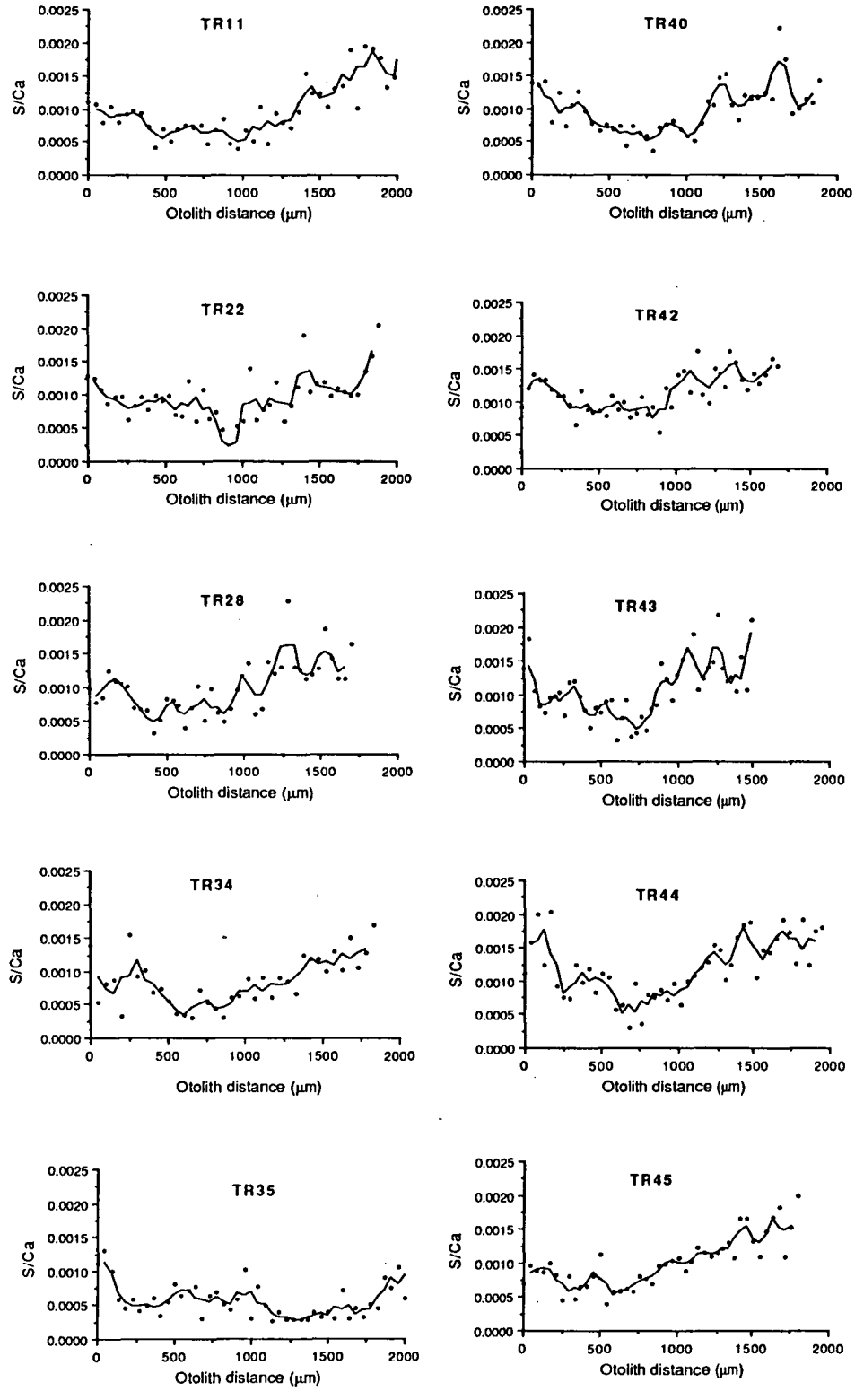

Fig. 4.12 Plots of S/Ca ratio data from microprobe transects across the sagittae (0 µm=primordium) of 20 Australian salmon collected near Vansitart Island in March 1986. Points are the raw data and the line represents data after smoothing with a 3-point moving average. Data on the length, weight, sex and age of these fish can be found in Table 4.3.

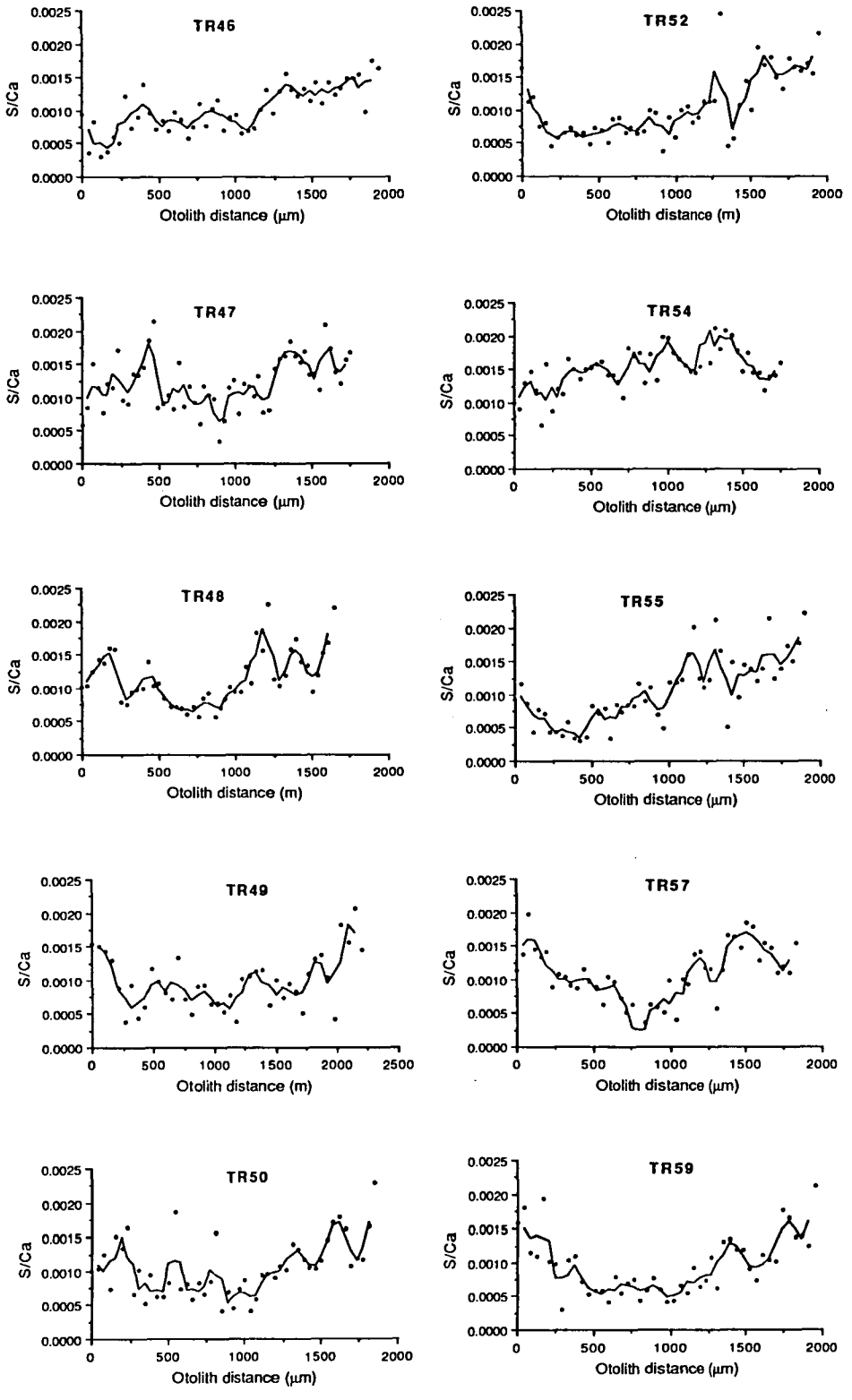

Fig. 4.12 (continued)

the cross correlations from the Sr/Ca, Na/Ca, K/Ca, S/Ca and the mean cross correlation data for the combined elements are shown in Fig. 4.13. A distance of 2.5 is significant at the 1% level and a distance of 3.3 is significant at the 5% level.

Comparison of the dendograms indicates that there is a great deal of variation in clustering among the 20 fish from the school based on the different elemental ratios. At the same time, a large percentage of the clusters are significant. The significant clusters in the strontium data at the 1% level are confined to groups of 2 or 3 fish, whereas at the 5% level there is evidence of 5 larger clusters (Fig. 4.13a). The degree of clustering is similar in the potassium data, but the individuals within the cluster are different (Fig. 4.13c). Both the sodium (Fig. 4.13b) and the sulphur data (Fig. 4.13d) are similar in that they show a much higher degree of significant clustering with the greatest degree of similarity evident in the dendogram based on the sulphur data. Cluster analysis based on the mean cross correlation for each element results in a level of organization similar to that found for the strontium and potassium data (Fig. 4.13e).

There is no clear relationship among the dendograms and evidence of fish that are clearly different from the others is not consistent among dendograms. For example, fish #54 is clearly "unrelated" to the other fish based on the sulphur data, whereas it shows relatively close associations in the other dendograms. Fish #47 is unrelated to the others based on the combined elemental data, but it is significantly correlated with other individuals based on the sodium ($p<0.01$), potassium ($p<0.01$), sulphur ($p<0.01$) and strontium ($p<0.05$) data.

Otolith microchemical data presented in this section are not adequate for making conclusions regarding the long term association of individuals within a fish school. However, the data do indicate the potential utility of this type of analysis and, at the same time serve to highlight the complexity of otolith microchemistry data.

The 20 individuals analysed in this section were undoubtedly contemporaneous in that they were collected in the same location and were approximately the same age. Australian salmon have a restricted distribution and their range is well defined. This information, combined with the fact that recognizable chemical patterns were evident among some of the younger juvenile Australian salmon, would seem to make this species a prime candidate for the study of environmentally influenced patterns in otolith chemistry. However, the lack of any periodicities which corresponded with the estimated fish age is further evidence that the factors effecting otolith trace element

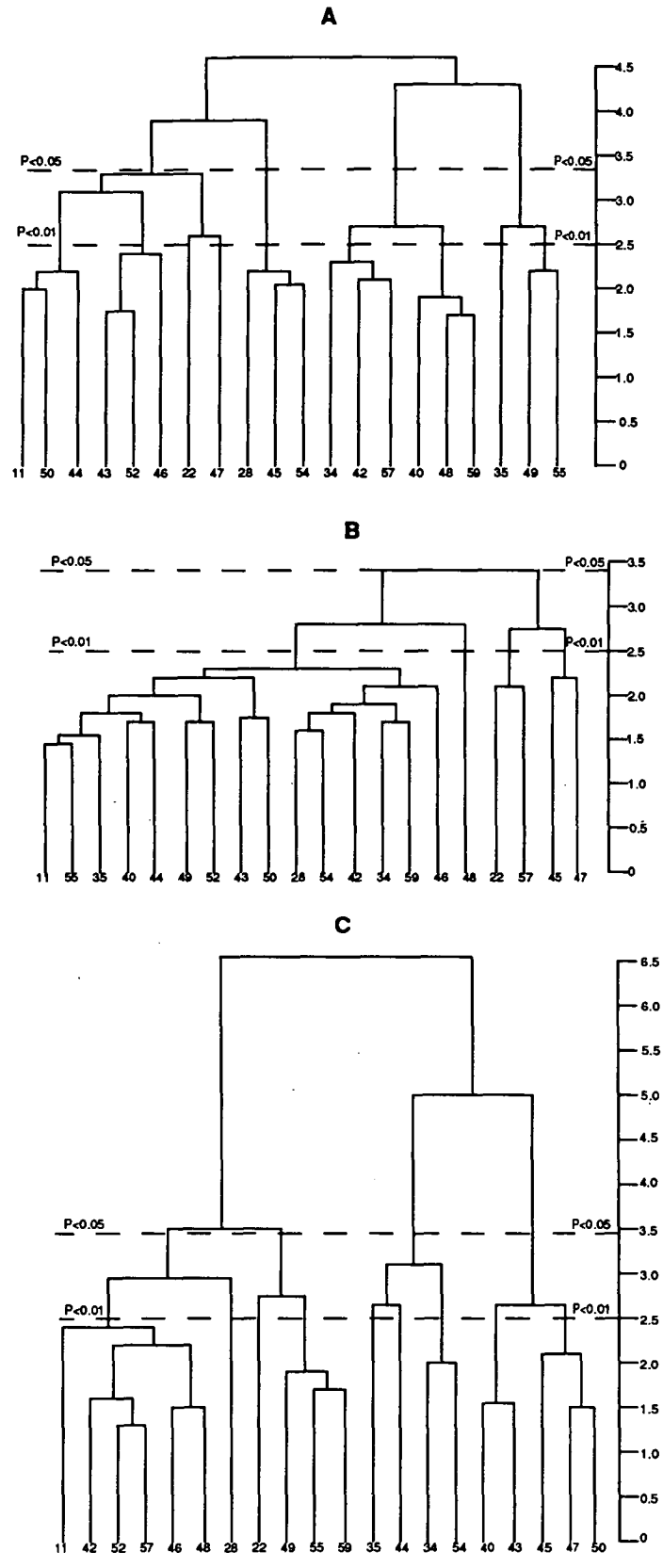

Fig. 4.13 Dendograms based on cross-correlation analysis of microchemical transects of Australian salmon sagittae. Integers refer to individual fish as in Figs. 4.9 to 4.12. Data on the length, weight, sex and age of these fish can be found in Table 4.3. (A) Sr/Ca data; (B) Na/Ca data; (C) K/Ca data.

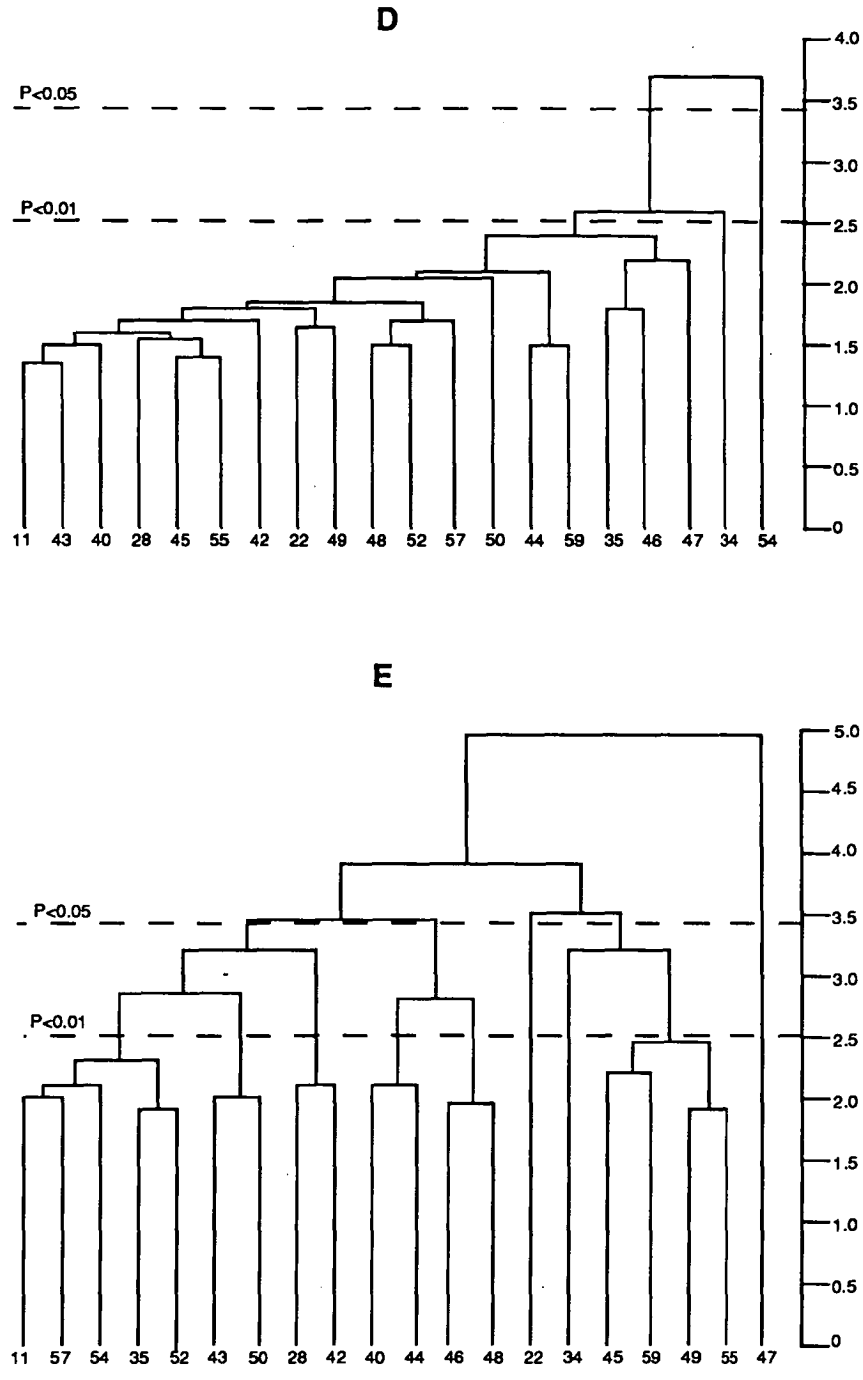

Fig. 4.13 (continued) Dendograms based on cross-correlation analysis of microchemical transects of Australian salmon sagittae. Integers refer to individual fish as in Figs. 4.9 to 4.12. Data on the length, weight, sex and age of these fish can be found in Table 4.3. (D) S/Ca data; (E) Sr/Ca, Na/Ca, K/Ca and S/Ca data combined as discussed in the text.

chemistry are complex and, that temperature does not significantly effect Australian salmon otolith chemistry in a direct manner.

Patterns were evident in the microchemical transects of the adult Australian salmon and the large number of significant correlations among these transects provides some indication of the degree of similarity among them. These data bring closer an approach that can be used to determine relationships among individuals within a school, but clearly, they do not present conclusive evidence regarding the nature of fish schools. The results can be used to refine the methods employed and help in directing future research in this area. Similar conclusions were arrived at by Dillon and Clark (1980) in their use of growth increments to determine contemporaneity in a population of scallops. However, the lessons from this research are somewhat different.

The major problem in comparative analysis of microchemical transects derives from the discrete nature of the samples and the need to reduce sample size because of both time and cost. Recognizable patterns were clearly evident in the juvenile Australian salmon, but duplication of the sampling frequency used would be extremely expensive. Even if the sample size were increased to a point where patterns were clearly defined, the chances of finding a similar pattern among different fish are small. This is obvious based on the low frequency of recognizable chemical patterns among small juveniles collected from a similar location. If it is difficult to find clear similarities among the small fish it would be far more difficult to find similarities among adults. This is due to the probable mixing of individuals within a school from widely different nursery grounds.

A major problem in the intercomparison of otolith life-history transects is the fact that the data collected are not continuous. Samples are integrated measures over a relatively small area with some degree of separation between each sample. Although these samples are uniformly spaced this does not insure that the regions analysed at each interval will correspond among individuals. The reasons for this are both biological and analytical in nature. From a specimen preparation viewpoint it is difficult to section large numbers of otoliths in precisely the same plane, even with the aid of a precision low-speed diamond saw (blade thickness approximately 150 μm). This is related to both the set-up of the otolith specimen in the saw and the fact that otoliths from different fish will probably differ, albeit slightly, in their dimensions. As a result, individual measurements of otolith microchemistry might be

made along slightly different axes in different otoliths.

In section 4.2, I discuss the variability that exists in otolith microchemistry life-history transects taken from the same otolith. These data show the problems that are encountered when transects along different planes are compared. Although there is generally considerable agreement among multiple transects from the same otolith, the differences that are apparent clearly make intercomparison among individuals difficult.

The biologically related problems that might make intercomparison of otolith chemistry transects problematic are even more confounding than the problems related to sample preparation. Even if it were possible to sample along precisely the same plane in each specimen, this would obviously not guarantee that the axes sampled were uniform in regard to their individual growth rates, increment widths and related phenomena. Therefore, even if the responses of otolith chemistry to physiological and environmental phenomena were quantifiable in a precise manner, this would not necessarily mean that microchemical life-history transects from various individuals would correspond, even if the fish were precisely the same length, weight and age. This, of course, is related to the varying growth rates that may be manifested by individuals even when exposed to what appear to be similar environmental conditions. These differences may result from genetics, disease or small-scale environmental variability.

Regardless of the potentially confounding properties of fish otolith growth, it is still be possible to recognize, among different fish, patterns in the variations in fish otolith microchemistry. This has been established from the data presented on juvenile Australian salmon in Section 4.4. This section attempted to extend these properties to adult Australian salmon.

It is important to realize that the goal of the study outlined in this section is to develop a method for interpreting an individual's environmental history, and to use this data as an index of association. Unfortunately, several basic factors discussed in earlier sections serve to confound this goal. Not only are the variations in otolith microchemistry difficult to explain, but there is also a large degree of variability even among transects within an otolith. In many cases, relatively sophisticated statistical methods would be required to determine that two different transects were from the same individual. Certainly, this makes it virtually impossible to use otolith chemistry as an index of, for example, temperature. Alternatively, it is conceivable that otolith

microchemistry can be used as an indicator of relative changes in the physiology of fish and, perhaps, these relative changes can be used to determine interactions and associations among individuals.

4.6 Juvenile *Acanthachromis polyacanthus*: characterization of nursery grounds

4.6.1 Introduction

Acanthachromis polyacanthus is unique among the pomacentrids because it does not have a planktonic larval phase (Robertson, 1973; Allen, 1975). Individuals hatch from demersal eggs and the newly hatched juveniles are subject to a relatively high degree of parental care (Thresher, 1985). The young are defended by the parents and remain in their care until they reach a length of from 20-25 mm TL, at which point they disperse from the territory of the parents and move out onto the reef with other individuals of their cohort (Thresher, 1985).

Because of the unique reproductive biology of this damselfish, combined with certain characteristics of it's distribution, it was felt that it would be useful in an investigation of the effect of small scale habitat variation on otolith microchemistry. *A. polyacanthus* is found in a wide range of habitats on the Great Barrier Reef. At Heron Island Reef and Wistari reef, *A. polyacanthus* is common on both the outer reef slope and within the shallow lagoon. Individuals from the two habitats would, at the very least, experience different water temperatures and salinities. Other features characteristic of shallow lagoons versus the reef slope might also play a role in the chemistry of the otoliths formed within juveniles while they remained part of a brood associated with a single location on the reef. This investigation seeks to determine if there are differences in the chemical composition of otolith primordia/nuclei from *A. polyacanthus* collected in these two different habitats.

4.6.2 Materials and methods

Acanthachromis polyacanthus were collected from both the reef slope and lagoon of Heron Island Reef and Wistari Reef in the Capricorn Group of the Great Barrier Reef, Australia from 10-14 December, 1986. Individuals from a brood were collected by anaesthetizing them with quinaldine and were then captured in a hand net. Samples from individual broods were placed in plastic bags and frozen upon return to the laboratory.

Temperature and salinity data were collected to determine if there were notable differences in the physical characteristics of the water from the various collection sites. Temperature was measured within the reef lagoons and along the reef slope with hand held mercury thermometers. Maximum/minimum thermometers were moored in the lagoons of Heron Island Reef and Wistari Reef from the 10-14 December and the temperatures were checked each day. Water samples were collected and returned to Hobart where they were analysed using an autosalinometer by the CSIRO Marine Laboratories.

Sagittae and lapilli were extracted from defrosted fish, washed in deionized water and then oven dried at 40°C. Otoliths were mounted sulcus side up in Cryobond 509 (Aremco Industries, Inc.), a heat labile thermoplastic polymer. Otoliths were ground to the level of the primordium and the remaining preparation steps before microprobe analysis were similar to those used for other species.

Wavelength dispersive electron microprobe analyses were carried out as for Australian salmon and blue grenadier with a low beam current (10 nA on copper) and relatively long counting times as employed in Chapter 2.

4.6.3 Results and Discussion

Physical data collected from Heron Island Reef and Wistari Reef are shown in Table 4.4. There are differences in the temperatures and salinities measured on the different reefs and in the different habitats, but they are not extreme. Although the maximum temperatures in the lagoon of Heron Island Reef are relatively high during mid afternoon low tides, the relatively cool temperatures that occur in the evening at low tides may balance the effect of the higher temperatures. The salinities of the lagoons are consistently higher during afternoon low tides, but these differences are small.

Table 4.4 Summary of temperature and salinity data collected from the lagoon and reef edge of Heron Island Reef and Wistari Reef. Temperatures are at a depth of 2 meters.

Location	Salinity (‰)	Temperature (°C) Maximum	Minimum	Mean
Heron lagoon		32.0	24.5	28.3
low tide	35.523			
high tide	35.436			
Heron reef edge	35.436	26.5	26.0	26.3
Wistari lagoon		27.5	24.5	26.0
low tide	35.582			
high tide	35.478			
Wistari reef edge	35.448	26.5	26.0	26.3

Analysis of the otolith chemistry in the nuclear region of sagittae from 30 different individual *A. polyacanthus* indicates that there were no significant differences in Sr/Ca, Na/Ca, K/Ca or S/Ca (Table 4.5).

Table 4.5 Elemental ratios obtained from the otolith nuclear region of *Acanthochromis polyacanthus* collected from lagoon and reef slope of Heron Island Reef and Wistari Reef. Values are based on 5 microprobe measurements on each otolith obtained from 15 fish from the two environments. Results of unpaired 2-tailed t-tests to determine if differences among habitats were significant are shown.

Element ratio	Lagoon (n=30)	Reef slope (n=30)	t	P
Sr/Ca	0.0029±0.0005	0.0030±0.0007	0.647	>0.5
Na/Ca	0.0158±0.0055	0.0149±0.0031	0.913	>0.2
K/Ca	0.0008±0.0004	0.0007±0.0005	0.721	>0.4
S/Ca	0.0009±0.0003	0.0011±0.0003	1.107	>0.2

The data collected from juvenile *A. polyacanthus* indicate that there is inadequate inter-site variability to distinguish fish from broods raised on the reef edge from those raised in the lagoon environment. Although there are significant differences in the temperatures of these two environments other segments of this study have shown that temperature alone is probably not capable of mediating a significant change in otolith chemistry.

4.7 Adult *Hoplostethus atlanticus*: age estimation

4.7.1 Introduction

Orange roughy, *Hoplostethus atlanticus*, is a species of considerable commercial importance in southeast Australian and New Zealand waters. Despite the value of this resource little is known of the biology of this bericyform fish which is generally caught at depths of from 800 to 1200 m. Although it is generally accepted that these fish are very long-lived, perhaps 100 years or older, a satisfactory method of age estimation for these species has not been developed. Ages of the smaller juveniles have been estimated on the basis of the counting of annuli and these data have been verified by data from length-frequency distributions (unpublished data, Mr. D. Smith, Marine Science Laboratories, Queenscliff, Victoria; unpublished data Dr. P. Mace, New Zealand Ministry of Agriculture and Fisheries), although no form of validation has been established.

Spectral analysis

Microchemical transects across an otolith are spatial series because they are ordered with respect to a position on the otolith. In many instances a spatial time series can be regarded as a generalization of a time series. This relationship is particularly apt in the case of spatially organized mineralized tissue because of the time related nature of otolith production. As such, it is reasonable to consider data collected across an otolith, be it derived from measurements of chemical composition, increment width, densitometry or a range of other variables, as a *de facto* time series.

When applying methods of time series analysis to otolith microchemical transects it is important to be aware of several factors. Most important is the basic assumption of time series analysis which states that discrete data must be separated by equal units of time. This assumption also applies to continuous time series data. Continuous data were not collected in this study primarily because of the need for

long counting times when dealing with elements that are only present in trace (<0.5 weight %) quantities. However, it is logistically feasible to collect continuous data series from otoliths if only Ca is measured and high beam currents are used. In such instances the assumption would state that the spatial axis of the otolith is linearly related to time and this relationship is constant across the entire otolith. In the majority of fish species somatic growth and otolith growth are clearly not uniform with time. Therefore, even though the microprobe measurements were uniformly spaced across the otolith in a spatial sense, it seems likely that, in most instances that they were not equally spaced in time.

In order to make individual measurements of an otolith microchemical transect equally spaced in time it is necessary to apply a model of otolith growth to the time series. Such a manipulation of the time series would be called "warping", primarily because different portions of the series would be manipulated to varying degrees. For example, during the juvenile growth phase otolith growth may be linearly related to time, whereas growth may decrease at the onset of maturity. At this point it would be necessary to apply a warping function to the time series so that points are uniform in a temporal sense. Unfortunately, the application of such a warping function implies some knowledge regarding the age, and, concomitantly, the growth rate of the species being studied. In the majority of research situations which might deal with otolith microchemistry this would result in a circular argument, as fish age and growth are the variables we hope to predict from microchemical transects. However, in the interests of identifying significant periodicities I used several simple models of otolith growth as time series warping functions.

Several studies have attempted to use spectral analysis to determine the frequency of chemical periodicities in calcified structures, usually in relation to environmental or geophysical phenomena such as the tides. Dolman (1975) discusses the use of normalized power spectra to quantify the periodicities in optical density or increment width present in molluscan shells and stromatolites. He was primarily interested in extracting environmental information from growth records and was not specifically interested in the age of the organisms. With this in mind, he subjectively identified regions where growth rate had changed, developed a growth trend model on the basis of these data and used this model to uniformly space (in a temporal sense) increment width data. Rosenberg and Jones (1975) measured chemical periodicities in molluscs and stromatolites and used Fourier analysis to smooth the

chemical series based on recombination of the major harmonics (>50% of the total power spectrum). However, they do not discuss the relative power of the various harmonics, whether or not they are significant and they do not consider the significance of varying growth rate in an individual over time. Rosenberg et al. (1980) discuss the use of spectral analysis to determine patterns in the chemistry and growth of skeletal structures. They state that "variations in growth rate in the time domain appear as variations in wavelength in the frequency domain," and indicate that this fact may be useful in studies involving allometry. Rosenberg and Simmons (1980a, 1980b) used this principle to investigate circadian, ultradian and infradian cycles in the growth and chemistry of rabbit teeth and they were able to identify a range of significant periodicities. Unfortunately, in those cases where the discrimination of significant periodicities by spectral analysis may be difficult at the outset, additional variations attributable to growth rate would only serve to make the discrimination of significant periodicities even more elusive. In fact, changes in growth rate may obscure certain periodicities through interference as discussed in Bloomfield (1976). The extent of these complications in spectral analysis of fish otolith microchemical transects cannot be determined unless we have a full understanding of both otolith growth rate and otolith chemical variability.

A second major problem in dealing with spectral analysis of otolith microchemical transects is based on the frequency of sampling, particularly in fish that are presumed to be slow growing and old. Even if it were possible to estimate the fish growth rate and apply this model to the microchemical data, it could still be difficult to identify cyclical variations in otolith composition. This is based on the simple concept of the Nyquist frequency (Bloomfield, 1976), which relates to the highest frequency about which meaningful information can be obtained from a data set. Expressed in terms of time the Nyquist frequency, $f_N = 1/2\Delta t$. This estimate is valid in ideal situations, but the variation in natural systems, coupled with sampling errors makes this rarely the case. It would be more realistic to expect to extract information regarding a particular frequency if the sampling rate was 5 times the frequency. Because the minimum acceptable sample size when measuring the chemistry of calcium carbonate with the wavelength dispersive electron microprobe is on the order of 10 μm x 10 μm, at least 50 μm of otolith growth would be required to obtain meaningful information regarding a periodicity. This is not a problem in fish that grow rapidly, but may be a problem in older, slow growing individuals.

Several other factors associated with both data collection and data analysis may adversely affect interpretation of power spectra obtained from microchemical data. These include identification of harmonics of fundamental frequencies, leakage, aliasing and, as discussed above, variations in growth. Detailed discussions of these problems can be found in Jenkins and Watts (1968) and Bloomfield (1976) and, in relation to increment data from molluscs and stromatolites, in Dolman (1975).

4.7.2 Materials and methods

Orange roughy otoliths were obtained from fish collected by the Tasmanian Department of Sea Fisheries. Otoliths were removed from frozen fish after defrosting, cleaned and stored dry in envelopes. Data on collection, weight, length, sex and maturity were recorded. Specimen preparation was similar to that of blue grenadier otoliths (Chapter 2) and the protocol for electron microprobe analyses is similar to that used for other microprobe transects (Section 4.2.1). Spacing between individual microprobe analyses was consistent within otoliths, but ranged from 15 to 30 μm, among individuals. The spacing of samples is evident from examination of the plots of chemical ratios against otolith distance.

Despite the numerous complications discussed in the introduction I attempted to obtain power spectra from orange roughy otolith microchemical data. Data were collected at intervals of 15 μm with each sample including an area of 100 μm^2. Generally a central portion of a sampling record was used and this included up to 512 points. Detrending of orange roughy data sets was not necessary because the central portions of the microchemical record appeared to be free of significant trends and, there was no evidence of trends dominating the spectral analysis. A fast Fourier transform (FFT) routine was employed with a triangular spectral window (Bloomfield, 1976). Significance of harmonics resulting from spectral analysis was determined using the test described by Shimshoni (1971) and discussed by Rosenberg et al. (1980). The test was developed by Shimoshoni (1971) to help in the identification of significant peaks in seismic records. Each harmonic is normalized relative to the total power present in the spectrum, the various normalized harmonics are then ranked according to their power (amplitude), and then compared with the amplitude that would be expected from a similarly ranked peak obtained from a random series of normally distributed points with a similar sample size (Rosenberg et al., 1980). The tabled values used for the determination of significance appear in

Shimshoni (1971).

4.7.2 Results and Discussion

The relationship between otolith length and fish length in orange roughy indicates that, up to a fish length (SL) of about 40 cm, otolith length increases proportionally to fish length (Linkowski and Liwoch, 1986). However, the fact that otolith growth appears proportional to growth in length up to a relatively large size in orange roughy (≈40 cm SL) does not indicate that somatic growth or otolith growth are constant over time. This is an important distinction when investigating rhythms in otolith microchemistry that may be derived from environmental phenomena and when considering growth in general.

Microchemical transects from 9 orange roughy are illustrated in Figs. 4.14 and 4.15. Figure 4.14 shows Sr/Ca, Na/Ca, K/Ca and S/Ca data for an individual fish, whereas Fig. 4.15 shows only Sr/Ca data from 8 roughy. Sr/Ca ratio transects from orange roughy generally show a similar basic form. Ratios start out at relatively high levels, 0.006 to 0.008, and drop down to approximately 0.004 after 750 μm of otolith growth. Sr/Ca ratios vary around this level until late in life. In the larger fish (>45 cm SL) otolith Sr/Ca ratios were found to increase markedly after otoliths reached a length of 8000 μm (primordium to edge on the major growth axis). In some of the larger fish Sr/Ca ratios above 0.007 were measured at the otolith margin. Na/Ca, K/Ca and S/Ca ratio data are characterized by a high level of variability (Fig. 4.14).

Variations in orange roughy otolith Sr/Ca ratios that could be related to otolith structural features were evident in the first 1000 μm of the transects. Eight of the 10 orange roughy otoliths analysed by microprobe showed a drop in Sr/Ca ratios in the first 1000 μm of the transect (Fig. 4.16). A notable feature of this drop was a slight increase in Sr/Ca ratio around 500 μm. This increase in Sr/Ca ratio at 500 μm is associated with a hyaline zone in the otolith. This zone is typically visible in both whole and sectioned orange roughy otoliths. Some researchers believe that this hyaline zone at 500 μm is an annulus laid down in the first year of life (personal communication, Mr. D. Smith, Victorian Institute of Marine Science, Queenscliff, Victoria).

The highest levels of Sr that I have measured in fish otoliths were found in a single orange roughy otolith (ORR33) (Fig. 4.15 and 4.16). In this individual,

Table 4.6 Data on orange roughy *Hoplostethus atlanticus* used in the investigation of age estimation based on microprobe transects of otolith trace element chemistry. All fish were caught at depths of 800 to 1200 m along the continental slope off Tasmania. The relevant microprobe data appear in Figs. 4.14, 4.15 and 4.16.

Fish no.	Sex	Length (cm)	Weight (g)	Date of capture
ORR9	M	35.4	1101	23/9/86
ORR10	F	39.5	1761	2/2/88
ORR14	M	24.0	428	2/2/88
ORR15	M	25.0	467	2/2/88
ORR16	F	49.4	2984	29/11/85
ORR20	M	46.7	2365	29/11/85
ORR33	IMM	21.0	181	23/9/86
ORR57	F	47.9	2470	29/11/85
ORR75	M	30.2	656	9/9/86

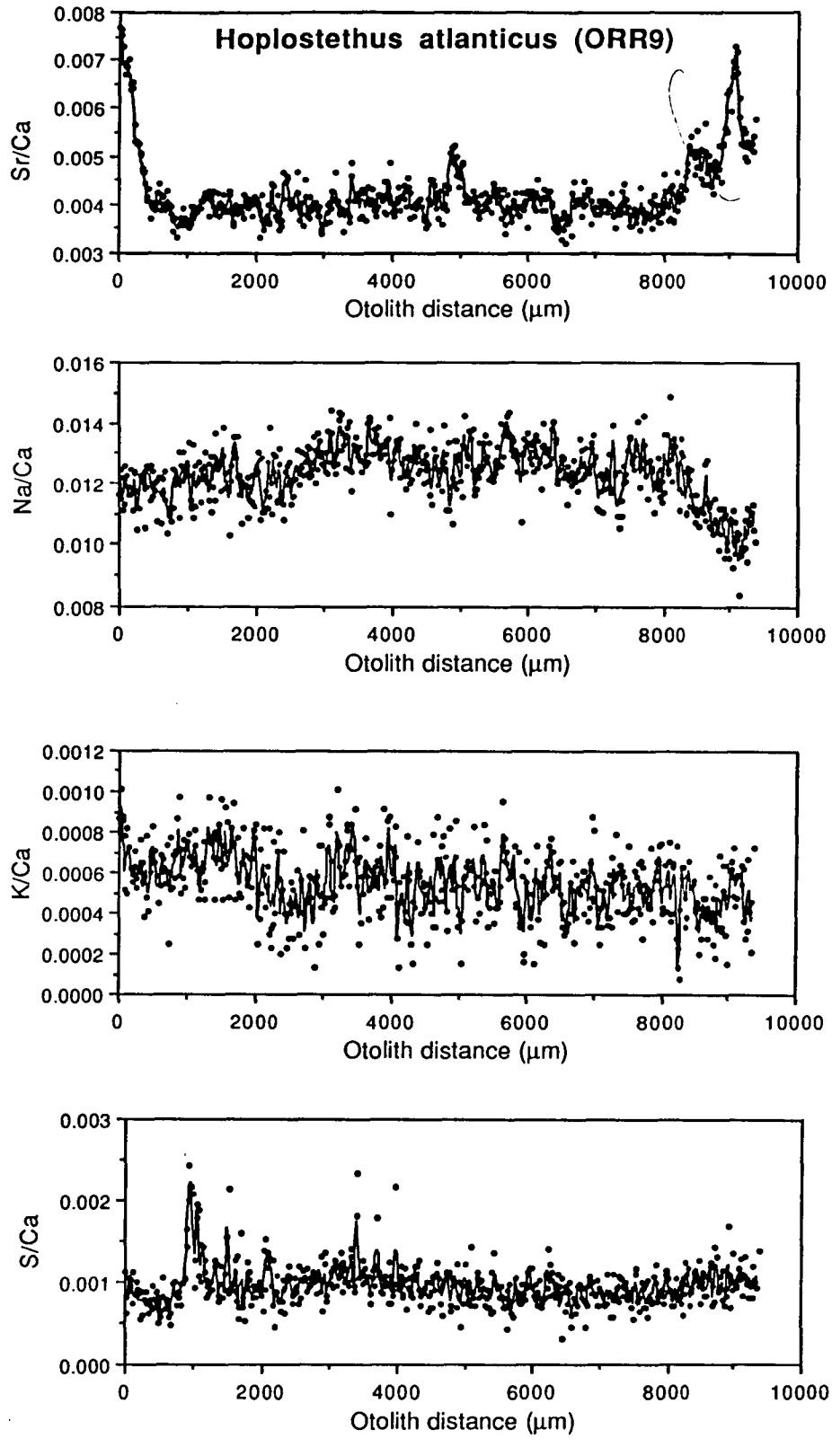

Fig. 4.14 Plots of Sr/Ca, Na/Ca, K/Ca and S/Ca data from a microprobe transect across a sagitta (section along the frontal plane, transect from the primordium to the postrostrum) from a mature *Hoplostethus atlanticus* (male, 35.4 cm SL, 1101 g) collected 23 September 1986 off the west coast of Tasmania. Points are raw data and line is based on a 3-point moving average.

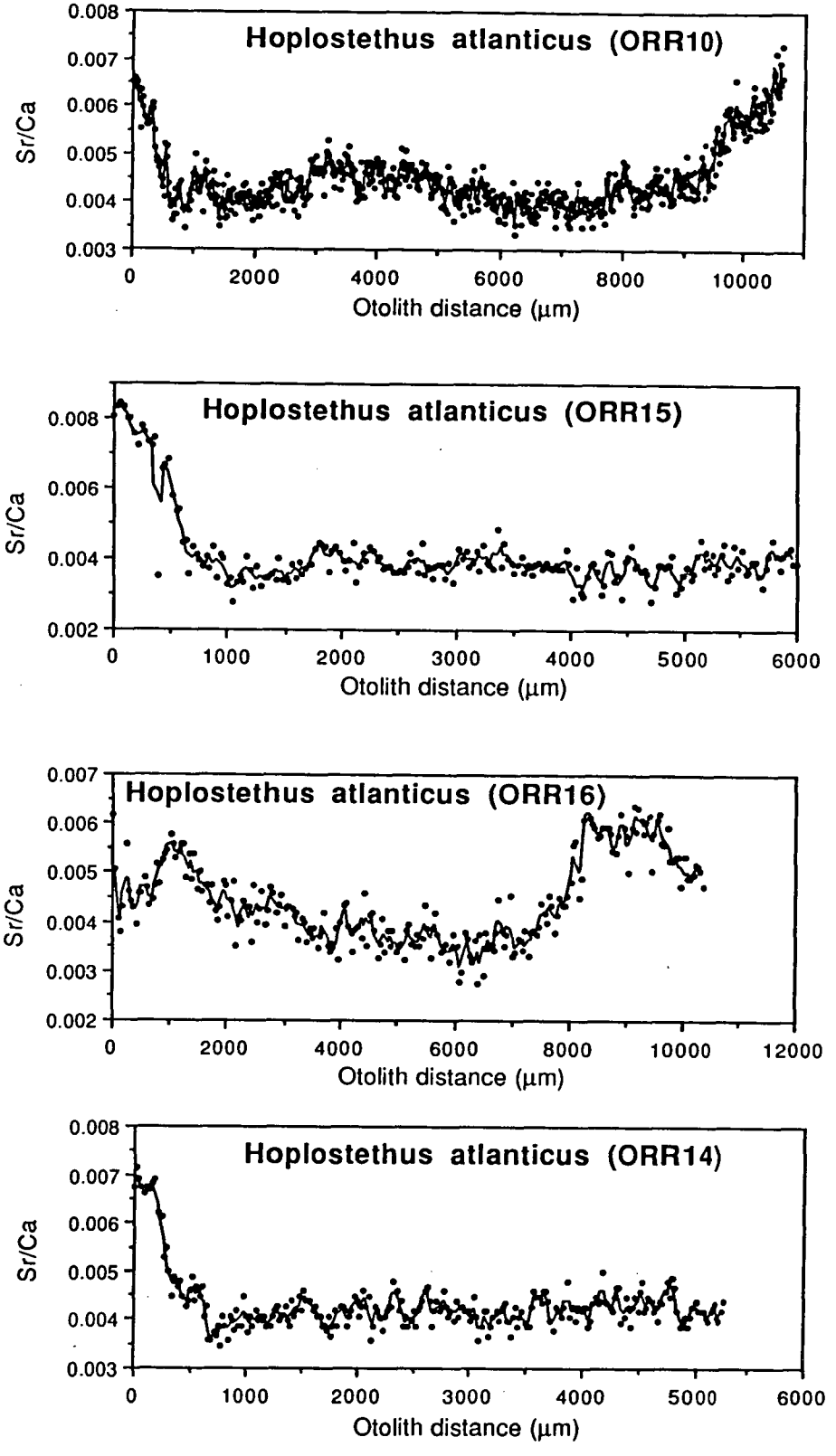

Fig. 4.15 Plots of Sr/Ca data from microprobe transects across sagittae (section along the frontal plane, transect from the primordium to the postrostrum) from 8 *Hoplostethus atlanticus* collected in waters around Tasmania. Points are raw data and the line is based on a 3-point moving average. Axes vary among fish to highlight the within fish variability. Data on fish length, weight, sex and capture date are presented in Table 4.6.

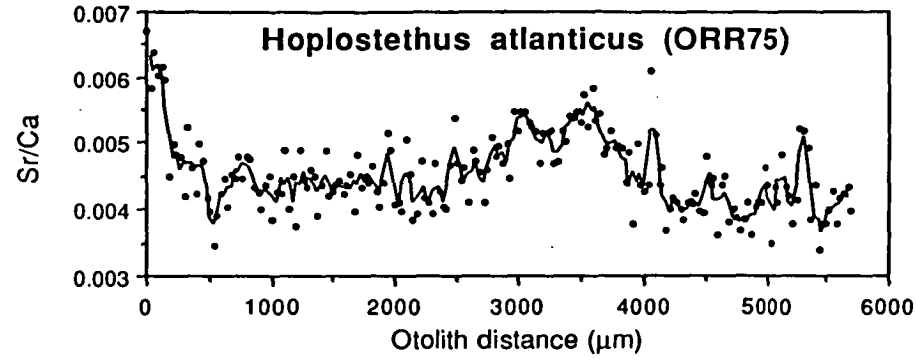

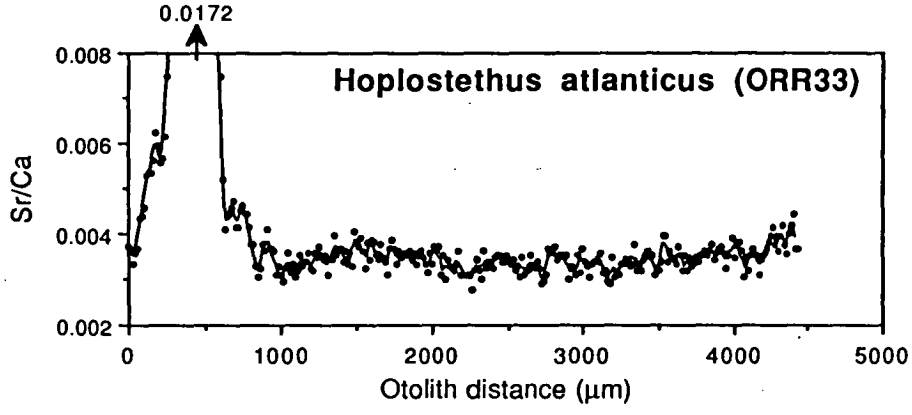

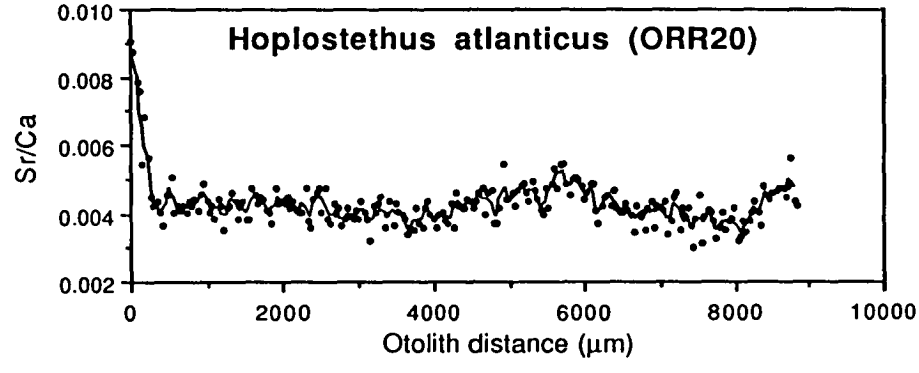

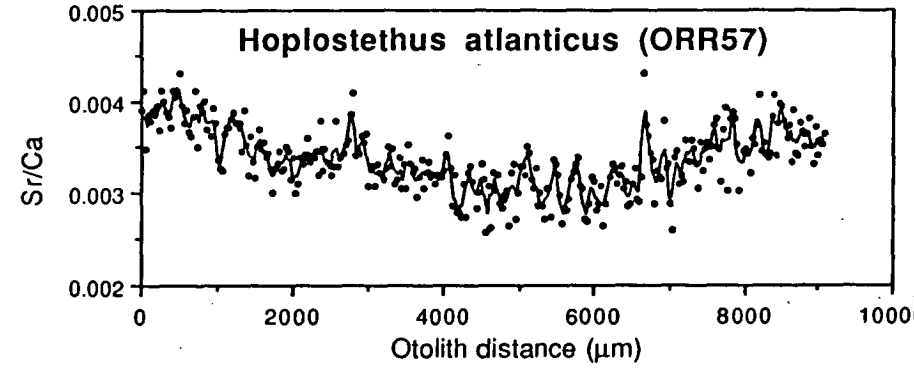

Fig. 4.15 (continued)

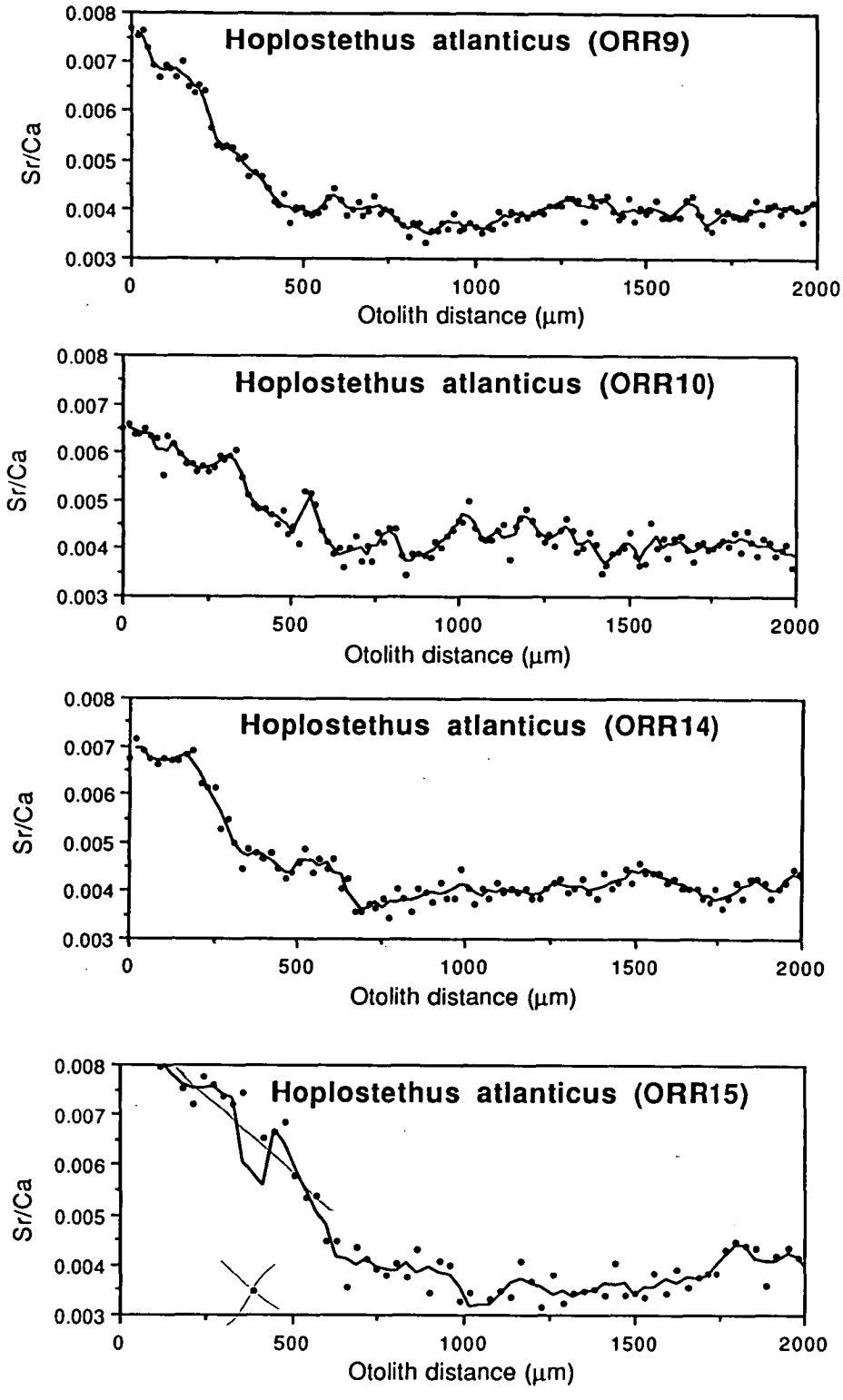

Fig. 4.16 Plots of Sr/Ca data from microprobe transects across sagittae (section along the frontal plane, transect from the primordium to the postrostrum) from 9 *Hoplostethus atlanticus* collected in waters around Tasmania (Table 4.6). Points are raw data and the line is based on a 3-point moving average. Same data as in Fig. 4.15 but only the first 2000 μm of the transects is shown to highlight common features. Note the increase in otolith Sr/Ca at an otolith distance of approximately 500 μm.

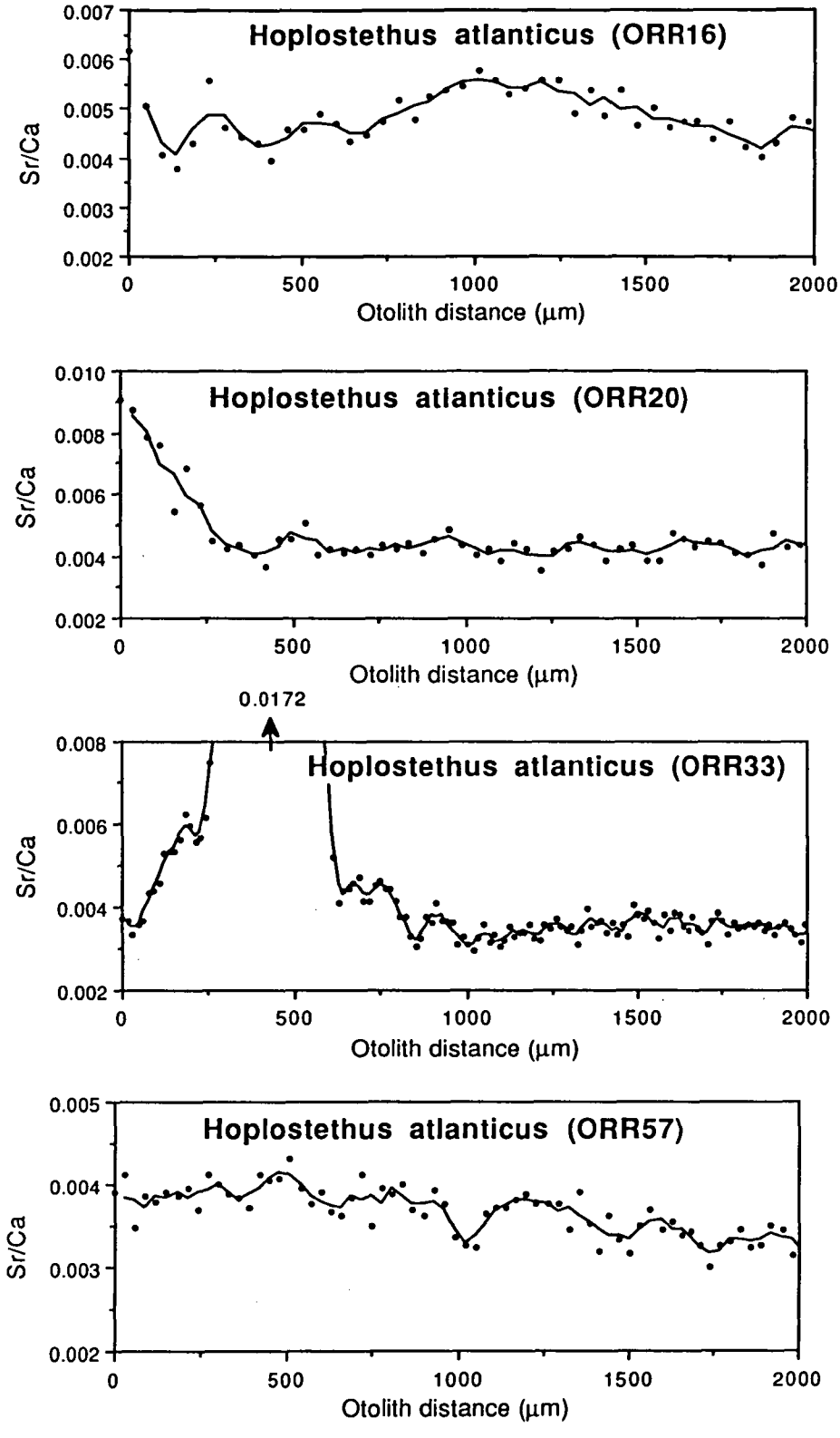

Fig. 4.16 (continued)

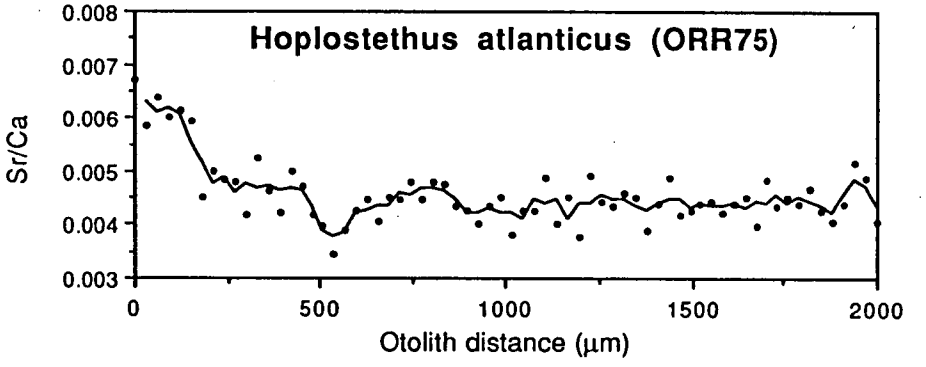

Fig. 4.16 (continued)

approximately 0.22 M/kg (20,000 mg/kg) of Sr was measured at a distance of around 500 μm from the otolith primordium. The increase across the otolith was gradual and there was no evidence of any structural changes in otolith in this region. In fact, the annulus that was generally detected at a distance of around 500 μm appeared to be located at a position about 750 μm from the primordium. Interestingly, there were no related extreme changes in otolith Na/Ca, K/Ca or S/Ca in this region.

The majority of spectra from microchemical transects of orange roughy otoliths failed to show evidence of significant periodicities even after applying a warping function to the series. Several spectra derived from Fourier analysis of orange roughy Sr/Ca, Na/Ca, K/Ca and S/Ca are illustrated in Appendix 4. In some cases, significant periodicities were detected (Fig. 4.17). The most significant periodicities were generally on the order of120 μm. If it is assumed that these periodicities are annual and then otolith growth is constant and linear over time, then in an otolith measuring 6000 μm from the primordium to the edge we would expect to find 50 cycles, corresponding to a fish of approximately 50 years of age. Otoliths of this size are found in orange roughy of about 40 cm SL. which have been estimated to be over 75 years old on the basis of radiometric ageing using $^{226}Ra/^{210}Pb$ decay series (personal communication, Dr. G. Fenton, Department of Zoology, University of Tasmania). Both methods indicate the extreme longevity of orange roughy. However, the fact that the fish are extremely old increases the probability of errors in the Fourier analysis of microchemical transects due to inadequate sampling frequency. On the basis of the results presented from the microchemical data, it seems that any relationship between microprobe transect ages and radiometric ages is probably a fortuitous occurrence as the various assumptions involved in the age estimate derived from the microchemical data are not likely to be fully satisfied.

Several features of orange roughy otoliths make them an interesting subject for study. Most notable are the features that are consistent among specimens, particularly the high Sr/Ca ratios that occur both early and late in life. Investigations into otolith composition of other species indicate that these changes are ultimately the result of changes in the composition of the endolymph. If this is so in the orange roughy, then extreme changes in physiology are probably occurring at this time. This hypothesis is plausible because, for instance, there are probably extreme changes in orange roughy growth rates both early and late in life. Unfortunately, data on this species is lacking and it is not possible to draw on existing knowledge to develop any significant

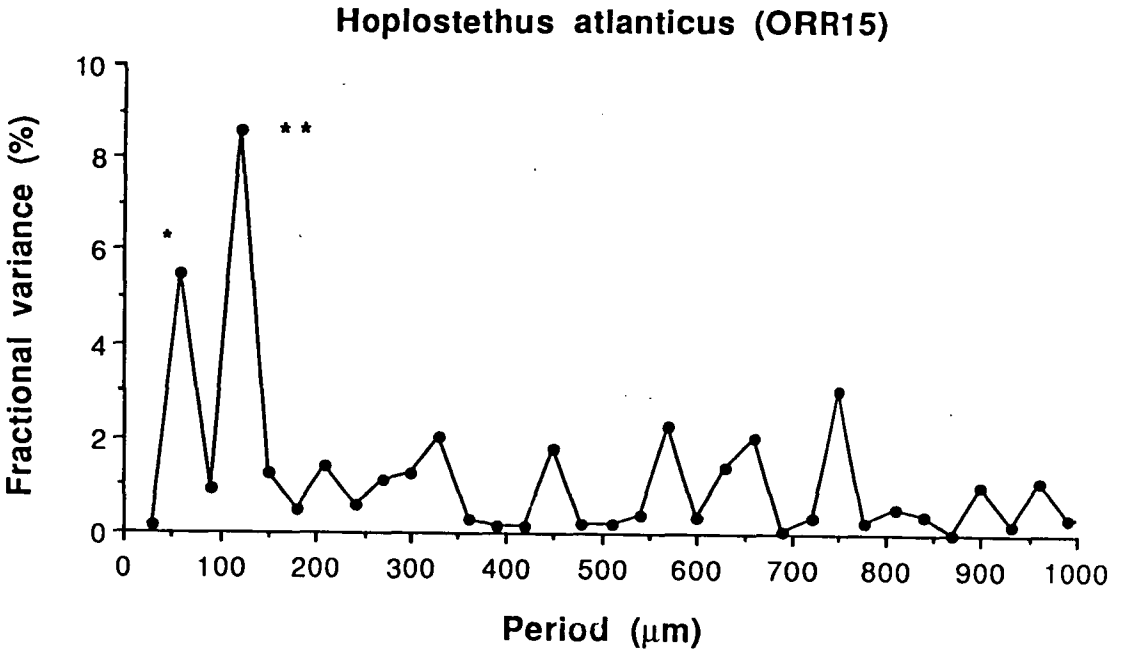

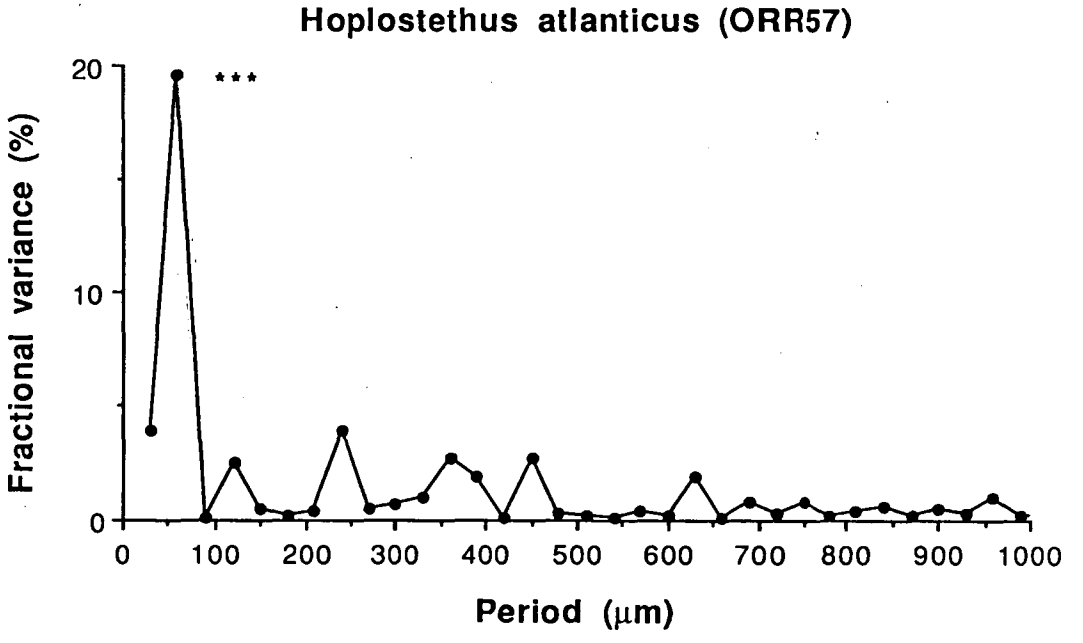

Fig. 4.17 Normalized power spectra for 2 microchemical series shown in Fig. 4.15. Significant harmonics are marked with asterisks (*, P<0.05; **, P<0.01; ***, P<0.001). Significance was determined on the basis of Shimshoni's (1971) test of significance in harmonic analysis. Other power spectra appear in Appendix 4.

arguments regarding the growth rates of orange roughy. Data presented in Chapter 7 on carbon isotope disequilibria may help elucidate some aspects of orange roughy biology, but further investigations are undoubtedly required.

4.8 Adult nothothenids: age estimation

4.8.1 Introduction

Time related changes in otolith microchemistry across otoliths were investigated in two Antarctic fish species to determine if clear cyclical patterns in otolith Sr/Ca ratios were a characteristic of notothenid fishes. Radtke and Targett (1984) presented Sr/Ca ratio data from a single electron microprobe transect across a sagitta from a pelagic notothenid, *Nototheniops larseni*. Despite a relatively low sampling frequency (1 sample every 28 μm), small beam size (5 μm), and considerable beam damage of the sample during data acquisition, these authors still found evidence for a clear periodicity in otolith Sr/Ca ratios. Furthermore, this periodicity was directly related to the estimated age of the fish based on counts of otolith annuli and microincrements. Although these periodicities cannot be related to temperature in the manner indicated by Radtke and Targett (1984) as discussed in Chapter 2, they still present valuable information on the manifestation of the effects of physiology and environment on the trace element composition of fish otoliths.

This investigation considers otolith Sr/Ca, Na/Ca, K/Ca and S/Ca ratios measured across the sagittal otoliths of two species of Antarctic fish, *Notothenia squamifrons* and *Nototheniops mizops*. These data will be used in an attempt to confirm the presence of clear cyclical periodicities in the otolith Sr/Ca ratios of Antarctic fish and will also determine if similar cycles are evident in data collected on other trace elements. Counts of otolith annuli and microincrements are also carried out in an attempt to provide further evidence that the periodicities, if any, are annual phenomena.

4.8.2 Materials and methods

Fish were collected by otter trawl from waters around Heard Island. The female *Nototheniops mizops* was collected on 5 October 1985. It was 146 mm in length (SL) and weighed 37.2 gm. The specimen of *Notothenia squamifrons*, a female, collected on 24 July 1987, was 153 mm long and weighed 48.0 gm. Sagittal otoliths were stored dry in paper envelopes.

Otoliths were mounted on glass slides in Cryobond 509 (Aremco Industries Inc.), sulcus side up and ground in the sagittal plane to the level of the primordium using 800 to 1200 grade carborundum wet/dry paper. After the primordium was reached otoliths were polished on a lapping wheel with Linde A in water and then finished with 0.25 μm diamond paste and prepared for microprobe analysis as discussed in Chapter 2. Analyses were done at a beam current of 25 nA (measured on Cu) and a accelerating voltage 15 kV. Counting times are the same as used for other otolith transects. Transects were made in the sagittal plane from the primordium to the otolith edge at the rostrum.

4.8.3 Results and Discussion

Microchemical data from *Notothenia squamifrons* and *Nototheniops mizops* are shown in Figs. 4.18 and 4.19. The Sr/Ca data from *N. squamifrons* clearly show evidence of some form of periodicity which could result from some seasonal variations in physiology that are related to environmental change (Fig. 4.18). The first four "cycles" with peaks at approximately 150, 700,1100 and 1600 μm are relatively obvious, while the last two cycles with peaks at 1900 and 2300 μm are less clear. Both the wavelength and amplitude of the Sr/Ca cycles appear to moderate after the third cycle and this may be indicative of a reduced physiological response to the environment and/or more uniform growth. Peaks similar to those in otolith Sr/Ca ratios are not apparent in the Na/Ca, K/Ca and S/Ca data.

Examination of the otolith sections using light microscopy showed that there was evidence of 6 annuli in the *N. squamifrons* sagitta with opaque zones at 275, 925, 1175, 1625, 2075 and 2350 μm from the primordium. Although the number of annuli corresponds with the estimated number of peaks in the Sr/Ca ratio data, the annuli do not correspond with the peaks in Sr/Ca ratio in all cases. The closest agreement for the position of annuli and Sr/Ca ratio peaks is found in the last 4 peaks. This indicates that peaks in Sr/Ca ratio in *N. squamifrons* sagittae are not necessarily associated with factors that result in changes in the appearance of the otolith.

The data from *Nototheniops mizops* show little evidence of cyclical variation (Fig. 4.19), but this is partly due to the graphical effects of the large amplitude peak in the first 200 μm of the section. However, if these data are graphed with a different vertical axis, peaks at 2100, 2400 and 2700 μm become more apparent. As for the *N. squamifrons* data, there is no evidence of periodicities in the Na/Ca, K/Ca and

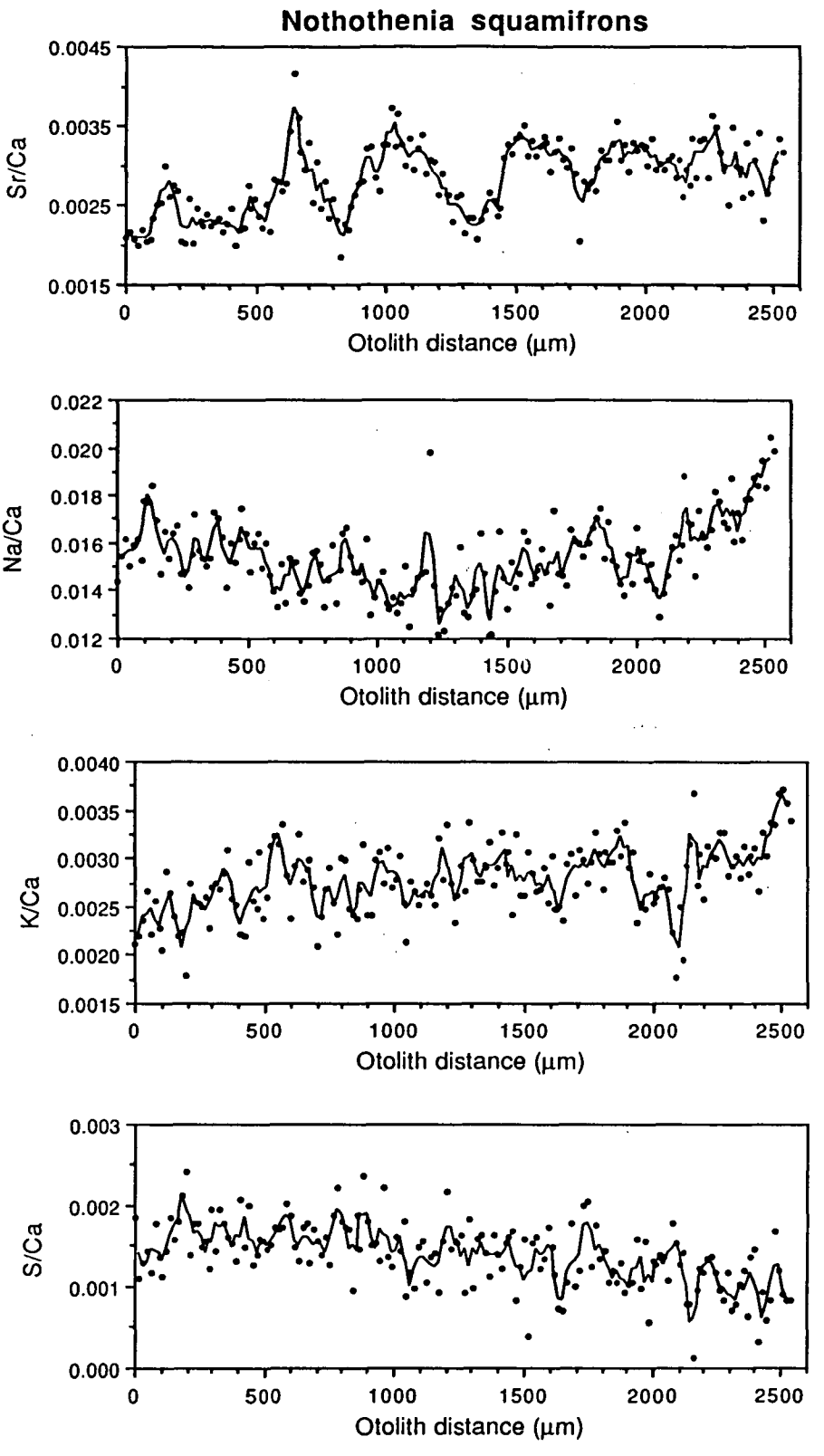

Fig. 4.18 Plots of Sr/Ca, Na/Ca, K/Ca and S/Ca data from a microprobe transect across a sagitta (section along the sagittal plane, transect from the primordium to the rostrum) from a specimen of *Notothenia squamifrons* (female, 153 mm SL, 48.0 g) collected off Heard Island 24 July 1987. Points are raw data and the line is based on a 3-point moving average.

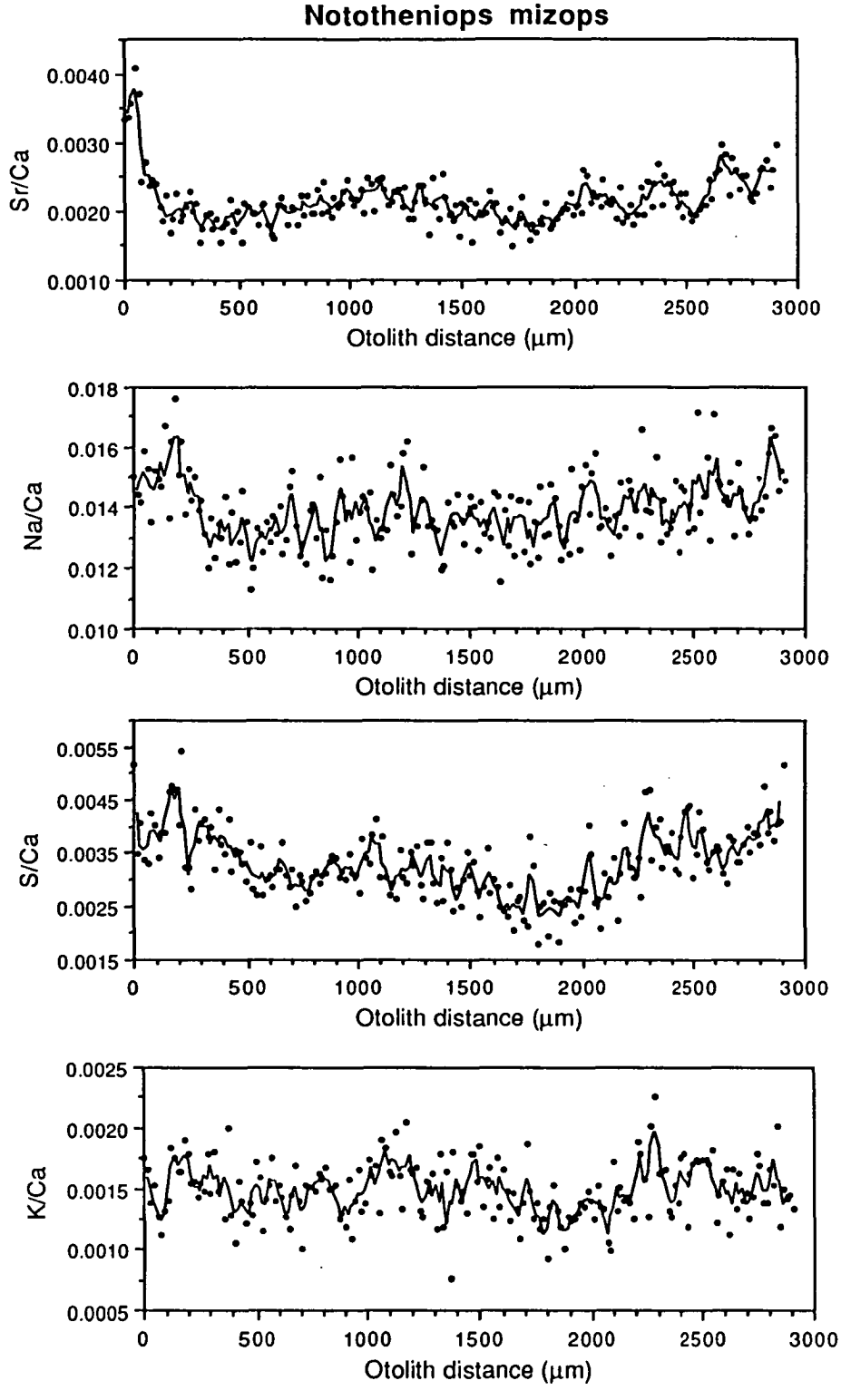

Fig. 4.19 Plots of Sr/Ca, Na/Ca, K/Ca and S/Ca data from a microprobe transect across a sagitta (section along the sagittal plane, transect from the primordium to the rostrum) from a specimen of *Nototheniops mizops* (female, 146 mm SL, 37.2 g) collected off Heard Island 5 October 1985. Points are raw data and the line is based on a 3-point moving average.

S/Ca data.

Examination of the *N. mizops* sagitta using light microscopy indicates the presence of 7 annuli with opaque zones at 725, 1150, 1475, 1875, 2100, 2375 and 2600. The 3 relatively distinct Sr/Ca peaks are in the same or similar positions as the opaque zones of the last 3 annuli, but there is no evidence of Sr/Ca peaks associated with the first 4 annuli.

Otolith microchemistry data from two species of Antarctic notothenids indicates that the presence of periodicities in otolith Sr/Ca ratios is not a phenomena common to all notothenids. However, the data do confirm the existence of these periodicities in some cases.

The data presented here provide an interesting comparison with the data from Radtke and Targett (1984). Firstly, it is important to note that Radtke and Targett (1984) have probably presented the otolith Sr/Ca data from *N. larseni* as the ratio of the weight fractions of Sr and Ca and not as the generally accepted atomic ratios. If this is the case then the range of their Sr/Ca ratio data is approximately 0.0011 to 0.0038 which is similar to that found here for *N. squamifrons* (0.0018 to 0.0042) and *N. mizops* (0.0015 to 0.0041).

The initial decision to compare *N. mizops* Sr/Ca ratio data with the data on *N. larseni* was based on the fact that these two species belonged to the same genus. However, *N. larseni* is a pelagic species, whereas *N. mizops* is a benthic fish. On this basis, it seemed important to also make a comparison with another pelagic notothenid species, *N. squamifrons*. With this information in mind, it is interesting that a microprobe transect of *N. mizops*, the congener of *N. larseni*, yields a series of Sr/Ca ratios that is different from that found for *N. larseni*, whereas data from a species, *N. squamifrons*, from a related genus yields a Sr/Ca ratio transect comparable to that from *N. larseni*. This may be due to the fact that *N. larseni* displays similar habits to *N. squamifrons*. Both these species are pelagic and consume pelagic prey, whereas *N. mizops* is a benthic species (Fischer and Hureau, 1985). Therefore, these Antarctic species provide evidence that niche and ecological relationships have a significant influence on otolith Sr/Ca ratios.

4.9 Otolith microchemical transects: characteristics of miscellaneous species

4.9.1 Introduction

Otolith microchemical data in the form of transects from the primordium to the otolith edge were collected from a range of species to investigate the range of forms that these data may take. The greatest amount of data was collected from blue grenadier and cod sagittae because of the background knowledge developed on the otolith microchemistry of these species. Sr/Ca ratio data are stressed because they generally show the most recognizable structure both among and within individuals.

4.9.2 Materials and methods

Otoliths were collected from a range of sources in southeast Australian waters. Sagittae were removed from fresh specimens, cleaned and stored dry in glass vials or paper envelopes. Transverse sections of otoliths were prepared for electron microprobe analysis as discussed in Chapter 2 and counting procedures are as outlined in Chapter 4.

4.9.3 Results and Discussion

Microchemical transect data from the sagittae of 5 fish species are illustrated in Figs. 4.20 to 4.25. Generally, these data confirm results presented elsewhere in this chapter regarding the problems in interpreting microchemical data.

In both blue grenadier and cod (Appendix 5) it appears impossible to relate the seasonal changes in otolith microchemistry based on microprobe analysis of the otolith margins (Chapter 2 and Chapter 3) to the variation measured along otolith transects in individuals. Also, it is not possible to relate the chemistry of the otoliths to any readily apparent structural features. In some instances there are similarities in the general appearance of a transect as in the case of 2 female cod, C11 and C21 (Appendix 5). The fish were both collected in Variety Bay, C11 on 25 March and C21 on 17 April 1988.

Jack mackerel, *Trachurus declivis*, are one of the few species investigated that do show changes in otolith microchemistry that can be related to changes in otolith structure. *Trachurus declivis*#2 and *Trachurus declivis*#3 (Fig. 4.20 and 4.21) collected by line fishing in Storm Bay on 25 March 1988 were both female fish 31 cm SL. The two fish were in the same school. Both show peaks in otolith Sr/Ca ratios

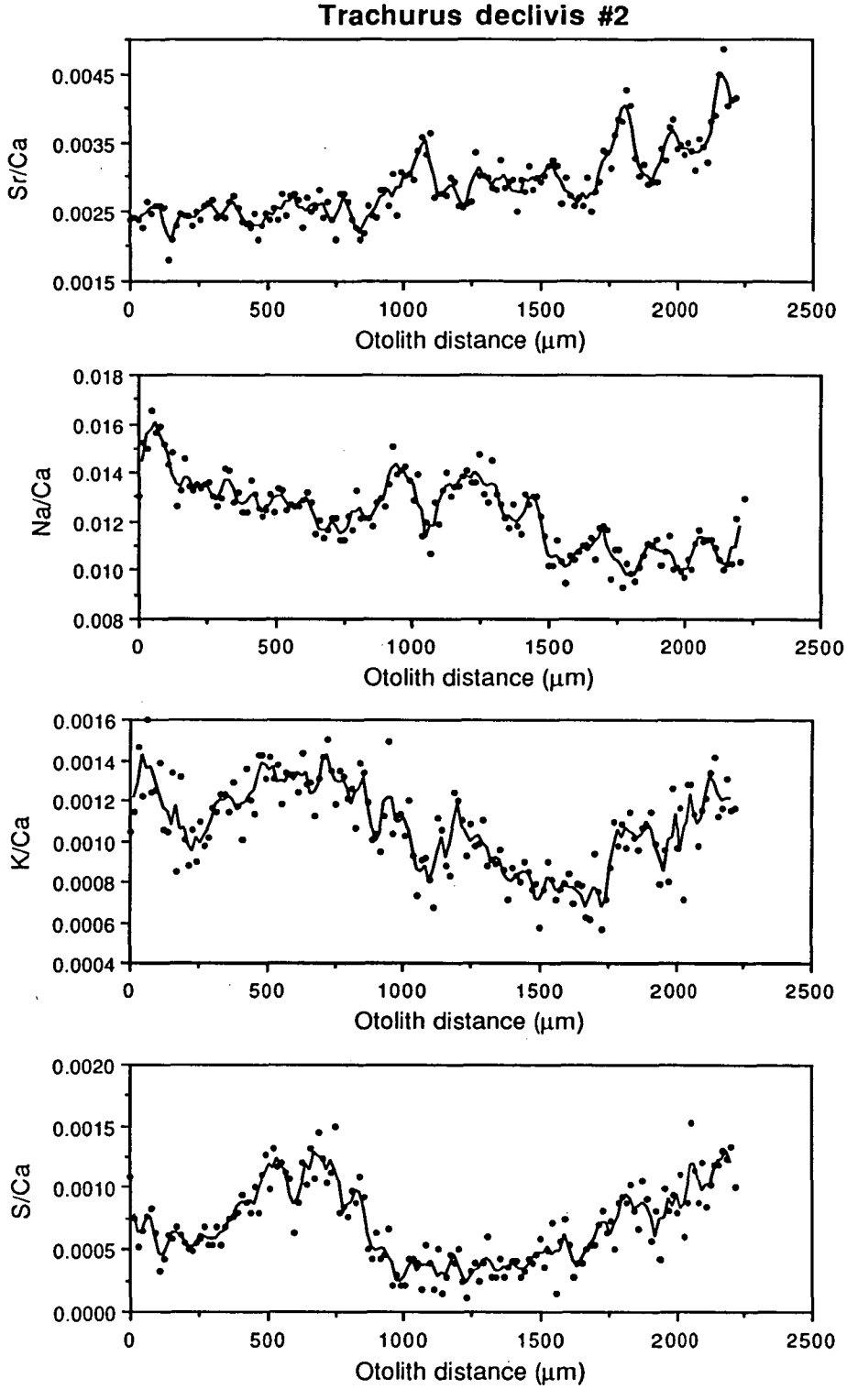

Fig. 4.20 Plots of Sr/Ca, Na/Ca, K/Ca and S/Ca data from a microprobe transect across a sagitta (section along the transverse plane) from a specimen of *Trachurus declivis* (female, 31 cm SL) collected in Storm Bay 25 March 1988. Points are raw data and the line is based on a 3-point moving average.

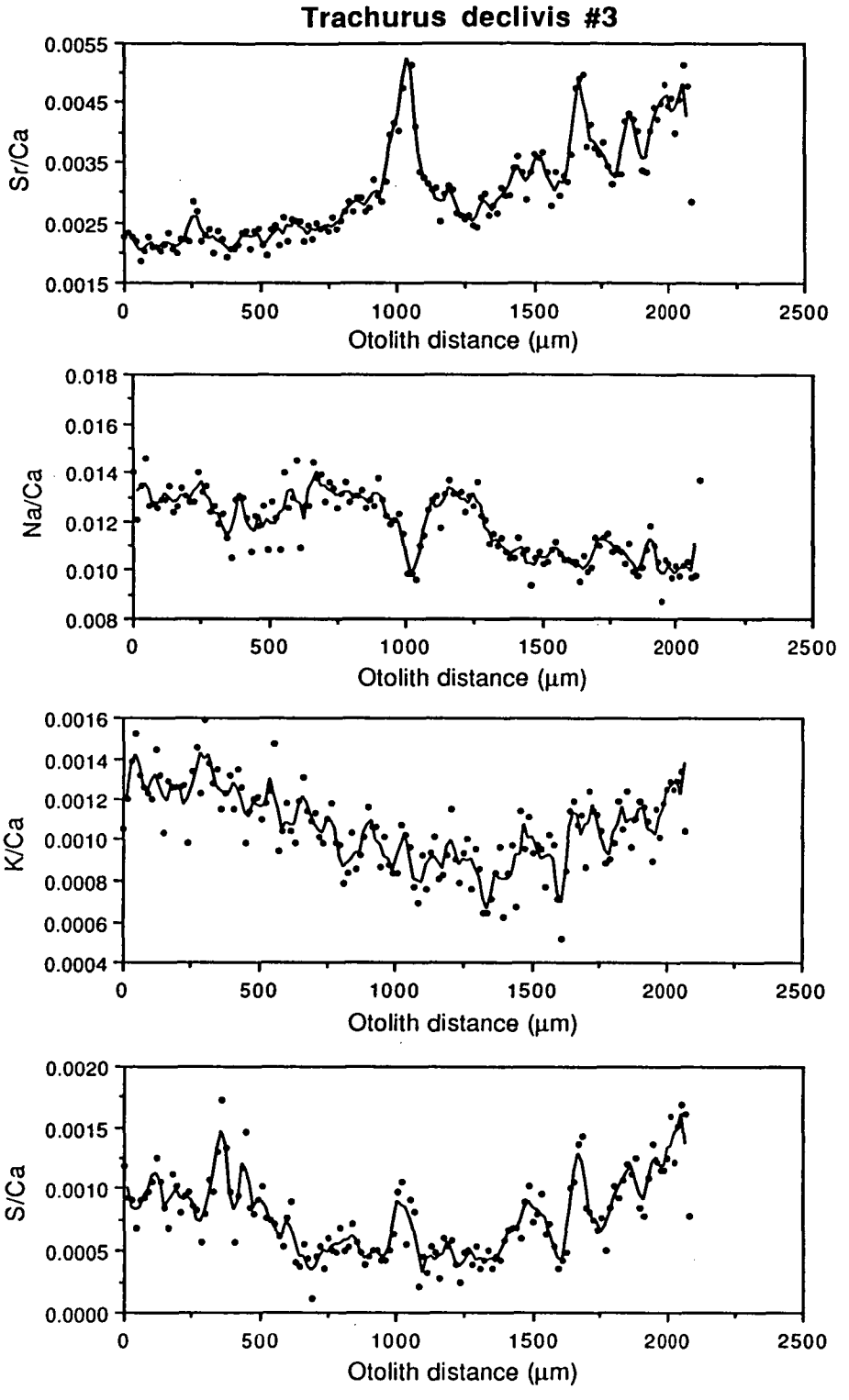

Fig. 4.21 Plots of Sr/Ca, Na/Ca, K/Ca and S/Ca data from a microprobe transect across a sagitta (section along the transverse plane) from a specimen of *Trachurus declivis* (female, 31 cm SL) collected in Storm Bay 25 March 1988. Points are raw data and the line is based on a 3-point moving average.

at an otolith distance of about 1000 μm and 1750 μm, as well 2 additional peaks around 2000 μm. The peaks in Sr/Ca ratios at 1000 μm and 1750 μm are associated with changes in increment widths (Fig. 4.22) and these may be due to major changes in life-history stage, physiology and environment. Based on the nature of the changes in increment width and otolith structure the peaks in otolith Sr/Ca in these instances may be related to winter growth. However, the peaks cannot be attributed to cold temperatures alone as otolith Sr/Ca ratios attained similar, or even greater levels when the fish were captured on 25 March at a water temperature of 17.3°C. Although the Sr/Ca ratio peaks occur at the same location on the otoliths, the peaks are of very different heights. For example, in *Trachurus declivis*#2 the peak Sr/Ca ratio at 1000 μm is about 0.0036, whereas the related peak in *Trachurus declivis*#3 is approximately 0.0052. This difference is evident even though the first 500 μm of the 2 of jack mackerel Sr/Ca transects varies around a similar value (0.0025). The Na/Ca data also show a fair degree of similarity.

Elemental ratio data from the blue throated wrasse (*Pseudolabrus tetricus*) (Fig. 4.23), gemfish (*Rexea solandri*) (Fig. 4.24), southern bluefin tuna (*Thunnus maccoyii*) (Fig. 4.25), and albacore tuna (*Thunnus alalunga*) (Fig. 4.25) do not show variations in otolith microchemistry that are related to structural changes in the otoliths, based on observations with light microscopy. Evidence for seasonal cycles or changes that might be clearly related to physiological or environmental phenomena are not readily apparent.

Comparison of the transects of the southern bluefin tuna and the albacore tuna otoliths presents evidence for the influence of physiological changes related to maturity on otolith composition. Both fish were caught near the Hippolytes, a series of rock pinnacles off the east coast of Tasmania, on 25 April 1988. The southern bluefin was an immature fish of 102 cm, whereas the albacore was 96 cm mature female. Based on the estimated size at first maturity and other growth data on albacore, it is likely that this individual would have spawned at least once (González-Garcés and Fariña-Perez, 1983; Laurs *et al.*, 1985). Although the two fish and their sagittal otoliths were almost exactly the same size the chemical records from the two microprobe transects are very different. For example, at the otolith margin the Sr/Ca ratio is 0.0036 in the albacore and 0.0020 in the southern bluefin despite the fact that these two fish were collected at the same location on the same date. Light micrographs of the otoliths from the two individuals show that the microstructure of

Fig. 4.22 Light micrographs of otolith sections used for microprobe analysis (magnification 55x). (A) *Trachurus declivis*#2 (female, 31 cm SL) sagitta transverse section, arrows indicate locations of Sr/Ca ratio peaks shown in Fig. 4.20; (B) *Trachurus declivis*#3 (female, 31 cm SL) sagitta transverse section, arrows indicate locations of Sr/Ca ratio peaks shown in Fig. 4.21; (C) *Thunnus maccoyii* (immature, 102 cm SL) sagitta frontal section, showing multiple spherulitic primordia, the arrow indicates the direction of the microprobe transect; (D) *Thunnus alalunga* (female, 96 cm SL) sagitta frontal section, showing multiple spherulitic primordia, the arrow indicates the direction of the microprobe transect; (E) *Thunnus maccoyii* (same otolith as in C) showing the sagitta postrostrum, the finishing point of the microprobe transect in Fig. 4.25; and (F) *Thunnus alalunga* (same otolith as in D) showing the sagitta postrostrum, the finishing point of the microprobe transect in Fig. 4.25. The arrow shows the point 2000 μm from the starting point of the microprobe transect in Fig. 4.25 where the Sr/Ca ratio increases sharply.

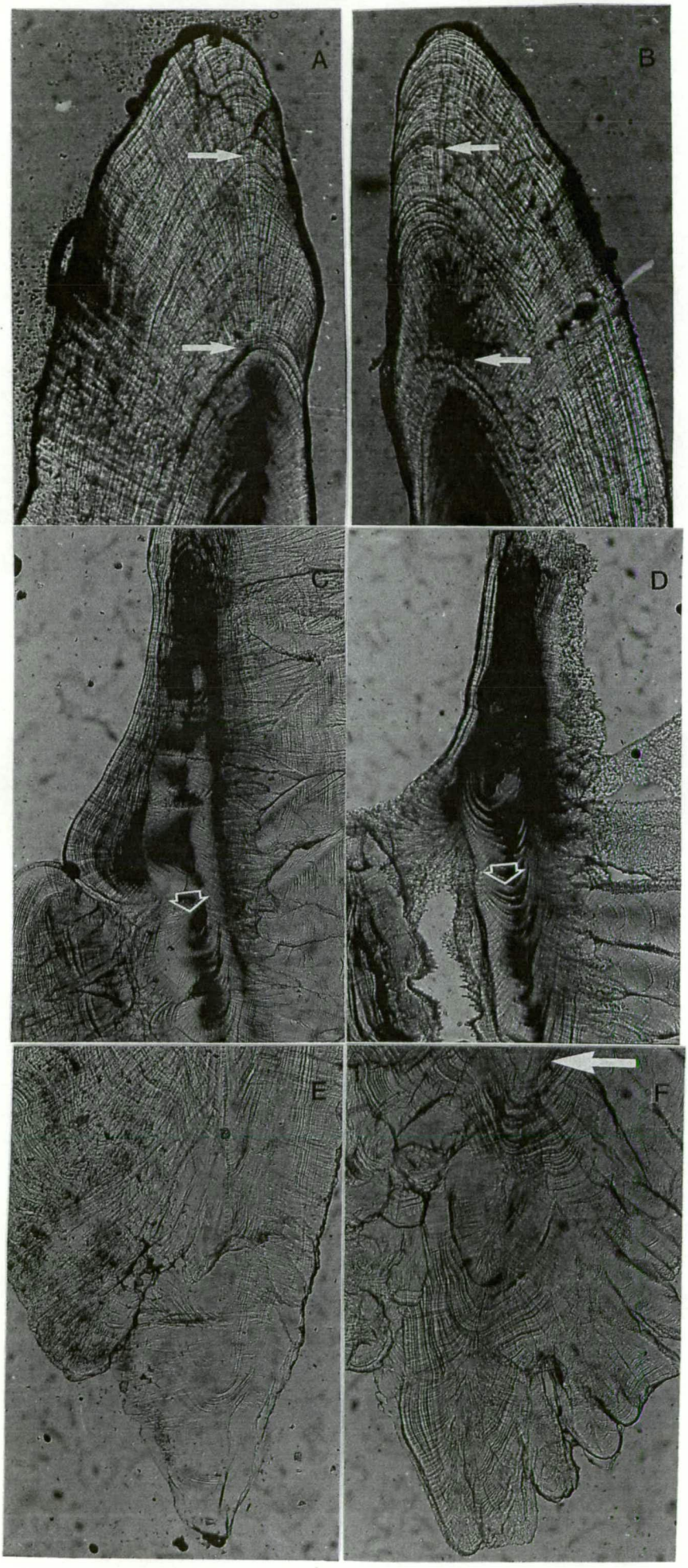
A
B
C
D
E
F

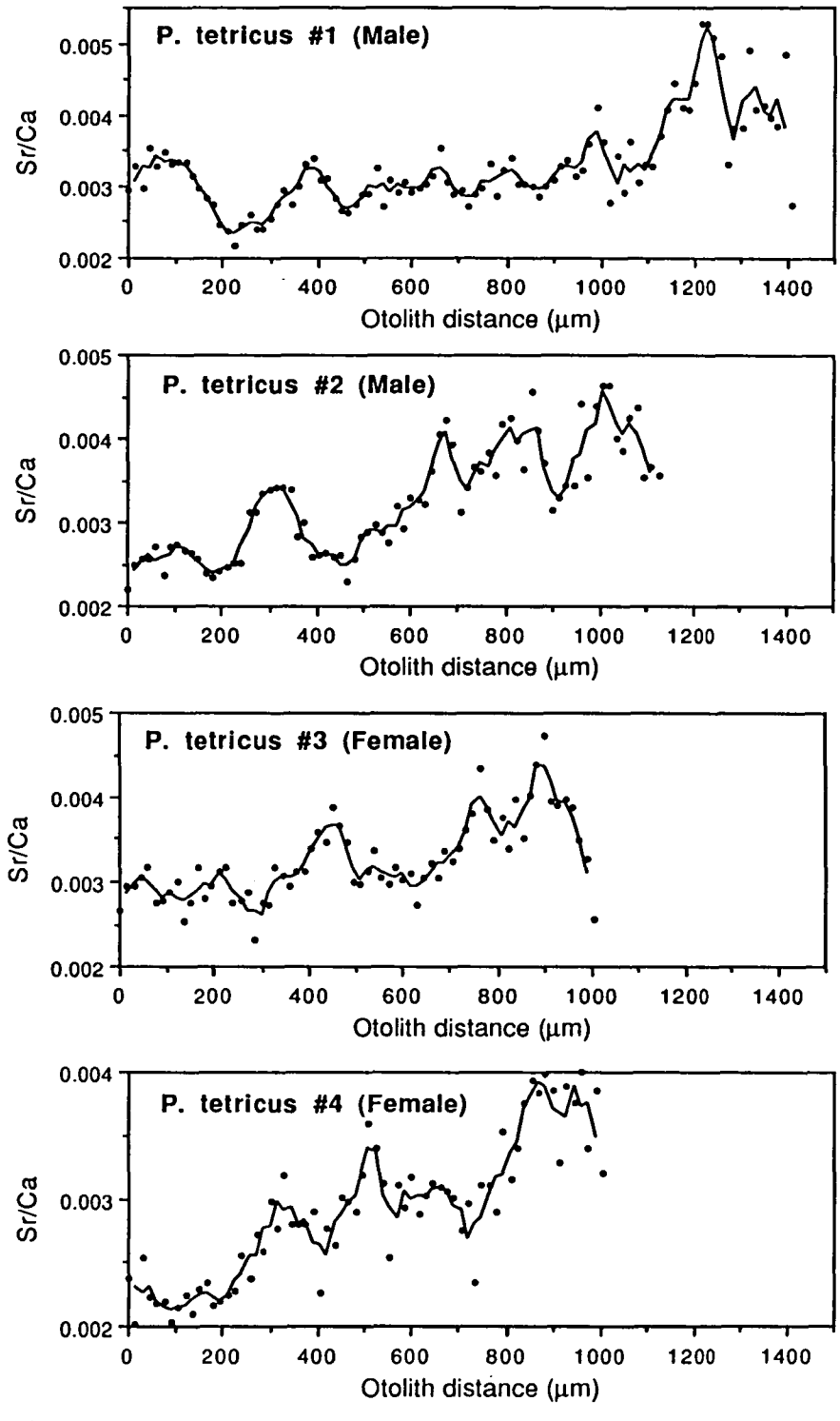

Fig. 4.23 Plots of Sr/Ca data from microprobe transects across sagittae (sections along the transverse plane) from 4 *Pseudolabrus tetricus* (male#1, 43 cm SL; male#2, 37 cm SL; female#1, 31 cm SL; female#2, 32 cm SL) collected in Variety Bay 22 June 1988. Points are raw data and the line is based on a 3-point moving average.

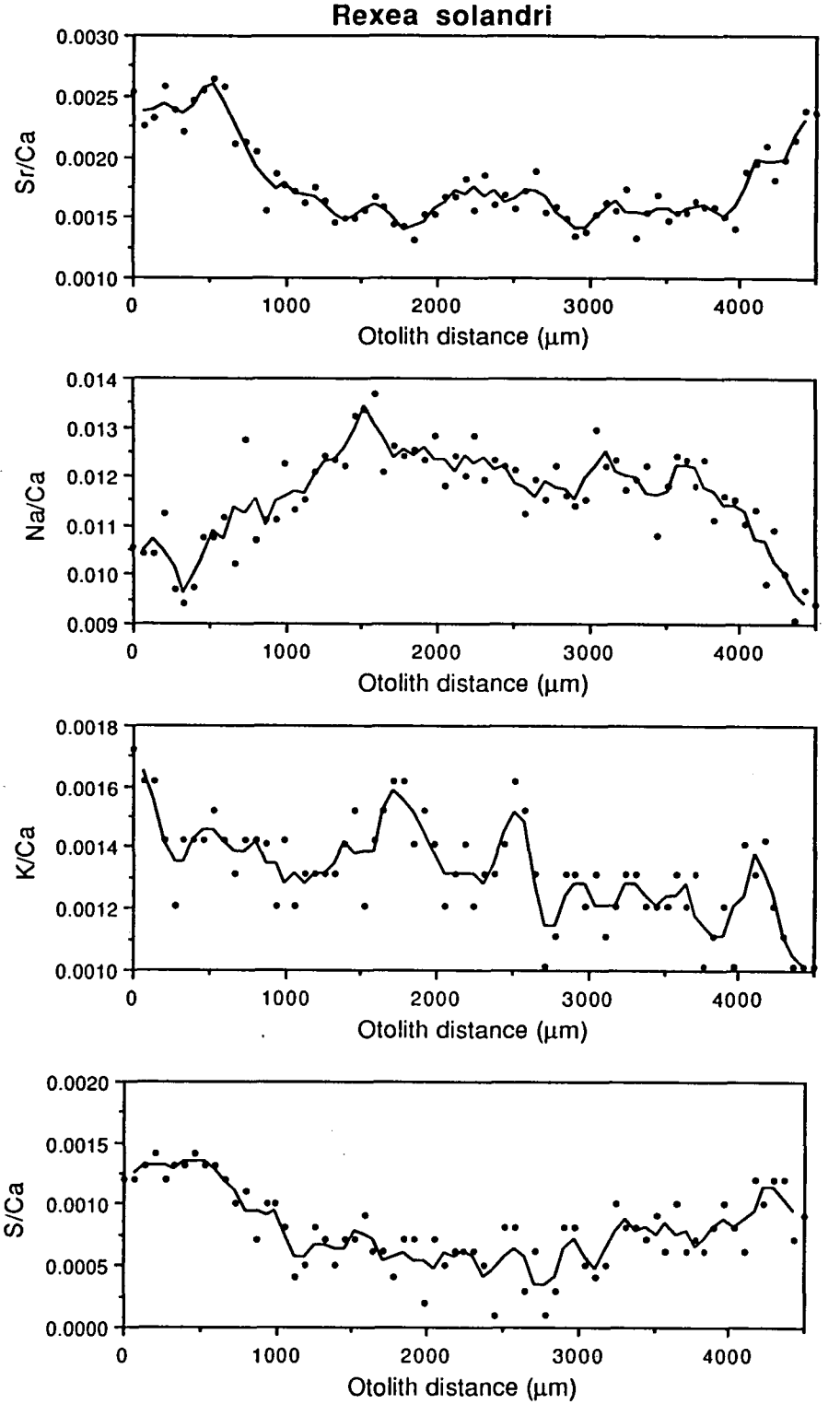

Fig. 4.24 Plots of Sr/Ca, Na/Ca, K/Ca and S/Ca data from a microprobe transect across a sagitta (section along the transverse plane) from a specimen of *Rexea solandri* (male, 623 mm SL, 2000 g) collected off Maria Island, Tasmania 20 February 1985. Points are raw data and the line is based on a 3-point moving average.

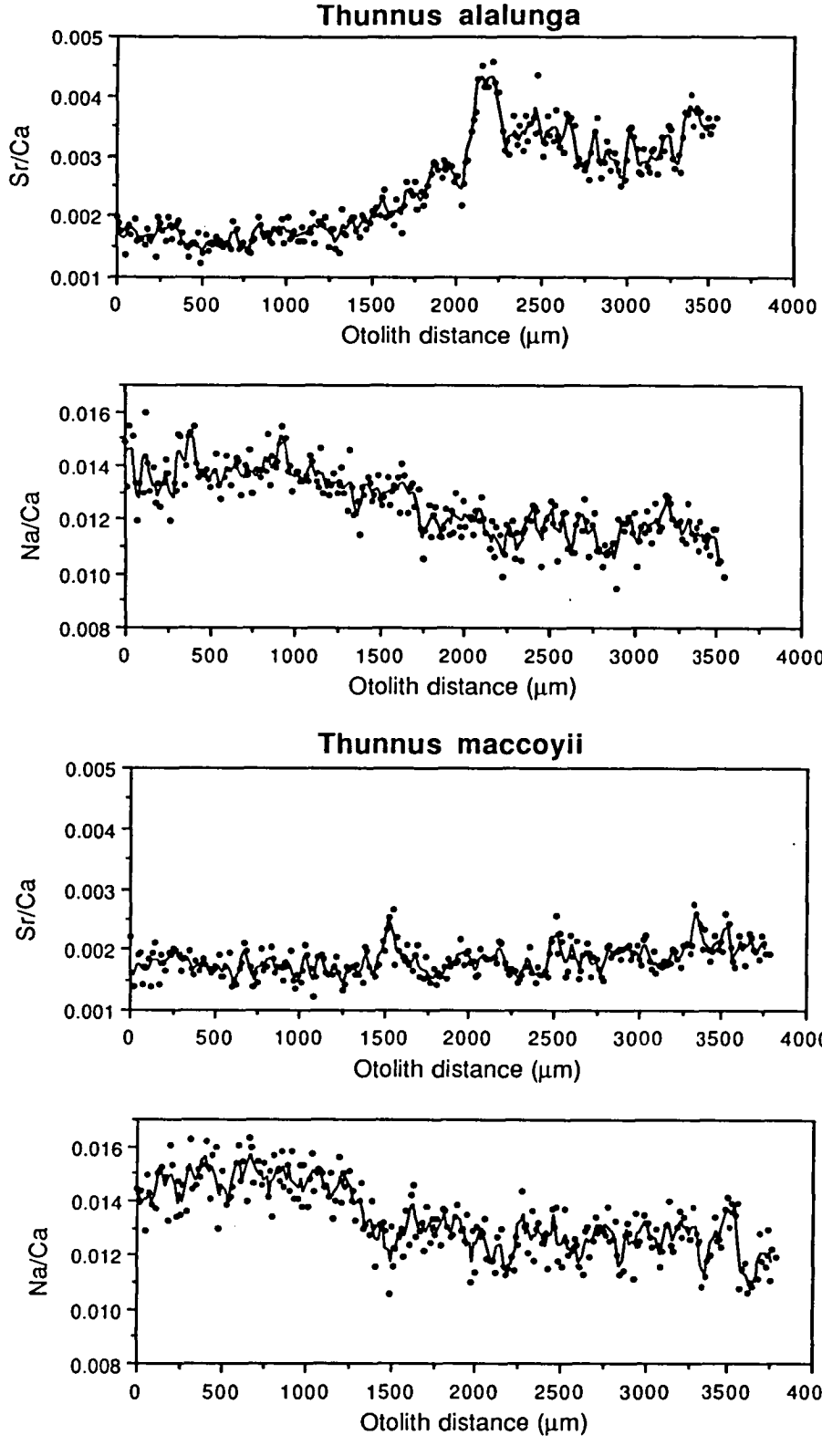

Fig. 4.25 Plots of Sr/Ca and Na/Ca data from microprobe transects across sagittae (section along the frontal plane, transect from the primordium to the postrostrum) from one *Thunnus alalunga* (female, 96 cm SL) and one *Thunnus maccoyii* (immature, 102 cm SL) collected near the Hippolytes off eastern Tasmania 25 April 1988. Points are raw data and lines are based on a 3-point moving average.

the two otoliths is similar (Fig. 4.22). Both possess multiple spherulitic (see Chapter 8) nuclei and have, what appear to be, very irregular growth increments or checks. This suggests that microchemical differences in these two individuals are due to either interspecific physiological differences or, physiological differences associated with age, growth rate and the level of maturity. As these are two closely related species (Sharp and Pirage, 1978), it is unlikely that there are significant differences in basic physiology. The Sr/Ca ratios from the albacore sagitta were very similar to those measured in the southern bluefin until the fish approached a size that would be close to maturity. Therefore, it seems likely that the differences in otolith microchemistry in these two species of tuna are due to life history stage and concomitant differences in the growth rate and level of maturity. Otoliths from mature southern bluefin tuna were unavailable for study because of political reasons.

The otolith microchemistry of several species has been considered and it is evident that there are large differences among species. These differences relate to both the absolute level of the elements present and the degree of variability that is found within individuals of a species. In most cases it is very difficult to draw conclusions as to the reasons for changes in otolith chemistry. Characteristic features can occasionally be found among individuals collected at the same time and location, but it can be difficult to determine if these are ontogentic or environmentally related features. As stated previously, it is essential to have a sound understanding of physiological responses to life history and environmental changes and these should be coupled with an understanding of the concomitant alterations in the chemistry of the blood plasma and the endolymph.

4.10 SUMMARY

Investigation of otolith microchemistry in a range of species indicates that the factors that ultimately effect otolith composition are generally not under strong environmental control. This is evident from the lack of clear periodicities in otolith composition in all species tested except for *N. squamifrons*. These findings are to be expected in light of the data presented in the previous chapters based on laboratory rearing of fish and investigations of plasma, endolymph and otolith composition. In both *N. squamifrons* and *T. declivis* the extreme changes in otolith Sr/Ca ratios were related to visible changes in otolith structure. However, I have presented evidence which indicates that extreme changes in otolith chemistry are not always

associated with changes in otolith structure and visa versa.

Variations in otolith chemistry can be useful in studies aimed at determining distributional relationships among contemporaneous individuals, particularly in studies seeking to identify nursery grounds or where there is an interest in fine resolution "stock" discrimination. In most cases the sample sizes required and the cost and time involved would be prohibitive. A similar situation exists with regard to the study of school cohesion, but similar problems apply.

The data from wild fish present strong evidence for the complex interaction of both environmental and physiological phenomena in mediating changes in otolith chemistry. This was particularly evident in a sample of stressed juvenile Australian salmon collected from a warm, brackish water lagoon. The otoliths of these fish responded in a uniform manner to the extreme environment and this response was different from that of other juvenile Australian salmon collected from a typical habitat at the same time of the year. However, it is important to be aware that, although the direction of the response to the environmental stress was uniform, the magnitude of the response was not. A similar situation existed with the 2 individuals of *Trachurus declivis* where major changes in otolith chemistry occurred at similar locations in the microchemical record, but the magnitude of these changes was different. This also occurs when comparing multiple transects within a single otolith. Therefore, when making comparisons among fish relative, and not absolute changes, should be stressed.

Some aspects of the Sr/Ca microchemical record are strongly influenced by ontogenetic factors. This is based on the fact that otolith Sr/Ca ratios are frequently high in both relatively young and old individuals. This may be related to relative growth rates as was discussed in Chapter 2. Also, differences in the composition of the otoliths from albacore and southern bluefin tuna are probably due to differences in maturity and growth rates. It is important to be aware of any ontogenetic factors that would result in similar chemical changes among otoliths from different individuals. These changes could be accidentally used as "stock" markers when attempting to identify the signature of a group of fish. Such errors could result in the grouping of individuals that do not necessarily belong to the same subpopulation unit.

In most species there appears to be little information that can be gained directly from the interpretation of otolith Sr/Ca, Na/Ca, K/Ca and S/Ca ratios. The complex interaction of factors affecting trace element levels in fish otoliths makes it virtually

impossible to determine those factors which result in a particular quantity of Sr, Na, K or S in an otolith or, to use these elements as indicators of physiological or environmental change. This is a common feature of complex synergistic systems. We could just as well predict the form of the waves on a confused sea.

CHAPTER 5

USE OF OTOLITH MICROCHEMISTRY TO DISTINGUISH THE PROGENY OF SYMPATRIC ANADROMOUS AND NONANDROMOUS SALMONIDS

5.1 INTRODUCTION

The ability to differentiate between juvenile anadromous salmonids and their sympatric nonanadromous conspecifics is essential for management of these species. However, stock discrimination between sea-run and resident freshwater salmonids has been limited to the adults upon their return from the sea to spawn. Furthermore, for those species where diadromy is a facultative, and not an obligate behavior, such as brown trout (*Salmo trutta*), rainbow trout (*Oncorhynchus mykiss*), Atlantic salmon (*Salmo salar*), cutthroat trout (*Salmo clarkii*) and Arctic char (*Salvelinus alpinus*), it has been impossible to distinguish between the co-occurring forms on the basis of meristic or morphometric characters (Nordeng, 1983; Jonsson, 1985; Neilson et al., 1985). Mckern *et al.*, (1974) were able to distinguish between winter and summer races of steelhead trout, anadromous rainbow trout, from rivers in British Columbia, Washington and Oregon on the basis of sagittal otolith nuclear dimensions that they believed to be affected by both qualitative and quantitative differences in yolk. Rybock *et al.* (1975) concluded that differences in the size of female resident nonanadromous rainbow trout and steelhead trout were adequate to result in differences in egg size and, concomitantly, the size of the otolith nucleus in the progeny. However, both Neilson *et al.* (1985) and Currens *et al.* (1988) found that measurements of otolith nuclear dimensions were of questionable value in distinguishing juvenile nonanadromous and anadromous rainbow trout.

Development of ova in anadromous salmonids is virtually complete through vitellogenesis or yolk formation before the fish enter fresh water. On the basis of this information, I hypothesized that egg composition would, in some way, reflect the chemical composition of the seawater environment and that this would ultimately affect the composition of the otoliths of the progeny, particularly the otolith nuclei that are formed in the early stages of development and well before yolk utilization is complete. Yolk is formed through the deposition of a phospholipoprotein-calcium complex yolk precursor, vitellogenin, in the developing oocyte (Mommsen and

Walsh, 1988). Solubility and transport of vitellogenin through the circulatory system of the female and to the developing ovaries may be dependent on the presence of calcium which has been shown to increase markedly in female salmonids (Bailey, 1957; Booke, 1964; Elliot *et al.*, 1979) and other fishes (Oguri and Takada, 1967; Woodhead, 1968) during gonad development. Vitellogenin has a very high affinity for calcium due to the significant negatively charged phosphate component of the molecule (Hara and Hirai, 1978; Hara *et al.*, 1980). This calcium binds to the vitellogenin molecule and, in this complexed form the vitellogenin and calcium are deposited in the oocyte. Clearly, yolk deposition is a conservative process in that the overall composition of the yolk is more dependent on the genetic programming of the female parent than the environment. However, in many calcium-binding proteins, such as vitellogenin, the calcium moiety of the complexed molecule can be substituted for by strontium due to the similar structural features of Ca^{++} and Sr^{++}(Skoryna 1981). The relative degree of this substitution would be largely dependent on the relative concentrations of calcium and strontium in the ambient environment. Typical Sr/Ca ratios in marine waters (salinity 35‰) are 0.0087 (0.09 $mM \cdot kg^{-1}$Sr:10.3 $mM \cdot kg^{-1}$Ca) (Bruland, 1983) and average 0.0019 (0.00068 $mM \cdot kg^{-1}$Sr:0.35 $mM \cdot kg^{-1}$Ca) in fresh water (Rosenthal *et al.*, 1970). These differences would be expected to effect the Sr/Ca ratio of the yolk and, ultimately, the composition of the developing embryo and it's otoliths.

In a study of otolith and endolymph composition, Kalish (1989) showed that the quantity of strontium incorporated into the otolith was directly related to the quantity of strontium present in the endolymph and, that anadromous brown trout collected in an estuary had higher levels of strontium in both the endolymph and otolith than nonanadromous brown trout (see Chapters 2 and 3). On this basis, it seems possible that differences in the elemental constituents of the yolk and embryos of anadromous and nonanadromous salmonids would result in differences in otolith composition. This hypothesis is supported by research that shows little or no exchange of calcium between prehatch salmonid embryos and the environment (Hayes *et al.*, 1948; Zeitoun *et al.*, 1976). This would be expected since calcium present in the yolk of the developing embryo is probably present in a protein-bound form and is destined for the tissues of the fry. Craik and Harvey (1984c) found that the calcium composition measured in whole rainbow trout eggs was indistinguishable from the calcium measured in protein precipitate obtained from the egg. This, of course,

excludes calcium that would be present in the fluid of the perivitelline space following fertilization (Laale, 1980; Alderdice, 1988). Strontium would probably behave similarly and there would be minimal loss of seawater derived yolk protein-bound ions to the freshwater environment where the development of salmonid embryos takes place.

In this chapter, I discuss investigations into variations in the elemental composition of the otoliths of nonanadromous and anadromous salmonids with emphasis on the composition of the sagittal otolith nucleus. Several "life history" transects, scans of elemental composition across an axis of an otolith made with a wavelength dispersive electron microprobe, are presented to indicate the variety of forms that these data may take in salmonids with differing life histories. I also present the results of an experiment designed to test the hypothesis that otolith primordia of the progeny of anadromous rainbow trout contain higher levels of strontium than the otolith primordia of nonanadromous rainbow trout. These data are examined in view of their usefulness in distinguishing the progeny of sympatric nonanadromous and anadromous salmonids and in investigations of diadromous behavior.

5.2 MATERIALS AND METHODS

Brown trout (nonanadromous *Salmo trutta*) and sea trout (anadromous *Salmo trutta*) were collected by gill net from the Derwent River and estuary, southeast Tasmania, Australia. Sea run and resident freshwater fish were distinguished on the basis of coloration. Juvenile and adult rainbow trout were obtained from both wild (freshwater) and hatchery (sea-farmed) stock. Atlantic salmon were obtained from hatcheries. Otoliths were removed from fresh fish, cleaned and stored in glass vials. Details of otolith preparation and microprobe analyses are described below.

Ripe ova were obtained from ovulating freshwater rainbow trout and sea-farmed rainbow trout and frozen in plastic bags for later analyses of calcium and strontium. The sea-farmed rainbow trout had been maintained in fresh water for 3 weeks, at the same hatchery as the freshwater rainbow trout, before ova were obtained from these fish. Whole rainbow trout eggs were used for the determinations. Groups of 10 eggs from 4 freshwater and 4 sea-farmed trout were used. Preparation of eggs was modified from the methods employed by Craik and Harvey (1984c). All solutions were made up with Milli-Q water (Millipore Corp.). Groups of eggs were weighed wet and then oven dried at 50°C for 24 h to estimate dry weight. The dried whole

eggs were ashed at 500°C for 24 h and then digested in 2.0 ml Aristar ultrapure hydrochloric acid at 100°C for 2 h. Samples were separated into two equal aliquots for separate calcium and strontium determinations. Sample digests for estimation of calcium were diluted in 10 mM lanthanum chloride to suppress interference due to phosphate binding. Calcium concentrations were determined by flame atomic absorption spectrophotometry using an air-acetylene flame.

Strontium concentrations in eggs were determined by the method of standard additions using graphite furnace atomic absorption spectrophotometry on a Varian AA-1475 spectrophotometer equipped with a GTA-95 graphite furnace and an autosampler. Argon was used as the purging gas in the graphite furnace. Samples were diluted with a 0.25% solution of an ionic detergent, Triton X-100, and 20 µl of diluted sample were injected by autosampler into a walled, pyrolytically coated graphite tube. Furnace conditions were: drying at 90°C for 60 sec; ramp ashing from 90 to 700°C for 20 sec; ashing at 2600°C for 1 sec; and atomization, with no gas flow, at 2600°C for 3 sec.

To confirm the hypothesis regarding otolith nucleus composition, eggs were obtained from sea-farmed and freshwater broodstock rainbow trout which originated from a similar hatchery stock (Cressy, Tasmania). These two groups of hatchery fish derive from similar stocks of rainbow trout imported into Tasmania and, because of minimal gene flow, inbreeding is relatively great and the diversity of the gene pool is low. Both freshwater and sea-farmed adults had been maintained on jack mackerel (*Trachurus declivis*) based pellets throughout the period of egg development. Sea-farmed broodstock were kept at the same hatchery as freshwater broodstock for three weeks before stripping and all eggs were fertilized with sperm from a male of freshwater stock. The developing embryos from sea-farmed and freshwater broodstock were maintained in separate baskets in the same channel of a recirculating water system where temperature was maintained at 10°C. A natural photoperiod was maintained throughout the experiment. A random sample of 20 freshwater progeny and 20 sea-farmed progeny was taken 20 days after hatching and these fish were frozen for later removal of otoliths. Sagittae and lapilli were removed from fry, the adhering otolith capsule was removed and otoliths were rinsed in deionized water. Otoliths were oven dried at 40°C. The length of sagittae and lapilli was measured with an ocular micrometer.

Otoliths from adults were embedded in Araldite D epoxy resin (Ciba-Geigy) and

polymerized in an oven at 40°C for 48 h. Several transverse sections of approximately 200 μm thickness were obtained from otoliths, including one section containing the primordium, with a low speed saw (Struers Accutom) equipped with a diamond cut-off wheel. Sections were affixed to glass slides with epoxy. After drying, sections were ground with several grades of carborundum paper (wet/dry paper 600-1200 grade) until the primordia were reached. The much smaller otoliths from fry were mounted, sulcus side up, in Crystalbond 509 (Aremco Products, Inc.), a heat labile thermoplastic polymer, and ground in the sagittal plane to the level of the primordia with 1200 grade wet-dry paper. All otoliths were then ground to the precise level of the primordia on a lapping wheel with 0.25 μm aluminium paste (Linde A) and then finished with 0.25 μm diamond paste. Polished specimens were ultrasonically cleaned in reagent grade mineral spirits followed by ultrasonic cleaning in deionized water and oven drying at 60°C. Samples were then coated in a high-vacuum evaporator with a 25 nm carbon layer and stored in a dessicator.

Otolith elemental analyses were carried out with a Cameca SX-50 wavelength dispersive electron microprobe. Analyses were made with a square raster of 10 x 10 μm. Probe current and accelerating voltage were 10 nA (measured on Cu) and 15 kV, respectively. Elements analyzed included Ca, Sr, Na, K and S. Salmonid otoliths are very susceptible to damage from the electron beam and it was necessary to utilize a low beam current and reduced counting times for all analyses. In conjunction with these conditions that reduce the the total number of x-ray counts from a specimen it is important to be aware of detection limits and counting statistics. A treatment of these subjects can be found in Goldstein *et al.* (1981) and references therein. Details of the microprobe counting procedures, precision and standards employed in this study are outlined in Table 5.1. Background was measured at offsets both above and below peak position for 50% of the peak counting time. The average counts from these two background measurements were subtracted from the peak. Background measurements were made with each analysis. Corrected X-ray intensity ratios were calculated using the ZAF method (Reed, 1975) and the final elemental ratios are normalized atom ratios based on concentrations derived from the standards.

Elemental data for otolith life history transects from adult salmonids were collected with approximately 40 μm separating each 10 μm x 10 μm sample region (50 μm separating the center point of each sample). This sampling spatial frequency was judged to be adequate because it was desired to collect data relating to major life

Table 5.1 Electron microprobe analytical data for salmonid otolith analyses. Details of counting times, counting precision and materials used as standards. Calcuation of the counting precision is discussed in Goldstein et al. (1981) Precision values are for the 95% confidence level.

Spectrometer/ Crystal	Element	Peak counting time (sec)	Counting precision	Standard Material	Source
1/PET	Ca-K_α	10	~28,000 counts collected 1.0%	Calcite	USNM 136321 Jarosewich & MacIntyre (1983)
1/PET	K-K_α	30	15% when K/Ca=$2x10^{-3}$	Anorthite	USNM 137041 Jarosewich et al. (1980)
2/PET	S-K_α	40	36% when S/Ca=$1x10^{-3}$	Troilite	BMR Museum (Australia) Ramdohr and Goresy (1971)
3/TAP	Na-K_α	20	8.1% when Na/Ca=$2x10^{-2}$	Anorthite	same as for K above
3/TAP	Sr-L_α	20	9.9% when Sr/Ca=$3x10^{-3}$	Strontianite	USNM 10065 Jarosewich & White (1987)

history changes only and not recurring or seasonal events.

For a comparison of otolith composition among the progeny of sea-farmed fish and freshwater fish microprobe data were collected from five individual primordia within each sagitta or lapillus. In some lapilli it was necessary to make multiple measurements on individual primordia because 5 primordia were not always exposed or visible. In addition, five microprobe measurements were made on each otolith at points near the otolith edge that were indicative of the otolith composition at a time after the completion of yolk absorption.

5.3 RESULTS

5.3.1 Life-history transects

Otolith life history transects representative of several types of adult salmonids are presented in Fig. 5.1. Differences in otolith transects among anadromous or sea-farmed fish and nonandromous individuals are only evident in the Sr/Ca data. An example of Sr/Ca, Na/Ca, K/Ca and S/Ca transects from a single anadromous *Salmo trutta* are shown in Fig. 5.2. Sea trout, sea-farmed Atlantic salmon and sea-farmed rainbow trout exposed to the marine environment display an increase in otolith Sr/Ca that is coincident with entry into seawater. The rate of increase in Sr/Ca across the otolith is greater in the sea-farmed fish than in the wild anadromous sea trout. This is probably due to the relatively rapid transfer of sea-farmed hatchery stock from freshwater to sea cages when compared with the seaward migration of sea trout.

There is an initial peak, associated with the otolith nucleus, in the Sr/Ca ratio of the sea trout and Atlantic salmon, but this peak does not appear in the sea-farmed or freshwater rainbow trout. It must be noted that in Tasmania freshwater broodstock are used for the production of sea-farmed rainbow trout. This peak in otolith Sr/Ca in the otolith nucleus of some individuals is presumably due to the presence of strontium sequestered in the egg yolk proteins during the seawater phase of ovarian development of the fishes female parent.

5.3.2 Otolith nucleus composition in experimental fish

The hypothesis that the seawater strontium contribution to the egg would result in increased otolith strontium was confirmed by the results of the rearing experiment. Results of this experiment are presented in Table 5.2. Mean Sr/Ca ratios based on

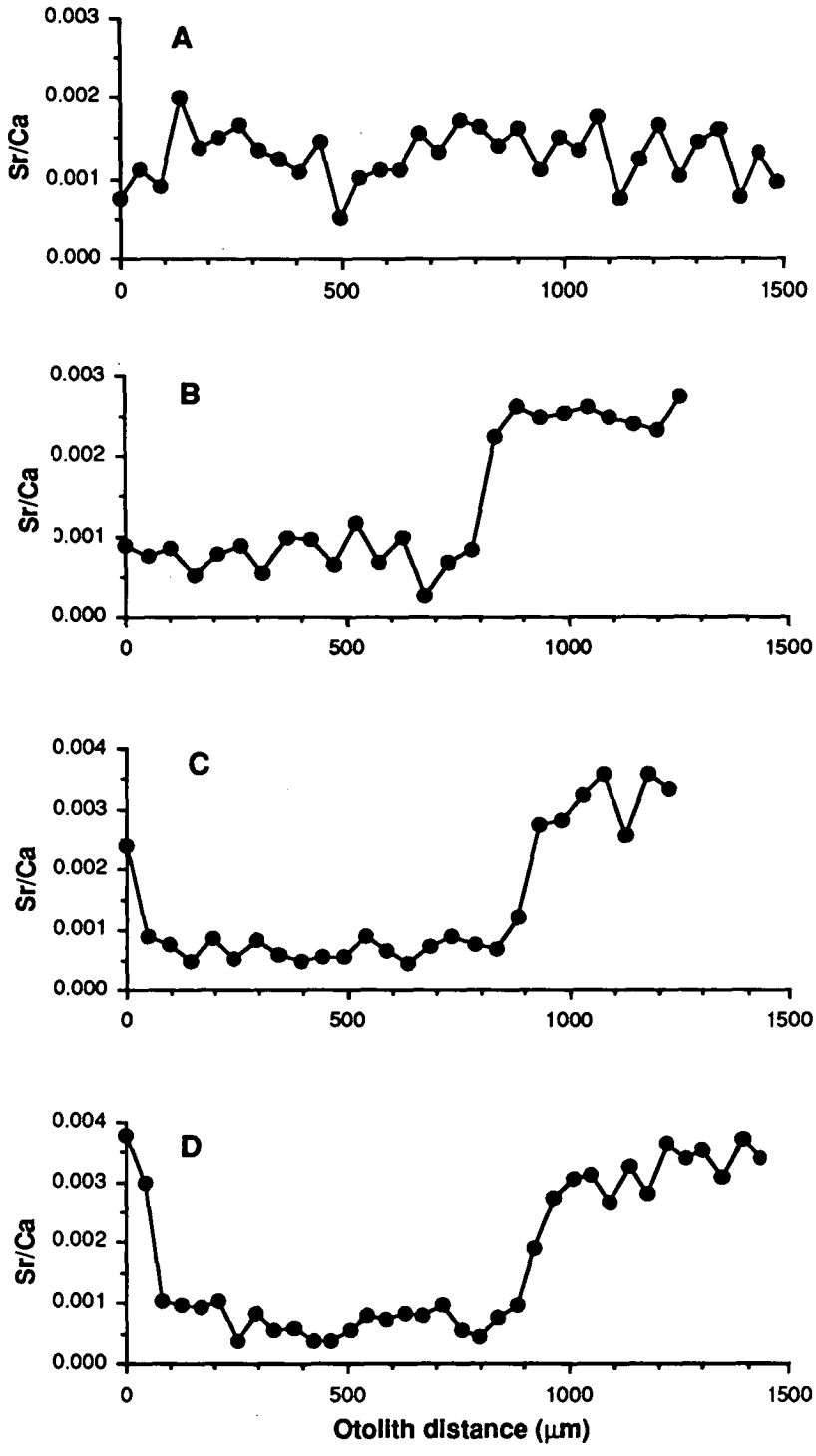

Fig. 5.1 Transects of otolith Sr/Ca ratios measured with a wavelength dispersive electron microprobe from the primordium (0 μm) to the otolith edge along transverse sections of sagittae from 4 female adult salmonids with differing life-histories. Each point represents a single measurement made over an area of 100 μm^2. (A) Wild nonanadromous *Oncorhynchus mykiss* from Great Lake, Tasmania; (B) sea-farmed *Oncorhynchus mykiss*; (C) sea-farmed *Salmo salar*; and (D) wild anadromous *Salmo trutta* from the Derwent River estuary.

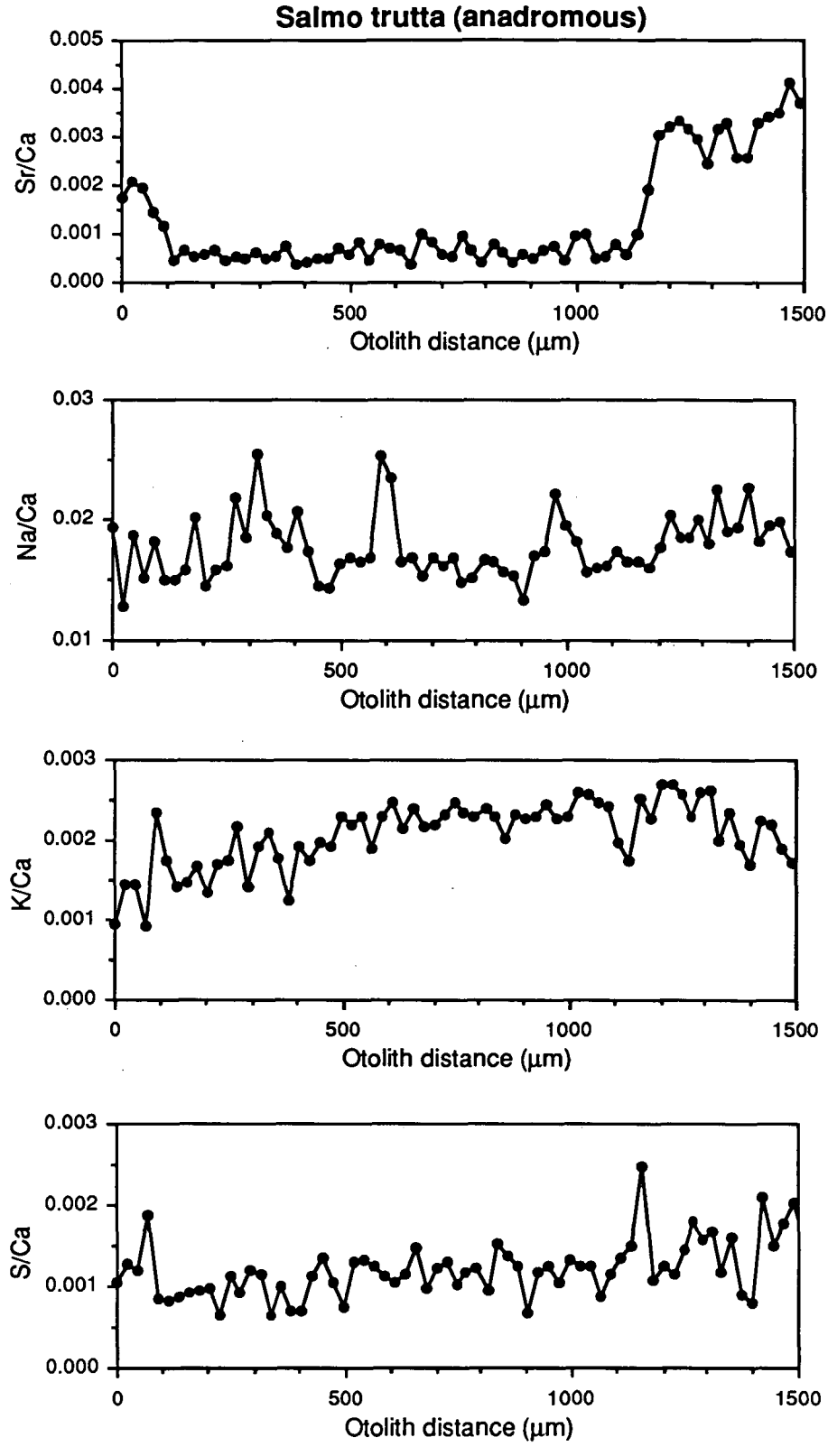

Fig. 5.2 Elemental ratios obtained from a transect across a transverse section of a sagitta from an anadromous *Salmo trutta (female,* 824 g, 445 mm SL) collected on 22/4/86 from the Derwent River near Bridgewater.

measurements in five primordia from each of the 20 sea-farmed broodstock progeny is 0.00313±0.00068, significantly greater than the mean value of 0.00114±0.00014 measured in the primordia of the freshwater broodstock progeny (unpaired one-tailed t-test, t=12.69, P<0.0001). One-way analysis of variance showed that there were no significant differences in mean otolith primordia Sr/Ca ratios among individuals from either seawater (F=0.88, P=0.476) or freshwater broodstock (F=1.29, P=0.279). Differences in otolith primordia composition between sea-farmed progeny and freshwater progeny were not significant for Na/Ca (unpaired two-tailed t-tests, t=-1.82, P=0.076) and S/Ca (t=-0.58, P=0.568), but were significant for K/Ca ratios (t=-3.88, P=0.0004). Similar results were obtained for measurements made in lapilli primordia from five freshwater and five marine progeny (Table 5.2).

A histogram of the frequency distribution of Sr/Ca ratios determined for five primordia in the sagittae of 20 progeny of sea-farmed rainbow trout and 20 progeny of freshwater rainbow trout shows that there is little overlap between individual measurements from the two groups (Fig. 5.3a). Only 5% of the measurements from the sea-farmed progeny overlap with 13% of the freshwater progeny measurements. A frequency histogram of the mean Sr/Ca ratios obtained from each sagitta nucleus shows that the sea-farmed and freshwater progeny are clearly separated on the basis of otolith primordia Sr/Ca ratios (Fig. 5.3b). On the basis of these results, five wavelength dispersive microprobe measurements of Sr/Ca ratios made within the sagitta nucleus of an individual would be adequate to determine if the female parent was an anadromous or nonanadromous individual.

Measurements of otolith composition made in regions of the sagittae formed after the completion of yolk sac absorption and corresponding with a period soon after first feeding corroborated data that showed the influence of yolk on otolith composition. There were no significant differences in Sr/Ca (unpaired two-tailed t-tests, t=1.30, P=0.201), S/Ca (t=-2.02, P=0.051) or K/Ca (t=1.09, P=0.282) ratios measured in the later formed regions of the otoliths from the two groups of fry and only slightly significant differences for Na/Ca ratios (t=2.70, P=0.010). Differences between the Sr/Ca ratio of the sagitta edge and primordium were highly significant in the sea-farmed broodstock progeny (paired two-tailed t-tests, t=10.38, P<0.0001) , and only slightly significant in the progeny of the freshwater broodstock (t=3.13, P=0.003).

Six electron microprobe transects over a sagitta from a single *Oncorhynchus mykiss* fry of sea-farmed broodstock origin were made to show Sr/Ca ratios over the

Table 5.2 Mean elemental ratios measured in primorida and post-yolk absorption regions in the sagittae and lapilli of progeny of sea-farmed and freshwater rainbow trout (*Oncorhynchus mykiss*). Values are means±1 standard deviation based on 5 microprobe measurements in each otolith region. N=20 for sagittae and N=5 for lapilli. Significance tests along sagittae primordia data are the results of paired two-tailed t-tests between those sagittae primordia and the post-yolk regions of the same otoliths. Significance tests alongside the lapilli data are the results of paired two-tailed t-tests between those lapilli data and the corresponding data from sagittae.

	Sr/Ca ($x10^3$)	Na/Ca ($x10^2$)	K/Ca ($x10^3$)	S/Ca ($x10^3$)
Sea-farmed progeny				
Sagittae (N=20)				
Primordia	3.13±0.68 ***	2.03±0.16 ***	2.07±0.47 ***	1.65±0.63 **
Post-yolk absorption	1.07±0.31	1.86±0.16	2.62±0.52	1.08±0.21
Lapilli (N=5)				
Primordia	4.34±0.80 ns	1.98±0.09 *	1.84±0.30 ns	1.30±0.35 ns
Post-yolk absorption	0.83±0.24 ns	1.74±0.06 ns	2.30±0.07 ns	1.00±0.14 ns
Freshwater progeny				
Sagittae (N=20)				
Primordia	1.14±0.14 ns	2.10±0.08 ***	2.61±0.41 ns	1.75±0.38 ***
Post-yolk absorption	0.96±0.19	1.73±0.15	2.46±0.37	1.21±0.21
Lapilli (N=5)				
Primordia	1.20±0.18 ns	1.95±0.04 *	2.43±0.25 ns	1.32±0.14 ns
Post-yolk absorption	1.06±0.13 ns	1.72±0.06 ns	2.68±0.26 ns	1.27±0.27 ns

*=P≤0.01; **=P≤.001; ***P≤0.0001

ns=not significant (P>0.05)

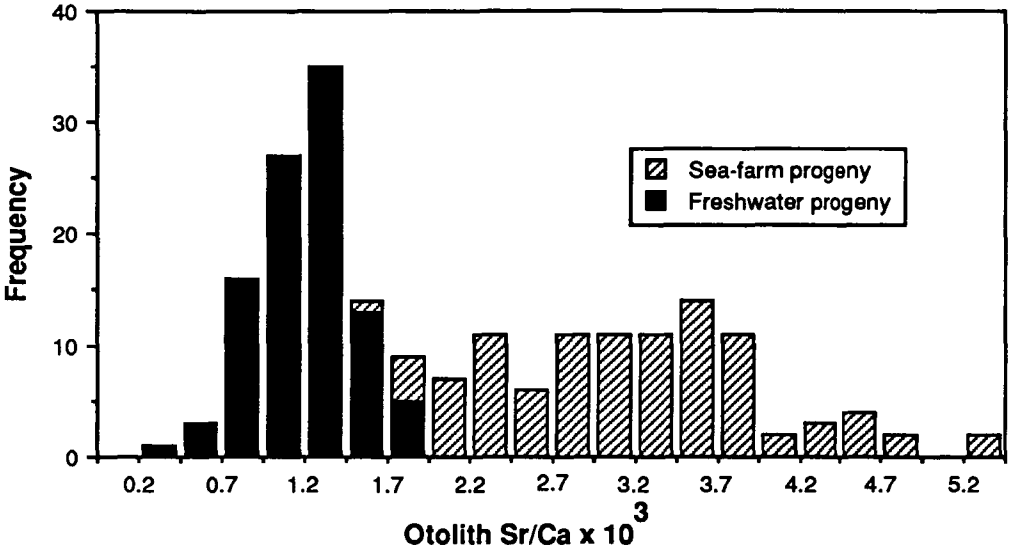

Fig. 5.3a Frequency distribution of individual otolith Sr/Ca measurements made in the primordia of 20 sagittae from *Oncorhynchus mykiss* fry of sea-farmed broodstock and 20 sagittae from fry of freshwater broodstock (N=200).

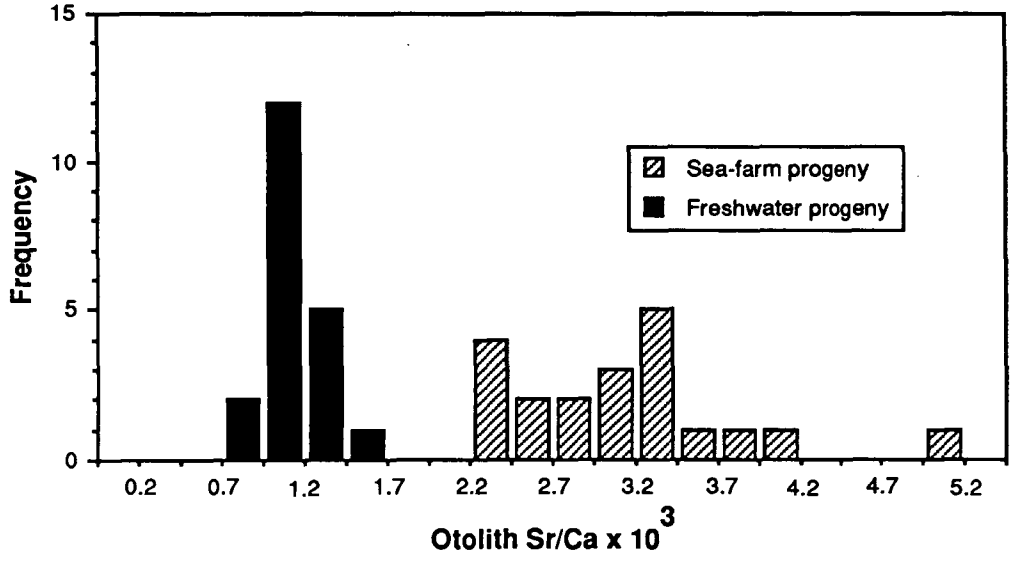

Fig. 5.3b Frequency distribution of mean otolith Sr/Ca ratios from the same 40 sagittae primordia as in Fig. 5.3a.

entire otolith including the nucleus and pre- and post-yolk absorption regions (Fig. 5.4). The outermost points towards the otolith rostrum and posterior show the sagitta Sr/Ca ratios after the completion of yolk sac absorption and provide evidence for much reduced otolith Sr/Ca ratios compared with the period of yolk sac utilization. The data also indicate that, in general, high Sr/Ca ratios prevail throughout the region of the nucleus and are not confined to the primoridia alone. A similar plot of Sr/Ca ratios derived from a sagitta of freshwater *Oncorhynchus mykiss* progeny would be relatively flat.

5.3.3 Egg composition

Measurements of egg calcium and strontium composition show that ova of the sea-farmed rainbow trout contain higher levels of strontium than their freshwater conspecifics. The mean strontium content was 0.054±0.013 μM/gm of ova (dry weight) for ova that had developed in seawater and 0.010±0.002 μM/gm for ova from freshwater fish, and the difference between these values was significant (unpaired two-tailed t-test, t=6.60, P=0.0006). Mean calcium content of yolk was 0.035±0.005 mM/gm from sea-farmed broodstock and 0.026±0.004 mM/gm from freshwater fish and these values were also significantly different (t=3.06, P=0.022).

5.4 DISCUSSION

The results present clear evidence that the Sr/Ca ratios of otolith primordia formed during embryonic development are directly influenced by the strontium content of the individual's yolk and that yolk composition is also influenced by the composition of the waters where vitellogenesis took place. These findings are important to the study and management of salmonid species where anadromy is a facultative behavior. They may also be important to studies of other diadromous species, but it remains to be seen whether the relatively small nutritive contribution of the yolk in these fishes is adequate to influence otolith composition. However, it seems probable that, since otolith primordia develop very early in the ontogeny of fishes (Brothers, 1984), there may be detectable differences in otolith strontium content within other species that display facultative diadromy. In many cases, the analysis of otolith primordium composition should make it possible to investigate the relationships between genetics and environment on diadromous behavior.

The basis for the differences in otolith primordium composition among

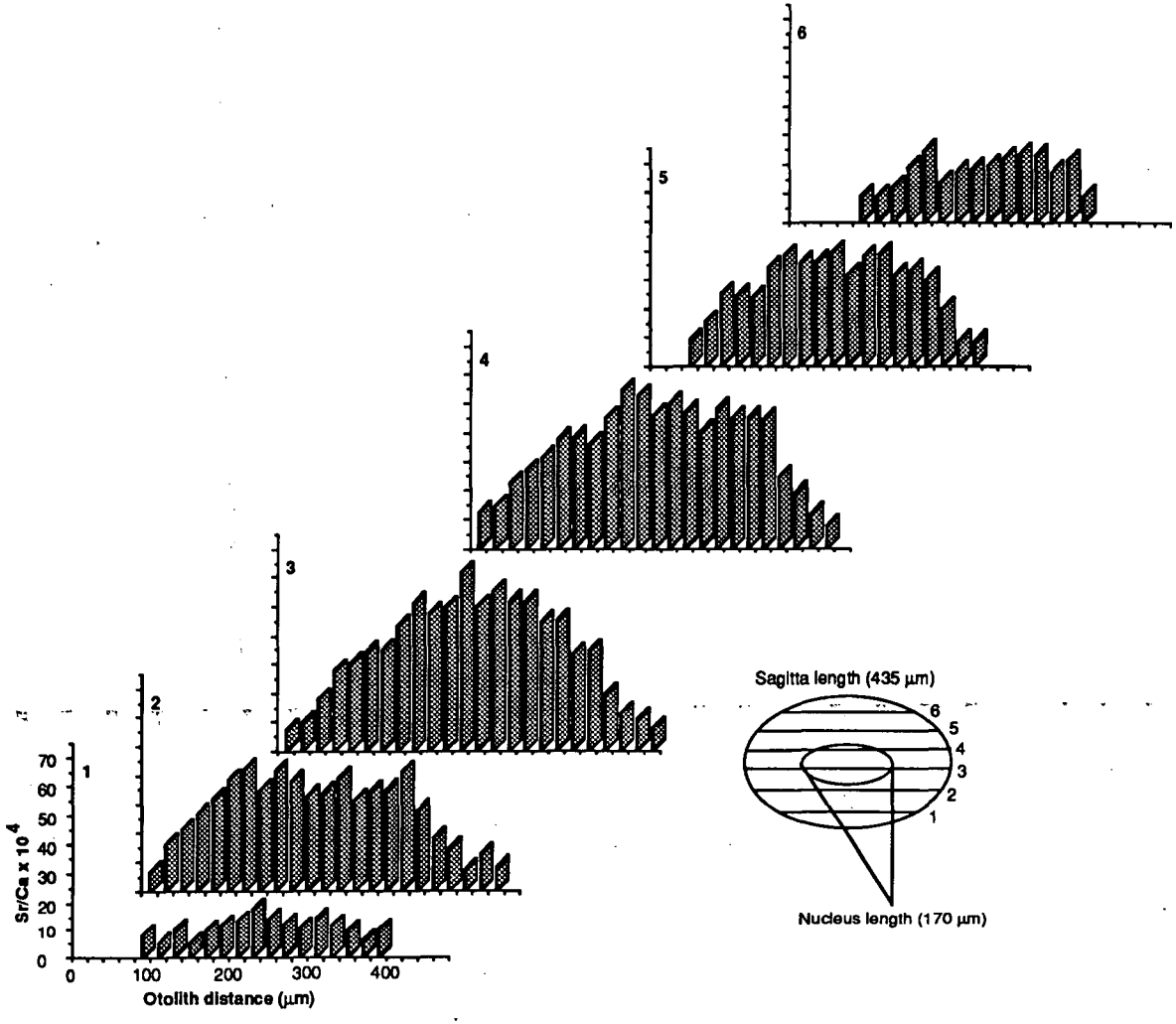

Fig. 5.4 Six transects of otolith Sr/Ca ratios made with a wavelength dispersive electron microprobe on a single sagitta from an *Oncorhynchus mykiss* fry of sea-farmed broodstock origin. The otolith was ground to the level of the primordia in the sagittal plane. Each column in the histograms represents an individual microprobe measurement (N=120). Outermost points show the sagitta Sr/Ca ratios after the completion of yolk sac absorption.

anadromous and nonanadromous fishes is such that there is probably little, if any, effect of race or population. Both wild and hatchery salmonids involved in this study displayed similar ranges of elemental ratios, depending on habitat (freshwater or marine) indicating that different salmonid species may incorporate into their otoliths a similar proportion of the ions present in the endolymph. Furthermore, this indicates that the relationship between endolymph and blood plasma composition is regulated in a similar manner in each of these species. Kalish (1989) showed that there was a tendency for both endolymph and otolith Sr/Ca ratios to be similar among individuals of a species, whereas differences were greatest among species. On the basis of the data presented here and in Kalish (1989) it seems likely that freshwater and marine salmonid otolith Sr content could be predicted on the basis of endolymph composition.

The results of this study confirm that differences in the composition of freshwater and seawater can be reflected in the composition of fish otoliths. These findings are similar to those obtained by Casselman (1982), Radtke *et al.* (1988) and Kalish (1989). Wavelength dispersive electron microprobe analyses of strontium content in diadromous fish otoliths can provide information on the rates of migration to and from the sea, residence times at sea and in freshwater, the age at which migrations take place and, they can also provide confirmation of data obtained from scales.

Confirmation of data obtained from scale reading is important because of the possibility of scale resorption (Bilton, 1974) and the equivocal nature of data obtained from scales in the discrimination of adult anadromous and nonanadromous salmonids. Bagenal *et al.* (1973) used the strontium content of whole scales to distinguish between brown trout and sea trout and Moreau and Barbeau (1979) used a similar rationale to discriminate anadromous from nonanadromous whitefish (*Coregonus clupeaformis*). However, Castonguay and FitzGerald (1982) found that this method was unreliable for distinguishing between anadromous and nonanadromous brook char (*Salvelinus fontinalis*) and Gausen and Berg (1988) had similar results when investigating migratory and nonmigratory Atlantic salmon. Measurements of otolith Sr may provide a more reliable means of determining migratory behavior in these species because otoliths are not resorbed during periods of stress (Simkiss, 1974; Campana, 1983). Also, otolith Ca and, most likely, Sr are derived from ions taken up by the gills (Simkiss, 1974) and any variations in the Sr

content of the diet would not be reflected in the composition of the otoliths. This is not the case for scales and differences in the Sr content of the diet as well as the effect of different levels of discrimination against Sr would be manifested in scale composition.

The elemental analysis of otolith primordia should provide an objective criterion for assessing if an individual is the progeny of an anadromous or nonanadramous female. This information alone, or in combination with data from life history transects, should make it possible to investigate the relationship between genetics and environment on diadromous behavior and aid in the management of species that display facultative diadromy. However, as with any new method, it is important to confirm the validity of these results for the particular species and habitat in question.

5.5 SUMMARY

Otolith microchemistry of anadromous and nonanadromous salmonids was investigated to determine if differences existed among migratory and nonmigratory individuals and to determine if the habitat where vitellogenesis took place affects the composition of the otolith primoridia of the progeny. Significant differences in otolith Sr/Ca ratios existed among adult anadromous and nonanadromous individuals but no detectable differences occur in Na/Ca, K/Ca and S/Ca ratios. The hypothesis that otolith Sr/Ca ratios in the primordia of the progeny of anadromous salmonids would be greater than Sr/Ca ratios in the primordia of the progeny of nonanadromous individuals because of differences in the composition of ova was tested and confirmed by the results of a controlled experiment. Also, the ova of anadromous *Oncorhynchus mykiss* were found to contain 5 times more Sr than their nonanadromous conspecifics. On the basis of these data it was concluded that otolith nucleus Sr/Ca ratios can be used to distinguish the progeny of sympatric anadromous and nonanadromous salmonids.

CHAPTER 6

OXYGEN AND CARBON STABLE ISOTOPES IN THE OTOLITHS OF WILD AND LABORATORY MAINTAINED AUSTRALIAN SALMON (*ARRIPIS TRUTTA*)

6.1 INTRODUCTION

Carbon and oxygen isotope chemistry of biogenic calcium carbonates is a powerful tool in studies of ocean palaeoenvironments and the life histories of marine organisms and may be a valuable source of information in studies of fish biology. Data on the oxygen isotopic composition of carbonates can be used to estimate the temperatures at which carbonates were formed. The carbon isotopic composition of calcium carbonate can be used to infer the past carbon isotopic composition of the oceans and, thus, may reflect changes in global carbon budgets and ocean circulation (Shackleton, 1977; Broecker, 1982). Carbon isotope data from calcareous tests can also provide information relating to metabolic processes and the sources of carbon involved in calcification (Craig, 1953; Tanaka *et al.*, 1986; Spero and Willams, 1988). However, interpretation of carbon isotope data is not well understood due to large and variable isotopic fractionation effects (Williams *et al.*, 1977; Shackleton and Vincent, 1978; Duplessy, 1978; Berger *et al.*, 1978; Swart, 1983; McConnaughey, 1989a, 1989b).

Oxygen isotope thermometry is, at present, the most effective method for the estimation of palaeotemperatures in the oceans. Since Urey (1947) proposed a temperature dependent fractionation of oxygen isotopes, specifically ^{18}O and ^{16}O, between calcium carbonate and water, the study of palaeooceanography has flourished. McCrea (1950) determined a palaeotemperature scale from theoretical calculations based on statistical thermodynamics and Epstein *et al.* (1953) derived a palaeotemperature equation for calcite by using data collected from molluscs grown under known environmental conditions (7° to 30°C). O'Neil *et al.* (1969) measured the equilibrium fractionation factor for ^{18}O between calcium carbonate and water in an inorganic system over a wide range of temperatures (0° to 500°C) and obtained results that are in agreement with Epstein *et al.* (1953). Shackleton (1974) developed a low temperature (-1° to 7°C) calibration equation for calcite based on the benthic foraminifera, *Uvigerina* sp., that is in good agreement with the relationship derived

by O'Neil *et al.* (1969) and, less so, with Epstein *et al.* (1953). Temperature dependent oxygen isotope fractionation in aragonitic carbonates has been investigated more recently by Grossman (1984a), Aharon and Chappell (1983), Dunbar and Wefer (1984) and Grossman and Ku (1986). In general, aragonite has received considerably less attention because the organisms of interest to palaeooceanographers typically have calcite tests.

Carbonate isotope geochemistry has been, most notably, concerned with temperature reconstruction of past oceans and these data are largely dependent upon the palaeotemperature equations, particularly that derived by Epstein *et al.* (1953). Emiliani (1954, 1955, 1966) is credited with the foundation work in the field of isotope palaeooceanography and his research is notable for the development of our present understanding of the time scale of periods of glaciation and deglaciation. Analyses of the oxygen stable isotope composition of the shells of foraminifera (Berger *et al.*, 1981), bivalves (Rye and Sommer, 1980), gastropods (Killingley and Rex, 1985), coccolithophorids (Dudley and Goodney, 1979) and other organisms have aided in the reconstruction of both ancient and modern ocean temperatures, with foraminifera making, by far, the largest contribution. Devereux (1967) suggested the potential utility of fish otoliths to the reconstruction of ocean temperatures, although they have been little used for this purpose because of their relative rarity in sediments when compared with foraminiferan tests or molluscan shells. It is probably for this reason that palaeooceanographers have not carried out detailed studies of oxygen isotope ratios in fish otoliths.

Interest in the biology of marine organisms provides an additional impetus for the study of oxygen and carbon isotopes in marine biogenic carbonates. Stable isotopes may be useful in determining the ages of marine animals by helping to discern seasonal cycles of temperature, approximating past environmental temperatures experienced by an individual, and in investigations of growth rates, metabolism and diet. Data on the oxygen and carbon stable isotopes in carbonates have been applied to investigations of the biology of corals (Weber and Woodhead, 1970), foraminifera (Spero and Williams, 1988), gastropods (Killingley and Rex, 1985), cephalopods (Taylor and Ward, 1983), whales (Killingley, 1980) and turtles (Killingley and Lutcavage, 1983), to mention a few. Several studies have investigated, albeit briefly, the isotopic composition of fish otoliths, primarily to aid in developing an understanding of fish biology (Devereux, 1967; Degens *et al.*,

1969; Mulcahy *et al.*, 1979; Radtke, 1984a, 1984b, 1987; Radtke *et al.*, 1987). Only one of these studies (Radtke, 1984a) includes any laboratory controlled validation. However, isotopic studies of fish otoliths have been flawed by use of inappropriate equations for conversion of $\delta^{18}O$ data to temperature and this has resulted in the incorrect interpretation of data in relation to both environmental temperature and isotopic fractionation. Relatively little attention has been given to the significance of $\delta^{13}C$ values obtained from fish otoliths. Degens *et al.* (1969) stated that fish otolith aragonite was derived, almost exclusively, from seawater bicarbonate, whereas Radtke (1984a, 1987) concluded that metabolic processes resulted in the fractionation of carbon isotopes in fish otoliths

This study investigates the stable oxygen and carbon isotopic composition of aragonitic fish otoliths from both captive and wild Australian salmon (*Arripis trutta*), a percoid teleost. Specifically, it is concerned with validation of the effects of temperature on isotopic fractionation and the departure, if any, from isotopic equilibrium and, the potential utility of oxygen and carbon isotopes in studies of fish biology. The problem of variability in isotopic composition between the sagittae pairs from an individual and among individuals collected from the same site is also addressed.

6.2 MATERIALS AND METHODS

6.2.1 Experimental design

Validation of environmental effects on the isotopic composition of fish otoliths is difficult because of the problems involved in maintaining marine fish under constant conditions for long periods of time. This is particularly true if one is interested in these relationships in the juvenile and adult stages. Potential stable isotope validation experiments would typically require analyses of whole otoliths, the pooling of otoliths from many fishes, or the grinding away of portions of the otolith formed in captivity. An alternative form of validation involves the use of a simple mass balance relationship that makes it possible to calculate the average isotopic composition of new material added during the period in captivity:

$$\delta^{18}O_{total} = \delta^{18}O_{wild}\left(\frac{M_{bc}}{M_{ac}}\right) + \delta^{18}O_{captive}\left(\frac{M_{ac} - M_{bc}}{M_{ac}}\right) \qquad \text{Eq. 6.1}$$

where $\delta^{18}O_{total}$, $\delta^{18}O_{wild}$ and $\delta^{18}O_{captive}$ refer to isotopic ratios measured in whole otoliths after completion of the fish rearing experiments and estimated during the precaptive wild phase and the captivity period. M_{bc} and M_{ac} refer to the otolith mass before and after captivity. A similar relationship can be used to determine the carbon isotopic composition of otolith material produced during captivity.

In order to apply the mass balance relationship to determine the stable isotopic composition of the new otolith material it is necessary to estimate the weight and isotopic composition of the fish's otolith before captivity. Estimation of the pre-captivity otolith length by visualization of an oxytetracycline hydrochloride derived fluorescent band and the collection check mark were determined to provide the best estimate of pre-captivity otolith length and, ultimately, pre-captivity otolith weight, as discussed below. The stable isotope composition of the pre-captivity otolith material was estimated from the isotopic composition of a sample of Australian salmon otoliths collected from fish captured at the same time as the experimental fish. The isotopic composition of the pre-captivity material is designated as the "baseline" otolith composition. These fish must be captured at the same time and location and be of similar size to the fish destined for experimental aquaria. These points are discussed in greater detail in Section 6.2.3.

6.2.2 Constant-Temperature Experiments

Juvenile Australian salmon were collected by beach seine in April 1987 off Cremorne Beach in southeastern Tasmania. Healthy juveniles were placed in seawater-filled plastic drums and transported to the laboratory within 2 h of capture and acclimated to the laboratory temperature (15±1°C).

Otoliths were marked for later measurements of otolith growth, and for discrimination between old (growth in the sea) and new (growth in the laboratory) otolith material by keeping the fish in ambient temperature filtered seawater containing 250 $mg \cdot l^{-1}$ oxytetracycline hydrochloride (OTC) for 16 h (1800 to 1000), after which they were transferred to drums with fresh seawater.

After the immersion period in OTC, individuals were selected at random and anesthetized in a solution of 0.1g MS-222 l^{-1} of seawater, measured to the nearest 0.1 mm SL with vernier calipers, and weighed to the nearest 0.01 g after being blotted dry on absorbent paper. Using iris scissors, each fish was given a unique combination of dorsal fin spine clips and placed in a plastic drum with fresh seawater and designated for a particular experimental aquarium. The fish were then transferred to the aquarium facility, acclimated to a selected temperature within 10 h and transferred to the appropriate experimental aquarium. At the beginning of the experiment 20 fish were placed in each aquarium and they were maintained in captivity for periods that varied from 19 to 66 days.

Constant-temperature rearing experiments were carried out with one aquarium each at 13.0, 16.0, 19.0 and 22.0 ± 0.2°C and salinity of 34.8 ± 0.2‰. A 14 h light : 10 h dark photoperiod was provided, incorporating a gradual change from light to dark, with light intensities of 2000 and <20 lx, respectively. Fish were maintained in 250 l insulated, opaque polypropylene aquaria with separate recirculating water filter systems and temperature control. Temperature was recorded twice each day and pH, salinity, ammonia, nitrite, nitrate and phosphate levels were determined once each week. Before experimental fish were placed in aquaria, ammonia and nitrite-nitrogen levels were stabilized below 1.0 $mg \cdot l^{-1}$ while pH fluctuated between 7.8 and 8.1. A 10% water change was carried out each day in order to maintain water quality.

Fish were fed to satiation once each morning (0900) with freshly caught live mysids, predominantly *Tenagomysis* sp., a regular item in the diet of Australian salmon. There were no fish mortalities during the course of these constant-temperature experiments. At the end of each experiment, fish were killed in a benzocaine/seawater solution, weighed, measured and then frozen for later extraction of sagittal otoliths.

Sagittae were extracted from thawed specimens, the adhering otolith capsule was removed using fine forceps and the otoliths were further cleaned in a sodium hypochlorite solution (12 $g \cdot l^{-1}$ available chlorine), then ultrasonically cleaned in deionized water and finally rinsed several times in deionized water. Cleaned otoliths were placed on glass slides and oven dried at 50°C for 10 h. After cleaning and drying otolith rostral length was measured to the nearest 0.01 mm with a binocular microscope equipped with a graticule and otolith weight was determined to the nearest 0.1 mg. Otoliths were stored in glass vials in a light proof box.

Before further processing, whole otoliths were observed using both reflected and transmitted light with a binocular dissecting microscope and with incident ultraviolet light excitation on a Leitz Diaplan microscope to determine the rostral length of otoliths before the fish were placed in aquaria. The fluorescence microscope was equipped with a PLOEMOPAK 4 incident light illuminator and OTC bands in the otoliths were made visible with a D filter block incorporating a 355-425 nm excitation filter, a 455 nm dichroic mirror and 460 nm barrier filter (Leitz-Wetzlar). New otolith material formed in captivity at all four temperatures was discriminated from older material laid down before the captive phase as a transparent hyaline zone with transmitted light illumination. Material produced in the period before capture was generally opaque in transmitted light. Otolith size before captivity could be determined both by visualization of the fluorescent band resulting from immersion of fish in OTC before fish were put into aquaria and the presence of the capture check mark (a highly opaque zone of about 15 μm width) between the old and new growth material.

Figure 6.1 shows the relationship between fish length and otolith weight and otolith length and otolith weight. It is evident that otolith length is a better predictor of otolith weight despite the relative difficulty of estimating this variable for the pre-captivity period. To avoid any bias in the prediction of otolith weight from otolith length, only the smaller otolith length classes that encompass those of the captive fish were used for the regression to predict otolith weight (Fig. 6.1). The pre-captivity weight of otoliths was estimated from the otolith rostral length measurements using the regression relationship between otolith weight (gm) and otolith length (mm), where $W = 0.000133 \times L^{2.907}$, ($r^2$=0.89, n=154). The estimated otolith lengths and the predicted otolith weights for the experimental fish appear in Table 6.1.

Otoliths were roasted in a vacuum at 370°C for 1 h and then reacted with 100% phosphoric acid at 24°C for 24 h under vacuum. The CO_2 resulting from the reaction with phosphoric acid was purified and any non-condensables removed by a series of three freezing/transfer steps. The purified CO_2 samples were analysed on a VG Micromass 602C mass spectrometer. The "cold finger" was required for analysis of all samples because of their small size. All values are reported in standard δ notation relative to the PDB-1 standard (Epstein *et al.*, 1953):

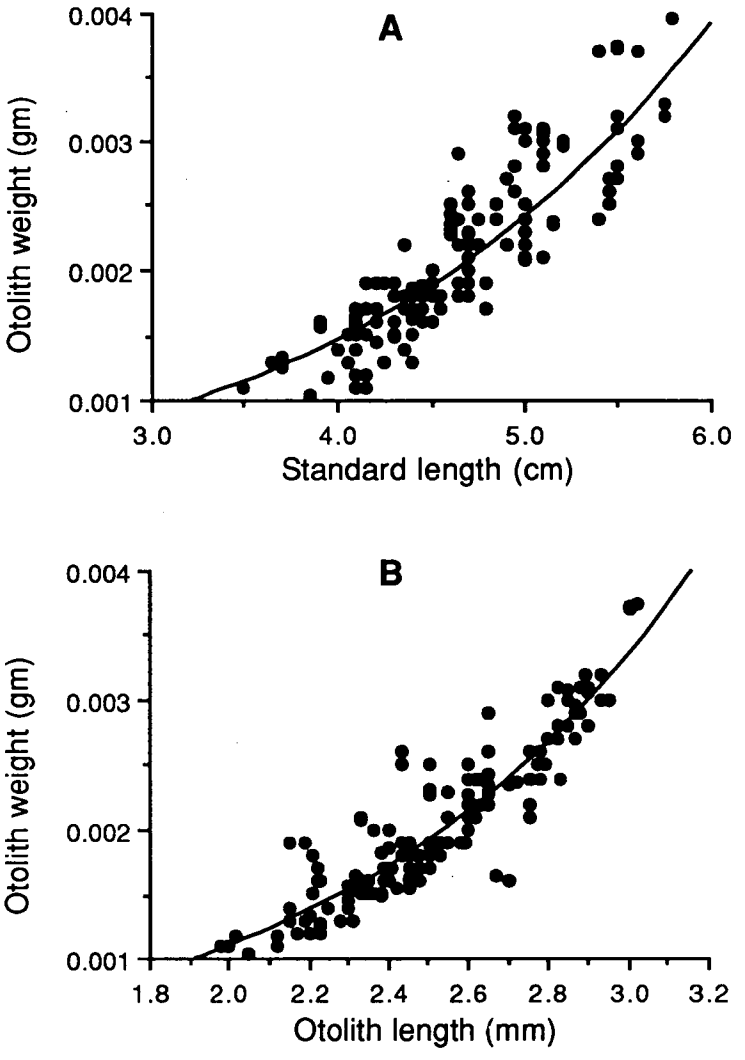

Fig. 6.1 Plots of (A) sagittal otolith weight versus fish standard length and (B) sagittal otolith weight versus sagitta length for Australian salmon. These relationships were used to estimate the pre-captivity otolith weight. $W_{oto} = (0.000043)(SL^{2.522})$, ($r^2 = 0.80$, n=154) and $W_{oto} = (0.000133)(OL^{2.907})$, ($r^2 = 0.89$, n=154), where W_{oto} is the otolith weight (gm) and SL and OL are the fish standard length (cm) and otolith rostral length (mm).

Table 6.1 Somatic and otolith growth data for laboratory reared *Arripis trutta* used in isotope studies. Fish # identifies temperature treatment: C=13°; D=16°; B=19°; A=22°C.

Fish #	$Length_{BC}$[1] (mm)	$Weight_{BC}$ (gm)	$Length_{AC}$[2] (mm)	$Weight_{AC}$ (gm)	Growth (mm/day)	Growth (gm/day)	Condition factor[3]	Otolith $length_{BC}$ (mm)	Otolith $weight_{BC}$[4]. (gm)	Otolith $weight_{AC}$ (gm)
C1	44.5	1.8	51.5	3.3	0.13	0.03	0.024	2.21	0.0013	0.0024
C2	45.0	2.0	51.5	3.5	0.12	0.03	0.026	2.24	0.0014	0.0022
C3	53.0	2.9	58.5	4.4	0.22	0.06	0.022	2.32	0.0015	0.0026
C4	47.5	2.2	52.5	3.5	0.20	0.05	0.024	2.49	0.0019	0.0024
C5	46.0	2.0	47.5	2.5	0.06	0.02	0.023	2.25	0.0014	0.0022
C6	47.0	1.9	55.5	3.6	0.23	0.04	0.021	2.45	0.0018	0.0026
C7	45.5	1.7	54.5	3.3	0.24	0.04	0.020	2.28	0.0015	0.0025
C8	46.0	1.9	57.0	3.8	0.30	0.05	0.021	2.45	0.0018	0.0026
C9	43.0	1.8	52.5	3.0	0.26	0.03	0.021	2.25	0.0014	0.0023
C10	48.0	2.2	57.0	4.1	0.24	0.05	0.022	2.38	0.0017	0.0020
C11	49.0	2.3	56.0	4.2	0.28	0.08	0.027	2.38	0.0017	0.0026
C12	43.5	1.6	51.5	2.9	0.22	0.03	0.021	2.23	0.0014	0.0024
D1	46.0	1.9	64.0	5.5	0.33	0.07	0.021	2.35	0.0016	0.0032
D2	44.5	1.9	66.5	6.1	0.33	0.06	0.021	2.58	0.0021	0.0036
D3	48.5	1.9	62.0	4.7	0.39	0.08	0.020	2.45	0.0018	0.0030
D4	43.0	1.5	57.0	3.9	0.40	0.07	0.021	2.20	0.0013	0.0028
D5	41.5	1.6	55.5	3.9	0.40	0.07	0.023	2.52	0.0020	0.0029
D6	49.0	2.1	60.0	4.6	0.31	0.07	0.021	2.48	0.0019	0.0034
D7	49.5	2.4	66.0	6.3	0.47	0.11	0.022	2.63	0.0022	0.0036
D8	44.5	1.7	52.5	3.4	0.35	0.07	0.023	2.33	0.0016	0.0026
D9	44.0	1.6	58.0	4.0	0.40	0.07	0.021	2.39	0.0017	0.0022
D10	44.0	1.7	54.5	3.8	0.46	0.09	0.024	2.38	0.0017	0.0022
B1	48.5	2.2	67.5	6.7	0.61	0.15	0.022	2.45	0.0018	0.0035
B2	49.0.	2.3	65.5	5.8	0.53	0.11	0.021	2.66	0.0023	0.0040
B3	42.5	1.5	62.5	5.1	0.65	0.11	0.021	2.18	0.0013	0.0034
B4	45.5	2.1	67.0	7.0	0.69	0.16	0.023	2.40	0.0017	0.0039
B5	50.5	2.4	65.5	5.4	0.79	0.16	0.019	2.28	0.0015	0.0031
B6	42.5	1.5	62.0	5.2	0.63	0.12	0.022	2.13	0.0012	0.0032
B7	50.5	2.4	67.0	6.1	0.53	0.12	0.020	2.68	0.0023	0.0038
A1	45.5	1.6	65.0	5.9	0.63	0.14	0.021	2.49	0.0019	0.0031
A2	46.0	1.8	68.0	6.9	0.71	0.16	0.022	2.25	0.0014	0.0040
A3	44.0	1.6	66.5	6.0	0.73	0.14	0.020	2.26	0.0014	0.0040
A4	44.0	1.8	65.5	5.7	0.69	0.13	0.020	2.30	0.0015	0.0034
A5	41.0	1.4	61.5	4.7	0.66	0.11	0.020	2.18	0.0013	0.0031
A6	45.5	1.7	67.0	6.4	0.69	0.15	0.021	2.58	0.0021	0.0030
A7	48.5	2.4	71.0	7.7	0.73	0.17	0.022	2.62	0.0022	0.0041
A8	48.0	1.9	62.5	5.5	0.47	0.11	0.022	2.49	0.0019	0.0035
A9	43.0	1.6	67.0	4.7	0.67	0.09	0.016	2.29	0.0015	0.0023

[1] before captivity

[2] after captivity

[3] condition factor = (W/L^3) 1000; (based on data after captivity)

[4] otolith $weight_{B.C.} = (0.000133) \times (\text{otolith } length_{B.C.})^{2.907}$

$$\delta = \left(\frac{R_{sample}}{R_{standard}} - 1 \right) \times 1000 \qquad \text{Eq. 6.2}$$

where R is the mass ratio (46-44) of the sample or standard. Isotopic ratios were related to the PDB standard through analysis of Biggenden calcite (BCS) which had been calibrated to the PDB standard via the international standards NBS-19 (Craig, 1957) and TKL (Blattner and Hulston, 1978). Analytical precision of the reported measurements is ±0.03‰ (1 s.d.) or better.

6.2.3 Estimation of isotopic temperatures

Numerous equations have been proposed to describe the temperature dependent fractionation of oxygen isotopes in calcium carbonate. This study employs the empirical relationship derived by Grossman (1982) using the aragonitic foraminifera *Hoeglundina elegans* to calculate isotopic temperatures:

$$T\,(°C) = 20.19 - 4.56\left(\delta^{18}O_{ar} - \delta^{18}O_w\right) + 0.19\left(\delta^{18}O_{ar} - \delta^{18}O_w\right)^2 \qquad \text{Eq. 6.3}$$

where $\delta^{18}O_{ar}$ and $\delta^{18}O_w$ represent the oxygen isotopic composition measured in the aragonitic sample and the oxygen isotopic composition of the seawater from which the aragonite was precipitated, respectively. It can be seen that the $\delta^{18}O$ of aragonite formed in equilibrium with seawater is a function of the water temperature and the seawater $\delta^{18}O$ represented as δ_w in palaeotemperature equations such as the one above.

Before continuing it is important to point out the exact nature of the δ_w factor that appears in palaeotemperature equations as it is often a source of confusion and can result in significant errors when applying the palaeotemperature equation or when considering deviations from equilibrium precipitation. The value δ_w refers to the oxygen isotopic composition of CO_2 gas equilibrated with the water sample relative to

the isotopic composition of a sample of CO_2 produced by the reaction of the international standard PDB calcite with 100% phosphoric acid at 25°C. If the relationship between salinity and $\delta^{18}O$ from Epstein and Mayeda (1953) is used than the resulting value does not require conversion to δ_w because Epstein and Mayeda used CO_2 produced from the acidification of PDB with phosphoric acid at 25°C as their standard. In many cases, such as the present study and Romanek *et al.* (1987), the $\delta^{18}O$ and salinity data from Craig and Gordon (1965) are used to estimate seawater $\delta^{18}O$. Craig and Gordon (1965) reported their data relative to CO_2 equilibrated with Standard Mean Ocean Water (SMOW) at 25°C and, therefore it is necessary to convert $\delta^{18}O_{SMOW}$ to δ_w before using palaeotemperature equations. The relationship between $\delta^{18}O_{SMOW}$ and δ_w is (Friedman and O'Neil, 1977) :

$$\delta_w = 0.99978\ (\delta^{18}O_{SMOW}) - 0.22 \qquad \text{Eq. 6.4}$$

In order to measure the $\delta^{18}O$ and $\delta^{13}C$ of water it is necessary to equilibrate a volume of carbon dioxide gas with the water sample and then analyse an aliquot of the gas (Epstein and Mayeda, 1953; Kroopnick, 1974), but facilities for this type of analysis were not available. Alternatively, the $\delta^{18}O$ of seawater can be estimated from the known relationship between salinity and $\delta^{18}O$. There are no published data relating the $\delta^{18}O$ and salinity from the Tasman Sea. However, data relating $\delta^{18}O$ to salinity in South Pacific Ocean surface waters (Craig and Gordon,1965) probably provide a suitable approximation for Tasman Sea surface waters:

$$\delta^{18}O_{SMOW} = 0.6956S - 24.04 \qquad \text{Eq. 6.5}$$

where S is equal to salinity (‰) and the $\delta^{18}O_{SMOW}$ value is converted to δ_w as discussed above.

6.2.4 Contribution of metabolic carbon

It is possible to estimate the percentage of metabolically derived carbon (M%[$\delta^{13}C$]) in the otolith with data on otolith $\delta^{13}C$, seawater $\delta^{13}C$ and carbon reservoirs in the form of metabolic carbon using a mass balance model:

$$\delta^{13}C_{oto} = \left(\delta^{13}C_{b,sw} + \varepsilon_{s\text{-}b}\right)\left(1 - \frac{M\%[\delta^{13}C]}{100}\right) + \left(\delta^{13}C_{meta} + \varepsilon_{s\text{-}a}\right)\left(\frac{M\%[\delta^{13}C]}{100}\right) \qquad \text{Eq. 6.6}$$

where $\delta^{13}C_{oto}$, $\delta^{13}C_{b,sw}$ and $\delta^{13}C_{meta}$ are the carbon isotopic ratios measured in the otolith, seawater bicarbonate and metabolically derived CO_2. The variables $\varepsilon_{s\text{-}b}$ and $\varepsilon_{s\text{-}a}$ are fractionation factors between HCO_3^- and $CaCO_3$ and, CO_2 and $CaCO_3$, respectively (Tanaka *et al.*, 1986). These variables are discussed in greater detail below. A similar type of relationship has been used by several authors (Weber and Woodhead, 1970; Williams *et al.*, 1977; Erez and Honjo, 1981; Williams *et al.*,1981) to estimate the contribution of metabolically derived bicarbonate to the makeup of calcium carbonate tests.

The value for the calcium carbonate-bicarbonate enrichment factor, $\varepsilon_{s\text{-}b}$, is from Emrich *et al.* (1970) as modified by Grossman (1984b):

$$\varepsilon_{s\text{-}b}\ (‰) = 12.40 - \frac{2980}{T(°K)} \qquad \text{Eq. 6.7}$$

Grossman and Ku (1986) empirically determined two equations for ^{13}C fractionation in aragonite, one based on the benthic foraminifera *H. elegans* and the other on coeval molluscs, both of which result in ^{13}C fractionation factors about 3‰ lower than in Equation 7 above. The ^{13}C fractionation relationships from Grossman and Ku (1986) indicate decreasing skeletal $\delta^{13}C$ with increasing temperature whereas Equation 7 predicts increasing skeletal $\delta^{13}C$. The use of these two alternate equations for ^{13}C fractionation does not result in significant changes in the estimates of the metabolic contribution to otolith carbon, but should be considered when

discussing deviations from equilibrium fractionation.

The fractionation factor between aqueous CO_2 and $CaCO_3$ ($\varepsilon_{s\text{-}b}$) involves two steps as $CaCO_3$ is actually formed from bicarbonate and calcium ions. Therefore, it is necessary to sum $\varepsilon_{s\text{-}b}$, just discussed, and $\varepsilon_{b\text{-}c}$, the fractionation factor between aqueous CO_2 and HCO_3^-:

$$\varepsilon_{s\text{-}a} = \varepsilon_{s\text{-}b} + \varepsilon_{b\text{-}c} \qquad \text{Eq. 6.8}$$

The value for $\varepsilon_{b\text{-}c}$ is also temperature dependent and is determined from Mook *et al.* (1974) (see their table 4) with the relationship:

$$\varepsilon_{b\text{-}c} = -\left(\frac{9866}{T}\right) + 24.12‰ \qquad \text{Eq. 6.9}$$

The carbon isotopic composition of Tasman Sea surface water ($\delta^{13}C_{sw}$) is estimated to be approximately 2.0‰ using the relationship between AOU (apparent oxygen utilisation) and $\delta^{13}C$ of the total dissolved CO_2 (Kroopnick, 1974; Williams *et al.*, 1977). AOU is the difference between the saturated O_2 content of water at a particular salinity and temperature and the measured O_2 content (Williams *et al.*, 1977). Surface waters are typically saturated with O_2 in the first few meters and this was assumed to be the case for the habitat of juvenile Australian salmon. This is in agreement with values typically measured in surface waters at similar latitudes (Kroopnick, 1974, 1980). Because the value of $\delta^{13}C_{met}$, that is $\delta^{13}C$ for metabolic aqueous CO_2 cannot be measured directly, the $\delta^{13}C$ value obtained from isotopic measurements of whole juvenile Australian salmon (20.1‰) was used (Fenton, 1985).

6.3 RESULTS

6.3.1 Estimation of baseline $\delta^{13}C$ and $\delta^{18}O$ values

The mean oxygen and carbon isotopic ratios for the baseline fish were 0.31±0.91‰ and -5.76±0.65‰, respectively. However, there were significant variations in oxygen and carbon isotopes from the Australian salmon otoliths used to estimate the isotopic baseline with several outliers in both oxygen and carbon isotopic ratios (Fig. 6.2). Furthermore, several replicate analyses of Australian salmon otolith pairs indicate that there is significant variation in the isotopic composition between the two sagittae of an individual fish as discussed below.

Calculation of a mean isotopic temperature using oxygen isotope data from the baseline Australian salmon and the empirically derived relationship from Grossman (1982) for aragonite yielded a mean temperature of 19.0°C, which would be within the range of expected mean temperatures experienced by these juvenile fish. Australian salmon are known to spawn along the coasts of New South Wales and Victoria in the spring and summer. Juvenile recruits (<35mm standard length) first appear in the environs of Storm Bay around January and continue to appear through about April (J. M. Kalish, unpublished data and Dr. Peter Last, C.S.I.R.O. Division of Fisheries Research, Hobart, unpublished data). The mean temperature experienced by a larval Australian salmon during the passive drift from the spawning grounds to Storm Bay, Tasmania can be estimated by calculating the mean temperature in southeast Australian waters from Eden, New South Wales to Hobart, Tasmania over the combined months of January to April using sea surface temperature data averaged over 10 years from Edwards (1979). If it is assumed larvae drift at a constant rate from the spawning grounds to recruitment in the environs of Storm Bay during the summer, the fish would have experienced a mean temperature of approximately 18.6°C, in excellent agreement with the calculated mean oxygen isotopic temperature of 19.0°C. On the basis of these relationships it was considered valid to utilise the mean oxygen and carbon isotopic ratios from the baseline data for further calculations.

6.3.2 Isotopic composition of otoliths from experimental fish

Analytical results for individual experimental fish are presented in Table 6.2.

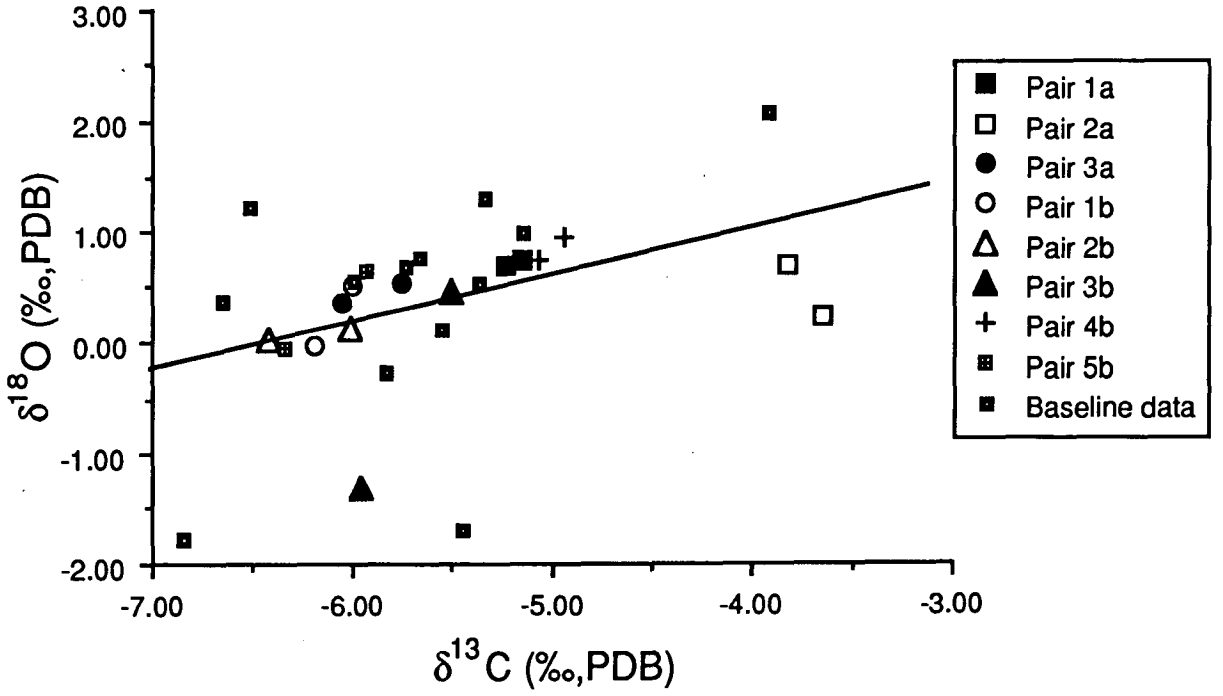

Fig. 6.2 Plot of oxygen versus carbon isotopic values for 8 pairs of sagittae used to estimate isotopic variation within an individual and data used to estimate isotopic baseline. Pairs AS52, AS53, AS56, AS57 and AS59 were used to determine the isotopic baseline and to investigate within fish variability in otolith isotopic ratios. Details of the fish used to investigate variation within individuals are presented in Table 6.6.

Table 6.2 Stable isotope data from laboratory reared *Arripis trutta* including results of mass balance calculations and isotopic temperatures based on 3 different empirically derived relationships which are discussed in the text. Fish # identifies temperature treatment: C=13°; D=16°; B=19°; A=22°C.

Fish #	$\delta^{18}O_{PDB}$(‰)	$\delta^{13}C_{PDB}$(‰)	Mass balance $\delta^{18}O_{PDB}$(‰)	Isotopic temp1 (°C) Grossman (1982)	Isotopic temp2 (°C) Horibe and Oba (1972)	Isotopic temp3 (°C) Epstein *et al.* (1953)	Mass balance $\delta^{13}C_{PDB}$(‰)
C1	0.78	-5.29	1.37	15.4	8.1	11.2	-4.70
C2	0.18	-5.56	-0.04	21.5	14.4	17.1	-5.22
C3	0.07	-6.01	-0.28	22.6	15.5	18.1	-6.37
C4	0.55	-5.61	1.43	15.1	7.8	11.0	-5.06
C5	-0.17	-5.80	-1.02	26.2	18.9	21.4	-5.87
C6	1.16	-5.98	3.07	9.0	0.7	4.9	-6.47
C7	1.05	-5.50	2.09	12.5	4.9	8.4	-5.13
C8	0.92	-5.81	2.29	11.8	4.0	7.7	-5.92
C9	1.26	-4.86	2.75	10.1	2.0	6.0	-3.45
C10	0.66	-5.45	2.34	11.6	3.8	7.5	-3.97
C11	1.07	-5.54	2.40	11.4	3.6	7.3	-5.16
C12	1.13	-5.38	2.22	12.0	4.3	8.0	-4.88
Mean	0.72±0.47	-5.57±0.32	1.55±1.31	14.9±5.5	7.3±5.9	10.7±5.3	-5.18±0.90
D1	0.85	-6.08	1.39	15.3	8.0	11.1	-6.40
D2	0.66	-5.95	1.15	16.3	9.1	12.1	-6.21
D3	0.75	-5.49	1.41	15.2	7.9	11.1	-5.09
D4	0.80	-5.47	1.23	15.9	8.7	11.7	-5.21
D5	0.92	-5.32	2.18	12.2	4.5	8.1	-4.41
D6	0.69	-5.79	1.15	16.3	9.1	12.1	-5.83
D7	1.04	-4.88	2.20	12.1	4.4	8.0	-3.48
D8	0.90	-5.45	1.78	13.7	6.3	9.6	-4.99
D9	0.83	-5.24	2.49	11.0	3.2	7.0	-3.58
D10	0.74	-5.33	2.04	12.7	5.1	8.6	-4.03
Mean	0.82±0.12	-5.50±0.36	1.70±0.50	14.1±2.0	6.6±2.2	9.9±1.9	-4.92±1.04
B1	0.05	-5.12	-0.23	22.3	15.3	17.9	-4.44
B2	0.61	-5.07	1.01	16.8	9.7	12.6	-4.15
B3	0.39	-5.44	0.44	19.3	12.3	15.0	-5.25
B4	0.70	-4.73	1.00	16.9	9.7	12.7	-3.94
B5	0.93	-6.00	1.48	14.9	7.6	10.8	-6.21
B6	1.25	-4.82	1.81	13.6	6.1	9.5	-4.26
B7	-0.06	-5.15	-0.65	24.4	17.2	19.7	-4.18
Mean	0.55±0.47	-5.19±0.43	0.70±0.89	18.3±3.9	11.1±4.0	14.0±3.7	-4.63±0.81
A1	0.05	-5.28	-0.35	22.9	15.9	18.4	-4.53
A2	0.29	-5.00	0.28	20.0	13.0	15.7	-4.59
A3	-0.37	-5.10	-0.75	24.8	17.7	20.2	-4.74
A4	-0.14	-5.68	-0.49	23.6	16.5	19.0	-5.62
A5	-0.41	-5.35	-0.92	25.7	18.4	21.0	-5.06
A6	-0.17	-5.39	-1.28	27.5	20.1	22.6	-4.54
A7	-0.15	-5.46	-0.68	24.5	17.3	19.9	-5.12
A8	-0.14	-5.92	-0.67	24.4	17.3	19.8	-6.11
A9	-0.27	-6.29	-1.31	27.7	20.3	22.8	-7.25
Mean	-0.15±0.21	-5.50±0.41	-0.68±0.48	24.6±2.3	17.4±2.2	19.9±2.2	-5.28±0.91
Σmean	0.51±0.51	-5.46±0.38	0.90±1.30				-5.04±0.92

The oxygen and carbon isotopic data from the experimental fish otoliths are plotted against temperature in Fig. 6.3 and 6.4. Separate graphs are shown for the data before and after the mass balance calculations. Lines representing equilibrium deposition of oxygen isotopes in calcite (Epstein *et al.*, 1953) and aragonite (Horibe and Oba, 1972; Grossman, 1982) are shown so that comparisons can be made with established isotopic temperature scales as well as a temperature scale frequently used in the fish otolith literature. A significant temperature effect ($F=14.28$, $df=3,34$, $P<0.0001$) was evident in the oxygen isotope data even when considering whole otolith composition and not only the otolith material produced during captivity (Table 6.3). However, there was no evidence for a linear relationship among these data ($F=5.34$, $df=1,2$, $P>0.10$) (Table 6.3). Carbon isotope data from the same samples showed no evidence of a temperature effect (Fig. 6.4).

After applying the mass balance relationship to the oxygen isotope data there was not a large change in the relative position of the data points at each temperature because both somatic and otolith growth rates were similar among fish at a single temperature (Fig. 6.3) (Table 6.1). Therefore, the amount of new otolith material formed in fish at a single temperature was a similar proportion of the total otolith material. However, scatter in the data is greater after application of the mass balance relationship, particularly in the data from fish maintained at 13°C and 16°C. This may be due to imprecision in the estimation of the isotopic baseline for some of the experimental fish. For example, underestimation of the degree of depletion in the heavy oxygen isotope by the isotopic baseline would result in subsequent overestimation of the magnitude of depletion in the newly formed otolith material. This effect would be particularly extreme in fish maintained at the lower temperatures because of the relatively small quantity of new otolith material. Despite this increase in the range of $\delta^{18}O$ at each temperature there was still a very significant effect due to temperature ($F=14.04$, $df=3,34$, $P<0.0001$). Again, there was no evidence for a linear relationship among the data ($F=9.18$, $df=1,2$, $0.05<P<0.10$) (Table 6.4).

The failure of the $\delta^{18}O$ data to show a linear relationship versus temperature was due to the presence of 3 outliers from the 13°C treatment. These data were clearly divergent from the other data points from the 13°C treatment both before and after the application of the mass balance model. These data may be significantly different from the other 13°C values because the fish may have experienced different environmental conditions before capture (see Chapter 4). If this were true than the pre-captivity

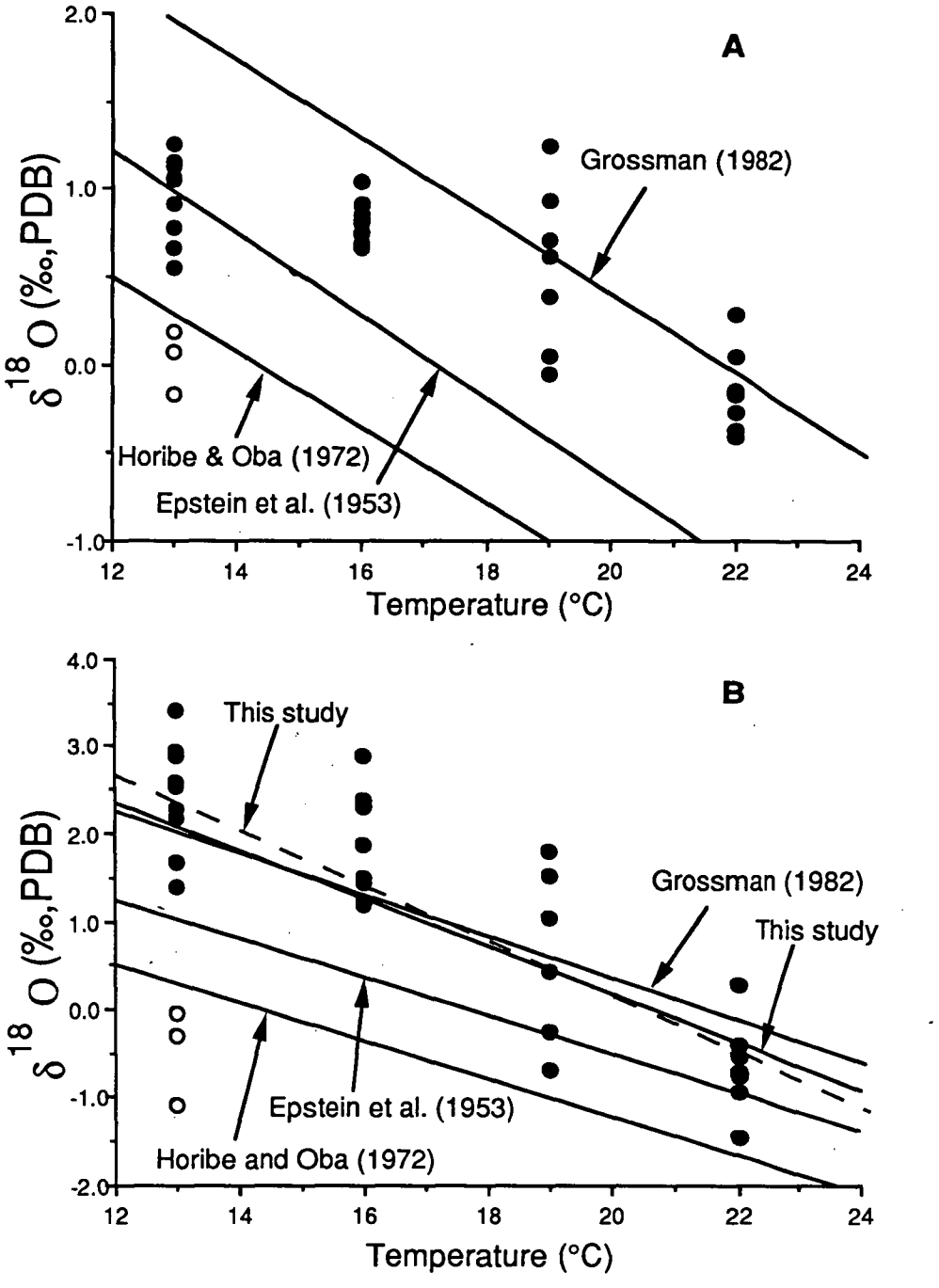

Fig. 6.3 Plots of oxygen isotope values versus temperature for otoliths from fish maintained at constant temperatures. Several lines based on isotopic temperature relationships frequently cited in the literature are shown for comparison. The line from Epstein *et al.* (1953) is based on calcite and the other two are based on aragonite (Horibe and Oba, 1972; Grossman, 1982). Open points are outliers discussed in text. (A) Data before mass balance calculations. Data are significantly correlated but linear regression is not significant. (B) Data after mass balance calculations. Solid line labelled "This study " includes outliers and is not significant ($F=9.18$, $df=1,2$, $0.05<P<0.10$); dashed line excludes outliers and the linear regression, $\delta^{18}O=6.69-0.326T$ ($r^2=0.77$, $P<0.0001$) is significant ($F=58.89$, $df=1,2$, $P<0.02$). See Section 6.3.2 and Table 6.3, 6.4 and 6.5.

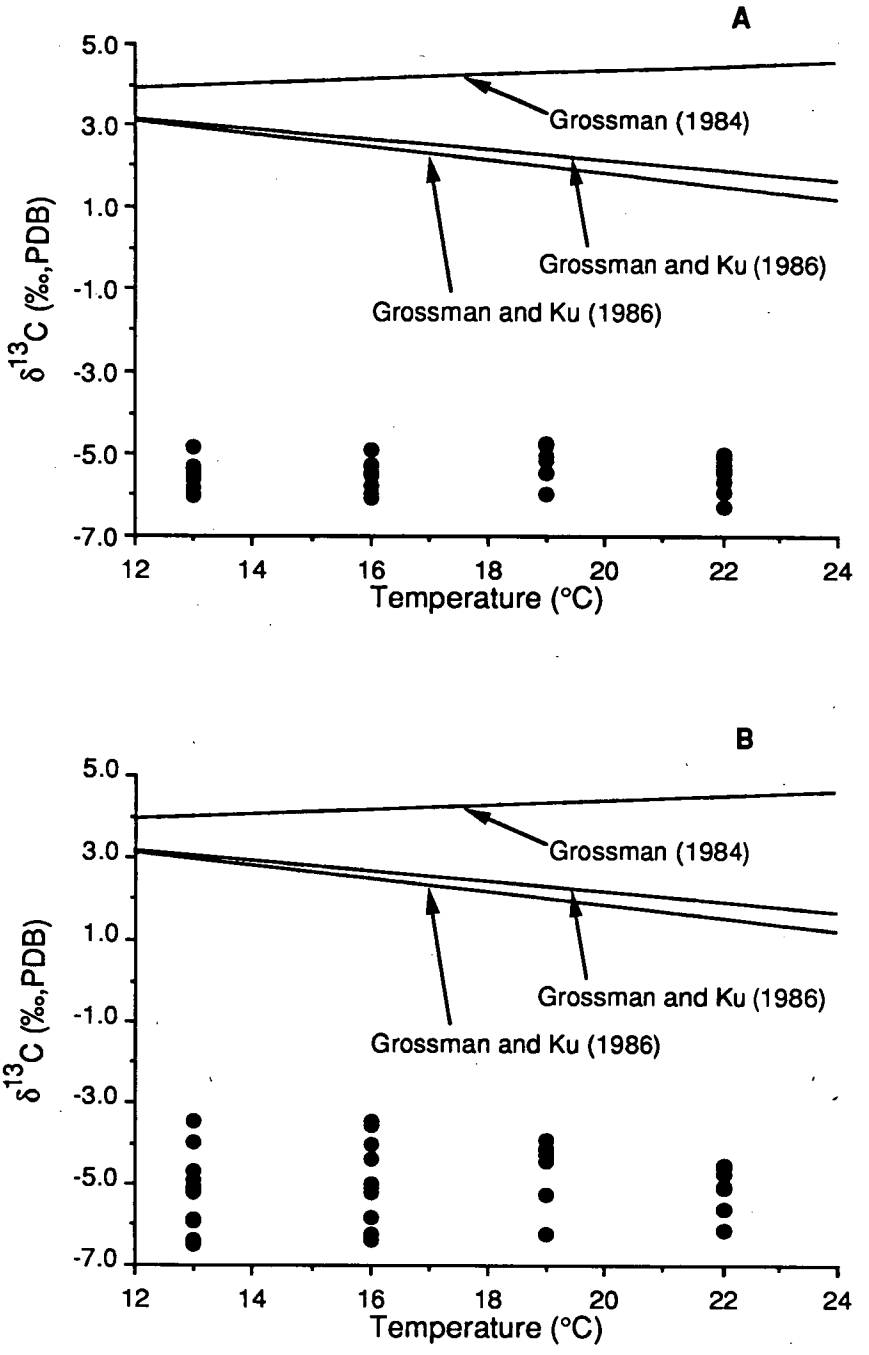

Fig. 6.4 Plot of carbon isotope values versus temperature for otoliths from *Arripis trutta* maintained at constant temperatures. The lines from the literature are all based on aragonite and are considered to be indicative of equilibrium fractionation of carbon isotopes. The data show that otolith carbon is depleted in the heavy carbon isotope relative to equilibrium both before (A) and after (B) the mass balance calculations.

Table 6.3 Results of one-way analysis of variance and Model I regression analysis examining the relationship among $\delta^{18}O$ values in *Arripis trutta* otoliths from fish maintained at 4 temperatures. Results are based on the raw $\delta^{18}O$ data before applying the mass balance relationship. See Fig. 6.3a.

Source of variation	df	SS	MS	F	P
Among temperatures	3	5.367	1.789	$14.28_{(3,34)}$	P<0.0001
Linear regression	1	3.903	3.903	$5.34_{(1,2)}$	0.10<P<0.25
Deviations from regression	2	1.463	0.732	$5.84_{(2,34)}$	0.005<P<0.01
Within temperatures	34	4.260	0.125		
Total	37	14.993			

Table 6.4 Results of one-way analysis of variance and Model I regression analysis examining the relationship among $\delta^{18}O$ values in *Arripis trutta* otoliths from fish maintained at 4 temperatures. Results are based on the $\delta^{18}O$ data after applying the mass balance relationship. See Fig. 6.3b.

Source of variation	df	SS	MS	F	P
Among temperatures	3	34.43	11.48	$14.04_{(3,34)}$	P<0.0001
Linear regression	1	28.27	28.27	$9.18_{(1,2)}$	0.05<P<0.10
Deviations from regression	2	6.16	3.08	$3.77_{(2,34)}$	0.025<P<0.05
Within temperatures	34	27.80	0.818		
Total	37	96.66			

Table 6.5 Results of one-way analysis of variance and Model I regression analysis examining the relationship among $\delta^{18}O$ values in *Arripis trutta* otoliths from fish maintained at 4 temperatures. Results are based on the $\delta^{18}O$ data after applying the mass balance relationship and the elimination of 3 outliers from the 13°C treatment See Fig. 6.3b.

Source of variation	df	SS	MS	F	P
Among temperatures	3	44.45	14.82	$40.59_{(3,31)}$	P<0.0001
Linear regression	1	42.99	42.99	$58.89_{(1,2)}$	0.01<P<0.025
Deviations from regression	2	1.460	0.730	$2.00_{(2,31)}$	0.10<P<0.25
Within temperatures	31	11.33	0.365		
Total	34	100.23			

$\delta^{18}O$ values for these otoliths could have deviated significantly from the estimated isotopic baseline. This is plausible given the large variations that were evident in the baseline oxygen isotope data. If it is accepted that these fish are aberrant in some way it is reasonable to eliminate them from the data set. If these individuals are eliminated from the data set there is a highly significant correlation between $\delta^{18}O$ and temperature (r^2=0.77, df=35, P<0.0001) and a significant linear regression (F=58.89, df=1,2, 0.01<P<0.025) (Table 6.5) (Fig. 6.3b), where, $\delta^{18}O$=6.69-0.326(T°C).

6.3.3 Variability between sagittae from individual fish

Eight pairs of sagittae from juvenile Australian salmon were analysed for carbon and oxygen isotopes in random order to eliminate any instrument and/or operator bias and it was found that there were significant differences within pairs of otoliths (Fig. 6.2). Data from these fish appear in Table 6.6. Three of the fish, collected in the same net haul, were almost identical in body length and weight and otolith length and weight. The other 5 pairs of sagittae, among the 23 sagittae used in the estimation of the $\delta^{18}O$ and $\delta^{13}C$ baseline, were from fish collected in a different net haul; they differed only slightly in length and weight (Table 6.6).

In the case of the three fish of almost identical weight and length it is evident that the sagittae from individuals had similar values for $\delta^{18}O$ and $\delta^{13}C$, although two of the pairs showed notable differences, one in $\delta^{18}O$ and the other in $\delta^{13}C$ (Fig. 6.2). $\delta^{18}O$ ranged from 0.22‰ to 0.75‰ equivalent to a temperature difference of approximately 2.4°C for the three otolith pairs. The difference in $\delta^{18}O$ from one of the otolith pairs (AS94) was almost as great as the range measured for all three pairs. The range of $\delta^{13}C$ for the three otolith pairs was -3.65‰ to -6.05‰, much greater than the range found for $\delta^{18}O$, although the greatest variation within a pair of sagittae was only 0.30‰, less than the range of $\delta^{18}O$ within a pair.

Values of $\delta^{18}O$ from the set of 5 otolith pairs were not significantly different from that found for the three previous pairs if a single outlier at -1.31‰ that was run at a low gas pressure (approximately half normal) due to a low gas yield from the sample is ignored. $\delta^{13}C$ values also displayed a similar, but somewhat narrower range than the previous 3 otolith pairs. The one notable difference between these five pairs and the previous three was that values from individual otolith pairs were not as tightly clumped. This implies even greater analytical imprecision and/or

Table 6.6 Results of Australian salmon otolith pair analyses. AS52-AS59 were collected on 4/19/87 and AS89-AS100 on 8/6/87.

Fish#	Length (mm)	Weight (gm)	Otolith length (mm)	Otolith weight (mg)	$\delta^{18}O_{PDB}$(‰)	$\delta^{13}C_{PDB}$(‰)
AS52a	45.5	1.83	2.51	1.80	-0.20	-6.19
b			2.51	1.80	0.52	-6.00
AS53a	43.0	1.67	2.51	1.85	0.02	-6.42
b			2.51	1.85	0.13	-6.01
AS56a	47.0	1.74	2.59	1.95	-1.31	-5.95
b			2.51	1.90	0.47	-5.50
AS57a	47.0	1.84	2.55	2.00	0.96	-4.94
b			2.61	2.11	0.74	-5.06
AS59a	42.0	1.34	2.49	1.65	0.63	-5.93
b			2.43	1.54	-0.50	-6.34
Mean					0.21±0.64	-5.83±0.51
AS89a	48.0	1.72	2.50	1.92	0.75	-5.14
b			2.52	1.90	0.69	-5.22
AS94a	47.0	1.68	2.45	1.91	0.22	-3.65
b			2.45	1.94	0.69	-3.82
AS100a	47.0	1.65	2.45	1.86	0.53	-5.75
b			2.45	1.83	0.35	-6.05
Mean					0.54±0.21	-4.94±0.99

greater variability at the level of the otolith pair from an individual.

6.3.4 Estimation of the contribution of metabolic carbon

Calculation of the contribution of metabolic carbon indicated that 31.7% to 34.9% of the carbon in otoliths from the laboratory reared Australian salmon was derived from metabolic CO_2 (Table 6.7).

Table 6.7 Results of calculations used to estimate the percentage of metabolically derived carbon (M%) in fish otoliths. $\delta^{13}C_{b,sw}$ = 2.0‰ as estimated from AOU and $\delta^{13}C_{met}$ = 20.1‰ based on whole juvenile Australian salmon.

Temperature (°C)	ε_{s-b} (‰)	ε_{b-c} (‰)	ε_{s-a} (‰)	Metabolic carbon (%)
13	1.98	10.38	12.36	31.9
16	2.09	10.02	12.11	31.7
19	2.20	9.67	11.87	31.7
22	2.30	9.32	11.62	34.9

There was no evidence for a relationship between temperature, somatic growth, and otolith growth and the relative proportion of metabolically derived CO_2 incorporated in the otoliths of juvenile Australian salmon. However, the greater depletion in ^{13}C at 22°C, resulting in the estimation of a larger contribution of metabolic carbon to the otolith may be indicative of a significantly higher metabolic rate in these fish.

A positive correlation between $\delta^{13}C$ and $\delta^{18}O$ is generally considered to be an indication of the incorporation of metabolically derived CO_2 into the carbonate structure (Grossman, 1984a) or due to kinetic effects during the hydration and hydroxylation of CO_2, where there is a discrimination against the heavier isotopes (McConnaughey, 1984a, 1984b). There was a positive correlation between the oxygen and carbon isotope data (r^2=0.27, n=23, $p<0.01$) used to estimate the isotopic baseline (Fig. 6.2), but a similar effect was not apparent in the laboratory maintained fish (Fig. 6.5) despite the wide range of temperatures. Further research is

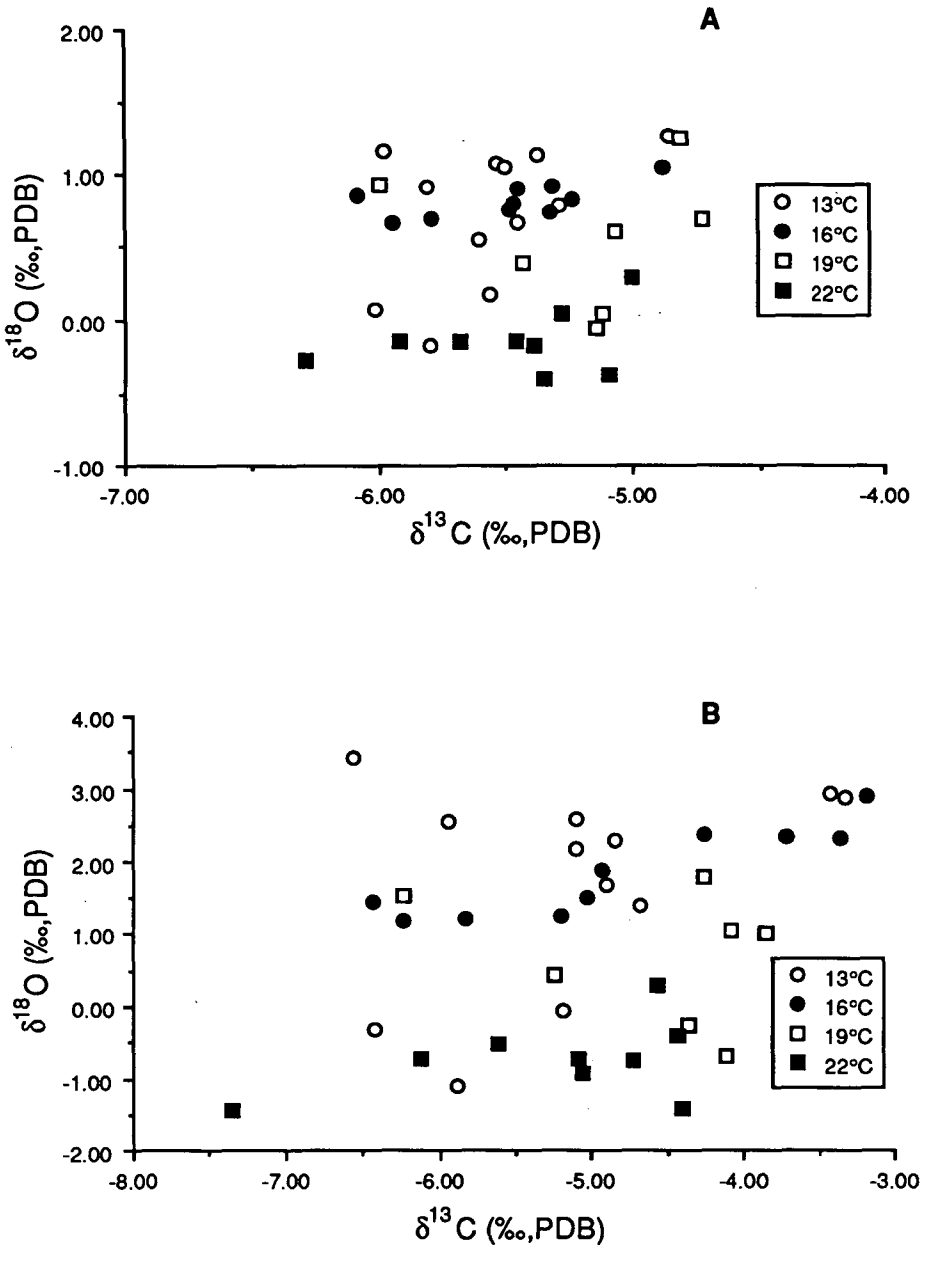

Fig. 6.5 Plots of oxygen versus carbon isotopes for otoliths from *Arripis trutta* maintained at four different temperatures before (A) and after (B) the mass balance calculations. Unlike the data from the baseline fish (Fig. 6.2), no trend is evident when data from the four controlled temperature groups are combined.

required to ascertain if there is any effect related to metabolism or calcification rate in the carbon and oxygen isotopes of fish otoliths (see Chapter 7).

6.4 DISCUSSION

6.4.1 Variability in otolith isotope data

There was considerable variability in both $\delta^{18}O$ and $\delta^{13}C$ from the baseline and aquarium fish. Standard deviations for $\delta^{18}O$ and $\delta^{13}C$ were 0.51‰ and 0.38‰ for aquarium fish at all four temperatures (data before mass balance calculations) and 0.91‰ and 0.65‰ for the baseline fish. The higher standard deviation for $\delta^{18}O$ and $\delta^{13}C$ data from the baseline fish may be due to environmental and metabolic variability experienced in the wild compared with the constant conditions experienced by fish in aquaria. Of course, it was assumed that the isotopic variability of the aquarium fish before the captive period would be equal to that of the baseline fish. The controlled environment period has resulted in a large reduction in the overall variability in the isotope data. Therefore, the controlled variables that would probably have the greatest effect on the isotopic composition of the otolith aragonite included temperature, salinity and diet.

Killingley *et al.* (1981) reported standard deviations of up to 0.5‰ in $\delta^{18}O$ and 0.6‰ in $\delta^{13}C$ and ranges of 2.0‰ for both $\delta^{18}O$ and $\delta^{13}C$ for the inter-shell variability of the tests of the planktonic foraminifera *Orbulina universa* collected in sediment samples from the same stratigraphic level, variability that is similar to what is reported here for otoliths from wild Australian salmon. They concluded that variation among shells of the same species and size was almost as great as the variability in the means among species.

Variability in isotopic ratios from planktonic foraminifera collected at the same stratigraphic level can result from (modified from Killingley *et al.*,1981): (1) geological and biological disturbance of sediments causing mixing of sediment layers; (2) variations in the temperature and isotopic composition of the waters in which the foraminifera grew; (3) differences in the depth distribution of individuals during life which would again expose the organism to different temperatures and seawater levels of oxygen and carbon isotopes; (4) variations in biological fractionation resulting from metabolic effects and, perhaps, genetic

differences; and (5) differences in diet (not applicable to foraminifera). Only the last three sources of variability are applicable to otoliths collected from living fish. However, the relative effect of these variables can be much greater than in foraminifera because of the longer life span, greater mobility, and more heterogeneous diet of fishes. The increased variability that may be associated with longevity can be minimised by analysing the otoliths from young fish or analysing only small portions of otoliths. Of course the latter procedure of analysing only small portions of otoliths drilled or chipped from specimens results in the additional complication of selecting animals of the same age and accurately removing similar segments from the otoliths.

Differences in otolith oxygen and carbon isotopes measured in the otoliths from fish that were identical in both somatic and otolith length and weight as well as time and location of capture (Fig. 6.2) are more difficult to understand than the relatively small differences between the two sagittae from individuals. These differences are particularly great in the measurements of $\delta^{13}C$, with $\delta^{18}O$ data being spread over a narrow range except for the single outlier mentioned previously. Considering that fish of the size used in this study were estimated to be about 120 days old on the basis of otolith microincrement counts, and that three of the fish appeared identical, it would be plausible to conclude that they had spent their lives in close proximity to one another (see Chapter 4). This is probably a valid assumption for the remaining 5 otolith pairs, as well. Variability in $\delta^{13}C$ within an otolith pair might best be explained by metabolic differences at the otolith level and analytical error. However, differences in $\delta^{13}C$ among pairs are too great to be explained on this basis alone. Because a large component of otolith carbon is derived from metabolic carbon, differences among individuals with similar environmental histories could result from differences in diet. The effect of diet $\delta^{13}C$ on the composition of body tissues is well established (DeNiro and Epstein, 1978). In the case of small juvenile Australian salmon, differences in otolith $\delta^{13}C$ might result from individual dietary preferences for, perhaps, crustacea versus polychaetes, two of the more common components of the diet for individuals collected from Cremorne Beach (J. M. Kalish, unpublished data). Gearing *et al.* (1984) investigated the $\delta^{13}C$ of a wide range of benthic and zooplanktonic organisms and found total $\delta^{13}C$ values that ranged from -23.0‰ to -15.8‰ with herbivorous zooplankton (e.g., mysids, euphausiids, copepods) having the lowest $\delta^{13}C$ and carnivorous benthic organisms (e.g., polychaetes, gastropods,

nemerteans) having the highest. Dietary differences before recruitment to the estuary should also be considered although the relative weight of the otolith would be quite small when compared with the final weight of the otolith used in isotopic analyses.

On the basis of stable isotope data obtained from otolith pairs the range and variation of the data used to establish a baseline reference for the mass balance calculations is understandable. It is clear that a relatively large number of samples is required to establish the isotopic baseline with a reasonable degree of reliability and even then, the potentially large variation in the otolith isotopic composition before captivity, in those fish used in the aquarium experiments, reduces the probability of that baseline being an accurate indicator of the pre-captivity otolith composition. All these factors accentuate the need for large sample sizes when carrying out studies relating to fish otolith stable isotope composition.

In order to reconstruct the environmental history of individuals, a stock or population and, thereby, the species in general, it is necessary to estimate the mean value of $\delta^{18}O$ and $\delta^{13}C$ at a given age with a high level of accuracy while taking a finite sample. This would involve taking otoliths from a finite number of individuals over a finite number of estimated ages. Time constraints place a limit on the number of individuals that might be used and, the level of accuracy that is achieved when estimating the mean isotopic temperature at each age. The isotopic data presented here for Australian salmon indicate that too small a sample can result in large errors, particularly when the sensitivity of the oxygen isotope palaeothermometer, where a change in $\delta^{18}O$ of 1.0‰ is equivalent to approximately 4.8°C, is considered.

The following statistical considerations (Sokal and Rohlf, 1981; Killingley *et al.*, 1981) are useful for estimating an appropriate sample size for otolith oxygen isotope analyses and may help to develop an appreciation for the number of analyses that might be required to satisfactorily estimate the temperature history of a stock of fishes. For simplicity it can be assumed that there are only two sources of variability in the estimation of otolith $\delta^{18}O$, variance due to mass spectrometer measurement error σ^2_m and, intraspecific variation σ^2_s. The total variance, σ^2_t resulting from these two independent sources is:

$$\sigma_t^2 = \sigma_m^2 + \sigma_s^2 \qquad \text{Eq. 6.10}$$

The variance of the mean associated with a sample of otolith isotopic measurements is a function of the variance associated with an individual otolith and the sample size:

$$\sigma_s^2 = \frac{\sigma_i}{n} \qquad \text{Eq. 6.11}$$

and substituting into the previous equation results in:

$$\sigma_t^2 = \sigma_m^2 + \frac{\sigma_i^2}{n} \qquad \text{Eq. 6.12}$$

The baseline oxygen isotope data for Australian salmon have a standard deviation, σ_i, of 0.91 (n = 23). The maximum value for σ_m = 0.03‰. In this example, σ_t = 0.19 and the 95% confidence limits would encompass values differing by 0.77‰, equivalent to approximately 3.7°C. If we assume that the size/age range of Australian salmon used in this example was sufficiently narrow then, to achieve 95% confidence limits equivalent to a temperature range of 1°C (σ_t = .05) would require 518 measurements. This is a large data requirement, but it is not an unmanageable sample size using the automated sample preparation lines and mass spectrometers which are now available. Furthermore, the standard deviation of oxygen isotope data measured in the otoliths of wild juvenile Australian salmon is somewhat greater than that estimated for other species (see Chapter 7), and this may be due to the three outliers with $\delta^{18}O$ values below -1.00‰.

6.4.2 Fish otolith $\delta^{18}O$ as an environmental thermometer

The data presented here show that Australian salmon otolith $\delta^{18}O$ is deposited very near to equilibrium relative to aragonite $\delta^{18}O$ and can act as a recorder of environmental temperature during the life of a fish. As expected, experimental data from this study did not conform to the predicted calcite equilibrium of Epstein *et al.* (1953) and the aragonite equilibrium relationship obtained by Horibe and Oba (1972),

which are both considered unacceptable for the estimation of aragonite isotopic equilibrium (Grossman and Ku, 1986).

Mulcahy *et al.* (1979), Radtke (1984a, 1984b, 1987) and Radtke *et al.* (1987) used Horibe and Oba's (1972) aragonite oxyen isotope fractionation equation resulting in erroneous interpretation of their results. Other authors (Devereux, 1967; Degens *et al.*, 1969; Mulcahy *et al.*, 1979) have used the oxygen isotope fractionation relationship for calcite (Epstein *et al.*, 1953) despite the fact that most fish otoliths are composed of aragonite (Carlstrom, 1963, Radtke, 1984a). In general, use of the calcite equation (Epstein *et al.*, 1953) would result in a more accurate interpretation of the results than Horibe and Oba's (1972) relationship for aragonite. Isotopic temperatures calculated using the Grossman (1982) palaeotemperature equation would be 6.3°C and 3.7°C higher than those calculated with the palaeotemperature equations of Horibe and Oba (1972) and Epstein *et al.* (1953), respectively. Where adequate data are presented (Mulcahy *et al.*, 1979; Radtke, 1984a, 1987), the isotopic temperatures calculated with Grossman (1982) are closer to the expected temperatures than the calculations in these studies suggest. This provides further evidence that, for the species investigated to date, fish otolith oxygen isotopes are deposited in, or near to, equilibrium.

6.4.3 Contribution of metabolic carbon

The very significant metabolically derived carbon component in Australian salmon otoliths (>30%) shows that metabolic rate and diet may have a very great effect on the $\delta^{13}C$ measured in fish otoliths. During the life cycle of an individual fish dietary items may range from phytoplankton to carnivorous fishes with $\delta^{13}C$ values between -25.0‰ to -15.0‰ in a phytoplankton-based marine ecosystem (Fry and Sherr, 1984). Because more than 30% of the otolith carbon is derived from these sources, dietary changes can be extremely important. These results indicate that, for Australian salmon, a change of 10.0‰ in the $\delta^{13}C$ of food (e.g. a change from consuming phytoplankton or herbivorous zooplankton to carnivorous invertebrates or fishes) would result in a 3.0‰ variation in the $\delta^{13}C$ of the otoliths. This is equivalent to the range of $\delta^{13}C$ values measured in the otoliths of wild juvenile Australian salmon. The dietary changes required to result in these variations in otolith $\delta^{13}C$ can occur within a single life history stage (e.g. juvenile or adult) or through development. Therefore, ontogenetic changes in otolith $\delta^{13}C$ could also be largely

attributable to age-related changes in diet.

6.5 SUMMARY

Stable isotope analyses of the otoliths of Australian salmon maintained under constant temperature conditions in the laboratory show the utility of these data for the estimation of the environmental temperature experienced by fishes in the wild. Isotopic temperatures calculated from data collected from Australian salmon otoliths used to determine an isotopic baseline are in agreement with the estimated mean temperatures that would have been experienced by these fish and provide additional evidence for the equilibrium fractionation of oxygen isotopes in otoliths. These otolith data are in agreement with both empirical and theoretical evidence used to determine oxygen isotopic equilibrium in aragonite. The highly negative value for $\delta^{13}C$ indicated that a large proportion of fish otolith calcium carbonate, approximately 33%, is composed of carbon derived from metabolic sources.

The importance of large sample sizes in studies of environmental temperatures derived from oxygen isotope data was emphasized. However, due to the variability of the data presented here, it would be valuable to carry out further validation studies relating to the deposition of stable isotopes in fish otoliths. Ideally, validation studies should be carried out with newly hatched individuals and over longer periods of time so that whole otoliths can be readily analysed for their isotopic composition. This would eliminate variability due to mass balance related problems. Alternatively, if large enough constant temperature facilities are available, larger fish could be maintained in captivity and the outermost portion of the otolith produced in captivity could be removed for isotopic analysis.

CHAPTER 7

ISOTOPIC DISEQUILIBRIA IN FISH OTOLITHS: METABOLIC AND KINETIC EFFECTS

7.1 INTRODUCTION

An understanding of the factors that effect the distribution of oxygen and carbon stable isotopes in marine biogenic carbonates can provide information on the biology of marine organisms and insight into mechanisms of calcification. This principle has been widely applied to studies of marine invertebrates and has only received minor attention in relation to fishes. Mulcahy *et al.* (1979), Radtke (1984a, 1984b), Radtke *et al.* (1987) and Chapter 6 have all shown the potential applications of fish otolith oxygen isotope data to studies of fish ecology and physiology. However, the suitability of these data and carbon isotope data, to studies of most marine fish species is still uncertain, particularly when the range of potential isotopic fractionation effects is considered.

During the precipitation of calcium carbonate from solution thermodynamic relationships exert the primary influence on the partitioning of oxygen and carbon isotopes (O'Neil *et al*, 1969). However, precipitation of biological carbonates frequently results in the deposition of both carbon and oxygen isotopes out of predicted equilibrium. Non-equilibrium deposition of oxygen and carbon isotopes in biogenic carbonates can be attributed to "metabolic" or "kinetic" isotope effects. Metabolic effects result from changes in $\delta^{13}C$ and $\delta^{18}O$ of CO_2 and HCO_3^- in the region of the calcium carbonate precipitate, due to biological processes such as respiration or photosynthesis. Kinetic effects result from the discrimination against heavy carbon and oxygen isotopes during diffusion of the carbonate isotopic species to the crystal surface (Turner, 1982; Grossman, 1984b) or, during the hydration and hydroxylation of CO_2, which results in HCO_3^- (McConnaughey, 1989a,1989b). Most researchers have not differentiated between metabolic and kinetic effects and have simply referred to biological fractionation or vital effects (Weber and Woodhead, 1970; Land *et al.*, 1977; Kahn, 1979; Kahn and Williams, 1981). Deviations from equilibrium deposition of oxygen and carbon isotopes have been attributed to the relative contributions of seawater versus metabolically derived carbon

and oxygen, with metabolically derived carbon and oxygen being depleted in the heavier isotopes. Using this assumption it becomes possible to estimate the relative contributions of metabolic carbon and seawater derived carbon to the makeup of biogenic carbonates (Williams *et al.*, 1977; Tanaka *et al.*, 1986; Chapter 6).

The study reported within Chapter 7 considers the theoretical and empirical basis for the estimation of isotopic equilibrium in calcium carbonate and applies this information to isotopic data collected on fish otoliths from a wide range of species. These data are critical in determining the utility of isotopic data to studies of a fish's environment and physiology. Data collected from different fish species living at a wide range of temperatures are used to investigate the utility of oxygen isotope thermometry to studies of fish biology and carbon isotope data is considered in light of it's potential as a source of information on metabolic processes and somatic and otolith growth. Finally, the relationship between oxygen and carbon isotopes collected from a wide range of species is investigated with respect to current theories on isotopic fractionation and in relation to physical and biological processes.

7.1.1 Determination of equilibrium fractionation in aragonite

Before discussing, in detail, the basis for isotopic disequilibria in fish otoliths it is important to consider the problems encountered in estimating carbon and oxygen isotopic fractionations in biogenic carbonates, particularly aragonite. Epstein *et al.* (1953) estimated oxygen isotope fractionation in biogenic calcite by determining isotopic ratios in molluscs collected from environments of known temperature and from shell material grown in laboratories under controlled temperature conditions. They obtained results which are in close agreement with determinations of oxygen isotope fractionation in inorganically precipitated calcite (O'Neil *et al.*, 1969). The close agreement between these studies of inorganic and biogenic calcite indicate that the biogenic carbonate of the mollusc shells was formed in isotopic equilibrium with the seawater environment and that there was no biological fractionation of oxygen isotopes.

The fractionation of ^{18}O in inorganic aragonites has only been estimated at a single temperature (25°C) (Tarutani *et al.*, 1969). Tarutani *et al.* (1969) found that the aragonite polymorph of calcium carbonate was enriched in ^{18}O by 0.6‰ relative to calcite at 25°C. Several relationships describing the temperature dependent fractionation of oxygen isotopes in biogenic aragonite have been determined since the

study of Tarutani *et al.* (1969):

$$\delta_{ar} - \delta_w = 3.05 - 0.220\ (T°C) \qquad \text{Eq. 7.1}$$

from Horibe and Oba (1972), based on shells of the mollusc *Anadara* sp.;

$$\delta_{ar} - \delta_w = (1.39 + 3.84) - \left[(0.038 + 0.233)\ (T°C)\right] \qquad \text{Eq. 7.2}$$

from Sommer and Rye (1978) and Rye and Sommer (1980), based on the fractionation between aragonite/calcite foraminifera shell pairs, their data actually show the fractionation between aragonite and calcite and these results must be combined with data on calcite fractionation (e.g. Epstein *et al.*, 1953) as has been done in Equation 2;

$$\delta_{ar} - \delta_w = 4.42 - 0.219\ (T°C) \qquad \text{Eq. 7.3}$$

from Grossman (1982), based on the foraminifera *Hoeglundina elegans*;

$$\delta_{ar} - \delta_w = 4.70 - 0.228\ (T°C) \qquad \text{Eq. 7.4}$$

from Grossman and Ku (1986), based on the foraminifera *H. elegans*;

$$\delta_{ar} - \delta_w = 4.65 - 0.213\ (T°C) \qquad \text{Eq. 7.5}$$

from Grossman and Ku (1986), based on a series of coeval molluscs;

$$\delta_{ar} - \delta_w = 5.10 - 0.268\ (T°C) \qquad \text{Eq. 7.6}$$

from Dunbar and Wefer (1984), based on the foraminifera *H. elegans*;

$$\delta_{ar} - \delta_w = 4.82 - 0.226\ (T°C) \qquad \text{Eq. 7.7}$$

from Aharon and Chappell (1983), based on tridacnid clams; and

$$\delta_{ar} - \delta_w = 6.69 - 0.326\ (T°C) \qquad \text{Eq. 7.8}$$

from Chapter 6, based on the otoliths of the percoid teleost *Arripis trutta*. δ_{ar} is the $\delta^{18}O$ of the carbonate sample and δ_w is the $\delta^{18}O$ of CO_2 gas equilibrated with a water sample, from which the carbonate was precipitated.

Lines representing the isotopic temperature scales for each of the above relationships and the data from Tarutani *et al.* (1969) are plotted in Fig. 7.1. Although these relationships are based on different organisms from far removed higher taxa, all but one are in agreement, on average, to within about 1.0‰ and, with the ^{18}O fractionation determined by Tarutani *et al.* (1969) at 25°C. The oxygen isotope fractionation equation determined by Horibe and Oba (1972) shows a significant depletion in ^{18}O relative to the other calibrations and, furthermore, indicates that aragonite is depleted in ^{18}O relative to calcite. This result disagrees with theoretical determinations of relative isotopic fractionation in calcite and aragonite and inorganic precipitate studies (Tarutani *et al.*, 1969). Horibe and Oba's (1972) data, obtained from the mollusc *Anadara* sp., are probably the result of disequilibrium fractionation due to biological effects (Grossman and Ku, 1986).

Equations for equilibrium ^{13}C fractionation in biogenic aragonite include:

$$\delta^{13}C_{ar} - \delta^{13}C_{DIC} = 12.40 - \frac{2980}{(T°C)} \qquad \text{Eq. 7.9}$$

from Grossman (1984a), based on *H. elegans*;

$$\delta^{13}C_{ar} - \delta^{13}C_{DIC} = 2.40 - 0.108\ (T°C) \qquad \text{Eq. 7.10}$$

from Grossman and Ku (1986), based on *H. elegans*; and

$$\delta^{13}C_{ar} - \delta^{13}C_{DIC} = 2.66 - 0.131\ (T°C) \qquad \text{Eq. 7.11}$$

from Grossman and Ku (1986), based on a series of coeval molluscs. Equations 10 and 11 are in close agreement whereas Equation 9, results in ^{13}C fractionations enriched in the heavier isotope by about 3.0‰. The effect of temperature on carbon

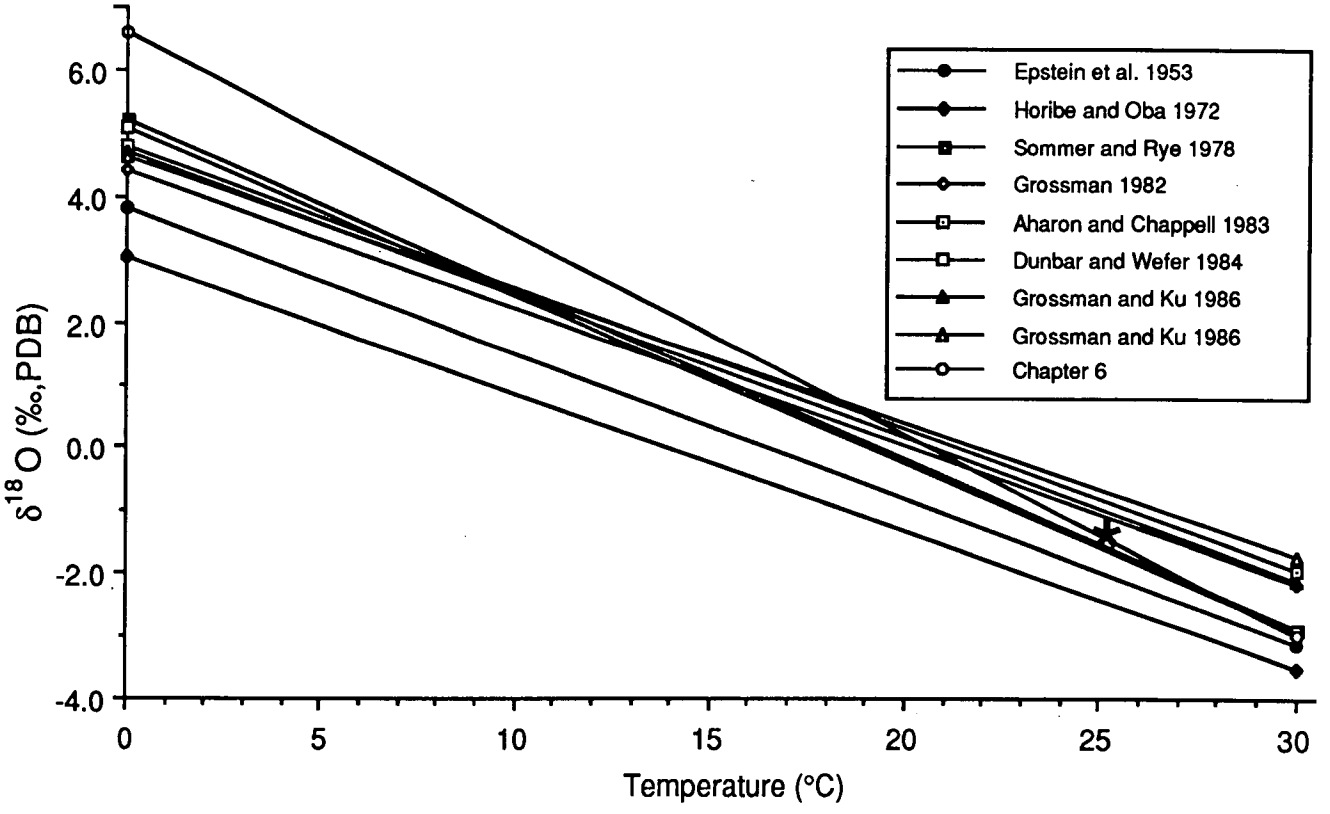

Fig. 7.1 Relationships describing the temperature dependent fractionation of oxygen isotopes in biogenic aragonite. One line, Epstein *et al.* (1953), is based on biogenic calcite. The star shows the oxygen isotope fractionation datum measured in an inorganic system by Tarutani *et al.* (1969). Details of these relationships appear in the text.

isotope fractionation in carbonates is both small and uncertain. Equation 9 indicates that aragonite enrichment in ^{13}C increases with increasing temperature, while Equations 10 and 11 predict the opposite effect.

7.2 MATERIALS AND METHODS

Otolith material used in this study was obtained during 1986 and 1987 from fish caught in Storm Bay, Tasmania and along the continental slope of Tasmania by line fishing or trawling. Antarctic fish were collected by trawl in the Southern Ocean off Heard Island in July, 1987. Otoliths were extracted, the adhering otolith capsule removed and the otoliths were cleaned ultrasonically in deionised water, oven dried at 50°C and stored in glass vials. In some cases, where isotope data is reported from both the juveniles and adults of a species, portions of otolith material were removed by grinding with a dental drill. For example, to determine the isotopic composition of otolith material produced during the adult phase of life, the outer portion of the otolith was ground away and for juveniles the central portion of the otolith was removed for isotopic analysis.

Otoliths were roasted in a vacuum at 370°C for 1 h and then reacted with 100% phosphoric acid at 24°C for 24 h under vacuum. The CO_2 resulting from the reaction with phosphoric acid was purified and any non-condensables removed by a series of three freezing/transfer steps. The purified CO_2 samples were analysed on a VG Micromass 602C mass spectrometer. All values are reported in standard δ notation relative to the PDB-1 standard (Epstein *et al.*, 1953):

$$\delta = \left(\frac{R_{sample}}{R_{standard}} - 1 \right) x\ 1000 \qquad \text{Eq. 7.12}$$

where R is the mass ratio (46-44) of the sample or standard. Isotopic ratios were related to the PDB standard through analysis of Biggenden calcite (BCS) which had been calibrated to the PDB standard via the international standards NBS-19 (Craig, 1957) and TKL (Blattner and Hulston, 1978). Analytical precision of the reported measurements is ±0.03‰ (1 s.d.) or better.

It is evident that the precise determination of equilibrium ^{18}O and ^{13}C

fractionation in aragonite is open to question. However, it is possible to make adequate estimations for the purpose of discussing general trends and relationships. Values for seawater $\delta^{18}O$ (δ_w) and $\delta^{13}C$ ($\delta^{13}C_{DIC}$) for each of the species investigated was approximated on the basis of data available in the literature (Epstein and Mayeda, 1953; Craig and Gordon, 1965; Kroopnick *et al.*, 1972; Kroopnick, 1974a, 1974b, 1980; Kroopnick and Craig, 1976; Williams *et al.*, 1977; Grossman, 1984a, 1984b) and, isotopic equilibrium for aragonite ($\delta^{18}O_{eq}$ and $\delta^{13}C_{eq}$) in each of the environments was calculated using Equation 7.3 for oxygen and Equations 7.9 and 7.10 for carbon. The oxygen isotope versus temperature relationship from Grossman (1982) was used, rather than the relationship between *Arripis trutta* otoliths and temperature (Chapter 6) to avoid any potential bias in the estimation of isotopic equilibrium. The resulting values are shown in Table 7.1, which presents the mean isotope data for otoliths ($\delta^{18}O_m$ and $\delta^{13}C_m$) from each species considered in this study. For example, for shallow-dwelling fishes from southeast Australian waters (e. g. *Arripis trutta*) the isotopic composition of aragonite precipitated in equilibrium ($\delta^{18}O_{eq}$ and $\delta^{13}C_{eq}$) with Tasman Sea surface water varying from 10° to 20°C was estimated as follows. $\delta^{13}C_{DIC}$ was estimated to be 2.0‰, based on depth and apparent oxygen utilization (Williams *et al.*, 1977), and, δ_w as 0.086‰ for Tasman Sea surface water (using data from the South Pacific Ocean from Craig and Gordon, 1965) as discussed in Chapter 6. Using Equations 7.9, 7.10 and 7.11, $\delta^{13}C_{eq}$ of otolith aragonite is estimated to range from 2.04‰ to 4.23‰ and, $\delta^{18}O_{eq}$ ranges from 0.13‰ to 2.32‰ based on Equation 7.3. The departures from isotopic equilibrium ($\Delta^{18}O_{eq} = \delta^{18}O_m - \delta^{18}O_{eq}$ and $\delta^{13}C_{eq} = \delta^{13}C_m - \delta^{13}C_{eq}$) also appear in Table 7.1.

7.3 RESULTS

Plots of $\delta^{18}O$ as a function of $\delta^{13}C$ for the sagittal otoliths of 35 marine fish species and the statoliths of one squid species appear in Figs. 7.2 and 7.3; the mean values are tabulated by species in Table 7.1. Data are broken down into two graphs (Fig. 7.2 and 7.3) so that it is possible to distinguish which data are attributable to a particular species. The bulk of the data are from isotopic measurements made in this study with the remainder of the data being obtained from the literature. Despite the fact that the data are from numerous species encompassing

Table 7.1 Summary of isotopic composition of fish otoliths, water, and dissolved inorganic carbon for species used in Figs. 7.2-7.7 and data used to estimate deviations from equilibrium isotopic fractionation. Values are means based on the number of replicates of each species. Full species names appear in Figs. 7.2 and 7.3. Isotopic values are reported in ‰ notation relative to the PDB standard. Headings are defined in the text.

Species[a]	Depth (m)	Temp. (°C)	$\delta^{18}O_m$	δ_w	$\delta^{18}O_{eq}$[h]	$\Delta^{18}O_{eq}$	$\delta^{13}C_m$	$\delta^{13}C_{Dic}$	$\delta^{13}C_{eq}$[i]	$\delta^{13}C_{eq}$[j]	$\Delta^{13}C_{eq}$[i]	$\Delta^{13}C_{eq}$[j]
C. acrolepis (23)[b]	991	4	3.37	-0.25	3.53	-0.16	-0.84	0	1.24	1.57	-2.09	-2.41
Ariomma[c]	200	15	0.80	-0.30	0.98	-0.18	-5.50	0	2.05	0.78	-7.55	-6.28
Norneus[c]	200	15	-0.10	-0.30	0.98	-1.08	-4.60	0	2.05	0.78	-6.65	-5.38
Cubiceps[c]	200	15	0.00	-0.30	0.98	-0.98	-4.50	0	2.05	0.78	-6.55	-5.28
Pampus[c]	50	15	0.20	-0.30	1.25	-1.05	-4.00	1	3.05	1.78	-7.05	-5.78
Peprilus[c]	50	15	-1.10	-0.30	1.25	-2.35	-4.60	1	3.05	1.78	-7.65	-6.38
Stromateus[c]	50	15	0.90	-0.30	1.25	-0.35	-0.80	1	3.05	1.78	-3.85	-2.58
Psenopsis[c]	200	15	1.10	-0.30	0.98	0.12	-0.90	0	2.05	0.78	-2.95	-1.68
Seriolella[c]	200	15	1.00	-0.30	0.98	0.02	-0.60	0	2.05	0.78	-2.65	-1.38
Schedophilus[c]	200	15	-0.10	-0.30	0.98	-1.08	-3.60	0	2.05	0.78	-5.65	-4.38
Centrolophus[c]	200	15	1.30	-0.30	0.98	0.32	-3.20	0	2.05	0.78	-5.25	-3.98
Hyperglyphe[c]	200	10	-0.20	-0.30	2.12	-2.32	-1.20	0	1.87	1.32	-3.07	-2.52
Stenotomus[c]	50	15	-1.80	-0.03	1.25	-3.05	-4.90	1	3.05	1.78	-7.95	-6.68
Roccus[c]	50	25	-4.40	-0.03	-1.03	-3.37	-4.40	1	3.40	0.70	-7.80	-5.10
Centropristes[c]	50	25	0.10	-0.03	-1.03	1.13	-0.80	1	3.40	0.70	-4.20	-1.50
Prionotus[c]	50	15	-0.20	-0.03	1.25	-1.45	-0.20	1	3.05	1.78	-3.25	-1.98
Merlucclus[c]	150	12	1.40	-0.20	1.76	-0.36	-0.80	0	1.99	1.15	-2.79	-1.95
Melanogrammus[c]	150	12	1.50	-0.20	1.76	-0.26	0.50	0	1.99	1.15	-1.49	-0.65
Gadus[c]	150	10	1.90	-0.20	2.22	-0.32	0.30	0	1.92	1.37	-1.62	-1.07
Ceratoscopelus[c]	250	12	2.00	-0.20	1.76	0.24	-4.10	0	1.94	1.10	-6.04	-5.20
Osmerus[c]	10	15	-1.50	-0.03	1.25	-2.75	-2.50	2	4.05	2.78	-6.55	-5.28
M. cephalus (2)[d]	0	23	-1.65	-1.80	-2.35	0.70	-3.96	2	4.34	1.92	-8.30	-5.88
T. thynnus (6)[e]	50	25	-1.32	-0.03	-1.03	-0.29	-8.03	2	4.40	1.70	-12.43	-9.73
P. filamentosus (3)[f]	30	20	1.01	0.05	0.19	0.82	-3.36	1	3.23	1.24	-6.59	-4.60
I. illecebrosus (3)[g]	20	12	0.57	-0.03	2.04	-1.47	-6.77	2	3.73	2.95	-10.50	-9.72
A. trutta (25)	3	16	0.25	0.05	1.10	-0.85	-5.61	2	4.09	2.67	-9.70	-8.28
H. atlanticus (10)	1040	4	2.39	-0.25	3.59	-1.19	-1.04	0	1.23	1.59	-2.27	-2.63
T. atun (4)	10	15	0.80	0.05	1.33	-0.53	-5.32	2	4.05	2.78	-9.37	-8.10
N. macropterus (4)	10	15	0.38	0.05	1.33	-0.96	-6.07	2	4.05	2.78	-10.12	-8.85
T. declivis (2)	10	15	1.05	0.05	1.33	-0.28	-5.39	2	4.05	2.78	-9.44	-8.17
B. brama (2)	100	10	0.35	0.05	2.47	-2.13	-6.48	0	1.87	1.32	-8.35	-7.80
M. novaezelandiae(4)	400	8	1.71	0.05	2.93	-1.23	-2.61	0	1.77	1.51	-4.38	-4.12
P. barbata (4)	10	12	1.10	0.05	2.01	-0.91	-1.44	2	3.94	3.10	-5.38	-4.54
T. maccoyii (2)	50	22	-1.63	0.05	-0.27	-1.36	-7.92	2	4.30	2.02	-12.22	-9.94
A. esper (2)	10	16	0.56	0.05	1.10	-0.54	-3.97	2	4.09	2.67	-8.06	-6.64
N. squamifrons (2)	10	1	2.65	0.05	4.52	-1.87	-3.75	1	2.92	3.69	-6.67	-7.44

[a] Number of replicates in parentheses.

[b] Mulcahy *et al.* (1979); [c] Degens *et al.* (1969); [d] Radtke (1984a); [e] Radtke *et al.* (1987); [f] Radtke (1987); [g] Radtke (1983).

[h] Using Grossman (1982).

[i] Using Grossman (1984a).

[j] Using Grossman and Ku (1986).

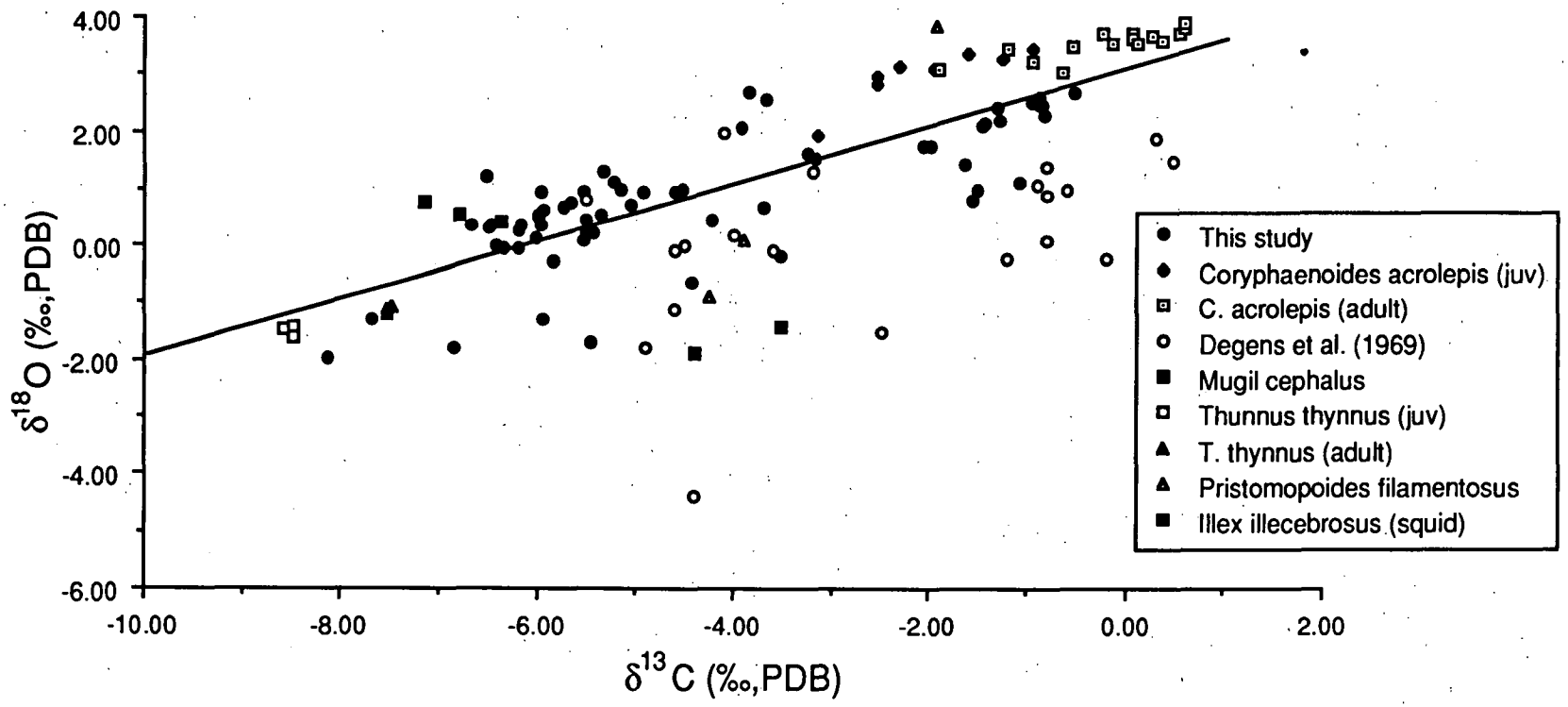

Fig. 7.2 Plot of $\delta^{18}O$ versus $\delta^{13}C$ for the aragonitic otoliths of 35 fish species and the aragonitic statoliths of one squid species. The data identified by species in this graph are from the literature. The data sources are indicated in Table 7.1. Data from this study are plotted on the graph for comparison and are identified to species in Fig. 7.3.

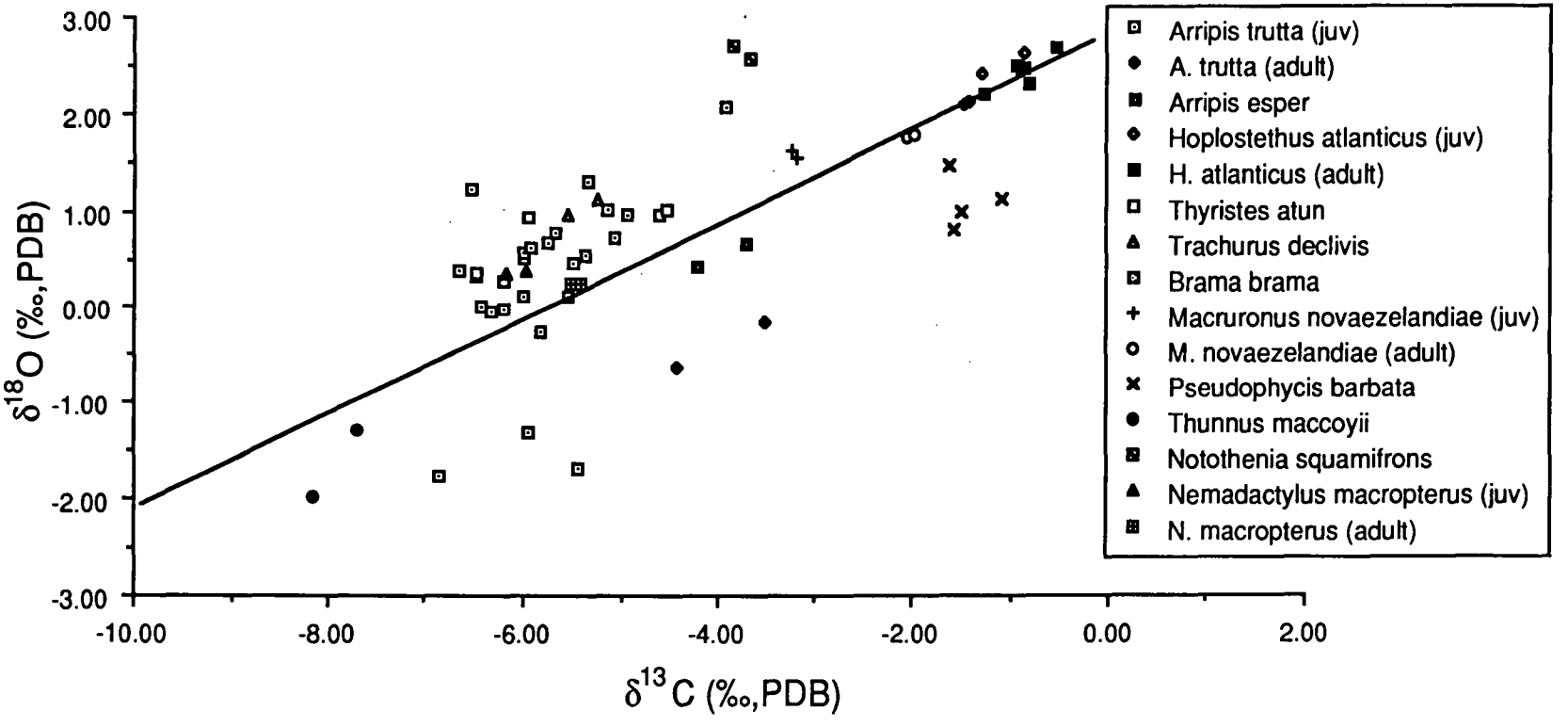

Fig. 7.3 Plot of $\delta^{18}O$ versus $\delta^{13}C$ for the aragonitic otoliths of 11 fish species. For some species data were collected from both juveniles and adults and this is indicated in the legend. All these data were collected in this study.

a wide range of higher taxa, collected in different oceans and at different depths and, that the samples were analysed by several different laboratories, there is still a strong correlation between $\delta^{13}C$ and $\delta^{18}O$. The least squares regression line for all data is $\delta^{18}O = 2.73 + (0.45)\delta^{13}C$, ($r^2=0.50$, $p<0.001$) and, for data collected in this study only, it is $\delta^{18}O = 2.64 + (0.41)\delta^{13}C$, ($r^2=0.58$, $p<0.001$). The majority of the $\delta^{18}O$ and $\delta^{13}C$ data from the various fish species fall close to the regression line, with the greatest scatter attributable to the data of Degens *et al.* (1969) who only made a single isotopic measurement for each species. Data on mullet (*Mugil cephalus*) from Radtke (1984a) also fall relatively far from the regression line, perhaps due to the fact that these data are from fish reared at a salinity of 32‰. In general, it must be assumed that intercalibration through the international standard PDB is satisfactory and that these deviations are real. The significance of the relative distribution of the various species along the regression line will be considered further in the discussion.

Plots of carbon isotopes against temperature show that otolith carbonate becomes more depleted in ^{13}C with increasing temperature (Fig. 7.4). Although the data show a negative correlation with temperature ($r^2=0.50$, $p<0.001$) as described by Grossman and Ku (1986) (Equations 7.10 and 7.11), the slope of the otolith carbon data versus temperature is approximately two times what they observed for a single species of foraminifera and several related mollusc species. If the deviations from equilibrium precipitation ($\Delta^{13}C_{eq}$) are plotted against temperature (Fig. 7.5) there is an even stronger negative correlation ($r^2= 0.62$, $p<0.001$), indicating that changes in $\delta^{13}C$ with temperature are due to isotopic fractionation and are not due to the influence of $\delta^{13}C_{DIC}$ although other studies have shown such a relationship in foraminifera (Williams *et al.*, 1977; Grossman, 1984b) and molluscs (Mook and Vogel, 1968; Fritz and Poplawski, 1974).

Otolith oxygen isotopes become more depleted in the heavy isotope (^{18}O) at higher temperatures (Fig. 7.6), similar to the trend for carbon isotopes. Least squares linear regression shows that the relationship between oxygen isotopes and temperature for all otolith data is, $\delta^{18}O_m = 3.58 - 0.196$ (T°C), ($r^2=0.69$, $p<0.001$) This line is in reasonable agreement with inorganic precipitate data from Tarutani *et al.* (1969) and relationships derived from other studies of biogenic aragonites shown in Fig. 7.1. However, it must be remembered that $\delta^{18}O_m$ values for individual fish otolith data points represent a mean value accumulated over the life of a fish, which,

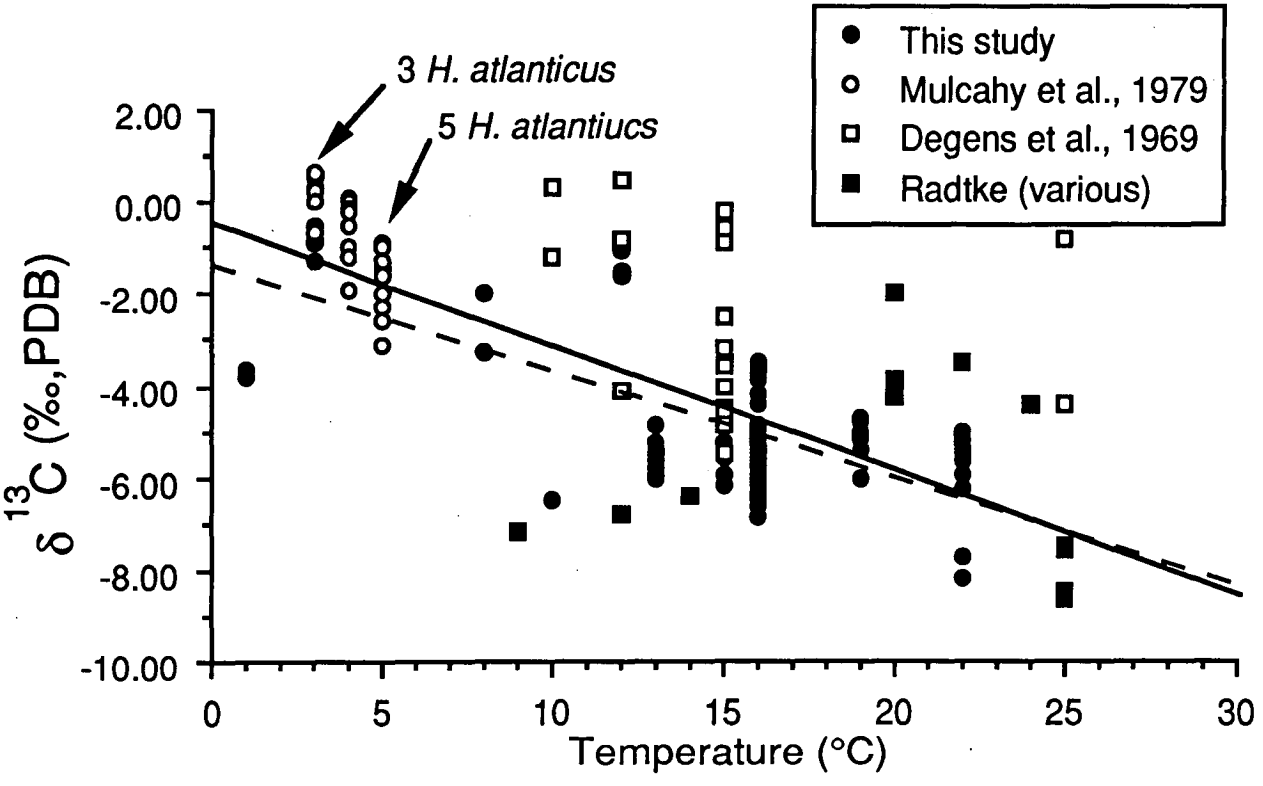

Fig. 7.4 Relationship between $\delta^{13}C$ and ambient water temperature. The solid line is based on linear regression for all data points and the dashed line is based only on data collected in this study. Eight data points from *Hoplostethus atlanticus* are obscured and their location is indicated in the figure.

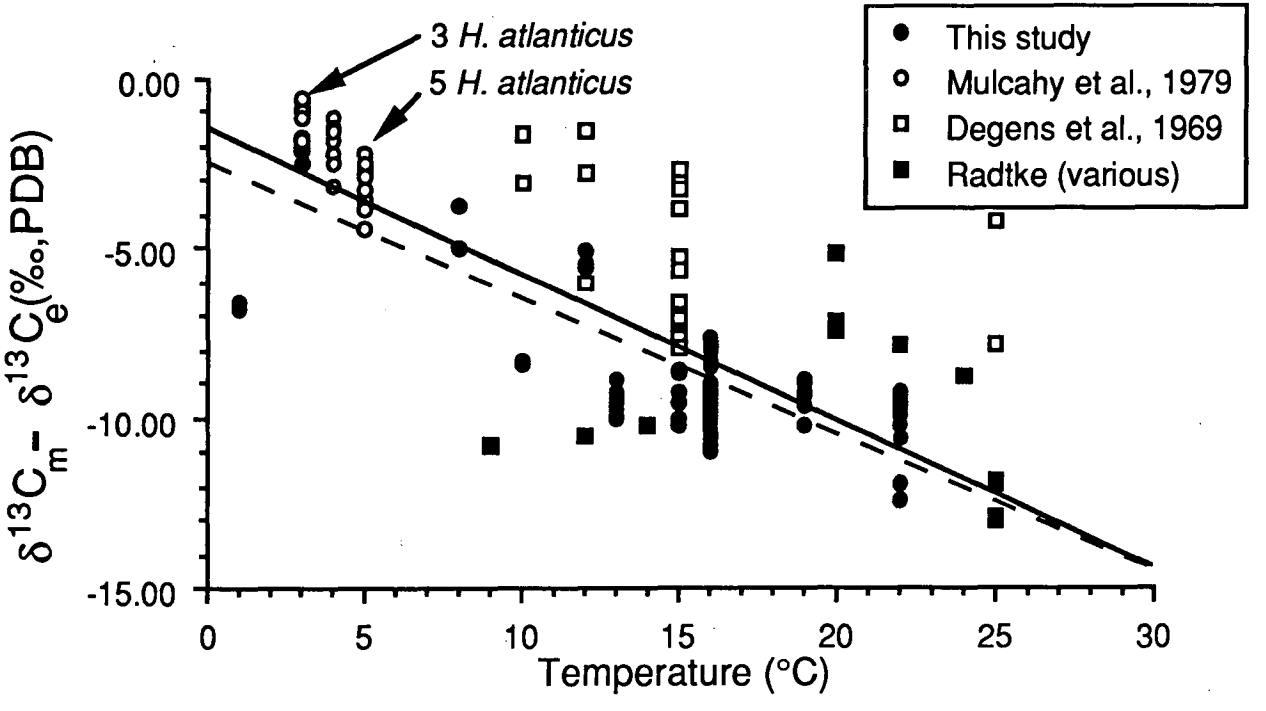

Fig. 7.5 Carbon isotope enrichment between otolith aragonite and estimated equilibrium aragonite as a function of temperature. Data used to estimate equilibrium appear in Table 7.1. The solid line is based on linear regression for all the data points and the dashed line is based only on data collected in this study. Eight data points from *Hoplostethus atlanticus* are obscured and their location is indicated on the figure.

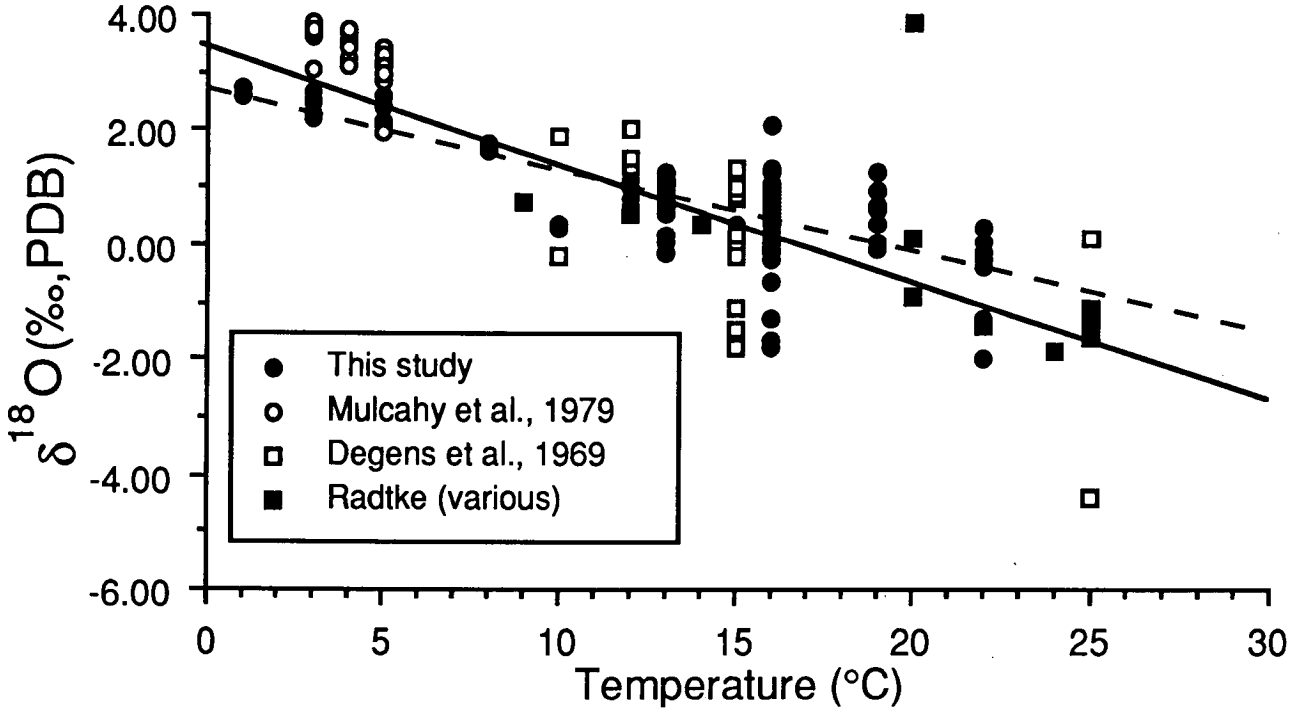

Fig. 7.6 Relationship between $\delta^{18}O$ and ambient water temperature. The solid line is based on linear regression for all data points and the dashed line is based only on data collected in this study.

in this study, might range from some fraction of a year to, perhaps, over 20 years. Furthermore, the estimates of temperature are based on current knowledge on the distribution of each species over the fish's lifetime, and, of course, have not been measured. Under these circumstances, the strong correlation appears to provide good evidence for a relationship between the $\delta^{18}O$ measured in fish otoliths and temperature. These points also apply to the carbon isotope data above, but it is clear that differences between the carbon data presented here and data appearing in the literature (Grossman, 1984a, Grossman and Ku, 1986) are more extreme than differences between oxygen isotopes measured in otoliths and literature values for other biogenic carbonates.

A plot of the differences between $\delta^{18}O_m$ and $\delta^{18}O_{eq}$ for all data (Fig. 7.7) shows that deviations from oxygen isotopic equilibrium ($\Delta^{18}O_{eq}$) are not related to temperature (r^2=0.03, p>0.08)and the mean deviation from equilibrium fractionation approaches zero. However, when data from this study are considered alone (Fig. 7.7), there is some evidence for a positive correlation between $\Delta^{18}O_{eq}$ and temperature (r^2=0.27,p<0.01) with relatively large depletions in the heavier oxygen isotope occurring at the lower temperatures. However, closer examination of these data indicate that this relationship is largely the result of a few data points at the extreme high and low temperatures. Furthermore, there was no evidence of a linear relationship among these data (F=1.23, df=1,59, P>0.25).

7.4 DISCUSSION

7.4.1 The relationship between $\delta^{13}C$ and $\delta^{18}O$

The interpretation of the relationship between $\delta^{13}C$ and $\delta^{18}O$ (Fig. 7.8) has been open to debate since Keith and Weber (1965) first suggested that the correlation might be due to calcification processes incorporating carbon and oxygen compounds originating from two isotopically different sources or, the incorporation of specific portions of oxygen and carbon compounds that displayed a correlation between $\delta^{13}C$ and $\delta^{18}O$. In those corals that contain symbiotic algae (hermatypic corals) the correlation between $\delta^{13}C$ and $\delta^{18}O$ is not always evident because only carbon is fractionated during photosynthesis (Swart, 1983). Furthermore, the combined effect of respiration, which depletes both oxygen and carbon heavy isotopes and,

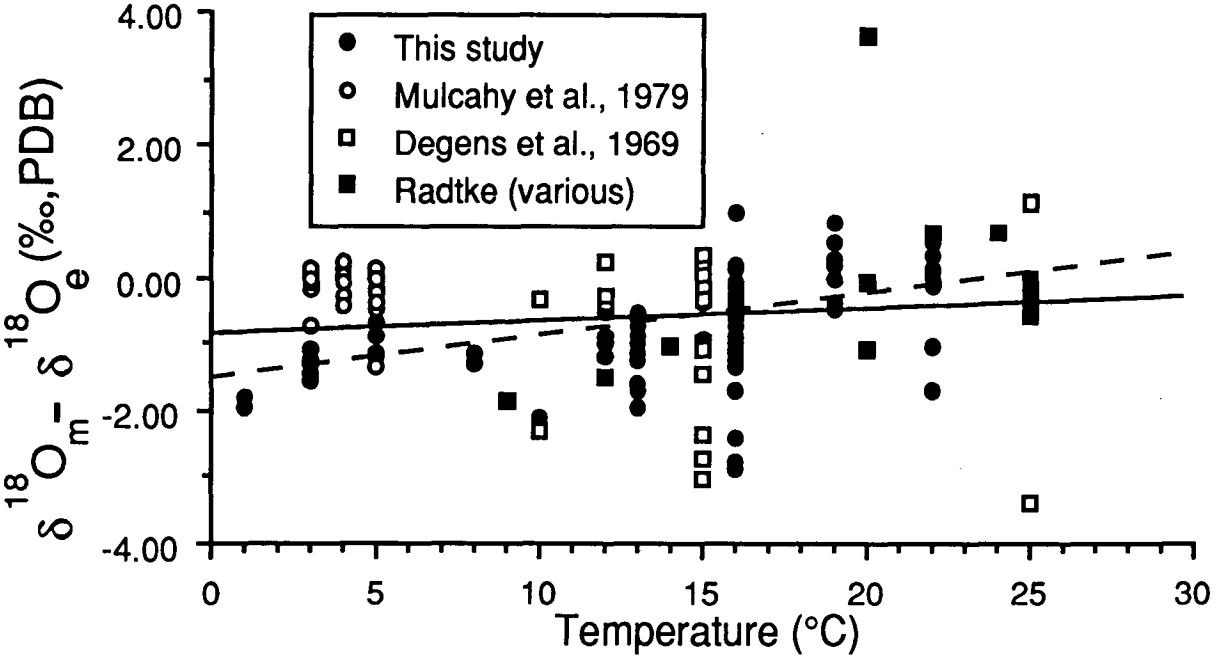

Fig. 7.7 Oxygen isotope enrichment between otolith aragonite and estimated equilibrium aragonite as a function of temperature. Data used to estimate equilibrium appear in Table 7.1. The solid line is based on linear regression for all the data points and the dashed line is based only on data collected in this study.

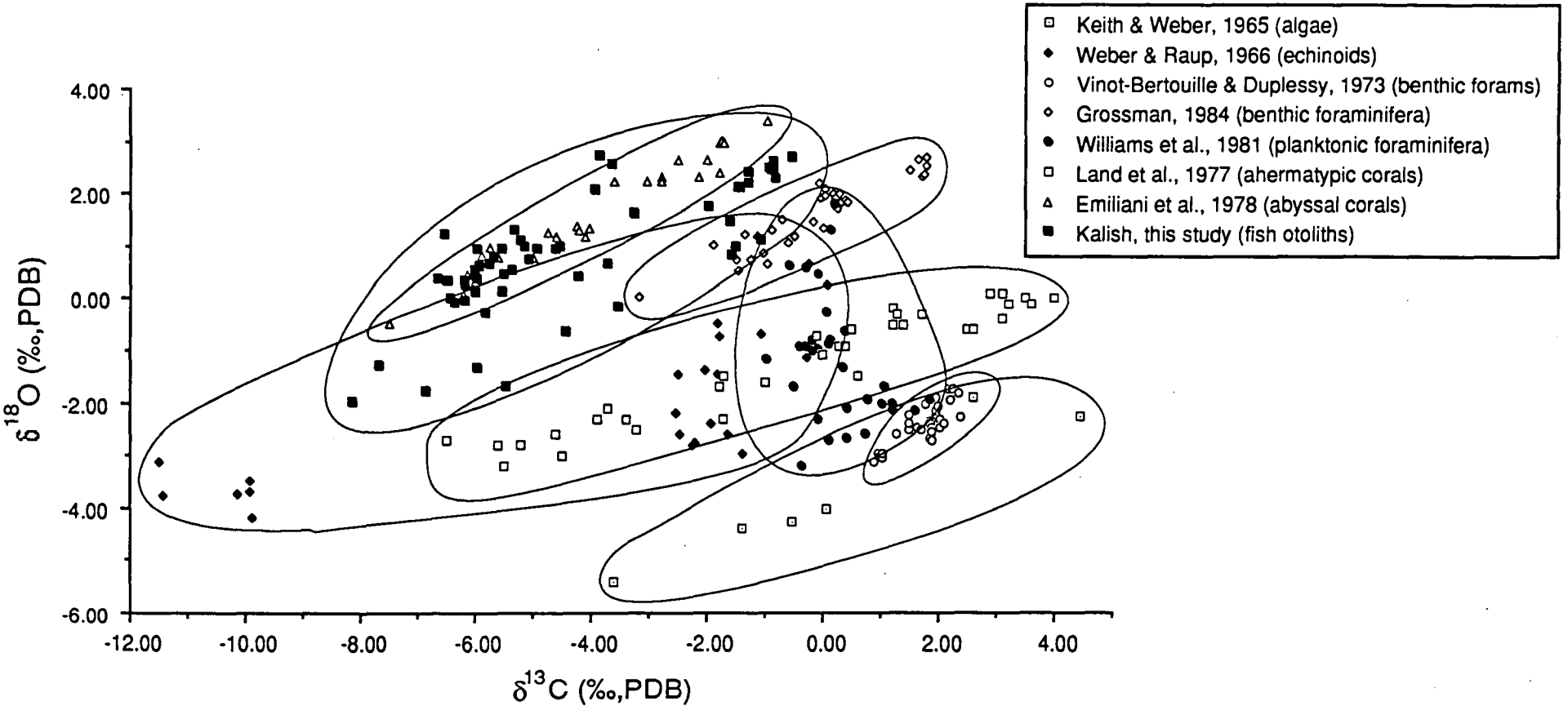

Fig. 7.8 Plot showing general trend in $\delta^{18}O$ versus $\delta^{13}C$ from several taxa using data reported in the literature and from fish otoliths analysed in this study. Only data from the photosynthetic planktonic foraminifera (Williams *et al.*, 1981) deviate from the general pattern. Of the remaining groups, only the algae are photosynthetic.

photosynthesis results in there often being no apparent relationship between $\delta^{13}C$ and $\delta^{18}O$ in hermatypic corals (Weber and Woodhead, 1970; Goreau, 1977; Swart and Coleman, 1980; Swart, 1983). Most researchers have concluded that the correlation between carbon and oxygen isotopes in ahermatypic corals and other organisms is the result of the incorporation of metabolically derived CO_2 (Keith and Weber, 1965; Weber and Woodhead, 1970; Vinot-Bertouille and Duplessy, 1973; Land *et al.*, 1977; Kahn, 1979; Kahn and Williams, 1981; Williams *et al.*, 1981a; Williams *et al.*, 1981b; Grossman, 1984b) in the biogenic carbonate.

Turner (1982) suggested that kinetic fractionation due to varying weights and, thus, diffusion rates of the different isotopes, could result in the depletion of the heavier carbon and oxygen isotopes, rather than incorporation of metabolic CO_2 alone. He found that calcium carbonate, specifically calcite, precipitated in an inorganic system, could be depleted in ^{13}C by 0.35‰ to 3.37‰ depending on the rate of carbonate precipitation with the magnitude of the ^{13}C depletion increasing with increased rate of precipitation. Unfortunately, he was only able to measure $\delta^{13}C$ and, thus, it is not possible to directly interpret these data with respect to the relationship between $\delta^{18}O$ and $\delta^{13}C$.

However, the magnitude of the kinetic fractionations due to different rates of diffusion can be approximated by estimating the ratio of diffusivities of the CO_3^{-2} isotopic species involved in carbonate precipitation (Turner, 1982). The ratio of diffusivities, D/D' is approximated by:

$$\frac{D}{D'} = \sqrt{\frac{m^L}{m^H}} \qquad \text{Eq. 7.13}$$

where D and D' and, m^L and m^H are the diffusivities and masses of the light and heavy carbonate isotopic species, respectively. ^{13}C and ^{18}O fractionation factors due to diffusion are 0.992 ($^{12}C^{16}O_3^{-2}/^{13}C^{16}O_3^{-2}$) and 0.984 ($^{12}C^{16}O_3^{-2}/^{12}C^{18}O^{16}O_2^{-2}$) .The ratios of the molecular velocities during diffusion indicate that depletions of 8.0‰ and 16.0‰ occur in $\delta^{13}C$ and $\delta^{18}O$, which corresponds to a slope of 2.0 for the regression of $\delta^{18}O$ against $\delta^{13}C$. Grossman (1984b) rejected the kinetic hypothesis, as outlined above, on the basis that his data did not have the

required slope. However, this calculation fails to consider the relative abundance of ^{13}C: ^{12}C versus ^{18}O:^{16}O, where the heavy isotopes are approximately 1.1% (Nier, 1950) and 0.2% (Garlick, 1969) of the total carbon and oxygen, respectively. The net result is that a CO_3^{-2} molecule with ^{13}C is 5 times more likely to occur at the crystal surface than a molecule with ^{18}O, indicating net depletions of 8‰ and 3.2‰ for carbon and oxygen, and a slope of 0.4. The mean slope of $\delta^{18}O$ versus $\delta^{13}C$ data obtained from the literature for several higher taxa (Fig. 7.8) is approximately 0.37 and, for the fish otolith data the slope is 0.45, very close to the approximations based on the kinetic/diffusion hypothesis.

The significance of a different kinetic effect, during the hydration and hydroxylation of CO_2, in altering $\delta^{13}C$ and $\delta^{18}O$ and causing isotopic disequilibria in biogenic carbonates, has recently been investigated by McConnaughey (1989a, 1989b). He concluded that the linear relationship between $\delta^{18}O$ and $\delta^{13}C$ indicates the influence of a kinetic mechanism that would result in simultaneous depletions and that such a mechanism is responsible for mediating isotopic disequilibria in biogenic carbonates, particularly during rapid precipitation. McConnaughey's (1989a) data from photosynthetic and non-photosynthetic corals show extreme departures from isotopic equilibrium and he states that isotopic disequilibria increase with increased growth rate in these organisms. He does not consider the additional effects of a kinetic/diffusion effect acting at the crystal face.

Other sources present evidence that contradicts the kinetic hypotheses. Fritz and Poplawski (1974) cultured freshwater molluscs in water with $\delta^{13}C_{DIC}$ of -35.5, -13.1, and +5.4‰. Those animals cultured in aquaria with $\delta^{13}C_{DIC}$ of -35.5‰ were enriched in ^{13}C relative to the water, while animals cultured in water with $\delta^{13}C_{DIC}$ of -13.1 and +5.4‰ were depleted in ^{13}C relative to the culture media. This result implies the inclusion of carbon with an isotopic composition of between -35.5‰ and -13.1‰, which is within the range of $\delta^{13}C$ measured for molluscan tissue (Gearing *et al.*, 1984), tissue $\delta^{13}C$ being an accepted estimator of the $\delta^{13}C$ of metabolically derived CO_2 present in the body fluids.

Studies by Pearse (1970), Sikes *et al.* (1981) and Tanaka *et al.* (1981) on sea urchins, corals, molluscs and barnacles have all shown that both metabolic carbon and DIC are incorporated into shell calcium carbonate. Pearse (1970) and Sikes *et al.* (1981) showed the importance of metabolic carbon by providing organisms with ^{14}C-labelled food which was subsequently detected in the shell. Tanaka *et al.*

(1986) looked at naturally occurring levels of ^{14}C in DIC and, various food sources in a natural system and concluded that up to 85% of the carbon in shell carbonate was derived from metabolic sources.

The fish otolith isotope data presented here, when plotted with isotope data from other organisms follows a similar trend to that described by McConnaughey (1989a) (Fig. 7.8) and the overall distribution of the otolith isotope data is very similar to that of the ahermatypic corals (Swart, 1983). However, my estimates of $\delta^{13}C$ and $\delta^{18}O$ for aragonite precipitated in isotopic equilibrium with the various fish environments represented in this data set (Table 7.1), indicate that carbon isotopes only, and not oxygen, are fractionated out of isotopic equilibrium. This point is illustrated by graphs of the carbon isotope enrichment between biogenic fish otolith aragonite and seawater dissolved inorganic carbon as a function of temperature (Fig. 7.5) and oxygen isotope enrichment between the otoliths and seawater $\delta^{18}O$ (Fig. 7.7). As mentioned previously, otolith $\delta^{18}O$ values do not differ significantly from predicted equilibrium values. Despite this dichotomy between $\delta^{18}O$ and $\delta^{13}C$, a highly significant regression between $\delta^{13}C$ and $\delta^{18}O$ is apparent, indicating that some mechanism, perhaps related to temperature (e.g. metabolic rate) is resulting in this relationship in fish otoliths, and not one related to the kinetics of CO_2 hydration and hydroxylation as described by McConnaughey (1989a, 1989b) or, kinetics in relation to diffusion of isotopes to the crystal surface (Turner, 1982).

On the basis of the relationships described to this point it seems reasonable to draw the same conclusion as Grossman (1984b), Tanaka *et al.* (1986) and many others, that carbon isotopic disequilibria, in fish otoliths in this case, are due to the incorporation of metabolically derived CO_2. This further supports calculations made to estimate the relative contributions of DIC and metabolic carbon to fish otoliths in Chapter 6.

7.4.2 Variations in carbon and oxygen stable isotopes among species

There are several trends, potentially relevant to the relationship between $\delta^{13}C$ and temperature, among the species investigated. Those species that display the smallest departures from $\delta^{13}C$ equilibrium are slow growing, live in deep, cold waters and possess relatively large otoliths, most notably the macrourid, *Coryphaenoides acrolepis* and orange roughy, *Hoplostethus atlanticus*. At the

opposite end of the spectrum are the fast growing, highly active, homeothermic tunas, which have, relative to body size, small otoliths. It is notable that the older macrourids are at the point most opposite from the tunas, whereas the younger, presumably faster growing individuals display a greater tendency to be more depleted in ^{13}C, thus, showing that the potential relationship between $\delta^{13}C$ and temperature/metabolic rate may also be manifested within a species. A similar relationship is also evident among samples from juvenile and adult Atlantic bluefin tuna (*Thunnus thynnus*) (Radtke *et al.*, 1987), Australian salmon (*Arripis trutta*), jackass morwong (*Nemadactylus macropterus*) and blue grenadier (*Macruronus novaezelandiae*). In each of these species, ^{13}C was more depleted in the otoliths of juveniles than in the adults. The differences in both $\delta^{13}C$ and $\delta^{18}O$ between juvenile and adult orange roughy are very small and may be directly related to the biology of these deepwater fishes.

The isotopic data from the otoliths of other fish species readily falls within the spectrum of growth/metabolic rates and $\delta^{13}C$ values outlined by *Coryphaenoides acrolepis* and *Thunnus* spp. (Figs. 7.2 and 7.3). Slow growing species with large otoliths, such as red cod (*Pseudophycis barbatus*) and blue grenadier have $\delta^{13}C$ values about 4.0‰ depleted in ^{13}C relative to equilibrium. $\delta^{13}C$ values measured in a wide range of pelagic species that might be classified as moderately fast growing and with medium sized otoliths are clustered towards the tuna end of the range and show a depletion of approximately 7.0‰ to 12‰ relative to $\delta^{13}C_{eq}$.

Differences between $\delta^{13}C$ measured in juveniles and adults of a single species are very small when compared with differences among species such as *Thunnus maccoyii*, *Coryphaenoides acrolepis* and *Hoplostethus atlanticus*. This is probably due to the relatively small differences in metabolic rates between juveniles and adults when compared with the metabolic rates of other species. Information on the metabolic rates of each of these species is not available but, in many cases, these rates can be inferred from data available on other species. The mean oxygen consumption rate (VO_2) for *Coryphaenoides acrolepis* , *Coryphaenoides armatus* and *Sebastolobus altivelis* measured at depths of more than 1200 m was 2.8±0.5 $\mu l \cdot g^{-1} \cdot h^{-1}$, (Smith and Hessler, 1974; Smith, 1978; Smith and Brown, 1983). Oxygen consumption rates for skipjack (*Katsuwonus pelamis*) and albacore (*Thunnus alalunga*) tuna have been measured as 505 (at 23 to 25°C) and 212

$\mu l \cdot g^{-1} \cdot h^{-1}$ (at 15 to 19°C), respectively (Gooding *et al.*, 1981; Graham and Laurs, 1982), more than 75 times the rate measured for the 3 deepwater species. Brett and Groves (1979) calculated a mean VO_2 of 62±24 $\mu l \cdot g^{-1} \cdot h^{-1}$ with a range of 18 to 160 $\mu l \cdot g^{-1} \cdot h^{-1}$ for 34 fish species (not including tunas or deep-sea species). Clearly, the fish represented in the isotope data cover the widest possible extremes of metabolic rates. Taking this range into consideration, it is not surprising that differences in metabolic rates within a species are not always resolved by the $\delta^{13}C$ data.

A notable exception to the relationship between temperature/ $\delta^{18}O$ and metabolism/$\delta^{13}C$ in this study is the data collected from the Antarctic fish *Notothenia squamifrons*, where the deviation from equilibrium $\delta^{13}C$ is much greater than would be expected on the basis of habitat temperature and the postulated relationship between metabolic rate and $\delta^{13}C$ (Fig. 7.5). The mean $\delta^{13}C$ value for *N. squamifrons* otoliths, collected in the Southern Ocean off Heard Island (mean temperature approximately 1°C), is -3.75±0.13, a value that would be expected for fishes living at a temperature of about 11.5°C and with oxygen consumption rates between those determined for the deep-sea species (2.8±0.5 $\mu l \cdot g^{-1} \cdot h^{-1}$) and the estimated mean for a range of species (62±24 $\mu l \cdot g^{-1} \cdot h^{-1}$). This deviation can be explained by the fact that cold-adapted fishes have metabolic rates above what would be expected on the basis of temperature and size alone (Macdonald *et al.*, 1987). This property is frequently attributed to metabolic cold adaptation (MCA), although the exact nature of this phenomenon is still open to debate (Macdonald *et al.*, 1987). There are no published data on the VO_2 of *N. squamifrons*, but an estimate can be derived by calculating the mean VO_2 from oxygen consumption data (measured below 3°C) on 10 species in the genus *Notothenia* appearing in Macdonald *et al.* (1987). The mean value for VO_2 for these ten species is 43.4±17.0 $\mu l \cdot g^{-1} \cdot h^{-1}$, placing these species within the range of metabolic rates and $\delta^{13}C$ values expected for fishes occurring in warmer waters.

The data presented above provide the framework for the development of a relationship between $\delta^{13}C$ and oxygen consumption. Although few data are available, I have plotted $\delta^{13}C$ versus oxygen consumption ($\mu l \cdot g^{-1} \cdot h^{-1}$) in Fig. 7.9. The data for *Coryphaenoides acrolepis*, *Notothenia* spp. and *Thunnus* spp. are based on multiple observations of both metabolic rates and otolith isotopic composition. An additional point, representative of a mean value for "all fish", is also plotted. This point is based on the mean oxygen consumption for 34 species (62±24

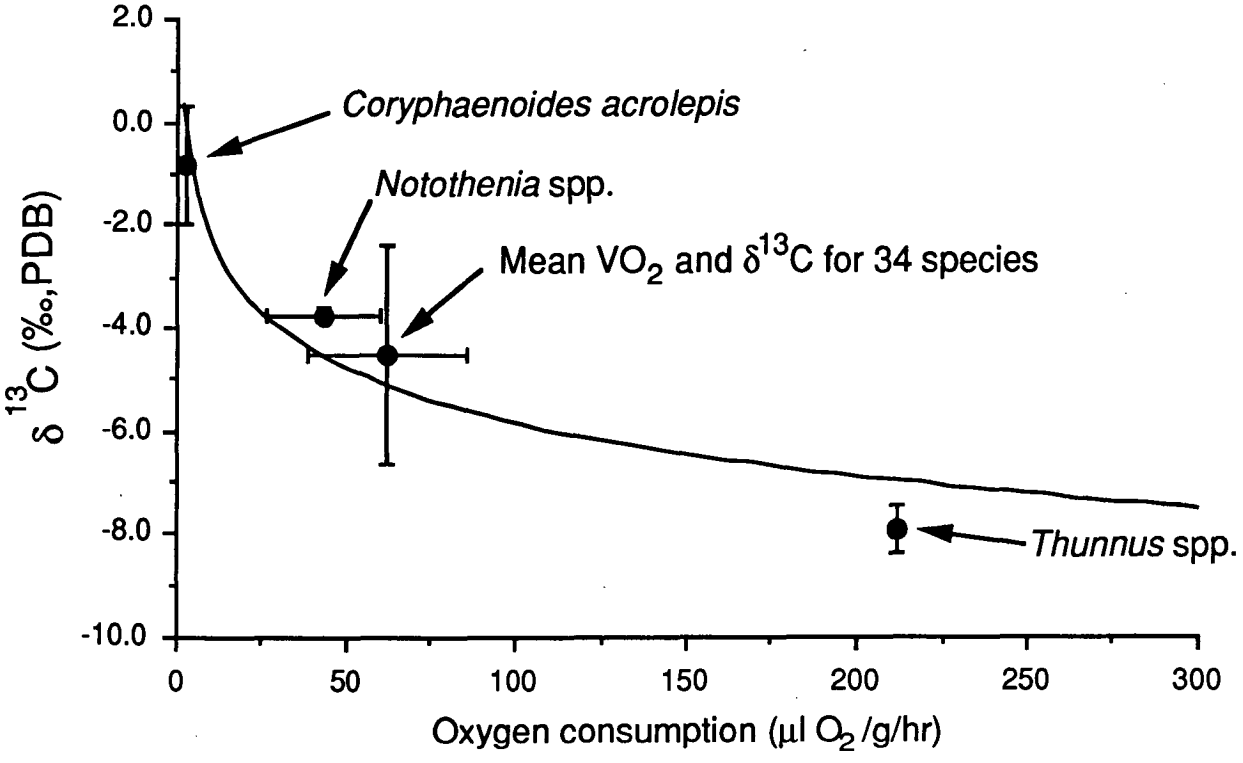

Fig. 7.9 Relationship between $\delta^{13}C$ and oxygen consumption (VO_2). Data points are explained in the text. There is a significant correlation between $\delta^{13}C$ and oxygen consumption ($r^2 = 0.92$, n=4, $P<0.05$). The logarithmic curve is described by the equation $\delta^{13}C=1.1979+(-3.5161)\log(VO_2)$. The logarithmic form of the relationship is similar to that representing the relationship between temperature and metabolic rate (Brett and Groves, 1979).

$\mu l \cdot g^{-1} \cdot h^{-1}$) from Brett and Groves (1979) and the mean value for $\delta^{13}C$ obtained from isotope data collected in this study (-4.51±2.15). If the data from the isotope studies of Mulcahy *et al.* (1979), Radtke (1984a, 1987) and Radtke *et al.* (1987) are included the mean value for $\delta^{13}C$ is 4.25±2.32. I have chosen not to include the data from Degens *et al.* (1969) because they did not do replicate analyses, thus, reducing the reliability of their data. The resultant relationship (Fig. 7.9) is a reasonable approximation of models that relate temperature to metabolic rate (Brett and Groves, 1979). On the basis of this initial result, it would be worthwhile to investigate further the significance of interspecific variations in $\delta^{13}C$.

The relationship between $\delta^{13}C$ and temperature, the potential association with metabolic rate and the fact that, in many cases, otolith size relative to body size decreases as the otolith aragonite becomes more depleted in $\delta^{13}C$, are points not consistent with the isotope fractionation theories of McConnaughey (1989a, 1989b). There are several points that support this conclusion with regard to fish otoliths. Firstly, although there is a strong correlation between $\delta^{18}O$ and $\delta^{13}C$, the departures of $\delta^{18}O$ and $\delta^{13}C$ from equilibrium do not seem to be attributable to the same mechanism. The $\delta^{18}O$ values are satisfactorily explained on the basis of the temperature fractionation effects first discussed by Urey (1947). The kinetic/hydration and hydroxylation mechanism of isotope fractionation would result in simultaneous depletions in oxygen and carbon isotopes independent of temperature. Furthermore, the kinetic effect is postulated to result in greater isotopic disequilibria in those calcium carbonate structures that are growing rapidly. In the extreme case of the tuna, otolith growth is probably slow despite very rapid somatic growth, because the otoliths are relatively small. Nevertheless, the tuna otoliths are the most depleted in ^{13}C of those measured. Of course, in drawing this conclusion it is necessary to assume that a unit of otolith material, such as a microincrement (Campana and Neilson, 1985) is produced over a similar time frame in all species, e.g., both tuna and orange roughy otolith microincrements are formed over a period of 8 hours.

The kinetic effect of isotope fractionation, and its link to isotopic disequilibria, is based on the idea that simultaneous depletions in ^{18}O and ^{13}C occur during CO_2 hydration and hydroxylation, presumably in the presence of some catalyst such as carbonic anhydrase. In fish, it seems unnecessary to carry out the process of CO_2 hydration and hydroxylation given the very large pool of available HCO_3^-.

Mugiya (1977, 1986) and Mugiya *et al.* (1979) investigated the roll of the enzyme carbonic anhydrase in fish otolith formation by a combination of *in vivo* and *in vitro* experiments. In a study of otolith formation in goldfish it was found that moderate doses of acetazolamide (Diamox), a carbonic anhydrase inhibitor, did not effect otolith growth, whereas large dose multiple injections reduced otolith growth by less than 17%. He concluded that the catalyzed hydration and hydroxylation of CO_2 was not necessary for otolith formation in goldfish (Mugiya, 1977). A subsequent study on *in vitro* prepartions of intact rainbow trout sacculi found relatively low levels of carbonic anhydrase activity, and it was concluded that, perhaps, carbonic anhydrase was not required at low rates of otolith deposition (Mugiya *et al.*, 1979). These studies indicate that carbonic anhydrase and CO_2 may play a non-essential role in fish otolith formation. If this is so than kinetic/hydration-hydroxylation effects would not be significant in carbon and oxygen isotope disequilibria, thus, providing further evidence that the correlation between $\delta^{13}C$ and $\delta^{18}O$ for fish otolith data is not due to kinetic isotope fractionation mechanism as proposed by McConnaughey (1989a, 1989b). Furthermore, in light of our present knowledge on processes of otolith growth and otolith growth rates it seems unlikely that isotopic disequilibria are due to the kinetic/diffusion mechanism.

7.5 SUMMARY

There is a strong correlation between $\delta^{18}O$ and $\delta^{13}C$ from fish otolith aragonite and these data display a slope very similar to that for various marine biogenic carbonates occurring in non-photosynthetic organisms. The range of the otolith data are very similar to that of ahermatypic corals.

Otolith oxygen isotopes were found to be deposited in, or close to isotopic equilibrium for a wide range of species. Variations in $\delta^{18}O$ could largely be explained on the basis of temperature related fractionation effects alone and, therefore, are the result of thermodynamic properties acting during the aragonite precipitation process. The utility of oxygen isotopes as an indicator of environmental temperatures is confirmed by equilibrium precipitation of otolith aragonite for a wide range of fish species.

Carbon isotopes were not precipitated in equilibrium. Non-equilibrium fractionation of carbon isotopes is hypothesized to be the result of differences in

metabolic rate and, in most cases, these differences appear to be related to temperature. There were consistent differences in $\delta^{13}C$ among juveniles and adults of a species with the faster growing juveniles showing a greater depletion in the heavy carbon isotope and this is consistent with the metabolic rate hypothesis. Carbon isotope data from fish otoliths may be useful in approximating the metabolic and, perhaps, growth rates of fishes and, thus, may also be of value in age estimation.

CHAPTER 8

CHARACTERIZATION OF OTOLITH ULTRASTRUCTURE BY SCANNING AND TRANSMISSION ELECTRON MICROSCOPY

8.1 INTRODUCTION

The use of otoliths in the estimation of fish age is based largely on the hypothesis that otolith deposition is a continuous process. Investigations of microstructural features such as daily increments must also assume that microincrements are circadian features that consist of two components; a "protein rich" discontinuous zone and "calcium carbonate rich" incremental zone (Campana and Neilson, 1985). The literature on these structures is extensive and increasing rapidly due to the usefulness of microincrements or daily increments in ageing fish. In some instances, the validity of the daily increment method has been questioned (Geffen, 1982), but more recent studies have shown that the supposed non-daily formation of microincrements is frequently an artefact of the limited resolution of light microscopy techniques (Campana *et al.*, 1987; Jones and Brothers, 1987).

The bipartite structure of otolith microincrements implies that cyclical changes in physiology must mediate the otolith deposition process. Investigations by Mugiya (1974, 1987), Mugiya *et al.* (1981) and Gauldie and Nelson (1988) have presented evidence for circadian physiological changes in relation to otolith deposition. Although there is good evidence for the interaction of daily physiological rhythms and the formation of otolith microincrements, the role of the organic matrix in otolith formation is still unknown. The mechanism of biogenic calcification in molluscs, corals, fish otoliths and other organisms is still a matter of considerable debate with the basic arguments centering around the role of an organic matrix in the calcification process. The question that is generally asked, particularly in work on calcification in corals and bivalves, is whether or not the organic matrix acts as a template for the calcification process, actually ordering the ions and facilitating nucleation (Bevelander and Nakahara, 1969; Johnston, 1977, 1980), or if it merely acts as an inhibitor of crystallization by attaching to specific crystal surfaces (Barnes, 1970). Numerous reviews are available on the calcification process in corals (Chalker, 1981, 1983; Barnes and Chalker, 1988), algae (Borowitzka, 1977, 1982) and molluscs (Wilbur and Saleuddin, 1983). Studies of the otolith calcification process are more limited,

but generally assume that an organic matrix plays a major part in otolith formation (Mugiya, 1964, 1987; Morales-Nin, 1987).

Although several studies have considered the physiological processes involved in otolith deposition, particularly in relation to the growth of daily increments, relatively little attention has been given to the structure of the components that constitute a microincrement, and the interaction of these subunits. Degens *et al.* (1969), Dunkelberger *et al.* (1980), Watabe *et al.* (1982) and Morales-Nin (1987) considered the structural interaction of otolith organic matrix and calcium carbonate within the otolith. Mann *et al.* (1983), Ross and Donovan (1986), Davies *et al.* (1988) and Gauldie and Nelson (1988) placed greater emphasis on the crystallographic nature of otolith aragonite and those factors which could affect otolith structure. These studies reinforced the view that otoliths are complex, aragonitic polycrystalline structures which incorporate varying quantities of protein in a cyclical manner. Morales-Nin (1987) hypothesized a model of otolith ultrastructure that shows otoliths as being composed of discrete prisms which are, in turn, composed of "microcrystals". Organic matrix is distributed irregularly over the surface of the microcrystals and prisms with increasing concentrations of protein occurring in the region of the discontinuous zones. Morales-Nin (1987) did not clearly define the distinction between microcrystals and prisms.

Because of the significance of mineralogy to the incorporation of trace elements and, the probable importance of the organic matrix in altering the level of certain elements, specifically sulphur, it was considered important to investigate certain aspects of otolith ultrastructure. This approach can provide insight into the mineralogical and crystallographic factors that may alter otolith trace element content. This chapter incorporates a variety of techniques, some which have already been employed in studies of otoliths, and others that are new to investigations of otolith ultrastructure. The combination of methodologies employed provides new information regarding the structure of otolith microincrements and the nature of the interaction between otolith aragonite and the organic matrix. The data are used to examine the model of otolith structure as postulated by Morales-Nin (1987) and are also considered in light of the variations in the levels of trace elements incorporated into fish otoliths.

8.2 MATERIALS AND METHODS

Otoliths from orange roughy, *Hoplostethus atlanticus*, were used to investigate the interaction of organic matrix and otolith carbonate. Sagittae were obtained from orange roughy collected by demersal trawling along the east coast of Tasmania in 1987 and 1988. Otoliths were removed at sea from freshly caught specimens, cleaned and rinsed in distilled water. Otoliths were then fixed in 2.5% glutaraldehyde in a 0.15 M sodium cacodylate buffer with 2.0% cetylpyridinium chloride adjusted to pH 7.8. Otoliths were placed in the fixative whole or after fracturing by hand. Otoliths remained in the fixative for periods of 3 to 5 days. Both Watabe *et al.* (1982) and Morales-Nin (1987) added 2.0% paraformaldehyde to the otolith fixative, but it was not included in this study because of the fact that paraformaldehyde can dissolve otolith material which would introduce artefacts. After removal from the fixative whole otoliths and fractured otoliths were critical point dehydrated.

Otoliths of orange roughy (*Hoplostethus atlanticus*), cod (*Pseudophycis barbatus*) and southern bluefin tuna (*Thunnus maccoyii*) were also removed from fresh specimens, cleaned and stored dry in vials. These otoliths were prepared by hand fracturing or by sectioning. The sectioning procedure was similar to that employed in the preparation of blue grenadier sagittae for electron microprobe analysis (Chapter 2). Some fractured otoliths and otolith sections were etched with 0.2 M EDTA or 0.1 M HCl adjusted to pH 7.4 to facilitate observation of otolith structure. Both fixed and unfixed otoliths and otolith sections were mounted on SEM stubs or portions of glass slides and coated with gold for observation with a Phillips 505 SEM.

Several sections of orange roughy otoliths were also prepared for high resolution TEM. Dry sagittae were embedded in Araldite D epoxy resin and polymerized in an oven at 40°C for 48 h. Transverse sections of approximately 200 μm thickness were cut in the anterior-posterior otolith plane with a Strueurs Accutom low-speed saw equipped with a diamond cut-off wheel. Otolith sections were cemented onto ground glass slides with Lakeside, a balsam compound that becomes labile at approximately 150°C. Sections were polished on a lapping wheel with 0.25 μm diamond paste and then removed from the slides by heat softening the balsam and then reattached to the slide polished face down. The sections were then ground to a thickness of approximately 20 μm and polished with diamond paste. Copper disks 3 mm O.D., 1 mm I.D. were then attached to the sections in the region of interest with

epoxy. The copper disks and associated otolith material below the disks were cut from the section with a special cutting tool. The disk and thin section material was then removed from the slide and the remaining section material by heat softening the balsam cement. These small sections were cleaned in xylene and then prepared for high resolution TEM analysis by argon plasma etching, also known as ion beam thinning. During the etching process the specimen was tilted at an angle of approximately 20° to the ion beam and etched with an accelerating voltage of 5.0 kV. The otolith aragonite was easily thinned by the ion beam and a hole was made in the specimen in about 1 hour. Specimens were then observed in a Phillips EM430 TEM operating at 300 kV.

8.3 RESULTS

Initial observations of otolith sections from orange roughy and cod indicated that the general structure of the aragonite crystals and the form of microincrements was similar to that observed in otoliths from other species (Figs. 8.1b and 8.6a). This observation is important to ensure that these otoliths are not grossly different from those of other species and, thus, ultrastructural observations in orange roughy and cod can safely be used as a model for other fish species. The frequency of microincrements observed by light microscopy was confirmed by comparison of the same sections after etching with EDTA and observation by SEM (Figs. 8.1a and 8.1b). When operating near the limit of resolution of light microscopy it is important to confirm that the microincrements that are observed are not due to diffraction or other artefacts.

8.3.1 Crystal prisms and microcrystals

Examination of a combination of etched and unetched pressure fractured sections of orange roughy, cod and southern bluefin tuna otoliths highlights the difficulty in determining the hierarchy of crystal organization in fish otoliths. Fractured otoliths showed sharply truncated structures that appeared to be composed of masses of irregularly shaped crystals along their length (Figs. 8.1c and 8.1d). It was not possible to distinguish bundles of microcrystals that could be classified as unique prism subunits from lathes that were single crystals. The shape of the crystal lathes was variable and ranged from acicular or needle-like to a more regular orthorhombic structure characteristic of aragonite. A large number of the truncated

surfaces appeared to be fractures along a single lattice plane of a crystal or, perhaps, a common lattice plane among two or more crystals. However, when analysing the ultrastructure evident in these images it is impossible to determine if fracturing was occurring within a crystal or among several crystals. There was no evidence that the planes of fracture were different from other regions of the otolith The truncated surfaces of the fracture were variable in size, and ranged from about 0.5 to 20.0 μm wide along their short axis. Those structures that appeared to be individual crystals were from 0.5 to 2.0 μm wide along the short axis (Figs. 8.1c and 8.1d). The long axes of the crystals appeared to be extremely irregular, but the general orientation of the crystals was uniform. Generally, it was not possible to determine which boundaries were the edges of discrete crystal subunits in these fractured specimens.

A fractured and HCl etched orange roughy otolith showed a combination of irregular needle-like crystals, as well as group of more uniform crystals that might be interpreted as polycrystalline prisms, along the surface of a 'smooth' fracture (Figs. 8.1e and 8.1f). The nature of these smooth fractures is discussed in more detail in Section 8.3.2. The fractured surface etched in an irregular manner and displays several "forms" of crystals. The acicular crystals in the right foreground (Fig. 8.1f) were similar to those typically observed in etched otolith sections (Fig. 8.1a). The structures that seem to resemble prisms (indicated by the arrow in Fig. 8.1f) are about 1.0 μm wide and, therefore, are of approximately the same size as the crystals observed in Figs. 8.1c and 8.1d.

Cod are unusual, although not unique among fish, because voids frequently develop within their sagittae. In these situations crystal growth appears to continue within the void, but, of course, ceases before the crystals come into contact with other crystal surfaces. By sectioning or fracturing the otolith in the region of these voids it becomes possible to observe individual crystal prisms without extensive sample preparation and the potential introduction of artefacts. A typical void within a cod sagitta is shown in Fig. 8.1g. The orientation of crystal growth appears to be similar to that of adjacent regions of the otolith, but the individual aragonite crystals are clearly visible.

Crystals of aragonite from within voids observed in cod otoliths were photographed using both SEM (Figs. 8.1g, 8.1h and 8.2a) and light microscopy (Fig. 8.2b). Some of the crystals clearly show forms characteristic of the orthorhombic system with 3 mutually perpendicular diad axes and interfacial angles

Fig. 8.1

a) Microincrements near the margin of a cod *Pseudophycis barbatus* sagitta. Otolith was sectioned, polished and then etched with EDTA. Needle-like crystals are visible throughout and, in many cases, these crystals cross over several microincrements. The arrows are presented for orientation so that this image can be compared with Fig. 8.1b.

b) Light micrograph showing the same cod otolith microincrements that are visible in the SEM in Fig. 8.1a. This photograph was taken before etching with EDTA. The arrows point to the same increments as in Fig. 8.1a. The magnification is 618x. It was impractical to make Fig. 8.1a and 8.1b the same magnification due to limitations imposed by the different size negatives.

c) Fractured orange roughy *Hoplostethus atlanticus* sagitta. There is no evidence of distinctive polycrystalline units. The arrow indicates a typical crystal lathe of about 1.5 μm wide.

d) Fractured orange roughy sagitta. A wide range of truncated surfaces are visible with no evidence of hierarchical structure. The arrow indicates a typical crystal lathe of about 1.5 μm wide and very similar to the crystal highlighted in Fig. 8.1c.

e) Fractured and HCl etched orange roughy sagitta. Zones parallel and perpendicular to the direction of crystal growth have been exposed. The left side of the micrograph shows a plane parallel to the direction of crystal growth. A distinct check mark is visible in the upper left and microincrements are evident further down. The plane perpendicular to the axis of crystal growth is dominated by needle-like crystals.

f) Higher magnification of Fig. 8.1e. The acicular crystals are still evident, but more regular prism-like structures can be seen in the area indicated by the arrow. These prisms are similar to those highlighted in Figs. 8.1c and 8.1d.

g) Void in a cod otolith. This section has been etched with EDTA.

h) Higher magnification of Fig. 8.1g. Crystals characteristic of aragonite are visible.

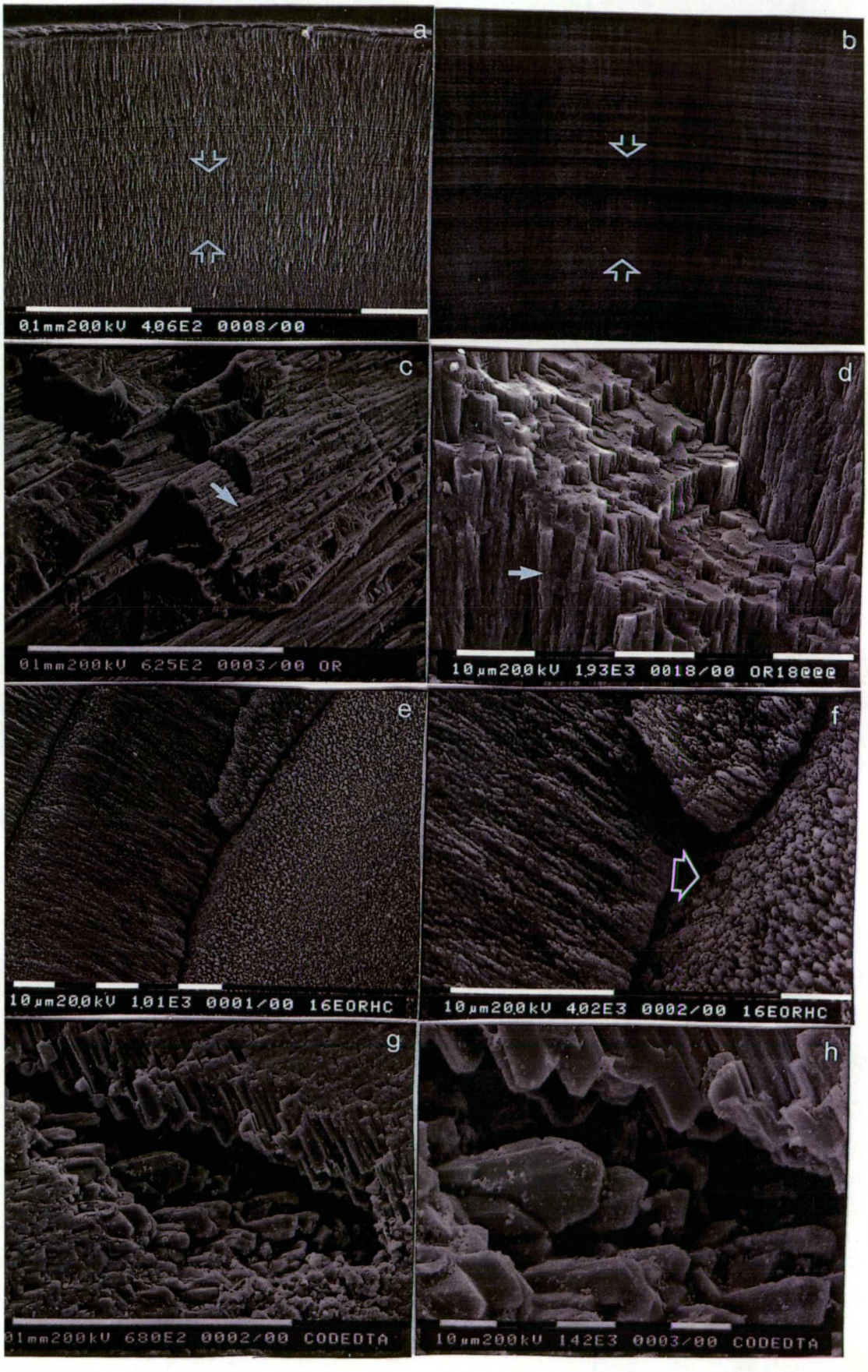
a
0.1mm20.0kV 4.06E2 0008/00
b
c
01mm20.0kV 6.25E2 0003/00 OR
d
10µm20.0kV 1.93E3 0018/00 OR18@@@
e
10µm20.0kV 1.01E3 0001/00 16EORHC
f
10µm20.0kV 4.02E3 0002/00 16EORHC
g
01mm20.0kV 6.80E2 0002/00 CODEDTA
h
10µm20.0kV 1.42E3 0003/00 CODEDTA

Fig. 8.2

a) Large crystals within the void of a cod otolith. This specimen has not been etched. A large range of crystal sizes is evident and many show features characteristic of aragonite. The crystal highlighted by the arrow is twinned and also shows increment-like structures with a width of approximately 0.5μm.

b) Light micrograph of a cod otolith thin section in the region of a void. The large crystals within the void are transparent and do not show any internal structure. Needle-like crystals generally seen in otolith sections are visible in the upper and lower portions of the micrograph. Magnification 150x.

c) EDTA etched cod otolith section perpendicular to the plane of crystal growth. There is a wide range of crystal morphologies and sizes.

d) Light micrograph of an orange roughy sagitta transverse section. The region of thickening over the distal lateral otolith surface can be seen at the top of the micrograph. The 'pinnacle' of the otolith in the upper middle of the micrograph, below the region of thickening, is the otolith primordium. Magnification 45x. The region highlighted by the arrow is shown at higher magnification in Fig. 8.2e.

e) Higher magnification of Fig. 8.2d. Light micrograph showing the region of thickening where the crystal orientation has changed (Light region near the top of the micrograph). Increments are visible in this region running parallel to the bottom of the page. The dark region in the central portion of the micrograph is the area of rapid otolith growth (see Fig. 8.6a) and microincrements can be seen almost perpendicular to the previously discussed increments. Magnification 290x.

f) Distal lateral surface of an orange roughy sagitta showing the surface of the region of otolith thickening, fixed in glutaraldehyde and etched with EDTA. Region A shows the large irregular prisms over the region of the otolith nucleus and region B shows more 'typical' crystals. The crystals in region B are very similar to those seen in etched cod otolith sections (Fig. 8.2c). The arrow marks the sharp boundary between the two regions.

g) Section through region A in Fig. 8.2f, fixed in glutaraldehyde and etched with EDTA. What appears to be a large irregular prism is marked with the lower arrow. The upper arrow shows the prism emerging on the otolith surface.

h) Surface structure of prisms shown in Fig. 8.2g. The arrow highlights the region shown at higher magnification in Fig. 8.3a. Otolith fixed in glutaraldehyde and etched with EDTA.

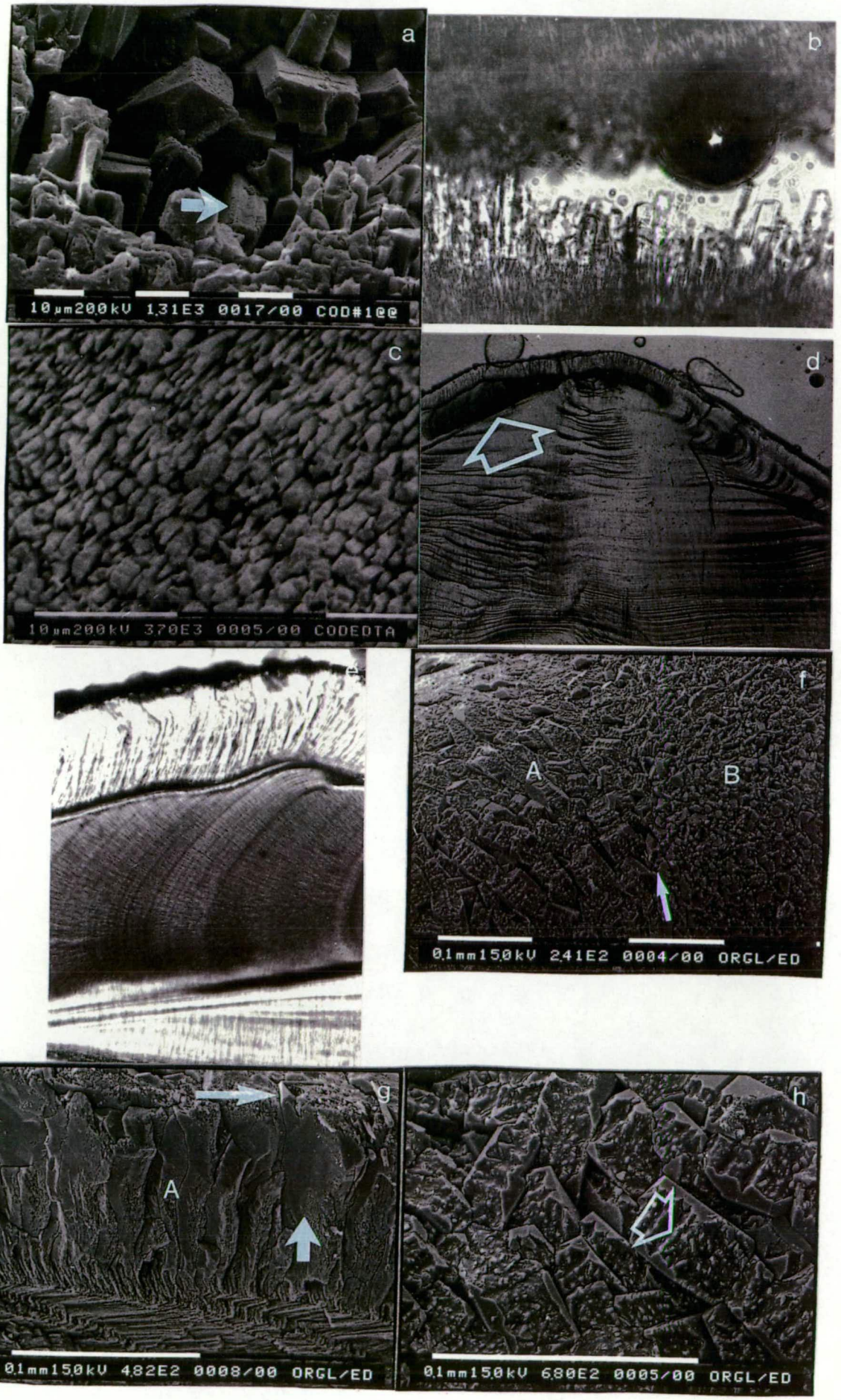
a
10µm20.0kV 1.31E3 0017/00 COD#1@@
b
c
10µm20.0kV 370E3 0005/00 CODEDTA
d
f
A
B
0.1mm15.0kV 2.41E2 0004/00 ORGL/ED
g
A
0.1mm15.0kV 4.82E2 0008/00 ORGL/ED
h
0.1mm15.0kV 6.80E2 0005/00 ORGL/ED

that approach 60°. Many of the crystals also show the characteristic doming that occurs in prisms in the orthorhombic system (Figs. 8.1h and 8.2a). One crystal showed clear evidence of twinning (Fig. 8.2a). This same crystal exhibited what might be interpreted as growth increments, each with a width of less than 0.5 μm. Etching of these crystals with EDTA indicated that they were not polycrystalline (Figs. 8.1g and 8.1h). Furthermore, observation of the crystals with light microscopy confirmed this point (Fig. 8.2b) since there was no evidence of the acicular crystals typically evident throughout cod otoliths (Fig. 8.1a, 8.1b). In light micrographs the crystals appear clear and devoid of any structure (Fig. 8.2b). These data provide evidence for the production of large individual crystals (>10 μm width) in some fish otoliths.

An SEM of a fractured cod otolith after etching with EDTA showed that the size of aragonite crystals was variable (Fig. 8.2c). This otolith fractured perpendicular to the plane of crystal growth and after etching it was possible to observe the form of the individual crystals. The morphology of the crystals ranged from prismatic to needle-like and crystal width varied from less than 0.5 μm to about 2.0 μm. This is similar to the estimated size of crystals observed in the fractured orange roughy sagittae (Figs. 8.1c and 8.1d).

Light micrographs and SEM of transverse sections of orange roughy sagittae indicate that there are extreme changes in the orientation of the aragonite crystals along the distal lateral otolith surface (Figs. 8.2d, 8.2e, 8.2g, 8.3b and 8.3c). This change in crystal orientation is characteristic of otoliths from larger (<35 cm SL) orange roughy and can be classified as a region of otolith thickening. Similar changes in crystal orientation were visible along the slow growth regions of albacore tuna, *Thunnus alalunga*, and southern bluefine tuna, *Thunnus maccoyii*, otoliths (i.e. regions other than the ventral terminal edge (Lee *et al.*, 1983)) (Figs. 4.22c and 4.22d) and, undoubtedly exist in other species. The appearance of these areas is very similar to the crossed-lamellar structure found in bivalves (Taylor *et al.*, 1969; Carter, 1980). Despite the extreme change in the appearance and orientation of these regions, electron microprobe analysis indicated that the Sr, Na, K and S content was similar to that of other otolith regions. In orange roughy and albacore otoliths, the slow growth region had a composition similar to that measured in the most recently formed portion of the otolith terminal edge.

The form of crystals in these regions of thickening is different from that found

Fig. 8.3

a) Surface detail of region A in Fig. 8.2f. Orange roughy otolith fixed in glutaraldehyde and etched with EDTA. There is a high density of organic matrix and the crystal morphology and orientation are variable.

b) Region of thickening (below region B in Fig. 8.2f) in an orange roughy otolith section etched with HCl. The crystals, highlighted by the large arrow, show the more typical needle-like structure of otolith aragonite. The smaller arrow identifies the sudden change in crystal orientation seen at higher magnification in Fig. 8.3c.

c) Orange roughy otolith section etched with HCl showing cross-lamellar structure.

d) Check mark in an orange roughy otolith section etched with HCl. The wide band ($\approx$ 5.0 μm) in the center of the micrograph appears to be predominantly organic matrix. Microincrements are visible on the right side of the micrograph. This check mark was approximately 80 μm from the primordium.

e) Fractured, unetched orange roughy sagitta. A uniform, concentric shell of organic matrix is visible.

f) Fractured, unetched orange roughy sagitta. A higher magnification micrograph of Fig. 8.3e showing the interface between the concentric shell of organic matrix and the aragonite lathes formed subsequent to the production of the organic shell. There is some evidence of a gap between the organic layer and the renewed crystal growth.

g) Fractured orange roughy sagitta, fixed in glutaraldehyde and etched with EDTA. The relationship between the aragonite crystals and the concentric organic layer, similar to that shown in Figs. 8.3e and 8.3f is evident. The organic layer has been partially removed by the etching process and, in some areas, it has peeled up from the aragonite crystal needles below (see left foreground). A gap can be seen between the organic layer and the renewed crystal growth.

h) Fractured orange roughy sagitta fixed in glutaraldehyde and not etched. This micrograph shows the globular form of the organic matrix that comprises the concentric shells shown in Figs. 8.3e, 8.3f and 8.3g.

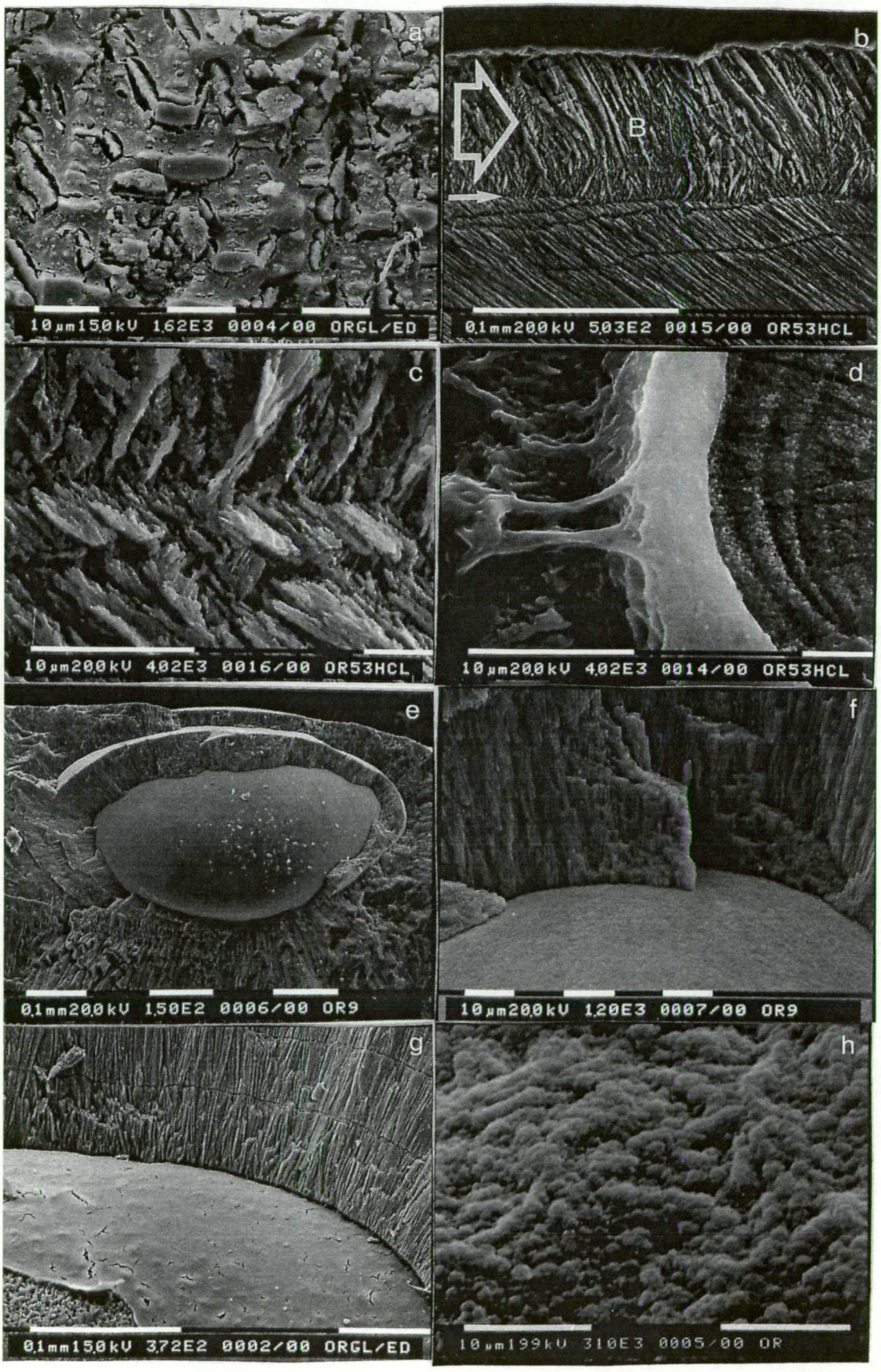
a
10µm15.0kV 1.62E3 0004/00 ORGL/ED
b
B
0.1mm20.0kV 5.03E2 0015/00 OR53HCL
c
10µm20.0kV 4.02E3 0016/00 OR53HCL
d
10µm20.0kV 4.02E3 0014/00 OR53HCL
e
0.1mm20.0kV 1.50E2 0006/00 OR9
f
10µm20.0kV 1.20E3 0007/00 OR9
g
0.1mm15.0kV 3.72E2 0002/00 ORGL/ED
h
10µm19.9kV 3.10E3 0005/00 OR

in other portions of the otolith and is also variable within this region. The change in prism size and form over the otolith lateral surface was sudden (Fig. 8.2f) and did not appear to be associated with any significant changes in the overall otolith morphology or chemistry.What appeared to be prisms over the region of the nucleus (region A in Fig. 8.2f), were actually composite structures. They appeared to be very large irregular prisms spanning the entire zone of otolith thickening (Fig. 8.2g) with only a small segment of the crystal being exposed on the surface of the otolith. These exposed portions of the prisms had a very regular structure (Fig. 8.2h). However, it appeared that the interior of these prisms had been invested with a complex matrix of protein and aragonite crystals of a wide range of sizes (Fig. 8.3a). The individual crystals within the 'hollow' of these prisms were over 10 μm wide in some cases. Prisms on the lateral otolith surface, but not in the immediate region of the nucleus, were much smaller than prisms over the nuclear region (region B in Fig. 8.2f). The appearance of this surface was very similar to that found in the etched cod otoliths (Fig. 8.2c) and displayed a similar range of crystal morphologies and sizes. These prisms were also similar in size to the prisms seen in the interior of the orange roughy otoliths (Fig. 8.1d). In cross section these crystals appeared identical to those typically seen in etched otolith sections (Figs. 8.3b and 8.3c).

8.3.2 Ultrastructure of check marks and the interaction between otolith organic matrix and aragonite

Check marks, discontinuities in the sequence of microincrements (Campana, 1983) are a common feature of orange roughy and cod otoliths. Checks of up to 5 μm were frequently observed in orange roughy sagittae (Fig. 8.6a) and HCl etching of these check marks revealed that there were large differences between the otolith material within the check and the material surrounding the check. On the basis of etching sections with acid and EDTA it was evident that these check marks are composed of protein rich material. An example of a relatively thick check is shown after etching in Fig. 8.3d.

Fracturing otoliths with thumb pressure in the region of such check marks often resulted in the exposure of a concentric surface of relatively smooth and uniform material (Figs. 8.3e and 8.3f). The exposed spherical surface was free of any significant macrostructure and appeared uniform at relatively low magnifications (<1500x) with the SEM. The surface also appeared to be free of any crystal-like

structures. At higher magnifications the glutaraldehyde-fixed surface displayed a fairly high degree of rugosity (Figs. 8.3h and 8.4a).

SEM of fractured and glutaraldehyde fixed sections of orange roughy otoliths confirm that the smoothed fractured surface was a continuous layer of organic matrix (Figs. 8.3g, 8.3h and 8.4a). In preparations where the fractured surface was briefly (<2 min) etched with EDTA after fixation, the organic layer has begun to peel away from the otolith surface and the aragonite crystals can be seen below the layer of organic matrix (Fig. 8.3g).

The organic layer in the fixed specimens had a different appearance in the various regions of the otolith. Where the otolith fractured along a concentric surface, presumably due to the presence of a check mark or relatively large discontinuous zone, the organic matrix appeared as tightly packed irregular globules, reminiscent of the florettes on a broccoli, with diameters ranging from approximately 0.1 to 0.5 μm (Figs. 8.3h and 8.4a). At a gap in the otolith, an interesting occurrence in this unetched specimen, there were thin fibers of organic matrix about 0.5 μm long and up to 0.16 μm wide (Fig. 8.4a). Along a fracture that occurred parallel to the plane of otolith growth, essentially perpendicular to the plane of the 'concentric sphere' of protein just discussed, the organic matrix appeared as a very dense mat or net (Figs. 8.4b and 8.4c). Microincrements are recognizable within this network as locations where there was a thickening of the organic matrix. In other areas the organic matrix seemed to be concentrated in bands at an angle to the direction of aragonite crystal growth and they appeared to affect the orientation of the crystals (Fig. 8.4d).

It is apparent that there are check mark regions in orange roughy otoliths where the deposition of aragonite stops completely. Campana (1983), in studies of check marks in stressed coho salmon, *Oncorhynchus kisutch*, concluded that a reduction in the rate of calcium deposition, with little or no change in the rate of organic matrix deposition, was responsible for the appearance of otolith check marks. The observations on orange roughy check marks partially support this conclusion and, furthermore, they showed what appears to be a complete cessation in the deposition of otolith aragonite. It is impossible to determine whether or not there had been an increase in the rate of organic matrix deposition since the period of time over which calcium carbonate deposition had ceased is unknown.

Further evidence that the deposition of organic matrix can halt the precipitation of otolith aragonite is shown in Figs. 8.4e and 8.4f. The direction of otolith growth

Fig. 8.4

a) Fractured orange roughy sagitta fixed in glutaraldehyde and not etched. The fracture occurred along a concentric shell of organic matrix (see Fig. 8.3e) and a perpendicular region, also with a high protein content. The globular form of the organic matrix can be seen in both regions. Thin fibers of organic matrix less than 0.16 μm wide can be seen across a gap between the regions. This gap appears to be similar to those that appear in Figs. 8.3f and 8.3g.

b) Fractured orange roughy sagitta fixed in glutaraldehyde and etched with EDTA. The plane of fracture was parallel to the axis of crystal growth. There is a thick mat of organic matrix over the whole surface, with lines of increased organic matrix in regions that would correspond with the discontinuous zones of the bipartite structure of microincrements.

c) Fractured orange roughy sagitta fixed in glutaraldehyde and etched with EDTA. The plane of fracture was parallel to the axis of crystal growth. A region similar to that in Fig. 8.4b, but with a less dense covering of organic matrix.

d) Fractured orange roughy sagitta fixed in glutaraldehyde and etched with EDTA. The plane of fracture was parallel to the axis of crystal growth. The quantity of organic matrix is much lower than in Figs. 8.4b and 8.4c. There an increase in organic matrix in the discontinuous zones. The arrows highlight bands of organic matrix that are at an angle to the general direction of crystal growth and appear to have altered the orientation of the aragonite crystals.

e) Fractured orange roughy sagitta fixed in glutaraldehyde and etched with EDTA. The plane of fracture was parallel to the axis of crystal growth. This micrograph shows aragonite needles that appear to have ceased growth in conjunction with the deposition of a dense layer of organic matrix. There is a gap between the layer of organic matrix and more recently formed aragonite needles.

f) Detail of Fig. 8.4e. The layer of organic matrix appears to have stopped growth of the uppermost aragonite crystals and is in direct contact with these crystals. The lower crystals are connected to the sheet of organic matrix by thin fibers of protein.

g) Light micrograph of two, of several, primordia in a southern bluefin tuna *Thunnus maccoyii* sagitta. The primordia show a distinct spherulitic morphology.

h) Scanning electron micrograph of primordia in a southern bluefin tuna sagitta, similar to Fig. 8.4g. The primordia show a distinct spherulitic morphology.

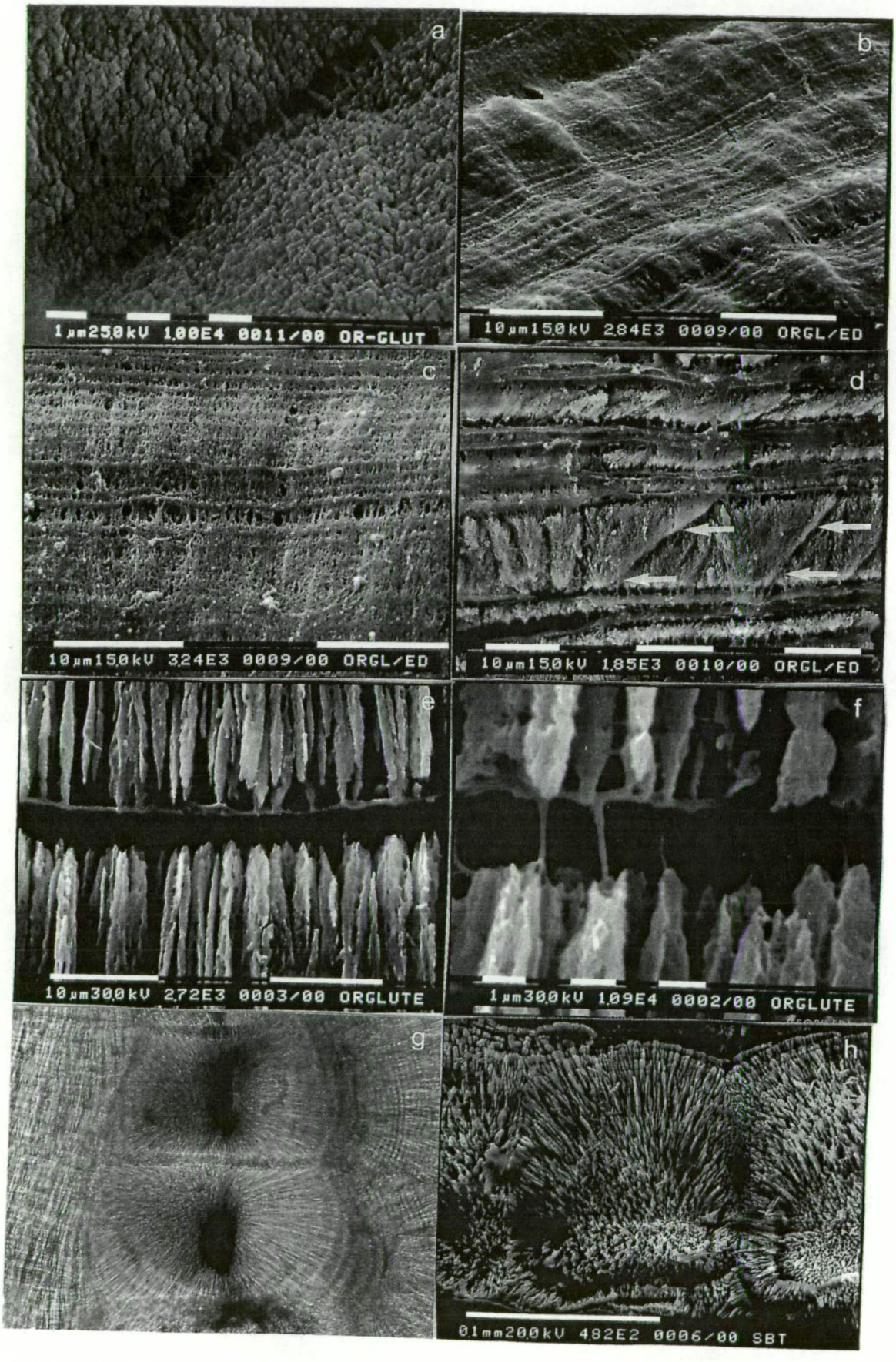
a
1 µm 25.0 kV 1.00E4 0011/00 OR-GLUT
b
10 µm 15.0 kV 2.84E3 0009/00 ORGL/ED
c
10 µm 15.0 kV 3.24E3 0009/00 ORGL/ED
d
10 µm 15.0 kV 1.85E3 0010/00 ORGL/ED
e
10 µm 30.0 kV 2.72E3 0003/00 ORGLUTE
f
1 µm 30.0 kV 1.09E4 0002/00 ORGLUTE
g
h
01 mm 20.0 kV 4.82E2 0006/00 SBT

is from the top towards the bottom. Aragonite needles can be seen flush against a zone of organic matrix which appears to have stopped their growth (Fig. 8.4e). There was a gap of approximately 1.5 μm between the layer of organic matrix and the point where aragonite started to precipitate again. While there were organic matrix fibers running from the zone of protein and across the gap to the newer lathes of aragonite, no such fibers are evident between the organic layer and the older aragonite needles (Fig. 8.4f).

8.3.3 Mineralogy of the primordium

Some of the fish species investigated in this study of otolith microchemistry, such as orange roughy, Australian salmon and southern bluefin tuna, frequently have relatively high levels of Sr in the otolith nuclear region. The basis for these elevated Sr levels is not known although ultrastructural features of the otolith nuclear region provide evidence for a precipitation rate based mechanism. Figures 8.4g and 8.4h show primordia of southern bluefin tuna sagittae (see Figs. 4.22c and 4.22d). Southern bluefin sagittae have multiple primordia and nuclei and in the specimen illustrated 8 primordia were visible. Each nucleus was approximately 110 μm in diameter and displayed a spherulitic structure. The structure of these spherulitic nuclei was similar to the aragonitic spherulites described by Blackwelder and Watabe (1977) from a freshwater snail (*Pomacea paludosa*), although the spherulites found in the snail were only 15 μm in diameter. Carter (1980) described spherulites from bivalves and these are about 20 μm in diameter. Bathurst (1975) illustrated 100 μm spherulites, called sclerodermites, which are a fundamental component of the skeleton of scleractinian corals.

Spherulites are considered high energy structures and they are believed to be formed during periods of rapid calcium carbonate precipitation. High precipitation rates have been hypothesized to be one of the mechanisms whereby increased levels of Sr would be incorporated into aragonite (Kinsman and Holland, 1969). These spherulite structures were also evident in the orange roughy and Australian salmon nuclei.

8.3.4 Transmission electron microscopy

The TEM is extremely useful for investigating the composition and orientation of crystalline materials because of both resolution and the nature of the TEM image.

The changes in contrast in a TEM image of a single compound (such as calcium carbonate) can result from 2 factors; differences in orientation of the crystals or changes in the thickness of crystals (Hirsch *et al.*, 1965). Of course, additional contrast changes will result if there are elements present of significantly different atomic weights. For example, $CaCO_3$ would be more electron luscent than $SrCO_3$. Differences in the orientation of crystals within a specimen result in changes in the percentage of the electron beam that passes through the objective aperture versus that which is diffracted due to Bragg reflections (based on the same Bragg's Law that allows the crystals of the wavelength dispersive electron microprobe to selectively diffract x-rays of different wavelengths). Portions of the direct beam that pass through the objective aperture form a bright-field image. Images can also be formed from the diffracted beam by tilting the beam so that it passes through the objective aperture or by changing the position of the objective aperture (Hirsch *et al.*, 1965). Both types of images were used to study the nature of the crystals present in otoliths of orange roughy.

An SEM photograph of an argon plasma etched portion of an orange roughy otolith that was used in otolith TEM studies is shown in Fig. 8.5a. The edges of the specimen immediately adjacent to the hole produced by thinning are the regions which are suitably thin (<100 nm) for TEM observation. Regions observed with the TEM are shown at higher magnification in Fig. 8.5b. The cobbled surface of the ion etched specimen is an artefact that is believed to be a function of the polished surface of the specimen before ion beam etching. However, the structures that are actually observed with the TEM are far smaller than these cobbles and should not be effected by them.

Argon plasma etching of portions of orange roughy otoliths produces specimens that are relatively free of structural artefacts, particularly when compared with the otolith sections produced by ultramicrotome sectioning (Gauldie and Nelson, 1988). The predominant feature in their sections were the large electron transparent fractures that resulted from sectioning. In those instances where a specimen is exposed to extremes of stress and shear which result in large fractures, numerous other artefacts may result. Therefore, interpretation of images is difficult and prone to errors. In comparison, argon plasma etched specimens provide a more readily interpreted image. Although differential etching of otolith aragonite and organic matrix is a potential problem, in some instances these differences can be useful in distinguishing features of otolith ultrastructure.

Fig. 8.5

a) Scanning electron micrograph of an orange roughy otolith section after completion of preparation for TEM by argon plasma etching. The hole is produced by the etching process. The distinct cobbled structure of the etched specimen is evident. Microincrements can still be seen in some areas of the specimen. The arrow highlights the region shown in Fig. 8.5b.

b) Higher magnification of specimen in Fig. 8.5a showing the regions viewed with the TEM (highlighted by the two arrows). These two regions of the thinned specimen were adequately thin (<100 nm) for viewing with the TEM.

c) Transmission electron micrograph of orange roughy otolith showing two 'size classes' of microincrements. Larger microincrements are composed of discontinuous zones that range in width from 0.40 to 1.00 μm and incremental zones as large as 2.0 μm. These are the microincrements that are usually seen by light microscopy in sections of orange roughy otoliths (Fig.8.6a). Smaller increments, such as those in the region highlighted by the arrow, had discontinuous zones of approximately 0.1 μm wide and incremental zones less than 0.3 μm in width. Magnification 4,600x.

d) Transmission electron micrograph of orange roughy otolith showing two 'size classes' of microincrements, similar to Fig. 8.5c. Magnification 4,600x.

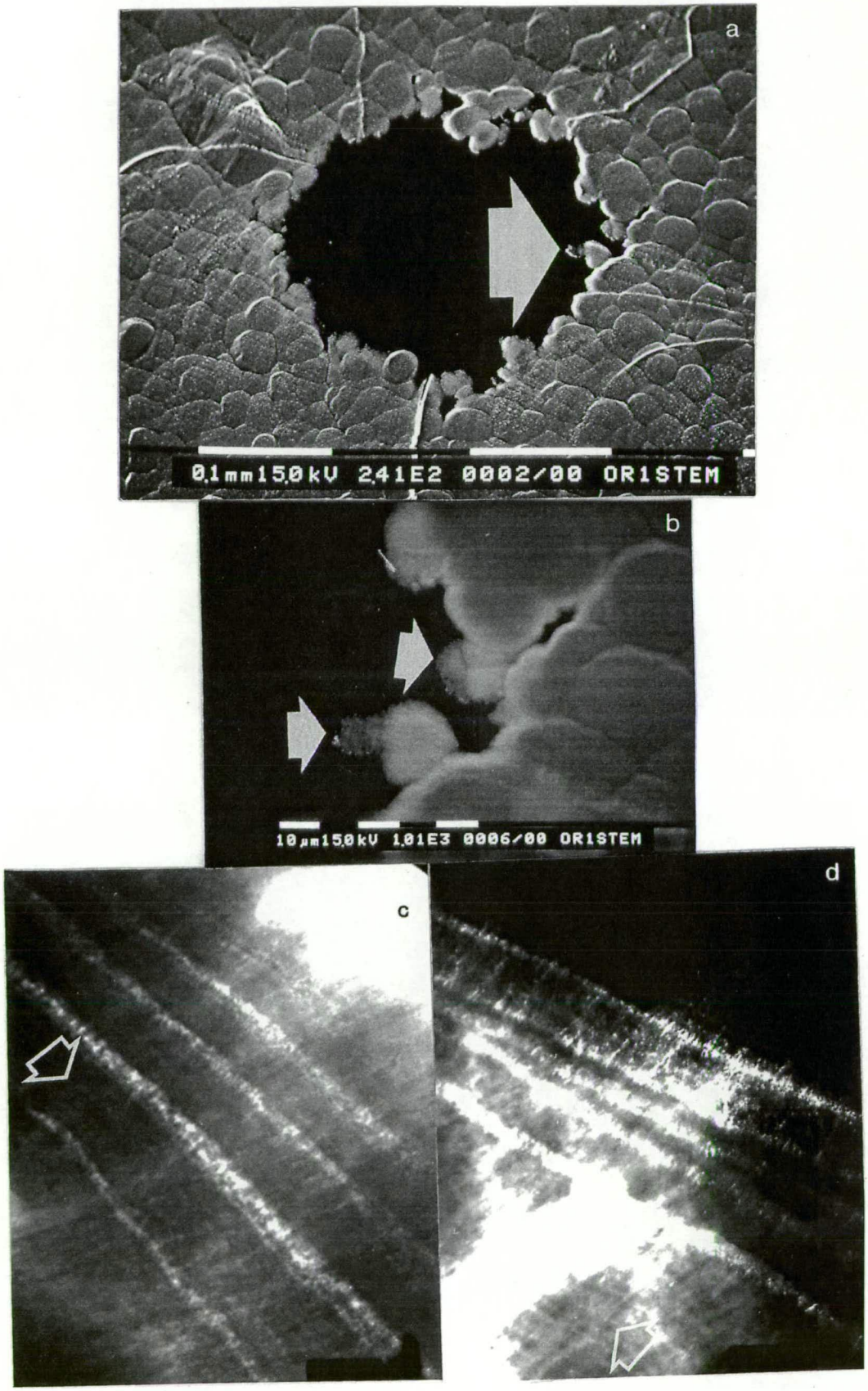
a
0.1mm15.0kV 241E2 0002/00 DR1STEM
b
10µm15.0kV 1.01E3 0006/00 DR1STEM
c
d

TEM is most useful in the investigation of structures of less than 5 μm in the largest dimension. For this reason the TEM images presented relate primarily to the ultrastructure of microincrements and of individual crystallites (*sensu* Mann *et al.*, 1983) or microcrystals (*sensu* Morales-Nin, 1987). However, as will be discussed later, the classification of crystalline structures in otoliths as microcrystals and prisms appears to be largely arbitrary.

Groups of microincrements are clearly visible in the lower magnification images (4,600x) (Figs. 8.5c and 8.5d). In many cases, all material was removed from the protein-rich discontinuous zone of the microincrements by ion beam thinning, and these regions were readily distinguishable as electron luscent white bands in the micrographs. The width of the larger bipartite microincrements varied widely in the sections. In Fig. 8.5c, the width of the more distinct discontinuous zones ranged from about 0.40 to 1.00 μm and the width of the corresponding calcium carbonate-rich incremental zones were as wide as 2.0 μm. These are the microincrements that are visible in many regions of the orange roughy otolith using light microscopy (Fig. 8.6a). However, closer inspection of TEM images revealed that among the distinct microincrements were numerous much smaller increments (Figs. 8.5c and 8.5d). These smaller increments had a discontinuous zone that was approximately 0.20 μm wide. The corresponding incremental zone was approximately 0.30 μm wide. Another low magnification TEM shows a similar arrangement of large and small microincrements (Fig. 8.5d). The more distinct electron luscent discontinuous zones ranged from 0.40 to 0.80 μm and the corresponding incremental zones varied from 0.40 to 1.50 μm. However, embedded within these larger microincrements were microincrements that were 0.20 μm wide and smaller. The relative widths of the two microincrement components were very different from that observed, in a similar region on the same orange roughy otolith, by transmitted light microscopy (Fig. 8.6a). In the light micrographs, the two components of the microincrements appeared to be of almost equal widths (≈1.0 μm each). Therefore, not only was it impossible to distinguish a large percentage of the orange roughy microincrements using light microscopy, but it was also difficult if not impossible to accurately measure the widths of individual microincrement components. These conclusions are similar to those that have been reached when comparing observations of otoliths made using light microscopy and SEM (Campana and Neilson, 1985; Campana *et al.*, 1987; Jones and Brothers, 1987) and also involving different otolith preparation techniques

Fig. 8.6

a) Light micrograph of thin section of an orange roughy sagitta. Arrow indicates small microincrements, with a width of approximately 2.0 μm, commonly seen in orange roughy sagittae. Magnification 450x.

b) Section of a southern bluefin tuna sagitta, etched with EDTA. Distinct increments are visible throughout the section. Smaller increments, only visible in a few regions, are highlighted. In this form of preparation it is impossible to determine if similar, small microincrements are visible throughout the section.

c) Transmission electron micrograph of an argon plasma etched orange roughy otolith. The single dark crystal in the center of the image (arrow) spans a discontinuous zone from which the organic matrix has been completely removed by the etching process. This aragonite crystal, approximately 2.2 μm long, was used to produce the selected area diffraction pattern in Fig. 8.6d. In some areas, irregular bundles of aragonite that had been thoroughly invested with organic matrix can be seen spanning the discontinuous zone. The mottled appearance throughout the micrograph is probably due to differential etching and shows the nature of the interaction between otolith organic matrix and aragonite in regions removed from the discontinuous zones. Magnification 18,900x.

d) Selected area diffraction pattern of individual aragonite crystal in Fig. 8.6c. The indices show the orientation of the **b (001)** and **c (010)** planes of the aragonite unit cell (see Fig. 8.8). The pattern is indicative of a single, perfect aragonite crystal.

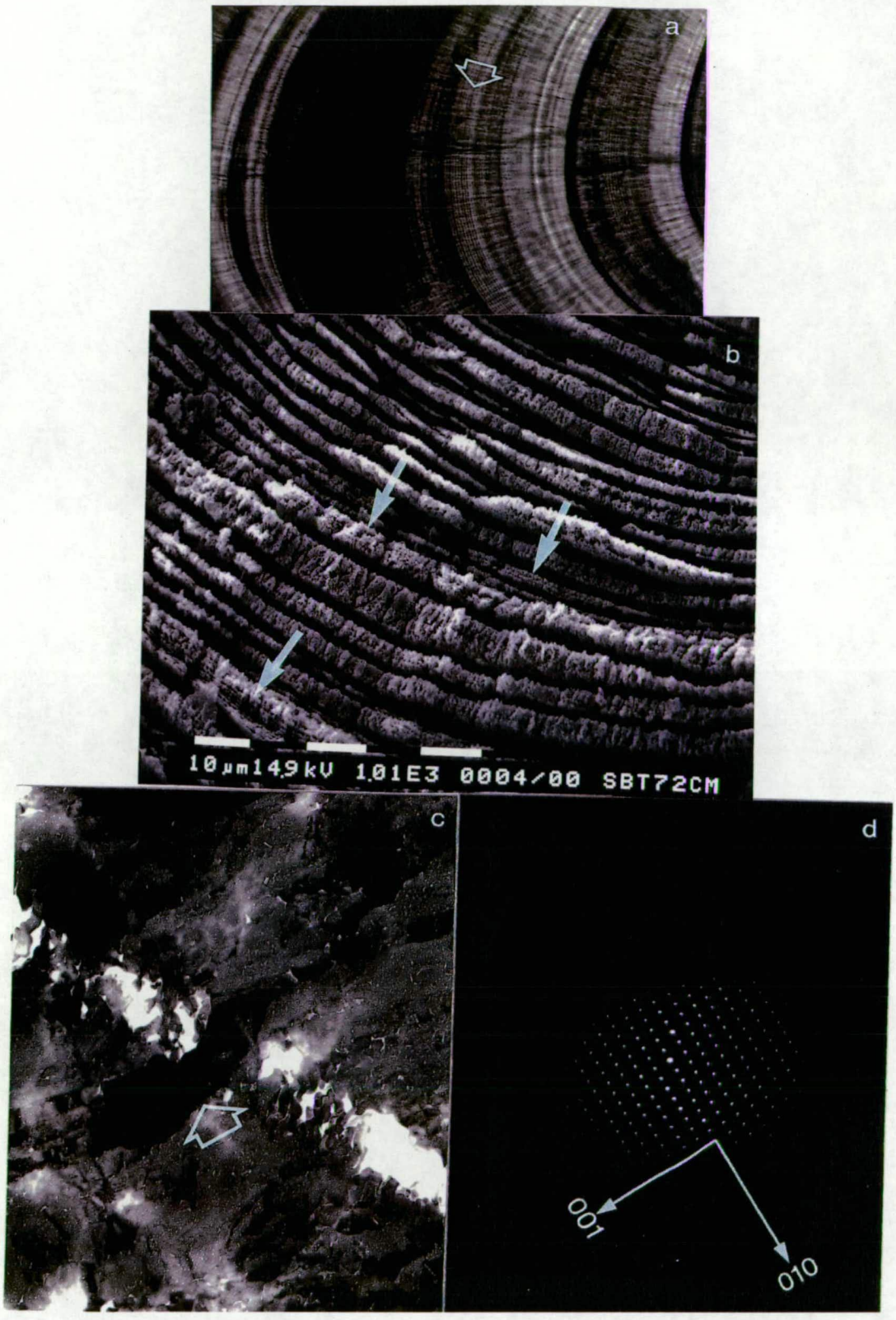
a
b
10µm14.9kV 1.01E3 0004/00 SBT72CM
c
d
001
010

for SEM (Morales-Nin, 1987).

It is important to realize that even when using SEM to observe EDTA or acid etched specimens it is still easy to overlook smaller microincrements. This is largely a function of the etching process, whereby it is difficult to differentially etch regions where the relative differences in otolith organic matrix are not great. An example of the potential problem and it's ramifications can be illustrated by initial attempts to enumerate otolith daily growth increments in the sagittae of southern bluefin tuna. The etched otolith section illustrated in Fig. 8.6b is from a southern bluefin tuna that had been captured, injected with oxytetracycline (OTC), tagged and released. The individual was recaptured after 429 days at liberty and the sagittae were sectioned and the position of the uv-fluorescent OTC derived mark was determined. Initial counts from the fluorescent band to the otolith edge were on the order of 147 increments. However, subsequent etching of other sections indicated that at least some of the poorly etched incremental zones were actually composed of smaller increments, and in some cases these increments were less than 0.5 μm. Because of the potential probability of overlooking such increments when ageing older or slower growing fish, it would be valuable to confirm that SEM observations of etched otoliths were accurate. For example, initial SEM observations of orange roughy otoliths failed to detect the finer (<0.5 μm) microincrements seen in TEM.

The otolith crystals display a perfect aragonite lattice based on electron diffraction patterns. Electron diffraction patterns result from differential diffraction by the lattice planes of a crystal, again a function of Bragg's Law (see Chapter 1). Discussions on the formation and analysis of diffraction patterns are presented in Hirsch *et al.* (1965) and Beeston *et al.* (1973). A selected area electron diffraction pattern from a single crystal of otolith aragonite spanning a discontinuous zone (Fig. 8.6c) is shown in Fig. 8.6d This diffraction pattern is a perfect example of the aragonite unit cell projected on a plane parallel to the *b* and *c* directions and can be compared with a schematic diagram of the same projection (Fig. 8.8).

Bright-field images show that both the shape and size of the individual crystals is highly variable, despite the fact that they have lattices that are perfect examples of aragonite. The single aragonite crystal used to create the diffraction pattern in Fig. 8.6d had an irregular shape, but appeared to be typical of fish otolith aragonite crystals (Fig. 8.6c). Another example of the irregular shape of the otolith crystals appears in Fig. 8.7a. This crystal varied in width from 1.3 to 2.5 μm and is more

Fig. 8.7

a) Bright-field image showing the variability in crystal size in an orange roughy sagitta. The large open arrow indicates a crystal that varies in width from 1.3 to 2.5 μm and is greater than 8.0 μm in length. The two smaller arrows show the position of the discontinuous zone spanned by the aragonite crystal. Magnification 8,200x.

b) Bright-field image showing needle-like crystals that are most frequently observed in fish otoliths. Arrows highlight two typical crystals. The width of the crystals varies from 0.1 to 0.7 μm and their lengths are up to, at least, 6.3 μm. Magnification 8,200x.

c) Bright-field image showing needle-like crystals and the variability in their orientation. Three crystals with different orientations are highlighted with arrows. Magnification 8,200x.

d) Dark-field image showing a region of predominantly needle-like crystals. Small differences in crystal orientation are evident. Magnification 5,150x.

e) Dark-field image showing rotational moiré patterns in an orange roughy otolith. Moiré patterns explained in Fig. 8.9 and in the text. These patterns were used to estimate the angle or rotation between overlapping aragonite lattices in the orange roughy otoliths. Magnification 18,000x.

f) Dark-field image showing rotational moiré patterns in an orange roughy otolith, similar to Fig. 8.7e. Magnification 21,000x.

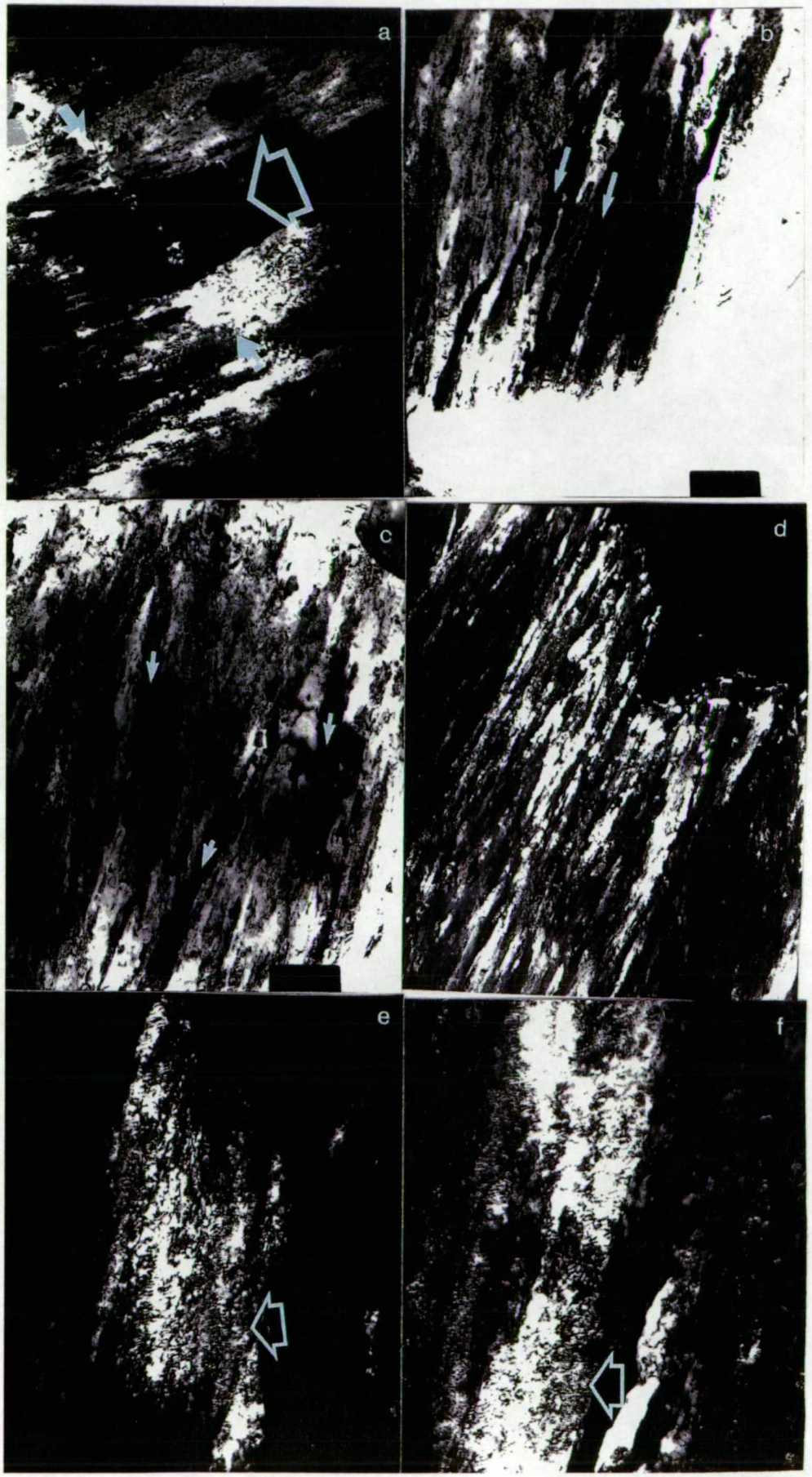
a
b
c
d
e
f

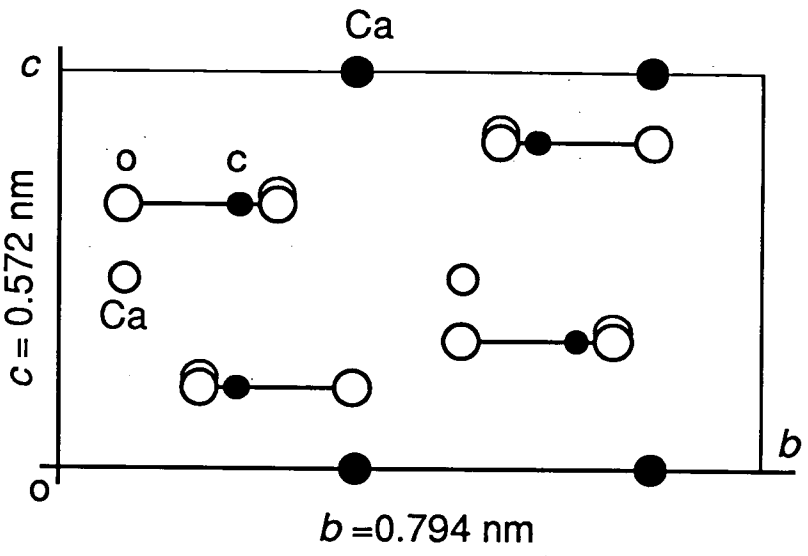

Fig. 8.8 Projection of the unit cell of aragonite on a plane parallel to the **b** and **c** directions. The carbon atoms are in coordination with three oxygen atoms and the (CO_3) groups lie in planes parallel to (**001**) and perpendicular to (**010**). The Ca atoms that occur at the bottom and top of the unit cell are shown in black, while the Ca atoms that occur at half the height of the cell (c/2) are shown as open circles (from Phillips and Phillips, 1980).

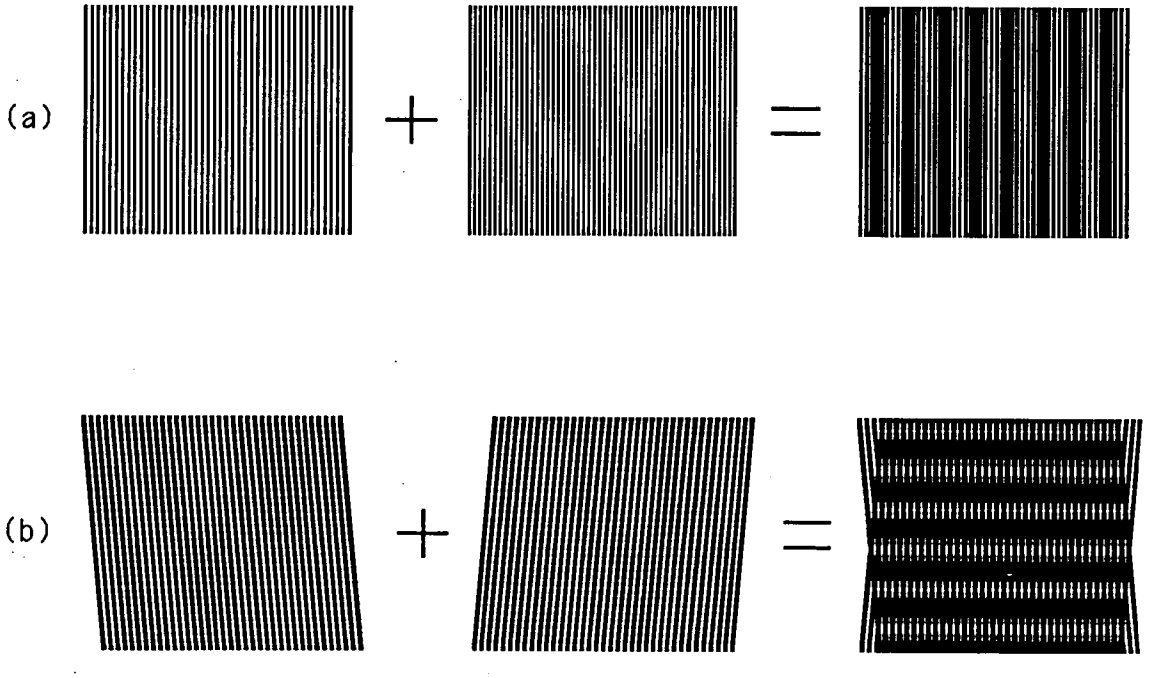

Fig. 8.9 An optical analogue demonstrating the formation of moiré patterns by two overlapping gratings : (a) parallel moiré patterns; (b) rotation moiré patterns. (Hirsch et al., 1965)

than 8.0 μm in length. Other crystals appeared more needle-like as in Figs. 8.7b, 8.7c and 8.7d and appear, in some cases, to be less than 0.2 μm wide. The outer edges of individual crystals frequently show jagged edges and have needle-like terminations as is seen in etched specimens observed with the SEM (Fig. 8.1a). These are typical examples of otolith aragonite crystals and they highlight the irregularity of the crystal shape and surface.

Bright field TEM, provides information that can be related to the interaction between otolith organic matrix and aragonite. The mottled appearance of the otolith surface in Fig. 8.6c, due to numerous small white (electron luscent) spots is an artefact of differential ion beam etching. This has probably resulted because protein was present in those regions and may have been 'anchored' to the aragonite crystals at those points. This indicates that, for the most part, organic matrix did not deeply penetrate the aragonite crystals, except in the protein rich discontinuous zones. At the discontinuous zones protein may completely penetrate single aragonite crystals, but does not necessarily halt crystal growth (Figs. 8.6c and 8.7a).

The interaction of the organic matrix and calcium carbonate microcrystals among microincrements is not well understood. The extension of aragonite microcrystals across discontinuous zones has been observed using SEM (Morales-Nin, 1987) and can be readily detected in etched otolith sections such as in Fig. 8.1. However, such studies cannot conclusively determine if the structures that are observed extending across an increment are single crystals, several crystals aligned lengthwise or, perhaps, several crystals fused within the region of the discontinuous zone.

TEM observations of crystals within the region of the discontinuous zones clearly showed the continuity of individual crystals across microincrements (Fig. 8.6c and Fig 8.7a). Two properties of TEM help to define these structures as single crystals. Firstly, these crystals were of relatively uniform contrast throughout, indicating that the crystal lattice had a uniform orientation. Furthermore, the selected area diffraction pattern of the crystal shown spanning a discontinuous zone in Fig. 8.6c, indicated that the crystal was a perfect single crystal of aragonite (Fig. 8.6d). Similar crystals were found across other discontinuous zones and in all cases the selected area diffraction patterns were characteristic of single crystals of aragonite. This point is discussed in more detail below.

There was no evidence of beam damage in any region of the orange roughy

otolith specimens on the basis of selected area diffraction patterns. Mann *et al.* (1983) and Ross and Donovan (1986) indicated that fish otolith aragonite (from plaice *Pleuronectes platessa*) was unstable in the electron beam and stated that exposure to the beam resulted in a lowering of the lattice symmetry and reversion to a more primitive lattice. This did not occur in orange roughy otoliths. Furthermore, recalculation of lattice parameters for the electron diffraction patterns generated by undamaged and, supposedly, damaged plaice otoliths (see Fig. 9 and 10, Mann *et al.*, 1983) indicated that the two patterns were both representative of aragonite, one was merely in a different orientation (personal communication, Dr. A. C. McLaren, Research School of Earth Sciences, Australian National University).

Examination of TEM indicates that the orientation of aragonite crystals in fish otoliths is not regular at ultrastructural scales. This can be clearly seen in both light field and dark field images (Figs. 8.7b, 8.7c and 8.7d). The relative orientation of aragonite crystals was highly irregular when compared with images of molluscan calcium carbonate (Taylor *et al.*, 1969; Travis and Gonsalves, 1969) and they appeared to vary in orientation by up to 20°. Of course, there was generally a high degree of organization within fish otoliths with the majority of crystals showing a similar general orientation.

The relative orientation or periodic structure of crystalline substances can be determined by the production of moiré patterns. Direct resolution of the spacing of the aragonite lattice (<0.6 nm) is beyond the resolution limit for periodic structures using the EM430 (Hirsch *et al.*, 1965). Moiré patterns, produced by two overlapping crystals can be used to indirectly resolve lattice images, which are based on the spacings and arrangement of the individual molecules of a crystal. Alternatively, in cases where the lattice spacing is known, the moiré patterns can be used to determine the relative orientation of overlapping crystals. Furthermore, it is possible to obtain information regarding deformations in the crystal lattice. Two forms of moiré patterns are illustrated in Fig. 8.9. When two crystals are oriented in the same direction, but the lattice spacing of the two crystals is different, than parallel moiré patterns will occur (Fig. 8.9a). The spacing between the beats of the parallel moiré pattern, D, are related to the two different spacings in the crystals, d_1 and d_2, by

$$D = \frac{d_1 d_2}{|d_1 - d_2|}$$

In many cases D can be readily resolved in the TEM, whereas the lattice spacing cannot. In some cases the moiré patterns are oriented in a direction that is almost perpendicular to the direction of the crystal lattice. These rotation moiré patterns (Fig. 8.9b) can be used to determine either the lattice spacing of a crystal or, if the lattice spacing of the crystal is known, to determine the angle which separates the two crystals. In this case, the distance between the moiré patterns, D, is related to spacing of the crystal lattice, d, and the angle between the crystals, a (in radians), by

$$D = \frac{d}{\left(2 \sin \frac{1}{2}\alpha\right)}$$

and this can be approximated as

$$D = \frac{d}{\alpha}$$

More detailed information on the significance of moiré patterns can be found in Hirsch *et al.* (1965) and references therein.

Rotation moiré patterns were evident in the TEM shown in Figs. 8.7e and 8.7f. They can be identified as rotation moiré patterns because of their orientation perpendicular to the aragonite crystals. Since the otolith material was confirmed to be aragonite, with a lattice spacing of 0.572 nm (Figs. 8.6d and 8.8), the moiré patterns can be used to estimate the offset between the crystals. The fringes of the moiré pattern in Fig. 8.7e have a spacing that ranges from 3.6 to 7.1 nm, which indicates that the angle between the two crystal lattices is from 9.1° to 4.6°. This wide range was probably due to the presence of impurities and imperfections or dislocations

within the crystal lattice. Dislocations were definitely present on the basis of the irregular form of some of the moiré patterns seen in Figs. 8.7e and 8.7f.

8.4 DISCUSSION

Observations of aragonite prisms and prism ultrastructure of orange roughy and cod do not fully conform with models of otolith structure illustrated by Morales-Nin (1987). This seems to be largely a problem of semantics as well as the flexibility of the model. The separation of the otolith into prisms, which are composed of microcrystals is a model that has been suggested for a range of molluscs (Travis and Gonsalves, 1969; Taylor *et al.*, 1969; Carter, 1980; Wilbur and Saleuddin, 1983). Data do show that protein is present between individual prisms or crystals, but it is difficult to confirm if these structures are polycrystalline. They may simply be large aragonite crystals. It seems plausible that there may be an 'illusion' that otoliths are polycrystalline (i.e. composed of prisms that are, in turn, composed of microcrystals) because of the wide range of prism sizes. Generally, it was not possible to detect any subdivision in the prisms or any discrete structures that were composed of smaller crystals.

From a functional viewpoint, the existence of large crystals in the otolith is not a problem. What appears to be critical in otoliths is their overall size and shape (Platt and Popper, 1981). Small crystal size would probably be a requirement if otoliths were involved in metabolic relationships. Small crystal size, combined with imperfect shape would increase the reactivity of the aragonite crystals (Posner and Betts, 1981), thus, making the materials in the otolith more readily available for metabolic processes. Because otoliths do not appear to be resorbed at any time (Simkiss, 1974; Campana, 1983) this would not be a factor in determining otolith crystal size and shape.

SEM and TEM observations of otolith microincrement form and ultrastructure provide information on the interaction between otolith organic matrix and aragonite. As discussed earlier, the role of otolith organic matrix in otolith formation is not understood. Discontinuous zones where organic matrix appeared to halt aragonite precipitation were common in orange roughy otoliths. Other discontinuous zones appeared to have only reduced aragonite precipitation coupled with an increase in protein deposition. Away from the discontinuous zones the aragonite crystals appeared to be invested with a relatively small amount of organic matrix. However,

SEM showed that some regions of the otolith contained much greater quantities of protein in both the incremental and discontinuous zones.

The complex microstructure of otoliths may not always be due to the combination of a large number of crystal forms (Davies *et al.*, 1988), but may also be due to the high degree of irregularity in the size of aragonite crystals. Differences in orientation, size and shape of crystals may result from several factors. Whatever these factors are, they do seem to indicate that, at the ultrastructural level, fish otoliths are not as uniform as is generally assumed. This structural complexity, combined with variations in precipitation rates and the composition of the endolymph environment can undoubtedly affect the quantities of trace elements that are incorporated into fish otoliths.

8.5 SUMMARY

SEM has been widely used in otolith studies to quantify microincrements with less attention given to the form and interaction of the otolith aragonite crystals and organic matrix. In this study, fractured and sectioned otoliths from several fish species were observed using SEM and TEM. The results suggest that the level of organization of fish otoliths may be lower than is generally assumed and that crystal size and shape are highly variable. The complex mineralogy of fish otoliths can be an important factor in explaining the small scale variability in their trace element chemistry.

CHAPTER 9

GENERAL DISCUSSION

This study has presented an integrated view of the processes involved in the incorporation of trace elements in aragonitic fish otoliths. Such an approach was necessary because of the general lack of understanding of the calcification mechanism, ultrastructure and chemistry of these structures. When compared with the predominant and more conspicuous biogenic calcification systems that occur in nature, such as those found in algae, foraminiferans, scleractinian corals, molluscs and the vertebrate skeleton, which are all poorly understood, the state of knowledge regarding fish otoliths is not surprising.

The majority of research on fish otoliths has concentrated on what is essentially a by-product of their growth, specifically their time keeping properties. The scientific literature dealing with the quantification of annuli and microincrements is extensive and seems to be increasing at an almost exponential rate. The concept of otoliths as recorders of physiological, environmental and life-history information is a logical extension of these time keeping properties. A similar rationale has resulted in an extensive literature on the chemistry of coral skeletons and molluscan shells as has been discussed in Chapter 1. The belief that the composition of biogenic carbonates, and their trace element chemistry in particular, would provide information about both past and present environments has further inspired investigations into carbonate precipitation and trace element incorporation in inorganically precipitated carbonates. Again, there is a large body of literature dealing with both artificial and natural systems involved in inorganic precipitation of calcium carbonate. The precipitation process, whereby the daily or cyclical accretion of biogenic calcium carbonate produces recognizable structures, is clearly linked to the final chemistry of that structure. Even with this most basic understanding, the concept of approaching the ontogenetic structural and chemical growth records in tandem seems reasonable. However, this study has served to underscore several important misconceptions and oversimplifications that are evident in the general approach to investigations of the ontogenetic chemical record in carbonates in general and, in fish otoliths in particular.

Biogenic calcification is clearly an important phenomena in the natural world. It occurs in plants, single cell organisms, a wide range of invertebrates and in all

vertebrates. Yet, the calcification process is not completely understood in any group of organisms. Fortunately, a full understanding of the calcification mechanism does not seem to be a prerequisite for investigating the incorporation of trace elements into calcium carbonate. This is evidenced by the success of the models used to predict Sr/Ca ratios in the otoliths of female cod (Chapter 3). However, many researchers have put a great deal of effort into studies that hoped to predict environmental salinity, temperature and, in some cases, life-history events and growth, without considering the basic features of the systems involved in calcification.

Basic to the comprehension of biogenic calcification systems is an understanding of the compartmentalized nature of biological systems. Williams (1983) described three ways in which biological systems divide space and his divisions can be extended to the organization of elements involved in calcification. The three compartments include:

1) inclusion of ions in an aqueous phase such as body fluids (plasma, endolymph) or within membrane enclosures (cells), the ions may be free, or part of a protein or chelate;

2) bound within proteins or other macromolecules and incorporated as a component of a cell; and

3) precipitation of largely inorganic forms, generally in the form of amorphous or crystalline pellets within cell vesicles.

By analogy, otoliths can be classified in the third category with the sacculus of the pars inferior functioning in a manner which is analogous to an individual cell. The analogy is particularly valid in this case, because, unlike most extracellular fluids which have a high Na/K ratio, the endolymph within the sacculus has a low Na/K ratio, similar to that within cells. With this in mind, it seems reasonable to conclude that many of the interactions involved in producing predominantly inorganic deposits within cell vesicles would also operate within the sacculus.

The idea that otoliths are precipitates within an internally regulated environment necessitates a new approach to the interpretation of microchemical data. To some extent, these principles would also be applicable to the deposition of biogenic carbonates by molluscs, corals, foraminiferans and other organisms. This is due to the fact that the ions which are used in the production of these structures are derived from an internal fluid environment. In the case of molluscs, this environment is the extrapallial fluid which contains inorganic ions derived primarily from the hemolymph

(Wilbur and Saleuddin, 1983). As is the case with the molluscan shell, the calcified structures of corals are in direct contact with the external environment, but this does not mean that ions that make up the skeleton do not pass through the tissues of the animal before precipitation. Hayes and Goreau (1977a, 1977b) located crystalline material within vesicles of the coral animal's ectodermal cells and claimed that these were crystals of aragonite destined for the coral skeleton. Essentially they were proposing intracellular calcification in corals. This interpretation of calcification in corals is not generally accepted (Barnes and Chalker, 1988). However, the calcium in these vesicles is believed to be discharged to the external environment along with additional skeletal components to produce the aragonite of corals (Johnston, 1980).

Despite difficulties in elucidating the nature of the calcification process in both molluscs and corals it is apparent that the mechanism is largely dependent on the production of a suitably supersaturated microenvironment with the appropriate mix of ions and organic material. Lowenstam and Weiner (1983) discuss similar relationships that exist between biogenic carbonates and the organism. Because of these relationships there is little basis for interpreting the trace element chemistry of biogenic carbonates without an understanding of the calcification environment be it endolymph, extrapallial fluid or the microenvironment created outside the body wall of a coral polyp. For this reason, I have stressed the importance of understanding the processes that alter the composition of fish blood plasma and endolymph. The basic relationship among these components, specifically as they relate to calcium and strontium, is shown schematically in Fig. 9.1. Clearly, these points were not considered by Townsend *et al.* (1989), since they calculated distribution coefficients for fish otolith strontium based on ambient seawater as the precipitating environment. Essentially, they have taken the otolith out of the fish and placed it into the sea.

Even though the composition of fish otoliths could be predicted to some degree, the unexplained variability of otolith Sr/Ca, Na/Ca, K/Ca and S/Ca still looms large. Here too, the compartmentalized nature of biological systems must also be understood. The fact that a system or process can be compartmentalized into discrete units or "black boxes" does not infer that the end product of that compartment is fully known. Clearly, the classical black box has always served to indicate that the exact nature of the process is unknown, even if we do know the end product. In the case of biogenic calcification and the related incorporation of trace elements, we do not understand the mechanisms leading to calcification. To add to this, the scale of the

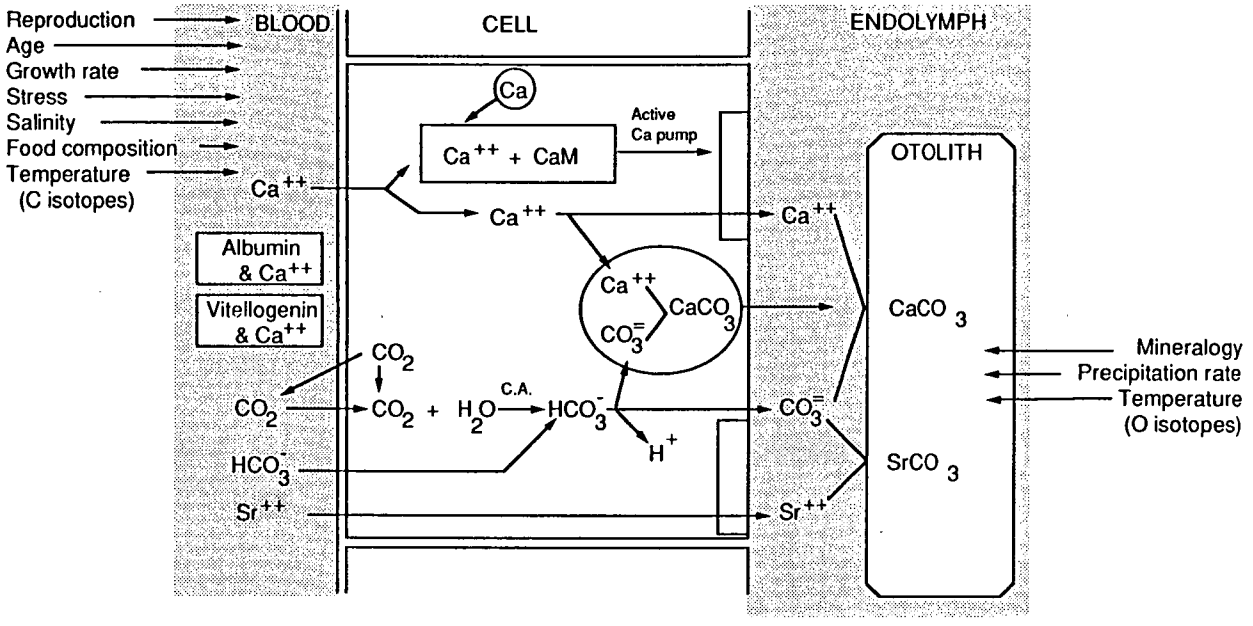

Fig. 9.1 Simplified model indicating the factors that influence blood and endolymph composition and, their interaction with possible metabolic pathways of calcium, strontium and carbonate to the otolith. The region between the blood and the endolymph, represented schematically as a simple cell in this diagram, is actually a series of membranes as discussed in the text. The diagram is largely adapted from Mugiya (1986) and is predominated by his proposed pathways for calcium via a calmodulin protein (CaM) and an active calcium pump. Also shown is the carbonic anhydrase (C.A.) catalyzed conversion of CO_2 to HCO_3^-. Calcium-binding proteins, albumin and vitellogenin, are shown in the blood but these must bind strontium to some degree, as well. Strontium is shown passing to the endolymph via an active calcium pump only, although it may also interact with the calmodulin substrate. There are both indendent and interactive factors which are shown acting on the composition of the blood plasma and the otolith.

process is not understood. For example, in the case of fish otoliths, the tendency would be to place these structures in the milieu of the sacculus and the endolymph therein. However, even if a perfect understanding of the processes that controlled endolymph composition was developed, it would still be difficult to account for the variability of trace elements incorporated in the otolith. And, of course, I am not referring to random variability in this instance.

At this point it would be instructive to return to the first investigative chapter, Chapter 2, and reconsider the 4 levels of variability that were hypothesized to affect otolith trace element chemistry. For clarity I will repeat those points here. On the scale of a single otolith, it is apparent that there are four levels of variability affecting trace element composition:

1) temporal variability which may be largely explained by the physiology of an individual fish and related changes in the composition of the endolymph;

2) spatial variability represented on scales of 5-10 μm as measured by the electron microprobe and within a single increment around an otolith that may be due to inhomogeneity in the distribution of proteins and trace elements in the endolymph;

3) submicron processes at the otolith-endolymph interface that may be dominated by such factors as the orientation of aragonite crystal faces, crystal surface area and the degree of solution saturation; and

4) processes at the molecular level and below relating to both the forces within aragonite crystals and kinetic and thermodynamic properties.

The data on the composition of cod blood plasma and endolymph produced satisfactory results in terms of the ability to deal with the first level of variability in relation to strontium. Also, the basis for variations in the stable isotopes of oxygen and carbon were readily explained, but it is important to remember that these data were collected from whole or, at least, a large portion of individual otoliths. In some cases otoliths were pooled to provide the requisite amount of calcium carbonate for the stable isotope analyses. While it was not possible to gauge the degree of small scale variability in relation to stable isotopes, this was readily accomplished for Sr, Na, K and S by using the electron microprobe. The conclusion was that small scale (within increment) variability was highly significant.

Again, I return to the concept of compartmentalization to assess the nature of the variability described above. There are several factors that could cause the observed variability. As will become apparent when discussing these questions, we are in

danger of becoming ensconced in an insolvable 'chicken or the egg' argument. Whether the small scale variability in otolith trace element chemistry is a function of the biological system or of otolith mineralogy. However, it is, most likely, a combination of the two.

Endolymph fluid is not a homogeneous environment. There will be concentration gradients for the various ions and proteins involved in calcification. The present body of information on the maculae and related secretory structures that surround the otoliths (Dunkelberger *et al.*, 1980; Saitoh and Yamada, 1989) suggests that there could be extreme differences in the nature of the otolith/fluid environment interface. This would be expected given the shape of the otolith, but the factors resulting in otolith shape do not appear to be responsible for the variations in otolith chemistry on scales of less than 10 μm. This conclusion is based on the lack of any relationship between otolith growth rate and otolith trace element composition. Otolith growth rate, in this case, can be directly related to location on the otolith.

Coral polyps are capable of precipitating calcium carbonate outside the confines of their body tissues. This feat appears to be accomplished by creating microenvironments supersaturated with respect to calcium carbonate adjacent to the animal. Compared with the volume of seawater moving over the coral polyp, the controlled volume is minute. Fish otoliths may also precipitate from a similar form of supersaturated microenvironment. The creation of this environment is necessary for the otolith to form because the endolymph usually contains less than 2.0 mM l^{-1} Ca^{++}, and 10 mM l^{-1} are probably required for precipitation. Thus, there appears to be a prerequisite for a supersaturated microenvironment at the otolith surface. Ultrastructural studies of the saccular epithelium, otolithic membrane and otolith indicate that these environments are not uniformly distributed over the otolith (Dunkelberger *et al.*, 1980; Saitoh and Yamada, 1989).

Further variability must be introduced due to the high degree of irregularity displayed by the aragonite crystals or prisms in otoliths. In fact, their irregularity is striking when compared with the uniform, interlocking structures frequently described from molluscs (Travis and Gonsalves, 1969; Clark, 1980). This irregularity accentuates the potential role of precipitation rates (Lorens, 1981) and surface effects (Morse, 1983; Morse, 1986) and how they can alter the levels of trace elements incorporated into calcium carbonate. Further discussion of these principles is beyond the scope of this thesis, but it is important to be aware of the variability that

can be introduced under these conditions.

Geochemists, when confronted with problems in the interpretation of mineralogy and trace element chemistry in biological systems, generally implicate "vital effects" or the presence of organic compounds as their source (Morse, 1983). In inorganic systems the factor of precipitation rates is frequently invoked to explain deviations from empirically based trace element incorporation models (White, 1977; Okumura and Kitano, 1986). Although the initial aim of this research was to interpret otolith trace element chemistry in relation to environmental events, it soon became clear that this was not possible. As a result, a large portion of this thesis has dealt with explanations for the variability of blood plasma and endolymph and how they may relate to the otolith. In part, I have attempted to explain the mystical "vital effects" of biogeochemical systems. From this synthesis it has become clear that complete answers to questions in biogenic calcification will require cooperation among a wide range of disciplines.

Despite the difficulties discussed above, otolith microchemistry may still be valuable to studies of fish biology. The area of stable isotope chemistry appears to have the greatest potential, particularly with the development of laser ablation mass spectrometers which will make it possible to analyse small portions of a sample as in microprobe based systems. Of the trace elements investigated, strontium clearly seems most useful to fish biologists, particularly in studies of diadromous fishes, small scale stock identification and, in some cases, fish ageing studies. These are discussed in detail in the relevant chapters. The use of otolith chemistry to determine the past physiological condition of a fish would be overly complex and there are too many factors operating simultaneously on the fish's physiology. The development of otolith trace element chemistry as a predictor of environmental temperatures or other environmental conditions seems unlikely on the basis of the species investigated here. This last point highlights the need to discriminate among variability that is the result of ontogenetic factors, physiological state and the environment. It is unlikely that these factors can ever be separated completely on the basis of otolith chemistry alone.

REFERENCES

Aharon, P. and J. Chappell. 1983. Carbon and oxygen isotope probes of reef environment histories. In, *Perspectives on coral reefs*, edited by D. J. Barnes. Brain Cloustin Publishers, Canberra, pp. 1-15.

Alderdice, D. F. 1988. Osmotic and ionic regulation in teleost eggs and larvae. In, *Fish Physiology, Vol. XI, Part A*, edited by W. S. Hoar and D. J. Randall. Academic Press, San Diego, p. 163-251.

Allen, G. R. 1975. *Damselfish of the South Seas*. Neptune, New Jersey: Tropical Fish Hobbyist

Amiel, A. J. , G. M. Friedman and D. S. Miller. 1973. Distribution and nature of incorporation of trace elements in modern aragonitic corals. *Sedimentology* 20: 47-64.

Andreasen, P. 1985. Free and total calcium concentrations in the blood of rainbow trout, Salmo gairdneri, during 'stress' conditions. *J. exp. Biol.* 118: 111-120.

Bagenal, T. B. (editor), 1974. *The ageing of fish*. Unwin Brothers, Ltd., England, 234 pp.

Bagenal, T. B., F. J. H. MacKereth, and J. Heron. 1973. The distinction between brown trout and sea trout by the strontium content of their scales. *J. Fish Biol.* 5: 555-557.

Bailey, R. E. 1957. The effect of estradiol on serum calcium, phosphorus, and protein of goldfish. *J. Exp. Zool.* 136: 455-469.

Barnes, D. J. 1970. Coral skeletons: an explanation of their growth and structure. *Science* 170: 1305-1308.

Barnes, D. J. and B. E. Chalker. In press. Calcification and photosynthesis in reef-building corals and algae. In, *Ecosystems of the world: Coral reefs*. Elsevier, Amsterdam.

Bathurst, R. G. C. 1975. *Carbonate sediments and their diagenesis* (2nd edition). Developments in Sedimentology 12, Elsevier Scientific Publ. Co., Amsterdam.

Beeston, B. E. P., R. W. Horne and R. Markham. 1973. *Electron difraction and optical diffraction techniques.* North-Holland Publishing Company, Amsterdam.

Berg, A. 1968. Studies on the metabolism of calcium and strontuim in freshwater fish I. - Relative contribution of direct and intestinal absorption. *Mem. Ist. Ital. Idrobiol.* 23: 161-196.

Berger, W. H., A. W. H. Bé and E. Vincent, (editors), 1981. Oxygen and carbon isotopes in foraminifera. *Paleogeogr., Palaeoclimatol., Palaeoecol.*, 33: 1-277.

Bergot, F. 1979. Effects of dietary carbohydrates and of their mode of distribution on glycaemia in rainbow trout (*Salmo gairdneri*, Richardson). *Comp. Biochem. Physiol.* 64A: 543-547.

Bertin, E. P. 1975. *Principles and practice of x-ray spectrometric analysis.* Plenum Press, New York.

Bevelander, G. and H. Nakahara. 1969. An electron microscopy study of the formation of the nacreous layer in the shell of certain bivalve molluscs. *Calcif. Tiss. Res.* 3: 84-92.

Bilinski, E. and L. J. Gardner. 1968. Effect of starvation on free fatty acid level in blood plasma and muscular tissues of rainbow trout (*Salmo gairdneri*). *J. Fish. Res. Bd. Can.* 25: 1555-1560.

Billings, G. K. and P. C. Ragland. 1968. Geochemistry and mineralogy of the Recent reef and lagoonal sediments south of Belize (British Honduras). *Chem. Geol.* 3: 135-153.

Bilton, H. T. 1974. Effects of starvation and feeding on circulus formation on scales of young sockeye salmon of four racial origins, and of one race of young kokanee, coho and chinook salmon. In, *Ageing of fish*, edited by T. B. Bagenal. Unwin Brothers Ltd, England, pp. 40-70.

Black, E. C. , A. C. Robertson, A. R. Hanslip and W.-G. Chiu. 1960. Alterations in glycogen, glucose and lactate in rainbow and Kamloops trout, *Salmo gairdneri*, following muscular activity. *J. Fish. Res. Bd. Can.* 17: 487-499.

Blacker, R. W. 1969. Chemical composition of the zones in cod (*Gadus morhua* L.) otoliths. *J. Cons. int. Explor. Mer* 33: 107-108.

Blacker, R. W. 1974 Recent advances in otolith studies. In, *Sea Fisheries Research*, edited by F. R. Harden Jones. Paul Eleck, London pp. 67-90.

Blake, D. F. and D. R. Peacor. 1981. Biomineralization in crinoid echinoderms: characterization of crinoid skeletal elements using TEM and STEM microanalysis. *Scanning Electron Microsc* 3: 321-328.

Blackwelder, P. L. and N. Watabe. 1977. Studies on shell regeneration. II. The fine structure of normal and regenerated shell of the freshwater snail *Pomacea paludosa. Biomineralisation* 9: 1-10.

Blattner, P. and J. R. Hulston. 1978. Proportional variations of geochemical $\delta^{18}O$ scales-an interlaboratory comparison. *Geochim. Cosmochim. Acta* 42: 59-62.

Bloomfield, P. 1976. *Fourier analysis of time series: An introduction.* John Wiley and Sons, New York.

Boehlert, G. W. 1985. Using objective criteria and multiple regression models for age determination in fishes. *U. S. Fish. Bull.* 83: 103-117.

Bondar, R. J. L and D. C. Mead. 1974. Evaluation of glucose-6-phosphate dehydrogenase from *Leuconostoc mesenteroides* in the hexokinase method for determining glucose in serum. *Clin. Chem.* 20: 586-590.

Booke, H. E. 1964. Blood serum protein and calcium levels in yearling brook trout. *Prog. Fish-Cult.* 26: 107-110.

Borowitzka, M. A. 1977. Algal calcification. In, *Oceanography and marine biology, annual reviews*, edited by H. Barnes. Aberdeen University Press, Aberdeen, pp. 189-223.

Borowitzka, M. A. 1982. Mechanisms in algal calcification. In, *Progress in phycological research*, edited by F. E. Round and D. J. Chapman. Elsevier Biomedical Press, Amsterdam, pp. 137-177.

Bottinga, Y. and H. Craig. 1969. Oxygen isotope fractionation between CO_2 and water, and the isotopic composition of marine atmospheric CO_2. *Earth Planet. Sci. Lett.* 5: 285-295.

Bradford, M. M. 1976. A rapid and sensitive method for the quantitation of microgram quantities of protein utilizing the principle of protein-dye binding. *Anal. Biochem.* 72: 248-254.

Brett, J. R. and T. D. D. Groves. 1979. Physiological energetics. In, *Fish Physiology, Vol. 8*, edited by W. S. Hoar, D. J. Randall and J. R. Brett. Academic Press, London, pp. 279-352.

Broecker, W. S. 1982. Ocean chemistry during glacial time. *Geochim. Cosmochim. Acta* 46: 1689-1705.

Brothers, E. B. 1984. Otolith studies. *ASIH Spec. Publ.* 1: 50-57.

Brothers, E. B., C. P. Mathews and R. Lasker. 1976. Daily growth increments in otoliths from larval and adult fishes. *U. S. Fish. Bull.* 74: 1-8.

Bruland, K. W. 1983. Trace elements in sea-water. In, *Chemical Oceanography, Vol. 8*, edited by J. P. Riley and R. Chester. Academic Press, London, p. 157-220.

Buchardt, B. and P. Fritz. 1978. Strontium uptake in shell aragonite from the freshwater gastropod *Limnaea stagnalis*. *Science* 199: 291-292.

Buckley, L. J. and F. J. Bulow, 1987. Techniques for the estimation of RNA, DNA and protein in fish. In, *Age and growth of fish*, edited by R. C. Summerfelt and G. E. Hall. Iowa State University Press, Ames,pp. 345-354.

Bulow, F. J., 1987. RNA-DNA ratios as indicators of growth in fish: A review. In, *Age and growth of fish*, edited by R. C. Summerfelt and G. E. Hall. Iowa State University Press, Ames, pp. 45-64.

Burton, W. K., N. Cabrera and F. C. Frank. 1951. The growth of crystals and the equilibrium structure of their surfaces. *Royal Soc. London Phil. Trans.* A243: 299-358.

Busenberg, E. and L. N. Plummer, 1985. Kinetic and thermodynamic factors controlling the distribution of SO_4^{-2} and Na^+ in calcites and selected aragonites. *Geochim. Cosmochim. Acta* 49: 713-725.

Cadot, H. M., J. R. Van Schmus and R. L. Kaesler. 1972. Magnesium in calcite of marine Ostracoda. *Geol. Soc. Amer. Bull.* 83: 3519-3522.

Campana, S. E. 1983. Calcium deposition and otolith check formation during periods of stress in coho salmon, Oncorhynchus kisutch. *Comp. Biochem. Physiol.* 75A: 215-220.

Campana, S. E. , J. A. Gagne and J. Munro. 1987. Otolith microstructure of larval herring (*Clupea harengus*): Image or reality? *Can. J. Fish. Aquat. Sci.* 44: 1922-1929.

Campana, S. E. and J. D. Neilson, 1985. Microstructure of fish otoliths. *Can. J. Fish. Aquat. Sci.* 42: 1014-1032.

Carlstrom, D. 1963. A crystallographic study of vertebrate otoliths. *Biol. Bull.* 125: 441-463.

Carter, J. G. Environmental and biological controls of bivalve shell mineralogy and microstructure. In, *Skeletal growth of aquatic organixms*, edited by D. C. Rhoads and R. A. Lutz. Plenum Press, New York, pp. 69-113.

Casselman, J. M. 1974. Analysis of hard tissue of pike Esox lucius L. with special reference to age and growth, edited byT. B. Bagenal. Unwin Brothers, Ltd., pp. 13-27.England

Casselman, J. M. 1982. Chemical analyses of the optically different zones in eel otoliths. In, *Proc. 1980 North American Eel Conference*, edited by K. H. Loftus. Ont. Minist. Nat. Resour., Ont. Fish. Tech. Rep. Ser. No. 4 pp. 74-82.

Casselman, J. M. 1983. Age and growth assessment of fish from their calcified structures: Techniques and tools. *U. S. Dep. Commer., NOAA Tech. Rep. NMFS* 8: 1-17.

Castaing, R. and A. Guinier. 1949. Sur l'exploration et l'analyse élémentaire d'un échantillon par une sonde électronique. In, *Proceedings of the 1st International Congress on Electron Microscopy*, Delft. pp. 60-66.

Castonguay, M., and G. J. FitzGerald. 1982. Critique de la méthode de distinction entre poissons anadromes et dulcicoles de la même espèce par la teneur en strontium de leurs écailles. *Can. J. Fish. Aquat. Sci.* 39: 1423-1425.

Chalker, B. E. 1981. Skeletogenesis in scleractinian corals: the transport and deposition of strontium and calcium. In, *Handbook of stable strontium*, edited by S. C. Skoryna. Plenum Press, New York pp. 47-63.

Chalker, B. E. 1983. Calcification by corals and other animals on the reef. In, *Perspectives on coral reefs*, edited by D. J. Barnes. Brain Cloustin Publishers, Canberra, pp. 29-45.

Chave, K. E. 1954a. Aspects of the biogeochemistry of magnesium. 1. Calcareous marine organisms. *J. Geol.* 62: 266-283.

Chave, K. E. 1954b. Aspects of the biogeochemistry of magnesium. 2. Calcareous sediments and rocks. *J. Geol.*. 62: 587-599.

Chavin, W. and J. E. Young. 1970. Factors in the determination of normal serum glucose levels of goldfish, *Carassius auratus* L. *Comp. Biochem. Physiol.* 33: 629-653.

Chivas, A. R. , P. De Dekker and J. M. G. Shelley. 1986. Magnesium content of non-marine ostracod shells: A new palaeosalinometer and palaeothermometer. *Palaeogeogr., Palaeoclimatol., Palaeoecol.* 54: 43-61.

Clark, G. R. II. 1968. Mollusk shell: Daily growth lines. *Science* 161: 800-802.

Clark, G. R. II. 1975. Periodic growth and biological rhythms in experimentally grown bivalves. In, *Growth rhythms and the history of the earth's rotation*, edited by G. D. Rosenberg and S. K. Runcorn. John Wiley, London, pp. 103-117.

Comar, C. L., 1967. Some principles of strontium metabolism: implications, applications, limitations. In, *Strontium metabolism*, edited by J. M. A. Lenihan, J. F. Noutit and J. F. Martin. AcademicPress, London, pp. 17-31.

Craig, H. 1953. The geochemistry of the stable carbon isotopes. *Geochim. Cosmochim Acta* 3: 53-92.

Craig, H. 1957. Isotopic standards for carbon and oxygen and correction factors for mass-spectrometric analysis of carbon dioxide. *Geochim. Cosmochim. Acta* 12: 133-149.

Craig, H. 1961. Standard for reporting concentrations of deuterium and oxygen-18 in natural waters. *Science* 133: 1833-1834.

Craik, J. C. A. and S. M. Harvey. 1984a. The magnitudes of three phosphorus-containing fractions in the blood plasma and mature eggs of fishes. *Comp. Biochem. Physiol.* 78B: 539-543.

Craik, J. C. A. and S. M. Harvey. 1984b. A biochemical method for distinguishing between the sexes of fished by the presence of yolk protein in the blood. *J. Fish Biol.* 25: 293-303.

Craik, J. C. A., and S. M. Harvey. 1984c. Egg quality in rainbow trout: the relation between egg viability, selected aspects of egg composition, and time of stripping. *Aquaculture* 40: 115-134.

Crenshaw, M. A. 1972. The inorganic composition of molluscan extrapallial fluid. *Biol. Bull.* 143: 506-512.

Currens, K. P., C. B. Schreck, and H. W. Li. 1988. Reexamination of the use of otolith nuclear dimensions to identify juvenile anadromous and nonanadromous rainbow trout, *Salmo gairdneri. U.S. Fish Bull.* 86: 160-163.

Daly, J. A. and G. Ertingshausen. 1972. Direct method for determining inorganic phosphate in serum with the "centrifiChem". *Clin. Chem.* 18(3): 263-265.

Dannevig, E. H. 1956. Chemical composition of the zones in cod otoliths. *J. Cons. perm. int. Explor. Mer* 21: 156-159.

Das, B. C. 1965. Age-related trends in the blood chemistry and haematology of the Indian carp (*Catla catla*). *Gerontologia* 10: 47-64.

Davies, N. M. , R. W. Gauldie, S. A. Crane and R. K. Thompson. 1988. Otolith ultrastructure of smooth oreo, *Pseudocyttus maculatus*, and black oreo, *Allocyttus* sp., species. *U. S. Fish. Bull.* 86: 499-515.

Degens, E. T. , W. G. Deuser and R. L. Haedrich. 1969. Molecular structure and composition of fish otoliths. *Mar. Biol.* 2: 105-113.

DeNiro, M. J. and S. Epstein. 1978. Influence of diet on the distribution of carbon isotopes in animals. *Geochim. Cosmochim. Acta* 42: 495-506.

Devereux, I. 1967. Temperature measurements from oxygen isotope ratios of fish otoliths. *Science* 155: 1684-1685.

Dillon, J. F. and G. R. Clark II. 1980. Growth-line analysis as a test for contemporaneity in populations. In, *Skeletal growth of aquatic organixms*, edited by D. C. Rhoads and R. A. Lutz. Plenum Press, New York, pp. 395-414.

Dodd, J. R. 1965. Environmental control of strontium and magnesium in *Mytilus*. *Geochim. Cosmochim. Acta* 29: 385-398.

Dodd, J. R. 1967. Magnesium and strontium in calcareous skeletons: A review. *J. Paleontol.* 41: 1313-1329.

Dolman, J. W. 1975. A method for the extraction of environmental and geophysical information from growth records in invertebrates and stromatolites. In, *Growth rhythms and the history of the earth's rotation*, edited by G. D. Rosenberg and S. K. Runcorn. John Wiley, London, pp. 191-222.

Doumas, B. T., W. A. Watson and H. G. Biggs. 1971. Albumin standards and the measurement of serum albumin with bromcresol green. *Clin. Chim. Acta* 31: 87-96.

Draper, N. R. and H. Smith. 1966. *Applied regression analysis*. John Wiley and Sons, Inc., New York.

Dudley, W. C. and D. E. Goodney. 1979. Oxygen isotope content of coccoliths grown in culture. *Deep-Sea Res.* 26A: 495-503.

Dunbar, R. B. and G. Wefer. 1984. Stable isotopic fractionation in benthic foraminifera from the Peruvian continental margin. *Mar. Geol.* 59: 215-225.

Dunkelberger, D., J. M. Dean and N. Watabe. 1980. The ultrastructure of the otolithic membrane and otolith in the juvenile mummichog, *Fundulus heteroclitus*. *J. Morphol.* 163: 367-377.

Duplessy, J. C. , C. Lalou and A. C. Vinot. 1970. Differential Isotopic fractionation in benthic foraminifera and paleotemperatures reassessed. *Science* 168: 250-251.

Edmonds, J. S., M. J. Moran, N. Caputi, and M. Morita. 1989. Trace element analysis of fish sagittae as an aid to stock identification: pink snapper (*Chrysophrys auratus*) in Western Australian waters. *Can. J. Fish. Aquat. Sci.* 46: 50-54.

Edwards, R. J. 1979. Tasman and Coral Sea ten year mean temperature and salinity fields, 1967-1976. *CSIRO (Australia) Div. Fish. Ocean. Report* No. 88 40 pp.

Elliot, J. A. K., N. Bromage, and C. Whitehead. 1979. Effects of oestradiol 17δ on serum calcium and vitellogenin levels in the rainbow trout. *J. Endocrinol.* 83: 54-55.

Emiliani, C. 1954. Depth habitats of some species of pelagic foraminifera as indicated by oxygen isotope ratios. *Am. J. Sci.* 252: 149-158.

Emiliani, C. 1955. Pleistocene temperatures. *J. Geol.* 63: 538-578.

Emiliani, C. 1966. Paleotemperature analysis of Caribbean cores P6304-8 and P6304-9 and a generalized temperature curve for the past 425,000 years. *J. Geol.* 74: 109-126.

Emiliani, C. J. H. Hudson, E. A. Shinn and R. Y. George. 1978. Oxygen and carbon isotopic growth record in a reef coral from the Florida Keys and a deep-sea coral from Blake Plateau. *Science* 202: 627-629.

Emrich, K. D. H. Ehhalt and J. C. Vogel. 1970. Carbon isotope fractionation during the precipitation of calcium carbonate. *Earth Planet. Sci. Lett.* 8: 363-371.

Enger, P. S. 1964. Ionic composition of the cranial and labyrinthine fluids and saccular D. C. potentials in fish. *Comp. Biochem. Physiol.* 11: 131-137.

Epstein, S. and T. Mayeda. 1953. Variation of ^{18}O content of waters from natural sources. *Geochim. Cosmochim. Acta* 4: 213-224.

Epstein, S. R. Buchsbaum, H. A. Lowenstam and H. C. Urey. 1953. Revised carbonate-water isotopic temperature scale. *Bull. Geol. Soc. Amer.* 64: 1315-1326.

Epstein, S. R. Buchsbaum, H. Lowenstam and H. C. Urey. 1951. Carbonate-water isotopic temperature scale. *Bull. Geol. Soc. Amer.* 62: 417-426.

Erez, J. and S. Honjo. 1981. Comparison of isotopic composition of planktonic foraminifera in plankton tows, sediment traps and sediments. *Palaeogeogr., Palaeoclimatol., Palaeoecol.* 33: 129-156.

Fabricand, B. P. , E. S. Imbimbo, M. E. Brey and J. A. Weston. 1966. Atomic absorption analyses for Li, Mg, K, Rb, and Sr in ocean waters. *J. Geophys. Res.* 71: 3917-3921.

Fabricand, B. P., E. S. Imbimbo and M. E. Brey, 1967. Atomic absorption analyses for Ca, Li, Mg, K, Rb, and Sr at two Atlantic Ocean stations. *Deep-Sea Res.*, Vol. 14, pp. 785-789.

Fabricand, B. P., E. S. Imbimbo, M. E. Brey and J. A. Weston, 1966. Atomic absorption analyses for Li, Mg, K, Rb, and Sr in ocean waters. J. Geophys. Res., Vol. 71, pp. 3917-3921.

Fänge, R. A. Larsson and U. Lidman. 1972. Fluids and jellies of the acousticolateralis system in relation to body fluids in *Coryphaenoides rupestris* and other fishes. *Mar. Biol.* 17: 180-185.

Fenton, G. 1985. Ecology and taxonomy of mysids (Mysidacea: Crustacea). Doctoral dissertation, University of Tasmania.

Fischer, W. and J. C. Hureau (editors). 1985. FAO species identification sheets for fishery purposes. Southern Ocean (Fishing areas 48, 58 and 88). FAO, Rome, 2: 233-470.

Fletcher, D. J. 1984. Plasma glucose and plasma fatty acid levels of *Limanda limanda* (L.) in relation to season, stress, glucose loads and nutritional state. *J. Fish. Biol.* 25: 629-648.

Friedman, I. and J. R. O'Neil. 1977. Compilation of stable isotope fractionation factors of geochemical interest. edited by6th ed. *U.S. Geol. Surv. Prof. Pap.* 440 pp.

Fritts, H. C. 1976. *Tree rings and climate.* Academic Press, London

Fritz, P. and S. Poplawski. 1974. ^{18}O and ^{13}C in the shells of freshwater molluscs and their environments. *Earth Planet. Sci. Lett.* 24: 91-98.

Fry, B. and E. B. Sherr. 1984. $\delta^{13}C$ measurements as indicators of carbon flow in marine and freshwater ecosystems. *Contrib. Mar. Sci.* 27: 13-47.

Garrels, R. M. and C. L. Christ. 1965. *Solutions, minerals, and equilibria.* Harper, New York.

Gauldie, R. W., D. A. Fournier, D. E. Dunlop and G. Coote, 1986. Atomic emission and proton microprobe studies of the ion content of otoliths of chinook salmon aimed at recovering the temperature life history of individuals. *Comp. Biochem. Physiol.* 84A: 630-636.

Gauldie, R. W. , E. J. Graynoth and J. Illingworth. 1980. The relationship of the iron content of some fish otoliths to temperature. *Comp. Biochem. Physiol.* 66A: 19-24.

Gauldie, R. W. and A. Nathan. 1977. Iron content of the otoliths of tarakihi (Teleosti: Cheilodactylidae). *N. Z. J. Mar. Freshwater Res.* 11: 179-191.

Gauldie, R. W. and D. G. A. Nelson. 1988. Aragonite twinning and neuroprotein secretion are the cause of daily growth rings in fish otoliths. *Comp. Biochem. Physiol.* 90A: 501-509.

Gausen, D., and O. K. Berg. 1988. Strontium levels in scales and vertebrae of wild and hatchery-reared Atlantic salmon, *Salmo salar* L., smolts. *Aquaculture Fish. Manag.* 19: 299-304.

Gearing, J. N. , P. J. Gearing, D. T. Rudnick, A. G. Requejo and M. J. Hutchins. 1984. Isotopic variability of organic carbon in a phytoplankton-based, temperate estuary. *Geochim. Cosmochim. Acta* 48: 1089-1098.

Geffen, A. J. 1982. Otolith ring deposition in relation to growth rate in herring (*Clupea harengus*) and turbot (*Scophthalmus maximus*) larvae. *Mar. Biol.* 71: 317-326.

Geller, J. D. 1977. A comparison of MDL limits using energy dispersive and wavelength dispersive detectors. *Scanning electron microsc.* 2: 281-287.

Goldstein, J. I., D. E. Newbury, P. Echlin, D. C. Joy, C. Fiori, and E. Lifshin. 1981. Scanning electron microscopy and x-ray microanalysis. Plenum Press, New York.

Gonzales-Garces, A. and A. C. Farina-Perez. 1983. Determining age of young albacore, Thunnus alalunga, using dorsal spines. *U.S. Dep. Commer., NOAA Tech. Rep. NMFS* 8: 117-122.

Goreau, T. J. 1977. Seasonal variations of trace metals and stable isotopes in coral skeleton: physiological and environmental controls. Rosenstiel School of Marine and Atmospheric Science, University of Miami, pp. 425-430.

Graham, J. B. and R. M. Laurs. 1982. Metabolic rate of albacore tuna *Thunnus alalunga. Mar. Biol.* 72: 1-6.

Gross, H. 1976. Calcium und Phosphatgehalt im Blutserum von Forellen in Beziehung zum Teichchemismus. *Fisch u. Umwelt* 2: 93-109.

Grossman , E. L. 1982. Stable isotopes and live benthic foraminifera from the Southern California Borderland. Doctoral dissertation, University of Southern California.

Grossman, E. L. 1984. Carbon isotopic fractionation in live benthic foraminifera-comparison with inorganic precipitate studies. *Geochim. Cosmochim. Acta* 48: 1505-1512.

Grossman, E. L. 1984. Stable isotope fractionation in live benthic foraminifera from the Southern California Borderland. *Palaeogeogr., Palaeoclimatol., Palaeoecol.* 47: 301-327.

Grossman, E. L. and T.-L. Ku. 1986. Oxygen and carbon isotope fractionation in biogenic aragonite: Temperature effects. *Chem. Geol. (Isotope Geoscience Section)* 59: 59-74.

Gunn, J. S., B. D. Bruce, D. M. Furlani, R. E. Thresher and S. J. M. Blaber, 1989. Timing and location of spawning of blue grenadier, Macruronous novaezelandiae (Teleostei: Merlucciidae), in Australian coastal waters. Aust. J. Mar. Freshw. Res. 40: 97-112.

Hallam, A. and N. B. Price. 1968. Environmental and biochemical control of strontium in shells of *Cardium edule*. *Geochim. Cosmochim. Acta* 32: 319-328.

Hara, A. 1987. Studies on female-specific serum proteins (vitellogenin) and egg yolk proteins in teleosts: Immunochemical, physicochemical and structural studies. *Mem. Fac. Fish., Hokkaido University* 34: 1-59.

Hara, A., and H. Hirai. 1978. Comparative studies on immunochemical properties of female specific serum proteins in rainbow trout (*Salmo gairdneri*). *Comp. Biochem. Physiol.* B 59: 339-343.

Hara, A., K. Yamauchi, and H. Hirai. 1980. Studies on female-specific serum protein (vitellogenin) and egg yolk protein in Japanese eel (*Anguilla japonica*). *Comp. Biochem. Physiol.* B 65: 315-320.

Harriss, R. C. 1965. Trace element distribution in molluscan skeletal material I. Magnesium, iron, manganese, and strontium. *Bull. Mar. Sci.* 15: 265-273.

Hayes, F. R., D. A. Darcy, and C. M. Sullivan. 1946. Changes in the inorganic constituents of developing salmon eggs. *J. Biol. Chem.* 163: 621-631.

Hayes, R. L. and N. I. Goreau. 1977a. Intracellular crystal-bearing vesicles in the epidermis of scleractinian corals, *Astrangia danae* (Agassiz) and *Porites porites* (Pallas). *Biol. Bull.* 152: 26-40.

Hayes, R. L. and N. I. Goreau. 1977b. Cytodynamics of coral calcification. In, *Proceedings of the Third International Coral Reef Symposium Vol. 2*, edited by D. L. Taylor. Rosenstiel School of Marine and Atmospheric Science, University of Miami, Miami, pp. 433-438.

Heinrich, K. F. J. 1981. *Electron probe microanalysis.* Van Nostrand, New York.

Heming, T. A. and E. J. Paleczny. 1987. Compositional changes in skin mucus and blood serum during starvation of trout. *Aquaculture* 66: 265-273.

Hille, S. 1982. A literature review of the blood chemistry of rainbow trout, *Salmo gairdneri* Rich. *J. Fish Biol.* 20: 535-569.

Hirsch, P. B. , R. B. Nicholson, A. Howie, D. W. Pashley and M. J. Whelan. 1965. *Electron microscopy of thin crystals.* Butterworths, London.

Horibe, Y. and T. Oba. 1972. Temperature scales of aragonite-water and calcite-water systems. *Fossils* 23/24: 69-79.

Houck, J. E., R. W. Buddemeier, S. V. Smith and P. L. Jokiel, 1977. The response of coral growth and skeletal strontium content to light intensity and water temperature. In, *Proceedings: Third International Coral Reef Symposium, Miami*, edited by D. L. Taylor, pp. 425-431.

Ichikawa, R. 1960. Strontium-calcium discrimination in the rainbow trout. *Rec. Oceanographic Works Jap.* 5: 120-131.

Irie, T. 1955. The crystal texture of the otolith of a marine teleost Pseudosciaena. *J. Fac. Fish. Anim. Husb. Hiroshima Univ.* 1: 1-13.

Irie, T. 1960. The growth of the fish otolith. *J. Fac. fish. Anim. Husb. Hiroshima Univ.* 3: 203-229.

Isa, Y. and M. Okazaki. 1987. Some observations on the Ca -binding phospholipid from scleractinian coral skeletons. *Comp. Biochem. Physiol.* 87B: 507-512.

Jarosewich, E. and I. G. Macintyre, 1983. Carbonate reference samples for electron microprobe and scanning electron microscope analyses. *J. Sed. Petrology*, 53: 677-678.

Jarosewich, E., J. A. Nelen, and J. A. Norberg. 1980. Reference samples for electron microprobe analysis. Geostand. Newslett. 4: 43-47.

Jarosewich, E. and J. S. White, 1987. Strontianite reference sample for electron microprobe and SEM analyses. *J. Sed. Petrology* 57: 762-763.

Jenkins, G. M. and D. B. Watts. 1968. *Spectral analysis and its application.* Holden-Day, San Francisco.

Johnston, I. S. 1977. Aspects of the structure of a skeletal organic matrix, and the process of skeletogenesis in the reef coral *Pocillopora damicornis*. In, *Proceedings: Third International Coral Reef Symposium, Miami*, edited by D. L. Taylor, pp. 447-453.

Johnston, I. S. 1980. The ultrastructure of skeletogenesis in hermatypic corals. *Inter. Rev. Cytology* 67: 171-214.

Jones, C. and E. B. Brothers. 1987. Validation of the otolith increment aging technique for striped bass, *Morone saxatilis*, larvae reared under suboptimal feeding conditions. *U. S. Fish. Bull.* 85: 171-178.

Jonsson, B. 1985. Life history patterns of freshwater resident and sea-run migrant brown trout in Norway. *Trans. Am. Fish. Soc.* 114: 182-194.

Joshi, B. D. 1980. Sex related cyclic variations in blood glucose and cholesterol contents of catfish, *Heteropneustes fossilis*. *Comp. Physiol. Ecol.* 5: 13-16.

Kahn, M. K. 1979. Non-equilibrium oxygen and carbon isotopic fractionation in tests of living planktonic foraminifera. *Oceanol. Acta* 2: 195-208.

Kalish, J. M. 1989. Otolith microchemistry: validation of the effects of physiology, age and environment on otolith composition. *J. Exp. Mar. Biol. Ecol.* 132:

Keith, M. L. and J. N. Weber. 1965. Systematic relationships between carbon and oxygen isotopes in carbonates deposited by modern corals and algae. *Science* 150: 498-501.

Kenchington, T. J. and O. Augustine. 1987. Age and growth of blue grenadier, *Macruronous novaezelandiae* (Hector), in south-eastern Australian waters. *Aust. J. Mar. Freshw. Res.* 38: 625-646.

Killingley, J. S. 1980. Migrations of California gray whales tracked by oxygen-18 variations in their epizoic barnacles. *Science* 207: 759-760.

Killingley, J. S. , R. F. Johnson and W. H. Berger. 1981. Oxygen and carbon isotopes of individual shells of planktonic foraminifera from Ontong-Java Plateau, equatorial Pacific. *Palaeogeogr., Palaeoclimatol., Palaeoecol.* 33: 193-204.

Killingley, J. S. and M. A. Rex. 1985. Mode of larval developement in some deep-sea gastropods indicated by oxygen-18 values of their carbonate shells. *Deep-Sea Res.* 32: 809-818.

Killingley, J. S. and M. Lutcavage. 1983. Loggerhead turtle movements reconstructed from ^{18}O and ^{13}C profiles from commensal barnacle shells. *Estuar., Coast. Shelf Sci.* 16: 345-349.

Kingsley, G. R. 1939. The determination of serum total protein, albumin, and globulin by the biuret reaction. *J. Biol. Chem.* 131: 197-200.

Kinsman, D. J. J. 1969. Interpretation of Sr^{+2} concentrations in carbonate minerals and rocks. *J. Sediment. Petrol.* 39: 486-508.

Kinsman, D. J. J. and H. D. Holland. 1969. The co-precipitation of cations with CaCO -IV. The co-precipitation of Sr with aragonite between 16° and 96°C. *Geochim. Cosmochim. Acta* 33: 1-17.

Kitano, Y. M. Okumura and M. Idogaki. 1975. Incorporation of sodium, chloride and sulfate with calcium carbonate. *Geochem. J.* 9: 75-84.

Korcock, D. E. , A. H. Houston and J. D. Gray. 1988. Effects of sampling conditions on selected blood variables of rainbow trout, *Salmo gairdneri* Richardson. *J. Fish Biol.* 33: 319-330.

Kroopnick, P. 1974. Correlations between ^{13}C and CO_2 in surface waters and atmospheric CO_2. *Earth Planet. Sci. Lett.* 22: 397-403.

Kroopnick, P. 1974. The dissolved O_2-CO_2-^{13}C system in the eastern equatorial Pacific. *Deep-Sea Res.* 21: 211-227.

Kroopnick, P. 1980. The distribution of ^{13}C in the Atlantic Ocean. *Earth Planet. Sci. Lett.* 49: 469-484.

Kroopnick, P. and H. Craig. 1976. Oxygen isotope fractionation in dissolved oxygen in the deep sea. *Earth Planet. Sci. Lett.* 32: 375-388.

Kroopnick, P. R. F. Weiss and H. Craig. 1972. Total CO_2, ^{13}C, and dissolved oxygen-^{18}O at GEOSECS II in the North Atlantic. *Earth Planet. Sci. Lett.* 16: 103-110.

Kulp, J. L., K. K. Turekian and D. W. Boyd. 1952. Sr content of limestones and fossils. *Bull. Geol. Soc. Amer.* 63: 701-716.

Laale, H. W. 1980. The perivitelline space and egg envelopes of bony fishes: a review. *Copeia* 210-226.

Land, L. S. , J. C. Lang and D. J. Barnes. 1977. On the stable carbon and oxygen isotopic composition of some shallow water, ahermatypic scleractinian coral skeletons. *Geochim. Cosmochim. Acta* 41: 169-172.

Land, L. S. and G. K. Hoops. 1973. Sodium in carbonate sediments and rocks: A possible index to the salinity of diagenetic solutions. *J. Sed. Petrol.* 43: 614-617.

Larsson, A. and R. Fänge. 1977. Cholesterol and free fatty acids (FFA) in the blood of marine fish. *Comp. Biochem. Physiol.* 57B: 191-196.

Last, P. R. 1983. Aspects of the ecology and zoogeography of fishes from soft-bottom habitats of the Tasmanian shore zone. Doctoral dissertation, University of Tasmania.

Laurs, R. M., R. Nishimoto and J. A. Wetherall. 1985. Frequency of increment formation on sagittae of North Pacific albacore (*Thunnus alalunga*). *Can. J. Fish. Aquat. Sci.* 42: 1552-1555.

Leach, G. J. and M. H. Taylor. 1977. Seasonal measurements of serum glucose and serum cortisol in a natural population of *Fundulus heteroclitus* L. *Comp. Biochem. Physiol.* 56A: 217-223.

Lech, J. J. 1970. Glycerol kinase and glycerol utilization in trout (*Salmo gairdneri*) liver. *Comp. Biochem. Physiol.* 34: 117-124.

Lee, D. W. , E. D. Prince and M. E. Crow. 1983. Interpretation of growth bands on vertebrae and otoliths of Atlantic bluefin tuna, *Thunnus thynnus*. *U. S. Dep. Commer., NOAA Tech. Rep. NMFS* 8: 61-69.

Lehninger, A. L. 1975. *Biochemistry* (2nd edition). Worth Publishers, Inc., New York.

Levine, B. A. and R. J. P. Williams. 1982. The chemistry of calcium and its biological relevance. In *The role of calcium in biological systems*, Vol. 1., edited by L. J. Anghileri and A. M. Tuffet-Anghileri. CRC Press, Inc., Boca Raton, pp. 3-26.

Linkowski, T. B. and M. Liwoch. 1986. Variations in morphology of orange roughy *Hoplostethus atlanticus* (Trachichthyidae) otoliths from New Zealand waters. *Reports of the Sea Fisheries Institute Gdynia* 21: 43-59.

Lockhart, W. L. and D. A. Metner, 1984. Fish serum chemistry as a pathology tool. In, *Contaminant effects on fisheries*, edited by V. W. Cairns, P. V. Hodson and J. O. Nriagu. John Wiley and Sons, New York, pp. 73-85.

Lorens, R. B. 1978. A study of biological and physical controls on the trace metal content of calcite and aragonite. Doctoral dissertation, University of Rhode Island.

Lorens, R. B. 1981. Sr, Cd, Mn and Co distribution coefficients in calcite as a function of calcite precipitation rate. *Geochim. Cosmochim. Acta* 45: 553-561.

Lorens, R. B. and M. L. Bender. 1980. The impact of solution chemistry on Mytilus edulis calcite and aragonite. Geochim Cosmochim Acta 44: 1265-1278.

Love, R. M. 1970. *The chemical biology of fishes.* Academic Press, London.

Love, R. M. 1980. *The chemical biology of fishes, Vol. 2.* Academic Press, London.

Love, R. M. , I. Robertson and I. Strachan. 1968. Studies on the North Sea cod VI. Effects of starvation. 4. Sodium and potassium. *J. Sci. Fd. Agric.* 19: 415-422.

Lowenstam, H. A. 1954a. Environmental relations of modification compositions of certain carbonate-secreting marine invertebrates. *Proc. Natl. Acad. Sci. U. S. A.* 40: 39-48.

Lowenstam, H. A. 1954b. Factors affecting the aragonite:calcite ratios in carbonate secreting marine organisms. *J. Geol.* 62: 284-322.

Lowenstam, H. A. and S. Weiner. Mineralization by organisms and the evolution of biomineralization. In, *Biomineralization and biological metal accumulation*, edited by P. Westbroek and E. W. de Jong. D. Reidel Publishing Company, pp. 191-203.

Macdonald, J. A., J. C. Montgomery and R. M. G. Wells, 1987. Comparative physiology of Antarctic fishes. In, *Advances in Marine Biology*, edited by J. H. S. Blaxter and A. J. Southward. Academic Press, London, 24: 321-388.

Mann, S. S. B. Parker, M. D. Ross, A. J. Skarnulis and R. J. P. Williams. 1983. The ultrastructure of the calcium carbonate balance organs of the inner ear: an ultra-high resolution electron microscopy study. *Proc. R. Soc. Lond. B* 218: 415-424

McCartney, T. H. 1967. Monthly variations of the serum total cholesterol and serum total lipid-phosphorus of mature brown trout. *Fish. Res. Bull. N. Y.* 30:42-45.

McConnaughey, T. 1989a. ^{13}C and ^{18}O isotopic disequilibrium in biological carbonates: I. Patterns. *Geochim. Cosmochim. Acta* 53: 151-162.

McConnaughey, T. 1989b. ^{13}C and ^{18}O isotopic disequilibrium in biological carbonates: II *In vitro* simulation of kinetic isotope effects. *Geochim. Cosmochim. Acta* 53: 163-171.

McCrea, J. M. 1950. On the isotopic chemistry of carbonates and a paleotemperature scale. *J. Chem. Phys.* 18: 849-857.

McKern, J. L., H. F. Horton, and K. V. Koski. 1974. Development of steelhead trout (*Salmo gairdneri*) otoliths and their use for age analysis and for separating summer from winter races and wild from hatchery stocks. *J. Fish. Res. Board Can.* 31: 1420-142.

Milliman, J. D., 1974. *Marine carbonates.* Springer-Verlag, Berlin.

Moberly, Jr R. 1968. Composition of magnesian calcites of algae and pelecypods by electron microprobe analysis. *Sedimentology* 11: 61-82.

Mommsen, T. P., and P. J. Walsh. 1988. Vitellogenesis and oocyte assembly. In, *Fish Physiology, Vol. XI, Part A*, edited by W. S. Hoar and D. J. Randall. Academic Press, San Diego p. 347-406.

Mook, W. G. , J. C. Bommerson and W. H. Staverman. 1974. Carbon isotope fractionation between dissolved bicarbonate and gaseous carbon dioxide. *Earth Planet. Sci. Lett.* 22: 169-176.

Morales Nin, B. 1986. Chemical composition of the otoliths of the sea bass (*Dicentrarchus labrax*) Linnaeus, 1758) (Pisces, Serranidae). Cybium 10: 115-120.

Morales-Nin, B., 1987. Ultrastructure of the organic and inorganic constituents of the otoliths of the sea bass. In, *Age and growth of fish*, edited by R. C. Summerfelt and G. E. Hall. Iowa State University Press, Ames, pp. 331-343.

Moreau, G., and C. Barbeau. 1979. Différenciation de populations anadromes et dulcicoles de Grands Corégones (Coregonus clupeaformis) par la composition minerale de leurs écailles. *J. Fish. Res. Board Can.* 36: 1439-1444.

Moreau, J. 1987. Mathematical and biological expression of growth in fishes: Recent trends and further developments. In, *Age and growth of fish*, edited by R. C. Summerfeltand G. E. Hall. Iowa State University Press, Ames, pp. 81-113.

Morse, J. W. 1983. The kinetics of calcium carbonate dissolution and precipitation. In, *Carbonates: mineralogy and chemistry*, edited by R. J. Reeder. Mineralogical Society of America, New York, pp. 227-264.

Morse, J. W. 1986. The surface chemistry of calcium carbonate minerals in natural waters: an overview. *Mar. Chem.* 20: 91-112.

Mugiya, Y. 1964. Calcification in fish and shell-fish III. Seasonal occurrence of a prealbumin fraction in the otolith fluid of some fish, corresponding to the period of opaque zone formation in the otolith. *Bull. Jap. Soc. Sci. Fish.* 30: 955-967.

Mugiya, Y. 1965. Calcification in fish and shell-fish-IV. The differences in nitrogen content between the translucent and opaque zones of otolith in some fish. *Bull. Japan. Soc. Sci. Fish.* 31: 896-901.

Mugiya, Y. 1966a. Calcification in fish and shell-fish-V. A study on paper electrophoretic patterns of the acid mucopolysaccharides and PAS-positive materials in the otolith fluid of some fish. *Bull. Jap. Soc. Sci. Fish.* 32: 117-123.

Mugiya, Y. 1966b. Calcification in fish and shell-fish VI. Seasonal change in calcium and magnesium concentrations of the otolith fluid in some fish, with special reference to the zone formation of their otolith. *Bull. Jap. Soc. Sci. Fish.* 32: 549-557

Mugiya, Y. 1974. Calcium-45 behavior at the level of the otolithic organs of rainbow trout. *Bull. Jap. Soc. Sci. Fish.* 40: 457-463.

Mugiya, Y. 1977. Effect of acetazolamide on the otolith growth of goldfish. *Bull. Jap. Soc. Sci. Fish.* 43: 1053-1058.

Mugiya, Y. 1978. Effects of estradiol-17β on bone and otolith calcification in the goldfish, *Carassius auratus*. *Bull. Japan. Soc. Sci. Fish.* 44: 1217-1221.

Mugiya, Y. 1986. Effects of calmodulin inhibitors and other metabolic modulators on in vitro otolith formation in the rainbow trout, *Salmo gairdnerii*. *Comp. Biochem. Physiol.* 84A: 57-60.

Mugiya, Y. 1987. Phase difference between calcification and organic matrix formation in the diurnal growth of otoliths in the rainbow trout, *Salmo gairdneri*. *U. S. Fish. Bull.* 85: 395-401.

Mugiya, Y. and H. Iketsu, 1987. Uptake of aspartic acid and sulfate by calcified tissues in goldfish and tilapia. *Bull. Fac. Fish. Hokkaido Univ.* 38: 185-190.

Mugiya, Y. H. Kawamura and S. Aratsu. 1979. Carbonic anhydrase and otolith formation in the rainbow trout, *Salmo gairdneri*: enzyme activity of the sacculus and calcium uptake by the otolith *in vitro*. *Bull. Jap. Soc. Sci. Fish.* 45: 879-882.

Mugiya, Y., S. Hirabayashi and T. Ohsawa. 1985. Microradiography of otoliths and vertebral centra in the flatfish *Limanda herzensteini* : Hypermineralization in the hyaline zones. *Bull. Japan. Soc. Sci. Fish.* 51: 219-225.

Mugiya, Y. and K. Takahashi, 1985. Chemical properties of the saccular endolymph in the rainbow trout, *Salmo gairdneri*. *Bull. Fac. Fish. Hokkaido Univ.* 36: 57-63.

Mugiya, Y., N. Watabe, J. Yamada, J. M. Dean, D. G. Dunkelberger and M. Shimizu. 1981. Diurnal rhythm in otolith formation in the goldfish, *Carassius auratus*. *Comp. Biochem. Physiol.* 66A: 659-662.

Mulcahy, M. F. 1967. Serum protien changes in diseased Atlantic Salmon. *Nature* 215: 143-144.

Mulcahy, S. A. , J. S. Killingley, C. F. Phleger and W. H. Berger. 1979. Isotopic composition of otoliths from a benthopelagic fish, *Coryphaenoides acrolepis*, Macrouridae: Gadiformes. *Oceanol. Acta* 2: 423-427.

Mulligan, T. J. , F. D. Martin, R. A. Smucker and D. A. Wright. 1987. A method of stock identification based on the elemental composition of striped bass *Morone saxatilis* (Walbaum) otoliths. *J. Exp. Mar. Biol. Ecol.* 114: 241-248.

Munro, H. N. and A. Fleck, 1966. The determination of nucleic acids. In, *Methods of biochemical analysis Vol. 14*, edited by D. Glick. Interscience Publishers, New York, pp. 113-176.

Neilson, J. D., G. L. Geen, and B. Chan. 1985. Variability in dimensions of salmonid otolith nuclei: implications for stock identification and microstructure interpretation. *U. S. Fish. Bull.* 83: 81-89.

Nordeng, H. 1983. Solution to the char problem based on Arctic char (*Salvelinus alpinus*) in Norway. *Can. J. Fish. Aquat. Sci.* 40: 1372-1387.

Norrish, K. and B. W. Chappell. 1977. X-ray fluorescence spectrometry. In, *Physical methods in determinative mineralogy*, edited by J. Zussman. Academic Press, London, pp. 201-272.

North, A. W. 1988. Age of Antarctic fish: Validation of the timing of annuli formation in otoliths and scales. *Cybium* 12: 107-114.

O'Neil, J. R. , R. N. Clayton and T. K. Mayeda. 1969. Oxygen isotope fractionation in divalent metal carbonates. *J. Chem. Phys.* 51: 5547-5558.

Odum, H. T. 1957. Biogeochemical deposition of strontium. *Publ Inst. Mar. Sci. Univ. Texas* 4: 39-106.

Oguri, M. and N. Takada. 1967. Serum calcium and magnesium levels of goldfish, with special reference to the gonadal maturation. *Bull. Japan. Soc. Sci. Fish.* 33: 161-166.

Ohara, M. and R. C. Reid. 1973. *Modelling crystal growth rates from solution.* Prentice-Hall Int'l Series, New York.

Okumura, M. and Y. Kitano. 1986. Coprecipitation of alkali metal ions with calcium carbonate. *Geochim. Cosmochim. Acta* 50: 49-58.

Onuma, N. F. Masuda, M. Hirano and K. Wada. 1979. Crystal structure control on trace element partition in molluscan shell formation. *Geochem. J.* 13: 187-189.

Pannella, G. 1971. Fish otoliths: daily growth layers and periodical patterns. *Science* 173: 1124-1127.

Petersen, I. M. and B. K. Emmersen. 1977. Changes in serum glucose and lipids, and liver glycogen and phosphorylase during vitellogenesis in nature in the flounder (*Platichtys flesus*, L.). *Comp. Biochem. Physiol.* 58B: 167-171.

Phillips, W. J. and N. Phillips. 1980. *An introduction to mineralogy for geologists.* John Wiley and Sons Ltd., Chichester, England.

Pilkey, O. H. and H. G. Goodell. 1963. Trace elements in recent mollusk shells. *Limnol. Oceanogr.* 8: 137-148.

Pitcher, T. J. 1986. Functions of shoaling behavior. In, *The behavior of teleos fish*, edited by T. J. Pitcher. Crown Melor, London pp. 294-337.

Pitcher, T. J., and P. D. M. Macdonald. 1973. Two models for seasonal growth in fishes. *J. Appl. Ecol.* 10: 599-606.

Platt, C. and A. N. Popper. 1981. Fine structure and function of the ear. In, *Hearing and sound communication in fishes*, edited by W. N. Tavolga, A. N. Popper and R. F. Richard. Springer-Verlag, New York, pp. 3-38.

Plummer, L. N. and E. Busenberg. 1987. Thermodynamics of aragonite-strontianite solid solutions: Results from stoichiometric solubility at 25 and 76°C. *Geochim. Cosmochim. Acta* 51: 1393-1411.

Posner, A. S. and F. Betts. Molecular control of tissue mineralization. In, *The chemistry and biology of mineralized connective tissue,* edited by A. Viels. Elsevier North Holland, Inc., Amsterdam, pp. 257-266.

Prince, E. D., and L. M. Pulos (editors), 1983. Proceedings of the international workshop on age determinations of oceanic pelagic fishes: Tunas billfishes, and sharks. *NOAA Tech. Rep. NMFS* 8, 211 pp.

Pytkowicz, R. M. 1983. *Equilibria, nonequilibria, and natural waters.* John Wiley and Sons, New York.

Radtke, R. L. 1983. Chemical and structural characteristics of statoliths from the short-finned squid *Illex illecebrosus. Mar. Biol.* 76: 47-54.

Radtke, R. L. 1984a. Formation and structural composition of larval striped mullet otoliths. *Trans. Amer. Fish.* Soc. 113: 186-191.

Radtke, R. L., 1984b. Cod fish otoliths: Information storage structures.In, The propogation of cod *Gadus morhua* L. *Flodevigen Rapp.*, 1: 273-298.

Radtke, R. L. 1987. Age and growth information available from the otoliths of the Hawaiian snapper, *Pristipomoides filamentosus. Coral Reefs* 6: 19-25.

Radtke, R. L. 1989. Strontium-calcium concentration ratios in fish otoliths as environmental indicators. *Comp. Biochem. Physiol.* 92A: 189-193.

Radtke, R. L., R. A. III Kinzie, and S. D. Folsom. 1988. Age at recruitment of Hawaiian freshwater gobies. *Environ. Biol. Fish.* 23: 205-213.

Radtke, R. L. and B. Morales-Nin. 1989. Mediterranean juvenile bluefin tuna: life history patterns. *J. Fish. Biol.* 35: 485-496.

Radtke, R. L. and T. E. Targett, 1984. Rhythmic structural and chemical patterns in otoliths of the Antarctic fish *Notothenia larseni*: Their application to age determination. *Polar Biol.* 3: 203-210.

Radtke, R. L. , D. F. Williams and P. C. F. Hurley. 1987. The stable isotopic composition of bluefin tuna (*Thunnus thynnus*) otoliths: evidence for physiological regulation. *Comp. Biochem. Physiol.* 87A: 797-801.

Ramdohr, P., and A. El Goresy. 1971. Einiges über den meteoriten von Mundrabilla in Westaustralien. *Chem. Erde* 30: 269-285.

Reed, S. J. B. 1976. *Electron microprobe analysis*. Cambridge University Press, Cambridge.

Reed, S. J. B., and N. G. Ware. 1972. Escape peaks and internal fluorescence in x-ray spectra recorded with lithium drifted silicon detectors. *J. Phys. E: Sci. Inst.* 5: 582-585.

Reeder, R. J. (editor). 1983. *Carbonates: Mineralogy and chemistry*. Reviews in Mineralogy Vol. 11, Mineralogical Society of America, New York.

Rhoads, D. C. and R. A. Lutz, (editors), 1980. *Skeletal growth of aquatic organisms*. Plenum Press, New York, 750 pp.

Robertson, D. R. 1973. Field observations on the reproductive behaviour of a pomacentrid fish, *Acanthochromis polyacanthus*. *Z. Tierpsychol.* 32: 319-324.

Robinson, P. 1980. Determination of calcium, magnesium, manganese, strontium, sodium and iron in the carbonate fraction of limestones and dolomites. *Chem. Geol.* 28: 135-146.

Robinson, J. and J. Mead. 1973. Lipid absorption and deposition in rainbow trout (*Salmo gairdneri*). *Can. J. Biochem.* 51: 1050-1058.

Romanek, C. S. , D. S. Jones, D. F. Williams, D. E. Krantz and R. Radtke. 1987. Stable isotopic investigation of physiological and environmental changes recorded in shell carbonate from the giant clam *Tridacna maxima*. *Mar. Biol.* 94: 385-393.

Rosenberg, G. D. 1980. An ontogenetic approach to the environmental significance of bivalve shell chemistry. In, *Skeletal growth of aquatic organixms*, edited by D. C. Rhoads and R. A. Lutz. Plenum Press, New York, pp. 133-168.

Rosenberg, G. D. , M. Ashton, R. Hewitt and D. J. Simmons. 1980. Application of normalized power spectra to the analysis of chemical and structural growth patterns. In, *Skeletal growth of aquatic organixms*, edited by D. C. Rhoads and R. A. Lutz. Plenum Press, New York, pp. 675-686.

Rosenberg, G. D. and C. B. Jones. 1975. Approaches to chemical periodicities in molluscs and stromatolites. In, *Growth rhythms and the history of the earth's rotation*, edited by G. D. Rosenberg and S. K. Runcorn. John Wiley, London, pp. 223-242.

Rosenberg, G. D. and D. J. Simmons. 1980a. Rhythmic dentinogenesis in the rabbit incisor: circadian, ultradian, and infradian periods. Calcif. Tissue Int. 32: 29-44.

Rosenberg, G. D. and D. J. Simmons. 1980b. Rhythmic dentinogenesis in the rabbit incisor: allometric aspects. Calcif. Tissue Int. 32: 45-53.

Rosenthal, H. L. 1981. Content of stable strontium in man and animal biota. In, *Handbook of stable strontium*, edited by S. C. Skoryna. Plenum Press, New York pp. 503-514.

Rosenthal, H. L., M. M. Eves, and O. A. Cochran. 1970. Common strontium of mineralized tissues from marine and sweet water animals. *Comp. Biochem. Physiol.* 32: 445-450.

Ross, M. D. and K. M. Donovan. 1986. Otoconia as test masses in biological accelerometers: what can we learn about their formation from evolutionary studies and from work in microgravity. *Scanning Electron Microscopy* 4: 1695-1704.

Rubinson, M. and R. N. Clayton. 1969. Carbon-13 fractionation between aragonite and calcite. *Geochim. Cosmochim. Acta* 33: 997-1002.

Rybock, J. T., H. F. Horton, and J. L. Fessler. 1975. Use of otoliths to separate juvenile steelhead trout from juvenile rainbow trout. *U. S. Fish. Bull.* 73: 654-659.

Rye, D. M. and M. A. Sommer. 1980. Reconstructing paleotemperature and paleosalinity regimes with oxygen isotopes. In, *Skeletal growth of aquatic organixms*, edited by D. C. Rhoads and R. A. Lutz. Plenum Press, New York, pp. 169-202.

Saitoh, S. and J. Yamada. 1989. Ultrastructure of the saccular epithelium and the otolithic membrane in relation to otolith growth in tilapia, *Oreochromis niloticus* (Teleostei: Cichlidae). *Trans. Am. Microsc. Soc.* 108: 223-238.

Saxena, S. K. 1973. *Thermodynamics of rock-forming crystalline solutions.* Springer-Verlag, New York, 188 pp.

Schneider, R. C. and S. V. Smith. 1982. Skeletal Sr content and density in *Porites* spp. in relation to evnvironmental factors. *Mar. Biol.* 66: 121-131.

Sena, S. F. and G. N. Bowers, Jr. 1988. Measurement of ionized calcium in biological fluids: ion-selective electrode method. In, *Methods in enzymology, Vol 158*, edited byJ. F. Riordan and B. L. Vallee. Academic Press, San Diego, pp. 320-334.

Shackleton, N. J. 1974. Attainment of isotopic equilibrium between ocean water and the benthonic foraminifera genus *Uvigerina*: isotopic changes in the ocean during the last glacial. *Colloq. Int. C. N. R. S.* 219: 203-209.

Shackleton, N. J. 1977. Carbon-13 in Uvigerna: tropical rainforest history and the equatorial Pacific carbonate dissolution cycles. In, *The fate of fossil fuel CO_2 in the oceans*, edited by N. R. Anderson and A. Malahoff. Plenum Press, New York, pp. 401-428.

Shackleton, N. J. , J. D. H. Wiseman and H. A. Buckley. 1973. Non-equilibrium isotopic fractionation between seawater and planktonic foraminiferal tests. *Nature* 242: 177-179.

Shackleton, N. J. and E. Vincent. 1978. Oxygen and carbon isotope studies in Recent foraminifera from the southwest Indian Ocean. *Mar. Micropaleontol.* 3: 1-13.

Sharp, G. D. 1978. Behavioral and physiological properties of tunas and their effects on vulnerability to fishing gear. In, *The physiological ecology of tunas*, edited by G. D. Sharp and A. E. Dizon. Academic Press, San Francisco, pp. 397-449.

Sharp, G. D. and S. W. Pirages. 1978. The distribution of red and white swimming muscles, their biochemistry, and the biochemical phylogeny of selected scombrid fishes. In, *The physiological ecology of tunas*, edited by G. D. Sharp and A. E. Dizon. Academic Press, San Francisco, pp. 41-78.

Shimshoni, M. 1971. On Fisher's test of significance in harmonic analysis. *Geophys. J. R. Astron. Soc.* 23: 373-377.

Shul'man, G. E. 1974. *Life cycles of fish: Physiology and biochemistry*. John Wiley and Sons, New York, 258 pp.

Simkiss, K. 1974. Calcium metabolism of fish in relation to ageing. In, *Ageing of fish*, edited by T. B. Bagenal. Unwin Bros. Ltd., London, pp. 1-12.

Skoryna, S. C. (editor), 1981. *Handbook of stable strontium*. Plenum Press, New York.

Smith, Jr K. L. and N. O. Brown. 1983. Oxygen consumption of pelagic juveniles and demersal adults of the deep-sea fish *Sebastolobus altivelis*, measured at depth. *Mar. Biol.* 76: 325-332.

Smith, K. L. , Jr. 1978. Metabolism of the abyssopelagic rattail *Coryphaenoides armatus* measured *in situ*. *Nature* 274: 362-364.

Smith, K. L. , Jr. and R. R. Hessler. 1974. Respiration of benthopelagic fishes: *in situ* measurements at 1230 meters. *Science* 184: 72-73.

Smith, S. V. , R. W. Buddemeier, R. C. Redalje and J. E. Houck. 1979. Strontium-calcium thermometry in coral skeletons. *Science* 204: 404-407.

Smith, S. V. and P. Kroopnick. 1981. Carbon-13 isotopic fractionation as a measure of aquatic metabolism. *Nature* 294: 252-253.

Snieszko, S. F., 1972. Nutritional fish diseases. In, *Fish nutrition*, edited by J. E. Halver. Academic Press, New York, pp. 403-437.

Sokal, R. R. and C. D. Michener. 1958. A statistical method for evaluating systematic relationships. *Univ. Kansas Sci. Bull.* 38: 1409-1438.

Sokal, R. R. and F. J. Rohlf, 1969. *Biometry* (1st edition). W. H. Freeman and Co., San Francisco.

Sokal, R. R. and F. J. Rohlf, 1981. *Biometry* (2nd edition). W. H. Freeman and Co., San Francisco.

Sokal, R. R. and P. H. A. Sneath. 1963 *Numerical taxonomy*. 1963. W. H. Freeman and Son, San Francisco.

Spero, H. J. and D. F. Williams. 1988. Extracting environmental information from planktonic foraminiferal $\delta^{13}C$ data. *Nature* 335: 717-719.

Stanley, C. A. 1978. Area of distribution, movements, age composition and mortality rates of the Australian salmon population in Tasmania, Victoria and New South Wales. *Aust. J. Mar. Freshwater Res.* 29: 417-433.

Stanley, C. A. and W. B. Malcom. 1977. Reproductive cycles in the eastern subspecies of the Australian salmon, *Arripis trutta marginata*. *Aust. J. Mar. Freshwater Res.* 28: 287-302.

Statham, P. J. 1981. X-ray microanalysis with Si (Li) detectors. *J. Microsc.* 123: 1-23.

Summerfelt, R. C. and G. E. Hall, (editors), 1987. *Age and growth of fish.* Iowa State University Press, Ames, 544 pp.

Swart, P. K. 1983. Carbon and oxygen isotope fractionation in scleractinian corals: a review. *Earth Sci. Rev.* 19: 51-80.

Tanaka, N. M. C. Monaghan and D. M. Rye. 1986. Contribution of metabolic carbon to mollusc and barnacle shell carbonate. *Nature* 320: 520-523.

Tarutani, T. R. N. Clayton and T. K. Mayeda. 1969. The effect of polymorphism and magnesium substitution on oxygen isotope fractionation between calcium carbonate and water. *Geochim. Cosmochim. Acta* 33: 987-996.

Taylor, B. E. and P. D. Ward. 1983. Stable isotopic studies of *Nautilus macromphalus* Sowerby (New Caledonia) and *Nautilus pompilius* L. (Fiji). *Palaeogeogr., Palaeoclimatol., Palaeoecol.* 41: 1-116.

Taylor, J. D., W. J. Kennedy and A. Hall. 1969. The shell structure and mineralogy of the bivalvia. Introduction. Nuculacea-Trigonacea. *Bull. Br. Mus. (Nat. Hist.)* 3: 1-125.

Thode, H. G. , M. Shima, C. E. Rees and K. V. Krishnamurty. 1965. Carbon-13 isotope effects in systems containing carbon dioxide, bicarbonate, carbonate, and metal ions. *Can. J. Chem.* 43: 582-595.

Thompson, G. and H. D. Livingston. 1970. Strontium and uranium concentrations in aragonite precipitated by some modern corals. *Earth Planet. Sci. Lett.* 8: 439-442.

Thompson, T. G. and T. J. Chow. 1955. The strontium-calcium atom ratio in carbonate-secreting marine organisms. *Deep-Sea Res*earch 3: 20-39.

Thresher, R. E. 1985. Brood-directed parental aggression and early brood loss in the coral reef fish, *Acanthochromis polyacanthus* (Pomacentridae). *Anim. Behav.* 33: 897-907.

Townsend, D. W. , R. L. Radtke, M. A. Morrison and S. D. Folsom. 1989. Recruitment implications of larval herring overwintering distributions in the Gulf of Maine inferred using a new otolith technique. *Mar. Ecol. Prog. Ser.* 55: 1-13.

Travis, D. F. and M. Gonsalves. 1969. Comparative ultrastructure and organization of the prismatic region of two bivalves and its possible relation to the chemical mechanism of boring. *Am. Zool.* 9: 635-661.

Turekian, K. 1955. Paleoecological significance of the strontium-calcium ratio in fossils and sediments. *Bull. Geol. Soc. Amer.* 66: 155-158.

Turekian, K. K. and R. L. Armstrong. 1960. Magnesium, strontium, and barium concentrations and calcite-aragonite ratios of some recent molluscan shells. J. Mar. Res. 18: 133-151.

Turekian, K. K. and K. H. Wedepohl. 1961. Distribution of the elements in some major units of the earth's crust. *Geol. Soc. Amer. Bull.* 72: 175-182.

Turner, J. V. 1982. Kinetic fractionation of carbon-13 during calcium carbonate precipitation. *Geochim. Cosmochim. Acta* 46: 1183-1191.

Umminger, B. L. 1969. Physiological studies on super-cooled killifish (*Fundulus heteroclitus*)-I. Serum inorganic constituents in relation to osmotic and ionic regulation at subzero temperature. *J. exp. Zool.* 172: 283-302.

Urey, H. C. 1947. The thermodynamic properties of isotopic substances. *J. Chem. Soc.* 562-581.

Urist, M. R., and A. O. Schjeide, 1961. The partition of calcium and protein in the blood of oviparous verterbrates during estrous. *J. Gen. Physiol.* 44: 743-756.

Ursin, E., 1963. On the seasonal variation of growth rate and growth parameters in Norway Pout *Gadus esmarkii* in the Stagerrak. *Meddr. Danm. Fisk. og Havunders N. S.* 4: 17-29.

Veizer, J. 1983. Trace elements and isotopes in sedimentary carbonates. In, *Carbonates: mineralogy and chemistry*, edited by R. J. Reeder. Mineralogical Society of America, New York, pp. 265-300.

Vinot-Bertouille, A. C. and J. C. Duplessy. 1973. Individual isotopic fractionation of carbon and oxygen in benthic foraminifera. *Earth Planet. Sci. Lett.* 18: 247-252.

Wada, K. and T. Fujinuki. 1976. Biomineralization in bivalve molluscs with emphasis on the chemical composition of the extrapallial fluid. In, *The mechanism of mineralization in the invertebrates and plants*, edited by N. Watabe and K. M. Wilbur. University of South Carolina Press, pp. 175-190.

Wadkins, C. L. and C. F. Peng, 1981. Strontium metabolism and mechanism of interaction with mineralized tissues. In, *Handbook of stable strontium*, edited by S. C. Skoryna. Plenum Press, New York, pp. 545-561.

Wahlefeld, A. W. 1974. Triglycerides: determination after enzymatic hydrolysis. In, *Methods of enzymatic analysis* 2nd English edition, edited by H. U. Bergmeyer. Academic Press, New York, pg. 1831-1835.

Wang, J., C. C. Chen and S. Osaki. 1983. Optimization of the phosphorus-UV reagent. *Clin. Chem.* 29: 1255.

Wardle, C. S. 1972. The changes in blood glucose in *Pleuronectes platessa* following capture from the wild: a stress reaction. *J. Mar. Biol. Ass. U. K.* 52: 635-651.

Warner, M. C. , A. M. Tomb and S. A. Diehl. 1979. Variability and stability of selected components in rainbow trout Salmo gairdneri serum and the precision of automated analysis in measuring these components. *J. Fish. Biol.* 15: 141-151.

Watabe, N. 1983. Shell repair. In, *The mollusca, Vol. 4*, edited by A. S. M. Saleuddin and K. M. Wilbur. Academic Press, New York, pp. 289-316.

Watabe, N., K. Tanaka, J. Yamada and J. M. Dean. 1982. Scanning electron microscope observations of the organic matrix in the otolith of the teleost fish *Fundulus heteroclitus* (Linnaeus) and *Tilapia nilotica* (Linnaeus). *J. Exp. Mar. Biol. Ecol.* 58: 127-134.

Watanabe, Y. and H. Miyamoto. 1973. Biochemical study of labyrinthine fluids (of the fish). *Med. J. Osaka Univ.* 23: 273-282.

Weber, J. N. 1973. Incorporation of strontium into reef coral skeletal carbonate. *Geochim. Cosmochim. Acta* 37: 2173-2190.

Weber, J. N. and D. M. Raup. 1966. Fractionation of the stable isotopes of carbon and oxygen in marine calcareous organisms-the Echinoidea: II. Environmental and genetic factors. *Geochim. Cosmochim. Acta* 30: 705-736.

Weber, J. N. and P. M. J. Woodhead. 1970. Carbon and oxygen isotope fractionation in the skeletal carbonate of reef-building corals. *Chem. Geol.* 6: 93-117.

Wedemeyer, G. A. 1981. The physiological response of fishes to the stress of intensive aquaculture in recirculating systems. In, *Aquaculture in heated effluents and recirculating systems* Vol. II, edited by K. Tiews. Heenermann, Berlin, pp. 3-18.

White, A. and T. C. Fletcher. 1985. Seasonal changes in serum glucose and condition of the plaice, Pleuronectes platessa L. *J. Fish Biol.* 26: 755-764.

White, A., T. C. Fletcher and J. A. Pope. 1986. Seasonal changes in serum lipid composition of the plaice, Pleuronectes platessa L. *J. Fish. Biol.* 28: 595-606.

White, A. F. 1977. Sodium and potassium coprecipitation in aragonite. *Geochim. Cosmochim. Acta* 41: 613-625.

Whitehead, C. and N. R. Bromage. 1978. Seasonal changes in the reproductive function of rainbow trout. *J. Fish. Biol.* 12: 601-608.

Whitehead, C., N. R. Bromage, R. Harbin and A. J. Matty. 1980. Oestradiol-17β, calcium and vitellogenin interrelationships during accelerated and biannual spawnings in rainbow trout. *Gen. Comp. Endocrinol.* 40: 329-330.

Wiechiers, H. N. S., P. Sturrock and G. V. R. Morais. 1975. Calcium carbonate crystallization kinetics. Water Res. 9: 835- 845.

Wilbur, K. M. and A. S. M. Saleuddin. Shell formation. In, *The mollusca, Vol. 4*, edited by A. S. M. Saleuddin and K. M. Wilbur. Academic Press, New York, pp. 235-287.

Williams, D. F. , A. W. H. Bé and R. G. Fairbanks. 1981. Seasonal stable isotopic variations in living planktonic foraminifera from Bermuda plankton tows. *Palaeogeogr., Palaeoclimatol., Palaeoecol.* 33: 711-102.

Williams, D. F. , M. A. Sommer and M. L. Bender. 1977. Carbon isotopic compositions of Recent planktonic formanifera of the Indian Ocean. *Earth Planet. Sci. Lett.* 36: 391-403.

Williams, R. J. P. 1983. Inorganic elements in biological space and time. *Pure and Appl. Chem.* 55: 1089-1100.

Wolf, K. H., G. V. Chilingar and F. W. Beals. 1967. Elemental composition of carbonate skeletons, minerals and sediments. In, *Carbonate rocks, developments in sedimentology*, Vol. 9B, edited by G. V. Chilingar, H. J. Bissel and R. W. Fairbridge. Elsevier, Amsterdam, pp. 23-150.

Woodhead, A. D., 1979. Senescence in fishes. *Sym. Zool. Soc. London* 44: 179-205.

Woodhead, P. M. J. 1968. Seasonal changes in the calcium content of the blood of arctic cod. J. Mar. Biol. Ass. U. K. 48: 81-91.

Woodhead, P. M. J. and P. A. Plack. 1968. On levels of calcium and of vitamin A aldehyde in the blood of Arctic cod. *J. Mar. Biol. Ass. U. K.* 48: 93-96.

Wydoski, R. S. , G. A. Wedemeyer and N. C. Nelson. 1976. Physiological response to hooking stress in hatchery and wild rainbow trout (Salmo gairdneri). *Trans. Am. Fish. Soc.* 5: 601-606.

Zeitoun, I. H., D. E. Ullrey, W. G. Bergen, and W. T. Magee. 1976. Mineral metabolism during the ontogenesis of rainbow trout (*Salmo gairdneri*). *J. Fish. Res. Board Can.* 33: 2587-2591.

APPENDIX 1

QUANTITATIVE DETERMINATION OF TRACE ELEMENTS IN FISH OTOLITHS BY X-RAY FLUORESCENCE SPECTROMETRY AND ATOMIC ABSORPTION SPECTROPHOTOMETRY

Investigations of otolith trace element chemistry by wavelength dispersive electron microprobe are limited to only a few elements, due to the relative insensitivity of the method when compared with readily available techniques such as flame atomic absorption spectrophotometry (FAAS), graphite furnace atomic absorption spectrophotometry (GFAAS) and x-ray fluorescence spectrometry (XRF). The advantage of the electron microprobe lies in the ability to nondestructively determine sample composition over very small spatial scales. However, in the interest of determining elements that could be detected with the electron microprobe several determinations of otolith trace metal content were made using FAAS and XRF techniques.

Details of the methods used can be found in Robinson (1980) and Norrish and Chappell. For FAAS analysis individual whole otoliths were dissolved in 1.0 M HCl at room temperature. FAAS analyses were carried out using an air-acetylene flame on a Varian AA6 spectrophotometer. Groups of otoliths were pooled by species for the XRF analyses due to the need for a mininum sample size of approximately 3 g. Samples were ground to a fine powder in a tungsten mill and then pressed into pellets with a boric acid backing by using a hydraulic press. XRF analyses were performed with a Philips PW1410 X-ray spectrometer. Species analysed included orange roughy *Hoplostethus atlanticus*, gemfish *Rexea solandri* and Australian salmon *Arripis trutta*. All samples were from Tasmanian waters.

Results are presented in the two tables below.

Table A1.1 Results of FAAS analyses of fish otoliths. All values are in ppm±1SD. N=5 for each value

Sample	Zn	Fe	Mg
H. atlanticus	6.2±0.6	18.6±1.5	12.4±0.7
R. solandri	5.9±0.5	12.2±1.1	15.1±1.4
A. trutta	7.4±0.8	20.9±0.8	15.9±0.6
A. esper	7.7±0.3	20.4±1.0	16.8±0.9

Table A1.2 Results of XRF analyses of fish otoliths. All values are in ppm. A value prefaced by a '<' sign indicates that the element was not detected by the instrument and in these cases the value tabulated is the minimum detection limit.

Sample	Zn	Cu	Cd	Ni	Cr	V	Ba
H. atlanticus (males and females<40 cm)	7	<1	<3	2	3	<3	7
H. atlanticus (males >40 cm)	7	1	<3	3	<2	<3	15
H. atlanticus (females >40 cm)	<1	2	<3	1	<2	<3	10
R. solandri (males)	4	<1	<3	2	4	<3	<3
R. solandri (females)	7	7	<3	2	<2	4	5
A. trutta (males)	4	3	<3	2	4	<3	4
A. trutta (females)	6	2	<3	2	2	5	7

These results indicate that most metals are present in fish otoliths at levels far below the detection limits of the wavelength dispersive electron microprobe. Levels of Cd were always below the level of detection by XRF and the other elements were frequently near the detection limit. In fact, the samples of otolith aragonite were generally of higher purity than the materials used as blanks for the x-ray spectrometer, and additional otolith samples were requested by the XRF analyst to be used as blanks in the future.

APPENDIX 2

MICROPROBE TRANSECTS FROM JUVENILE AUSTRALIAN SALMON

The Sr/Ca ratio transect data on the next 13 pages were collected in the investigation of microprobe analysis as a tool for 'stock discrimination' and the characterization of nursery grounds (Section 4.4). The transects show the Sr/Ca ratio data without any smoothing or manipulation. The collection sites are indicated on a map shown in Fig. 4.4 and they are referred to in Table 4.2 The collection site water temperature is also shown in Table 4.2. In this appendix the data have been grouped on the basis of collection date.

Marieville Esplanade (13 November 1985)

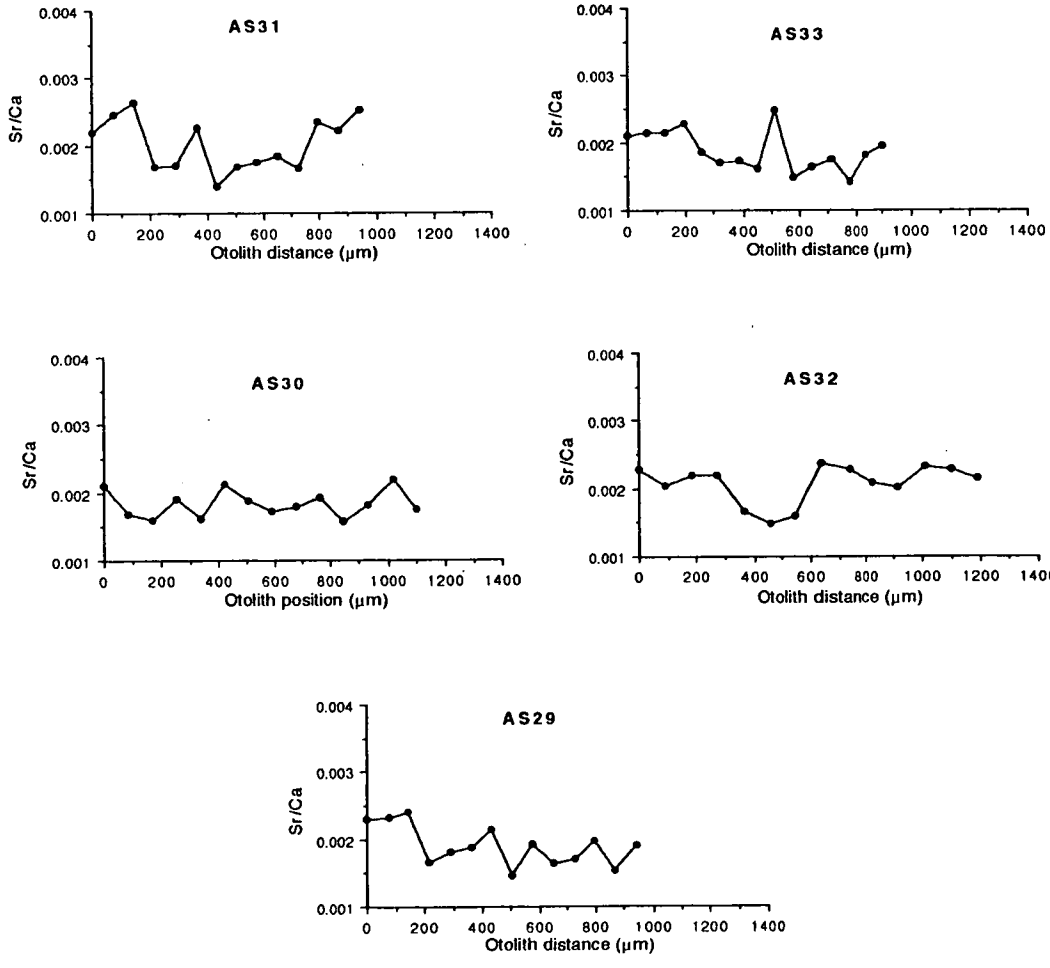

Nutgrove Beach (14 October 1986)

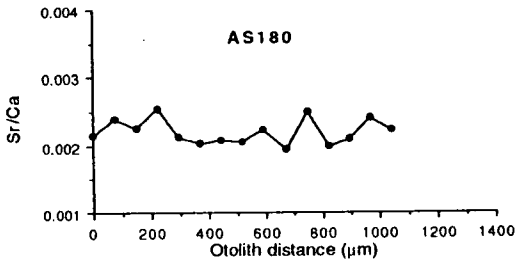

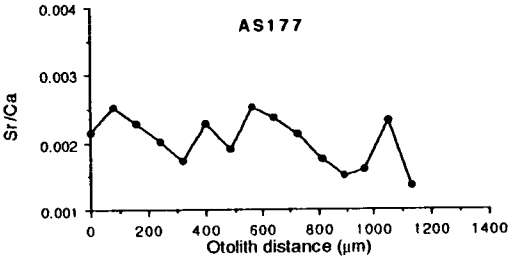

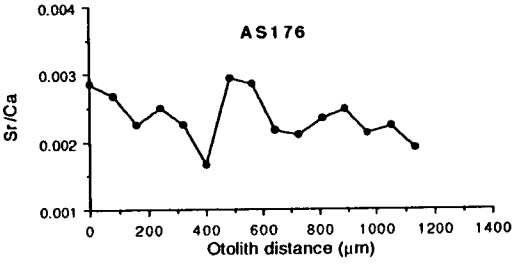

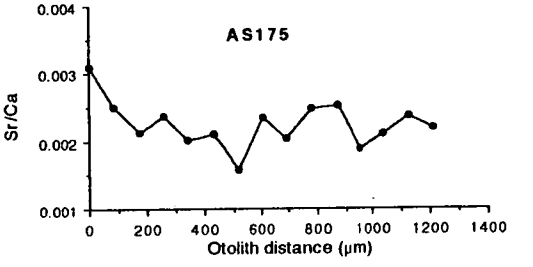

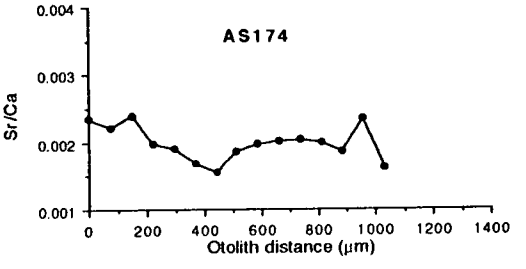

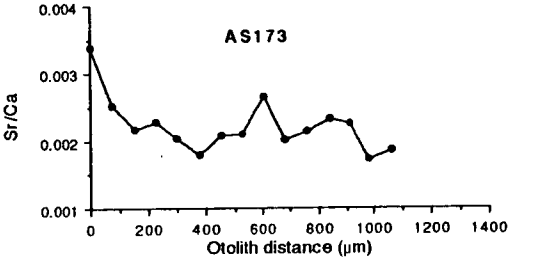

Cremorne Beach (28 March 1987)

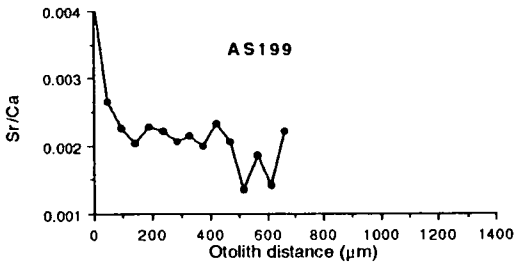

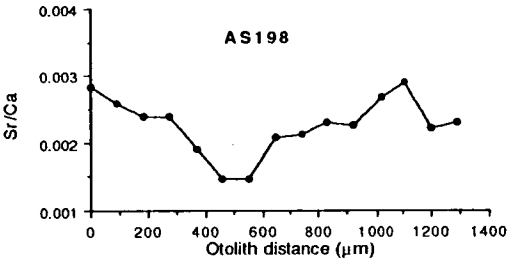

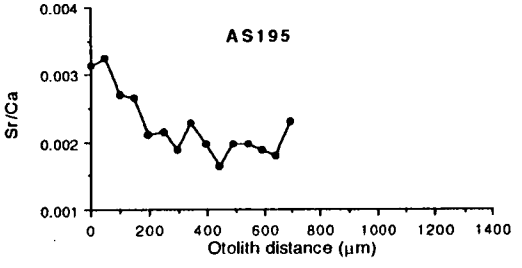

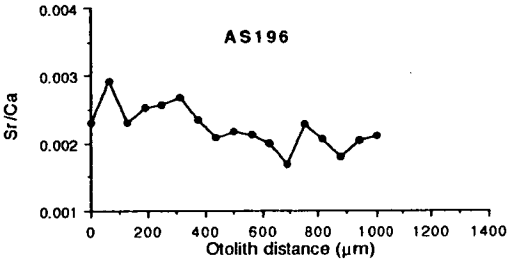

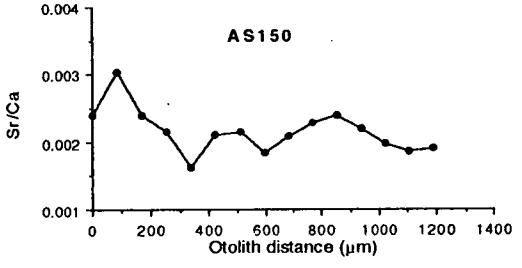

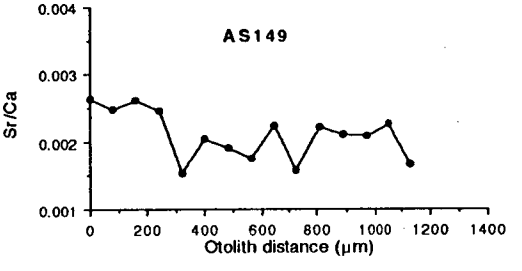

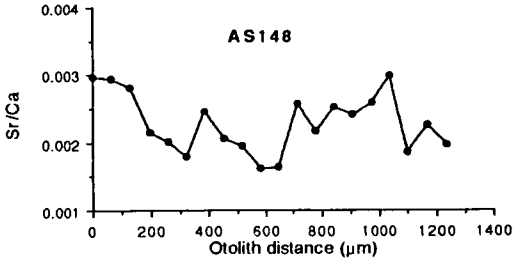

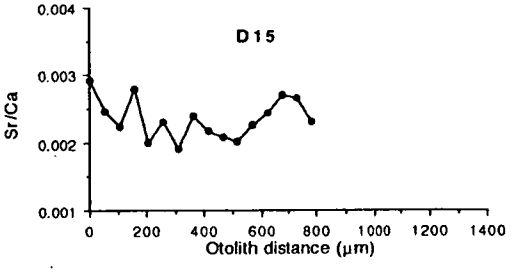

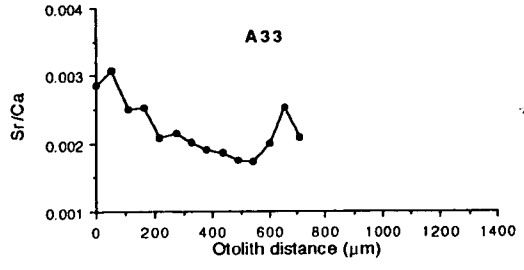

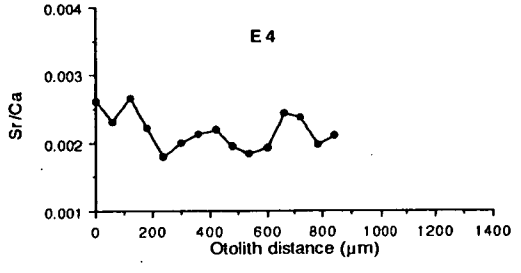

Cremorne Beach (19 April 1987)

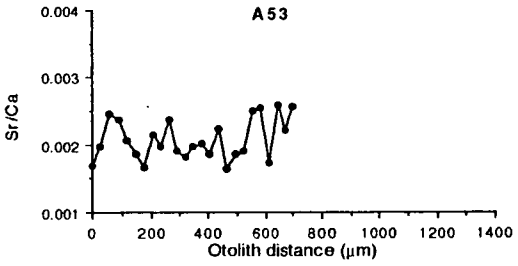

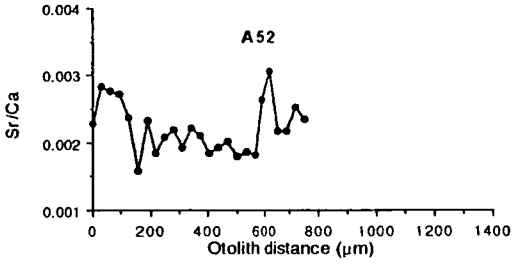

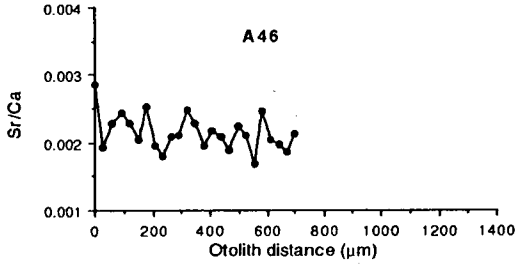

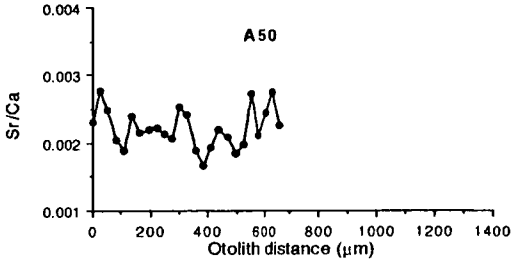

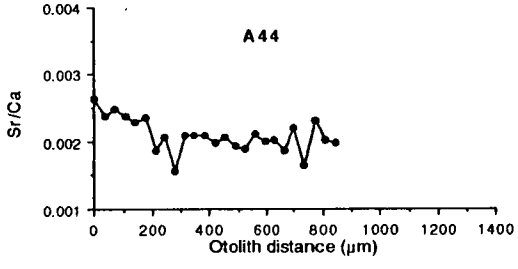

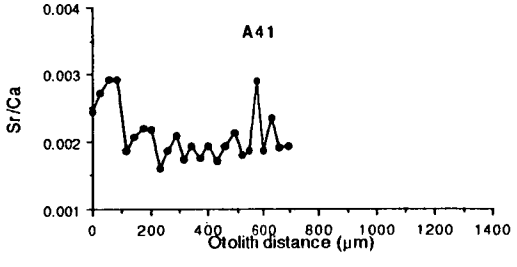

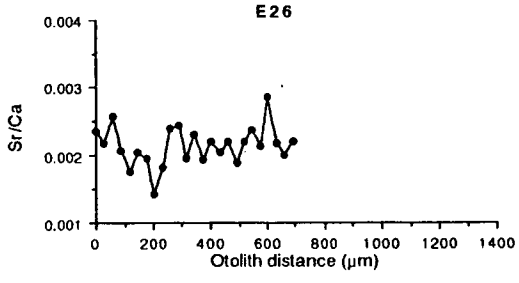

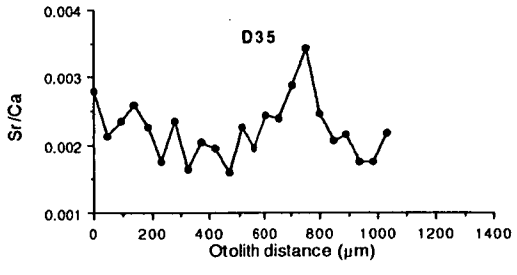

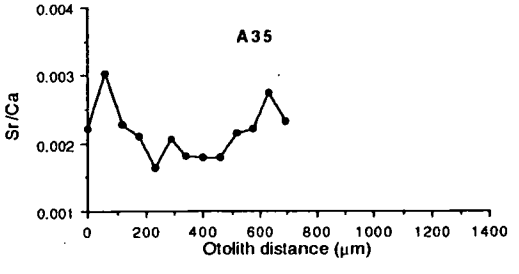

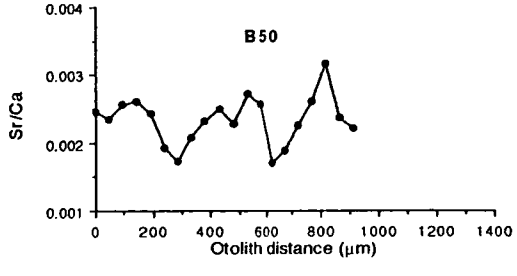

Cremorne Beach (19 April 1987) (continued)

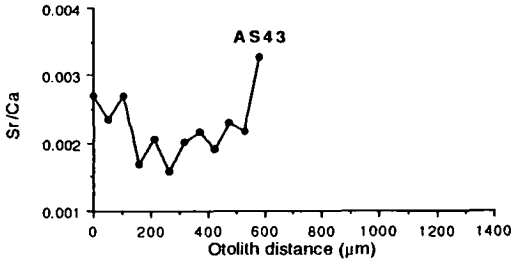

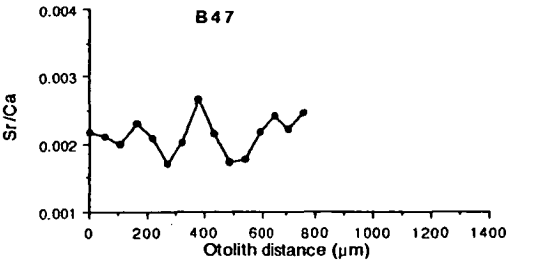

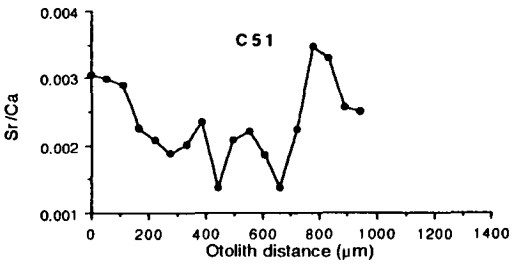

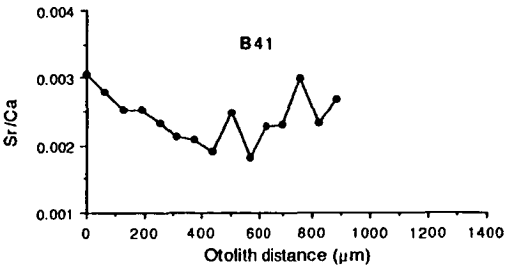

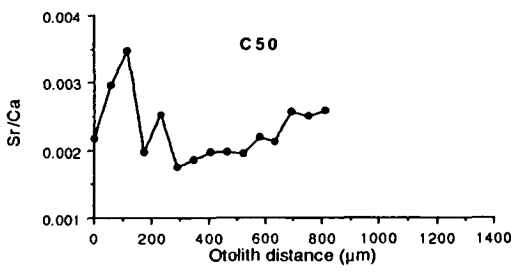

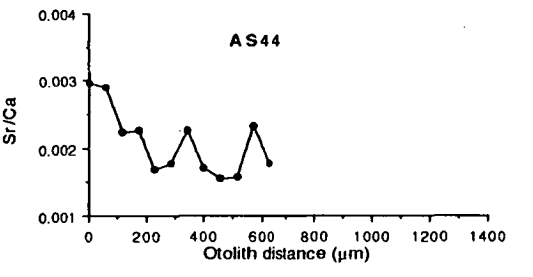

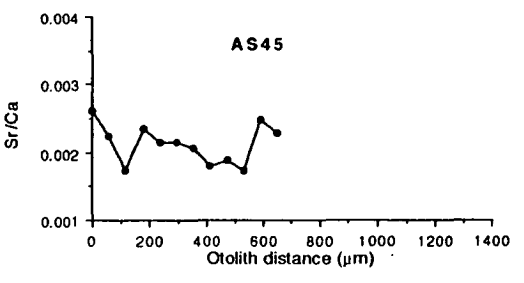

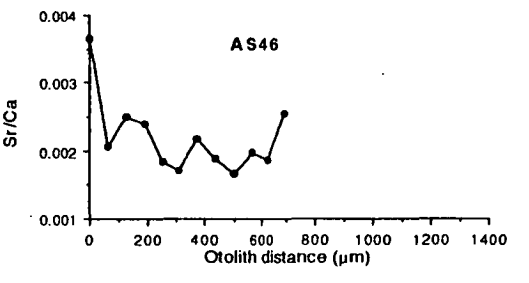

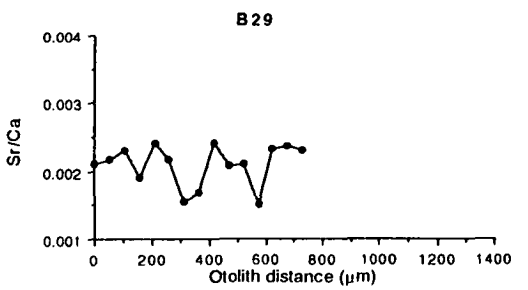

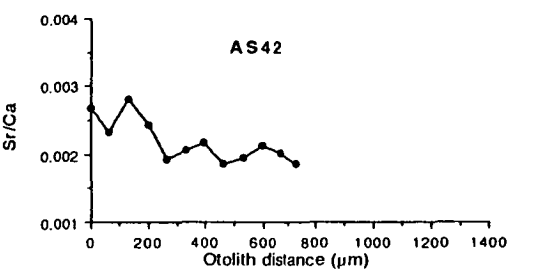

Cremorne Beach (8 June 1987)

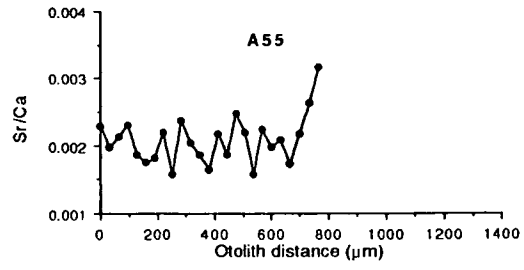

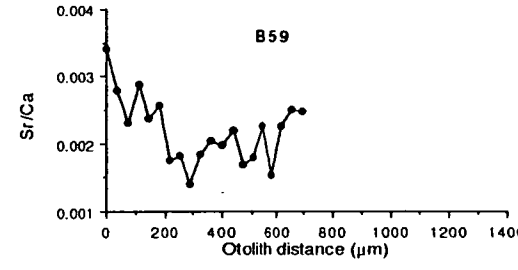

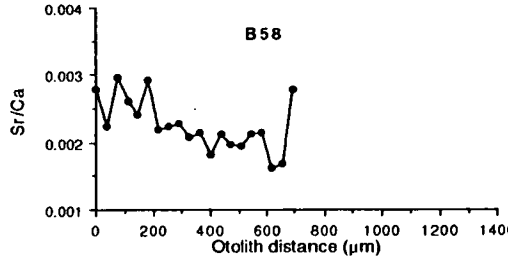

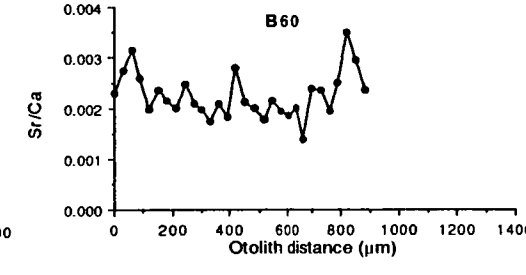

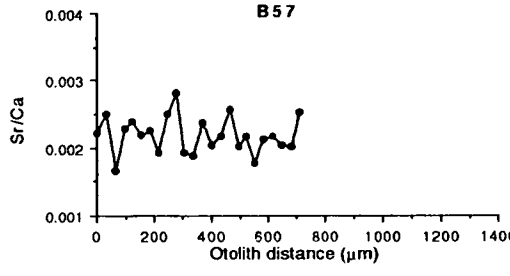

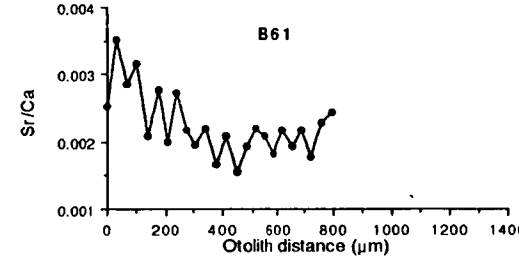

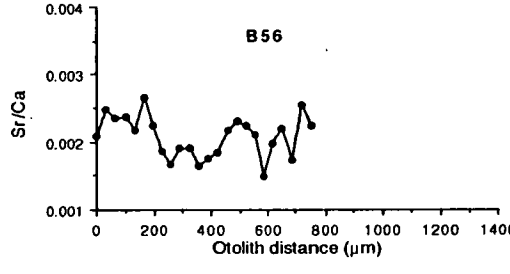

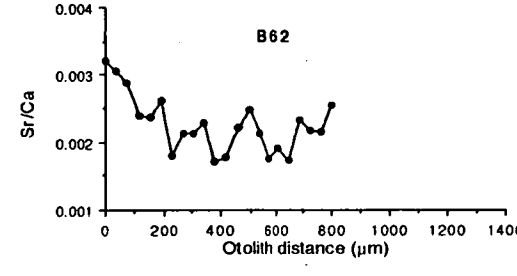

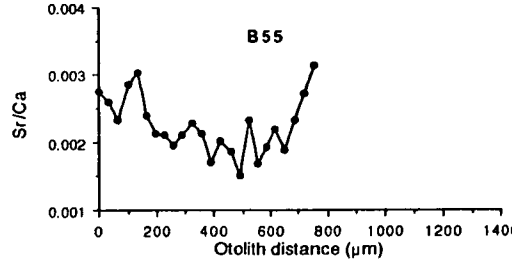

Cremorne Beach (26 September 1987)

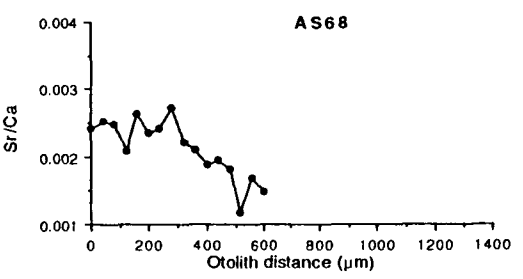

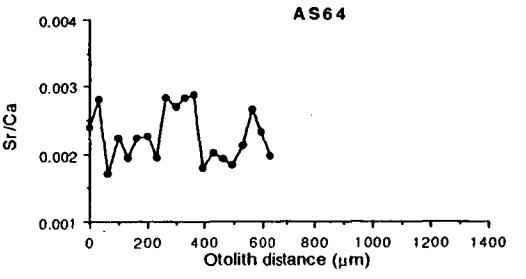

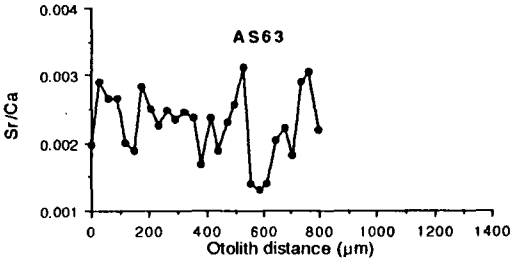

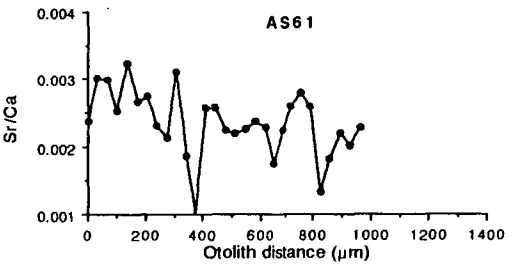

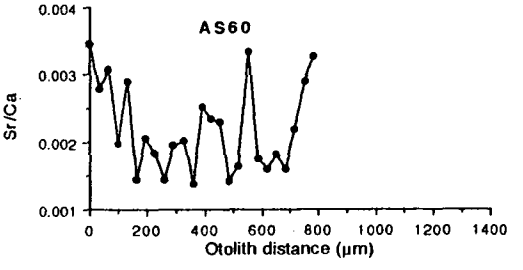

Cremorne Beach (9 January 1988)

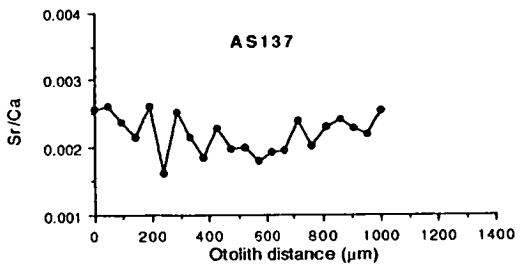

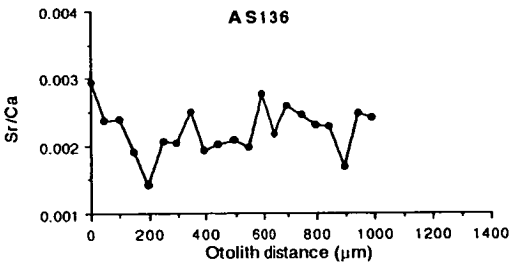

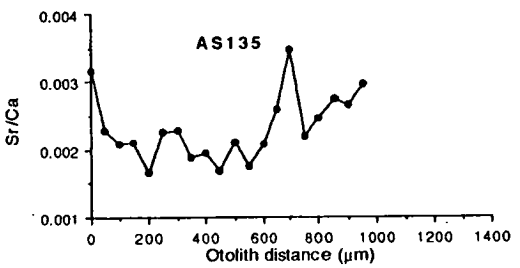

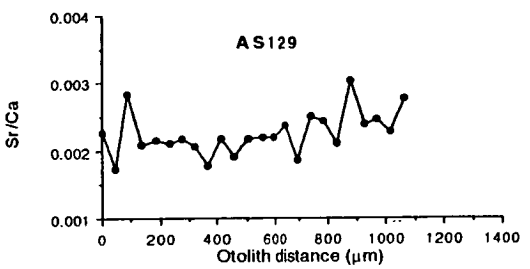

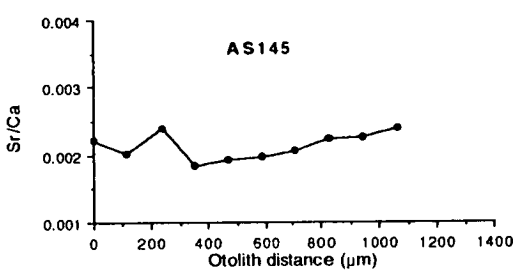

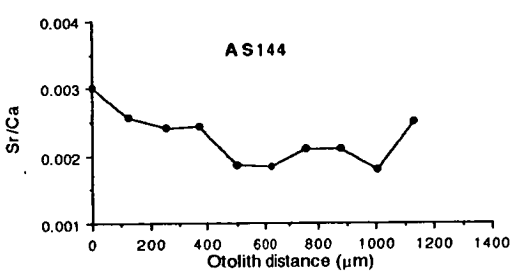

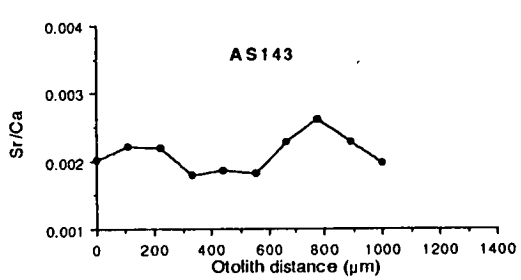

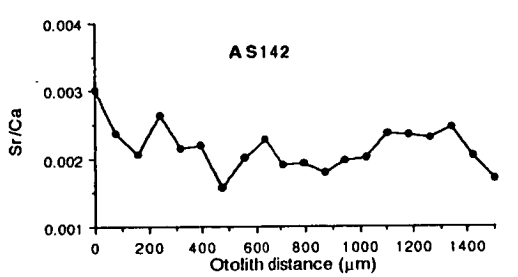

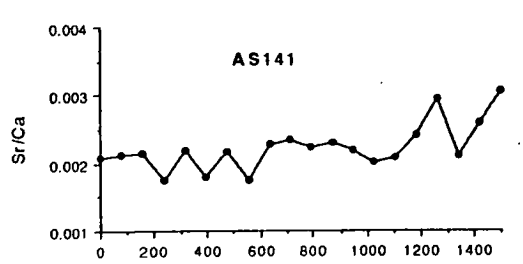

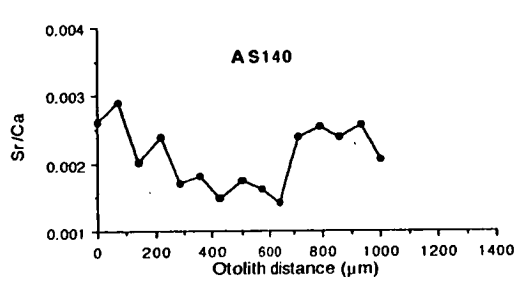

Cremorne Beach (9 January 1988) (continued)

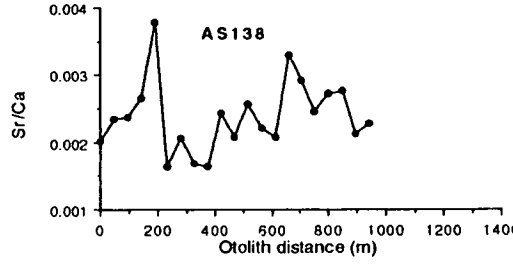

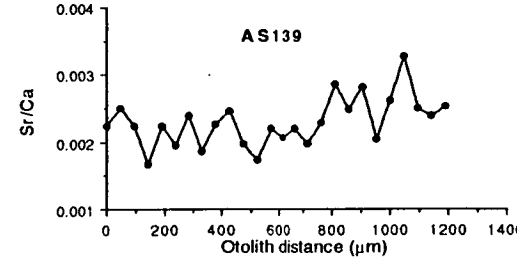

Cremorne Beach (10 February 1988)

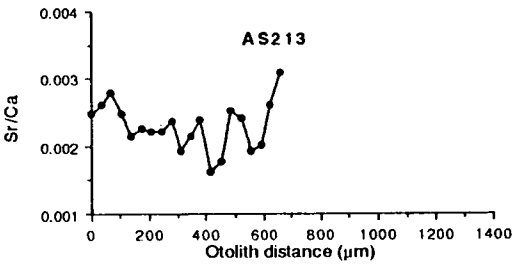

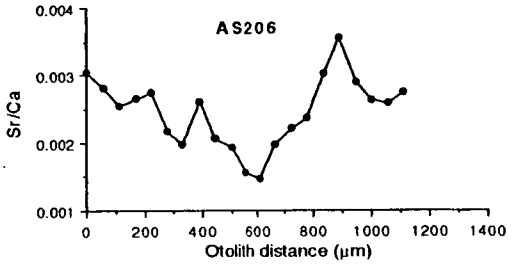

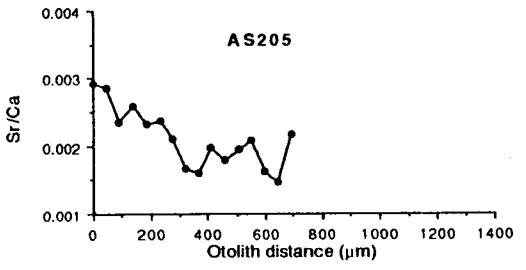

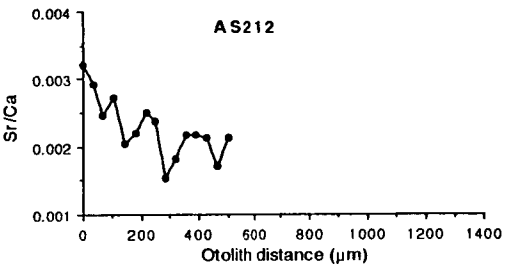

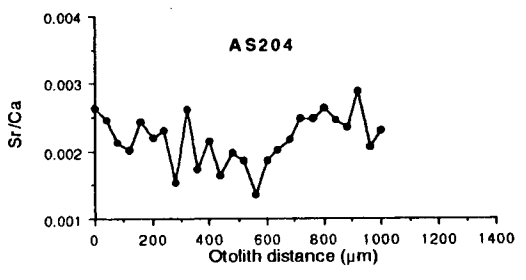

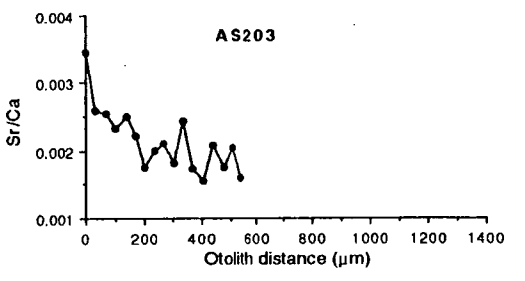

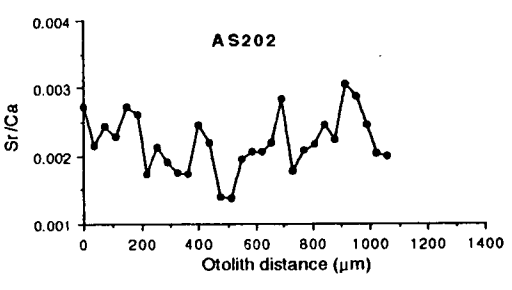

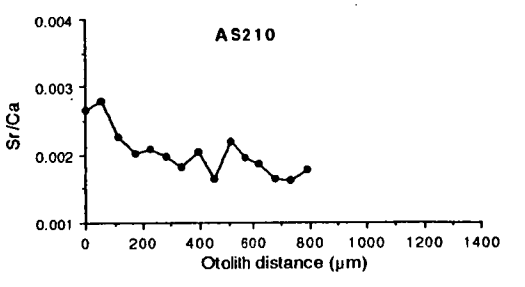

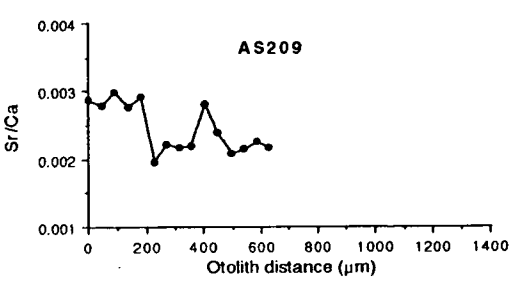

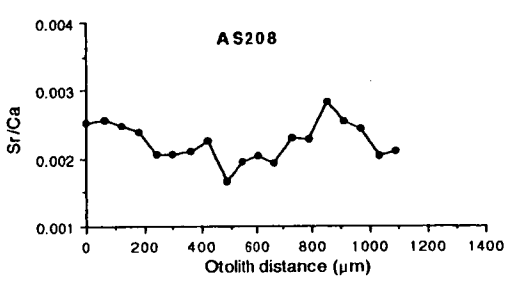

Cremorne Beach (10 February 1988) (continued)

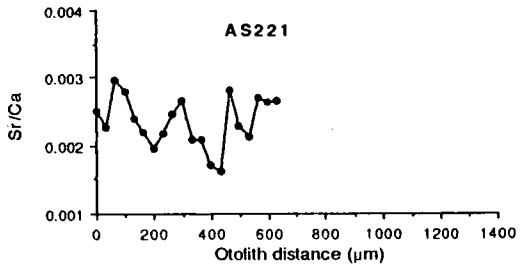

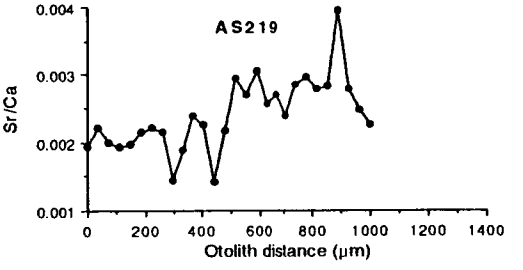

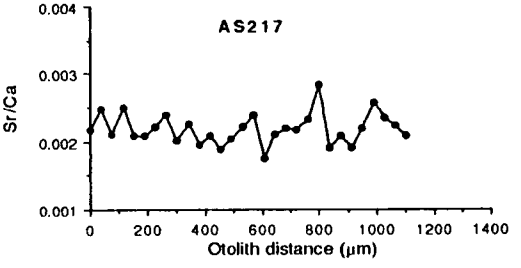

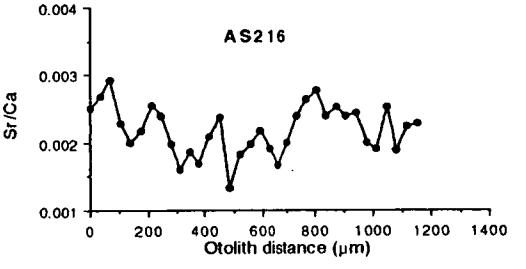

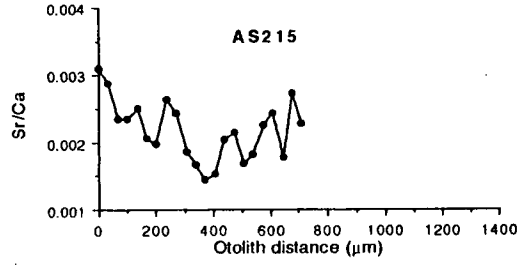

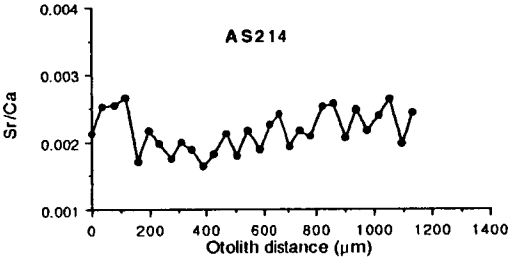

Cremorne Beach (1 April 1988)

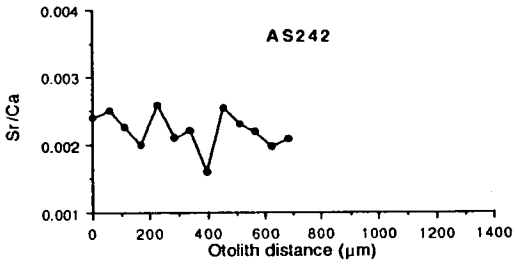

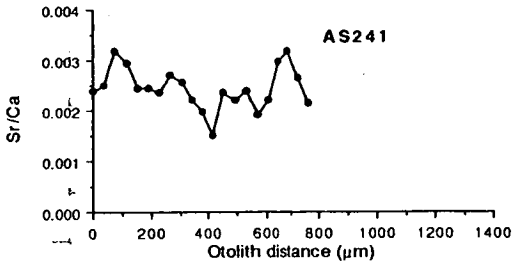

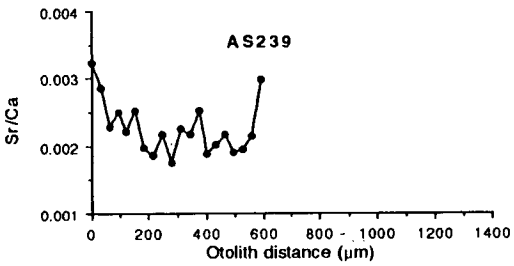

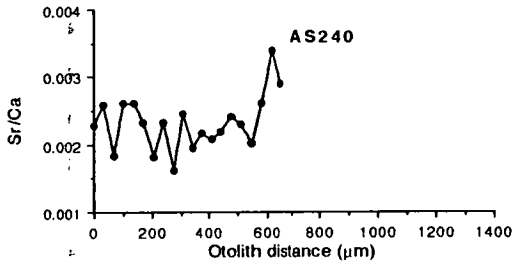

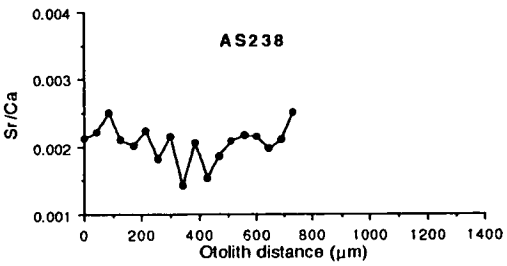

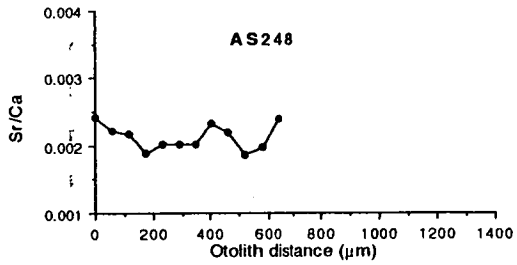

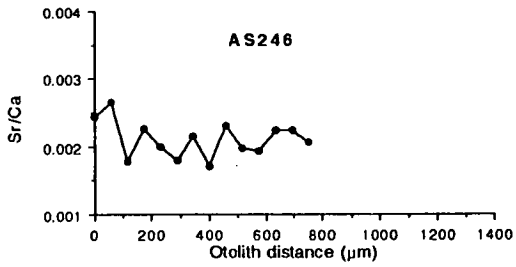

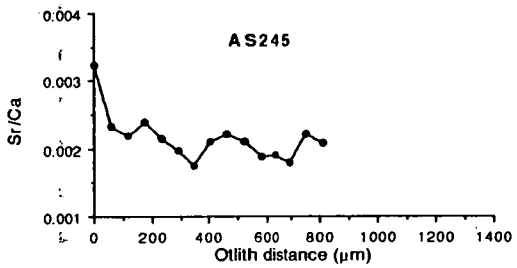

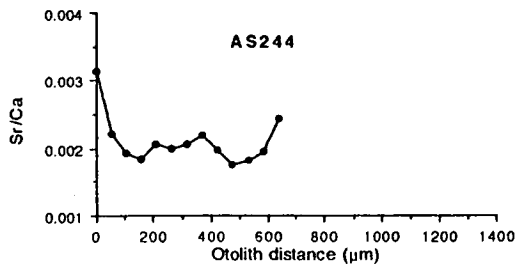

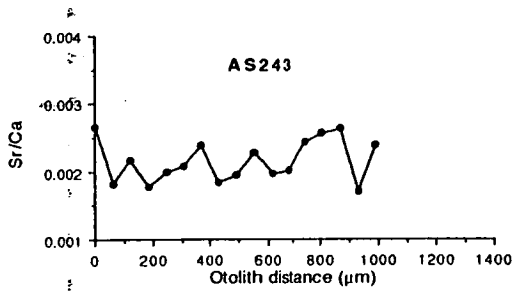

Cremorne Beach (1 April 1988) (continued)

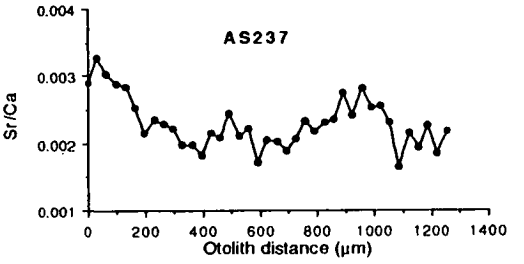

APPENDIX 3

CROSS-CORRELATION COEFFICIENT MATRICES

Cross-correlation data for Sr/Ca, Na/Ca, K/Ca, S/Ca and mean values calculated from these matrices are shown in Tables A3.1 to A3.5. These data were used in the investigation of *Arripis trutta* school cohesiveness (Section 4.5).

Table A3.1 Cross-correlations among Sr/Ca ratio data from *Arripis trutta* collected in a single school. All series were truncated to 46 measurements and a maximum lag of 7 was used. The number in parentheses is the lag for which the maximum cross-correlation was obtained.

	11	22	28	34	35	4	42	43	44	45	46	47	48	49	50	52	54	55	57	59
11	X	.35(-2)	.36(-6)	.35(1)	.36(1)	.40(-1)	NS	NS	.42(0)	.36(-7)	.42(-3)	.38(4)	.47(6)	.33(0)	.52(0)	.47(-5)	.51(-7)	NS	.51(3)	.40(0)
22		X	NS	.33(1)	NS	NS	-.47(-4)	.39(3)	NS	NS	NS	.39(0)	NS	NS	NS	.45(6)	NS	.34(0)	NS	NS
28			X	NS	NS	NS	-.34(-6)	.36(1)	NS	.49(0)	.35(0)	.35(0)	.35(4)	NS	.38(7)	.33(-5)	.42(-2)	-.34(2)	.45(0)	.45(-3)
34				X	NS	NS	.42(0)	NS	NS	NS	.33(-1)	NS	.35(-1)	.44(-1)	.39(-7)	NS	.34(5)	NS	.41(0)	NS
35					X	NS	NS	NS	.36(0)	NS	NS	NS	.40(-7)	.36(-6)	.37(-3)	.49(-3)	-.35(0)	.38(0)	.41(0)	.50(1)
4						X	.43(4)	NS	.34(1)	.32(3)	.38(-1)	NS	.56(7)	-.39(-7)	NS	NS	NS	-.36(-1)	.45(4)	.40(0)
42							X	-.40(7)	NS	NS	NS	NS	.37(4)	NS	.34(-1)	.57(4)	-.41(3)	NS	.49(0)	NS
43								X	NS	.46(2)	.43(5)	NS	.38(-6)	NS	.34(5)	.50(-5)	.41(0)	NS	NS	NS
44									X	-.34(-1)	.34(-1)	.38(4)	.38(-6)	NS	.49(-3)	NS	.50(0)	.38(1)	.34(3)	.36(2)
45										X	.35(6)	NS	-.48(-5)	.34(5)	.40(6)	.41(-4)	NS	NS	-.37(-6)	NS
46											X	NS	.58(7)	NS	NS	.44(-5)	NS	NS	NS	NS
47												X	.37(2)	.43(-4)	.38(-6)	NS	-.47(6)	.55(7)	.45(-3)	.59(-6)
48													X	.50(2)	.40(-2)	.34(0)	NS	.48(6)	NS	.44(-7)
49														X	.37(2)	.44(1)	.39(-7)	-.39(-7)	.37(-1)	NS
50															X	X	.37(-3)	NS	NS	.40(7)
52																	X	-.41(-4)	-.55(-4)	NS
54																		X	NS	NS
55																			X	.40(0)
57																				X
59																				

Table A3.2 Cross-correlations among Na/Ca ratio data from *Arripis trutta* collected in a single school. All series were truncated to 44 measurements and a maximum lag of 7 was used. The number in parentheses is the lag for which the maximum cross-correlation was obtained.

	11	22	28	34	35	4	42	43	44	45	46	47	48	49	50	52	54	55	57	59
11	X	.35(3)	.49(2)	.61(0)	.65(0)	.66(0)	.49(1)	.61(0)	.62(0)	.50(3)	.41(3)	NS	.45(-1)	.67(0)	.49(4)	.51(-2)	.60(-4)	.69(0)	.53(0)	.45(0)
22		X	.41(6)	NS	.39(0)	.32(3)	.34(3)	.32(1)	.39(-3)	.33(-1)	NS	.36(1)	NS	.40(3)	NS	.37(5)	NS	.44(-2)	.48(-2)	NS
28			X	.57(5)	.39(3)	.47(-2)	.56(-1)	.51(-1)	.40(0)	NS	.47(2)	NS	NS	.58(0)	.53(5)	.46(0)	.62(-4)	.43(3)	.40(-1)	.46(-1)
34				X	.64(-3)	.47(-5)	.53(0)	.59(-3)	.46(0)	.39(4)	.53(0)	NS	NS	.48(-1)	.52(-1)	.54(-4)	.55(-1)	.50(-3)	.39(-2)	.60(3)
35					X	.50(2)	.43(0)	.44(3)	.58(3)	.46(3)	.34(-6)	NS	.41(-3)	.52(4)	.46(1)	.40(-1)	.61(-6)	.67(0)	.43(3)	.49(6)
4						X	.46(1)	.46(0)	.58(3)	NS	.47(0)	NS	.49(2)	.54(0)	.43(4)	.41(2)	.41(-1)	.46(2)	.40(3)	.38(4)
42							X	.38(0)	.39(0)	NS	.44(-1)	NS	.37(1)	.46(0)	.51(1)	.43(-5)	.55(0)	.42(0)	NS	.48(3)
43								X	.50(3)	.34(3)	.38(6)	NS	.43(-6)	.51(4)	.57(4)	.37(1)	.51(-3)	.47(1	.43(-3)	.43(0)
44									X	.35(0)	.33(-4)	NS	.52(-1)	.58(0)	.41(1)	.48(-4)	.45(-4)	.52(-3)	.41(0)	.36(0)
45										X	NS	.45(4)	NS	NS	NS	NS	.38(-5)	.37(-2)	.39(-2)	.52(-1)
46											X	NS	.41(2)	.33(-3)	NS	.37(3)	.47(1)	NS	NS	.52(7)
47												X	-.41(0)	.37(0)	NS	NS	-,51(1)	.34(-6)	.38(-3)	-.55(6)
48													X	NS	NS	.33(3)	.46(-3)	.35(1)	.36(2)	.42(2)
49														X	.56(1)	.58(-2)	.44(-6)	.55(-2)	.47(-2)	.36(0)
50															X	.41(-1)	.50(-6)	.43(-1)	.45(-7)	.38(0)
52																X	.51(-6)	.40(1)	NS	.37(4)
54																	X	.56(7)	.39(4)	.60(2)
55																		X	.51(0)	.52(5)
57																			X	.54(0)
59																				X

Table A3.3 Cross-correlations among K/Ca ratio data from Arripis trutta collected in a single school. All series were truncated to 46 measurements and a maximum lag of 7 was used. The number in parentheses is the lag for which the maximum cross-correlation was obtained.

	11	22	28	34	35	40	42	43	44	45	46	47	48	49	50	52	54	55	57	59
11	X	NS	.33(-1)	NS	.43(-3)	NS	.40(0)	-.35(-1)	-.41(-3)	.38(-1)	.36(0)	.38(3)	.36(-2)	NS	-.46(-4)	.49(-2)	-.47(1)	NS	.49(-3)	-.36(-1)
22		X	NS	NS	-.37(3)	.39(-2)	.48(2)	NS	-.45(-4)	-.53(3)	.45(2)	NS	NS	.44(7)	NS	.35(2)	NS	NS	NS	.47(2)
28			X	NS	-.38(-1)	NS	.37(1)	NS	NS	NS	.37(5)	NS	NS	NS	-.38(-5)	.35(0)	NS	NS	.40(0)	NS
34				X	NS	NS	NS	NS	.38(-2)	-.39(0)	NS	NS	NS	NS	NS	NS	.36(-3)	.49(-1)	NS	.38(1)
35					X	NS	-.55(2)	.35(2)	.36(-3)	NS	-.51(3)	-.38(5)	-.45(3)	-.35(4)	.39(0)	-.67(0)	.51(2)	NS	-.66(0)	NS
40						X	NS	.65(0)	-.35(0)	.34(-6)	NS	.34(-3)	.40(0)	NS	NS	NS	NS	NS	-.32(-6)	-.37(-7)
42							X	-.41(0)	-.40(-3)	NS	.55(0)	-.46(-3)	.47(0)	.43(0)	-.64(-4)	.63(-2)	-.42(0)	NS	.60(1)	NS
43								X	-.32(0)	.43(-6)	-.45(1)	.51(-3)	-.58(1)	-.46(-2)	.52(-4)	-.35(-3)	.53(0)	-.34(-2)	-.45(1)	.42(4)
44									X	NS	NS	.39(-1)	.36(0)	NS	.34(-1)	.42(-6)	.35(3)	NS	.39(-6)	NS
45										X	NS	.62(0)	-.45(7)	-.62(4)	.39(1)	NS	NS	-.42(6)	.35(-6)	-.62(2)
46											X	-.35(-4)	.67(0)	.40(-3)	-.44(-4)	.48(-2)	-.34(0)	NS	.42(0)	NS
47												X	-.45(4)	-.48(1)	.66(0)	.52(-5)(	-.44(-5)	-.41(3)	.44(-5)	-.64(4)
48													X	.51(-2)	-.56(-6)	.43(0)	-.37(0)	.38(-3)	.45(-3)	NS
49														X	-.46(-1)	.35(-1)	NS	.56(-7)	.38(-1)	.51(-2)
50															X	-.49(0)	.35(3)	-.36(-4)	-.43(4)	NS
52																X	-.51(0)	.43(-6)	.76(0)	.39(-1)
54																	X	.34(3)	-.57(1)	.37(-6)
55																		X	.38(6)	.58(1)
57																			X	NS
59																				X

Table A3.4 Cross-correlations among S/Ca ratio data from Arripis trutta collected in a single school. All series were truncated to 46 measurements and a maximum lag of 7 was used. The number in parentheses is the lag for which the maximum cross-correlation was obtained.

	11	22	28	34	35	40	42	43	44	45	46	47	48	49	50	52	54	55	57	59
11	X	.55(3)	.65(-1)	.41(-6)	,54(3)	.64(-1)	.67(0)	.74(2)	.56(0)	.63(0)	.50(-1)	.54(7)	.60(3)	.58(6)	.55(4)	.66(2)	.39(-7)	.67(0)	.50(4)	.41(3)
22		X	.49(0)	.53(1)	.37(0)	.59(0)	.59(-6)	.63(-1)	.44(1)	.59(0)	.46(-3)	.34(0)	.53(0)	.61(-1)	.48(-3)	.48(-4)	NS	.68(-3)	.48(0)	.45(1)
28			X	.45(0)	.51(7)	.54(4)	.62(1)	.59(2)	.51(-2)	.62(-1)	.43(2)	.43(7)	.55(3)	.43(6)	.46(2)	.58(2)	.39(-2)	.67(-2)	.49(5)	.38(1)
34				X	NS	.53(-1)	.52(2)	.36(0)	.41(-1)	.52(-1)	.32(5)	NS	.43(-1)	.33(-2)	NS	.46(-3)	NS	.51(-3)	.33(-1)	.38(1)
35					X	.42(-1)	.45(-6)	.52(-5)	.41(-4)	.44(-3)	.56(-4)	.48(1)	.47(-3)	.56(6)	.53(-3)	.58(-4)	NS	.51(-3)	.39(-2)	NS
40						X	.58(1)	.71(-1)	.64(0)	.64(1)	.41(0)	.37(6)	.55(1)	.55(0)	.44(2)	.58(0)	NS	.69(-2)	.56(1)	.44(0)
42							X	.61(4)	.59(0)	.58(0)	.51(3)	.47(6)	.54(6)	.58(6)	.52(4)	.57(4)	NS	.57(-3)	.55(3)	.45(-2)
43								X	.64(2)	.62(2)	.49(0)	.45(5)	.62(1)	.58(1)	.62(4)	.70(0)	NS	.58(-2)	.65(2)	.47(0)
44									X	.56(0)	.42(6)	.39(5)	.58(0)	.49(0)	.53(4)	.61(-2)	-.35(3)	.48(0)	.62(1)	.67(0)
45										X	.54(0)	NS	.58(0)	.58(-1)	.45(7)	.60(-1)	.37(-6)	.73(-3)	.49(7)	.36(6)
46											X	.43(0)	.43(0)	.55(4)	.40(-1)	.54(0)	.32(-4)	.51(1)	NS	NS
47												X	.39(0)	.44(-1)	.44(0)	.34(-2)	NS	NS	.50(-3)	.52(0)
48													X	.43(1)	.59(1)	.68(1)	NS	.41(0)	.58(-3)	.40(0)
49														X	.42(0)	.62(-2)	NS	.52(-1)	.59(1)	.42(-2)
50															X	.57(-2)	NS	.42(-1)	.46(1)	.39(0)
52																X	.40(-5)	.65(1)	.59(3)	NS
54																	X	.64(7)	.36(3)	.43(4)
55																		X	.38(2)	.54(-1)
57																			X	X
59																				

Table A3.5 Mean cross correlation based on cross correlations from Sr/Ca, Na/Ca, K/Ca and S/Ca data from *Arripis trutta* collected in a single school. Negative or nonsignificant cross-correlations (P>0.05) were assigned a value of zero when calculating the mean cross correlation. All correlations are shown below. A value of 0.30 is significant at the P<0.05 level. Values in parentheses are standard deviations.

	11	22	28	34	35	40	42	43	44	45	46	47	48	49	50	52	54	55	57	59
11	X	.31(.23)	.45(.15)	.34(.25)	.49(.13)	.42(.31)	.39(.28)	.42(.33)	.50(.10)	.47(.12)	.42(.06)	.32(.23)	.47(.10)	.39(.30)	.50(.04)	.53(.10)	.49(.10)	.34(.39)	.51(.02)	.40(.04)
22		X	.22(.26)	.21(.26)	.28(.20)	.32(.24)	.47(.10)	.33(.26)	.32(.21)	.36(.26)	.23(.26)	.27(.18)	.13(.26)	.34(.23)	.2(.24)	.41(.06)	0(0)	.36(.28)	.24(.28)	.23(.26)
28			X	.25(.30)	.32(.22)	.25(.30)	.47(.14)	.36(.26)	.23(.27)	.28(.32)	.40(.05)	.19(.23)	.22(.27)	.25(.30)	.47(.10)	.43(.11)	.36(.26)	.36(.28)	.32(.22)	.21(.24)
34				X	.16(.32)	.25(.29)	.37(.25)	.24(.29)	.31(.21)	.32(.22)	.29(.22)	0(0)	.20(.23)	.31(.22)	.23(.27)	.25(.29)	.31(.23)	.24(.25)	.30(.20)	.45(.10)
35					X	.23(.27)	.22(.25)	.24(.28)	.43(.10)	.22(.26)	.35(.25)	.21(.25)	.43(.03)	.45(.11)	.44(.07)	.53(.12)	.37(.27)	.39(.28)	.47(.13)	.12(.21)
40						X	.37(.25)	.45(.32)	.48(.15)	.32(.26)	.31(.21)	.18(.28)	.50(.07)	.37(.26)	.22(.25)	.25(.29)	.10(.20)	.38(.29)	.43(.10)	.42(.06)
42							X	.25(.30)	.25(.29)	.15(.29)	.38(.25)	.12(.24)	.44(.08)	.37(.25)	.34(.24)	.41(.28)	.14(.28)	.25(.29)	.41(.28)	.33(.22)
43								X	.29(.33)	.46(.12)	.33(.22)	.24(.28)	.26(.31)	.27(.32)	.51(.12)	.41(.31)	.26(.30)	.26(.31)	.27(.32)	.33(.22)
44									X	.23(.28)	.27(.19)	.29(.19)	.46(.11)	.27(.31)	.44(.08)	.50(.08)	.20(.23)	.25(.29)	.44(.12)	.26(.32)
45										X	.22(.27)	.27(.32)	.38(.26)	.38(.28)	.31(.21)	.15(.30)	.31(.22)	.47(.17)	.40(.06)	.46(.13)
46											X	.19(.23)	.52(.12)	.32(.23)	.21(.24)	38(.07)	.28(.20)	.13(.25)	.10(.21)	.13(.26)
47												X	.40(.03)	.43(.04)	.37(.27)	.32(.23)	.24(.27)	.19(.22)	.33(.22)	.30(.34)
48													X	.36(.24)	.39(.27)	.36(.28)	.32(.22)	.42(.09)	.46(.09)	.38(.26)
49														X	.45(.08)	.46(.16)	.11(.22)	.53(.03)	.36(.25)	.43(.06)
50															X	.48(.07)	.31(.22)	.40(.03)	.43(.04)	.20(.23)
52																X	.45(.07)	.37(.27)	34(.39)	.39(.01)
54																	X	.49(.14)	.47(.11)	.24(.29)
55																		X	.32(.22)	.38(.26)
57																			X	.37(.25)
59																				X

APPENDIX 4

SPECTRAL ANALYSIS OF ORANGE ROUGHY, *HOPLOSTETHUS ATLANTICUS*, OTOLITH MICROCHEMICAL TRANSECTS

These spectra are presented to show results that were typically obtained from spectral analysis of orange roughy, *Hoplostethus atlanticus*, otolith microchemical data. Although significant harmonics were detected in two transects of otolith Sr/Ca ratios (Fig. 4.17) the majority of the spectra did not include any significant harmonics. In the following spectra, a signal of at least -25 DB would be required for a peak to be significant. These data are discussed in Section 4.7.

The following spectra were obtained from a microprobe transect of orange roughy ORR9 (see Fig. 4.14). A fast Fourier transform was used which required that the number of data points for analysis be a value raised to the power of 2 and 256 data points (2^8) were used in these analyses. The series were truncated at the beginning and end to remove the regions that showed a constant increase or decrease in an elemental ratio. A triangular spectral window was applied to the data.

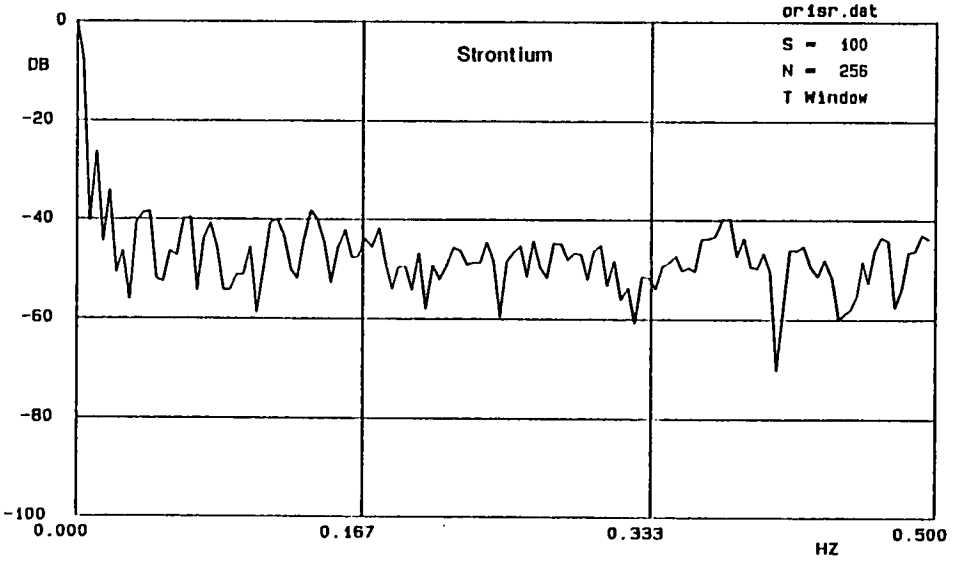

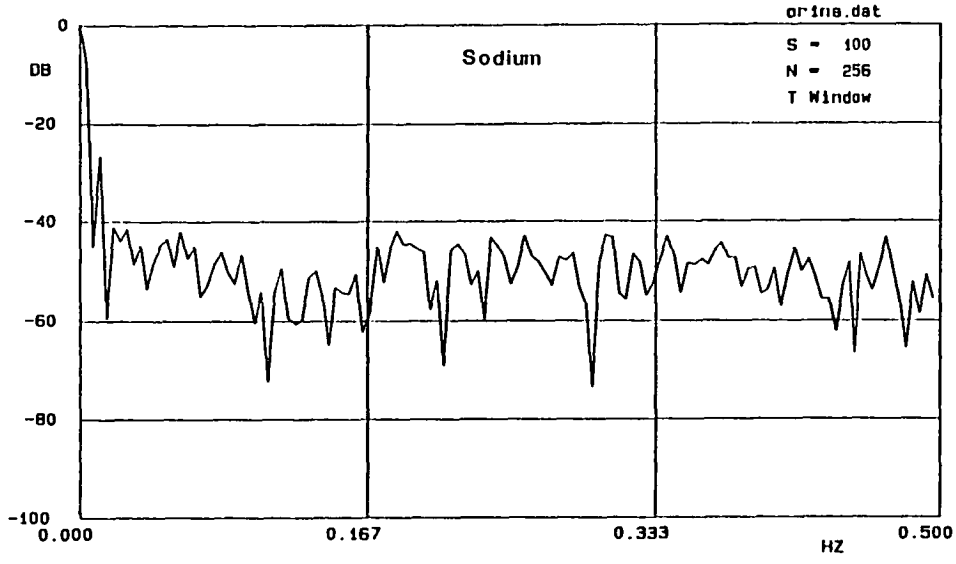
orine.dat
Sodium
S = 100
N = 256
T Window
DB
0
-20
-40
-60
-80
-100
0.000
0.167
0.333
0.500
HZ

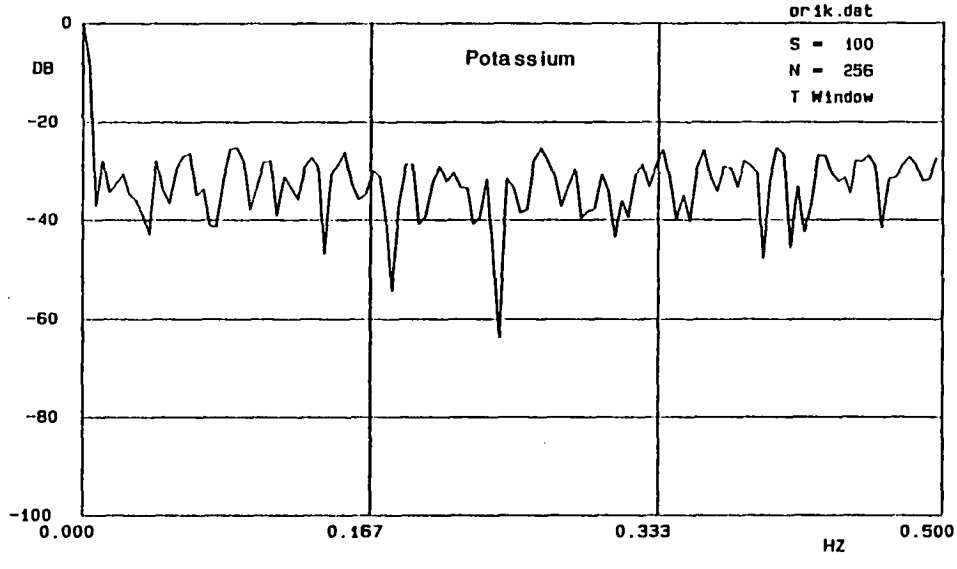
orik.dat
Potassium
S = 100
N = 256
T Window
DB
0
-20
-40
-60
-80
-100
0.000
0.167
0.333
0.500
HZ

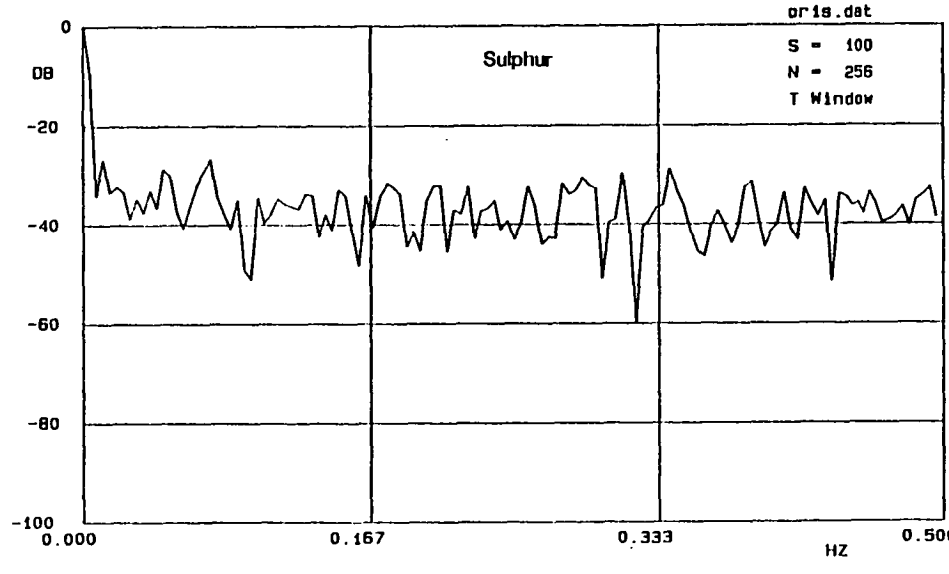
oris.dat
Sulphur
S = 100
N = 256
T Window
DB
0
-20
-40
-60
-80
-100
0.000
0.167
0.333
0.500
HZ

APPENDIX 5

LIFE-HISTORY TRANSECTS OF COD, *PSEUDOPHYCIS BARBATUS*, AND BLUE GRENADIER, *MACRURONUS NOVAEZELANDIAE*, OTOLITHS

The following pages contain additional microchemical transects of cod and blue grenadier sagittae. The transects were made from the primordium to the otolith edge on transverse sections of sagittae. The cod transects are of Sr/Ca data only, whereas the blue grenadier transects show Sr/Ca, Na/Ca, K/Ca and S/Ca data. As in previous transects, the points are the elemental ratios and the solid line is based on a 3-point moving average.

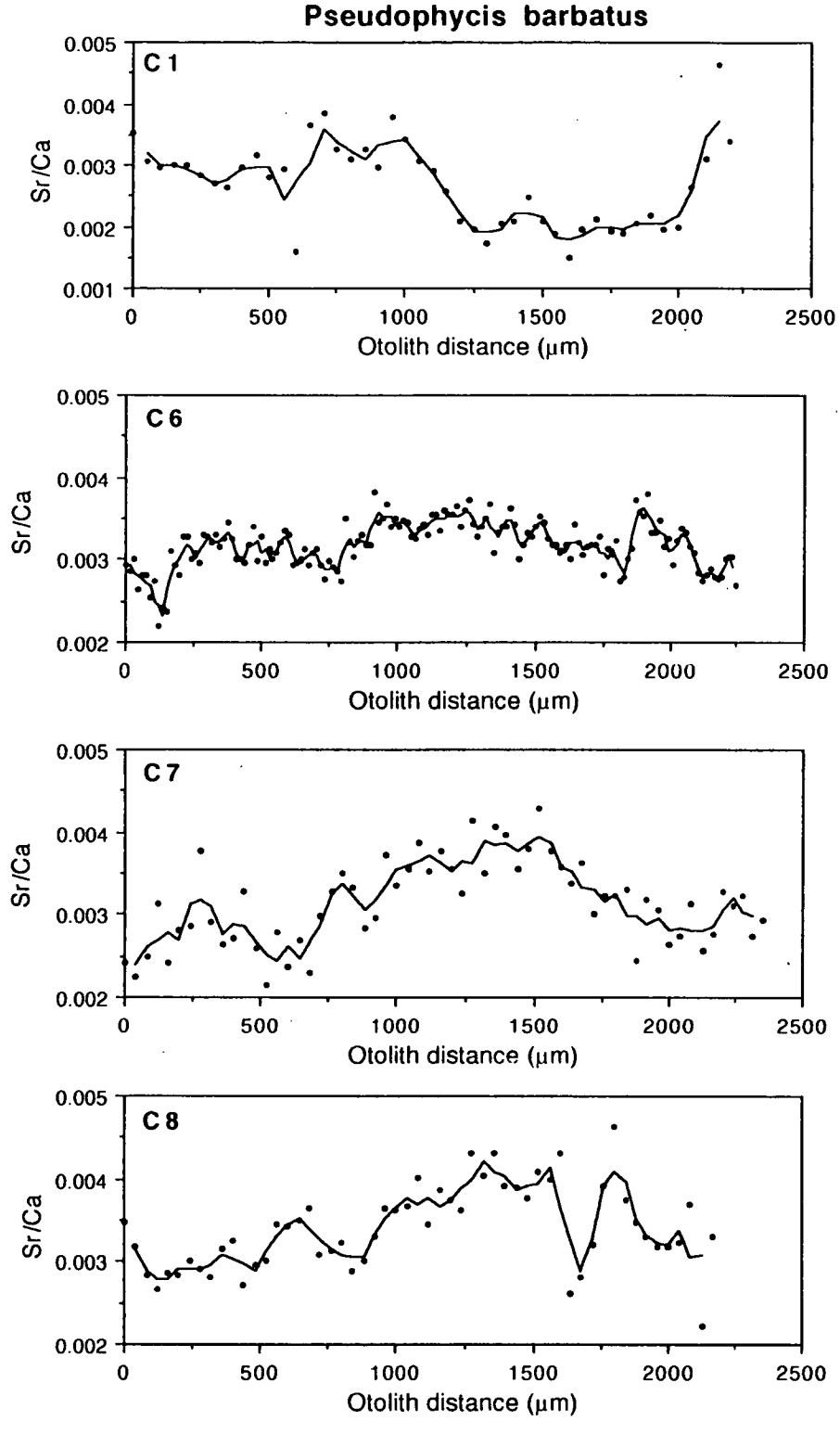

Fig. A5.1 Microprobe transects showing Sr/Ca data from 4 *Pseudophycis barbatus* collected from Variety Bay, 25 March 1988. C1 (female, 37 cm SL, 750 g); C6 (female, 29 cm SL, 450 g); C7 (female, 36 cm, 680 g); C8 (male, 34 cm SL, 650 g).

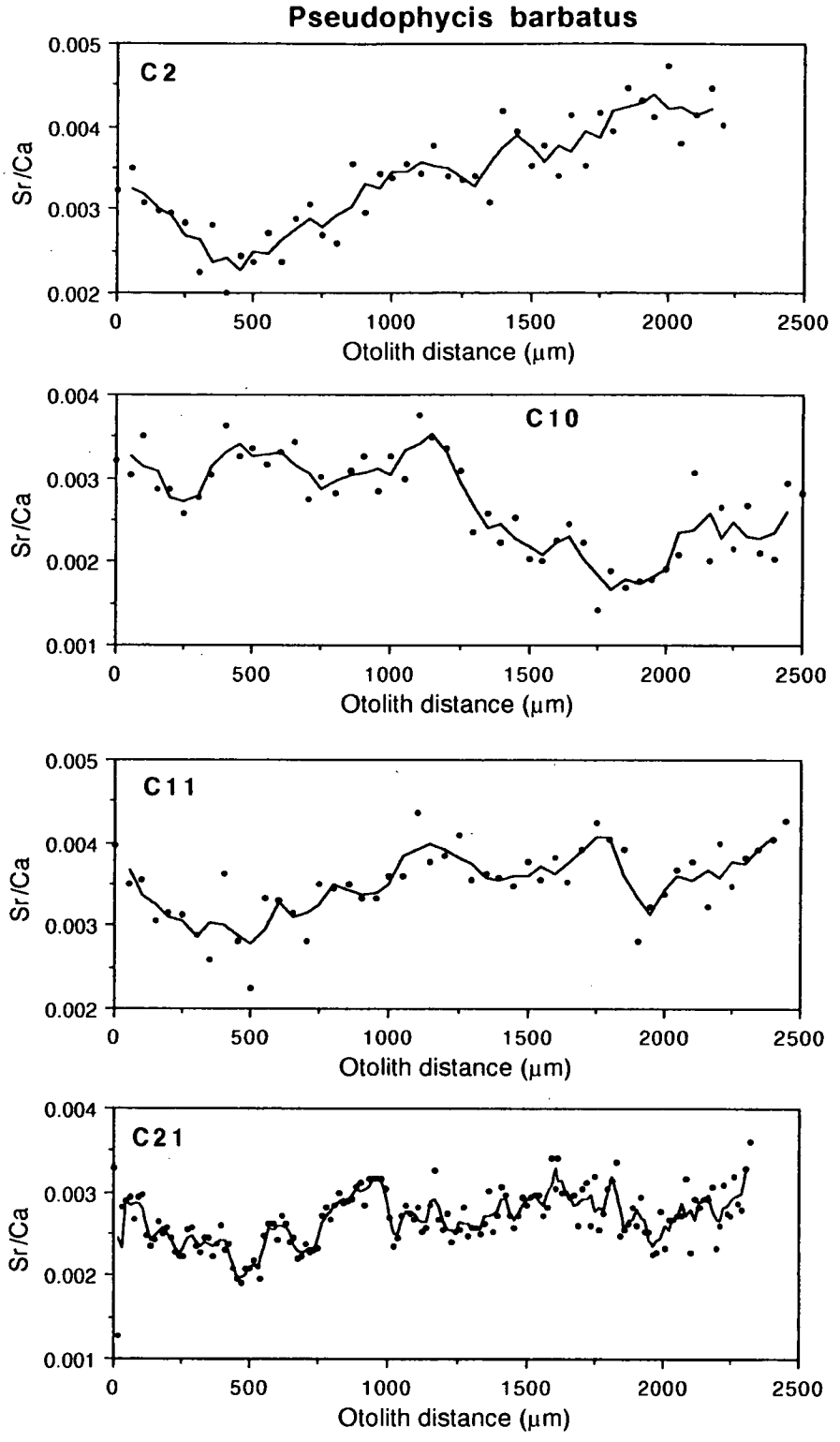

Fig. A5.2 Microprobe transects showing Sr/Ca data from 4 *Pseudophycis barbatus* collected from Variety Bay. Three were collected 25 March 1988: C2 (female, 32 cm SL, 480 g); C10 (female, 33 cm SL, 590 g); C11 (female, 35 cm, 630 g); and one was collected 17 April 1988, C21 (female, 36 cm SL, 610 g).

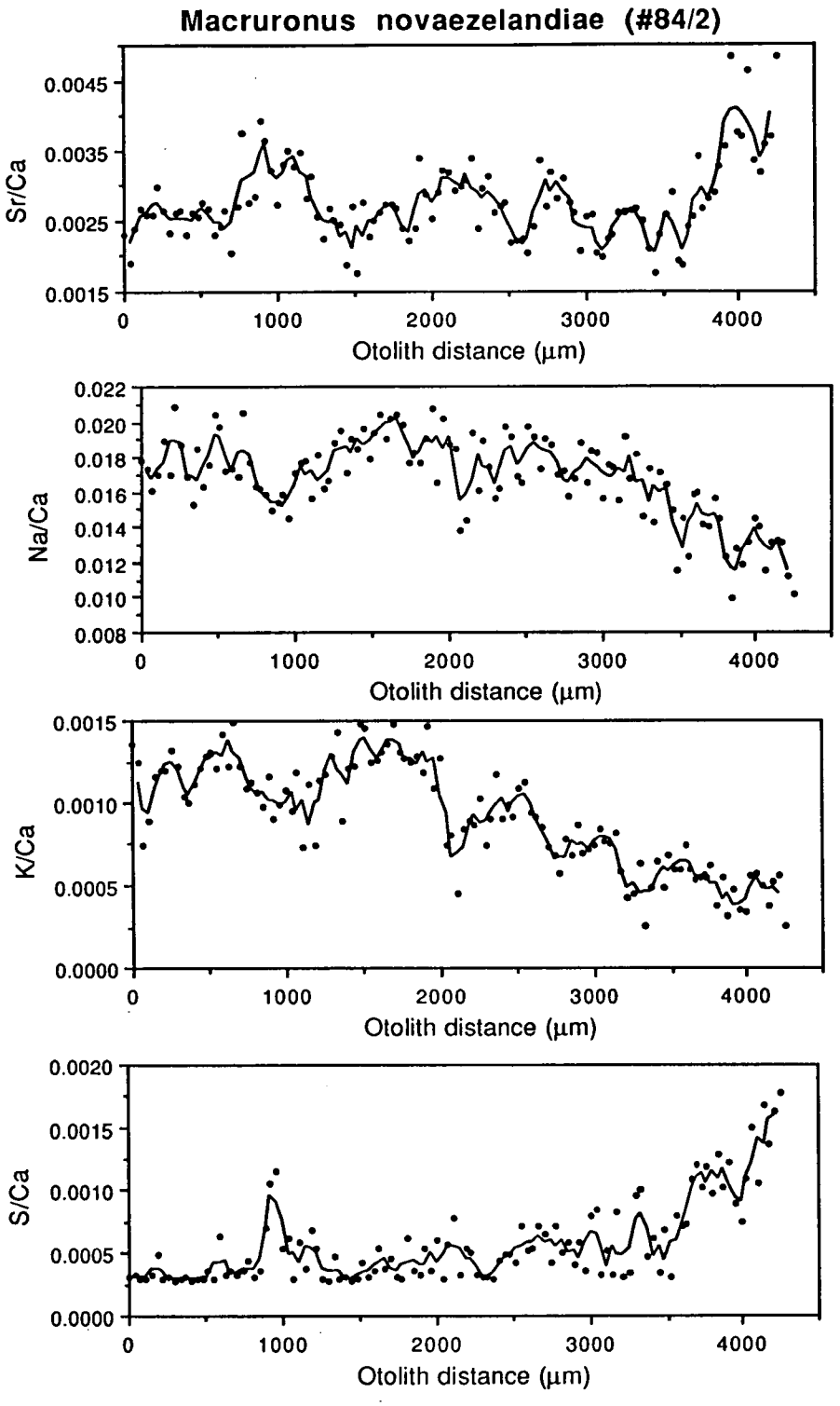

Fig. A5.3 Microprobe transect of a sagitta from a *Macruronus novaezelandiae* caught off the east coast of Tasmania, March 1985. Female, 90 cm SL, 2.5 kg. Estimated age based on otolith annuli was 15 years.

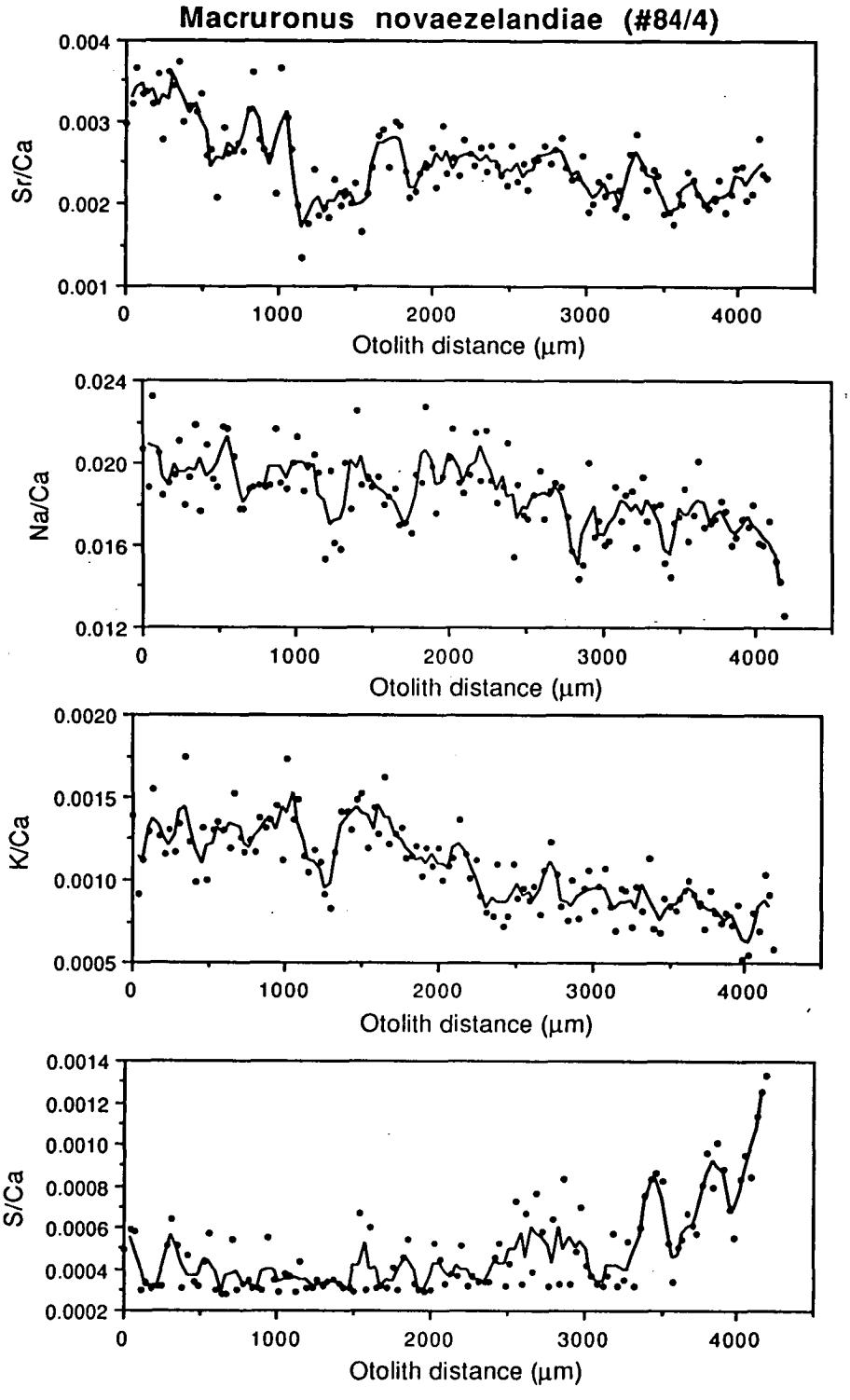

Fig. A5.4 Microprobe transect of a sagitta from a *Macruronus novaezelandiae* caught off the east coast of Tasmania, March 1985. Male, 75 cm SL, 1.7 kg. Estimated age based on otolith annuli was 6 years.

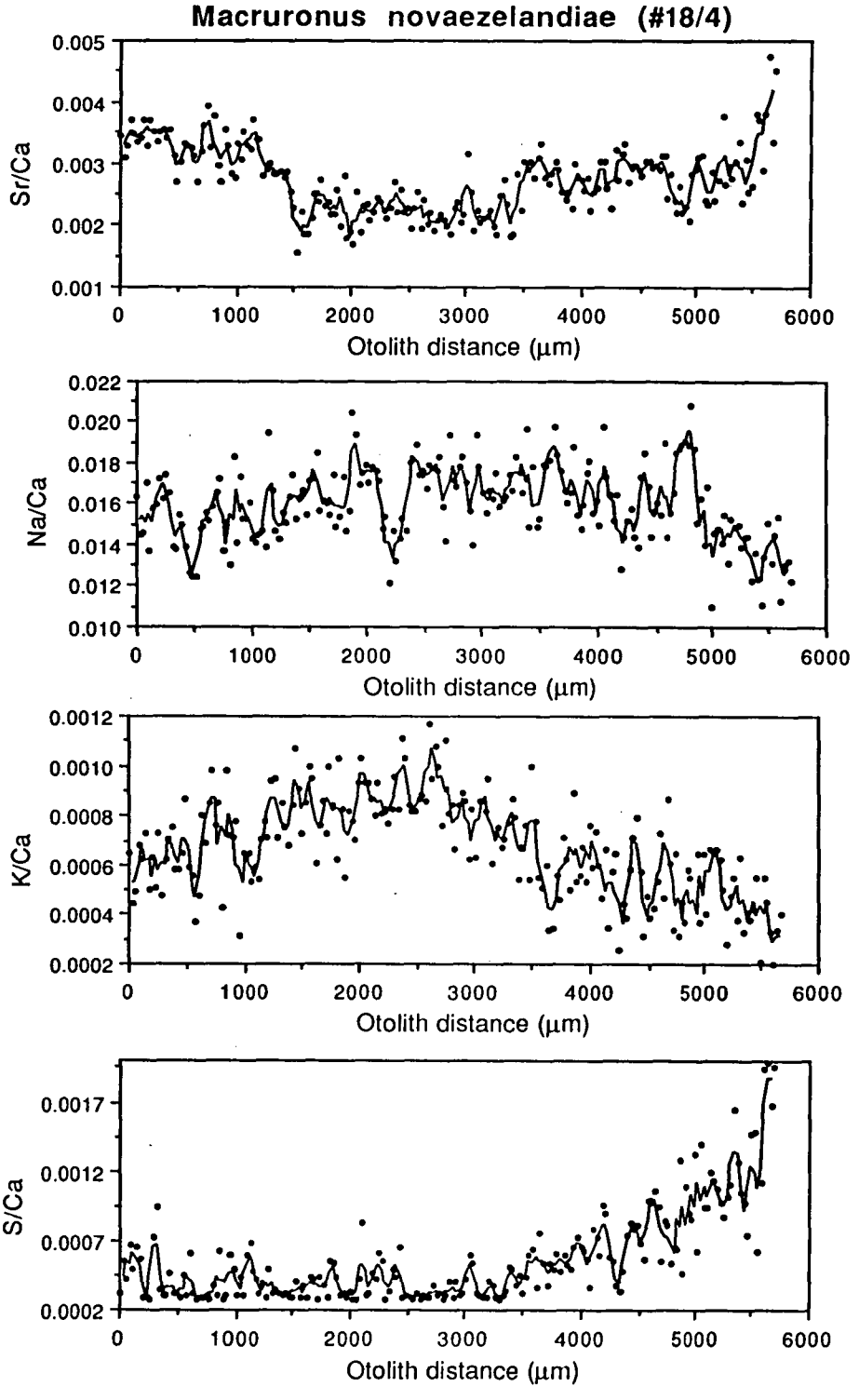

Fig. A5.5 Microprobe transect of a sagitta from a *Macruronus novaezelandiae* caught off the west coast of Tasmania, August 1985. Female, 99 cm SL, 4.4 kg, in spawning condition. Estimated age based on otolith annuli was 12 years.

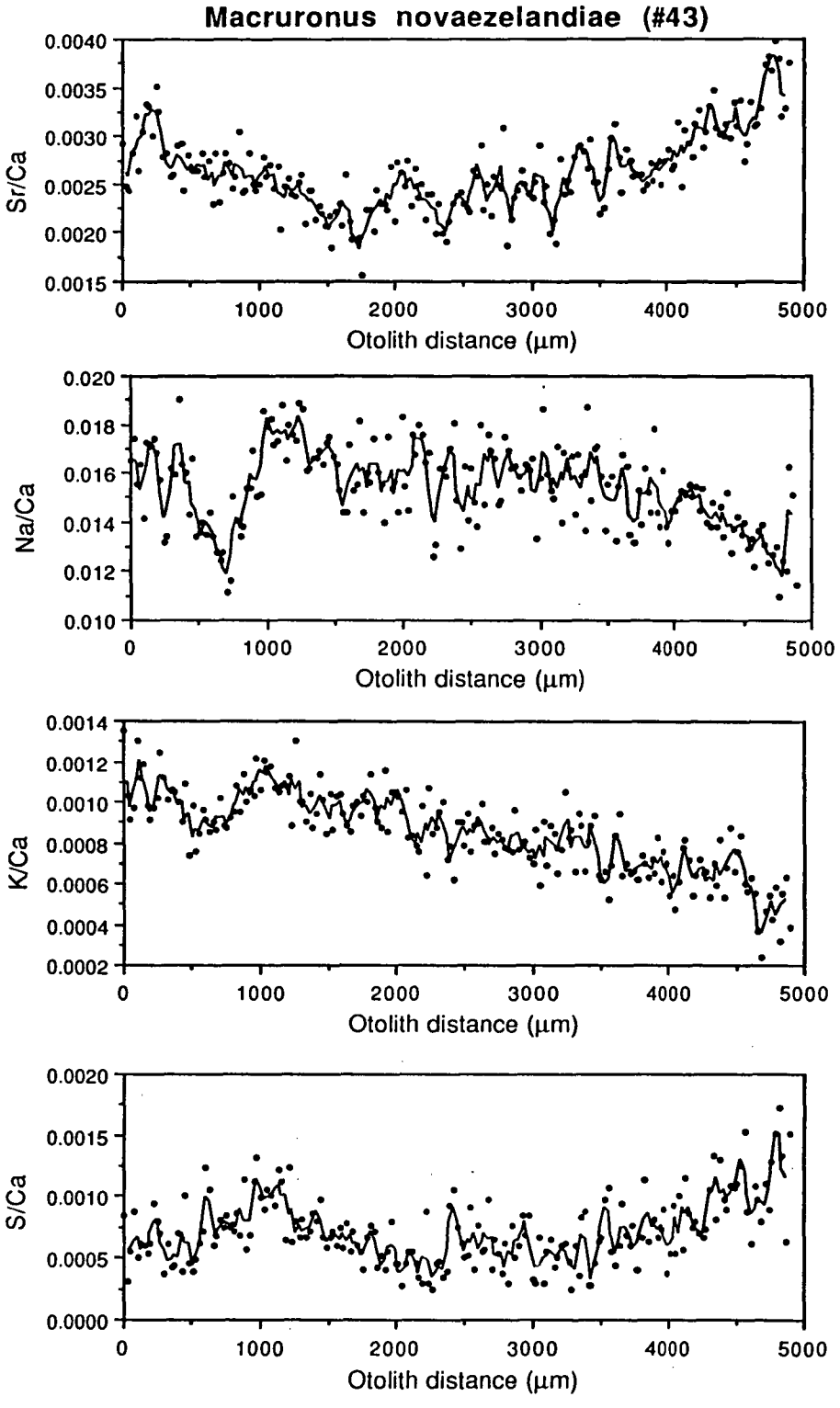

Fig. A5.6 Microprobe transect of a sagitta from a *Macruronus novaezelandiae* caught off the west coast of Tasmania, January 1985. Female, 91 cm SL, 3.2 kg. Estimated age based on otolith annuli was 13 years.

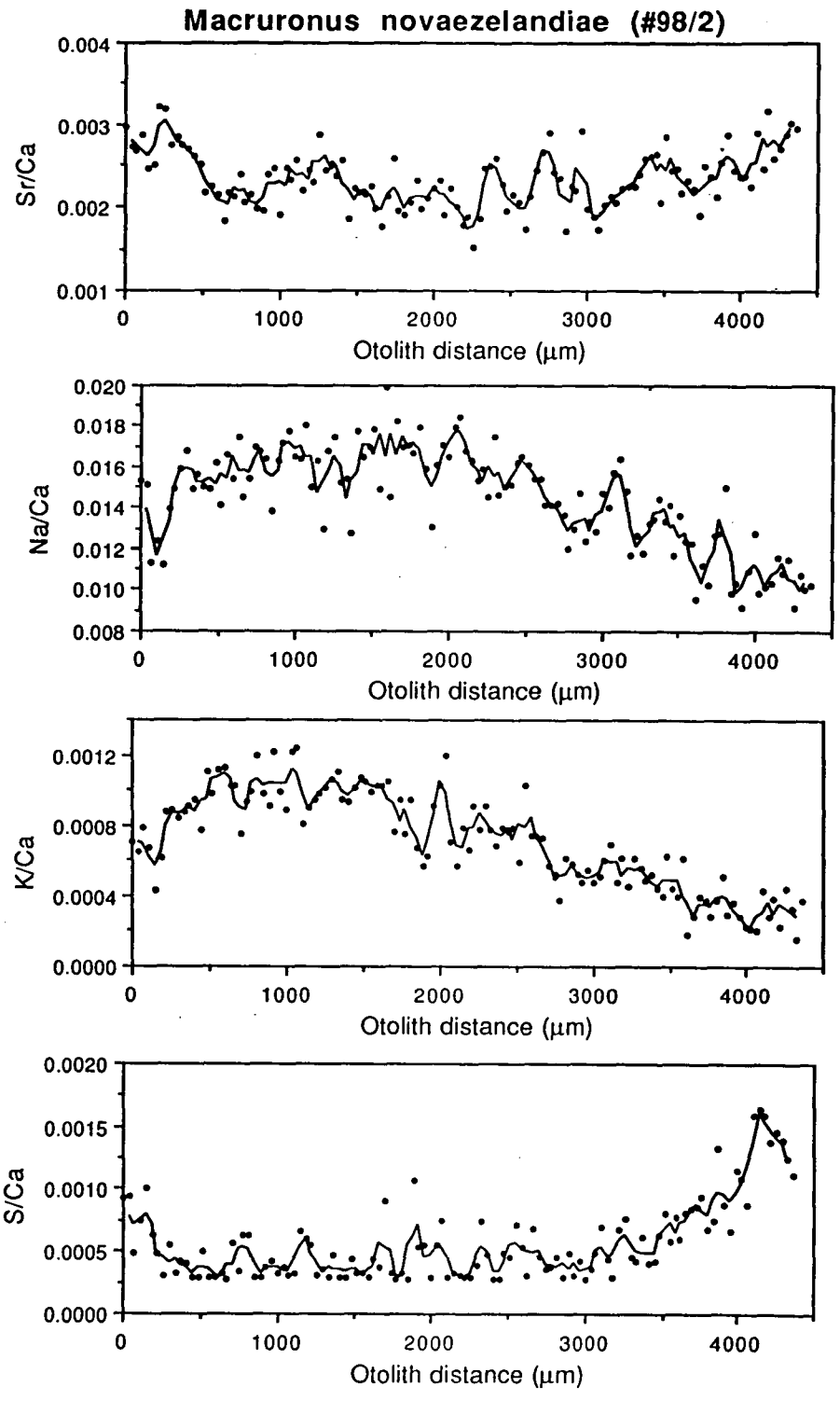

Fig. A5.7 Microprobe transect of a sagitta from a *Macruronus novaezelandiae* caught off the west coast of Tasmania, September 1984. Male, 81 cm SL, 2.2 kg. Estimated age based on otolith annuli was 8 years.

Journal of Experimental Marine Biology and Ecology 1989, Vol. 132, pp. 151-178